

Programme and Proceedings

SWIM 2014

23rd Salt Water Intrusion Meeting



June 16–20, 2014
Husum, Germany

Editors

Helga Wiederhold, Leibniz Institute for Applied Geophysics, LIAG

Johannes Michaelsen, CONSULAQUA

Klaus Hinsby, GEUS

Broder Nommensen, LLUR

Title**SWIM 2014**

23rd Salt Water Intrusion Meeting
Programme and Proceedings

Editors

Helga Wiederhold, Johannes Michaelsen, Klaus Hinsby, Broder Nommensen

Book compilation and formatting

Smart Abstract, Gabriele Köhn und schicker-sign, Regina Schicker

Printing

NEUE PERSPEKTIVEN Digital- und Offsetdruck

1st Edition

June 2014

ISBN 978-3-00-046061-6

Leibniz-Institut für Angewandte Geophysik
Stilleweg 2, 30655 Hannover

Table of Contents

Preface	5
Sponsor Recognition	6
Organizing Committee	7
Scientific Committee	7
Programme Agenda	8
Optional Field Trip	14
Poster Directory	15
Abstracts and Proceedings	20
Author Index	467



Welcome to the 23rd Saltwater Intrusion Meeting (SWIM), held from June 16 to 20 in Husum, Germany.

At SWIM23 you will experience a typical North Frisian town in the German-Danish border region. SWIM has been held on a biennial basis since 1968 SWIM held in Hannover (Germany). The next five meetings were organized by countries surrounding the North Sea, i. e. The Netherlands (1970), Denmark (1972), Belgium (1974), UK (1977) and again Germany (1979). But since then, SWIMs were held in a variety of locations across Europe (1981, 1996 Sweden; 1983, 1994, 2006 Italy; 1986, 2002 The Netherlands; 1988, 1998 Belgium; 1990, 2000 Poland; 1992, 2004 Spain; 2010 Portugal). Since 2008, every second SWIM is being held outside Europe (2008 USA; 2012 Brazil).

We are very glad to have SWIM back to our region after 35 years as a joint initiative of scientists from Denmark and Germany. The organizing committee includes colleagues from Geological Surveys (GEUS, LLUR, GLA HH, LBEG), a Research Institute (LIAG), a University (TU Hamburg-Harburg) and a consulting/engineering company (CONSULAQUA). As our venue, we chose the Husumhus ('Husum House'), event center of the Danish population of Southern Schleswig, situated in Germany in the city centre of Husum.

SWIM provides a great opportunity to raise awareness of fresh-/saltwater issues and the necessity for appropriate management tools to ensure fresh groundwater supply in a sustainable way. SWIM meetings are very successful in bringing together people who are interested in saline groundwater issues: well-known specialists, water managers and students. SWIMs are attended by a multi-disciplinary group of people with a wide variety of expertise including chemistry, engineering, geology and hydrogeology, geophysics, mathematics, physics, and management. SWIM is a chance to develop new initiatives and collaborative research projects.

In Northern Germany and Denmark, groundwater from porous Quaternary, Tertiary and Cretaceous aquifers is the primary source for fresh-water supply. Seawater intrusion along the shorelines of the North Sea and Baltic Sea, inland salinisation by Holocene marine deposits, upconing of deeper connate saltwaters, and salt diapir dilution pose the most dangerous threats to our fresh-water reservoirs. At SWIM23 we will discuss scientific progress and will raise awareness of saltwater intrusion in the public eye, as well as for managers involved in spatial planning administration and policy.

In this sense, we would like to carry on the inspiring idea presented by Gualbert Oude Essink at the last

SWIM concerning local climate-proof fresh groundwater supply. Our professional goal is generally restricted to developing a local solution – a small fish in relation to the huge shark representing climate and global change. However, many local solutions for climate-proof fresh groundwater supply have regional impact. We need to pool our expertise and local knowledge because only a wide effort of many people can open a chance to face the new challenges of climate and global change successfully. This challenge and responsibility of upcoming SWIMs should motivate us to increase our impact, communicate our showcases and work together on the development of sustainable and climate-proof water management in coastal regions around the world.

SWIM23 participants from 20 countries with 140 contributions show the increasing interest in SWIM. Themes concentrate on 10 topics: case studies from all around the world, variable-density flow and transport modelling, management of coastal aquifers, geophysics and hydraulic parameter estimation, dating of fresh and saline groundwater, saltwater intrusion monitoring, submarine groundwater, hydrogeology of islands, shallow processes, and sea level rise.

The keynote speech of Hans von Storch will give fresh input on science, policy decision and public participation in the context of the challenge of climate change at the coast. Hans von Storch is a director of the Institute for Coastal Research of the Helmholtz Center Geesthacht and professor at the Meteorological Institute of the University of Hamburg.

This proceedings book contains the papers submitted by participants and reviewed by the scientific committee. Not all took advantage of the chance to submit the extended abstract, but to have a permanent reminder of the 23rd SWIM we also included the short abstracts. We are grateful to all those who helped with this process. Digital copies of the proceedings book will be made available from the website after the meeting.

This meeting would not be possible without the efforts of numerous individuals. Special thanks to the team of Husum Tourist Information and the host of Husumhus, Witago for managing the registration and SMART ABSTRACT for managing the paper submission. We are particularly indebted to our sponsors.

On behalf of the Organizing Committee, we sincerely hope that we will have fruitful discussions leading to new ideas and collaborative efforts aiming towards increasing regional impact. Enjoy the SWIM23! Without your participation, SWIM would not be possible.

A special thanks to our sponsors

- Deutsche Forschungsgemeinschaft
- OOWV Oldenburg-Ostfriesischer Wasserverband
- Niedersachsen Wasser
- Hamburg Wasser
- Aarhus Geophysics
- Danish Ministry of the Environment
- KOWA SH Kooperation kommunaler Wasser- und Abwasserverbände Schleswig-Holsteins
- Danish Water Forum
- DHI-WASY
- OpenGeoSys

Organizing Committee

- **Klaus Hinsby**, Geological Survey of Denmark and Greenland GEUS, Copenhagen
- **Jörg Elbracht**, Geological Survey of Niedersachsen LBEG, Hannover
- **Johannes Michaelsen**, CONSULAQUA, Hamburg
- **Broder Nommensen**, Geological Survey of Schleswig-Holstein LLUR, Flintbek
- **Wilfried Schneider**, Hamburg University of Technology TU HH, Hamburg
- **Renate Taug**, Geological Survey Hamburg BSU, Hamburg
- **Helga Wiederhold**, Leibniz Institute for Applied Geophysics LIAG, Hannover
- **Gerson Cardoso da Silva Junior**, Federal University Rio de Janeiro, Rio de Janeiro
- **Adrian Werner**, Flinders University Adelaide, Adelaide

Scientific Committee

- **Giovanni Barrocu**, University of Cagliari, Cagliari, Italy
- **Michael Böttcher**, Leibniz Institut für Ost-seeforschung, Warnemünde, Germany
- **Emilio Custodio**, Real Academia de Ciencias, Barcelona, Spain
- **Perry De Louw**, Deltares, Utrecht, Netherlands
- **Georg Houben**, Federal Institute for Geosciences and Natural Resources BGR, Hannover, Germany
- **Rasmus Jakobsen**, Geological Survey of Denmark and Greenland GEUS, Copenhagen, Denmark
- **Reinhard Kirsch**, Geological Survey of Schleswig-Holstein LLUR, Flintbek, Germany
- **Christian D. Langevin**, US Geological Survey, Reston, USA
- **Flemming Larsen**, Geological Survey of Denmark and Greenland GEUS, Copenhagen, Denmark
- **Luc Lebbe**, Ghent University, Gent, Belgium
- **Gudrun Massmann**, Carl von Ossietzky Universität Oldenburg, Germany
- **Suzana Gico Montenegro**, University of Pernambuco UFPE, Recife, Brazil
- **Willard S. Moore**, University of South Carolina, Columbia, USA
- **Gualbert H.P. Oude Essink**, Deltares, Utrecht, Netherlands
- **Maurizio Polemio**, CNR-IRPI, Bari, Italy
- **Maria Pool**, Flinders University, Adelaide, Australia
- **Vincent Post**, Flinders University, Adelaide, Australia
- **Dieke Postma**, Geological Survey of Denmark and Greenland GEUS, Copenhagen, Denmark
- **Kai Radmann**, CONSULAQUA Beratungsgesellschaft mbH, Hamburg, Germany
- **Wilfried Schneider**, Hamburg University of Technology, Hamburg, Germany
- **Bernhard Siemon**, Federal Institute for Geosciences and Natural Resources BGR, Hannover, Germany
- **Shaul Sorek**, Ben-Gurion University of the Negev, Israel
- **Gerson Cardoso da Silva Junior**, University of Rio de Janeiro UFRJ, Rio de Janeiro, Brazil
- **Torben O. Sonnenborg**, Geological Survey of Denmark and Greenland GEUS, Copenhagen, Denmark
- **Alexander Vandenbohede**, Ghent University, Gent, Belgium
- **Clifford I. Voss**, US Geological Survey, Menlo Park, USA
- **Kristine Walraevens**, Ghent University, Gent, Belgium
- **Adrian Werner**, Flinders University, Adelaide, Australia
- **Ugur Yaramanci**, Leibniz Institute for Applied Geophysics LIAG, Hannover, Germany
- **Yoseph Yechieli**, Geological Survey of Israel and Ben Gurion University, Jerusalem, Israel

■ Monday, June 16, 2014

Monday, June 16, 2014 | 09:00 – 10:30

Welcome and Opening Ceremony

- **Robert Habeck**, Minister of Energy, Agriculture, the Environment and Rural Areas Schleswig-Holstein
- **Uwe Schmitz**, Mayor of Husum
- **Bjørn Kaare Jensen**, Deputy Director and Programme Director for Water Resources, Nature and Climate at GEUS
- **Peter Hansen**, Amtskonsulent, Sydslesvigsk Forening e.V.

09:00 - 09:45 Science, policy decision making and public participation – the challenge of climate change at the coast

Hans von Storch (featured speaker) **p. 442**

Monday, June 16, 2014 | 11:00 – 12:40

Effects of Sea Level Rise and Climate Change

- 11:00 - 11:25 Palaeo-climatic and Hydraulic control on Saline Groundwater in Holocene Delta Plains
Flemming Larsen (featured speaker) **p. 220**
- 11:25 - 11:40 Global Quick Scan of the Vulnerability of Groundwater systems to Tsunamis
Gualbert Oude Essink **p. 275**
- 11:40 - 11:55 Palaeo-modeling of coastal salt water intrusion during the Holocene:
an application to the Netherlands
Joost Delsman **p. 91**
- 11:55 - 12:10 Sea-level rise and seawater inundation of an atoll island, Roi-Namur,
Kwajalein Atoll, Republic of the Marshall Islands
Stephen Gingerich **p. 129**
- 12:10 - 12:25 Seawater intrusion overshoot - possible occurrence and cause
Leanne K. Morgan **p. 256**
- 12:25 - 12:40 Modelling the climate change impact on seawater intrusion in the coastal aquifer
of Bremerhaven, North Germany
Jie Yang **p. 457**

Monday, June 16, 2014 | 14:00 – 15:40

Local Small Scale and Shallow Processes

- 14:00 - 14:25 Saline seepage in deltaic areas: how local processes dominate salinization
Perry de Louw (featured speaker) **p. 83**
- 14:25 - 14:40 Predicting the effects of sea spray deposition and evapoconcentration on shallow
coastal groundwater salinity under various vegetation type
Pieter Jan Stuyfzand **p. 401**
- 14:40 - 14:55 The effect of saline gravel pit lakes (Ravenna, Italy) on ground water chemistry
Pauline N. Mollema **p. 248**
- 14:55 - 15:10 Tidal, spring-neap, and seasonal dynamics of a saltwater-freshwater mixing zone
in a beach aquifer
James W. Heiss **p. 158**
- 15:10 - 15:25 Geologic and hydrodynamic effects on shallow groundwater-surface water exchange
and chemical fluxes to an estuary
Holly A. Michael **p. 243**
- 15:25 - 15:40 Effect of forest fire on coastal aquifer salinisation and freshwater availability
Beatrice Maria Sole Giambastiani **p. 125**

Monday, June 16, 2014 | 16:00 – 17:30

Case Studies of Saltwater Intrusion 1

- 16:00 - 16:15 The effects of sea tides on fresh-saline water interface fluctuations and transient flow regime at coastal aquifers – field data and laboratory experiments
Elad Levanon p. 225
- 16:15 - 16:30 Can a large sand suppletion lead to a substantial increase in fresh water resources?: The Sand Motor Project
Sebastian Huizer p. 189
- 16:30 - 16:45 Controlled level drainage, a feasible measure to increase a fresh water lens in tidal creek deposits
Pieter Pauw p. 281
- 16:45 - 17:00 Development of a freshwater lens in a new strip of dunes
Ruben Caljé p. 54
- 17:00 - 17:15 3D-Modelling of the salt-/fresh water interface in coastal aquifers of Lower Saxony (Germany) based on airborne electromagnetic measurements (HEM)
Nico Deus p. 95
- 17:15 - 17:30 Coastal Water Resources Vulnerable to Climatic Change by Sea Level Rise (Gaza Strip Coastal Aquifer Case Study)
Ashraf M. Mushtaha p. 257
- 17:30 - 19:00 **Poster Session 1**

■ Tuesday, June 17, 2014

Tuesday, June 17, 2014 | 08:45 – 10:30

Variable Density Flow and Transport Modelling 1

- 08:45 - 09:00 Dupuit or Not Dupuit? That's the question
Mark Bakker p. 32
- 09:00 - 09:15 Simulation of seawater intrusion with standard groundwater codes
Frans Schaars p. 350
- 09:15 - 09:30 Comparison of different numerical models using a two-dimensional density-driven benchmark of a freshwater lens
Leonard Stoeckl p. 389
- 09:30 - 09:45 Density-driven flow modelling using d^{3f}
Anke Schneider p. 358
- 09:45 - 10:00 Experimental Investigation of Transient Saltwater Intrusion in Heterogeneous Porous Media
Gareth Robinson p. 323
- 10:00 - 10:15 The impact of tides on mixing and spreading in heterogeneous coastal aquifers
Maria Pool p. 309
- 10:15 - 10:30 SWIBANGLA: Managing salt water intrusion impacts in Bangladesh
Marta Faneca Sánchez p. 109

Tuesday, June 17, 2014 | 11:00 – 12:30

Submarine Groundwater

- 11:00 - 11:25 Biogeochemical consequences of seawater intrusion into coastal aquifers
Willard Moore (featured speaker) p. 252

Programme Agenda

- 11:25 - 11:40 Carbon Isotopes in Dissolved Inorganic Carbonate (DIC) trace Submarine Groundwater Discharge and Advective Pore water Circulation in Tidal Areas of the Southern North Sea
Michael E. Böttcher p. 42
- 11:40 - 11:55 Freshwater intrusion: Return of Meteoric Groundwater back to the Continent, San Diego, California, USA
Wesley R. Danskin p. 71
- 11:55 - 12:10 Submarine groundwater discharge in the southwestern Baltic Sea
Jan Scholten p. 362
- 12:10 - 12:25 Unstable flow patterns during submarine groundwater discharge: Changing the way we look at the freshwater-seawater interface
Janek Greskowiak p. 132

Tuesday, June 17, 2014 | 14:00 – 15:45

Case Studies of Saltwater Intrusion 2

- 14:00 - 14:15 Saltwater intrusion in fractured rock - a study of the proposed high-level nuclear waste repository at Forsmark, Sweden
Clifford I. Voss p. 444
- 14:15 - 14:30 Saltwater Intrusion in Karst aquifers along the Eastern Mediterranean
Grace Rachid p. 311
- 14:30 - 14:45 The interrelation between multi layered aquifer and the sea, examples from Gaza and the Carmel coastal areas
Said Ghabayen p. 121
- 14:45 - 15:00 Saltwater contamination in the lowlying coastland of the Venice Lagoon, Italy
Andrea Viezzoli p. 438
- 15:00 - 15:15 Seawater intrusion characterization in the coastal section of Sfax superficial aquifer (Tunisia)
Rouaida Trabelsi p. 411
- 15:15 - 15:30 Hydrogeological and Hydrogeochemical Investigation of the Coastal Area of Jifarah Plain, NW Libya
Kristine Walraevens p. 445
- 15:30 - 15:45 Hydrodynamic effects in the discharge zone of the Motril-Salobreña coastal aquifer due to the drilling of artesian wells
Juan Pedro Sánchez Úbeda p. 343

Tuesday, June 17, 2014 | 16:00 – 17:30

Geophysics and Hydraulic Parameter Estimation 1

- 16:00 - 16:25 Saltwater intrusions – a challenge for geophysics
Reinhard Kirsch (featured speaker) p. 211
- 16:25 - 16:40 Helicopter-borne electromagnetics: A powerful tool for the mapping of coastal aquifers
Annika Steuer p. 385
- 16:40 - 16:55 Actualization of a 40 year old salinization map of the eastern Belgian coast using airborne time-domain electromagnetic survey (SkyTEM)
Dieter Vandeveld p. 435

- 16:55 - 17:10 Investigating freshwater lenses with ground-penetrating radar (GPR): capabilities, limitations and perspectives
Jan Igel **p. 195**
- 17:10 - 17:25 Contribution of Nuclear Magnetic Resonance for feeding hydraulic models in saltwater problems
Thomas Günther **p. 150**
- 17:30 - 19:30 **Poster Session 2**

■ **Wednesday, June 18, 2014**

Wednesday, June 18, 2014 | 08:45 – 10:30

Management of Coastal Aquifers 1

- 08:45 - 09:00 Military inundations at the Yser front: the groundwater perspective
Alexander Vandenbohede **p. 431**
- 09:00 - 09:15 Overview: Management of groundwater at salinisation risk
Livia Emanuela Zuffianò **p. 466**
- 09:15 - 09:30 Integrated coastal aquifer and coastal zone management strategies
Giovanni Barrocu **p. 34**
- 09:30 - 09:45 Hydrogeological modeling for sustainable groundwater management under climate change effects for a karstic coastal aquifer (Southern Italy)
Maurizio Polemio **p. 305**
- 09:45 - 10:00 Quantifying the relative contribution of climatic and pumping impacts to coastal aquifer depletion using a highly parameterised groundwater model: Uley South Basin (South Australia)
Matthew Knowling **p. 215**
- 10:00 - 10:15 Assessing managed aquifer recharge (MAR) for coastal aquifer management in Asia, South America and Europe in a changing climate
Klaus Hinsby **p. 164**
- 10:15 - 10:30 Sharing precious water volumes in The Water Farm: from concept towards practice
Esther van Baaren **p. 417**

Wednesday, June 18, 2014 | 11:00 – 12:30

Monitoring Saltwater Intrusion

- 11:00 - 11:15 Measurements with an automated electrical resistivity tomography system in a freshwater/saltwater transition zone
Michael Grinat **p. 134**
- 11:15 - 11:30 Characteristics of real time variations of freshwater-saltwater interface using a new monitoring method at Jeju island, South Korea
Yongcheol Kim **p. 208**
- 11:30 - 11:45 The self-potential (SP) response to seawater intrusion: Evidence for the application of SP monitoring to the management of abstraction in coastal aquifers.
Donald John MacAllister **p. 239**
- 11:45 - 12:00 Monitoring inland salt-water intrusion with long-electrode ERT
Mathias Ronczka **p. 335**

Programme Agenda

- 12:00 - 12:15 Coastal aquifer monitoring and management from high frequency and autonomous downhole hydrogeophysical observatories
Philippe Adrien Pezard p. 288
- 12:15 - 12:30 Monitoring seawater intrusion by means of long-term series of EC and T logs (Salento coastal karstic aquifer, Southern Italy)
Maria Dolores Fidelibus p. 117

Wednesday, June 18, 2014 | 14:00 – 15:30

Hydrogeology of Islands

- 14:00 - 14:25 The use of multi-level pressure and salinity data to understand freshwater-lens dynamics
Vincent Post (featured speaker) p. 310
- 14:25 - 14:40 Freshwater lenses as archives for climate history and hydrochemical evolution – insights from depth-specific age dating and stable water isotope analysis, Langeoog Island, Germany
Georg Houben p. 172
- 14:40 - 14:55 The role of 3D volcanic structures on seawater intrusion in Grande Comore Island inferred from geophysical investigations and groundwater modelling
Anli Bourhane p. 50
- 14:55 - 15:10 Guiding Principles for Fresh Water Lens Development, Exploitation and Maintenance in Artificial Islands
Marloes van Ginkel p. 420
- 15:10 - 15:25 The fresh-saltwater distribution of the Island of Föhr – assembling of a data base for the assessment of climate change impact
Wolfgang Scheer p. 354

Wednesday, June 18, 2014 | 16:00 – 17:30

Geophysics and Hydraulic Parameter Estimation 2

- 16:00 - 16:15 Geophysical investigation of a managed freshwater lens on the North Sea island of Langeoog
Stephan Costabel p. 63
- 16:15 - 16:30 Cone Penetration Tests with electrical conductivity for fresh-salt water investigations
Kees-Jan van der Made p. 418
- 16:30 - 16:45 Hydrogeophysical inversion techniques for seawater intrusion models
Daan Herckenrath p. 163
- 16:45 - 17:00 Coupled hydrogeophysical inversion on synthetic example of seawater intrusion
Klara Steklova p. 381
- 17:00 - 17:15 Use of high-resolution tidal data and highly-parameterized inversion in managed coastal aquifers
Joseph Hughes p. 184
- 17:15 - 17:30 A flexible predictive tool for saltwater intrusion in the Red River Delta
Hoang Duc Nguyen p. 262
- 19:00 - 22:00 **Conference Dinner in Husums Brauhaus**

■ Friday, June 20, 2014

Friday, June 20, 2014 | 08:45 – 10:30

Dating of Fresh and Saline Groundwater & Case Studies of Saltwater Intrusion 3

08:45 - 09:10	Dating of saline groundwater from several Israeli aquifers, indication for paleo seawater intrusion and comparison with results of numerical simulations <i>Yoseph Yecheili</i> (featured speaker)	p. 461
09:10 - 09:25	Evaluating Remediation Potential of a Salinized Heterogeneous Aquifer System Using Three-Dimensional, Density-Dependent Groundwater Modeling <i>Marc Walther</i>	p. 449
09:25 - 09:40	Climate change effect on seawater intrusion evolution in Dar Es Salaam coastal plain, Tanzania <i>Giuseppe Sappa</i>	p. 344
09:40 - 09:55	Hydrological History of the Amsterdam Water Supply Dunes <i>Philip Nienhuis</i>	p. 265
09:55 - 10:10	Salinisation processes in the Kalahari Sediments of Western Zambia: Machile Basin <i>Kawawa Eddy Banda</i>	p. 33
10:10 - 10:25	Groundwater Freshening following Coastal Progradation and Land Reclamation of the Po Plain, Italy <i>Diana M. Allen</i>	p. 25

Friday, June 20, 2014 | 11:00 – 13:00

Variable Density Flow and Transport Modelling 2

11:00 - 11:15	Historical and projected saltwater distribution at the left bank of the Scheldt near the port of Antwerp, Belgium <i>Luc Lebbe</i>	p. 221
11:15 - 11:30	Salt groundwater distribution in the Pakistani Punjab based on simulation of historic events <i>Theo Olsthoorn</i>	p. 269
11:30 - 11:45	Seawater intrusion in fractured coastal aquifers: preliminary investigation using a discretely fractured Henry problem <i>Megan Sebben</i>	p. 363
11:45 - 12:00	Responses to Climate Change and Development Stressors on Small Oceanic Islands <i>Shannon T. Holding</i>	p. 168
12:00 - 12:15	Monitoring and modelling the dynamic behaviour of rainwater lenses and soil-, ground- and drain water salinities <i>Perry de Louw</i>	p. 87
12:15 - 12:30	Results of a Physical Experiment of Variable-Density Driven Flow and Transport in a Saturated Porous Media <i>Carlos Guevara</i>	p. 144
12:30 - 12:45	Saline water circulation beneath the fresh-saline interface: results of laboratory experiments and numerical modeling <i>Imri Oz</i>	p. 279
12:45 - 13:00	Requirements of modeling the freshwater lens of the Island of Sylt <i>Kai Radmann</i>	p. 315

Friday, June 20, 2014 | 14:00 – 15:00

Management of Coastal Aquifers 2

14:00 - 14:15	Problems and solutions when storing fresh water in brackish aquifers <i>Pieter Jan Stuyfzand</i>	p. 397
14:15 - 14:30	Effect of dispersivity on saltwater intrusion and removal processes <i>Masahiro Takahashi</i>	p. 405
14:30 - 14:45	Potential Consequences of Saltwater Intrusion at the German North Sea Coast for the water supply <i>Malte Eley</i>	p. 103
14:45 - 15:00	Fresh keeper without reverse osmosis: can we prevent upconing by pumping brackish water to a deeper aquifer? <i>Willem Zaadnoordijk</i>	p. 462

Optional Field Trip

Optional Field Trip – Thursday, June 19, 2014

A Visit to the Island of Sylt

- 8:00 Bus leaves at HusumHus SWIM-Conference Building
Travel by bus and train to the island of Sylt passing the landscapes of Marshland and Geest
- 9:30 Walk along the MORSUM KLIFF observing impact of glacier (ice-age), wind and sea; the geological outcrop provides insight to Quaternary and Tertiary formations.
- 12:00 Walk on the tidal flat, experience a part of the Wadden Sea listed as World Heritage
- Lunch**
- 14:30 Visit of the Water Division of the local company “EnergieVersorgung Sylt” EVS, which operates services and systems for water, wastewater and stormwater. Water supply depends on exploitation of the fresh water lens and faces an extreme seasonal fluctuation in water demand.
- 16:00 Dunes of Listland, overview on moving dunes and dune slacks
- 18:00 Westcoast Cliff, observing impacts of storm events causing high eroding rates of about 1 m per year and measures for coastal defence

Return to Husum

Poster Directory

- P-01** Quantify the Influence of the Ocean Current on the Submarine Groundwater Discharge
Wei-Ci Li — p. 229
- P-02** Estimation of preferential recharge and saltwater intrusion to a coastal groundwater system in the North Central Coast of Vietnam by means of 3D hydrostratigraphical modeling
Vu Thanh Tam — p. 409
- P-03** Hydrogeochemical Characterization of Groundwater in Soc Trang Province, Southern Vietnam
Hoang Thi Hanh — p. 154
- P-04** Origin of saltwater in the groundwater systems of Indian subcontinent
Naveed Alam — p. 24
- P-05** Salt Water Intrusion into the Tertiary Aquifers in North Qatar Peninsula, Arabian Gulf
Ali Elobaid Elnaiem — p. 107
- P-06** Assessment of saltwater intrusion in the aquifer of Tripoli Lebanon
Omar Kalaoun — p. 204
- P-07** Submarine groundwater discharge at the Dead Sea
Christian Siebert — p. 366
- P-08** Hydrogeological model of a complex coastal aquifers: the case of Sibari Plain (Southern Italy)
Maurizio Polemio — p. 297
- P-09** The coastal hydrogeological system of Mar Piccolo (Ionian Sea, Italy)
Pierpaolo Limoni — p. 235
- P-10** A peculiar case of coastal springs and geogenic saline groundwater: the Santa Cesarea Terme thermal springs (Southern Italy)
Maurizio Polemio — p. 301
- P-11** Geochemical and isotopic evidence of the aquifer-lagoon interaction during Holocene (Almería, SE Spain)
Fernando Sola — p. 379
- P-12** Evidence of Pleistocene submarine discharges in the Aguadulce cliffs (Almería, SE Spain)
Fernando Sola — p. 380
- P-13** Groundwater flow and salinity distribution near a tidal gully in the Zwin remnant, Belgium
Gert-Jan Devriese — p. 99
- P-14** Groundwater salinity patterns at the land-ocean boundary in the Netherlands
Pieter Pauw — p. 285
- P-15** Saltwater intrusion in porous aquifers in Northern Germany
Helga Wiederhold — p. 453
- P-16** Helicopter-borne electromagnetic surveys in Northern Germany
Bernhard Siemon — p. 375

Poster Directory

- P-17** Multi-isotope composition of freshwater sources for the southern North and Baltic Sea
Michael E. Böttcher — p. 46
- P-18** Airborne clay mapping at the East Frisian coast
Bernhard Siemon — p. 371
- P-19** Impact of tourism on groundwater extraction on the island of Langeoog, Germany
Georg Houben — p. 180
- P-20** Hydrogeological features of freshwater lenses on volcanic islands - physical and numerical modeling
Georg Houben — p. 176
- P-21** Application of airborne electromagnetics for groundwater investigations in the vicinity of salt structures
Florian Krause — p. 218
- P-22** Groundwater flow analysis in variable-density formation waters - a comparison of common approximations
Martina aus der Beek — p. 31
- P-23** The salinization of useful Cenozoic aquifers by ascending Mesozoic brines - characterization on the basis of hydrochemical data from northern and central Poland
Dorota Kaczor-Kurzawa — p. 200
- P-24** Origins of groundwater salinity and implications for the groundwater management of Emborê Aquifer, Rio de Janeiro State, Brazil
Gerson Cardoso da Silva Jr. — p. 67
- P-25** Towards groundwater security in coastal East Africa (UPGRO Programme): initiating a regional research network and integrated hydrogeologic, climatic & socio-economic observatories in coastal aquifers of the East African/Western Indian Ocean region
Jean-Christophe Comte — p. 62
- P-26** Seawater intrusion in the southern Po Plain, Italy: managing a geologic and historical heritage
Alexander Vandenbohede — p. 427
- P-27** Seawater intrusion vulnerability indicators for freshwater lenses in strip islands
Leanne K. Morgan — p. 255
- P-28** ASTER and WorldView-2 satellite data applications for recognition of salt water intrusion effects on forest vegetation
Michaela De Giglio — p. 75
- P-29** A geophysical approach for mapping and quantifying near-surface freshwater-saltwater transitions
Ercan Erkul — p. 108
- P-30** Resistivity tomography, an underestimated tool for mapping fresh salt groundwater interface
Michel Groen — p. 138

- P-31** Geoelectrical monitoring of freshwater-saltwater interaction in physical model experiments
Mathias Ronczka — p. 331
- P-32** Geophysical monitoring of brine and compressed air leakages in groundwater from deep energy storages
Said Attia al Hagrey — p. 20
- P-33** Evidence and causes of groundwater level fluctuations in a semiconfined mediterranean coastal aquifer. The ocean tide effect
Angela Vallejos — p. 415
- P-34** Application of the Base Pressure Method for the Correction of Water Level Data from Monitoring Wells influenced by Salt Water
Jörg Grossmann — p. 140
- P-35** Tide cleaning of heads in unconfined coastal aquifers via processing of signal wave components
Juan Pedro Sánchez Úbeda — p. 339
- P-36** Comparing transport parameters and PHREEQC simulation parameters of seawater intrusion experiments in columns filled with different porous media
Nuria Boluda-Botella — p. 38
- P-37** Modeling of gypsum dissolution driven by variable density flow in the coastal karst aquifer of Lesina Marina (southern Italy)
Maria D. Fidelibus — p. 113
- P-38** Cost-Effective Management of Sea Water Intrusion in Shallow Unconfined Aquifers
Mohammed Hussain — p. 191
- P-39** Saltwater upconing zone of influence
Danica Jakovovic — p. 199
- P-40** Evaluating hydraulic barriers for reducing and controlling saltwater intrusion in a changing climate
Per Rasmussen — p. 319
- P-41** Procedure to simulate the historical evolution of the fresh and salt water distribution in a highly dynamic coastal area
Jasper Claus — p. 58
- P-42** Stochastic Analysis of Saltwater Intrusion in Heterogeneous Aquifers using Local Average Subdivision
Gareth Robinson — p. 327
- P-43** Influence of geological heterogeneity on freshwater discharge in coastal aquifers – physical experiments and numerical modeling
Leonard Stoeckl — p. 393
- P-44** On the development of instabilities under density-driven flow conditions in saturated porous media: physical and numerical experiments
Carlos Guevara — p. 148

Poster Directory

- P-45** Technical Aspects relating to Salt Water Intrusion problems
Hoang Phuc — p. 292
- P-46** Optimisation of subsurface fresh water storage in new land developments
Marianne Tijss — p. 410
- P-47** Calibrating a seawater intrusion model using surrogate simulations
Daan Herckenrath — p. 162
- P-48** Lessons learned from a regional variable density groundwater flow model and implemented climate change scenarios: a Dutch case
Esther van Baaren — p. 416
- P-49** iMOD: A high performance open source framework for SEAWAT
Jarno Verkaik — p. 437
- P-50** eMOD : a MATLAB application for MODFLOW-based groundwater flow and solute transport models
Alexander Vandenbohede — p. 424
- P-51** Recent Updates to the SEAWAT Computer Program
Christian Langevin — p. 219
- P-52** Saltwater intrusion in the Crau coastal aquifer (South of France): validation of variable density modeling using geophysical and geochemical data
Bach Thao Nguyen — p. 261
- P-53** Combining numerical modelling and field-based methods to obtain spatially and temporally variable recharge to a semi-arid coastal aquifer: Uley South Basin, South Australia
Carlos Miraldo Ordens — p. 246
- P-54** In search for clay and salt, combining traditional techniques with airborne geophysics (SkyTEM) to optimize the 3D image of the subsurface
Sander de Haas — p. 79
- P-55** Integrating improved conceptual knowledge into a 3-D variable density numerical model for a heavily exploited coastal aquifer with submarine spring discharge in South Portugal
Rui Hagman (unable to attend the meeting) — p. 185

Conference Papers

Listed alphabetically by presenting author.
Presenting author names appear in **bold**.

Geophysical monitoring of brine and air leakages in groundwater from deep energy storages

Said A. al Hagrey*, Daniel Köhn, Carla E. Wieggers, Dirk Schäfer, Wolfgang Rabbel
 Institute of Geosciences, University of Kiel, 24118 Kiel, Germany, sattia@geophysik.uni-kiel.de

ABSTRACT

Injected compressed air energy storage (CAES) and brine may seep from deep reservoirs along weak zones upwards into shallow groundwater aquifers. These CAES and fluid phase leakages cause changes in the electrical resistivity, density and elastic moduli of the aquifers, and justify applications of various geophysical techniques. Applied geophysical techniques can resolve and monitor these brine and CAES anomalies of a sufficient size and contrast inside the aquifer. Our sensitivity study shows that an investigation depth of conductive brine anomalies is at least twice that of resistive CAES anomalies. Based on sensitivity contrasts, seismic and gravity techniques are more sensitive to CAES leakages whereas electric and electromagnetic to brine intrusions.

INTRODUCTION

Renewable energy resources are intermittent and need a buffer storage to bridge the time-gap between production and demand peaks. The North German Basin has favourable conditions and a very large capacity for compressed air/gas energy storage (CAES) in porous saltwater reservoirs and salt caverns. However, the injected CAES and even saltwater can seep along weak zones and fractures upwards and migrate into shallow groundwater aquifers. These gas and fluid phase leakages cause changes in the electrical resistivity, density and elastic moduli of these aquifers, and justify applications of various geophysical techniques. Our current interdisciplinary project ANGUS+ deals with impacts of using geologic subsurface as a thermal, electric or material reservoir in context with alternative energy resources. Our main task is to develop an integrative geophysical monitoring strategy for this geologic CAES and its possible leakages for almost realistic scenarios.

Using numerical simulations of almost realistic scenario we study the applicability of techniques of elastic full wave inversion (FWI), electric resistivity tomography (ERT), transient electromagnetic induction (TEM) and gravity in monitoring these leakages in shallow groundwater aquifers.

HYDROGEOLOGICAL SIMULATION

We simulated two scenarios (Fig. 1). The first is a saltwater intrusion of 4.2 g/s with different salinities for 10 years due to pressure increase into a near surface potable aquifer. In the model the aquifer is homogeneous with a thickness up to 40 m. The salt water is transported with natural groundwater flow.

The second is a leakage of 1 kg/s compressed air for 10 years into a 500 m thick Quaternary aquifer with alternating layers of different sands, silt and clay. The geological structure has been determined by the State Agency for Agriculture, Environment and Rural Areas. It was imported into the simulation code TOUGH2-MP (EOS3) with help of the user interface PetraSim. The air migrates

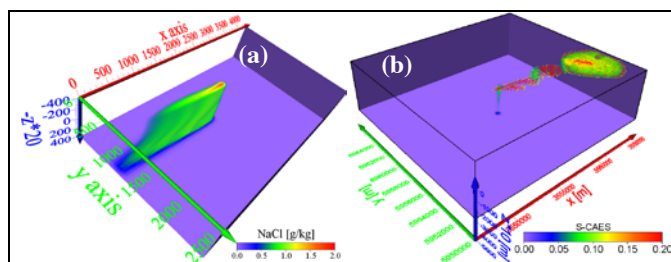


Figure 1: 3D saltwater and CAES leakages into shallow groundwater. After 10 years of leakage the density change of water is up to 4 kg/m³ for saltwater intrusion (salinity 4 g/l, a) and -340 kg/m³ for CAES (saturation 0.654, b).

buoyancy driven upwards, but accumulates below low permeable layers and searches its way upwards through better permeable areas.

GEOPHYSICAL MODELLING

Method	Petrophysical law	Forward - inverse codes	References
ERT	Archie	RES2DMOD - RES2DINV	Archie 1942, Loke et al 2003, Christiansen & Auken 2009, Tarantola 1986, Gassmann 1951, Köhn et al. 2012, Batzle & Wang 1992, Götz & Lahmeyer 1988
TEM	Archie	EM1DINV	
FWI	Gassmann, Patchy	DENISE	
Gravity	Mixing law for multiphase media	IGMAS+	

These hydrogeological leakage models, among others, are transferred in geophysical models (electric resistivity, seismic P and S-wave velocities and density) using almost realistic parameterization and adequate petrophysical laws (Table 1). Typical values for petrophysical parameters (e.g., porosity, density, TDS, elastic parameters) are considered from publications (e.g. Kunkel et al. 2002, Hese 2012). Using codes of Table 1, the forward modelling of this scenario generates synthetic datasets which in turn are inverted to reproduce the underground models. Surveys using optimized setups are conducted on land, in the air and in boreholes (e.g. Hagrey 2012). Data inversions are conducted without and with posing constraints on the initial model outside the leakage. We present here a part of the geophysical results for the sake of brevity.

GEOPHYSICAL MONITORING SALTWATER INTRUSION

Results reflect a varying sensitivity of the different applied techniques to resolve and monitor this saltwater intrusion (Figs. 2-3). ERT and TEM techniques are well capable to detect and monitor this intrusion already 0.5 year after intrusion. Gravity and FWI are unable to detect the anomaly of this saltwater intrusion with salinity contrasts up to 3.721 g/l (density up to 3.721 kg/m³, averaging 0.045

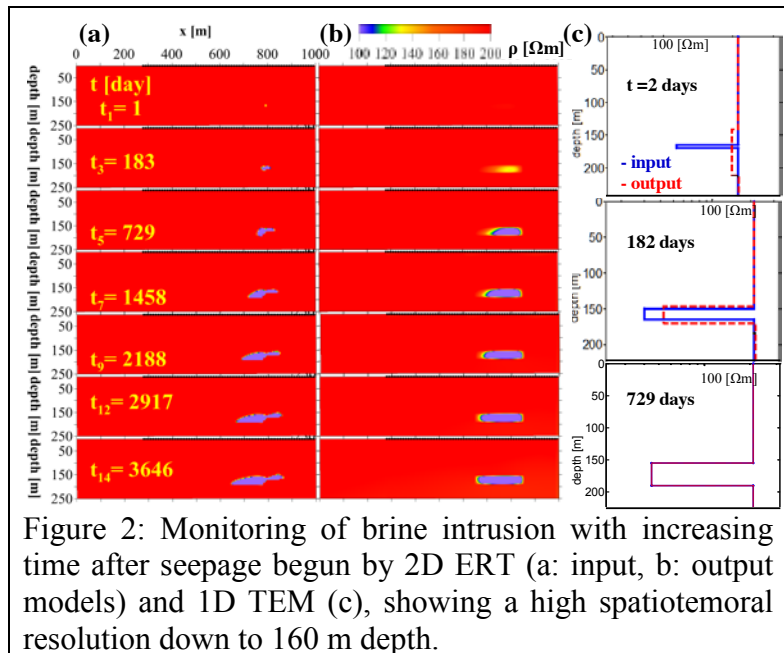


Figure 2: Monitoring of brine intrusion with increasing time after seepage begun by 2D ERT (a: input, b: output models) and 1D TEM (c), showing a high spatiotemoral resolution down to 160 m depth.

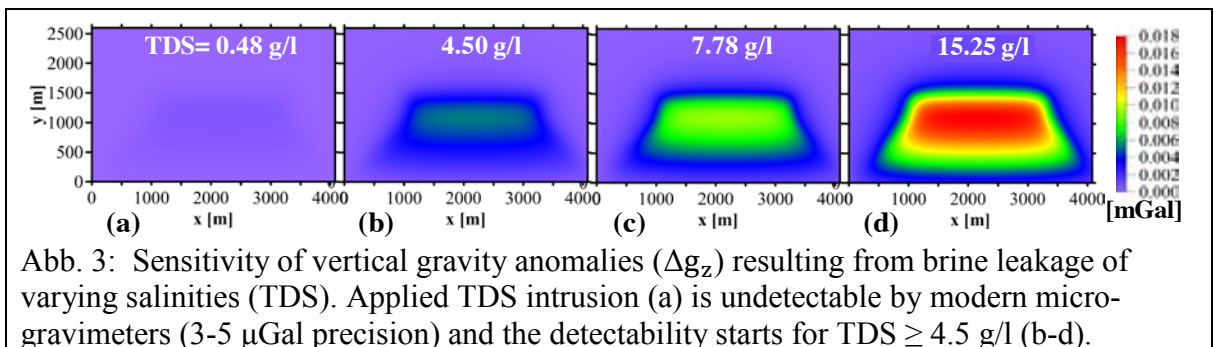


Abb. 3: Sensitivity of vertical gravity anomalies (Δg_z) resulting from brine leakage of varying salinities (TDS). Applied TDS intrusion (a) is undetectable by modern micro-gravimeters (3-5 μ Gal precision) and the detectability starts for TDS \geq 4.5 g/l (b-d).

kg/m³). Sensitivity analyses show that a plume as in figure 1 yields a measurable vertical gravity anomaly Δg_z (i.e. $> 5 \mu\text{Gal}$) when the density contrast approaches $\geq 4.5 \text{ kg/m}^3$, i.e. TDS contrast $\geq 4.5 \text{ g/l}$. Hence, only salt water intrusions with a TDS 10 times higher than in the presented scenario can be detected by gravity. Seismic sensitivity analyses using reverse time migration (RTM) show that a plume detection is possible with a TDS contrast is 50 times larger than in the scenario (not shown).

GEOPHYSICAL MAPPING CAES LEAKAGE

Reconstructed ERT models (Fig. 4) show the technique capability (of different surveys and inversion constraints) to resolve the resistive anomalies of the CAES leakage within the conductive aquifer. The inverted model resolution is enhanced by applying a combined surface-borehole survey (instead the single surface or borehole survey alone, cf. Figs. 4d and 4e) and by considering a constrained inversion (instead of no constraints, cf. Figs. 4d and 4f). We can see that the resolution of the surface survey decreases with increasing depth where the deep anomaly shows a smeared oversize and reduced amplitude.

Inverted 1D aero-TEM models show the technique capability to resolve these shallow and deep resistive anomalies. The shallow resistive anomaly is better resolved than the deep anomaly. Obviously, both ERT and TEM techniques can resolve these CAES anomalies. However, the resolution of resistive air plumes in conductive

medium is governed by the equivalence principle of the transverse resistance ($\rho h = \text{constant}$, $h = \text{layer thickness}$), where the smearing effect increases the thickness on expenses of the resistivity amplitude. i.e. the amplitude is underestimated.

Moreover, the 3D gravity technique applied here (not shown?) shows a high sensitivity to this shallow leakage in groundwater. For this leakage a negative anomaly approaches an amplitude of $>140 \mu\text{Gal}$ which is far higher than the least measurable value of $5 \mu\text{Gal}$ using micro-gravimeters.

Applying Gassmann eq. yields changes of the elastic material parameters of V_p , V_s and bulk density d_b (Fig.5a-c). Due to the free surface boundary condition the data of synthetic reflection seismic is dominated by the Rayleigh wave, which highly increases the nonlinearity of the inverse problem (Brossier *et al.* 2009). The synthetic seismic sections are the input data for the FWI. The initial model for the time-lapse waveform inversion at each time-step is the true elastic baseline model before the CAES leakage. No constraints to the time-lapse data, like sequential frequency/offset filtering or time windowing, are applied and all elastic model parameters are inverted simultaneously. The seismic inversion results (Fig. 5d-f) are compared with the true changes (Fig. 5a-c). Due to the dominance of the Rayleigh

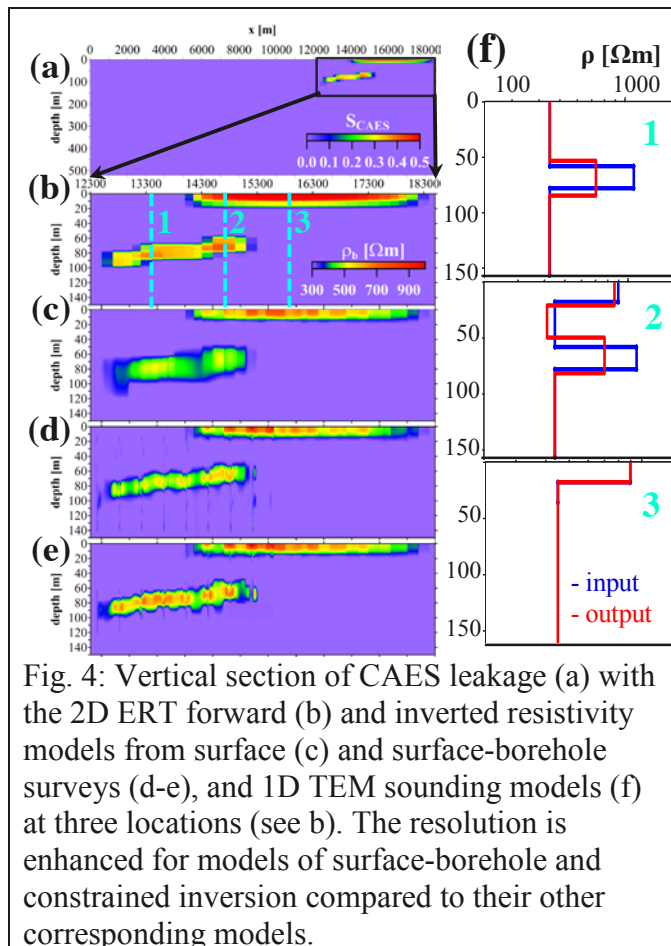


Fig. 4: Vertical section of CAES leakage (a) with the 2D ERT forward (b) and inverted resistivity models from surface (c) and surface-borehole surveys (d-e), and 1D TEM sounding models (f) at three locations (see b). The resolution is enhanced for models of surface-borehole and constrained inversion compared to their other corresponding models.

wave in the time-lapse data only V_s model variations could be recovered with some success, while the changes in V_p and d_b are underestimated.

CONCLUSION

Applied geophysical techniques are capable to detect and monitor saltwater or CAES leakage. A comparative interpretation of results for both leakages may facilitate the sensitivity evaluation of the single techniques applied to each of these leakages. The CAES leakage is characterized by its resistivity highs and mass deficit, and the saltwater intrusion by its resistivity lows and mass excess. The lower boundary value of detectability has been determined. FWI technique can map the CAES plume better than the saltwater plume based on impedance contrasts. Applied integrative techniques complement each other. Gravity and FWI methods are more sensitive to CAES plumes yielding stronger density contrast than saltwater intrusions, whereas ERT and TEM are more sensitive to the conductive saltwater than the resistive CAES. Also the investigation depth for the resistive CAES plume is far shallower than that for the conductive saltwater intrusion.

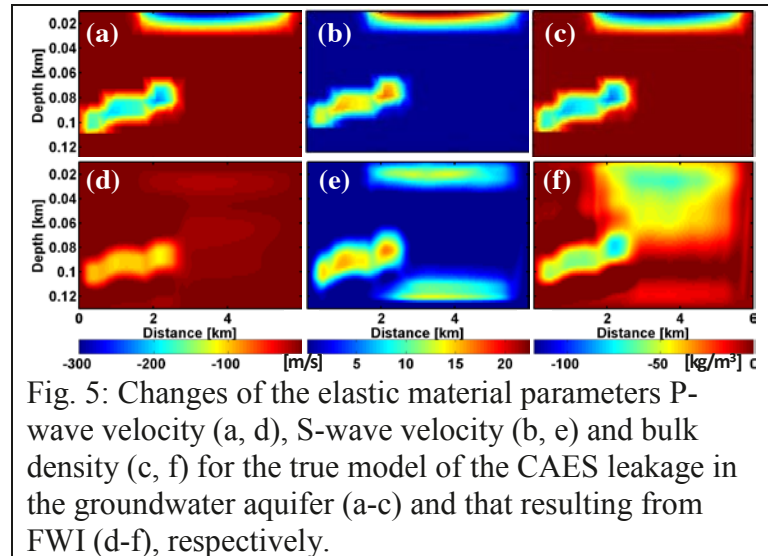


Fig. 5: Changes of the elastic material parameters P-wave velocity (a, d), S-wave velocity (b, e) and bulk density (c, f) for the true model of the CAES leakage in the groundwater aquifer (a-c) and that resulting from FWI (d-f), respectively.

ACKNOWLEDGEMENTS

This study has been carried out within the framework of ANGUS+ research project funded by the German Federal Ministry of Education and Research (BMBF).

REFERENCES

- Archie G.E. 1942. The electrical resistivity log as an aid in determining some reservoir characteristics. Transactions of the American Institute of Mining Engineers 146, 54-62.
- Batzle M. and Wang Z. 1992. Seismic properties of pore fluids. Geophysics 57, 1396-1408.
- Brossier, R., Operto, S. and Virieux, J. 2009. Seismic imaging of complex onshore structures by two-dimensional elastic frequency-domain full-waveform inversion. Geophysics 74(6), WCC63-WCC76.
- Christiansen A.V. and Auken E. 2009. Presenting a Free, Highly Flexible Inversion Code: Near Surface 2009, Dublin, Ireland, Expanded Abstract, B09.
- Gassmann, F. 1951. Über die Elastizität poröser Medien. Vierteljahrsschrift der Naturforschenden Gesellschaft in Zürich 96, 1-23.
- Götze H.-J. and Lahmeyer B. 1988. Application of three-dimensional interactive modeling in gravity and magnetism. Geophysics 53(8), 1096-1108.
- Hagrey S. A. al 2012, 2D optimized electrode arrays for borehole resistivity tomography and CO₂ sequestration modelling. Pure and Applied Geophysics 169(7), 1283-1292.
- Hese F. 2012. *3D Modellierungen und Visualisierung von Untergrundstrukturen für die Nutzung des unterirdischen Raumes in Schleswig-Holstein*. PhD thesis, University of Kiel, Kiel.
- Köhn D., De Nil D., Kurzmann A., Przebindowska A. and Bohlen T. 2012. On the influence of model parametrization in elastic full waveform tomography. Geophysical Journal International 191, 325-345.
- Kunkel R., Hannappel S., Voigt H.-J., Wendland F. 2002. Die natürliche Grundwasserbeschaffenheit ausgewählter hydrostratigraphischer Einheiten in Deutschland. Endbericht eines FuE-Vorhabens im Rahmen des Länderfinanzierungsprogramms „Wasser und Boden“ der Länderarbeitsgemeinschaft Wasser. 97 p.
- Loke H., Acworth I. and Dahlin T. 2003. A comparison of smooth and blocky inversion methods in 2D electrical imaging surveys. Exploration Geophysics 34, 182-187.
- Tarantola A. 1986. A strategy for non-linear inversion of seismic reflection data. Geophysics 51, 1893-1903.

Origin of saltwater in the groundwater systems of Indian subcontinent

N. Alam¹ and T. N. Olsthoorn^{1,2}

¹Department of Water Management, Delft University of Technology, Delft, Netherlands

²Waternet (Amsterdam Water Supply), Vogelenzang, Netherlands

ABSTRACT

Groundwater management and exploration in the important Indus Basin aquifer require discovering the mechanism of salt accumulation. It is undoubtedly clear that the infiltrating rivers in the Punjab are the cause of high evaporation gradually away from the rivers, which results into accumulation of saltwater in the Indus Basin aquifer. But, the presence of saltwater at greater depths confuses the Hydrogeologists working on the groundwater management of the area to build reliable models. In this paper, we explore the hypothesis of land formation in the Indian subcontinent, which unveils the noteworthy history as well as important origin of saltwater in the Indus Basin aquifer. A gigantic Himalayan's river called as "Siwalik" had been involved in the land formation of Indian subcontinent since a few million years ago as revealed by archeological records. A huge amount of debris and alluvium as transported from the Himalayas by this great river were deposited in the sea, where the present-day lands of Pakistan, Indian Punjab and Indian state of Rajasthan exist. In this paper, we simulate the hydrogeological processes of land formation to date back the origin of saltwater in the Indus Basin aquifer. Borehole logs, which were drilled up to bedrocks in the recent past, are used to evaluate the pattern of deposition. The analysis of chemical and isotope samples, as collected in the past, also indicates a possible relation between the deeper groundwater and ocean water.

Groundwater Freshening Following Coastal Progradation and Land Reclamation of the Po Plain, Italy

Marco Antonellini¹, **Diana M. Allen**², Pauline N. Mollema¹, D. Capo¹, N. Greggio¹

¹ Department of Biological, Geological and Environmental Sciences. University of Bologna, Ravenna RA, Italy

²Department of Earth Sciences, Simon Fraser University, Burnaby, BC, Canada

ABSTRACT

Many coastal areas historically were inundated by seawater, but have since undergone land reclamation to enable settlements and farming. This study focuses on the coastal unconfined aquifer in the Po Plain near Ravenna, Italy. Fresh water is present as isolated, thin (1-5 m) lenses on top of brackish-salt water. Historical maps show large areas of sea inundation until approximately 150-200 years ago when coastal progradation and construction of the drainage canals began. Since then, the aquifer has been freshening from recharge. A 3D SEAWAT model is used to simulate a 200 year freshening history, starting with a model domain that is saturated with sea water, and applying recharge across the top model layer. Calibration to the observed concentrations is remarkably good for discrete depths within many monitoring wells despite model simplicity. The distribution of fresh water at the end of the 200 year period, representing current conditions, is controlled by the drainage network. Within and adjacent to the drains, the groundwater has high salinity due to up-coning of salt water. Between drains, the surface layers of the aquifer are fresh due to the flushing action of recharge. The modeling results are consistent with cation exchange processes revealed in the groundwater chemistry.

Keywords: Land Reclamation, Groundwater Freshening, Coastal Aquifers, Numerical Modeling, Italy

INTRODUCTION

Coastal regions have experienced significant change due to human development as well as natural geological processes. The construction of extensive drainage networks has been a primary means to reclaim the land for agricultural development, to mitigate the effects of land subsidence, or a combination of both. In the literature (Stuyfzand 1989; de Louw et al. 2011), these drainage networks have been described as leading to upconing of the saltwater from depth, thereby leading to salinization of the freshwater lens (Mollema et al. 2012). However, some coastal aquifers show evidence of high salinity, not because of current anthropogenic activities, but rather because salt water has not been flushed completely by fresh water after the Holocene marine transgression (e.g. Custodio and Bruggeman 1987). The aquifers are in transition from an initial state of a salty aquifer to one that is now exposed at surface and subject to freshening processes. However, if the water table is close to surface due to the low elevation, the land floods readily and must be drained artificially to enable use of the land surface. Within this context, the role of the drainage network either as a means of freshening the aquifer or causing salinization is of interest (Vandenbohede et al. 2014).

In this paper, freshening of a coastal aquifer following coastal progradation and land reclamation activities (construction of a drainage network) is investigated. The study area is the Ravenna coastal plain in Italy, just to the south of the Po River Delta (Figure 1). Fresh water is present as isolated, thin (1-5 m) lenses on top of brackish-salt water. Examination of historical maps for the region has revealed that in 485 AC, a large portion of the coastal region was submerged below sea level. Submergence persisted through the 1000-1200 AC, and at least to 1780 AC in the area south of the city. Thus, the Ravenna territory has evolved over the last 300 years from a brackish lagoonal environment to a continental setting; in the southern area, a gulf was still present around the early- to mid-1800s (Ciabatti 1968). Since then, the coastline has prograded seaward up to 5 km in the area south of Ravenna, although most of the beaches along the Ravenna coastline are currently being eroded. This progradation and consequent transition to a continental setting has been further facilitated through the land reclamation drainage in the last 150-200 years (Stefani and Vincenzi 2005). Today, most of the Ravenna territory is kept dry by the land reclamation drainage system operated by the Land Reclamation Authority (LRA). This drainage system consists of a dense network of canals organized around centralized mechanical pumping machines that lift the water into a main canal and convey it to the sea (Stefani and Vincenzi 2005). The drainage system lowers the water table sufficiently to allow for urban and industrial settlements as well as for agriculture.

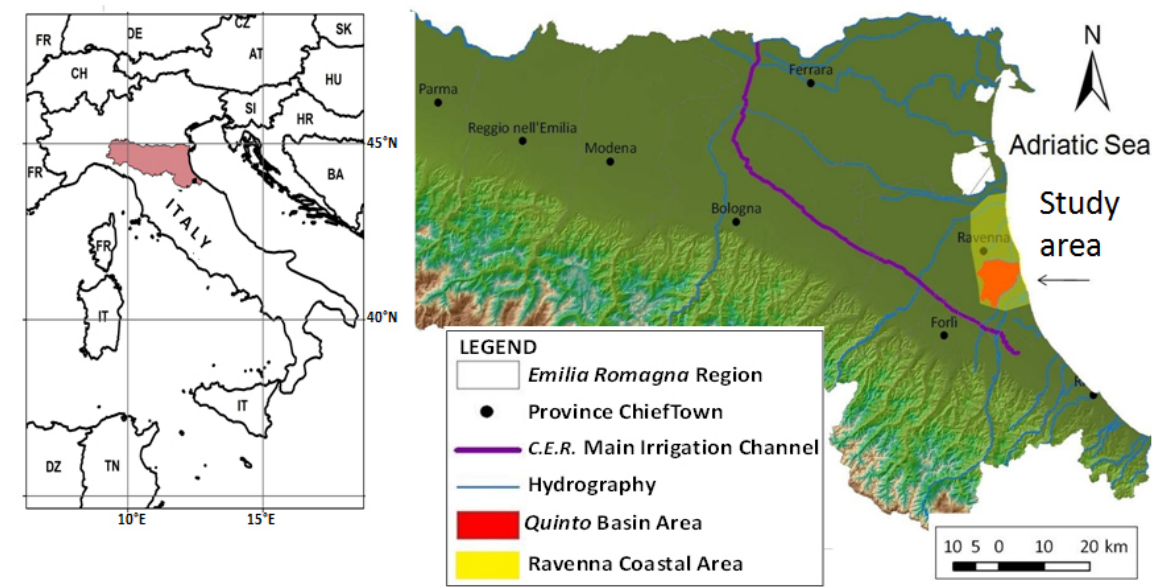


Figure 1. Location of the study region near Ravenna, Italy on the Po Plain

METHODS

Monitoring of the Ravenna coastal aquifer started in 2003 using a network of shallow piezometers belonging to the Ravenna municipality (20 piezometers with depths ranging from 4 to 20 m). In this study, water samples were collected using straddle-packers for full chemical analysis (pH, Eh, BOD, alkalinity, major cations, major anions; Mollema et al. 2013). Water level, electrical conductivity (EC) and temperature were also measured with continuous multi-parameter loggers in the piezometers and in surface waters (69 monitoring points). The BEX index of cation exchange (Stuyfzand 2008) was used to evaluate if there is a trend of salinization or freshening in the aquifer. The index quantifies the cationic exchange, in meq/L, according to the following relationship, which is specific for aquifers that also contain dolomite like the one considered in this study:

$$\text{BEX} = [\text{Na}^+ + \text{K}^+]_{\text{measured}} - 0,8768 * \text{Cl}^- \quad (1)$$

Where the BEX is equal to zero, the cations from sea water and fresh water are in equilibrium. Where $\text{BEX} > 0$, a freshening process is underway, and where $\text{BEX} < 0$ there is a salinization process underway.

The numerical code SEAWAT-2000 (Langevin et al. 2007) was used to simulate the freshening process in an attempt to explain the salinity distribution and the groundwater chemistry, and to evaluate the effects of the land drainage network on the freshening process. The model domain is approximately 14 km long and 9 km wide and extends to a depth of 30 m with 100x100 m cells. The model is discretized vertically into 16 layers with a thickness of 2 m per layer, with the exception of the upper two layers, which have a thickness of 0.5 and 1.0 m, respectively.

The geologic data used to construct the model were extracted from a 3D RockWorks model developed for the region. Three hydrostratigraphic units were identified: sand, silt and clay. Initial hydraulic conductivity (K) estimates were derived from slug tests, but were adjusted during model calibration. Vertical anisotropy was estimated at half an order of magnitude lower for all material types. Initial porosity (n), specific yield (Sy) and specific storage (Ss) values were estimated from the literature but were also adjusted during calibration. The longitudinal/transverse dispersivity was set to 10 m/ 1m.

The model boundary conditions included no flow (zero flux) at the bottom, western, northern and southern sides, to represent negligible fresh groundwater inflows to the system. A specified head and concentration boundary condition represents the easternmost sea boundary. To simulate the drainage system, drain (Cauchy) boundary conditions were assigned to the network of drainage canals. The conductance values were adjusted slightly during model calibration, but were only varied as a group to avoid over parameterization. Recharge (R) was applied to the top layer of the model according to material type: sand=30 mm/year and clay=20 mm/year. However, R was highly uncertain and was adjusted during model calibration. Zero evapotranspiration (ET) was included everywhere except along a narrow strip by the ocean where pine forests are present. Here ET was set to 40 mm/year (slightly higher than R) with an extinction depth of 2 m. The model was run for a period of 200 years, although longer and shorter periods were experimented with. The initial concentration was 25,000 mg/L.

RESULTS

Model calibration used both water levels and concentrations at 20 monitoring wells. The monitoring wells were multi-level; therefore, concentration data were available at discrete depths (3-5 depths in each well). Calibration to observed concentrations involved examining a) the time series results (e.g. Figure 2), b) the spatial distribution of concentrations at discrete depths (e.g. Figure 3), and c) the overall correlation at the end of the simulation.

The 3D numerical model was very challenging to calibrate given the uncertainties in many of the input parameters, not the least of which was the timing of the freshening process. Until the historic maps were found (Andraghetti 2007), which placed some constraint on the timing of land exposure, the potential end time for the simulation (i.e. the time to compare the observed concentrations against the simulated ones) was very uncertain. Based on the historic maps, a time frame of 200 years was considered a reasonable simulation period and this was invariant for the calibration simulations. The surface exposure of the sand and clay was generally well mapped, but the distribution of sediments at depth was less well

constrained and was based on interpolation from borehole lithology logs. Likewise, to keep the model as simple as possible, only three hydrostratigraphic units were modeled, and these were assigned uniform hydraulic properties. It is likely that this is a gross simplification of the actual geology at depth, and for this reason, the distribution of hydrostratigraphic units and their hydraulic properties is considered to be the greatest source of uncertainty, and likely a primary cause of poor model calibration at depth in most piezometers. Many piezometers showed insufficient flushing at depth, and it was tempting to increase the K value of some of the deeper clay units as they were actually mapped as clay with thin layers of sand. But to avoid over parameterization of the model, the simplified hydrostratigraphic model was adhered to.

The model calibration was found to be very sensitive to how close the piezometer was to a drain. The drainage canals were modeled as 100 m wide drain cells in the model, when in reality the drainage canals are much narrower (< 10 m). Therefore, while accurate GPS coordinates were used to position the piezometers in the model, their placement relative to the model drains may have been incorrect. Because the drains function to skim water off the surface of the aquifer, and this is fresh water, the result is an upconing of salt water from below along the length of the drain. If a piezometer is placed too close to a drain in the model, then the salinity distribution at depth will be too high. These effects of the drains are similar to those reported by de Louw et al. (2011) and Eeman et al. (2011) in the polders of The Netherlands.

The overall salinity distribution from the model is quite similar to what is observed in the corresponding area south of Ravenna. Three of the four model layers (Layers 1, 4 and 12 in Figure 3) show strong similarity to the observed salinity maps (not shown) lending support to the overall conceptual model of a freshening system for this southern area. Further support for a freshening process, at least in the south Ravenna area, is the dominance of $BEX > 0$. The only areas in the south where $BEX < 0$ were near the pine forests (PS5 and PS12) and along the coast near MF1,2,3. Interestingly, these piezometers were among the most challenging to calibrate suggesting that perhaps some other process (sea spray, vegetation?) may be influencing the salinity distribution.

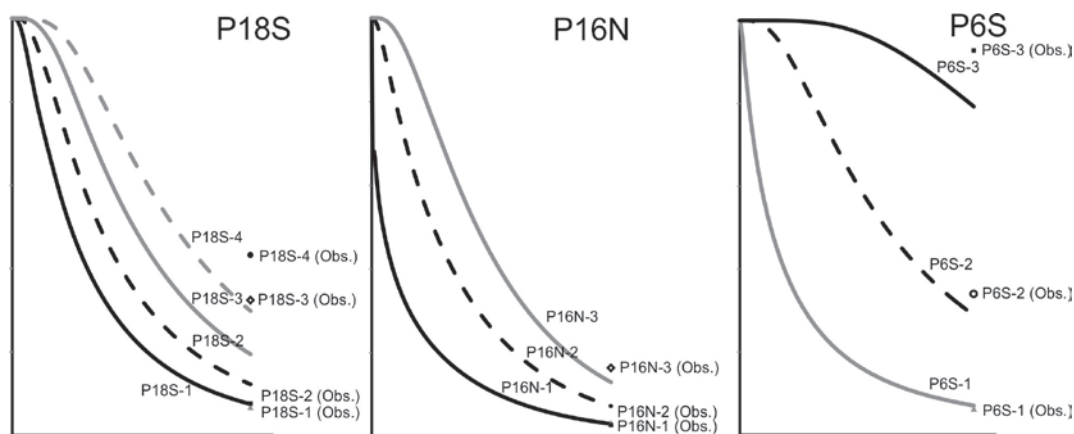


Figure 2. Concentration time series for selected monitoring wells. For all piezometers, the deepest monitoring port corresponds to the highest number (e.g. P18S-4)

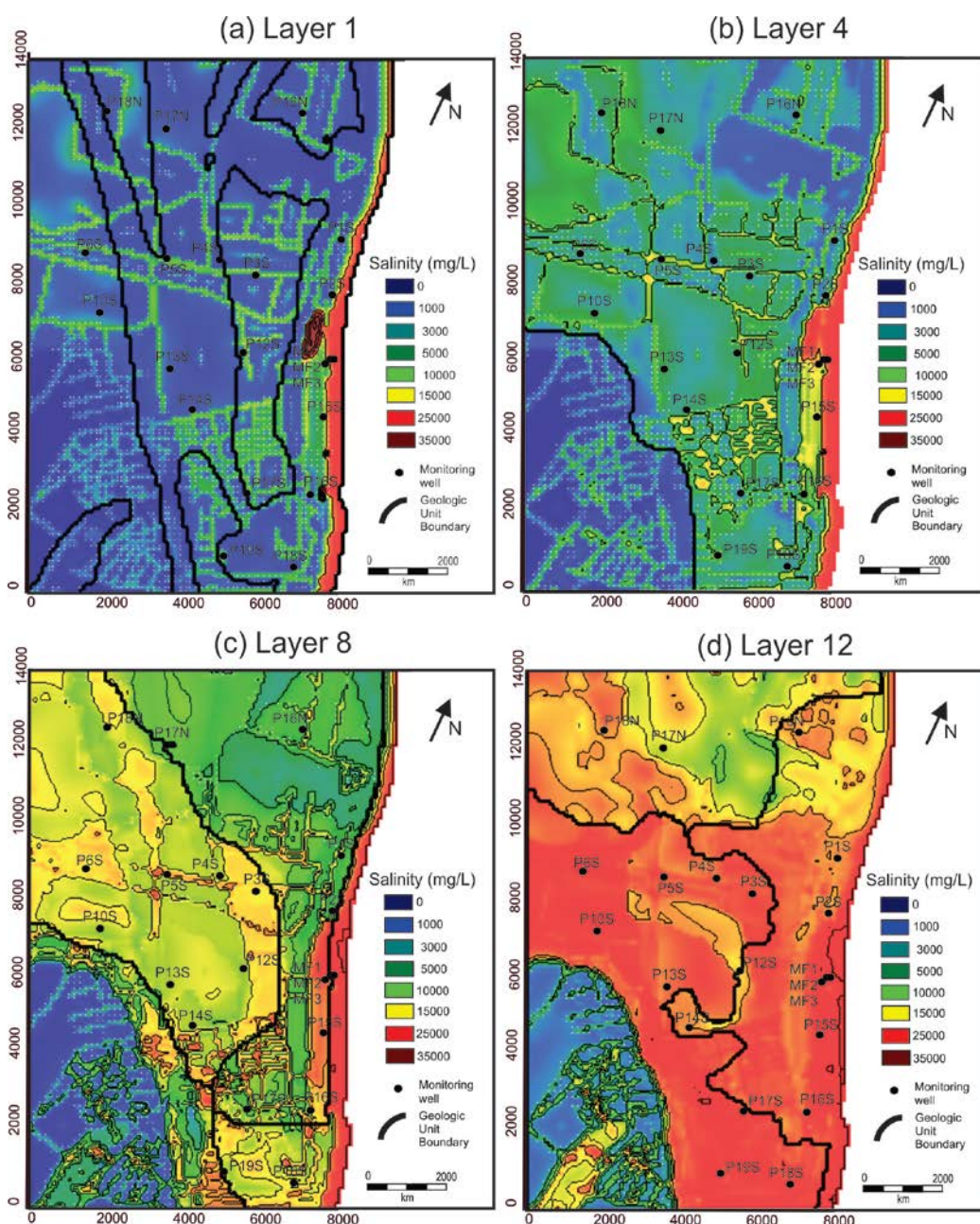


Figure 3. Salinity (mg/L) for four model layers after 200 years of simulation time (a) Layer 1, (b) Layer 4, (c) Layer 8, (d) Layer 12

CONCLUSIONS

The Ravenna coastal plain is very complex in terms of coastal evolution, surface water distribution, land use, coastal hazards (such as coast erosion and land subsidence), aquifer geology, and disaggregated management. A relatively simple 3D numerical model that captures the land development history of the area has been successful in explaining the distribution of freshwater and saltwater in the aquifer and the freshening trend. The freshening trend is also confirmed by the BEX geochemical indicator. The drainage canal network itself, however, has a salinity which is higher than in the surrounding aquifer pointing out that it is also causing upconing of the deeper salt water.

REFERENCES

Andraghetti, G.F. 2007. *Aquae condunt urbes*. Media Press, Ravenna, pp 143.

Ciabatti, M. 1968. Gli antichi delta del Po anteriori al 1600. In: Atti del convegno internazionale di studi sulle antichità di Classe- Ravenna, 14-17 ottobre 1967; Faenza, 23-33.

Custodio, E. and G.A. Bruggeman. 1987. Groundwater problems in coastal areas. Studies and Reports in Hydrology, UNESCO, International Hydrological Programme, Paris.

de Louw, P.G.B., Y. Van der Velde, and S.E.A.T.M. Van der Zee. 2011. Quantifying water and salt fluxes in a lowland polder catchment dominated by boil seepage: a probabilistic end member mixing approach. *Hydrol. Earth Syst. Sci.* 15: 2101–2117.

Eeman, S., A. Leijnse, P.A.C. Raats, and S.E.A.T.M. Van der Zee. 2011. Analysis of the thickness of a fresh water lens and of the transition zone between this lens and upwelling saline water. *Advances in Water Resources* 34: 291–302.

Langevin, C.D., D.T. Thorne Jr., A.M. Dausman, M.C. Sukop, and G. Weixing. 2007. SEAWAT Version 4: a computer program for simulation of multi-species solute and heat transport. U.S. Geological Survey Techniques and Methods Book 6, Chapter A22, 39 p.

Mollema, P., M. Antonellini, G. Gabbianelli, M. Laghi, V. Marconi, and A. Minchio. 2012. Climate and water budget change of a Mediterranean coastal watershed, Ravenna, Italy. *Environmental Earth Sciences* 65: 257-276.

Mollema, P.N., M. Antonellini, E. Dinelli, G. Gabbianelli, N. Greggio, and P.J. Stuyfzand. 2013. Hydrochemical and physical processes influencing salinization and freshening in Mediterranean low-lying coastal environments. *Applied Geochemistry* 34: 207–221.

Stefani, M., and S. Vincenzi. 2005. The interplay of eustasy, climate and human activity in the late Quaternary depositional evolution and sedimentary architecture of the Po Delta system. *Marine Geology* 222-223: 9-48.

Stuyfzand, P.J. 1989. A new hydrochemical classification of watertypes. *IAHS Publ.* 182: 262–265.

Stuyfzand, P.J. 2008. Base exchange indices as indicators of salinization or freshening of (coastal) aquifers. *Proceedings of 20th Salt water Intrusion Meeting: Naples FL USA, 23-27 June 2008.*

Vandenbohede, A., P.N. Mollema, N. Greggio, and M. Antonellini. 2014. Seasonal dynamic of a shallow freshwater lens due to irrigation in the coastal plain of Ravenna, Italy. *Hydrogeology Journal*. doi: 10.1007/s10040-014-1099-z.

Contact Information: Diana M. Allen, Simon Fraser University, Department of Earth Sciences, 8888 University Drive, Burnaby, BC, V5A1S6, Email: dallen@sfu.ca

Groundwater flow analysis in variable-density formation waters – a comparison of common approximations

M. aus der Beek¹, F. Krause¹ and S. Schäfer¹

¹K+S Aktiengesellschaft, Kassel, Germany

ABSTRACT

Calculating the direction and magnitude of groundwater flow from freshwater hydraulic heads is a common approach, yet decreasingly accurate with increasing density-variations of groundwater in sloping aquifers. The density of groundwater can vary significantly both laterally as well as vertically with increasing depths due to e.g. total dissolved solids, fluid temperature, fluid compressibility, and gravity. Aquifers are not always situated horizontally but can dip at certain angles and vary in thickness. Thus, buoyancy from density-variations and potential forces from pressure and elevation differences can play a major role in determining flow of formation waters (Bachu 1995)

Being confronted with the task of determining the direction of groundwater flow in a sedimentary rock basin with a surface area of app. 1220km², consisting of sloping saline and fresh water aquifers, we use this opportunity to quantify the components of the flow-driving forces. Despite the fact that common knowledge apparently suggests to re-calculate heads to a reference, defining this reference is not trivial in aquifers with great density variations. In this study we review and compare the most common approximations to calculate groundwater flow in variable-density formation waters (Davies 1987; Bachu and Michael 2002; Alkalali and Rostron 2003). We rely hereby on a great number of measured data, which were available from groundwater monitoring bores in the form of fluid-level measurements, pressure data measurements, and/or chemical analyses.

REFERENCES

Alkalali, A. and B. Rostron (2003). "Basin-scale analysis of variable-density groundwater flow: Nisku Aquifer, Western Canadian Sedimentary Basin." *Journal of Geochemical Exploration* 78-79: 313-316.

Bachu, S. (1995). "Flow of variable-density formation water in deep sloping aquifers: review of methods of representations with case studies." *Journal of Hydrology* 164: 19-38.

Bachu, S. and K. Michael (2002). "Flow of variable-density formation water in deep sloping aquifers: minimizing the error in the representation and analysis when using hydraulic-head distribution." *Journal of Hydrology* 259: 49-65.

Davies, P. B. (1987). Modeling areal, variable-density ground-water flow using equivalent freshwater head-analysis of potentially significant errors. NWWA-IGWMC Conference-Solving Groundwater Problems with Models, Denver.

Contact Information: Martina aus der Beek, K+S Aktiengesellschaft, Bertha-von-Suttner-Straße 7, 34131 Kassel, Germany, Email: Martina.ausderBeek@k-plus-s.com

Dupuit or Not Dupuit? That's the question

Mark Bakker

Water Resources Section, Civil Engineering and Geosciences, Delft University of Technology, Delft, The Netherlands

EXTENDED ABSTRACT

The basic idea behind the Dupuit approximation is that the head is approximated as hydrostatic within an aquifer. The main advantage of this approximation is that it reduces the spatial dimensions by one; the head at a certain elevation can be solved as a function of the two horizontal coordinates, and the head at any other elevation can be computed from the hydrostatic conditions. The modern interpretation of the Dupuit approximation is that 'the resistance to flow in the vertical direction is neglected'. A three-dimensional flow field and three-dimensional pathlines may be computed under this interpretation, as vertical flow within an aquifer is governed by continuity rather than by a head gradient.

The Dupuit approximation is often reasonable in cases of regional flow where flow is predominantly horizontal, but it remains an approximation. In this presentation, the accuracy of the Dupuit approximation is evaluated for a number of cases of interface flow in coastal aquifers, including the depth and shape of the interface, the size of the outflow face along the ocean bottom, and the effect of vertical anisotropy.

Contact Information: Mark Bakker, Water Resources Section, Civil Engineering and Geosciences, Delft University of Technology, Delft, The Netherlands, Phone: +31 15 2783714, Email: mark.bakker@tudelft.nl

Salinisation processes in the Kalahari Sediments of Western Zambia: Machile Basin

K.E. Banda^{1,3}, R. Jakobsen², F. Larsen², P. Bauer- Gottwein¹, I. Nyambe³

¹Department of Environment, Technical University of Denmark, 2500 Kgs-Lynby, Denmark

²Department of Geochemistry, Geological Survey of Denmark and Greenland (GEUS), 10, Øster Voldgade, DK-1350 Copenhagen K, Denmark

³Department of Geology, University of Zambia - Integrated Water Resources Management Centre, C/O School of Mines, Lusaka, Zambia

ABSTRACT

Approximately 18% of the earth's land drains to interior depressions such as inland seas, lakes or salt pans. In southern Africa, the Okavango and Lake Makgadikgadi is such an endorheic basin, occupying the northern parts of Botswana and southwest parts of Zambia. We have studied the salinization processes in this semi-arid Machile basin in Zambia, where high groundwater salinity has led to rural inhabitants drinking from polluted surface water or worse still brackish/saline groundwater. It is hypothesised that saline terrestrial sediments hosted in the Kalahari sediments from the Lake Palaeo-Makgadikgadi maybe the source of present saline groundwater in the Machile Basin. This study investigates the processes that have affected mobilization of large amounts of salts in the groundwater. To resolve this, various methods were used including borehole geophysical logging, sediment core characterisation, pore water hydrochemistry and stable isotopes. Further, X-Ray Diffraction (XRD) and Scan Electron Microscopy (SEM) were combined to establish the presence of evaporite minerals. Geophysical borehole logging and sediment characterisation showed a sediment pack with intercalations of sand and clay indicating a depositional environment of varied climatic conditions. A clayey-silt formation hosts the high salinity groundwater which terminates over impervious basalt rock. Comprehensive studies on sediment cores of pore water hydrochemistry and stable isotopes showed high concentration of Na^+ , SO_4^{2-} , Ca^{2+} and Mg^{2+} with precipitates of gypsum, calcite and dolomite formed by evapo-concentration. Geochemical modelling using PHREEQC suggests mixing of fresh water with saline connate groundwater in different amounts with depth dissolving predominantly gypsum. Besides these changes in recharge composition and mixing, chemical reaction including ionic exchange of Na^+ on the clay for Ca^{2+} and Mg^{2+} in solution and dissolution of carbonate minerals in response to the cation exchange have altered the hydrochemistry. This study demonstrates that the aquifer geochemistry within the saline groundwater region could be as a result of the interplay between physical and chemical changes.

Contact information: Kawawa E. Banda, e-mail: kawab@env.dtu.dk

Integrated Coastal Aquifer and Coastal Zone Management Strategies

G. Barrocu

Department of Civil Engineering, Environmental Engineering, and Architecture, University of Cagliari, Italy.

ABSTRACT

The majority of coastal aquifers are endangered by saltwater intrusion and pollution as a consequence of overexploitation and mismanagement. In fact, coastal zones are more and more intensely urbanized and groundwater of good quality is not sufficient to match the growing demand, especially in the dry areas of southern Mediterranean coasts, reliant on groundwater resources for their domestic, agricultural, irrigation and industrial water supplies (Figure 1).

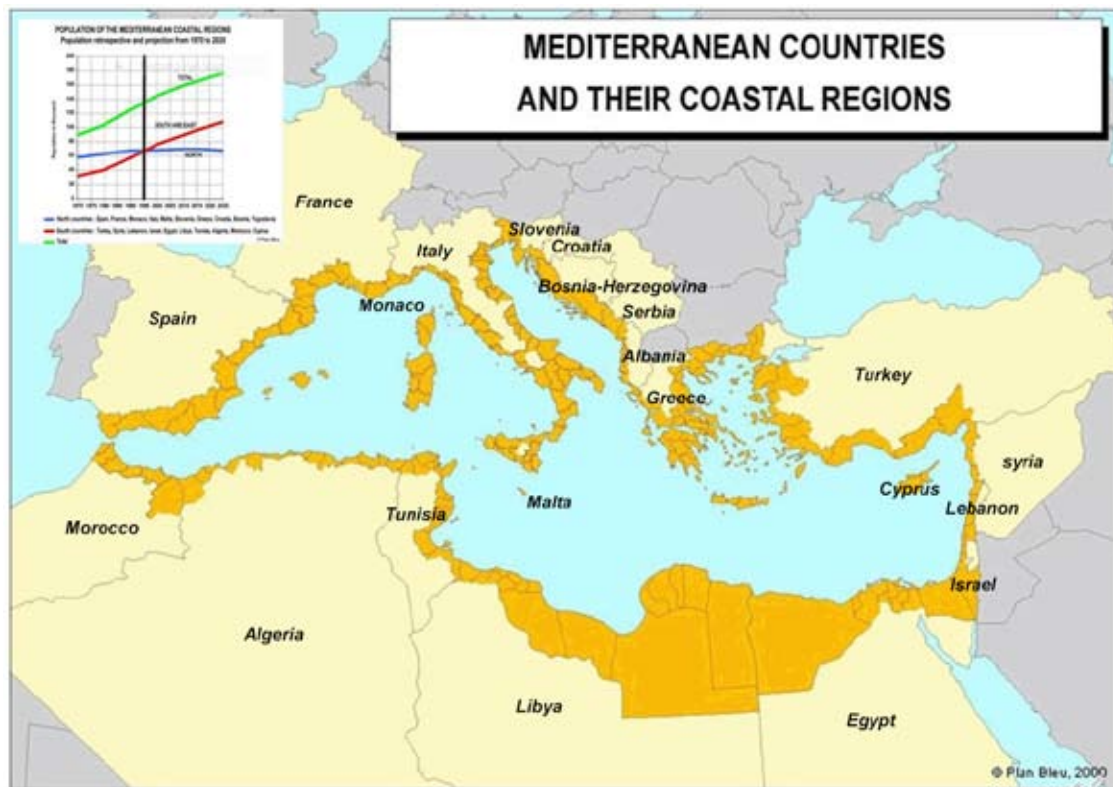


Figure 1. The total water resources of the Mediterranean area are estimated at 1.060 km³, of which 107.4 km³ (84.2% of the total) are in the south, 62.4km³ (5.8% of the total) in the east, and the remaining 894.6 km³ (84.2% of the total) in the north (data derived and map modified from EUWI MED 2007, Plan Bleu 2000, and UNEP MAP 2012).

The total population of the Mediterranean countries grew from 276 million in 1970 to 412 million in 2000 (a 1,35 % increase per year) and to 466 million in 2010. The population is predicted to reach 529 million by 2025. More than a third lives in coastal administrative entities totalling less than 12 % of the surface area of the Mediterranean countries. The population of the coastal regions grew from 95 million in 1979 to 143 million in 2000. It

could reach 174 million by 2025 (UNEP/MAP 2012). The concentration of population in coastal zones is heaviest in the western Mediterranean, the western shore of the Adriatic Sea, the eastern shore of the Aegean-Levantine region, and the Nile Delta. Overall, the concentration of population in the coastal zone is higher in the southern Mediterranean countries, where the variability of the population density is highest, ranging from more than 1000 people/km² in the Nile Delta to fewer than 20 people/km² along parts of coastal Libya. Many coastal areas are so heavily urbanized that the need for freshwater is even more acute and increasing.

Coastal areas represent the final part of the hydrogeological catchments, where the fragile interface equilibrium between fresh, brackish, and saltwater may be easily jeopardized also by natural processes, such as sea level variations due to climate cycles and subsidence, floods and tsunamis, and anthropic activities developed also inland upstream. Owing to sea level variations in time, the structure of major deltaic plains is rather complex, and fossil freshwater and salt water aquifer layers are interbedded in depth below sea level (Barrocu, Dahab 2010). Saltwater intrusion processes and their effects are quite well known and described in literature, particularly in previous SWIM proceedings. Saltwater intrusion is generally produced by overexploitation, due to excessive fresh groundwater development with respect to effective natural recharge, land-use change, climate variations, and sea level fluctuations. Short- and long-term climatic fluctuations influence the amount of recharge and consequently the groundwater resource available for use (Post 2005; Ferguson, Gleeson 2012; Werner et al. 2013).

Well pumping in coastal aquifer systems modifies hydrodynamic levels producing lateral saltwater ingression when their radius of influence, depending on terrain K rate, trespasses the fragile interface between fresh groundwater, coast saline water bodies, and the sea, even when aquifer recharge is higher than the yield extracted. It also produces upconing of seawater trapped in deep layers formed in geological past, such as syndepositional connate saltwater and dense brines, sometimes connected to salt domes, evaporitic deposits in thin beds or disseminated geologic formations. The upconing of brackish and saltwater, often consisting of fossil waters, caused by well drawdown, produces water-rock interactions difficult to control, affecting groundwater quality and aquifer hydraulic parameter values. Soil and groundwater salination may be due also to sea water spray and anthropogenic salt released from industries, roads, etc. Coastal aquifers may be particularly endangered by mining activities, industrial facilities, and unsuitable engineering works. Retoxification processes may be observed where accumulation of heavy metals in sediments and changes of the environmental conditions take place. Alluvial sediments act as long-term skins storing heavy metals, and through chemical processes of desorption and dissolution, they can revert into large sources of heavy metals in bioavailable form (Sodde, Barrocu 2008).

Under natural conditions, sea level variations due to surges, tides, and tsunamis determine temporary low coast land submersion, so that salt water infiltrates and produces groundwater and soil salination. Tsunamis effects on urbanized low areas may be counteracted by protecting them with physical barriers.

Floods, typical of arid and semiarid areas like the Mediterranean coasts, may be conveniently moderated by stocking them in reservoirs so as to mitigate excessive erosion effects, produce hydroelectricity, and surface water may be conveniently transferred downstream to match different demands when and where necessary. However, erosion cannot be completely blocked upstream without endangering coastal plains and beaches,

whose dynamic stability depends on continental water outflow and sea movements, especially in deltas. Upland river channel fragmentation by dams and water regulation resulting from reservoir operation, interbasin diversion, and irrigation generally affect river discharge and aquifer recharge.

Inland pollutants transported by floods partly outflow directly into the sea and are partly deposited with deltaic sediments. Floods and tsunamis may heavily devastate urbanized low coastal areas, where they generally mobilize pollutants of different diffused and point sources so that they infiltrate and endanger groundwater and soil, at grades depending on their vulnerability. Interaction effects of salination and pollution, depending on temperature, pH and Eh, are not easy to control. Inland pollution of transboundary aquifers, typical of karstic areas like Slovenia, Croatia, Bosnia and Herzegovina, Albania, Greece, Montenegro, Turkey, Israel, Palestine, and North-African countries, may affect coastal aquifers, where large volumes of water are discharged from the aquifer system through terrestrial and submarine springs.

Surface water and groundwater body boundaries to be considered in coastal land planning and management should be determined by the hydrogeological catchment, collecting both surface waters and groundwater, often different from the surface water basin. Such case is foreseen in the Article 8 of the Barcelona *“Convention for the Protection of the Marine Environment and the Coastal Region of the Mediterranean and its Protocols”*, saying that the *“Contracting Parties shall endeavor to ensure that their national legal instruments include criteria identifying and delimiting, outside protected areas, open areas in which urban development and other activities are restricted or, where necessary, prohibited for the sustainable use of the coastal zone”*. The concept of integrated water resource management implies an international approach to river conservation of entire river systems considering hydrogeological catchments irrespective of political borders. No other way is possible than the agreement between different water authorities and land administrators to find the best fitting method to rule land and water resources in an integrated way.

Coast urbanization implies soil consumption and should not endanger land safety and ecosystems. Agriculture practices are compatible with recycled and brackish water irrigation, the only available in areas with scanty water resources, considering real free global market requirements, as in the long run producers might not be able to rely on high public incentives. Aquaculture may be developed depending on water quality available and different type of fish exigencies.

A minimum stream flow including sediment transport is to be granted to preserve riparian and coastal areas ecosystems, and induce groundwater recharge. Natural recharge may be conveniently integrated with diffused and intensive artificial recharge. Saltwater intrusion and interface morphology may be modified and controlled by hydrodynamic and physical barriers so as to develop coastal aquifers in the best way.

Desalinization methods may be the only solution to grant water supply especially in small islands with scanty fresh water resources. A number of desalination plants are functioning in Mediterranean coasts, particularly in Israel, Spain, Algeria, Egypt, etc., mainly for the production of drinking water but also for agriculture demand. Production costs are variable, depending on local energy costs. In some countries, like Italy, desalination plants are not favoured by local rules on account of the impacts due to byproduct concentrates released into

the sea, soil salination caused by saltwater upconing when tapping saline groundwater from coastal aquifer wells, and high energy costs.

Conflicts among different users may not be resolved rationally and effectively only with technical remedies aiming at controlling saltwater intrusion from the sea and due to upconing. Major efforts are necessary to convince decision makers and users to evaluate and manage available groundwater and surface waters, land capability and susceptibility, human resources in an integrated way, so as to grant a real sustainable economic development for present coastal areas inhabitants and future generations. It is a responsibility of all scientists and professionals of disciplines involved in coastal aquifer and zone management are responsible for emphasizing the relevance of their activities. The integrated management of surface waters, groundwater, and biotic and abiotic environment components is essential to prevent and mitigate interest conflicts between people resident in hydrogeological catchments and outside resource users.

Research and university courses should be finalized to prepare high profile land managers.

REFERENCES

Barrocu, G., Dahab, K. 2010. Changing climate and saltwater intrusion in the Nile delta, Egypt, Proc. XXXVI IAH Congress, Toyama, Japan, Eds. M. Taniguchi, I.P. Holman, IAH Selected Papers, 16, Groundwater Response to Changing Climate, Chapt. 2, pp. 11-25, CRC Press Taylor & Francis Group, Balkema Book, ISBN: 978-0-415-54493-1 (Hbk), ISBN: 978-0-203-85283 (Ebook)

EUWI MED.2007. Mediterranean Groundwater Report.

<http://www.semide.net/initiatives/medeuwi/JP/GroundWater>

http://forum.europa.eu.int/Public/irc/env/wfd/library?l=/framework_directive/groundwater_library&vm=detailed&sb=Title

Ferguson, G., Gleeson, T. 2012. Vulnerability of coastal aquifers to groundwater use and climate change. *Nature Climate Change* 2: 342-344.

Margat, J., Vallée D. 2000. Water resources and uses in the Mediterranean countries. Blue Plan for the Mediterranean. Sophia-Antipolis: Regional Activity Centre.

Sodde, M., Barrocu, G. 2008. Seawater intrusion and arsenic contamination in the alluvial plain of the rivers Quirra and Flumini Pisale, south-eastern Sardinia. Ed. Barrocu, Proc. 1st SWIM-SWICA, Cagliari-Chia Laguna, Sept. 24-29, 2006, University of Cagliari, UNESCO, Regione Autonoma Della Sardegna, IAEA, IAH, Tipografia 3 ESSE, Serramanna (CA), pp. 165-173, ISBN 88-902441-2-7

UNEP/MAP .2012. State of the Mediterranean Marine and Coastal Environment, UNEP/MAP – Barcelona Convention, Athens, 2012.

Werner, A.D., Bakker M., Post, V.E.A., Vandenbohede A., Lu C., Ataie-Ashtiani, B., Simmons, C.T., Barry, D.A. 2013. Seawater intrusion processes, investigation and management: Recent advances and future challenges. *Advances in Water Resources* 51: 3-26, doi: 10.1016/j.advwatres.2012.1003.1004.

Contact Information: Giovanni Barrocu, University of Cagliari, Department of Civil Engineering, Environmental Engineering, and Architecture, 09123 Cagliari, Italy. Phone: +39 33540975 Email: barrocu@gmail.com

Comparing transport parameters and PHREEQC simulation parameters of seawater intrusion experiments in columns filled with different porous media

N. Boluda-Botella¹

¹Department of Chemical Engineering. University of Alicante. P.O. Box 99, E-03080 Alicante. Spain. Email: nuria.boluda@ua.es

ABSTRACT

The hydrogeochemistry of seawater intrusion is investigated from the results of column experiments with different porous media. A combination of greater interstitial velocity, shorter length and dispersion in the column filled with resin provides the Péclet number in the order of the other experiments with gypsum precipitation. Although the cation exchange capacity of the resin is great, gypsum precipitation/dissolution did not occur experimentally. The grain size of the porous medium or the surface of the resin could prevent gypsum precipitation, and this fact could occur in different porous media. On the other hand, theoretical simulations, with selectivity coefficients of the resin, indicate that gypsum precipitation – dissolution must have occurred when the gypsum saturation index is zero. Simulation results are improved in the first stages of the seawater intrusion by considering a gypsum saturation index of 0.65. Finally, selectivity coefficients in the best simulations with PHREEQC for the three porous media are compared with the usual range from literature: calcium is included but magnesium and potassium are out of range. The experimental determination of exchange coefficients and the simultaneous study of the precipitated cations are important to obtain an approximation to data from seawater intrusion experiments.

INTRODUCTION

Laboratory column experiments were carried out in previous papers to study the hydrogeochemistry of seawater intrusion, with focus on cationic exchange and gypsum precipitation (Boluda-Botella et al. 2008a). These studies were done by displacing synthetic freshwater with seawater along a sediment column 100 cm in length. Also, application of reactive models to the experimental data showed similar results but with several differences: sulphate (total S) is overpredicted and cations depend on the selected exchange coefficients (Boluda-Botella et al. 2014).

An attempt was made to study gypsum precipitation in a column 19 cm in length, filled with resin (Duolite C20), of a great cationic exchange capacity (CEC), and previously saturated with 2.8 mmol/L calcium chloride solution (Boluda-Botella et al. 2008b). When seawater displaces the resident solution from the column, the calcium concentration increases due to exchange with sodium of the seawater and, with high sulphate concentration; this could produce gypsum precipitation into the column, as in previous experiments (Gomis-Yagües et al. 2000). However, gypsum was not precipitated, as seen from the elution curve of sulphate, synchronous to that of conservative chloride.

In this paper, both types of experiments are studied, firstly comparing transport parameters obtained with ACUAINTRUSION TRANSPORT (Boluda-Botella et al. 2014, <http://hdl.handle.net/10045/2691>) and their influence in gypsum experimental precipitation

and later, the simulations with PHREEQC (Parkhurst and Appelo, 1999), with selected reactive parameters which take into account cationic exchange and gypsum precipitation.

METHODS

Four column experiments presented in previous papers are considered. Three in a stainless steel column, 1 m long: experiments I and II used natural sediment, taken from the Jávea Quaternary aquifer system, on the coast of Alicante (Spain) and experiment III used treated sediment. This latter was obtained by modifying the first sediment with hydrochloric acid, to reduce the carbonate content, increasing its CEC (natural sediment 7 meq/100 g and treated 10 meq/100 g). Experiment IV was carried out in an Omnifit glass column of 2.5 cm internal diameter and 19 cm length, with cationic resin Duolite C20, with CEC of 156 meq/100 g.

The hydrodynamic column parameters were determined using ACUAINTRUSION TRANSPORT, a program designed to calculate the transport parameters that fit the experimental chloride breakthrough curves using the analytical solution of the convection–dispersion equation. The square of the mean deviation between the experimental and calculated compositions is automatically minimised. The required experimental data are as follows: flow (Q), column length (L), column diameter, and experimental chloride concentration versus time (t). The software provides the calculated transport parameters that fit the experimental breakthrough curves: Darcy velocity (u), interstitial water velocity (v), mean residence time t_m (L/v), column Péclet number ($Pe=vL/D_L$), effective porosity ϵ , longitudinal dispersion coefficient (D_L) and dispersivity α (L/Pe).

PHREEQC (Version 2) is a reactive transport model, from the U.S. Geological Survey (Parkhurst and Appelo, 1999) which was applied to experiments I-III (Boluda-Botella et al., 2014) and to the resin experiment (Boluda-Botella et al., 2008b).

RESULTS AND DISCUSSION

Comparison of transport parameters from ACUAINTRUSION TRANSPORT

Table 1 includes hydrodynamic parameters of experiments with gypsum precipitation (I-III) and parameters of the resin experiment (IV), without gypsum precipitation.

Table 1. The transport parameters obtained during different experiments with ACUAINTRUSION TRANSPORT (Boluda-Botella et al. 2008a and 2008b)

Exp	Column Length (cm)	Column Diameter (cm)	Q (mg/min)	Porous media	u (cm/h)	t_m (h)	$Pe=vL/D$	ϵ	v (cm/h)	D_L (cm ² /h)	α (cm)
I	100	3.16	20	Natural	0.15	241	183	0.37	0.41	0.23	0.55
II	100	3.16	35	Natural	0.27	143	166	0.38	0.70	0.42	0.60
III	100	3.16	20	Treated	0.15	203	147	0.31	0.49	0.33	0.68
IV	19	2.5	50	Resin	0.61	14.7	168	0.47	1.29	0.15	0.11

Residence time in Exp. IV is 10 times less than in the other experiments, but a combination of greater interstitial velocity, shorter length and dispersion provide the Péclet number which is similar to experiments I-III, but gypsum precipitation did not occur. Calcium

concentration is greater than in experiments I-III (Figure 1) and the solubility product is reached but other reasons such as the grain size of the porous medium or the surface of the resin could prevent gypsum precipitation. As a consequence, it is necessary to analyze the seawater intrusion especially in the medium where it occurs.

A different case is observed in other column experiments, with materials from experiments I and II but with a higher flow rate (82 mg/min). The greater dispersion (27.3 cm²/h) and the smaller Pe (5.6) prevented a high calcium concentration from being attained, to reach gypsum solubility product and precipitation of this mineral (Boluda-Botella et al. 2008a).

Comparison of parameters used in PHREEQC

Table 2 includes transport and reactive parameters considered in simulations and shows cation exchange parameters in the different porous media. Definitions of cation exchange reactions and other details are in Boluda-Botella et al. 2014. The saturation Index (SI) for gypsum is zero in simulations for experiments I-III, when differences between the experimental S curve and the Cl breakthrough curve are considerable, and gypsum precipitation occurs. Differences between Cl and S (triangle symbols) are shown in Figure 1, for the experiment II. However, in experiment IV, although CEC=2.26 meq/L pore water (pw) is nearly 3 times greater in the resin, and Pe is similar to other column experiments, gypsum precipitation does not occur, and S are synchronous to that of Cl (Figure 1). The results with SI = 0 are not satisfactory, and simulations with SI gypsum=0.65 prevented the precipitation of gypsum and PHREEQC simulations are a good approximation to experimental results (symbols=experimental, lines=model).

Table 2. Input parameters included in the PHREEQC Transport data block and ionic exchange. Logarithm of the exchange coefficients (Log K): PHREEQC simulations; from batch experiments or data (*for resin) log K, calculated according the Gains-Thomas convention; range provided in Appelo and Postma (2005), as log K used in PHREEQC.

Exp.	Cells	Lengths	Shifts	Time step	α	CEC	PHREEQC simulations			Batch exp. or data (*)			Range Appelo and Postma (2005)		
							Log K			Log K			Log K		
		(cm)		(s)	(cm)	(eq/L pw)	K	Ca	Mg	K	Ca	Mg	K	Ca	Mg
I	50	2.0	620	17411	0.6	0.511	1.1	1.0	0.8	1.6	1.0	0.8			
II	50	2.0	1060	10218	0.6	0.497	1.1	1.0	0.8	1.6	1.0	0.8	0.60-	0.44-	0.44-
III	50	2.0	700	14587	0.7	0.871	1.2	0.8	1.4	1.1	0.4	0	0.82	1.05	0.80
IV	40	0.5	1200	1315	0.1	2.26	0.28	0.49	0.17	0.28	0.49	0.17			

The exchange coefficients used in the best PHREEQC simulations have been calculated from data of batch experiments (natural and treated sediment) or calculated with data from commercial products and literature, taking into account 16 % degree of crosslinking (Perry and Green. 2001). Exchange coefficients in the PHREEQC simulations are very different in the 3 porous media. Calcium exchange coefficients are within the “Range” considered in Appelo and Postma, but magnesium and potassium exchange coefficients are very far outside this range.

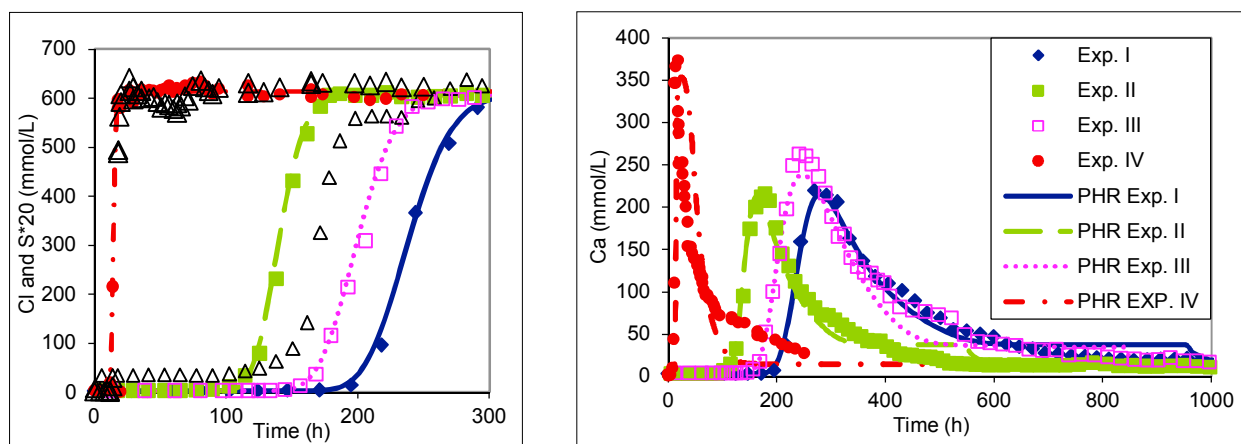


Figure 1. Experimental data from column experiments (Exp.) and PHREEQC simulated results (PHR). Cl and Ca concentration (mmol/L). 20 x S concentration (mmol/L) represented as Δ in Exp. II and IV.

CONCLUSIONS

Gypsum precipitation depends on the column hydrodynamic parameters, as demonstrated in seawater intrusion experiments with natural sediment (Boluda-Botella et al. 2008a), where great dispersion (small Pe) prevents a high calcium concentration and gypsum saturation index from being attained. Gypsum precipitation occurs in the column sediment with high Pe, but does not occur in the column resin with the same Pe, despite the great Cation Exchange Capacity (CEC) of the resin. In this case, gypsum oversaturation is considered in the best cation simulation with PHREEQC (SI= 0.65). The grain size of the porous medium or the surface of the resin could prevent gypsum precipitation, and this fact could be produced in different natural media.

The exchange coefficients used in the PHREEQC simulations were calculated from data of batch experiments (Boluda-Botella et al. 2014) or calculated with data from commercial products and literature, and provide an approximation to experimental data. Calcium exchange coefficients are within the range considered in literature, but magnesium and potassium exchange coefficients are not included in this range.

REFERENCES

- Appelo, C.A.J. and Postma, D. 2005. *Geochemistry, groundwater and pollution*. 2nd Ed. Balkema, 535 pp.
- Boluda-Botella, N., Gomis-Yagües, V. and Ruiz-Beviá, F., 2008a. Influence of the transport parameters and chemical properties of the sediment in experiments to measure reactive transport in seawater intrusion. *J. Hydrol.* 357, 29–41.
- Boluda-Botella, N., Gomis-Yagües, V. Pedraza Berenguer, R. and Torres Prieto, N. 2008b. Modelling seawater intrusion in a resin-filled column. 11th Mediterranean Congress of Chemical Engineering
- Boluda Botella, N., Valdes-Abellan, J. and Pedraza, R. 2014. Applying reactive models to column experiments to assess the hydrogeochemistry of seawater intrusion: Optimising ACUAINTRUSION and selecting cation exchange coefficients with PHREEQC. *J. Hydrol.* 510, 59–69.
- Gomis-Yagües, V., Boluda-Botella, N. and Ruiz-Beviá, F. 2000. Gypsum precipitation as an explanation of the decrease of sulphate concentration during seawater intrusion. *J. of Hydrol.*, 228, 48-55.
- Parkhurst, D.L. and Appelo, C.A.J., 1999. U.S. Geological Survey. *Water Res. Inv. Report 99-4259*, 312 pp.
- Perry, R.H. and Green, D.W. 2001. *Manual del Ingeniero Químico*. 7 Ed. McGRAW-HILL.

Carbon Isotopes in DIC trace Submarine Groundwater Discharge and Advective Pore water efflux in Tidal Areas of the southern North Sea

Vera Winde¹, Peter Escher¹, Bernd Schneider¹, Philipp Böning², Abdul M. Al-Raei³, Gerd Liebezeit², **Michael E. Böttcher**^{1*}

¹Leibniz Institute for Baltic Sea Research (IOW), D-18119 Warnemünde, FRG

²Institute for Chemistry and Biology of the Marine Environment, Wilhelmshaven/Oldenburg, FRG

³Max Planck Institute for Marine Microbiology, D-28359 Bremen, FRG

ABSTRACT

We report results from a study conducted in different tidal basins of the southern North Sea, here with a focus on the Jade Bay and the backbarrier tidal area of Spiekeroog Island. The present study combines the results from several seasonal sampling campaigns that investigated the tidal response of the pelagic carbonate system under different magnitudes of superimposition by mixing processes with fresh waters and *in-situ* transformation processes, like primary production and pelagic respiration. In addition, benthic processes were followed by the analyses of fresh water inlets, as well as intertidal pore waters recovered from short sediment cores. Finally, direct advective pore water efflux from permeable sediments during low tide was considered, too. Both, the concentration and the stable carbon isotope composition of DIC are shown to be valuable tools to follow and interpret the basic processes causing tidal and spatial variations in the pelagic carbonate system of the coastal waters, in particular when combined with parameters like salinity, nutrients and redox-sensitive metal analyses.

INTRODUCTION

The pelagic carbonate system in the southern North Sea may significantly be impacted by the intense biogeochemical processes taking place within the tidal areas of the southern North Sea (e.g., Brasse et al., 1999; Thomas et al., 2009), with only few studies carried out to understand the dynamics in the tidal basins (e.g., Hoppema, 1990; Moore et al., 2011; Winde et al., 2014). The sources for alkalinity (TA) and dissolved inorganic carbonate (DIC) may result from mixing with fresh waters originating from rivers, flood gates, submarine ground water discharge, or benthic-pelagic exchange of pore waters that were modified by oxidation of organic matter and/or methane (Billerbeck et al., 2006; Al-Raei et al., 2009; Moore et al., 2011) and *in-situ* processes. Here, we present results from studies conducted in two tidal basins of the southern North Sea. It was the aim of this study to investigate seasonal and tidal responses of the pelagic carbonate system in the basin without and under superimposition by *in-situ* transformation processes, like primary production and pelagic respiration. Both, the concentration and the stable carbon isotope composition of DIC are shown to be valuable tools to follow and analyze the tidal and spatial variations in the pelagic carbonate system of the tidal coastal waters. The composition of fresh water inlets at the Jade Bay coast as well as pore waters from selected intertidal surface sediments from both basins were investigated as examples for water and DIC sources draining into the basins. Results are evaluated by the combined consideration of mixing and carbon

transformation processes, demonstrating that different source-sink contributions are obtained as a function of season.

MATERIALS AND METHODS

Water samples from fresh water inlets, and coastal sediments were taken as described earlier (Al-Raei et al., 2009; Winde et al., 2014). Salinity, temperature and pH were immediately measured. Water aliquots were filtered (0.45 μm membrane filters) for further analyses by ICP-OES/MS (Thermo iCAP 6300 Duo, ElementII) for major and redox-sensitive trace elements, a QuAatro nutrient analyzer (SEAL Analytical). Analyses of TA and DIC were carried out via potentiometric and coulometric titration, respectively (Winde et al., 2014). The $\delta^{13}\text{C}$ values of DIC were measured by means of CF-irmMS using a Thermo Finnigan MAT 253 gas mass spectrometer coupled to a Thermo Gas Bench II via a Thermo Conflo IV split interface.

RESULTS AND DISCUSSION

Seasonal and tidal changes in the carbonate system of a tidal basin.

It has been shown that seasonal and tidal compositional variations occur in the investigation areas that indicate the mixing of North Sea with fresh waters of different sources, superimposed by benthic-pelagic coupling (Moore et al., 2011; Winde et al., 2014). The consideration of seasonal variations, here for the example of the Jade Bay (Figure 1), yields characteristic compositional variations that can be evaluated based a common evaluation of the concentration and stable isotope composition of DIC. Mixing with fresh and pore waters as well as photosynthesis are the dominant processes controlling observed co-variations.

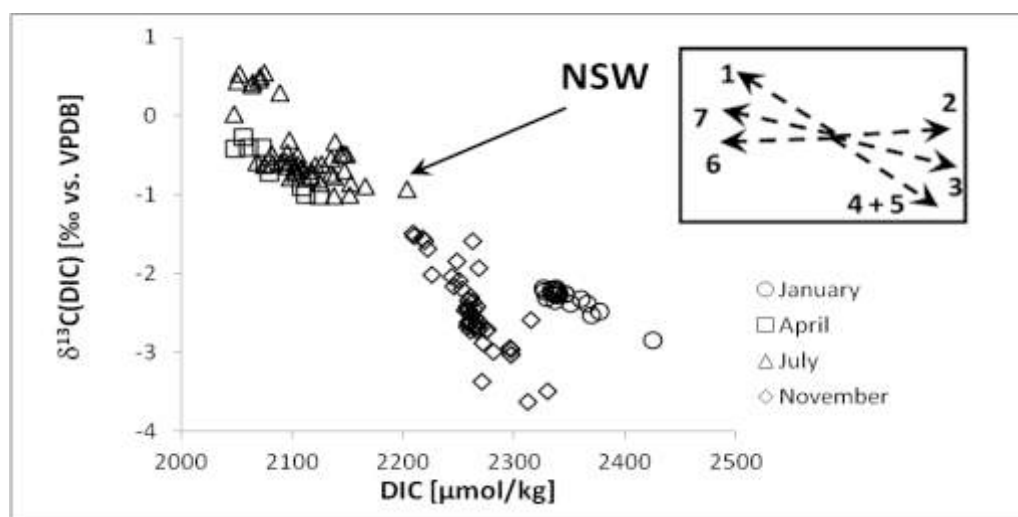


Figure 1a. Co-variations of the concentration and carbon isotopic composition of DIC in the upper water column of the Jade Bay (tidal cycles and transects), southern North Sea during 4 sampling campaigns in 2010. NSW: North Sea (surface) water as an end-member for winter mixing with fresh waters. DIC data from the July campaign were calculated from TA and pH values with CO2SYS (Lewis & Wallace, 1998). Arrows in the small window indicate the processes with potential impact on the pelagic coastal carbonate system according to the concept proposed by Winde et al. (2014), with: 1 Photosynthesis, 2 CaCO_3 dissolution, 3 CO_2 invasion, 4 OM mineralization, 5 mixing with anoxic pore water/fresh water, 6 CaCO_3 mineralization, 7 CO_2 degassing. The slope for #5 strongly depends on the composition of the pore/fresh water mixing compound. Winter data are taken from Winde et al. (2014). Fresh water inlets: October (DIC: 1373-6542 $\mu\text{mol/kg}$; $\delta^{13}\text{C}$: -14.9 to -16.1‰ VPDB; Winde et al., 2014), May (DIC: 1358-6279 $\mu\text{mol/kg}$; $\delta^{13}\text{C}$: -3.4 to -10.9‰ VPDB).

Efflux of anoxic pore waters from an intertidal sand plate.

Outflow of nutrient enriched anoxic pore waters has been shown for intertidal sand plates in the backbarrier tidal areas of the southern North Sea, a process that is driven by pressure differences during low tide and may impact the composition of the water column to extends depending on season and hydrological conditions (Billerbeck et al., 2006; Al-Raei et al., 2009; Dellwig et al., 2007; Moore et al., 2011). This is a further example for intense benthic-pelagic coupling providing an additional source for DIC and TA, besides nutrients and redox-sensitive elements.

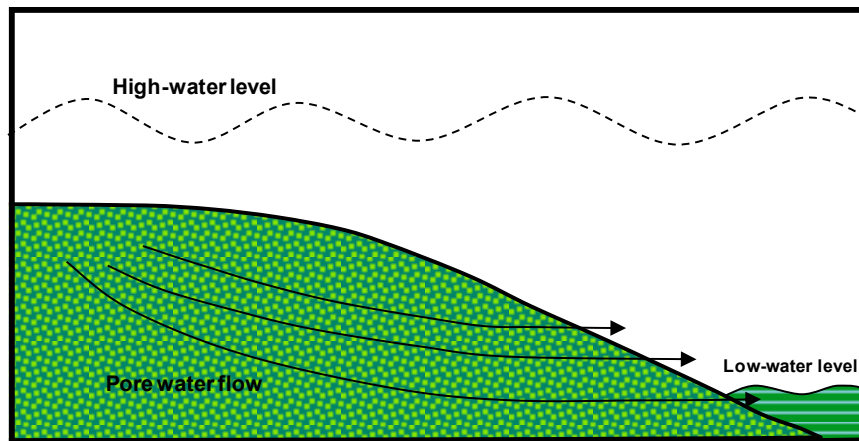


Figure 2a. A model scheme for the liberation of anoxic pore waters from permeable intertidal sands during low tide (modified after Billerbeck et al., 2006).

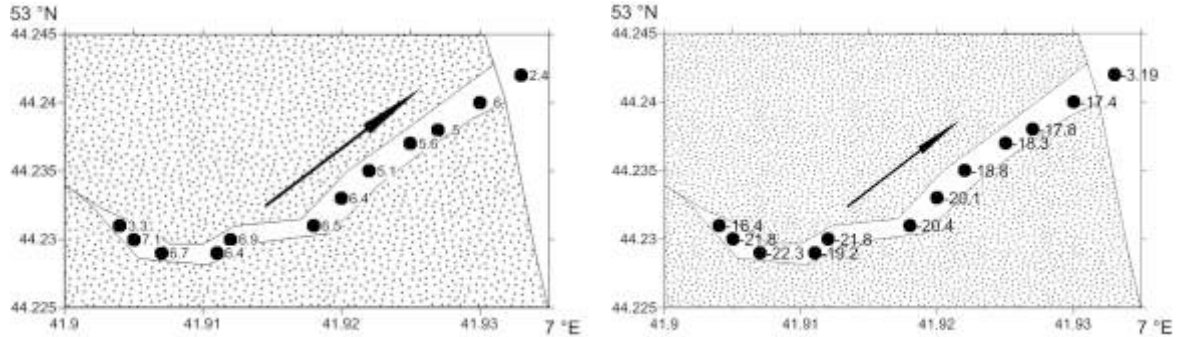


Figure 2b. Efflux of anoxic pore water from the Janssand (sand plate in the backbarrier tidal area of Spiekeroog Island) during low tide (31st October 2010) as shown by enhanced concentrations (left; in [mM]) of isotopically light (right; in [‰ vs. VPDB]) DIC, and dissolved sulfide and redox-sensitive trace metals (data not shown). Arrow: Flow direction towards the main tidal channel (right side). The enhancement of isotopically light DIC is mainly due to the oxidation of biogenic methane in the sediments (Böttcher et al., 2007).

ACKNOWLEDGEMENTS

Research was supported by BMBF within the Verbundprojekt BIOACID I, and Deutsche Forschungsgemeinschaft during the research group 'BioGeoChemistry of the Wadden Sea', and Leibniz IOW. Thanks are due to M. Schultz for help during on-board sampling in the Jade Bay.

REFERENCES

- Al-Raei, A.M., Bosselmann, K., Böttcher, M.E., Hespeneide, B., Tauber, F., 2009. Seasonal dynamics of microbial sulfate reduction in temperate intertidal surface sediments: Controls by temperature and organic matter. *Ocean Dynamics*, no. 59: 351-370.
- Billerbeck, M., Werner, U., Polerecky, L., Walpersdorf, E., de Beer, D., Hüttel, M., 2006. Surficial and deep pore water circulation governs spatial and temporal scales of nutrient recycling in intertidal sand flat sediment. *Marine Ecology Progress Series*, no.326: 61-76.
- Böttcher, M.E., Al-Raei, A.M., Hilker, Y., Heuer, V., Hinrichs, K.-U., Segl, M., 2007. Methane and organic matter as sources for excess carbon dioxide in intertidal surface sands: Biogeochemical and stable isotope evidence. *Geochimica et Cosmochimica Acta*, no. 71: A111.
- Brasse, S., Reimer, A., Seifert, R., Michaelis, W., 1999. The influence of intertidal mudflats on the dissolved inorganic carbon and total alkalinity distribution in the German Bight, southeastern North Sea. *Journal of Sea Research*, no. 42: 93-103.
- Dellwig, O., Bosselmann, K., Kölsch, S., Hentscher, M., Hinrichs, J., Böttcher, M.E., Reuter, R., Brumsack, H.-J., 2007. Sources and fate of manganese in a tidal basin of the German Wadden Sea. *Journal of Sea Research*, no. 57: 1-18.
- Hoppema, J.M.J., 1990. The distribution of alkalinity in the southern bight of the North Sea and in the western Wadden Sea. *Netherlands Journal of Sea Research*, no. 26: 11-23.
- Lewis, E., Wallace, D.W.R., 1998. Program developed for CO₂ system calculations. ORNL/CDIAC-105. Carbon dioxide information center, Oak Ridge National Laboratory, U.S. DE, Oak Ridge, Tenn.
- Moore, W.S., Beck, M., Riedel, T., Rutgers van der Loeff, M., Dellwig, O., Shaw, T.J., Schnetger, B., Brumsack, H.-J., 2011. Radium-based pore water fluxes of silica, alkalinity, manganese, DOC, and uranium: A decade of studies in the German Wadden Sea. *Geochimica et Cosmochimica Acta*, no. 75: 6535–6555.
- Thomas, H., Schiettecatte, L.-S., Suykens, K., Koné, Y.J.M., Shadwick, E.H., Prowe, A.E.F., Bozec, Y., de Baar, H.J.W., Borges, A.V., 2009. Enhanced ocean carbon storage from anaerobic alkalinity generation in coastal sediments. *Biogeosciences*, no. 6: 267–274.
- Winde, V., M.E. Böttcher, P. Escher, P. Böning, M. Beck, G. Liebezeit, and B. Schneider. 2014. Tidal and spatial variations of DI^{13}C and aquatic chemistry in a temperate tidal basin during winter time. *Journal of Marine Systems*, no.129: 394-402.
- Contact Information:** Michael E. Böttcher, Geochemistry & Isotope Geochemistry Group, Department of Marine Geology, Leibniz Institute for Baltic Sea Research (IOW), D-18119 Warnemünde, FRG, Phone: 0049-381-5197-351, email: michael.boettcher@io-warnemuende.de

Multi-isotope composition of freshwater sources for the southern North and Baltic Sea

Michael E. Böttcher¹, Marko Lipka¹, Vera Winde¹, Olaf Dellwig¹, Ernst O. Böttcher², Tillman M.C. Böttcher³ and Iris Schmiedinger¹

¹Geochemistry & Isotope Geochemistry, Department of Marine Geology, Leibniz Institute for Baltic Sea Research, D-18119 Warnemünde, FRG; ²D-21339 Lüneburg, FRG; ³D-26129 Oldenburg, FRG

ABSTRACT

We measured the stable hydrogen ($\delta^2\text{H}$) and oxygen ($\delta^{18}\text{O}$, $\delta^{17}\text{O}$) stable isotope composition of different fresh water sources for the coastal southern North and Baltic Sea (precipitation, river waters, fresh water inlets, coastal beach springs, fresh waters in and emerging from coastal marine sediments (SGD)) at sites in Germany, Poland and the Netherlands. Results are compared to the GNIP LMWL at Cuxhaven and the GMWL. The stable isotope results are complemented by the analysis of major and trace elements and nutrients in river and SGD samples to add information about ground water developments and mixing processes.

INTRODUCTION

The hydrological cycle is reflected by specific water isotope signatures found in precipitation, surface, and ground waters (e.g., Dansgaard, 1964; Craig & Gordon, 1965; Gat, 1996). Since fresh waters of different generation and ages may enter the coastal areas it is expected that they carry characteristic stable isotope signatures. Information about the specific composition of different fresh water sources allows for a use in mixing models for the origin of coastal waters and the deduction of benthic-pelagic coupling. Traditionally, investigations focused on the abundance of the isotopes H-1, H-2, O-16, and O-18 (e.g., Gat, 1996; Röpert et al., 2012). With the development of new analytical methods, also the O-17 isotope came into the focus of interest (e.g., Angert et al., 2004; Luz & Barkan, 2010).

We investigated the multi-isotope composition of different sources for fresh waters at sites with relevance for the southern coastal North and Baltic Sea areas (precipitation, rivers, fresh water inlets, coastal beach springs, fresh waters in and emerging from coastal marine sediments (SGD)). The composition of winter precipitation (rain, snow) at locations in Northern Germany (Warnemünde, Oldenburg (Oldb.), Lüneburg) and the Netherlands (Texel Island) was analyzed to derive local meteoric water lines in order to compare the measurements with the GNIP station in Cuxhaven (NW-Germany) and the GMWL. Precipitation in the towns of Oldenburg and Lüneburg is of relevance, since it may reach the North Sea coast-line via the Hunte/Weser and Ilmenau/Elbe systems, respectively. Selected precipitation events were resolved in enhanced time resolution. Stable isotope results for river and SGD (submarine groundwater discharge) samples were further complemented by on-site measurements (temperature, pH, salinity) and selected hydrogeochemical analyses (main and trace elements, nutrients, dissolved carbonate system).

MATERIALS AND METHODS

Water samples from fresh water inlets, and coastal sediments were taken as described earlier (Beck et al., 2011; Kotwicki et al., 2014; Winde et al., 2014). Water aliquots were immediately filtered (0.45 μm membrane filters) for further analyses by ICP-OES (Thermo

iCAP 6300 DuoThermo Fisher Scientific) and a QuAAtro nutrient analyzer (SEAL Analytical). Precipitation sampling was carried out using a Hellmann-type rain gauge (NE of the town Lüneburg) or otherwise with open plastic sampling devices. At the Lüneburg site, the amount of fallen rain (volume per area of surface) was additionally quantified on a regular daily base. Stable isotope measurements (H-1, H-2, O-16, O-17, O-18) were conducted by means of a CRDS system (Picarro L2140-i) giving results in the conventional δ -notation versus the V-SMOW standard. The international standards VSMOW, SLAP, and GISP, besides in-house standards, were used to scale the isotope measurements.

RESULTS AND DISCUSSIONS

Precipitation.

Short-term sampling of winter precipitation on the Dutch island Texel followed a non-amount-weighted correlation equation of $\delta^2\text{H} = 7.5 \cdot \delta^{18}\text{O} + 6.5$ ($n = 19$; $r^2 = 0.99$), close to the LMWL at the German coastal town Cuxhaven ($\delta^2\text{H} = 7.8 \cdot \delta^{18}\text{O} + 5.2$; Röper et al., 2012).

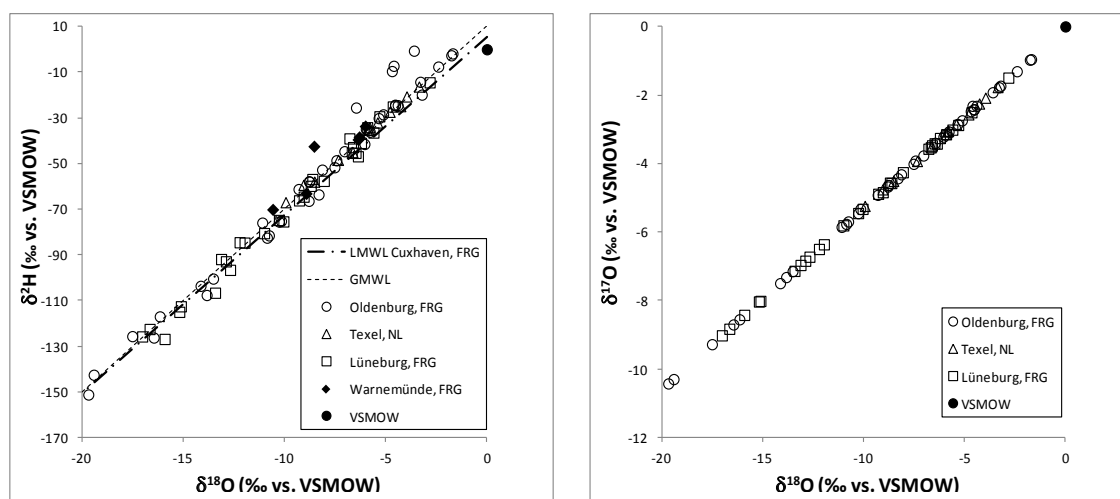


Figure 1. $\delta^{18}\text{O}$ - $\delta^2\text{H}$, and $\delta^{18}\text{O}$ - $\delta^{17}\text{O}$ co-variations in winter precipitation (December 2013 - March 2014). LMWL at Cuxhaven from Röper et al. (2012).

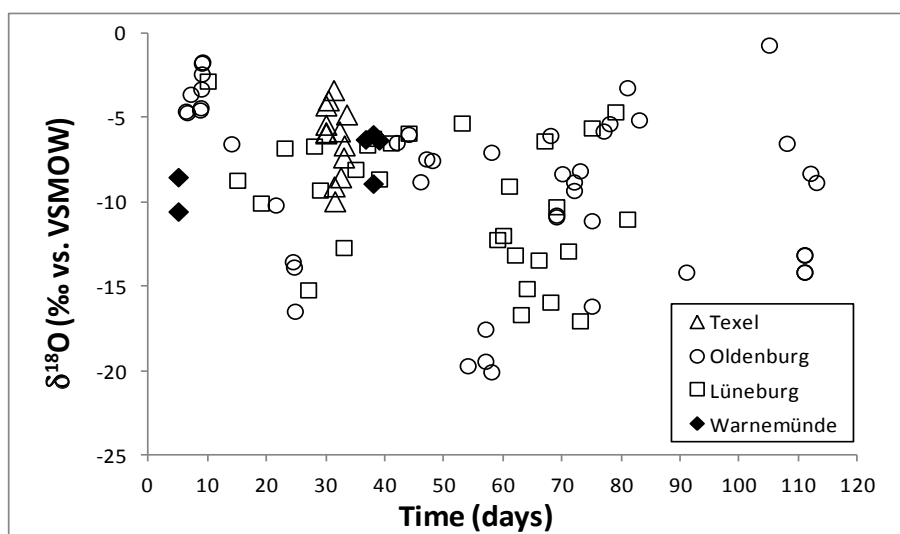


Figure 2. Temporal dynamics during short-time sampling of winter and spring precipitation at four Dutch and German sites (Start: December 1st, 2013).

The short-term sampling based LMWL at the Site Lüneburg ($\delta^2\text{H} = 8.2 \cdot \delta^{18}\text{O} + 10.8$; $n = 30$; $r^2 = 0.99$; December 2013 to March 2014) falls close to the GMWL. Results for the Site Warnemünde ($\delta^2\text{H} = 7.4 \cdot \delta^{18}\text{O} + 9.6$; $n = 6$; $r^2 = 0.84$) and Site Oldenburg ($\delta^2\text{H} = 8.5 \cdot \delta^{18}\text{O} + 16.5$ ($n = 39$; $r^2 = 0.98$)) demonstrate differences (Figures 1 and 2), that are caused by meteorological characteristics, like different water sources, temperature regimes, and precipitation amounts. Sites of SGD, fresh water beach springs, and coastal low-salinity pore waters were investigated at the North Sea (Janssand - backbarrier tidal area of Spiekeroog Island; northern beach of Texel Island) and the Baltic Sea (Meschendorf, Puck Bay). For a more detailed understanding, more prolonged time series with an amount-weighted evaluation are required, that are currently in progress.

Rivers, submarine groundwater discharge, beach springs & coastal low-salinity pore waters.

Samples from rivers draining into the North Sea (Elbe) and the Baltic Sea (Schwentine, Warnow) fall close to the LMWL established at Cuxhaven (Röper et al., 2012). The deep pore waters from a long drill core recovered on the Janssand, a sand flat in the backbarrier tidal area of Spiekeroog Island (Beck et al., 2010), are positioned on a mixing line between modern North Sea water and fresh waters positioned close to the modern LMWL at Cuxhaven. Fresh waters escaping on beaches of Texel Island are positioned on a mixing line between the LMWL and North Sea water (Figure 3).

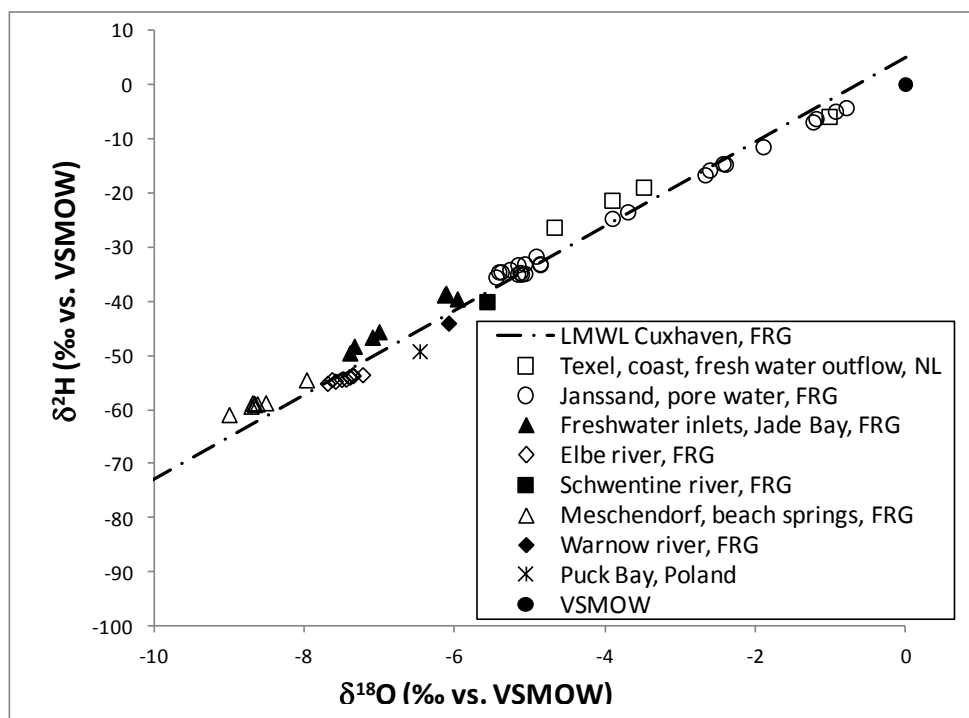


Figure 3. Stable oxygen and hydrogen isotope composition of different fresh water sources (rivers, fresh water springs at the shore line, pore waters from a long sediment core recovered from the Janssand in the backbarrier tidal area of Spiekeroog (Beck et al., 2010)) for the North Sea: Janssand, Elbe, Texel, Jade Bay, and the Baltic Sea: Meschendorf, Schwentine, Warnow. The sample of Puck Bay is a mixture between SGD ($\delta^{18}\text{O} \approx -10.3\text{‰}$, $\delta^2\text{H} \approx -76\text{‰}$; Vogler et al., unpublished) and Baltic Sea water.

Seasonal studies on different scales and more river and SGD sites are required to further develop quantitative balances for the impact of different fresh waters on the coastal regions of the North and Baltic Sea. Major and trace elements, including nutrients, of SGD samples further allow for the application of mixing models with more saline bottom waters and reflect the pathways of ground water evolution.

ACKNOWLEDGEMENTS

The research was supported by BMBF within the Verbundprojekt BIOACID I + II, the BONUS⁺ project AMBER, Deutsche Forschungsgemeinschaft during the research group 'BioGeoChemistry of the Wadden Sea', and Leibniz IOW. Thanks are due to K. Müller for technical support.

REFERENCES

- Beck, M., T. Riedel, T. Graue, J. Köster, N. Kowalski, C.S. Wu, G. Wegener, Y. Lipsevers, H. Freund, M.E. Böttcher, H.-J. Brumsack, H. Cypionka, J. Rullkötter, and B. Engelen. 2011. Imprint of past and present environmental conditions on microbiology and biogeochemistry of coastal Quaternary sediments. *Biogeosciences*, no.8: 55-68.
- Angert, A., C.D. Cappa, D.J. de Paolo. 2004. Kinetic ¹⁷O effects in the hydrological cycle: Indirect evidence and implications. *Geochimica et Cosmochimica Acta*, no.68: 3487-3495.
- Craig, H., and L.I. Gordon. 1965. Deuterium and oxygen-18 variations in the ocean and the marine atmosphere. In: *Stable Isotopes in Oceanographic Studies and Paleotemperatures* (ed. Tongiorgi, E.). 9-130, Laboratory of Geology and Nuclear Science.
- Dansgaard, W. 1964. Stable isotopes in precipitation. *Tellus*, no.16: 436-468.
- Gat, J.R. 1996. Oxygen and hydrogen isotopes in the hydrological cycle. *Annual Reviews in Earth and Planetary Sciences*, no.24: 225-262.
- Kotwicki, L., K. Grzelak, M. Czub, O. Dellwig, T. Gentz, B. Szymczycha, and M.E. Böttcher. 2014. Submarine groundwater discharge to the Baltic coastal zone: Impacts on the meiofaunal community. *Journal of Marine Systems*, no. 129: 118-126.
- Luz, B., and E. Barkan. 2010. Variations of ¹⁷O/¹⁶O and ¹⁸O/¹⁶O in meteoric waters. *Geochimica et Cosmochimica Acta*, no.74: 6276-6286.
- Röper, T., K.F. Kröger, H. Meyer, J. Sültenfuss, J. Greskowiak, and G. Massmann. 2012. Groundwater ages, recharge conditions and hydrochemical evolution of a barrier island freshwater lens (Spiekeroog, Northern Germany). *Journal of Hydrology*, no.454-455: 173-186.
- Winde, V., M.E. Böttcher, P. Escher, P. Böning, M. Beck, G. Liebezeit, and B. Schneider. 2014. Tidal and spatial variations of $\delta^{13}\text{C}$ and aquatic chemistry in a temperate tidal basin during winter time. *Journal of Marine Systems*, no.129: 394-402.

Contact Information: Michael E. Böttcher, Geochemistry & Isotope Geochemistry Unit, Department of Marine Geology, Leibniz Institute for Baltic Sea Research (IOW), D-18119 Warnemünde, FRG, Phone: 0049-381-5197-351, email: michael.boettcher@io-warnemuende.de

The role of 3D volcanic structures on seawater intrusion in Grande Comore Island inferred from geophysical investigations and groundwater modelling

A. Bourhane¹, J-C. Comte², J-L. Join¹ and T. Mara³

¹Laboratory Geosciences Reunion, UMR 7154 - IPGP, University of Reunion Island, France

²Groundwater Research Group, S.P.A.C.E., Queen's University Belfast, Northern Ireland

³Laboratoire de Physique et Ingénierie Mathématique pour l'Énergie et l'Environnement - University of Reunion Island, France

ABSTRACT

Grande Comore Island is located at the Northern end of the Mozambique Channel in the Southwestern Indian Ocean. Groundwater is the only safe water resource for drinking, but only one third of the population have access to this resource. Due to the steep slopes of this high and still active volcanic island, all existing wells are drilled in the coastal zone within 3 km from the shoreline and can reach up to more than 100m deep. Among them, only one third provide groundwater of acceptable salinity for drinking (less than 1 g/L), one third provide water of salinity comprised between 1 and 3 g/L, and the remaining third is generally disused due to salinities higher than 3 g/L. The development of groundwater in Grande Comore requires an improved understanding of the coastal volcanic aquifers, quantitatively and qualitatively. This work applies an integrated hydrogeological approach aiming at improving both the conceptual understanding of Grande Comore volcanic aquifers and the dynamics of seawater intrusion. This approach included (1) a review of the current hydrogeological knowledge regarding the structure, properties and conceptualisation of the island's volcanic aquifers, (2) the spatial characterisation of both aquifer structures and seawater intrusion in coastal areas, through the implementation of geophysical surveys comprising electrical resistivity tomography (ERT) and time-domain electromagnetic (TDEM) and (3) the quantification of the impact of typical volcanic heterogeneities on coastal groundwater salinity through numerical groundwater modelling. The simulations confirm the strong controls exerted by volcanic structures on saline intrusion dynamics as observed from geophysical investigations, in particular the presence of paleo-valleys filled by lava flows of contrasted hydrogeological properties.

INTRODUCTION

The Comoros volcanic archipelago is located midway between the west coast Madagascar and the African east coast, at the northern extremity of the Mozambique Channel, between Lat. S 11-13° and Long. N 43-46°. It covers a total area of 2033 km² including four main islands. The westernmost island of Grande Comore is geologically the most recent [most of the rocks have less than 1 Ma], the largest [1024 km²] and the highest [2361 m]. The volcanism is still active at the Karthala Volcano [2361 m]. The island is mainly composed of two recent shield volcanoes of dominant basaltic type: (1) the massif of La Grille [1087 m], which covers the northern half part of the island, is of intermediate age [Middle Pleistocene], with a morphology characterised by gentle slopes and scattered by several cinder cones; (2) the massif of the Karthala, which covers a surface of about two thirds of the island in its centre, is an active shield volcano [Quaternary] characterized by a near-absence of weathering.

This work is aiming to understand and simulate the role of structural heterogeneities on the seawater intrusion dynamics in the recent volcanic aquifers. Geophysical methods are used for imaging the salt wedge geometry and numerical simulations allowed understanding the relations between geological structures and saltwater intrusion extension.

HYDROGEOLOGICAL SETTING

The Comoros archipelago has a humid tropical climate, including a hot and wet season and a cool and dry season. The annual rainfall varies from less than 1.5 m in the north-east up to more than 5 m in the south-west of the island (western flank of the Karthala). Runoff is very low (estimated annually at 5% of rainfall) and there are no permanent rivers.

The renewable annual groundwater volume of Grande Comore is estimated between 0.5 and 2 billion (10^9) cubic meters, resulting from an effective rainfall infiltration estimated between 57% and 63% of the annual rainfall. The combined annual abstraction of the currently 11 operating wells (out of the 55 existing) can be estimated at about 7 millions of m^3 , which constitutes only 0.4 to 1.4% of the renewable annual groundwater resource. However, two thirds of the Island's water wells are naturally contaminated by saltwater concentrations higher than 1g/L.

In the coastal zone, the hydrodynamic properties of the basal aquifer, display exceptionally high values of transmissivities, hydraulic conductivities, diffusivities and well productivities. Most of the results, however, would not be representative of the most recent and highly productive units, where it is difficult to obtain significant drawdowns required for a reliable interpretation of the pumping tests. Aquifer storativities reflect unconfined to semi-confined conditions. Aquifers hydrodispersive properties that control solute transport, such as salt water, are not known. The high aquifer diffusivities result in both a low attenuation and a short time-lag of the tidal signal, which enhance the seawater encroachment, further exacerbated by a large tidal range [up to 3 m].

METHODS

A review of the available literature provided the current status of knowledge about the Grande Comore hydrogeological settings. Then, multi-techniques ground geophysical investigations carried out in 3 coastal zones enabled imaging the complexity of the geometry of the seawater interface in Grande Comore. These methods included Time Domain Electro-Magnetics [TDEM] soundings and Electrical Resistivity Tomography [ERT] profiles. These 2D measurements were taken with the Wenner-Schlumberger array, which has a relatively good signal/noise ratio (Dahlin and Zhou 2004) and is sufficiently sensitive to the geometrical features of seawater interface in coastal groundwater (Comte et al., 2010). Finally, a 3D numerical model using the code SEAWAT (Guo and Langevin 2002) was applied to investigate the theoretical effects of local aquifer heterogeneities associated to typical various volcanic structures on the patterns of seawater intrusion in the basal aquifer.

RESULTS

Geophysical investigations

The littoral domain in the most recent volcanic rock is characterized by variable resistivities resulting from both different lithologies and degree of seawater intrusion. On the flanks of the recent Karthala volcano, at shallow depths, the unsaturated basalts and the fresh groundwater are characterised by very high resistivities ($>1000 \Omega.m$ and $100-1000 \Omega.m$, resp.). At greater depths, the presence of saline/brackish groundwater results in very low

resistivities ($<100 \Omega.m$ for brackish water and $<10 \Omega.m$ for salt water). On transects normal to the coast (Figure 1a), the interface between fresh and saline groundwater displays a very low dipping angle towards the island resulting from low hydraulic gradients and high permeabilities. In such recent volcanic areas, this low dipping angle of the seawater interface explains the apparent wide transition zone between saline and fresh groundwater and the occurrence of high degrees of salinities at relatively large distances from the sea. Transects parallel to the coast (Figure 1b) reveal large resistivity variations in the saturated zone (about 10 to 500 $\Omega.m$), which suggests large variations of permeability, porosity and/or salinity associated to possible preferential flows resulting from the depositional structure of lava flows.

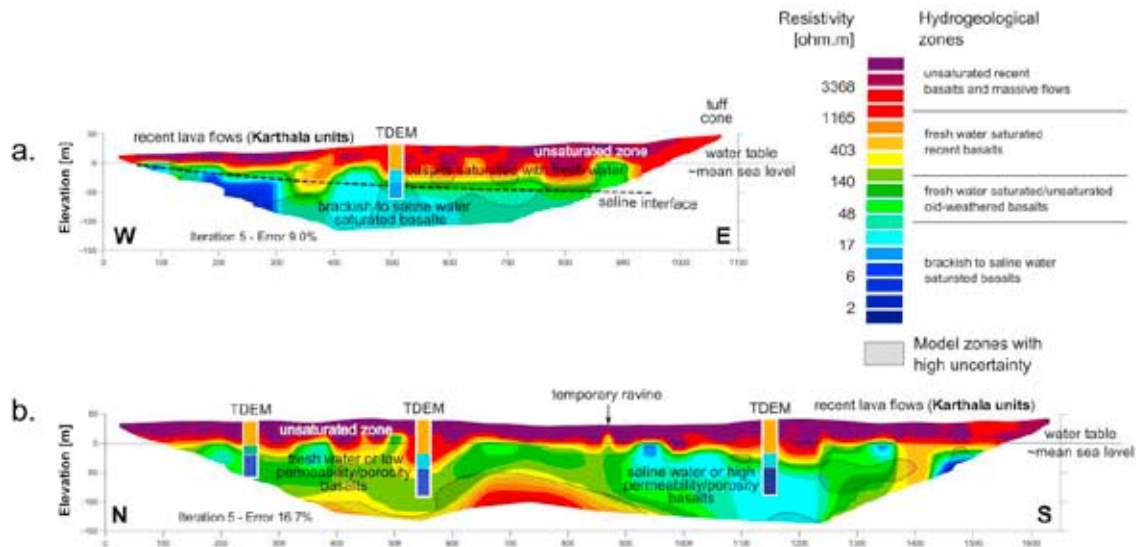


Figure 1 : Typology of the basal volcanic aquifers in Grande Comore interpreted from combining ERT and TDEM results – (a) section normal to the coast; (b) section parallel to the coast.

Theoretical simulation of the role of 3D volcanic structures on saline intrusion

The model hydrogeologic parameters and boundary conditions applied are representative of the youngest volcanic units of the Karthala volcano in Grande Comore. The homogeneous model ($K_h=10^{-3}$ m/s; $K_v=10^{-4}$ m/s) results in a smooth and regular transition zone between fresh and saline water displaying a low dipping angle towards the island (Figure 2a). The thickness of freshwater lying on transition levels reaches about 30m below sea level at 1.2 km from the shoreline, and about 75 m at 5 km. The local presence of a paleo-valley infilled with a massive, low permeability isotropic lava flow ($K_h=K_v=10^{-5}$ m/s) results in a deepening of the transition zone beneath the paleo-valley, where freshwater thickness appears almost double (~ 50 m) at 1.2 km from the shoreline (Figure 2b). In contrast, the local presence of a paleo-valley infilled with a high permeability isotropic lava flow ($K_h=K_v=10^{-2}$ m/s) results in the thinning of the freshwater levels, which disappear on a distance from the coast up to 2 km, particularly on the borders of the paleo-valley (Figure 2c). The width of the transition zone along the coast appears also significantly increased. Given the large diversity of volcanic units expected in young volcanic environment such as in Grande Comore, those theoretical simulations confirms the significant lateral variation of salinities observed in water wells along the coast in both La Grille and Karthala recent volcanoes. Those simulations support the hypothesis that local structures can strongly impact the seawater intrusion at the local/field scale.

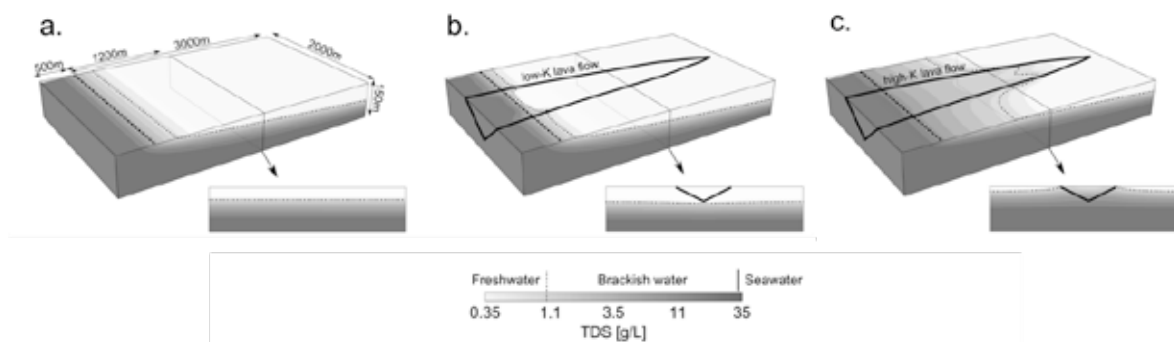


Figure 2 : Role of local heterogeneities on seawater intrusion in the coastal zone: (a) homogeneous model; (b) palaeovalley infilled with lower permeability (K) lava flow; (c) palaeovalley infilled with higher permeability lava flow. The top face is at mean sea level elevation. Dashed line is the coastline and dotted line is the contour 1 g/L corresponding to the WHO (2003) max salinity standard for drinking water. Vertical exaggeration x3.

DISCUSSION AND CONCLUSIONS

Strong hydrogeological heterogeneities have been observed in the recent volcanic aquifers. Geophysical results revealed a large diversity of geological heterogeneities and salinity variability in the coastal areas. Those areas are where all the water wells are located which is the result of the technical and economical difficulties for drilling boreholes in other areas where elevations are high and the water table is very deep. Groundwater modelling confirms that in the coastal zone the presence of channels of recent high-permeability lava flows enhances the saline invasion, while the presence of lower permeability lava flows tends to maintain the saline interface deeper. These findings reveal a potential for further developing the aquifers of the coastal zone of Grande Comore, where the knowledge of the geological structures appears crucial for accessing groundwater of acceptable salinity.

REFERENCES

- Comte J-C, Banton O, Join J-L, and Cabioch G (2010) Evaluation of effective groundwater recharge of freshwater lens in small islands by the combined modeling of geoelectrical data and water heads. *Water Resour Res* 46:n/a–n/a. doi: 10.1029/2009WR008058
- Dahlin T, and Zhou B (2004) A numerical comparison of 2D resistivity imaging with 10 electrode arrays. *Geophys Prospect* 52:379–398. doi: 10.1111/j.1365-2478.2004.00423.x
- Guo W, and Langevin CD (2002) A Computer Program for Simulation of Three-Dimensional Variable-Density Ground-Water Flow. *Tech. Water-Resour. Investig. Book 6 Chapter A7 77 P*
- WHO (2003) Total dissolved solids in drinking-water. Background document for preparation of WHO Guidelines for drinking-water quality. (WHO/SDE/WSH/03.04/16). World Health Organization, Geneva

Contact Information: Anli Bourhane, Laboratory Geosciences Reunion (LGSR) – IPGP UMR 7154 – University of Reunion Island - 15, Avenue René Cassin - CS 92003 - 97 715 Saint Denis – France - Phone: +262(262) 938208 - Fax: +262(262) 938266 - Email: anli.bourhane@univ-reunion.fr

Development of a freshwater lens in a new strip of dunes

Ruben J. Caljé¹, Wouter Beekman¹ and Frans Schaars¹
¹Artesia Water, Schoonhoven, the Netherlands

ABSTRACT

Part of the dune area close to Rotterdam was widened into the sea by about 300 meters in 2008. The purpose of the widening was compensation for lost nature area due to an extension of the harbor of Rotterdam. Now that some years have passed, the question arises whether the conditions are fit for the desired biotopes.

Groundwater level measurements show that the initial groundwater level increase due to a rainwater surplus has probably ceased. Groundwater quality and geo-electrical measurements were performed, to determine if the freshwater lens is still changing. A cross sectional groundwater flow and transport model was used to link these measurements to each other, in time and space. The model was calibrated on groundwater heads and the salinity decrease in some of the wells in the new dune strip.

These activities provided the opportunity to investigate the growth of a freshwater lens on a short time scale, and to test our transient models. The model showed that the initial head change took place in about 2 years, while the salinity distribution was still changing significantly.

The research is still going on and will be decisive for future intervention in the dune valley. If the groundwater heads are too low and the amount of surface water in the valley will be insufficient, measures will be taken.

INTRODUCTION

Close to the port of Rotterdam, near Hoek van Holland, the dunes are about 500 meters wide. This dune area was widened into the sea by about 300 meters in 2008 (Figure 1). The new strip of dunes was created on the sea side of the beach, enclosing the old beach as a valley. The purpose of the widening was compensation for lost nature area due to an extension of the harbor of Rotterdam (Figure 2). The geology consists mainly of sand, intersected by a few clay layers, of which the most important one is 1-5 meter thick at about -20 m below sea-level.

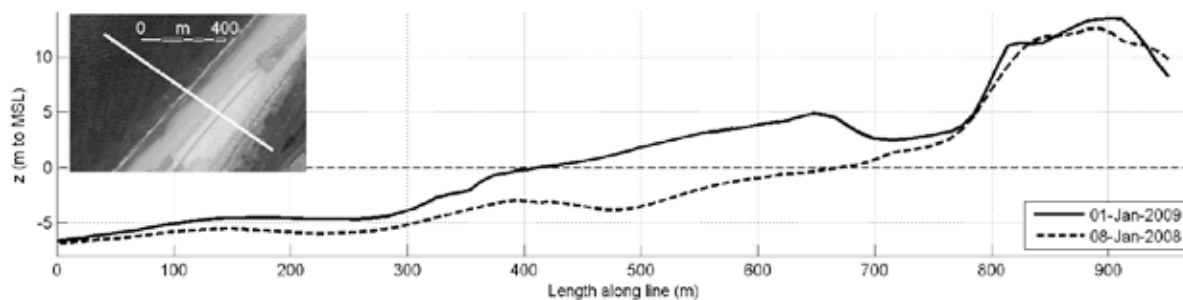


Figure 1. Two altitude profiles: after and before the construction of the new dune strip.

The design challenge was to determine the optimal elevation of the valley floor to meet the desired environment, while the influence of the dynamic dune-forming processes in creating and maintaining the valley was uncertain. Now that some years have passed, the question arises how the morphology and hydrology of the valley has changed and whether the conditions are fit for the desired biotopes.



Figure 2. A photograph from the top of the old dune, showing the harbor of Rotterdam on the left and the new strip of dunes on the right (<https://beeldbank.rws.nl>, Rijkswaterstaat / Harry van Reeken).

METHODS

Initially the area was monitored by groundwater level and salinity measurements in 8 shallow piezometers, grouped in 2 lines perpendicular on the coast. The filters were placed between 1.5 and 2 m below sea level. The rise in groundwater heads due to the construction of the new dune strip was difficult to separate from the seasonal fluctuations, but seems to have ceased after about 2 years. The water in the inland piezometers was already fresh at the start of the project, and by 2012 all other piezometers had also turned fresh.

To continue the monitoring of the freshwater lens, geo-electrical measurements were performed at the start of 2014. These geo-electrical measurements consisted of 4 CVES profiles. These profiles showed increasing salinity with depth, which was quite constant in the horizontal plane. In the CVES profile perpendicular to the coast, the influence of the sea was noticeable only at the most seaward part. Measuring the conductivity during a drilling by a hand auger to 5 meters depth showed similar resistance values as the CVES-profiles, getting more saline at the bottom of the auger hole.

A cross sectional groundwater flow and transport model was used to link these measurements to each other, in time and space. The model uses the SEAWAT model code (Langevin, et al., 2007) and consists of a cross-section of a few kilometers perpendicular to the coast, in the same direction as the piezometers and one of the CVES-profiles. The model reaches from the sea to the dunes and the polder behind the dunes, enclosing the entire fresh water lens below the dunes.

The simulation time consists of 2 periods: the original situation is simulated for 1000 years to calculate the equilibrium between fresh and saline groundwater. A shorter time period is modeled hereafter in which the new dune strip is present. The model was calibrated on groundwater heads and the salinity decrease in some of the wells in the new dune strip.

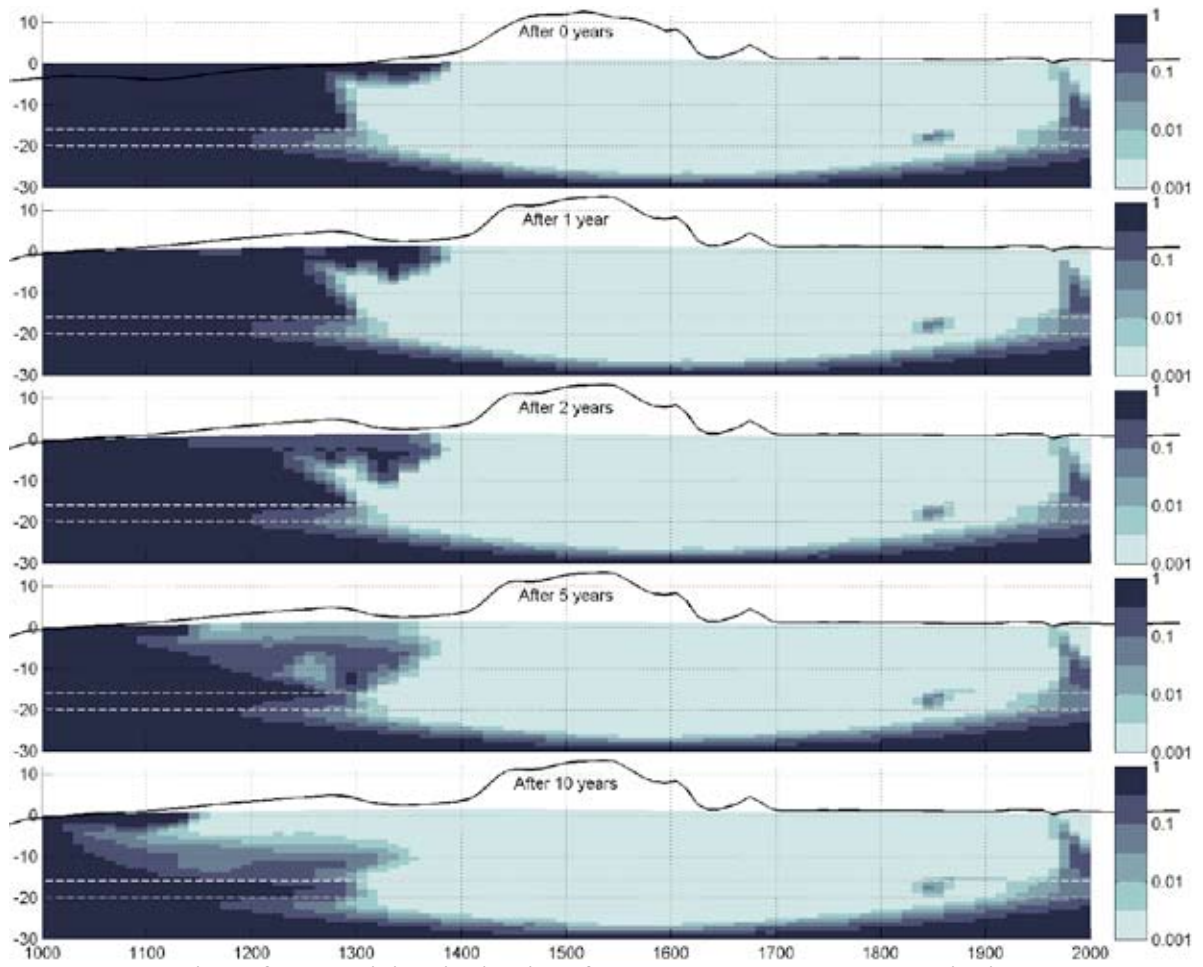


Figure 3. The salinity distribution of the model, at several moments in time.

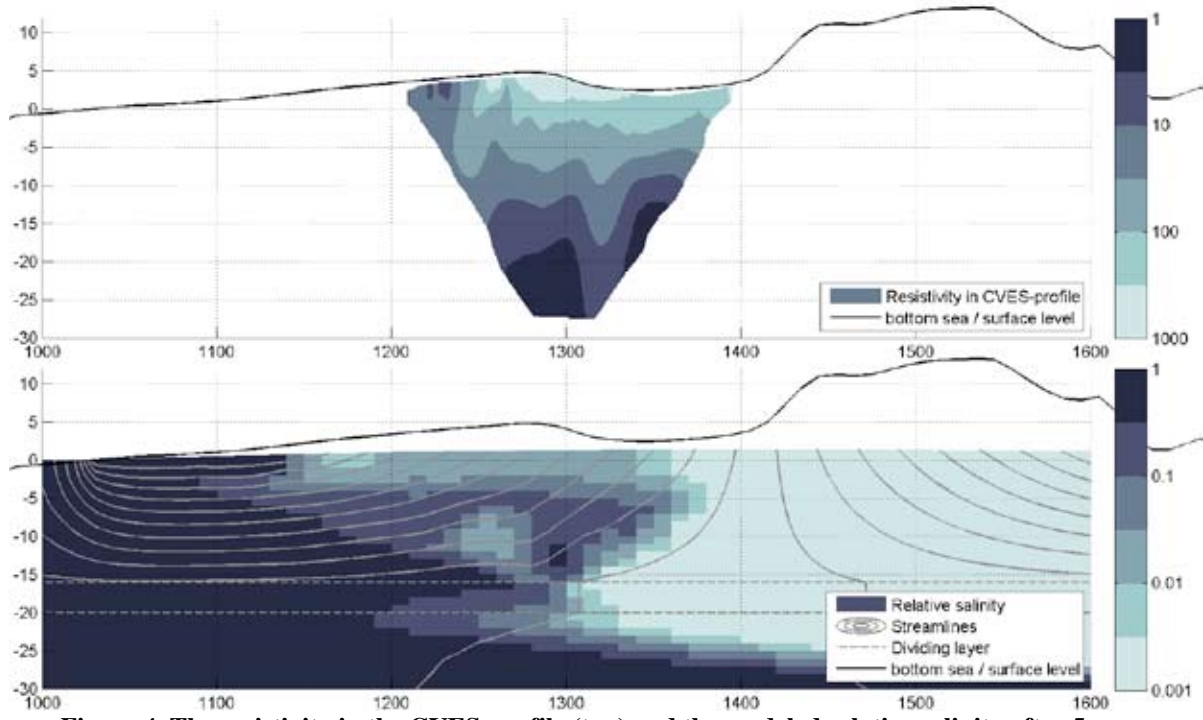


Figure 4. The resistivity in the CVES-profile (top) and the modeled relative salinity after 5 years (bottom).

RESULTS

The model shows that in the first 2 years after the construction of the new dune strip the groundwater levels are increasing fast due to a rainfall surplus. After this period the groundwater level increases only marginally, caused by the gradually changing salinity distribution (Figure 3).

Because of the nature of a cross-sectional model it was not possible to fully match the measured groundwater heads and salinity or the CVES-profiles. However, the model is able to simulate the mayor process: the fresh water lens is formed by new rainfall, mostly horizontal. This will continue in the coming years, until a new equilibrium is reached between rainfall and fresh water flowing to the sea and the polder. The model does not incorporate the tide at the seaward boundary. While the tide does not seem to influence the salinity distribution below the dunes, it can account for the differences between the model and the CVES-profile near the beach (Figure 4).

The CVES-profile shows an increasing salinity distribution with depth, with no inversions. The model however does show an inversion, caused by the fact that salt groundwater at the former location of the beach gets trapped between older and newer fresh water. Another difference between model and measurements is the speed in which the water in the piezometers gets fresh: in the model it takes a few years, while in reality it only takes a few months.

It turns out that the salinity distribution is quite sensitive to the manner in which sand was supplied along the coast. Part of the sand displacement was performed in dry conditions by excavator trucks, while other parts were supplied by rainboring of sand with salt water. This salt water infiltrated during the construction, constituting an additional salt load. The model showed that this salt load has a mayor influence on the salinity distribution during the first few years of simulation. Another aspect which was examined with the model was the occurrence of surface water at the landward side of the dunes, causing an extra in- or outflow of fresh water to or from the freshwater lens.

DISCUSSION AND CONCLUSIONS

These activities provided the opportunity to investigate the growth of a freshwater lens on a short time scale. The research is still going on and will be decisive for future intervention in the dune valley. If the groundwater heads are too low and the amount of surface water in the valley will be insufficient, measures will be taken. These measures will probably consist of the lowering of the surface level of the dune valley, towards the groundwater level. This will however imply that the ecological development of the valley has to start all over again.

REFERENCES

Langevin, C., Thorne, D. J., Dausman, A., Sukop, M., & Guo, W. 2007. SEAWAT Version 4: A Computer Program for Simulation of Multi-Species Solute and Heat Transport. USGS Techniques and Methods Book 6, Chapter A22.

Contact Information: Ruben J. Caljé, Artesia Water, Korte Weistraat 12, Schoonhoven, 2871 BP, the Netherlands, Phone +31628145830, Email: r.calje@artesia-water.nl

Reproducing the fresh-salt water distribution during the past millennium of a highly dynamic coastal groundwater system: the construction of the variable-density groundwater model

J. Claus¹, G. Oude Essink², G. Janssen², D. Vandeveld³, L. Kaland⁴ and L. Lebbe¹

¹Department Geology and soil science, Ghent University, Ghent, Belgium

²Deltares, Utrecht, the Netherlands

³Flemis Environment Agency (VMM), Brussels, Belgium

⁴Province of Zeeland, Middelburg, the Netherlands

ABSTRACT

The western part of the south bank of the Western Scheldt has, through its last thousand years of history, been known as a highly dynamic coastal groundwater system. It is a transboundary area located on the coastal plains of Belgium and the Netherlands. It is characterized by tidal mud-flats, tidal gullies, marshes and dunes that have been subject to natural developments (sea level rise and storm surges) and human influences (construction of dikes and drainage systems for land reclamation, construction of canals for shipping and military inundations). These historic events and their influence on the landscape are pretty well documented, especially from the year 1500 onward: written literature is available, as well as historical paintings of the area and reconstruction land maps. To be able to simulate the fresh-salt water distribution over the past 1000 year in this dynamic coastal area, representative sets of historical boundary conditions had to be derived. As the type of land and the topography appear to be main drivers of this hydrogeological setting, reconstruction maps of both these characteristics were created based on the available documentation and the know landscape forming processes. A combination of these reconstruction maps with the present day boundary conditions lead to the derivation of the historical conditions. Another important characteristic to incorporate in this model was the sea level fluctuation. A challenge this study entailed, was the transboundary nature of the study area (Belgium – The Netherlands). Both countries have their own specific datasets (e.g. hydrogeological classification of the subsoil, chloride concentration maps) which do not always show a perfect fit at the border. A correlation between the different datasets was necessary to construct a stable and representative model. This study focused on the different steps that had to be run through to construct a working groundwater model of this dynamic coastal area, rather than on the results of the model. The software used to construct the groundwater model is MOCDENS3D.

INTRODUCTION

The construction of a numerical variable-density groundwater model requires the input of hydraulic conductivities of the different depositional facies, external sources, boundary conditions and an estimate of the fresh water head and fresh-salt water distribution at the start of the simulation. In addition, a set of boundary conditions of a historical period have to be deduced: a possible technique to derive these historical boundary conditions is tested here.

This study was conducted in the western part of Zeeland Flanders (NL) and the northeastern part of West Flanders (BE) and the northern part of East Flanders (BE). In the north it is enclosed by the estuary of the Western Scheldt, in the south by the higher tertiary areas.

What makes this area perfectly suited for this research on palaeohydrogeological processes affecting the fresh-salt water distribution is that, in the past 1000 years, it has been known as a very highly dynamic coastal area. It is characterized by tidal mud-flats, tidal gullies, marshes and dunes that have been subject to natural developments (sea level rise and storm surges) and human influences (construction of dikes and drainage systems for land reclamation, construction of canals for shipping and military inundations). These historic events and their influence on the landscape are well documented, especially from 1500 onward. Written literature is available, as well as paintings of the area and reconstructed land use maps.

The subsoil consists of quaternary deposits which have a thickness of 20 to 25m. It consists out of clayey overbanked deposits, sandy creek deposits, peat layers, sand dunes, loam and pleistocene deposits. Beneath the quaternary deposits, the tertiary Bartoon clay occurs. The tertiary deposits consist of an alteration of predominately fine sandy aquifers and heavy clay aquitards.

METHODS

The historic evolution of flow and fresh-salt water distribution in this dynamic coastal environment is simulated using MOCDENS3D. This code enables the simulation of 3D-density dependent groundwater flow and coupled solute transport. For this modeling exercise in specific, special attention is given to the discretization of the historical boundary conditions and to the elaboration of the transboundary data sets.

Elaboration of transboundary data sets

Both Belgium and the Netherlands have their own available data which doesn't stretch out far into the other country, so a combination of both sets had to be made. Not all available datasets showed a perfect fit at the boundary and unconformities were corrected. A correlation was made between the hydrogeological subdivision of the subsoil in the Netherlands (REGIS II classification) opposed to the hydrogeological subdivision in Flanders (HCOV classification). This hydrogeology stays fixed throughout the model. For the correlation between the datasets on rivers, drainage and such, the available data of each country was accounted to their own respective areas.

Evolution during the past millennium: deriving historical boundary conditions

For a reliable reconstruction of the fresh-salt water distribution during the past millennium, it is essential to have a good understanding on the dynamics of the coastal area. The changing positions of the gullies, the tidal areas, the dunes and the reclaimed land, with its accompanying drainage systems, need to be translated into boundary condition for every stress period. These boundary conditions are main drivers controlling the ongoing dynamic processes in the coastal groundwater system (viz. fresh water recharge and upward salt groundwater flow).

All available **documentation** which contributes to the understanding of this landscape during the past millennium was collected (e.g. Wilderom 1973; Brand 1993). An appeal was made on sources from literature, reconstructed land maps and even historical paintings. Documentation on the period 1000 to 1500 is rather limited, available maps are mostly reconstructed in later periods. From 1500 on, more information is available. This lead to the following subdivision of the time: the timespan from the year 1000 till present has been subdivided into a total of fifteen stress periods: from 1000 till 1500 it is covered in steps of 100 years and from the year 1500 till present, it is subdivided into periods of about 50 years.

For each of the chosen years, a map is constructed on which six types of land at the surface are indicated. Each of these **land types** has its own characteristics with regard to the topography and will interact differently with the groundwater reservoir (they have different recharge rates, drainage levels, presence of rivers, ...). The six considered land types are: 1. *Sea or gully*: have a surface level beneath the lowest water level of the sea; 2. *tidal area*: due to tidal movements of the sea, this surface is only temporarily flooded; 3. *peat*: a very plane area with water levels close to the surface level, but the area is not flooded; 4. *reclaimed land (polder)*: water levels are determined by human interference; 5. *dune*: higher terrain with better permeable sediments, this area usually acts as replenishment for the groundwater reservoir with fresh infiltration waters; and 6. *a transition zone between reclaimed land and the higher inland tertiary zone*: located in the south of the study area, north of the higher sandy loam area, in which the water table is located deeper beneath the surface, as such no active drainage is needed to keep the area dry.

In order to make a good estimate of the historic upper boundary conditions, it is crucial to have a good view on the **topography**, as the topography acts as an essential factor controlling the groundwater flow in four of the indicated land types: *tidal area*, *peat land*, *reclaimed land* and *the transition zone between polders and higher inland tertiary area*. As no DEM files of the historic landscape are available, it was necessary to make an approach on the topography as it was at that time. This was realized by using the present DEM combined with the known landscape forming processes in each of the specific land types (e.g. subsidence of peat, inversion of topography at creek deposits).

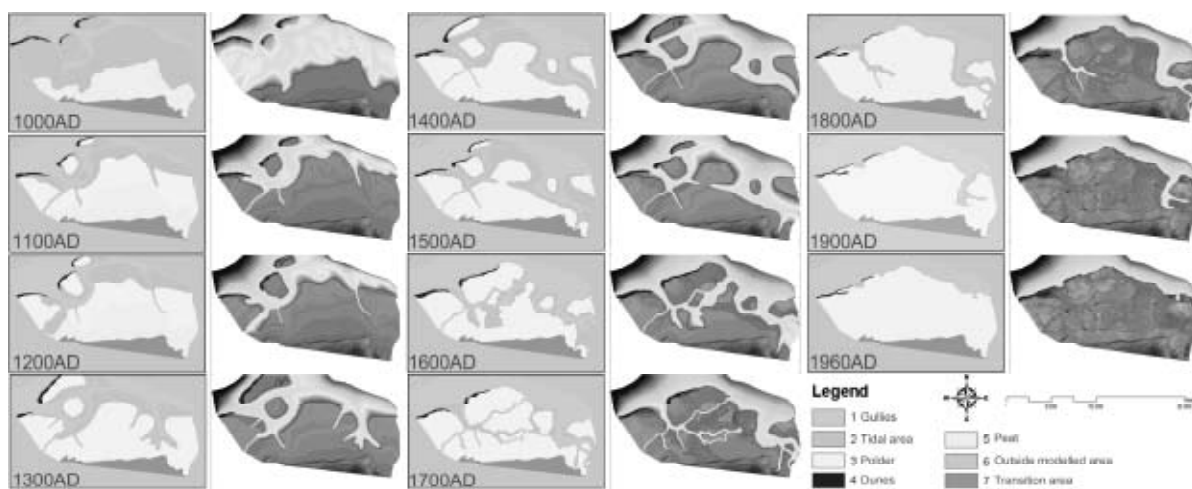


Figure 1. Historical upper boundary conditions: types of land at the surface (left) and DEM (right) from +6 to -8 mTAW (= around +4 to -6 m MSL).

The combination of the reconstructions maps of the land types, the historical topography reconstruction and the present day upper boundary conditions leads to a set of **historical upper boundary conditions** (recharge, drainage and rivers).

Sea level variation

When simulating the groundwater flow over longer periods of time, sea level rise is an important factor to incorporate into the model. Several sea level reconstructions that go back till the year 1000 were analyzed and the model of van Kemp et al. (2011) was chosen as the most suitable one.

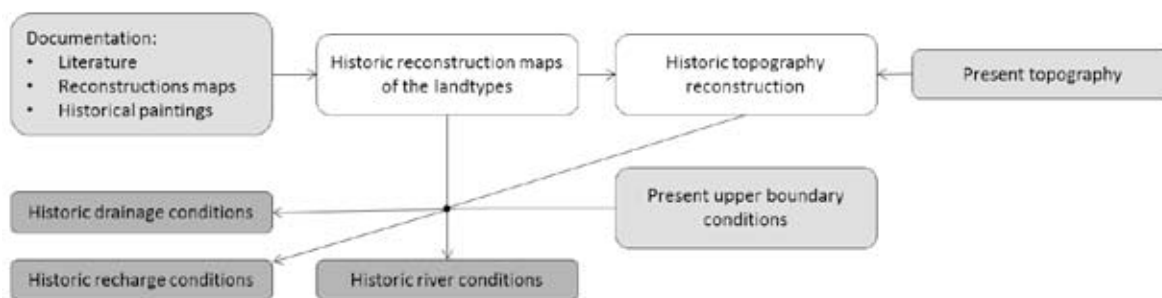


Figure 2. Methodology to derive historical boundary conditions. Light grey: available input, white: intermediate steps, dark grey: output of the historic boundary conditions.

RESULTS

The combination of the discretization of the hydrogeological setting of the area, the historical upper boundary conditions and sea level variation resulted in a simulated historical evolution of the fresh-salt water distribution in a dynamic coastal environment over the past millennium. However, these results are not discussed within this paper, which has its focus on the construction of the model. More information on the results can be found in Vandeveldel et al. 2012.

CONCLUSIONS

A model was constructed of the fresh-salt water distribution in the past millennium in a highly dynamic coastal groundwater system. The transboundary nature of the study area made a correlation of the different available datasets a necessity. Furthermore, a method to derive historical upper boundary conditions was presented. This method relied on the reconstruction of land maps where a subdivision into six types of land was made. Each type of land shows its specific hydrogeological characteristics responsible for its historical evolution of the fresh-salt water distribution.

ACKNOWLEDGEMENTS

This study was supervised by the Flemish Environmental Agency (VMM, Belgium) and the Province of Zeeland (the Netherlands) within the framework of ScaldWIN, a European project for a better quality of surface and groundwater bodies in the Scheldt River Basin.

REFERENCES

- Brand, K.J.J (1993). De ontwikkeling van het polderlandschap in de Vier Ambachten en omringend gebied, in: A.M.J. de Kraker, H. van Royen en Marc E.E. De Smet (red.) 'Over den Vier Ambachten' 750 jaar Keure 500 jaar Graaf Jansdijk (Kloosterzande), pg. 41-61.
- Kemp, A.C., Horton, B.P., Donnelly J.P., Mann M.E., Vermeer M., & Rahmstorf, S. (2011). Climate related sea-level variations over the past two millennia. PNAS., vol 108, no. 2, pg. 11017-11022.
- Vandeveldel, D., Kaland, L., Lermytte, J., Lebbe, L., Oude Essink, G.H.P., Vandenbohede, A., Janssen, G., Claus, J., D'Hondt, D., Thomas, P. (2012). Modelling the historic evolution of the fresh-salt water distribution in a Dutch-Flemish transboundary aquifer. 22nd Saltwater Intrusion Meeting (SWIM22). Armação dos Búzios, Rio de Janeiro, Brazil.
- Wilderom, M.H. (1973). Tussen Afsluitdam en Deltadijken: IV Zeeuwsch Vlaanderen. C.C. Drukkerij G.W. den Boer, Middelburg. ISBN 90 70027 41 0, 567p.
- Contact Information:** Claus Jasper, Ghent University, department of Geology and Soil science, Krijgslaan 281 (S8), B9000 Ghent, Belgium, Email: jasper.claus@ugent.be

Towards groundwater security in coastal East Africa: initiating a regional research network and integrated hydrogeologic, climatic & socio-economic observatories in coastal aquifers of the Comoros Islands, Kenya and Tanzania

Jean-Christophe Comte¹, Joy Obando², Rachel Cassidy¹, Olivier Banton³, Kassim Ibrahim⁴, Jean-Lambert Join⁵, Mary Makokha², Isaac Marobhe⁶, Simon Melchioly⁶, Ibrahimu Mjemah⁷, Ibrahim Mohamed⁴, Beatrice Mwege², Nicholas Robins¹, Halimu Shauri⁸ and Hamidou Soule⁴

¹Groundwater Research Group, Queen's University Belfast, Belfast, United Kingdom

²Department of Geography, Kenyatta University, Nairobi, Kenya

³Laboratory of Hydrogeology, University of Avignon, Avignon, France

⁴Faculty of Sciences, University of the Comoros Islands, Moroni, Comoros

⁵Laboratory Geosciences Reunion, University of Reunion Island, Saint Denis, France

⁶Department of Geology, University of Dar Es Salaam, Dar Es Salaam, Tanzania

⁷Department of Physical Sciences, Sokoine University of Agriculture, Morogoro, Tanzania

⁸Department of Social Sciences, Pwani University, Kilifi, Kenya

ABSTRACT

African coastal regions are expected to experience the highest rates of population growth in coming decades. Fresh groundwater resources in the coastal zone of East Africa (EA) are highly vulnerable to seawater intrusion. Increasing water demand is leading to unsustainable and ill-planned well drilling and abstraction. Wells supplying domestic, industrial and agricultural needs are or have become, in many areas, too saline for use. Climate change, including weather changes and sea level rise, is expected to exacerbate this problem. The multiplicity of physical, demographic and socio-economic driving factors makes this a very challenging issue for management. At present the state and probable evolution of coastal aquifers in EA are not well documented. The UPGro project 'Towards groundwater security in coastal East Africa' brings together teams from Kenya, Tanzania, Comoros Islands and Europe to address this knowledge gap. An integrative multidisciplinary approach, combining the expertise of hydrogeologists, hydrologists and social scientists, is investigating selected sites along the coastal zone in each country. Hydrogeologic observatories have been established in different geologic and climatic settings representative of the coastal EA region, where focussed research will identify the current status of groundwater and identify future threats based on projected demographic and climate change scenarios. Researchers are also engaging with end users as well as local community and stakeholder groups in each area in order to understanding the issues most affecting the communities and searching sustainable strategies for addressing these.

Contact Information: Jean-Christophe Comte, Queen's University Belfast - Groundwater Research Group, School of Planning Architecture and Civil Engineering, Stranmillis Road, Belfast, BT9 5AG, Northern Ireland (UK), Phone: +4428 9097 5633, Email: j.comte@qub.ac.uk

Geophysical investigation of a managed freshwater lens on the North Sea island of Langeoog

Stephan Costabel¹, Ursula Noell¹, Thomas Günther², Georg Houben¹, Wolfgang Voß¹, Bernhard Siemon¹

¹Federal Institute for Geosciences and Natural Resources (BGR), Hannover, Germany

²Leibniz Institute for Applied Geophysics (LIAG), Hannover, Germany

ABSTRACT

A case study is presented that demonstrates the benefit of combining different geophysical methods, in particular electromagnetic methods and the relatively new method of magnetic resonance sounding. The survey on the island of Langeoog shows that geophysics can reliably provide lithological characterization of the subsurface and estimates of groundwater salinity.

INTRODUCTION

Within the project Freshwater Lens Investigation (FLIN) of the German Federal Institute for Geosciences and Natural Resources (BGR), the freshwater lens on the North Sea island of Langeoog was investigated. Besides geochemical and hydrogeological methods (Houben et al. 2014), different geophysical techniques were applied: Frequency-domain helicopter-borne electromagnetics (HEM, e.g. Siemon et al. 2009), transient electromagnetics (TEM, e.g. Fitterman and Stewart 1986), electrical resistivity tomography (ERT, e.g. Ernstson and Kirsch 2006), and magnetic resonance sounding (MRS, e.g. Yaramanci and Müller-Petke 2009). While the first three methods provide the resistivity (ρ) distribution in the subsurface, the latter measures the water content (Φ_{MRS}) directly and is sensitive to pore size as it is based on the nuclear magnetic resonance of the proton spins in the groundwater molecules. The NMR relaxation time T_2^* increases with increasing pore size of the material investigated. Using this additional information, we expected a benefit regarding the lithological interpretation at places where boreholes are not available.

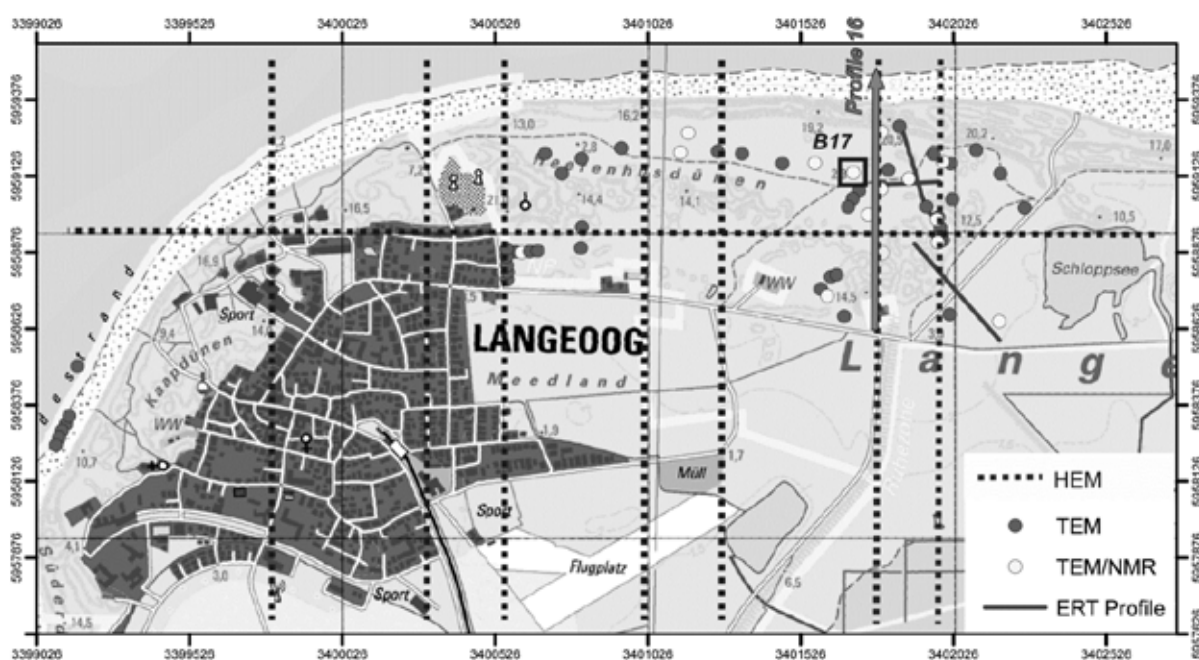


Figure 1: Map with locations of geophysical measurements on the island of Langeoog.

The interpretation of geophysical ρ measurements alone is naturally non-unique, because ρ is affected by both groundwater mineralization and lithology. On the other hand, the sensitivity of MRS to the ρ distribution in the subsurface is very low; so it cannot be used as stand-alone method regarding saltwater intrusion problems. The objectives of the survey on the island of Langeoog were 1) the localization and characterization of the freshwater-saltwater boundary, 2) the identification of clay layers inside the lens, 3) the prediction of the groundwater salinity over depth. Figure 1 shows an overview of the area of investigation and the measurement locations.

FRESHWATER-SALTWATER INTERFACE

The HEM method provides a regional overview of the freshwater/saltwater conditions (Siemon et al. 2014). Additional TEM measurements were conducted in the area of the managed freshwater lens to gain detailed information. Figure 2 compares the results of HEM and TEM along an S-N profile (Profile 16, see also Figure 1). Saltwater-bearing sediments ($\rho < 1.5 \Omega\text{m}$) are found in a depth of 40 to 50 m. In the middle of the lens, the freshwater ($\rho = 30\text{-}200 \Omega\text{m}$) extends down to a depth of 30 m, while at the edges, as expected, its thickness decreases. Interestingly, a transition zone between freshwater and saltwater with $\rho = 5\text{-}20 \Omega\text{m}$ and with a thickness of 10 to 20 m was detected. As the lithology interpretation from drillings and MRS measurements indicates, this zone cannot be related to lithology changes (dashed lines in Figure 2). In the North of the profile, a thin layer with $\rho = 1\text{-}3 \Omega\text{m}$ was found at a depth of 10 to 15 m. Compared to HEM, the TEM results reveal this layer with a similar resistivity, but 5 m deeper. We preliminary interpret this layer as saltwater on top of a thin clay layer, probably a relic of an ancient flooding. The clay layer itself could not be detected by the EM methods.

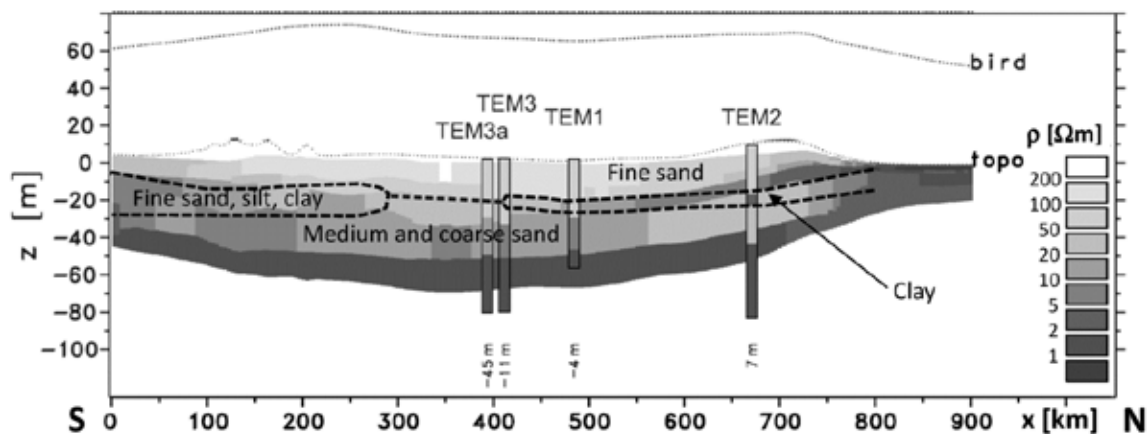


Figure 2: Comparison of HEM and TEM (loop size: 50 m) results, lithological interpretation from drillings and MRS measurements on Profile 16.

LITHOLOGICAL CHARACTERIZATION

With small TEM loops (25 m square), indications for thin clay layers above the saltwater were found at a depth of 20 to 30 m with a resistivity of about 7 to 10 Ωm (not shown), while larger TEM loops did not resolve these layers (Figure 2). Using ERT, we tried to track their lateral extent, but the bad coupling of the electrodes with the dry dune sand caused very inaccurate measurements and ambiguous results. Besides borehole interpretation, which is sparsely available on the island of Langeoog, also MRS measurements allowed for a lithological characterization to some extent. Figure 3 shows an example for a TEM (Figure 3a) and an MRS measurement (Figure 3b and c) at borehole B17 (see also Figure 1), both

measured with a square loop of 50 m side length. As at B17 no lithology interpretation was available, the lithological information over depth depicted in Figure 3d was taken from another borehole at a distance of about 150 m. The well screen of B17 ranges from 35 to 65m depth and so we took the opportunity to measure the groundwater salinity in the transition zone directly in this borehole (Figure 3e). We note that TEM does not reveal the clay layer at 22 to 26 m depth, whereas Φ_{MRS} is clearly underestimated in this region. This is because clay and silt exhibit T_2^* times smaller than the instrumental dead time. Consequently, the MRS signal from such fine-grained material is not detected completely and the corresponding Φ_{MRS} is underestimated. The differentiation between fine and coarse sand is possible due to different T_2^* times (fine sand: 100 to 250 ms and medium to coarse sand: 350 to 500 ms).

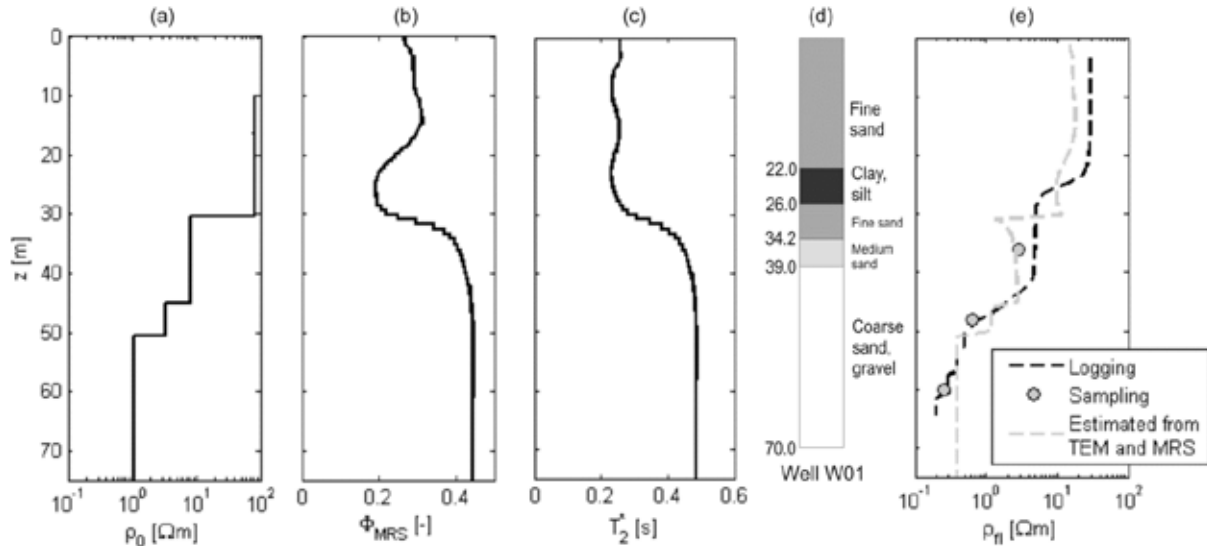


Figure 3: Results of a TEM and an MRS measurement at borehole B17: (a) resistivity distribution from TEM, (b) MRS water content distribution and (c) relaxation time distribution compared to (d) lithology interpretation from drilling, (e) estimated groundwater resistivity distribution compared to reference from salinity logging and sampling in B17.

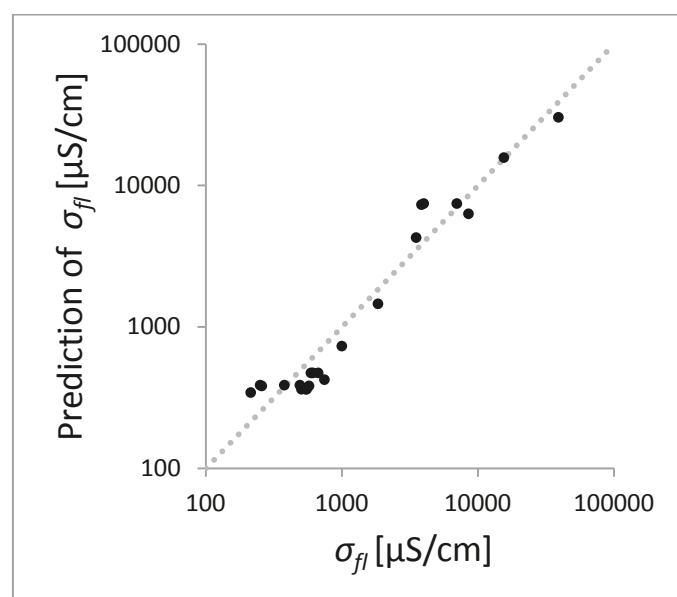


Figure 4: Comparison of predicted and measured electrical conductivity of groundwater.

ESTIMATING THE ELECTRICAL CONDUCTIVITY OF GROUNDWATER

Using the ρ distribution from TEM and the Φ_{MRS} distribution from MRS, the groundwater resistivity ρ_{fl} (and its inverse, the electrical conductivity σ_{fl} as a measure of groundwater salinity) was estimated using the equation of Archie (1942):

$$\rho_{fl} = a\rho\Phi_{MRS}^n$$

For our estimations, the Archie exponent n was set to 1.3 (literature value for unconsolidated sand) and the linear factor a was set to 1. Figure 3e shows the estimated ρ_{fl} resulting from the TEM/MRS data example in Figure 3a to c compared to ρ_{fl} as measured in B17. The estimated ρ_{fl} distribution is in good agreement with the reference. In Figure 4, we compare further σ_{fl} estimates from TEM/MRS measurements on the island with reference values from groundwater sampling. In total, at 22 sites of investigation both groundwater samples and TEM data were available. At some of these sites (8 points in Figure 4), MRS could not be applied due to intense EM noise. In such cases, we used the MRS water content of the nearest MRS measurement for estimation. The good correlation in Figure 4 shows that groundwater salinity can reliably and non-invasively be estimated by combining EM and MRS measurements.

CONCLUSIONS

The geophysical case study on the island of Langeoog demonstrates the successful combination of EM and MRS measurements, which provides additional information on both lithology and groundwater salinity. This information will be included in a hydrogeological model and will support the hydrodynamic modelling of the freshwater lens in the future.

REFERENCES

Archie G.E. 1942. The electrical resistivity log as an aid in determining some reservoir characteristics. Transactions of the American Institute of Mining, Metallurgical, and Petroleum Engineers 146: 54-62.

Ernstson, K., and R. Kirsch. 2006. Geoelectric methods In Groundwater Geophysics – A Tool for Hydrogeology, ed R. Kirsch, 86-108. Springer.

Fitterman, D.V., and M.T. Stewart. 1986. Transient electromagnetic sounding for groundwater. Geophysics 51: 995-1005.

Houben G. J., P. Koeniger, and J. Sültenfuß. 2014. Freshwater lenses as archives for climate history - insights from depth-specific age dating and stable water isotope analysis, Langeoog Island, Germany. In Proceedings of the 23rd Salt Water Intrusion Meeting, Husum, Germany.

Siemon, B., A.V. Christiansen, and E. Auken. 2009. A review of helicopter-borne electromagnetic methods for groundwater exploration. Near Surface Geophysics 7: 629-646.

Siemon, B., W. Voß, J. Elbracht, N. Deus, and H. Wiederhold. 2014. Airborne clay mapping at the East Frisian coast. In Proceedings of the 23rd Salt Water Intrusion Meeting, Husum, Germany.

Yaramanci, U., and M. Müller-Petke. 2009. Surface nuclear magnetic resonance - A unique tool for hydrogeophysics. The leading edge 28, no. 10: 1240-1247.

Contact Information: Stephan Costabel, Federal Institute for Geosciences and Natural Resources (BGR), Department Groundwater and Soil Science, Wilhelmstr. 25-30, 13593 Berlin, Germany, Phone: +49-30-36993391, Fax: +49-30-36993100, Email: stephan.costabel@bgr.de.

Origin of groundwater salinity and implications for groundwater management of the Emborê Aquifer, Rio de Janeiro State, Brazil

Z. Chrispim¹, M.G. Alves¹, M.T. Condesso de Melo², G.C. Silva Jr.³

¹ Univ. Estadual do Norte Fluminense Darcy Ribeiro, Campos dos Goytacazes, Brasil.

² CVRM, Instituto Superior Técnico, Universidade Técnica de Lisboa, Lisbon, Portugal.

³ Universidade Federal do Rio de Janeiro, Rio de Janeiro, Brasil.

ABSTRACT

The population of northern coastal area of Rio de Janeiro State (Brazil) relies on coastal groundwater resources as its main source of water supply. However, the increasing demand for groundwater resources in the last decade has increased the risk of aquifers' overexploitation and salinization. The Emborê aquifer is the most important aquifer in Rio de Janeiro State and the main source of freshwater for the region but still very little investigated. The aim of the present study is to investigate the water quality of the aquifer, to determine the origins of groundwater salinity and to identify early warning signs of seawater intrusion in order to prevent it. A detailed hydrochemical (major and some minor elements) and isotopic (²H and ¹⁸O) study of groundwater quality was carried out and allowed for: (1) the identification of distinct areas within the aquifer with different hydrochemical properties; (2) the identification of main patterns of hydrochemical evolution; and, (3) the identification of principal geochemical processes occurring in the aquifer. Regionally, the groundwater presents distinct geochemical signatures depending on its stratigraphic setting within the aquifer, the proximity to the coastline and the presence/ absence of palaeochannels. Distinct salinity distribution patterns were identified within the Emborê aquifer but seem to reflect the impact of local phenomena more than modern saline intrusion. Results indicate that groundwater infiltration and movement occurred without pronounced evaporative effects and that increasing salinities in the Emborê aquifer are mostly related to mixing with higher salinity waters flowing in interlayered aquifer levels with lower permeabilities and longer residence times.

INTRODUCTION

Brazil has large reserves of oil and groundwater resources in sedimentary basins along the coast. The Campos sedimentary basin is located in the northeast part of the Rio de Janeiro State, close to the delta of Paraíba do Sul river, with a total area of 115,000 km² (and an area of just 2000 km² onshore). Its oil reserves are one of the most important in the Southern Atlantic domain (Contreras, 2011). The Emborê Formation, which is part of the Campos sedimentary basin, is indeed the most important aquifer in Rio de Janeiro State and the main source of fresh water resources for a region, which includes the municipalities of Campos dos Goytacazes, São Francisco de Itabapoana, São João da Barra and Quissamã (Barreto et al., 2001). Other aquifer formations in the region include the Barreiras Formation and the Fluvial-Deltaic and Alluvial-Lacustrine Formations (Figure 1).

The increasing demand for groundwater resources in this region of the Rio de Janeiro State has increased the risk of aquifers' overexploitation and groundwater quality deterioration. The main aim of the present study is then to investigate the water quality of the Emborê

aquifer, to determine the origins of groundwater salinity and to identify early warning signs of seawater intrusion in order to prevent it.

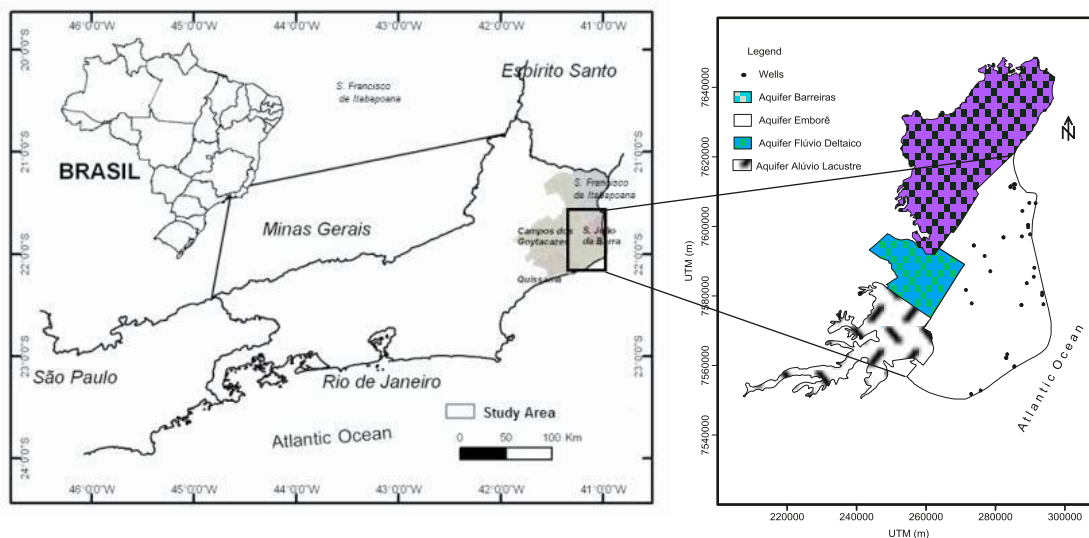


Figure 1. Map of the study area indicating the main aquifers in Campos sedimentary basin and the location of groundwater sampling wells in Emborê aquifer.

HYDROGEOLOGY

The depositional conditions varied within the Campos basin and in the Emborê Formation, sediments of marine influence alternate with predominant detrital infilling of continental origin. The Emborê Formation is composed of poorly calibrated sandstone deposits with conglomeratic and fossiliferous bands, sandy coquinas, calcarenites and organic sandy clays with traces of pyrite and the total thicknesses may vary from 100 to 2,000 m thick.

From the hydrogeological point of view, the Emborê Formation is a multilayer confined aquifer that underlies Quaternary fluvial-deltaic and alluvial-lacustrine aquifer formations. Permeability values change in depth and spatially according to the geology and the impact of local tectonics. Groundwater recharge occurs mainly through preferential flow along palaeochannels and from Paraíba do Sul River. Average transmissivity values for the aquifer vary from 150 to 250 m²/day and storage coefficient values are typical of a confined aquifer (10⁻⁵ to 10⁻⁴). Most boreholes drilled in the aquifer for water supply are at most 250 m deep.

METHODS

A detailed hydrogeochemical study was carried out in the Emborê aquifer to characterize the groundwater geochemical evolution. 28 groundwater samples were collected for major and some minor elements analysis and isotopic composition determination (²H and ¹⁸O). Field parameters (pH, temperature, electrical conductivity) were also determined.

RESULTS AND DISCUSSION

Regionally, the groundwater presents two distinct hydrochemical facies depending on its stratigraphic setting within the aquifer, the proximity to the coastline and the presence/

absence of palaeochannels where preferential flows may occur (Figure 2). In the southern portion of the study area, all the samples collected correspond to calcium-bicarbonate type groundwaters with electrical conductivity (EC) values that range from 307-640 $\mu\text{S}/\text{cm}$ and chloride concentrations varying from 10 to 102 mg/L. In the northern part, EC is generally higher than 640 $\mu\text{S}/\text{cm}$, reaching a maximum value of 1627 $\mu\text{S}/\text{cm}$, and groundwaters are mainly of sodium-chloride or sodium-bicarbonate type. The lower salinity values observed and the predominance of calcium-bicarbonate type waters in the southern most part is probably due to the mixing with the continental freshwaters recharged along the palaeochannels.

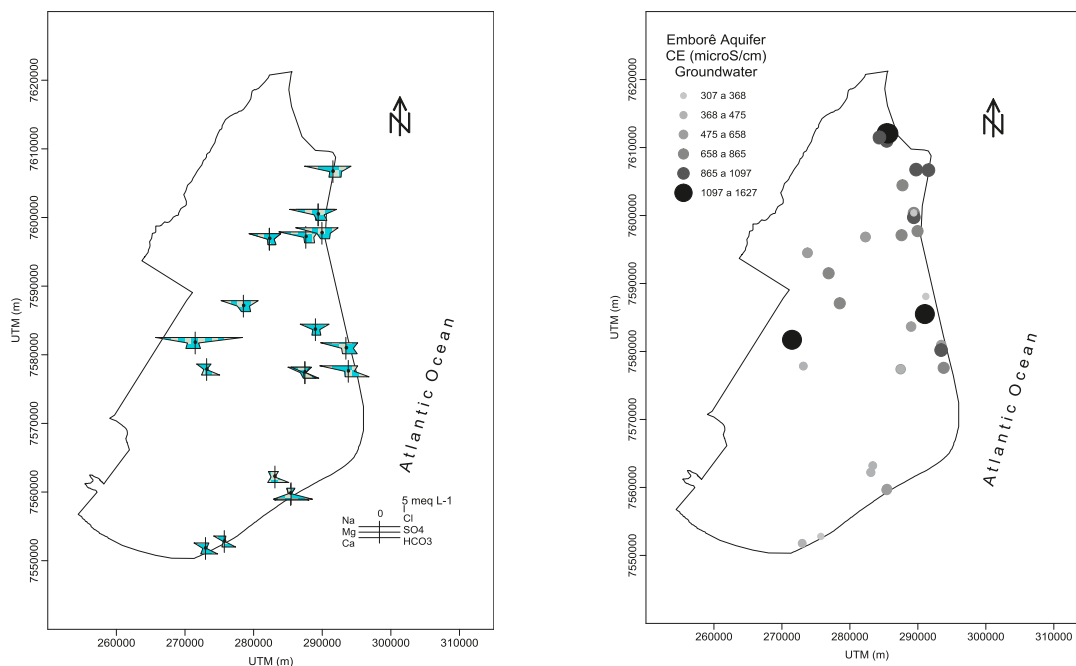


Figure 2. Distribution of the principal hydrochemical facies and electrical conductivity in the Emborê aquifer.

Ionic molar ratios (Cl/Br , Na/Cl and Na/Ca) were calculated to infer salinization or freshening patterns of groundwater evolution (Figure 3). Groundwater Br/Cl ratios align with seawater mixing line regardless of groundwater salinity and Na/Cl and Na/Ca indicate an enrichment of Na to Ca or Cl, indicating groundwater freshening patterns and discarding brine dissolution.

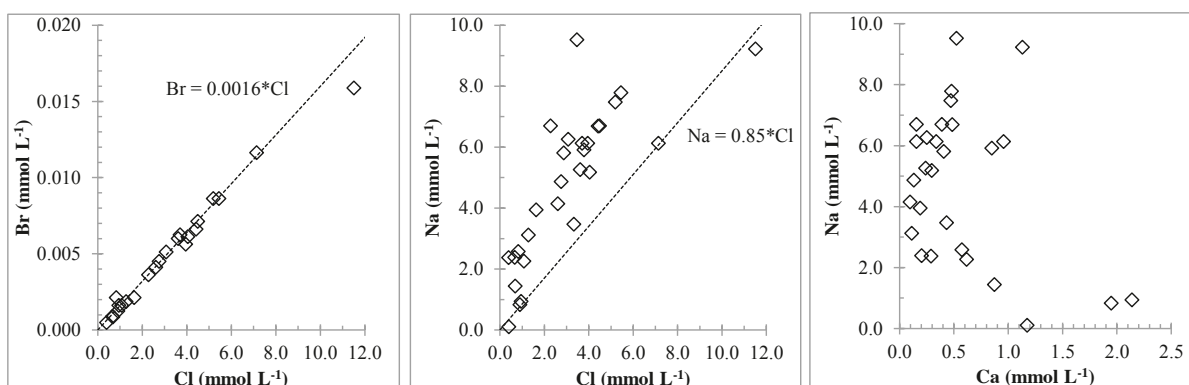


Figure 3. Calculation of some ionic ratios (Br/Cl , Na/Cl and Na/Ca) to infer salinization or freshening patterns of groundwater evolution.

Stable isotopic composition of groundwaters in the Emborê aquifer (oxygen-18 and deuterium) plot on the Local Meteoric Water Line (LMWL) discarding the hypothesis that some of the higher salinity groundwaters could be related to pronounced evaporative effects during recharge processes (Figure 4). Most groundwaters of calcium-bicarbonate facies and showing lower salinities are more depleted in ¹⁸O and ²H when compared to the rest of the aquifer.

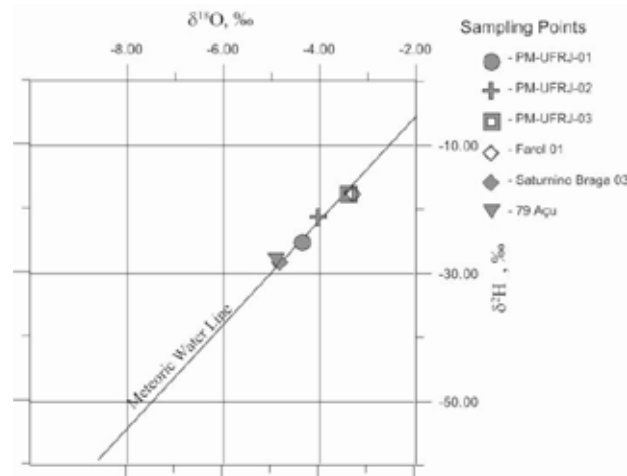


Figure 4. Relationship between $\delta^2\text{H}$ and $\delta^{18}\text{O}$ contents in groundwater samples.

CONCLUSIONS

The results show that increasing salinities in the north and central part of the aquifer are related to mixing processes with seawater (either modern or old seawater trapped in the sediments) but patterns of groundwater quality still indicate predominant freshening processes. Influence of evaporative effects during recharge or brine dissolution in the increasing salinities were discarded based on the isotopic composition and ionic molar ratios.

REFERENCES

- Barreto, A.B.C.; Monsore, A.L.M.; Leal, A.S. & Pimentel, J. 2001. Caracterização Hidrogeológica do Estado do Rio de Janeiro, Brasília/ CPRM. Mapa. CD-ROM. (Estudo Geoambiental do Estado do Rio de Janeiro).
- Contreras, J. 2011. Seismo-stratigraphy and numerical basin modeling of the southern Brazilian continental margin (Campos, Santos, and Pelotas basins). Inaugural Dissertation. Universität Heidelberg, 171 pp.

ACKNOWLEDGEMENTS

The authors would like to thank the Convênio Brasil-Portugal - FCT/CAPES – Projeto 344/13 and to the Emborê Project (Petrobrás).

Contact Information: Zélia Chrispim, Laboratório de Engenharia Civil, Universidade Estadual do Norte Fluminense Darcy Ribeiro (UENF), Av. Alberto Lamego, 2000, Parque Califórnia, Campos dos Goytacazes, RJ/Brasil. Phone: (22) 27397376, E-mail: zeliachrispim@terra.com.br.

Freshwater Intrusion: Return of Meteoric Groundwater back to the Continent, San Diego, California, USA

Wesley R. Danskin¹, Bert J. Stolp², Geoff Cromwell¹, Robert Anders¹, and Larry Feinson³

¹USGS, California Water Science Center, San Diego, CA, USA

²USGS, Utah Water Science Center, West Valley City, UT, USA

³USGS, New Jersey Water Science Center, Lawrenceville, NJ, USA

ABSTRACT

Water-level and water-quality data from multiple-depth monitoring-well sites, installed along the San Diego Bay, California, USA, indicate that fresh groundwater is moving through a sedimentary aquifer beneath the continental shelf, back toward production wells near the coastline. Each of these 12 well sites includes 4-6 separate piezometers, ranging in depth from 20 to 500 meters. Water-quality data from these piezometers show that part of the sedimentary aquifer is composed of a shallow highly saline zone about 60 meters thick, which is underlain by a freshwater zone about 200 meters thick, which is underlain by dilute seawater to a depth of more than 500 meters. Isotopic analyses indicate that the fresh groundwater was recharged during the last glacial period, likely filling the dewatered coastal sediment with relatively fresh groundwater, and then being over-topped by rising seawater. Additional lithologic and paleontological data, collected during installation of the well sites, were used to develop a three-dimensional geologic framework model of the coastal area. Ongoing work involves incorporating the geologic model and geochemical data in a density-dependent cross-sectional flow model to test concepts of groundwater flow, from the continent to the ocean, and then back onto the continent.

INTRODUCTION

The coastal area of San Diego, California, USA, has modest rainfall, runoff, and recharge. The Mediterranean climate provides an idyllic setting for residents and visitors, but water managers are challenged by the scant local water supplies and increasing population (fig. 1). Like other coastal areas throughout the world where the presence of saline groundwater reduces the supply of drinking water, future development of the local groundwater resources in the San Diego area of southern California is limited by the presence of saline-to-brackish groundwater in some parts of the coastal aquifer.

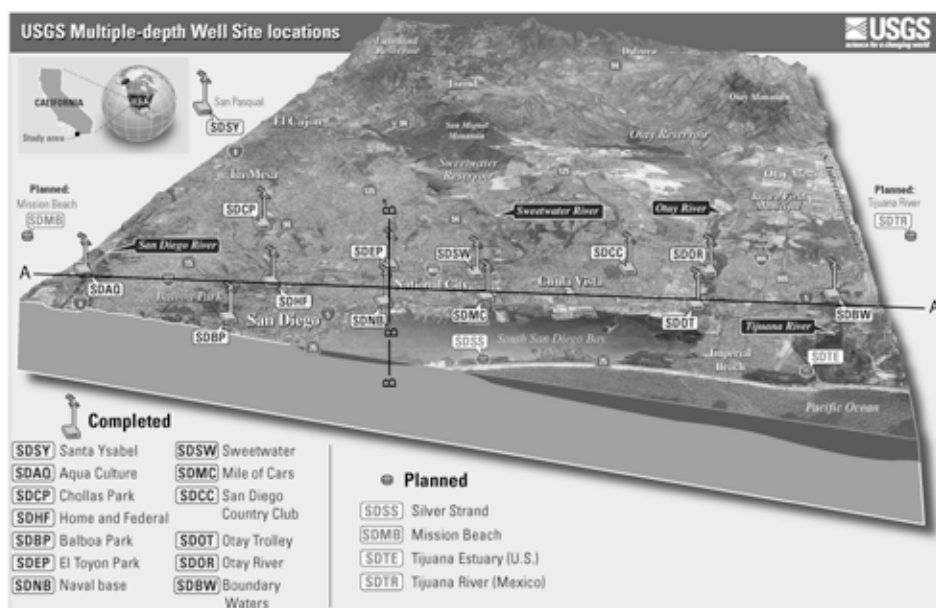


Figure 1. Study area of coastal San Diego County, California, USA.

METHODS

Local water agencies and the United States Geological Survey (USGS) are using a combination of techniques to provide the necessary understanding of the geology, geochemistry, and hydrology to develop the scant fresh, and much more abundant brackish, groundwater resources in the coastal San Diego area. The techniques include installation of twelve 500-meter-deep, multiple-depth, monitoring-well sites, each with 4 to 6 piezometers equipped with pressure-recording transducers (fig. 1). During installation of the well sites, drill cuttings were collected and analyzed for color, grain-size, provenance, and paleontological indicators of age and depositional environment. Geophysical logs were obtained to identify formations and depths of saline water. These data were combined to create a three-dimensional geologic framework model (Danskin 2012; fig. 2).

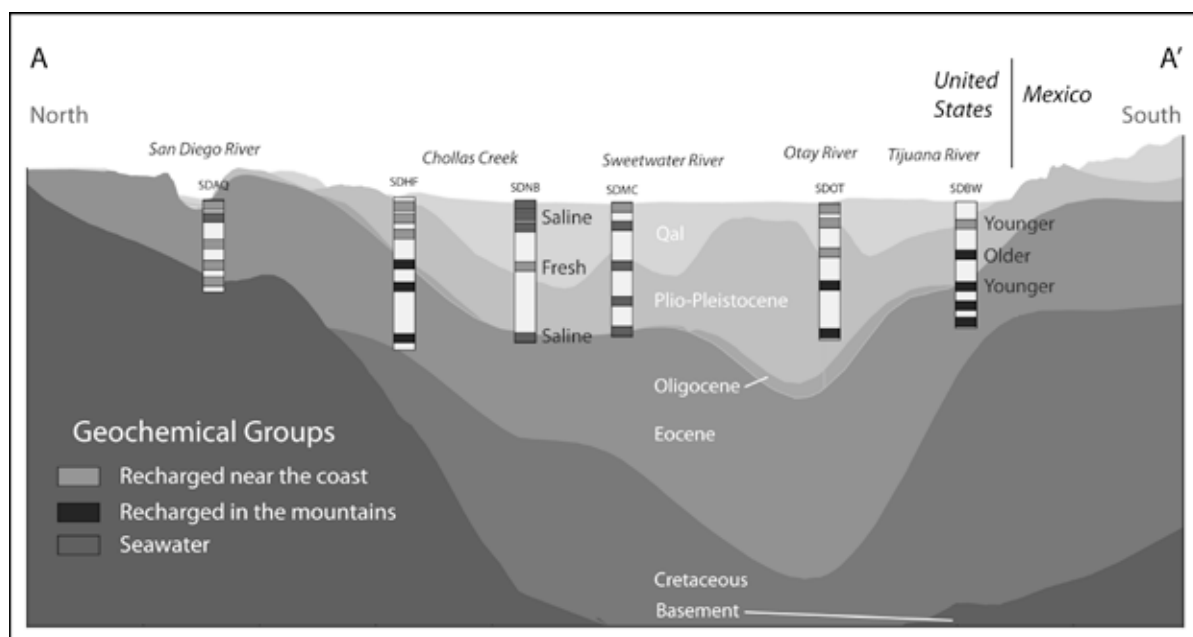


Figure 2. Section A-A' showing geologic formations and geochemical groups.

Water-quality samples collected from the depth-dependent piezometers were analyzed for a variety of chemical constituents including major and minor ions, trace elements, stable isotopes of hydrogen, oxygen, and strontium, and radioactive isotopes of tritium and carbon (Anders et al. 2013).

A suite of numerical models were used to integrate data and to test ideas about the geologic structure, arrangement of formations, location and quantity of recharge, quantity and flowpaths of groundwater, interaction of surface water and groundwater, configuration of fresh and saline water, and possible areas to extract additional fresh or brackish groundwater. These numerical models include a regional water-budget model using the BCM method (Flint et al. 2012), a regional groundwater flow model using the USGS MODFLOW code, and a coastal density-dependent groundwater flow model using the USGS SUTRA code.

RESULTS

Water-quality data collected from the twelve multiple-depth monitoring-well sites (fig. 1) indicate that most groundwater along the San Diego coast is brackish, with dissolved-solids concentrations ranging from 1,200 to 2,000 milligrams per liter (mg/L). Some coastal groundwater, however, has dissolved-solids concentrations as low as 700 mg/L. Indeed,

production wells near monitoring-well site SDEP have been producing fresh groundwater for more than 60 years.

The northwest-to-southeast trending section A-A' (fig. 1) shows the spatial distribution of three geochemical groups representing groundwater recharged near the coast, groundwater recharged further east in the mountains, and groundwater intruded with seawater (fig. 2). Ongoing work involves comparing the geologic framework model with the geochemical groups in order to distinguish different groundwater flowpaths.

Depth-dependent water-quality data collected from well site SDNB identifies three zones: a shallow highly saline zone about 60 meters thick, underlain by a freshwater zone about 200 meters thick, underlain by dilute seawater to a depth of more than 500 meters (Cronquist et al. 2011; fig. 2). Understanding how these vertical zones were formed is an important part of being able to manage coastal groundwater, including continued freshwater pumpage near well site SDEP and increased brackish pumpage for a desalination plant located near well site SDSW (fig. 1).

Density-dependent groundwater flow along the northeast-to-southwest trending section B'-B'' (fig. 1) was simulated using a cross-sectional SUTRA model (fig. 3). The initial simulations of the freshwater/seawater interface seemed plausible and matched the salinity data at well sites SDEP and SDNB. But the shallow saline zone (fig. 2) could not be generated even with a wide range of hydraulic characteristics. For these simulations, all boundary conditions for the model were fixed at present elevations and concentrations.

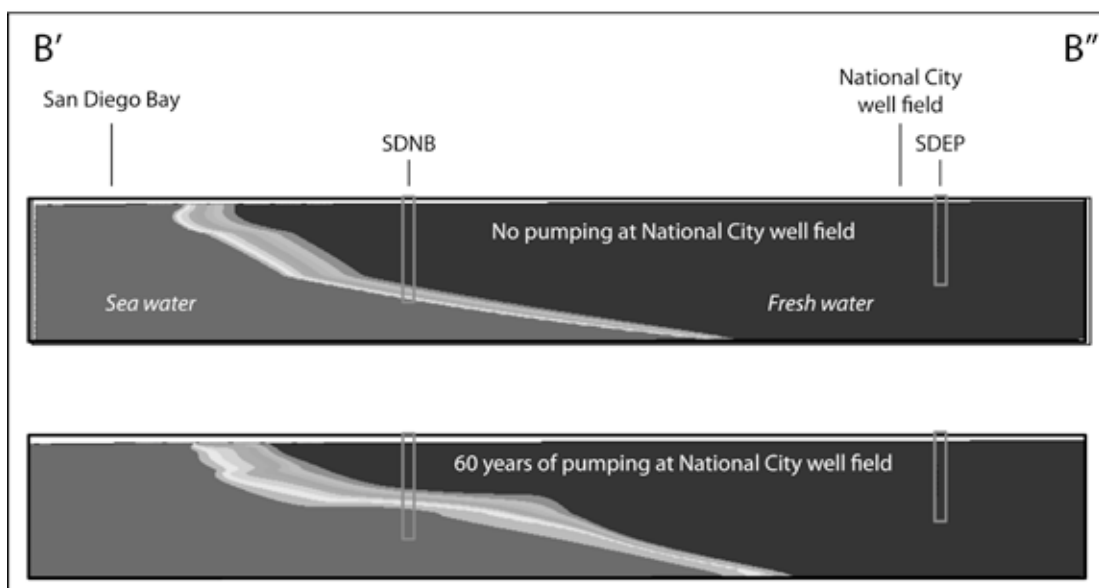


Figure 3. Section B'-B'' showing initial results of density-dependent model simulations.

DISCUSSION

Based on these data and simulations, the conceptual model of the San Diego coastal aquifer was revised to include the transient behavior of the ocean, in particular: (1) during the last glacial maximum about 20,000 years before present (ybp), sea level declined about 130 m; (2) the upper 100+ m of coastal sediment was drained of saline water and re-filled with fresh water; (3) the sea level rose to overtop the fresh groundwater, thereby creating the observed three-layer zone of saline, fresh, and saline groundwater found at well site SDNB. The

SUTRA model of section B-B'' is being used to test this conceptualization by including a variable pressure boundary condition along the seawater edge.

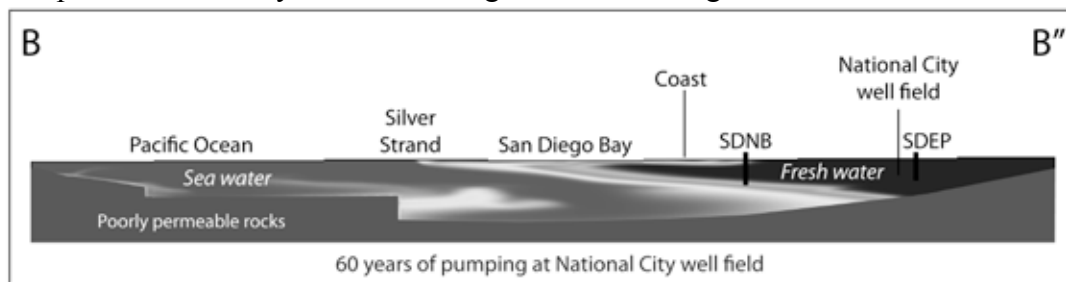


Figure 4. Section B-B'' showing results from simulating a variable sea-level boundary.

The revised conceptual model seems plausible, matches conditions found at well site SDNB (figs. 2 and 4), and is similar to other coastal parts of the world (Post et al. 2013). It is not understood, however, why other coastal well sites in San Diego do not demonstrate such a clear three-zone system. Possibly, the incised river drainages near these well sites contribute to greater mixing of groundwater when the sea rises. Historical pumping also may have affected present conditions. Well site SDBW has a middle zone with older water (20,000 ybp) than above or below (fig. 2), which may suggest piston flow of groundwater off the coast, then back onto the continent, prompted by the substantial groundwater pumping that occurred in the Tijuana River Valley between 1945 and 1970.

Future work includes additional simulations of fresh and saline water in order to test these hypotheses. To provide data for the simulations, fresh groundwater under San Diego Bay is being mapped via salinity, temperature, and electromagnetic techniques.

REFERENCES

- Anders, R., G.O. Mendez, K. Futa, and W.R. Danskin, 2013, A geochemical approach to determine sources and movement of saline groundwater in a coastal aquifer. *Ground Water*. doi: 10.1111/gwat.12108, 13 p.
- Cronquist, D.A., S.D. Banister, and R. Anders, 2011, Delineating zones of seawater intrusion in a coastal Southern California aquifer: H31G-1249, AGU fall meeting, San Francisco, California, December 5-9, 2011 [poster].
- Danskin, W.R., 2012, Gaining the necessary geologic, hydrologic and geochemical understanding for additional brackish groundwater development, coastal San Diego, California, United States: 22nd Salt Water Intrusion Meeting (SWIM), Buzios, Brazil, June 17-22, 2012. [ext. abstract].
- Flint, L.E., A.L. Flint, B.J. Stolp, and W.R. Danskin, 2012, A basin-scale approach for assessing water resources in a semiarid environment: San Diego region, California and Mexico, *Hydrol. Earth Syst. Sci.*, 16, 3817-3833, doi:10.5194/hess-16-3817-2012.
- Post, Vincent E.A., J. Groen, H. Kooi, M. Person, S. Ge and W.M. Edmunds, 2013, Offshore fresh groundwater reserves as a global phenomenon: *Nature*, v. 504, p. 71-78. doi:10.1038/nature12858

Brand names are for identification purposes only and do not imply endorsement by the USGS.

Contact Information: Wesley R. Danskin, United States Geological Survey, 4165 Spruance Road, Suite 200, San Diego, CA 92101 USA, Phone: 858-663-6832, Fax: 619-225-6101, Email: wdanskin@usgs.gov

ASTER and WorldView-2 satellite data applications for recognition of salt water intrusion on forest vegetation

Michaela De Giglio¹, Nicolas Greggio², Lorenzo Panciroli¹ and Maurizio Barbarella¹

¹DICAM - Civic, Chemical, Environmental and Materials Engineering Dep., University of Bologna, Italy

²CIRSA – Interdepartmental Research Centre for Environmental Sciences, University of Bologna, Italy

ABSTRACT

The salinization of the coastal aquifers is a worldwide issue affecting many delta areas. The low-lying Ravenna plain (Italy) is strongly drained, highly subsident with the only topography present in dune and paleodune areas. In this context, the underlying phreatic aquifer is completely brackish and salty and the only fresh water lenses are located below the historical pinewoods (paleodune) and along the actual dune belt. Changes in the water salinity are able to induce variations in the leaves properties and vegetation cover, recognizable by surveys carried out in different spectral bands. Furthermore, a comparison between remote sensing satellite images with different resolution, ASTER and Worldview-2, was carried out using the Normalized Difference Vegetation Index (NDVI). Inside the San Vitale pinewood (Ravenna, Italy), different sample areas were selected within the Thermophilic Deciduous Vegetation because it covers more than 80% of the studied pine forest. The NDVI, calculated with traditional bands, identified the same stressed areas shown by both satellite data. Instead, using the new Red Edge band of the Worldview-2 image, a greater correlation between NDVI and groundwater salinity was detected.

INTRODUCTION

The salt water intrusion analysis is mainly carried out through generally time-consuming and relatively expensive ground monitoring campaign (Pu and Landry, 2012). In contrast, satellite data allow periodic monitoring of large areas, although some field work is still necessary for the image validation.

The aim of this work is to identify portions of pinewood affected by groundwater salinization through the multispectral satellite data analysis, with different spatial and spectral resolution. In order to quantify the benefits of both higher spatial and spectral resolution, ASTER and Worldview-2 results were compared.

The association between remote sensing techniques and vegetal biophysical indicators is exploited for the diagnosis and monitoring of threatened habitats (Barton 2012). In particular, several studies have used the NDVI to analyze indirect effects of environmental changes (Aguilar et al. 2012), including those due to processes of salinization (Zhang et al. 2011). Increased water salinity induces changes in chlorophyll concentration and therefore a photosynthesis slowdown (DeLaune et al. 1987). In detail, by measuring the relative difference between responses of chlorophyll and cellular structure in red and near-infrared bands (Peñuelas, 1998), the NDVI analyzes the greenness and productivity (Reed et al. 1994) of the plants.

The study area is San Vitale roman-time pinewoods that have suffered from groundwater salinization for the past several years. The main causes of the widespread salt water intrusion in phreatic aquifers are: natural and anthropogenic land subsidence, low topography, low natural hydraulic gradients and artificial drainage (Antonellini et al. 2008).

The Vegetation map defines two main vegetation type “Thermophilic Deciduous Forest” (below TDF) and “Thermophilic Evergreen Forest” (below TEF) (Regione Emilia Romagna, 1999). Because TDF cover more of the 80% of San Vitale, the study was performed within this vegetation type. The pinewood vegetation has been classified, excluding *Pinus pinea*

species from the classification because they are not able to reproduce inside these natural areas (Piccoli et al., 1991).

METHODS

In this study, satellite images with different spatial and spectral resolution and groundwater salinity data were used. ASTER sensor acquires visible and infrared ranges with a spatial resolution of 15 m while Worldview-2 acquires data with spatial resolution of 2 m and has available in the same range four new bands. Both sets of data were acquired in the May 2011.

In the first step, the NDVI was implemented for both available remote sensed data using the same traditional bands: Red (0.630-0.690 μm) and NIR (0.780-0.860 μm) for ASTER image, Red (0.630-0.690 μm) and NIR1 (0.770-0.895 μm) for Worldview-2 image.

The NDVI was calculated for the same five Areas of Interest (AOIs) in both satellite data (CN1, CN2, CS1, CS2, S). For each AOI of every image, basic statistics of NDVI values were calculated. Consequently, the frequency histograms of AOIs were plotted to explain the data distributions and Skewness and Kurtosis (NIST/SEMATECH 2003) shape factors were obtained to evaluate deviation from the Gaussian trend.

In every image, the threshold of 5% for the AOI with higher NDVI was selected as criteria to compare the vegetation health status. Later, this value was used to quantify the percentages of pixel of the other AOIs corresponding to stressed vegetation that fall below this limit. This statistical analysis allowed for the identification of less green parts of the vegetation compared to the reference area. Therefore, in order to analyze possible advantages of high spatial resolution in respect to the medium resolution in this study, ASTER and Worldview-2 results were compared to verify if the same stressed areas were recognized.

In the second step, with the aim to study the greater spectral resolution contribution of Worldview-2 data, the same procedure with the new bands Red Edge (below RE, 0.705-0.745 μm) and NIR2 (0.860-1.040 μm) in NDVI index was applied.

The validation of these results was made by contemporaneous groundwater salinity measurements.

RESULTS

The main AOIs results are summarized in the Figure 1. The average groundwater salinity ranges between 1 and 7 g/l along an East-West gradient. The heterogeneous pine tree density goes from 6 to 25 individuals/hectare. The average NDVI values obtained by traditional bands (NDVI ASTER, NDVI WV-2) are coherent between the satellite data. For WV-2 image, the NDVI values computed as Red Edge-NIR1 and Red Edge-NIR2 combinations show a different discrimination between AOIs regardless of general different values due to the various bands used (Fig.1a). Considering the relative frequency histograms of the NDVI originated with traditional bands instead, the distribution values shows different behaviors for the two remote sensed data. In particular, for some WV-2 AOI the graph follows a bimodal trend (Fig.1b).

Finally, the AOIs ranking has been done in terms of salinity, pine tree density and both traditional (NDVI ASTER/WV-2) and new NDVI (NDVI WV-2 RE_NIR1/2), after the application of the whole procedure for all calculated NDVI (Fig.1c).

The overlays between groundwater salinity and NDVI results (Fig.2) show the different ability of traditional and new NDVI to recognize the areas stressed by groundwater salinity.

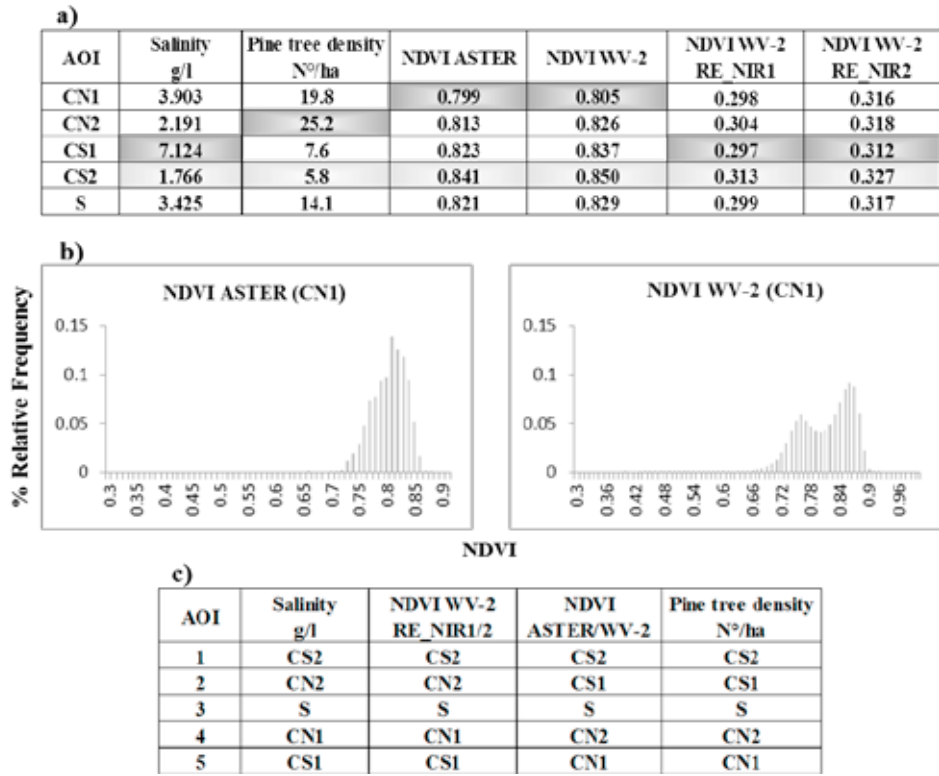


Figure 1.
 a) NDVI analysis results. Light gray color represent healthiest AOIs while dark gray color indicates the more stressed AOIs.
 b) Example of relative frequency histogram, related CN1 AOI, for traditional NDVI distribution values.
 c) AOIs, ordered from the healthiest AOI (1) to the most stressed (5), for each considered parameter.

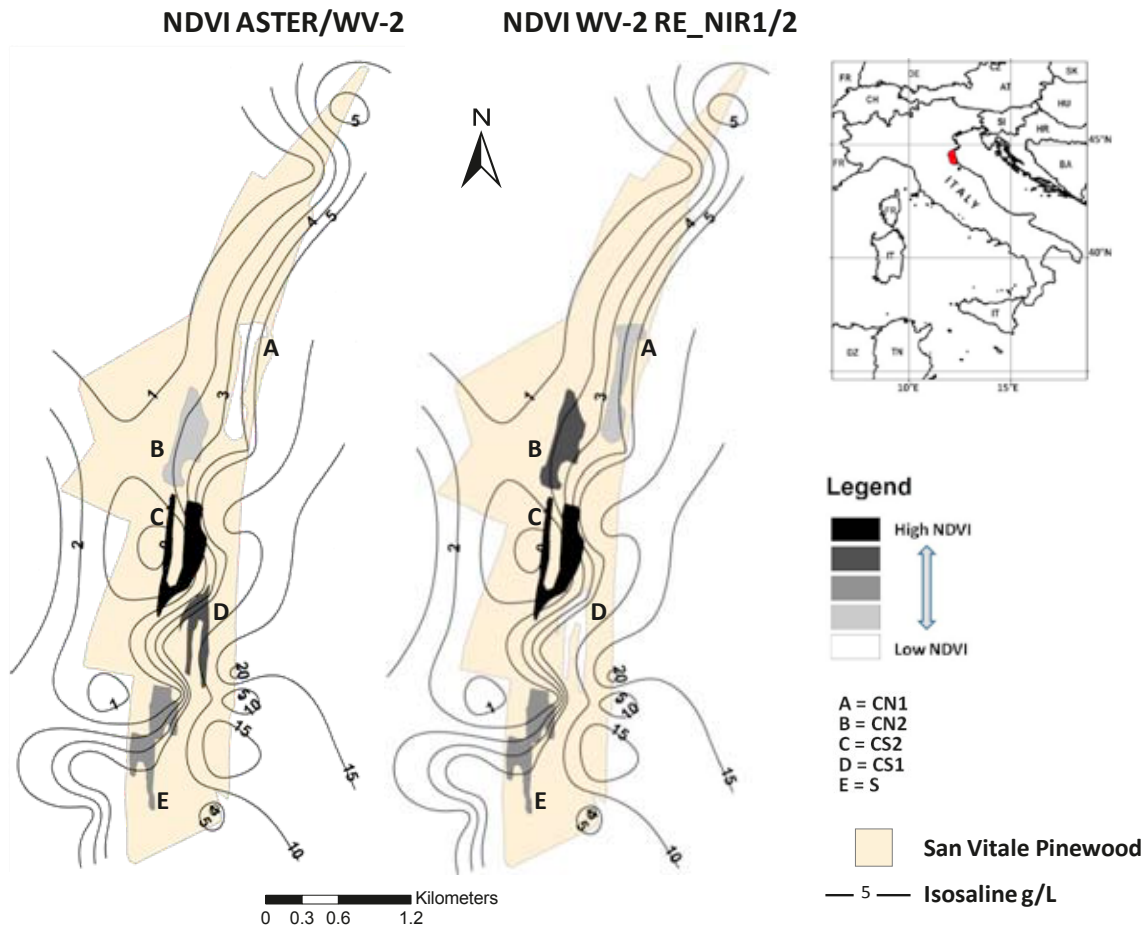


Figure 2. Overlay between groundwater salinity and NDVI results

DISCUSSION AND CONCLUSIONS

The NDVI results, calculated with same traditional red and infrared bands, are identical for ASTER and Worldview-2 data in term of AOIs discrimination.

Based on mean NDVI value, the south AOIs (CS2, CS1, S) were identified as less stressed areas compared to north samples (CN2, CN1). These results aren't agree with an increase in salinity along East-West gradient. The CN2 and CN1 areas are also the areas with the highest pine trees density and their low NDVI values confirm that the pine trees are a negative factor for the overall pine forest health.

In general, the response of the two satellite data seems to be influenced in the same way by pine trees density, but the contribution of the WV-2 higher spatial resolution is evident in the relative frequency histograms analysis. In fact, the CN1 and CN2 (partly S) NDVI values distribution have a bimodal trend, with the peak centered at lower NDVI values corresponding to pine species, as verified by further insights. The high spatial resolution, indeed, allows for the creation of sub-AOIs that exclude the pine trees.

Best results were obtained with the higher spectral resolution WV-2. New band Red Edge provides results less affected to pine trees density because it discriminates better evergreen and deciduous plants. The NDVI values obtained replacing the red band with Red Edge are perfectly consistent with the groundwater salinity of the considered AOIs.

REFERENCES

- Aguilar, C., Zinnertb, J.C., Poloa, M.R., Young, D.R. 2012. NDVI as an indicator for changes in water availability to woody vegetation. *Ecological Indicators*, 23: 290–300.
- Antonellini, M., Mollena, P., Giambastiani, B.M.S., Bishop, K., Caruso, L., Minchio, A., Pellegrini, L., Sabia, M., Ulazzi, E., Gabbianelli, G. 2008. Salt water intrusion in the coastal aquifer of southern Po Plain, Italy. *Hydrogeology journal*, 16: 1541–1556.
- Barton, C.W.M. 2012. Advances in remote sensing of plant stress. *Plant and Soil*, 354: 41–44.
- DeLaune, R.D., Pezeshki, S.R., Patrick Jr., W.A. 1987. Response of coastal plants to increase in submergence and salinity. *Journal of Coastal Research*, 3(4): 535–546.
- National Institute of Standards and Technology (NIST), 2003. NIST/SEMATECH e-Handbook of Statistical Methods. <http://www.itl.nist.gov/div898/handbook/>. Accessed 28 May 2013.
- Peñuelas, J. 1998. Visible and near-infrared reflectance techniques for diagnosing plant physiological status. *Trends in Plant Science*, 3: 151–156.
- Piccoli, F., Gerdol, R., Ferrari, C. (1991). Vegetation Map of St. Vitale pinewood (Northern Adriatic coast, Italy). *Phytocoenosis*, pp 337-342.
- Pu, R.; Landry, S. 2012. A comparative analysis of high spatial resolution IKONOS and WorldView-2 imagery for mapping urban tree species. *Remote Sens. Environ.*, 124: 516–533.
- Reed, B.C., Brown, J.F., Vander Zee, D., Loveland, T.R., Merchant, J.W., Ohlen, D.O. 1994. Measuring phenological variability from satellite imagery. *Journal of Vegetation Science*, 5:703–714.
- Regione Emilia Romagna - Servizio Cartografico e Geologico, 1999. Carta della Vegetazione del Parco Regionale del Delta del Po - Stazione “Pineta di San Vitale e Pialasse di Ravenna”. <http://geoportale.regione.emilia-romagna.it/it/catalogo/dati-cartografici/ambiente/carta-della-vegetazione/carta-della-vegetazione-parco-regionale-del-delta-del-po-stazione-pineta-di-san-vitale-e-piallasse-di-ravenna-digitale-edizione-1999>.
- Zhang, T., Zeng, S.L., Gao, Y., Ouyang, Z.T., Li, B., Fang, C.M., Zhao, B. 2011. Using hyperspectral vegetation indices as a proxy to monitor soil salinity. *Ecological Indicators*, 11: 1552–1562.

Contact Information: Michaela De Giglio, DICAM - University of Bologna, Viale Risorgimento 2, 40136 Bologna (Italy), Phone: +39 0512093109, Fax: +39 0512093114, Email: michaela.degiglio@unibo.it

In search for clay and salt, combining traditional techniques with airborne geophysics (SkyTEM) to optimize the 3D image of the subsurface

Sander de Haas¹, Harry Rolf¹ and Frans Schaars²

¹PWN Water Supply Company North-Holland, Velsbroek, The Netherlands

²Artesia Water, Schoonhoven, The Netherlands

ABSTRACT

The coastal dune area of North-Holland in The Netherlands has been used for the production of drinking water since the early 1900's. Because of this, the area has been thoroughly researched and measured using traditional measurement techniques such as piezometers, borehole logs, CPT's etc. Additionally in 2011 a large scale airborne geophysics survey (SkyTEM) was carried out in this area (HydroGeophysics Group - Aarhus University, 2012). The area around Bergen was chosen for further interpretation because it is known that a distinct confining layer is present within the fresh aquifer. This paper describes the interpretation of these geophysical measurements based on the large amount of existing information.

In the coastal dune area near Bergen there are almost 500 boreholes. Geophysical borehole logging has been carried out in 89 of these boreholes. Chloride concentration is measured at 48 locations 4 times a year. At 16 sites 'salt watcher' cables are present, which measure the conductivity of the groundwater at several depths. Recently 5 cone penetration tests (CPT's) with conductivity measurements have been carried out (Rolf and Schaars, 2012). Other sources of information on the fresh-salt interface are the groundwater model and (older) maps of hydrogeological studies. All this data covers the same area which has been measured using airborne geophysics (SkyTEM) and can therefore be used to verify and interpret the geophysical measurements.

Having this much information available presents several challenges: how to visualize and interpret data which is different in so many ways, yet all contains information on the fresh-salt interface? Some information is tens of years old so might not represent the current state of the fresh-salt interface. Combining similar data from different sources (databases) sometimes shows contradictions or differences caused by erroneous conversions. Even when all errors are removed the data still consist of different entities and units: resistivities (airborne geophysics, borehole logs), conductivities, chloride concentrations, and so one, all measured using different techniques.

The major step in the interpretation and validation of the data is the combined visualization. Several techniques have been used to jointly view and interpret different data types. Using MATLAB and GIS software (ESRI ArcGIS, ArcScene, Google Earth) many different maps, images and interactive maps and charts have been developed. Figures 1 to 3 show some examples of these.

Combining all this info it proved possible to map the extent of the confining clay layer and to determine the fresh/salt interface that corresponds well with most other sources. Besides this the combined interpretation of all these sources gave many insights in the

hydrogeological system and the developed tools, figures and maps are a great resource for other hydrogeological projects.

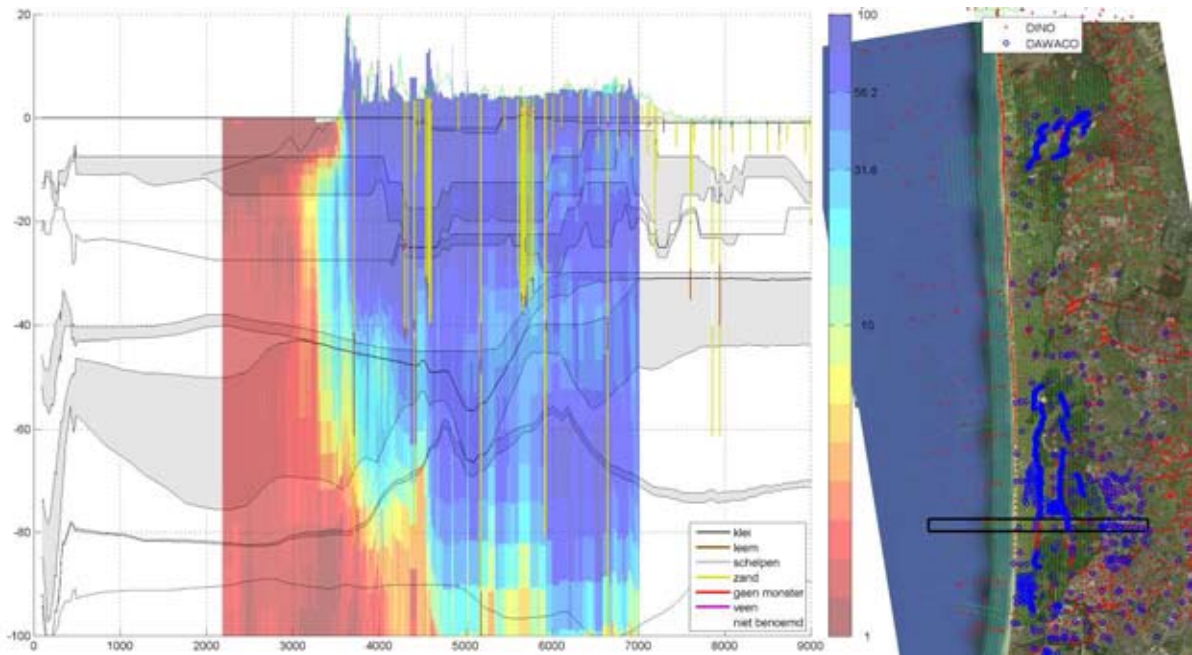


Figure 1 Cross-section (left) showing the resistivities from airborne geophysics (red = low resistivity, blue = high resistivity), geological information from boreholes in the bars (yellow = sand, brown/grey = peat and clay) and aquitards (gray) from the groundwater model in the background

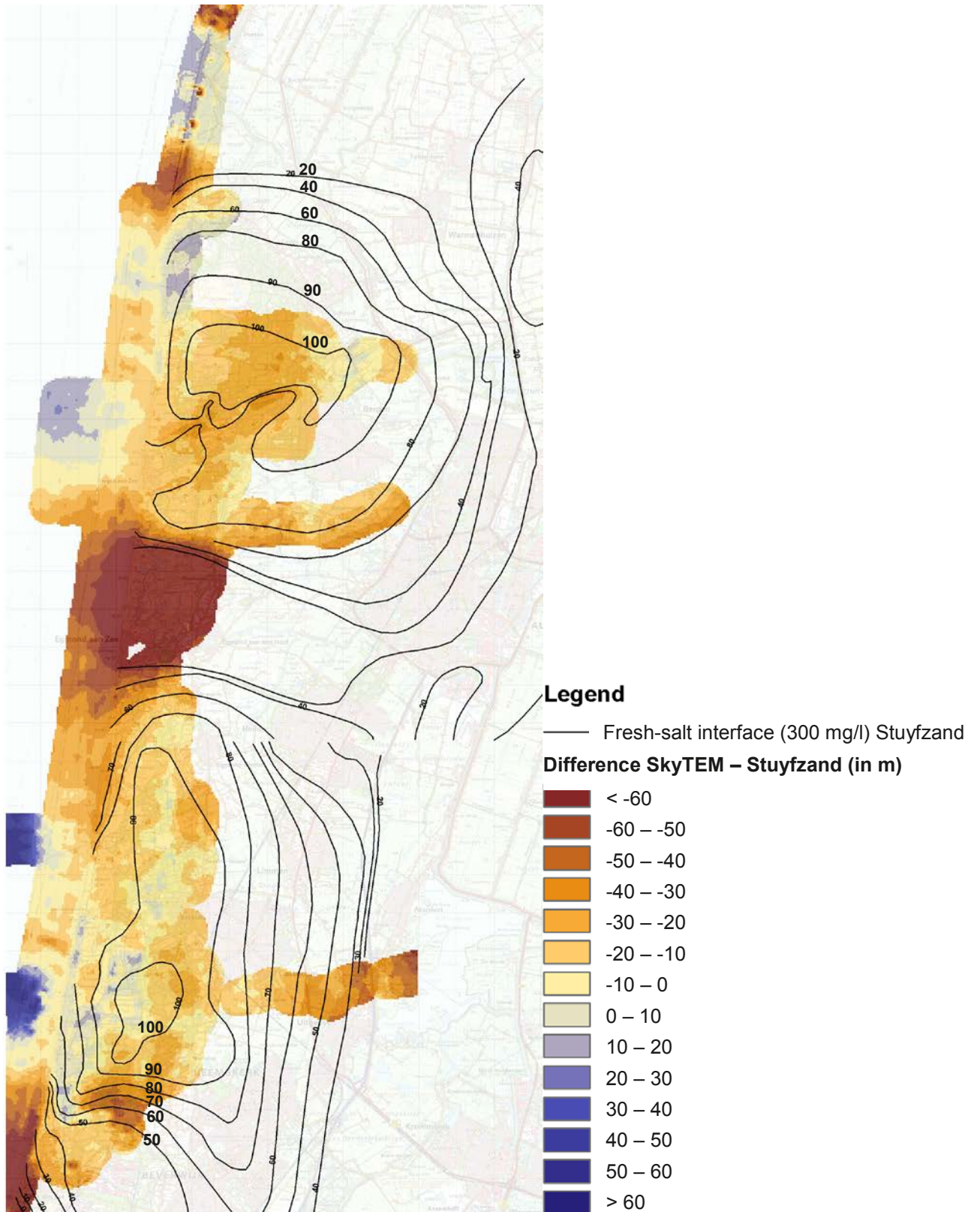


Figure 2 Difference in depth of the fresh-salt interface as determined by Stuyfzand (1985) and based on the SkyTEM data

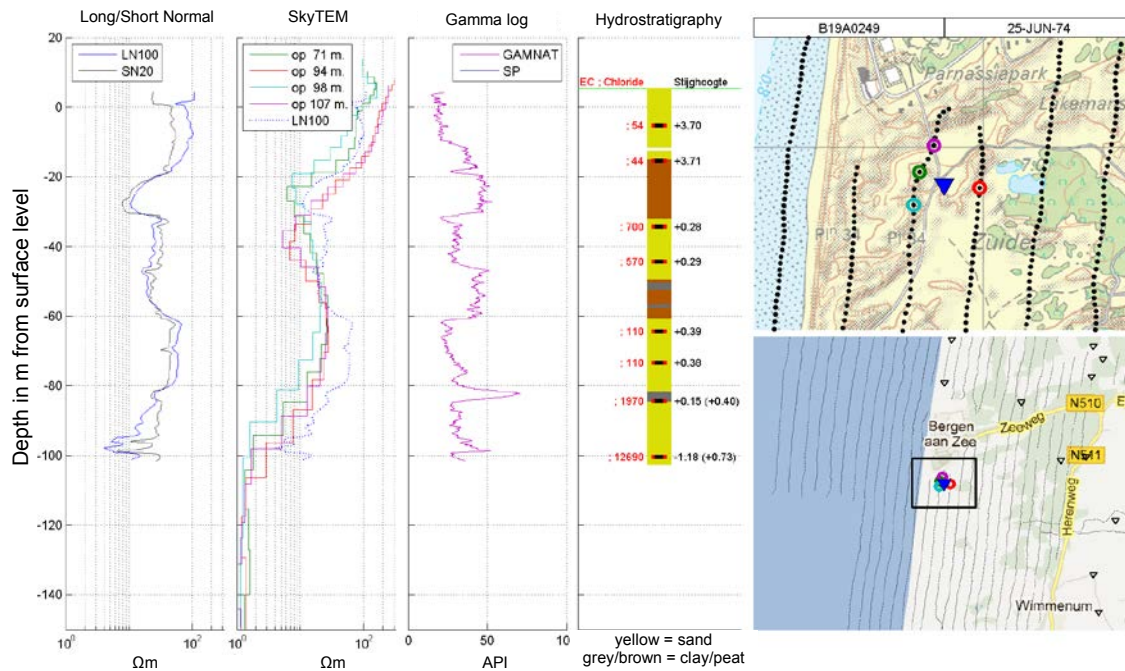


Figure 3 Several sources of hydrogeological information combined in one figure. From left to right: borehole logging (Long Normal/Short Normal), SkyTEM (time-domain electromagnetics) data for 4 nearby sites, borehole logging (Gamma ray logging), hydrostratigraphy and maps showing the location

References

HydroGeophysics Group - Aarhus University. 2012. SkyTEM Survey Noord-Hollands Duinreservaat 2011. Report number 2011-11-09.

Rolf, H. and Schaars, F. 2012. Verification of SkyTEM results on the Bergen clay by Cone Penetration Tests (CPT).

Stuyfzand, P.J. 1985. Hydrochemie en hydrologie van het duingebied tussen Egmond en Wijk aan Zee. SWE 85.012.

Contact Information: Sander de Haas, PWN Water Supply Company North-Holland, P.O. Box 2113, 1990 AC Velsbroek, The Netherlands, Phone: +31 6 13771915, Email: sander.de.haas@pwn.nl

Saline seepage in deltaic areas: how small scale processes dominate salinization

Perry G.B. de Louw¹

¹ Department of Soil and Groundwater, Deltares, Utrecht, The Netherlands

ABSTRACT

In low-lying coastal areas that lie below mean sea level, saline groundwater may reach the surface by upward groundwater flow leading to the salinization of surface waters, shallow groundwater and soil water in the root zone. This process is referred to as 'saline seepage' and was the main subject of a six-year term PhD-research in the Dutch delta. The most important results will be discussed and it will be demonstrated how small scale local processes dominate salinization of regional water systems.

INTRODUCTION

In many coastal areas, groundwater is brackish to saline which may pose problems for the sustainable exploitation of fresh groundwater. Saline seepage, the upward flow of saline groundwater, leads to the salinization of surface waters, shallow groundwater and soil water in the root zone. Climate change and future rise in sea level are expected to increase saline seepage and reduce the availability of both fresh surface water and groundwater. Predicting effects of future changes, defining effective water management strategies for a climate proof sustainable freshwater supply and successful implementation of any measure are only meaningful when all relevant processes involving saline seepage are fully understood. The main objective of my PhD-research was to address the knowledge gap that exists of the understanding and quantification of the dynamic processes involving saline seepage leading to the salinization of surface water, shallow groundwater and soil moisture.

The research focused on (i) the preferential saline seepage through boils leading to surface water salinization and (ii) the interaction between thin rainwater lenses and saline seepage leading to the salinization of shallow groundwater and the root zone. These two processes were identified as important contributors to the salinization of the Dutch delta which was the study area of the research. The results written in this extended abstract are taken from my PhD-thesis (De Louw, 2013) and five published papers (De Louw et al., 2010, 2011^{ab}, 2013^{ab}) of which the thesis is composed.

METHODS

The spatial variability and temporal dynamics of salinization processes involving saline seepage were analysed and quantified based on field campaigns supported by numerical and analytical methods. The study area was the south-western delta of the Netherlands Dutch delta and two deep polders (reclaimed lakes) in the western part of The Netherlands: the Noordplaspolder and the Haarlemmermeer Polder. The field campaigns involved field techniques applied at scales varying from local point (groundwater sampling, temperature and electrical soil conductivity (TEC)-probe measurements, electrical cone penetration tests (ECPT)) to field scale (continuous vertical electrical soundings (CVES), electromagnetic survey with EM31), and even to regional scale using helicopter-borne electromagnetic measurements (HEM). Time varying field data was collected at agricultural fields and polder catchment outlets to monitor the dynamic salinization processes. For a period of 3 years we collected monthly ground and soil water salinity in combination with hourly observations of

water table elevation, drain tile discharge and drain water salinity. Numerical modelling was applied to analyse the dynamic behaviour of the salinization processes.

RESULTS AND DISCUSSION

Preferential saline seepage through boils

Based on field observations and measurements, we distinguished three types of seepage in a deep polder which differ in flux and salt concentration (Figure 1): (i) diffuse, background seepage through the low permeability sediments (clay, peat) of the Holocene confining layer (HCL), (ii) preferential seepage through permeable, sandy paleochannel belts in the HCL, and (iii) intense preferential seepage via boils (De Louw et al., 2010). Boils are small conduits in the upper aquitard (HCL) connecting the aquifer with the surface through which water preferentially discharges at high velocities in the order of 10^2 to 10^4 m d⁻¹. The largest seepage fluxes and highest chloride concentrations are found in boils producing an average chloride concentration of 1100 mg L⁻¹ for the Noordplaspolder with a recorded maximum of 2850 mg L⁻¹. Boil water salinity is up to 5 to 30 times more saline than the other two forms of seepage. Based on field measurements and numerical modeling we conclude that saltwater upconing is the key mechanism leading to elevated salinities of boil water (De Louw et al., 2013a). Concentrated forms of seepage at higher rates tend to discharge groundwater from deeper strata with more saline groundwater than diffuse forms of seepage at low rates which discharge only fresh groundwater from the aquifer top (Figure 1).

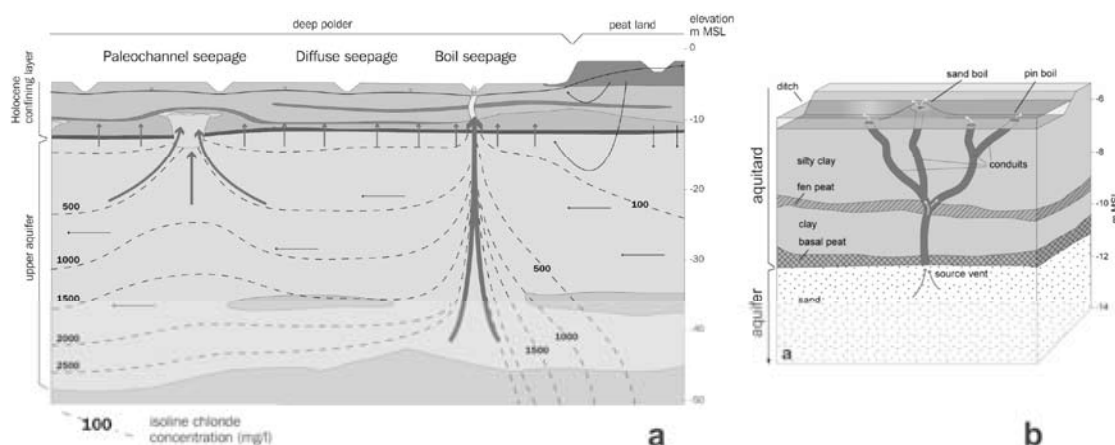


Figure 1. (a) Three seepage types with different fluxes and chloride concentrations: diffuse seepage, paleochannel seepage and boil seepage. (b) Boil with different conduits connecting the aquifer with the surface (adapted from De Louw et al., 2010).

To quantify the water and salt fluxes in a deep polder on a daily time scale, and taking into account the uncertainty of parameters, a probabilistic (GLUE) dynamic water and salt balance model on a daily time scale has been set up and successfully applied to Noordplaspolder (De Louw et al., 2011^a). The results showed that the far most dominant salinization source in the Noordplaspolder is boil seepage with an average contribution of 66% ($\pm 7.2\%$) to the total salt loads from only 15% ($\pm 4.7\%$) of the total water flux. Standard deviations are given between brackets. Regarding the omnipresence of saline boils in Dutch deep polders and the typical salinity distributions found below most deep polders (i.e. fresh above salt groundwater) we presume that boils are the most likely dominant salinization source in most Dutch deep polders.

Thin rainwater lenses in areas with saline seepage

Point measurements (TEC, ECPT) below 30 agricultural fields with saline seepage showed a gradual mixing zone between infiltrated rainwater and upward seeping saline groundwater (De Louw et al., 2011^b). The centre of this mixing zone (D_{mix}) was found at a median depth of 1.7 m below ground level and almost all mapped lenses lacked truly fresh groundwater. For the purpose of this study the thin rainwater lens in saline seepage areas was defined as the entire groundwater body from the base of the mixing zone (B_{mix} , which is the depth at which the salinity equals the salinity of regional groundwater) to the water table (Figure 2). With this definition, the rainwater lens (further referred to as RW-lens) is not purely a freshwater lens, and salinities within the RW-lens vary both in space and in time. B_{mix} was found at a median depth of 2.8 m and the ECPT measurements showed that below B_{mix} the salinity stayed virtually constant with depth until a depth of at least 25 m below ground level.

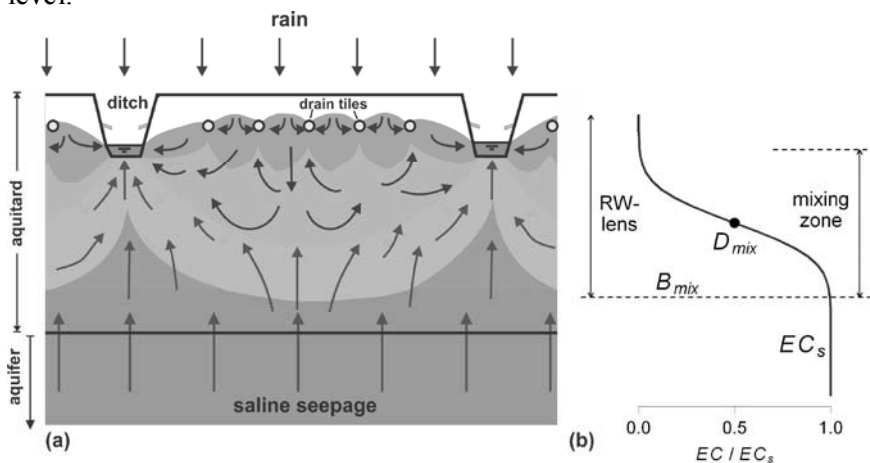


Figure 2. (a) Schematic visualization of a RW-lens in an area with upward seepage of saline groundwater. (b) Vertical profile of the electrical conductivity (EC) of groundwater at an arbitrary point in the RW-lens (adapted from De Louw et al., 2013^b)

The limited size of RW-lenses is primarily caused by the permanent regionally head driven upward groundwater flow from the upper aquifer into the HCL which prevents rainwater from reaching depths below the bottom of the HCL. Unlike RW-lenses in seepage areas, the vertical downward flow of rainwater in the infiltration areas is only limited (in absence of aquitards) by the buoyancy force of the surrounding saline groundwater and its density importantly determines lens thickness according to the Badon Ghyben Herzberg principle. These systems build up much thicker lenses (BGH-lenses), varying from 5-15 m thick lenses in sandy creek ridges to 100 m thick lenses in the dunes. As it was established that lenses in seepage areas are limited to the extent of the upper aquitard (HCL) due to permanent upward seepage, we subsequently examined the mixing mechanisms and flow processes within the aquitard and the factors controlling lens size and mixing zone properties with numerical modeling. We concluded that the transient oscillatory vertical flow regime in the aquitard driven by water table fluctuations is the main mechanism of mixing between infiltrating rainwater and upward saline seepage and determines the position and extent of the mixing zone in the aquitard. Recharge, seepage flux and drainage depth are the controlling factors.

The time varying field data showed that the change of the position of D_{mix} is small (< 0.25 m), and fluctuates at a seasonal time scale (De Louw et al., 2013^b). The base of the RW-lens (B_{mix}) stayed virtually at the same position. Numerical simulations showed that the small variations in the position of the mixing zone can be explained by the slow transient

oscillatory flow regime in the permanent saturated part of the RW-lens, which also controls the mixing between infiltrated rainwater and seepage water. The flow and mixing processes are much faster near the water table, which fluctuates on a daily basis in response to recharge and evapotranspiration, and conditions alternate between saturated to unsaturated. When the water table falls, most of the water with variable dissolved salt concentrations is retained as soil water, which will mix and become diluted with only a small amount of infiltrated rainwater when the soil saturates again. The salinity of the mixture will thus be close to that of the soil water before saturation, which explains the observed absence of very fresh groundwater. Although the mixing processes are fast, the temporary storage of salt in soil water has an important damping effect on groundwater salinity variations when the RW-lens grows due to the recharge by rainwater.

Salt migrates upwards into the root zone by capillary rise of the groundwater at the water table. As the water table falls during the summer, the water rising through the capillaries originates from deeper parts of the RW-lens and is therefore more saline. Salinities of soil water can become significantly higher than in the groundwater due to the unsynchronized effects of capillary rise of saline water during dry periods and the flow of infiltrated rainwater during wet periods being restricted to cracks in the soil. Preferential flow through cracks is thought to play an important role in the rapid response of the drain tile discharge to individual rain events. Groundwater of variable salinity, originating from different parts of the RW-lens, as well as infiltrated rainwater, contributes to the drain tile discharge in proportions that vary on a timescale of hours to days, and this causes the dynamic behaviour of drain water salinity.

CONCLUDING REMARK

The findings of the PhD-research demonstrate that small scale processes dominate salinization of regional water systems. These processes should therefore be taken into account when modelling salinization and predicting effects of climate change, defining effective water management strategies and successful implementation of any measure.

REFERENCES

- De Louw, P.G.B., Oude Essink, G.H.P., Stuyfzand, P.J., Van der Zee, S.E.A.T.M., 2010. Upward groundwater flow in boils as the dominant mechanism of salinization in deep polders, The Netherlands. *Journal of Hydrology* 394, 494-506.
- De Louw, P.G.B., Van de Velde, Y., Van der Zee, S.E.A.T.M., 2011^a. Quantifying water and salt fluxes in a lowland polder catchment dominated by boil seepage: a probabilistic end-member mixing approach. *Hydrology and Earth System Sciences* 15, 2101-2117.
- De Louw, P.G.B., Eeman, S., Siemon, B., Voortman, B.R., Gunnink, J., Van Baaren, S.E., Oude Essink, G.H.P., 2011^b. Shallow rainwater lenses in deltaic areas with saline seepage. *Hydrology and Earth System Sciences* 15, 3659-3678.
- De Louw, P.G.B., Vandenbohede, A., Werner, A.D., Oude Essink, G.H.P., 2013^a. Natural saltwater upconing by preferential groundwater discharge through boils, *Journal of Hydrology* 490, 74-87.
- De Louw, P.G.B., Eeman, S., Oude Essink, G.H.P., Vermue, E., Post, V.E.A., 2013^b. Rainwater lens dynamics and mixing between infiltrating rainwater and upward saline groundwater seepage beneath a tile-drained agricultural field. *Journal of Hydrology* 501, 133-145.
- De Louw, P.G.B., 2013. Saline seepage in deltaic areas. Preferential groundwater discharge through boils and interactions between thin rainwater lenses and upward saline seepage. PhD thesis, Vrije Universiteit Amsterdam. ISBN/EAN 9789461085429.

Contact Information: Perry G.B. de Louw, Department of Soil and Groundwater, Deltares, Utrecht, The Netherlands Phone: +31-6-3054800, Email: perry.delouw@deltares.nl

Monitoring and modelling the dynamic behaviour of rainwater lenses and soil-, ground- and drain water salinities

Perry G.B. de Louw¹, Sara Eeman², Gualbert H.P., Oude Essink¹, Esther Vermue², Vincent E.A. Post³

¹ Department of Soil and Groundwater, Deltares, Utrecht, The Netherlands

² Wageningen University, Environmental Sciences Group, Soil Physics, Ecohydrology and Groundwater Management, Wageningen, The Netherlands

³ School of the Environment / National Centre for Groundwater Research and Training, Flinders University, Adelaide SA, Australia

ABSTRACT

Thin rainwater lenses near the land surface are often the only source of freshwater in agricultural areas where saline groundwater migrates to the surface by upward groundwater flow. The dynamic behaviour of salinities within these rainwater lenses and the soil moisture in the unsaturated zone above them is of great importance from an agricultural perspective. Saline groundwater can reach the root zone via capillary rise, affecting crop growth.

The seasonal dynamics of these thin rainwater lenses are poorly known. The transient behavior of rainwater lenses in areas with upward saline seepage was studied beneath two tile-drained agricultural fields in the Netherlands. Evidence of rainwater lens dynamics was systematically collected by monthly ground- and soil water sampling, in combination with daily observations of water table elevation, drain tile discharge and drain water salinity. SEAWAT was used to simulate the dynamic mixing processes between rainwater, soil water, groundwater and drain water. The combination of field observation and numerical modeling allowed us to develop of a conceptual model of rainwater lens dynamics.

INTRODUCTION

In many coastal areas, groundwater is brackish to saline which may pose problems for the sustainable exploitation of fresh groundwater. Thin rainwater lenses near the land surface are often the only source of freshwater in agricultural areas upward saline seepage. Due to their limited size and nearby position to the surface, these thin rainwater lenses (further referred to as RW-lenses) are very vulnerable to changing recharge patterns (climate change). Also, it is expected that the characteristics and dynamics of RW-lenses may have an important impact on soil water salinities in the root zone of agricultural crops. To address the knowledge gap that exists on the temporal dynamics of RW-lenses and their relation to soil water salinity, RW-lens dynamics was monitored at two agricultural fields in the southwestern delta of The Netherlands. SEAWAT was used to simulate the dynamic behavior of these rainwater lenses to understand the mixing processes in RW-lenses. Parts of the results presented in this extended abstract were taken from De Louw et al, (2013). In the presentation and the extended abstract the focus will be on the method of simulating the observed dynamic processes with SEAWAT.

METHODS

The study area was the south-western delta of the Netherlands. Time varying field data was collected at two agricultural fields to monitor the dynamic salinization processes. For a period of 3 years we collected monthly ground and soil water salinity in combination with hourly observations of water table elevation, drain tile discharge and drain water salinity. Soil water was collected from soil moisture samplers (rhizons) at depth 0.15 m, 0.30 m, 0.45 m, 0.60 m and 0.75 m below ground level (BGL). Ground water salinity was collected from piezometers with 0.16 m long screens at depths (bottom of screen) of 0.8 m, 1.0 m, 1.3 m, 1.6 m, 2.0 m, 3.0 m and 4.0 m BGL.

SEAWAT version 4 (Langevin et al., 2007) was used to simulate the dynamic mixing processes between rainwater, soil water, groundwater and drain water. A RW-lens between two drain tiles was simulated with a length of 10 m and a thickness of 4.5 m. Since the RW-lenses are found near the surface, conditions of the unsaturated zone play an important role in their dynamic behavior and need to be accounted for in the model. Parameter values were adopted into SEAWAT in such a way (as described below) to account for the most important processes in the unsaturated zone. The moving water table was simulated through MODFLOW's cell wetting and drying option. For the highest active cells a specific yield (S) was used to account for storage changes due to a fluctuating water table. S was quantified based on measured water table fluctuations and rainfall amounts. A relation was found between S and the water table depth, which was implemented in the model by letting the specific yield vary with depth. By doing so, the dynamic conditions in the unsaturated zone were partly accounted for in SEAWAT. A constant value of S of 0.12 was applied at a depth below 0.7 m BGL and above this depth, S decreases to 0.05 for the upper 0.3 m. Cracks were observed in at the agricultural fields facilitating fast infiltration and drainage of rainwater. To simulate this process accurately we assigned a relatively-high K_h value (2.5 m/d) to the upper 0.4 m of the clayey subsoil. In combination with the adopted small values of S (0.05 – 0.09) the observed rapid response of the water table elevation and drain discharge were adequately reproduced. Evapotranspiration (negative recharge) constitutes a sink for both water and solutes in SEAWAT. Conceptually, negative recharge is considered to represent water loss from the saturated zone by capillary rise. In the field, depending on the salinity of groundwater at the water table, variable amounts of solutes are thereby moved into the unsaturated zone and temporarily stored. During recharge events, the solutes residing in the unsaturated zone are flushed. To replicate this behavior in the model, a Cl concentration of 1.25 g L⁻¹ was assigned to the water entering the system as recharge. This value was chosen such that the total salt mass leaving the model by capillary rise equaled the total salt mass entering the model by recharge.

RESULTS

Figure 1 shows the monthly observed groundwater and soil water salinity depth profiles. The results showed that variations in the position of the mixing zone and mixing zone salinities are small and vary on a seasonal timescale. Figure 2 shows the comparison between observations and model results. The observed dynamics of the water table, drain discharge and the groundwater salinity depth profiles could be reproduced quite well with the numerical model. However, the observed dynamics of drain water salinity could only be partially reproduced by the model. The largest discrepancy occurred directly after the summer period when drain tiles start discharging again. The lower simulated values of drain water salinity than observed is believed to be attributable to the fact the salinity of the recharge water after a period of drought is higher in the field than the constant Cl concentration of 1.25 g L⁻¹ used in the model.

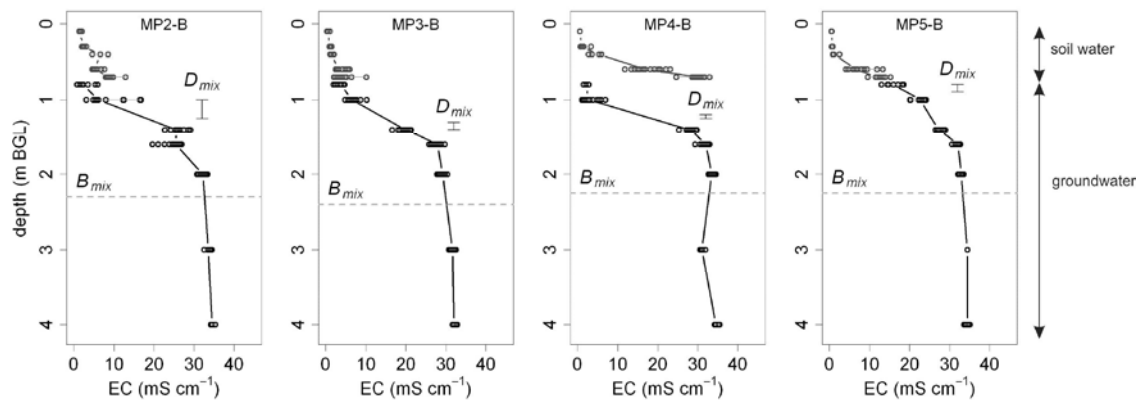


Figure 1. Depth profiles of soil water salinity and groundwater salinity based on monthly measurements during the period March 2009 – December 2010. The individual measurements are indicated by dots and median values are connected by a full line. The amplitude of the displacement of D_{mix} during the monitoring period and the depth of B_{mix} is indicated for each measurement point (adapted from De Louw et al., 2013).

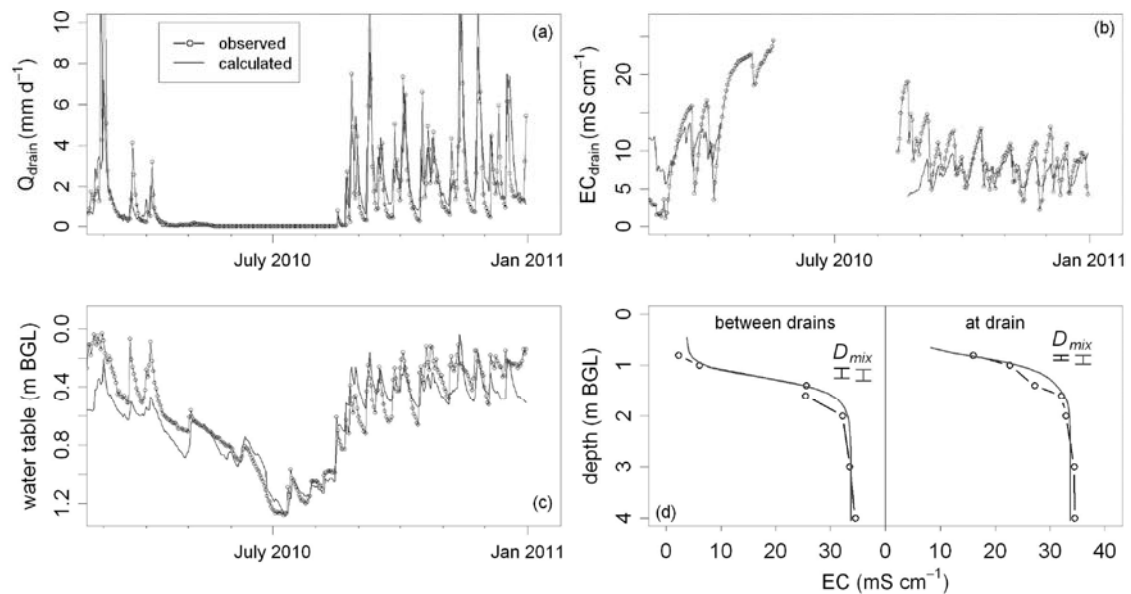


Figure 2. Comparison between observed and calculated (a) drain water discharge (Q_{drain}), (b) drain water salinity (EC_{drain}), (c) water table between the two drain tiles, and (d) salinity-depth profiles at and between the two drain tiles (from De Louw et al., 2013).

Based on both the field measurements and numerical simulations the following conceptual model of rainwater lens dynamics could be derived. Variations in the position of the mixing zone and mixing zone salinities are small and vary on a seasonal timescale, which is attributed to the slow transient oscillatory flow regime in the deepest part of the lens. The flow and mixing processes are much faster near the water table, which fluctuates on a daily basis in response to recharge and evapotranspiration, and conditions alternate between saturated to

unsaturated. Although the mixing processes are fast, the temporary storage of salt in soil water has an important damping effect on groundwater salinity variations when the RW-lens grows due to the recharge by rainwater. Salinities of soil water can become significantly higher than in the groundwater (MP4-B in Figure 2), due to the unsynchronized effects of capillary rise of saline water during dry periods and the flow of infiltrated rainwater during wet periods being restricted to cracks in the soil. Preferential flow through cracks is thought to play also an important role in the rapid response of the drain tile discharge to individual rain events. Modeling showed that groundwater of variable salinity, originating from different parts of the RW-lens, as well as infiltrated rainwater, contributes to the drain tile discharge in proportions that vary on a timescale of hours to days, and this causes the highly dynamic behavior of drain water salinity.

CONCLUSIONS

The observed dynamics of RW-lens salinities, water table fluctuations and drain water discharge could be well simulated by the numerical model SEAWAT. Although SEAWAT is a saturated flow model, the effect of the unsaturated zone on the shallow groundwater system (i.e. temporary storage of water and salt in the vadose zone and effects of cracks), could satisfactorily be reproduced by the model. As we now have unravelled the dynamic behavior of RW-lenses, the next step will be to predict soil water salinities in the root zone as they may limit the growth of agricultural crops. The challenge will be to obtain more field data of groundwater and soil water salinities and to correctly simulate the interaction between RW-lens dynamics and soil water salinity in the root zone using a variable saturated zone model that also incorporate the effect of cracks.

REFERENCES

- De Louw, P.G.B., Eeman, S., Oude Essink, G.H.P., Vermue, E., Post, V.E.A., 2013. Rainwater lens dynamics and mixing between infiltrating rainwater and upward saline groundwater seepage beneath a tile-drained agricultural field. *Journal of Hydrology* 501, 133-145.
- Langevin, C.D., Thorne, D.T., Dausman, A.M., Sukop, M.C., Guo, W., 2007. SEAWAT Version 4: A computer program for simulation of multi-species solute and heat transport: U.S. Geological Survey Techniques and Methods. Book 6, Chapter A22, 39pp.

Contact Information: Perry G.B. de Louw, Department of Soil and Groundwater, Deltares, Utrecht, The Netherlands Phone: +31-6-3054800, Email: perry.delouw@deltares.nl

Palaeo-modeling of coastal salt water intrusion during the Holocene: an application to the Netherlands

J.R. Delsman^{1,2}, K.R.M. Hu-a-ng^{1,3,*}, P.C. Vos¹, P.G.B. de Louw¹, G.H.P. Oude Essink¹, P.J. Stuyfzand^{2,4}, M.F.P. Bierkens^{1,3}

¹Department of Soil and Groundwater, Deltares, Utrecht, The Netherlands

²Critical Zone Hydrology Group, Department of Earth Sciences, VU University Amsterdam, Amsterdam, The Netherlands

³Department of Physical Geography, Utrecht University, Utrecht, The Netherlands

⁴KWR Watercycle Research Institute, Nieuwegein, The Netherlands

*now at: Acacia Water, Gouda, The Netherlands

ABSTRACT

Management of coastal fresh groundwater reserves requires a thorough understanding of the present-day groundwater salinity distribution and its possible future development. However, coastal groundwater often still reflects a complex history of marine transgressions and regressions, and is only rarely in equilibrium with current boundary conditions. In addition, the distribution of groundwater salinity is virtually impossible to characterize satisfactorily, complicating efforts to model and predict coastal groundwater flow. A way forward may be to account for the historical development of groundwater salinity when modeling present-day coastal groundwater flow. In this paper, we construct a palaeo-hydrogeological model to simulate the evolution of groundwater salinity in the coastal area of the Netherlands throughout the Holocene. While intended as a perceptual tool, confidence in our model results is warranted by a good correspondence with a hydrochemical characterization of groundwater origin. Model results attest to the impact of groundwater density differences on coastal groundwater flow on millennial timescales and highlight their importance in shaping today's groundwater salinity distribution. Not once reaching steady-state throughout the Holocene, our results demonstrate the long term dynamics of salinity in coastal aquifers. This stresses the importance of accounting for the historical evolution of coastal groundwater salinity when modeling present-day coastal groundwater flow, or when predicting impacts of e.g. sea level rise on coastal aquifers. Of more local importance, our findings suggest a more significant role of pre-Holocene groundwater in the present-day groundwater salinity distribution in the Netherlands than previously recognized. The implications of our results extend beyond understanding the present-day distribution of salinity, as the proven complex history of coastal groundwater also holds important clues for understanding and predicting the distribution of other societally relevant groundwater constituents.

A full version of this paper is currently under review for HESS, the discussion version (including a video animation) can be found online at:

<http://www.hydro1-earth-syst-sci-discuss.net/10/13707/2013/hessd-10-13707-2013.html>

Contact Information: Joost R. Delsman, Department of Soil and Groundwater, Deltares, PO Box 85467, 3508 AL Utrecht, The Netherlands, Email: joost.delsman@deltares.nl

SELECTED RESULTS

(for full results see HESSD paper)

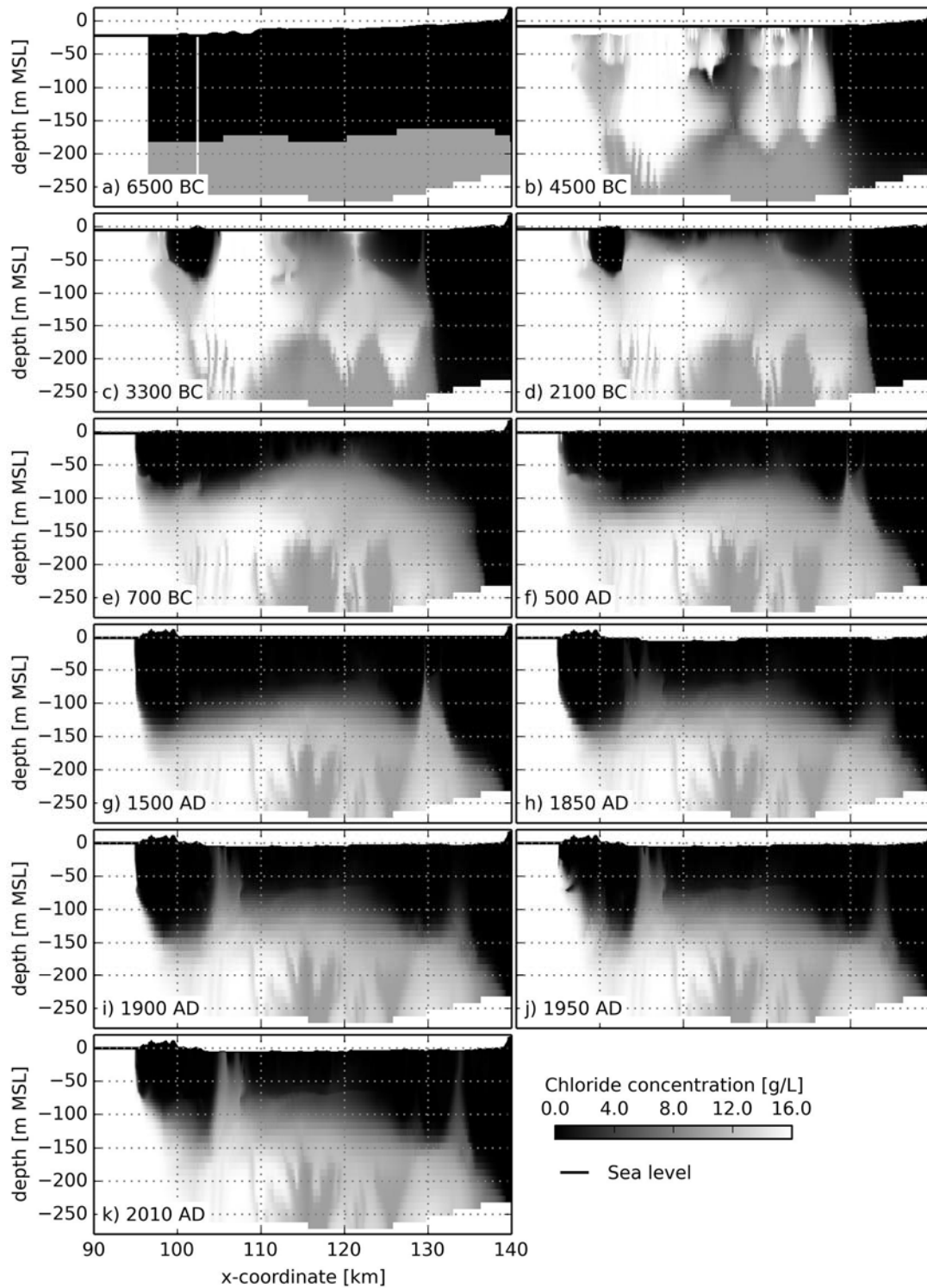


Figure 1: Modeled evolution of salinity distribution from 6500 BC to present. Note the rapid infiltration of seawater after the marine transgression lasting from 4500BC – 3300BC and the significance of non-continuous aquitards. Subsequent widespread peat development promoted the infiltration of fresh water until 1850 AD, after which lake reclamation and pumping caused the upward migration of deep saline groundwater. Not once in the modeled period is the salinity distribution in equilibrium with the contemporaneous flow situation.

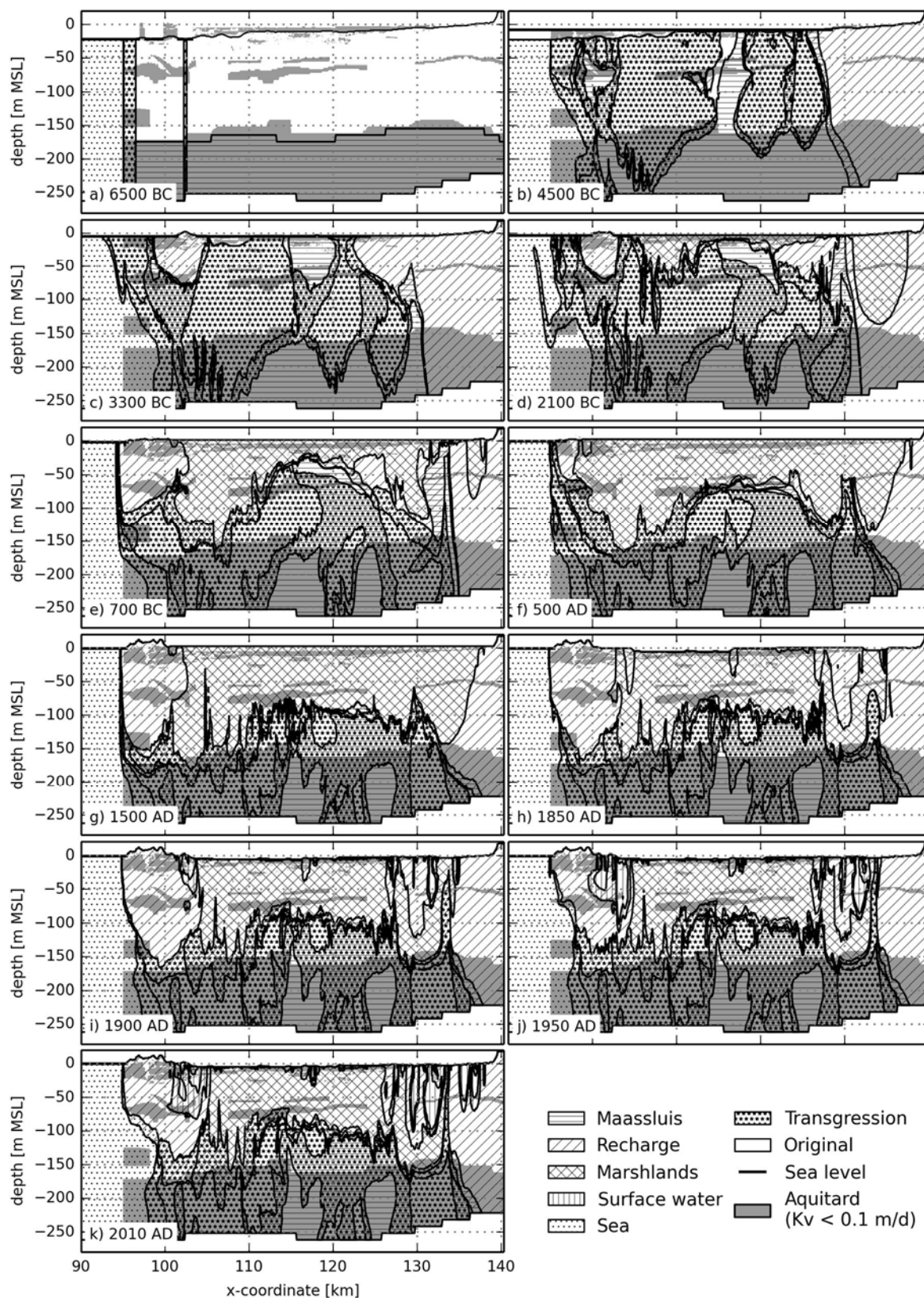


Figure 2: Evolution of groundwater origin from 6500 BC to present. The significance of seawater infiltrating during the transgression phase versus the ‘classic’ seawater intrusion is evident in the results, signifying the importance of accounting for historical evolution when modeling the groundwater salinity distribution. Also note the displacement of pre-transgression water by the infiltrating sea water during the marine transgression. Pleistocene

‘Maassluis’ water is displaced upwards, after which it slowly moves downward to its present location, where its presence has been determined using hydrogeochemical analyses (Stuyfzand, 1993). This evolution provides new insights in the role of Pleistocene groundwater in the present-day salinity distribution.

REFERENCES

Stuyfzand, P. J., 1993. Hydrochemistry and hydrology of the coastal dune area of the Western Netherlands, PhD thesis, 362 pp., Faculty of Earth Sciences, VU University Amsterdam.

3D-Modelling of the salt-/fresh water interface in coastal aquifers of Lower Saxony (Germany) based on airborne electromagnetic measurements (HEM)

Nico Deus¹, Jörg Elbracht¹

¹State Authority for Mining, Energy and Geology (LBEG), Hannover, Germany

Contact Information: Nico Deus, State Authority for Mining, Energy and Geology (LBEG), Department Hydrogeology, Stilleweg 2, 30655 Hannover, Germany, Phone: +49-511-6432819, Email: nico.deus@lbeg.niedersachsen.de

ABSTRACT

The public water management of Lower Saxony has to provide about 8 million people with fresh water. With a portion of 71% of the public water supply in Germany (BGR 2010), the fresh groundwater is the most important resource for urban, agricultural and industrial activities. Some of the aquifers used for groundwater extraction provide problems with intruding salt water from different sources (GRUBE et al. 2000). Especially the coastal aquifers may be vulnerable for sea water intrusion, which is the landward encroachment of sea water into fresh water aquifers (IVKOVIC et al. 2012). This process could be enhanced or initiated by anthropogenic activities. Because of the importance of the salt water intrusion problems, the State Authority for Mining, Energy and Geology (LBEG) planned, based on a pilot project in the area of Esens (see Fig. 1) (GÖSSMANN 2012), to generate a statewide “salt water map” for Lower Saxony with a focus on the coastal aquifers influenced by sea water intrusion.

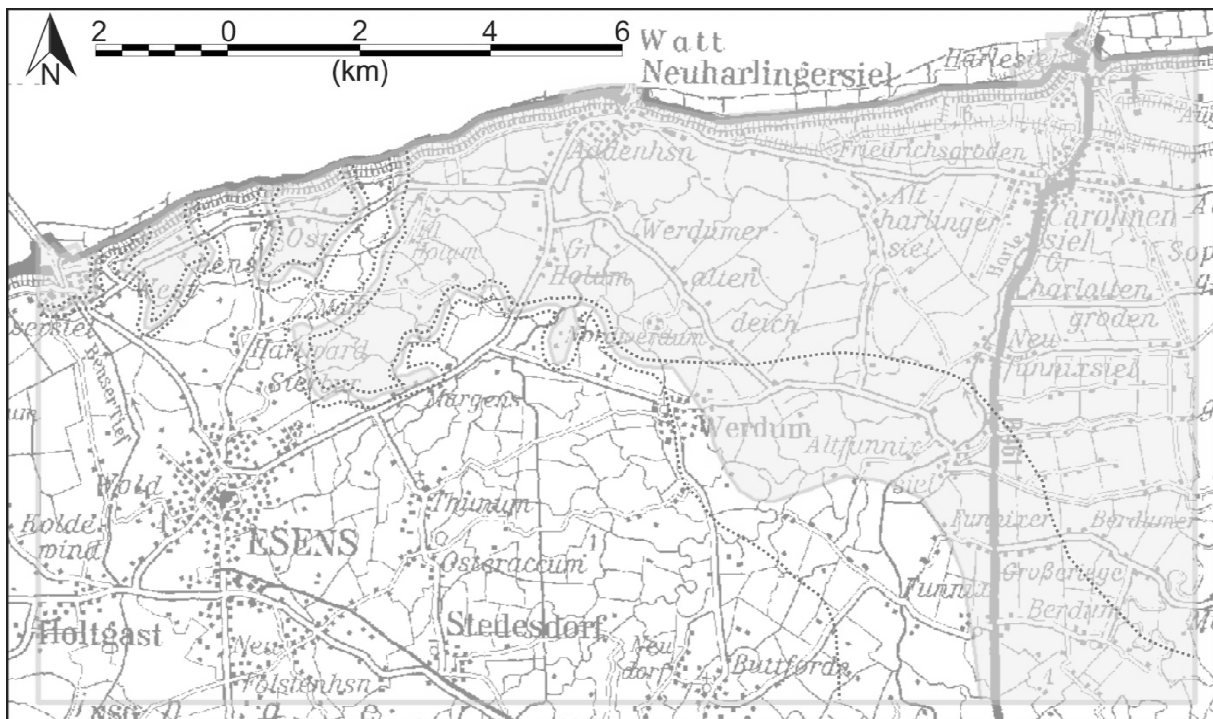


Figure 1: Groundwater salinization in the study area of Esens identified by airborne electromagnetic measurements combined with a geological 3D model (GÖSSMANN, 2012). The light grey zone marks the salinization area, the dotted line shows the uncertainty of this interpreted area caused by the heterogeneous database.

In Germany the use of fresh water as drinking water is limited through the thresholds for different parameters in the “Trinkwasserverordnung (German drinking water regulation)” (BMJ 2013). Those are 250 mg/l chloride, 250 mg/l sulfate and 200 mg/l sodium (BMJ 2013). The threshold for the electrical conductivity at 20°C is 2790 $\mu\text{S}/\text{cm}$ (BMJ 2013) which correlates with an electric resistivity of 4 Ωm . These parameters were used to characterize the groundwater and divide it into salt-/fresh water areas.

For the coastal regions of Lower Saxony we use airborne electromagnetic measurements (HEM) to get the electric resistivity of the underground (sediments and pore fluids) and combined them with groundwater analyses to detect the intrusion of sea water into the aquifers. The helicopter-borne system operated by the “Federal Institute for Geosciences and Natural Resources (BGR)” enables simultaneous measurements of electromagnetic, magnetic and gamma-ray spectrometry (SIEMON et al. 2012) For our interests on saltwater intrusion we used the electromagnetic data from the BGR measurements. Therefore, referring to the experiences and results of GÖSSMANN (2012), we combined the resistivity distribution with geological maps, profiles, wells and groundwater analyses to distinguish low resistivity’s caused by sea water intrusion, from those caused by clay materials which have the same resistivity. In addition to that, we generate linked geologic profiles and based on these profiles, a geologic 3D-model of the Pleistocene subsurface, to get reliable information of the clay distribution. After the inversion of the data we used horizontal resistivity maps in different depths to identify the intrusion of sea water (see Fig. 2).

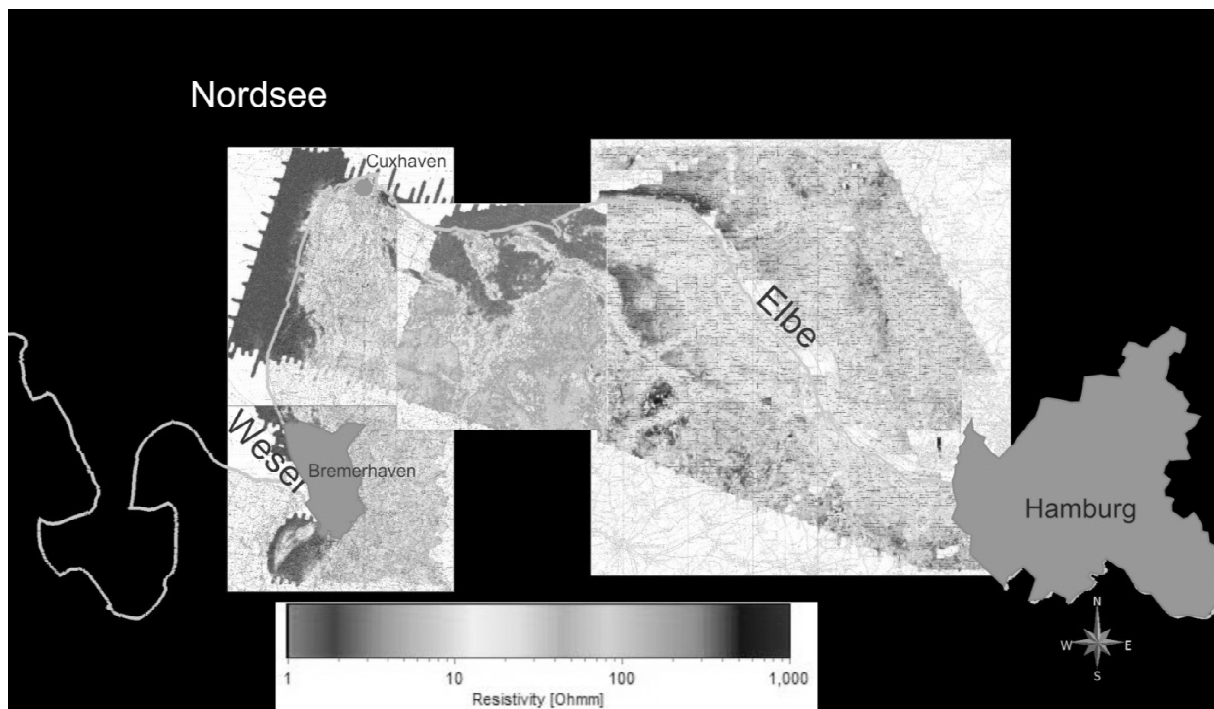


Figure 2: HEM-resistivity distribution for a depth of -10m NN in the "Elbe-Weser-Dreieck". The outline curve marks the coastline of Lower Saxony.

The resistivity maps were integrated in GOCAD® as a picture and the identified sea water intrusion were plotted as a curve on each map. Afterwards a vertical surface was built up from the several curves in various depths which illustrate the salt-/fresh water interface (see Fig. 3). Fig. 3 shows a preliminary construction of the salt-/fresh water interface, which is not based on the mentioned 3D-model, but only on wells, groundwater analyses and geologic maps. As soon as the linked geologic profiles and the 3D-model are available, the interface will be adapted to get a reliable final version.

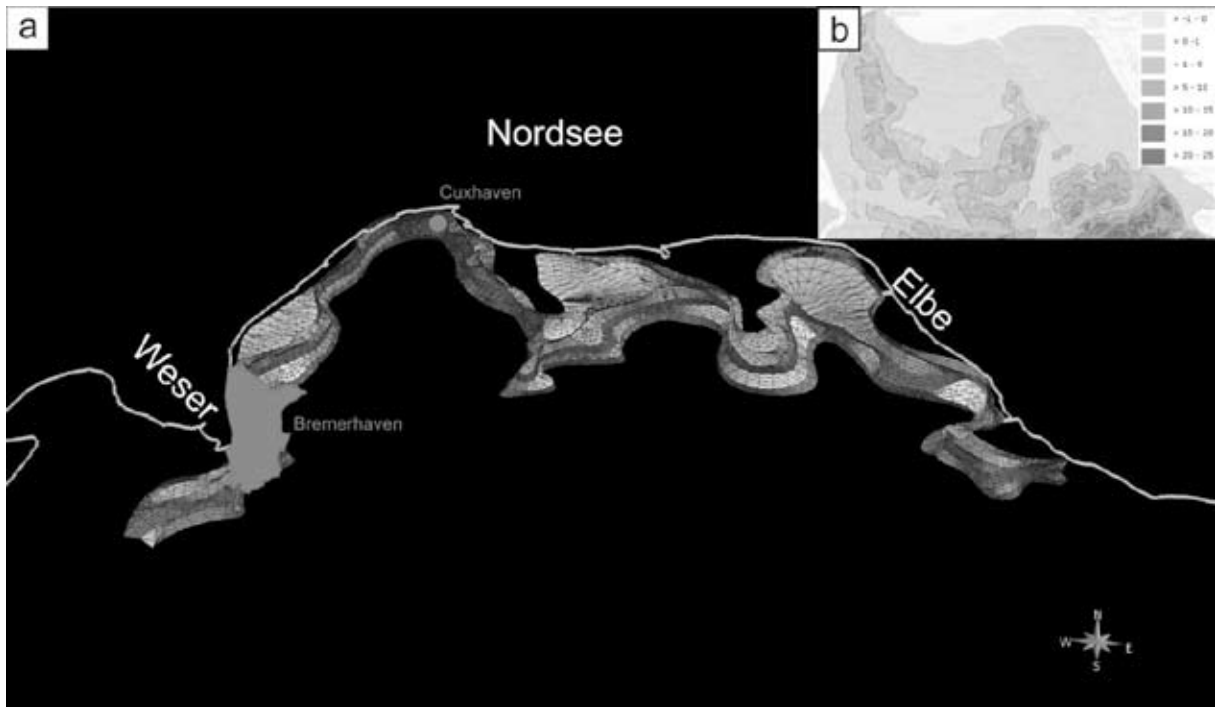


Figure 3: a) Identified salt-/fresh water interface in the „Elbe-Weser-Dreieck“ based on HEM data. The interface consists of different surface parts, which were each created through a top and a bottom curve that illustrates the saltwater front for a certain depth. b) Depth of the groundwater table in meter relative to the mean sea level (NN) for the project area.

With this illustration of the interface, we can show how dynamic and vertically irregular the salt-/ fresh water system is developed, especially in coastal regions. Additionally, through this growth of information, we are able to give precise specifications of the depth in which the groundwater is over salted.

BGR 2010. Grundwasseranteil an der öffentlichen Wasserversorgung der Bundesländer in 2007. http://www.bgr.bund.de/nn_322854/DE/Themen/Wasser/grundwasser__gewin__tab.html, Abruf 01.12.2010.

BMJ (Bundesministerium für Justiz) 2013. Trinkwasserverordnung in der Fassung der Bekanntmachung vom 2. August 2013 (BGBl. I S. 2977), die durch Artikel 4 Absatz 22 des Gesetzes vom 7. August 2013 (BGBl. I S. 3154) geändert worden ist. – Berlin.

Gössmann, N. 2012. Kartierung der Küstenversalzung mit Hilfe geophysikalischer Daten und 3D-Modellierung im Raum Esens (Ostfriesland). Hannover (unpublished Master thesis Univ. Hannover), 92pp.

Grube, A., Wichmann, K., Hahn, L. & Nachtigall, K.H.. 2000. Geogene Grundwasserversalzung in den Poren-Grundwasserleitern Norddeutschlands und ihre Bedeutung für die Wasserwirtschaft. TZW-Schriftenreihe, 9, Karlsruhe, 203 pp.

Ivkovic, K.M., Marshall, S.K., Morgan, L.K., Werner, A.D., Carey, H., Cook, S., Sundaram, B., Norman, R., Wallace, L., Caruana, L., Dixon-Jain, P. & Simon, D. 2012. National-scale vulnerability assessment of seawater intrusion: summary report. Waterlines Report Series No 85, Australia, 185 pp.

Simon, B., Steuer, A., Ibs-von Seht, M., Miensopest, M.P., Meyer, U. & Wiederhold, H. 2012. Airborne geophysical surveys in the Weser-Elbe area, Northern Germany. 21th International Workshop on Electromagnetic Induction in the Earth, 25.-31.8.2012, Darwin, Australia.

Groundwater flow and salinity distribution near a tidal gully in the Zwin remnant, Belgium

Gert-Jan Devriese¹, Jasper Claus¹ and Luc Lebbe¹

¹Department of Geology and Soil Science, Ghent University, Ghent, Belgium

ABSTRACT

To understand the hydrogeological processes in tidal flats as the Zwin remnant, the hydraulic heads, the groundwater flow and the salinity distribution near a side branch of the main gully were studied. This was done by collecting hydraulic heads for four months using automatic data loggers, by collecting soil and groundwater samples and by executing electromagnetic induction measurements in six boreholes which were located in a line perpendicular to the coastline near a side branch of the main gully in the Zwin remnant. The collected data were then implemented in a 2D density dependent groundwater model to get insights in the hydrogeological processes. The observations showed that the gullies and their vicinities are very dynamic environments due to the influence of both the tides and the wind direction and wind speed. Both factors induce significant head fluctuations which result in a variable groundwater flow and salinity distribution. The resulting base groundwater flow varies due to longer period variations such as neap and spring tide with a supplementary effect due to the variation in wind direction and speed. Closer to the gully additional variations are present due to shorter semidiurnal tidal cycles. According to the 2D density depended groundwater model, the salinity distribution is less sensitive to the variable hydraulic heads and forms a typical salinity distribution with higher salt concentrations under the gully and intertidal areas and lower salt concentrations under the supratidal areas. Next to this, a typical fresh water tongue arises from the supratidal area towards the gully creating a brackish water lens under the intertidal area.

INTRODUCTION

The Zwin natural reserve is an important mudflat and salt marsh area near the Belgian - Dutch border. It consists of a narrow dune ridge which is breached over a length of ca. 250 meters. Through this inlet the seawater can enter the hinterland through a branched network of (narrow) gullies forming a so-called 'slufter'. In the middle ages the Zwin formed the main entrance to the city of Bruges but since, the Zwin has been silting up due to the reclamation of surrounding lands and, since the 1980's, due to the sand replenishment at the beaches of Cadzand and Knokke-Heist.

In the past, the groundwater flow near tidal gully's has been studied by numerous researchers, and although this mostly happened from an ecohydrologic angle and without the incorporation of the salinity distribution insights have been gained about the general groundwater flow near tidal gully's. Some other researchers (e.g. Mao et al. 2006; Werner and Lockington 2006; Lenkopane et al. 2009) did incorporate the salinity distribution while studying the groundwater flow near tidal gully's leading to new insights in the contribution of the topography and the tidal fluctuations in the distribution of salt/brackish water near tidal gully's. We believe however that not all contributing factors have been fully investigated so far. From our observations at the Zwin nature reserve it seems that both the wind direction and wind speed can have a significant influence on the hydraulic heads at different distances and therefore influence the groundwater flow and salinity distribution.

METHODS

For this study six shallow observation wells were placed perpendicular to the coastline near a side branch of the main gully. In these observation wells, hydraulic heads and electromagnetic induction measurements were executed as well as water samples were collected. The hydraulic heads were measured with automatic data loggers for four months and coupled to the registered weather parameters from the same period in order to obtain insights in the relation between both parameters and the periodical inundations in parts of the Zwin remnant. The executed electromagnetic induction measurements allowed us to derive the salinity distribution along a vertical cross-section along the observation wells. Finally, some soil samples were taken to determine the soil characteristics using ROSETTA (Schaap et al. 2001). All collected data were then implemented in a 2D density dependent groundwater flow model. For this model the MOCDENS3D code (Lebbe and Oude Essink 1999) was used. Visual MOCDENS3D (Vandenbohede 2007) was used as a postprocessor.

RESULTS

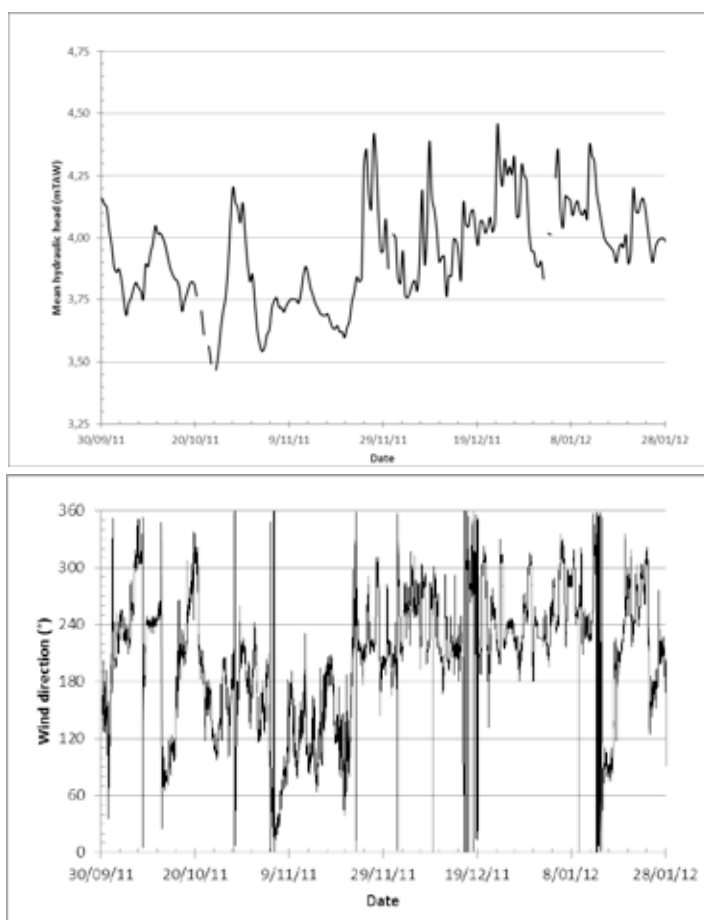


Figure 1 (upper): Mean hydraulic heads of observation well 1.

Figure 2 (lower): Registered wind direction at Zeebrugge.

From the analysis of the mean hydraulic heads of the tidal cycles two dominantly governing processes could be distinguished. The first one, observed during the whole observation period are the tides. During periods of full and new moon the observed hydraulic heads at all observation wells are clearly higher than at first and third quarter. The second process, which is (mainly) observed from 22 November 2011 until the end of the observations, is due the change in the dominating wind direction (Figure 2).

During longer periods of mainly westerly winds the average hydraulic head in the area will rise with up to 50 centimeters. The reason for this uniform rise lies in the fact that the wind forces an extra amount of water into the Zwin during high tide while it hampers water to flow out during low tide. Due to the morphology of the coast before the Zwin remnant parts of the wind generated surface waves are forced into the Zwin inlet during periods of mainly westerly winds therefore strengthening the inflow during high tide while diminishing the outflow during low tide. The relation between the wind direction and the registered hydraulic heads can be seen when comparing Figure 1 and Figure 2 from 22 November 2011 on. With the shift of the wind direction to 210-300° the average hydraulic head in observation well 1 rises with ca. 25-30 centimeters.

The frequency analysis of the observed hydraulic heads showed that the lunisolar synodic fortnightly signal is dominant in the study area with smaller contributions of the principal lunar semidiurnal and smaller solar elliptic signal. These signals have respectively a period of 14.765, 0.518 and 0.499 days. The first one is, together with the wind direction and speed, responsible for the base groundwater flow in the area, while the later ones are responsible for the supplementary variations closer to the gully.

Furthermore the electromagnetic induction measurements in the six observation wells showed that the groundwater reservoir is mainly filled with very brackish water with the exception of the upper few meters. Here, two areas can be distinguished. In the first one, which is located closest to the gully, periodical inundations occur leading to the presence of moderately brackish water in the upper few meters. In the area further away from the gully, the elevation is higher causing it to be inundated only very rarely. In this area brackish to moderately brackish water occurs above the very brackish water.

All collected data were implemented in a 2D density dependent groundwater flow model. For this model, a good fit was obtained with the observed hydraulic heads. The model showed that the hydraulic heads vary greatly within the considered period. Resulting in a clear outflow of groundwater to the gully at periods of low tides and inundations and infiltration at periods of high tide. The initial saltwater concentrations for the model were derived from the EM39 measurements as well as from earlier research by Lebbe and Courtens (2011). Despite the short modeling period (ca. 4 months) some changes in the saltwater distribution could be observed. Due to the mainly draining character of the gully the moderately salt water which was initially present under the gully has almost completely moved towards the gully. Besides this a typical water tongue has developed from the higher non (regular) inundated area towards the gully. This water tongue is similar to the one found under shores with gentle slopes and important tidal fluctuations before dunes with an important fresh groundwater flow towards the sea such as in De Panne (Vandenbohede and Lebbe, 2006).

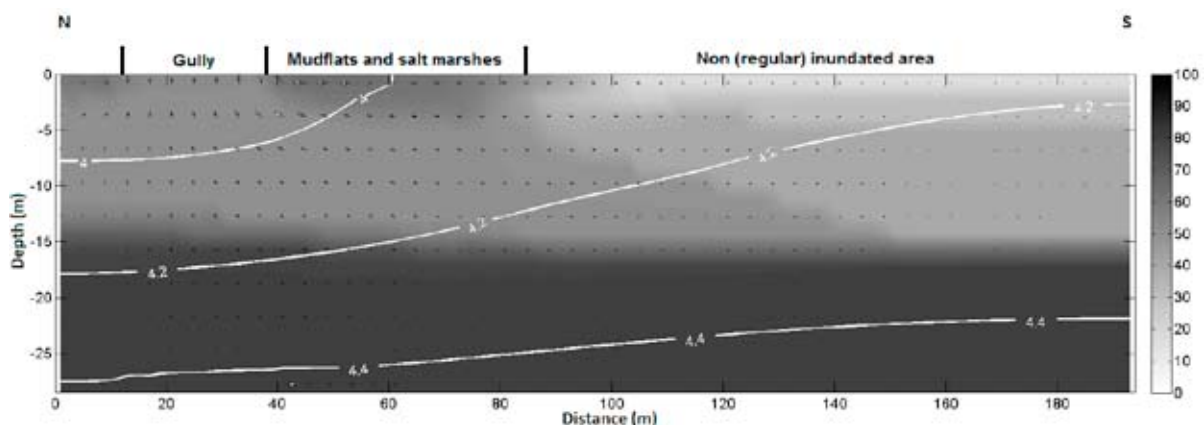


Figure 3: Modelled 2D cross-section through the observation wells. (Colour scale gives the saltwater percentages, black: 100% salt relative to North Sea water, white: 0% salt relative to North Sea water, white lines represent the contourlines of the hydraulic heads.)

CONCLUSIONS

The hydraulic heads at the Zwin remnant are not only governed by the variation in tides but also due to the wind direction and, to a lesser extent, by the wind speed. During longer

periods of mainly westerly winds the hydraulic heads in the area can rise with up to 50 centimeters. These changes are due to the morphology of the coast before the Zwin inlet. During periods of mainly westerly winds the wind forces an extra amount of water into the Zwin whereas it hampers the outflow during low tide. During longer periods without, or with very few, westerly winds the inverse occurs. The wind speed strengthens or weakens this process.

The conducted groundwater model allowed the simulation of the groundwater flow in the vicinity of the gully. The heads in the phreatic aquifer showed complex fluctuations which are induced by the water level fluctuations in the gullies and by the periodical inundations of parts of the adjacent mudflats and salt marshes. The head fluctuations result in a groundwater flow which varies strongly in time. The base groundwater flow depends mainly on the longer period variation in spring and neap tide with a supplementary effect due to the prevailing wind direction. This supplementary effect is caused by the drop in the water levels in the gully and the vicinity of the gully in periods where the prevailing winds differs from the dominant (south) westerly winds. Closer to the gully additional variations in the groundwater flow are visible due to the shorter semidiurnal tidal cycles.

REFERENCES

- Lebbe, L. and C. Courtens. 2011. Development of measures for mitigating the salinization in the adjacent polders due to the enlargement of the Zwin (in Dutch). Scientific report, GROMO.
- Lebbe, L., and G. Oude Essink. 1999. Section 12.11. MOC DENSITY / MOC DENS3D-code. 434-439, in Chapter 12. Survey of Computer codes and Case Histories.. Eds. Sorek, S. & Pinder, G.F. in: Seawater Intrusion in Coastal Aquifers, Concepts, Methods and Practices. Eds. Bear, J., Cheng, H-D, Herrera, I., Sorek, S. and Ouazar D. Kluwers Academic Publishers.
- Lenkopane, M., A. Werner, D. Lockington and L. Li. 2009. Influence of variable salinity conditions in a tidal creek on riparian groundwater flow and salinity dynamics, *Journal of Hydrology* 375 (3-4), 536-545.
- Mao, X., P. Enot, D.A. Barry, L. Li, A. Binley and D.-S. Jeng. 2006. Tidal influence on behaviour of a coastal aquifer adjacent to a low-relief estuary, *Journal of Hydrology* 327 (1-2), 110-127.
- Schaap, M.G., F.J. Leij, F.J. and M.T. van Genuchten. 2001. ROSETTA: a computer program for estimating soil hydraulic parameters with hierarchical pedotransfer functions, *Journal of Hydrology* 251 (3-4), 163-176.
- Vandenbohede, A. 2007. Visual MOC DENS3D: visualization and processing software for MOC DENS3D, a 3D density dependent groundwater flow and solute transport model. User Manual. Research Unit Groundwater Modeling, Ghent University.
- Vandenbohede, A. and L. Lebbe. 2006. Occurrence of salt water above fresh water in dynamic equilibrium in a coastal groundwater flow system near De Panne, Belgium, *Hydrogeology Journal* 14 (4), 462-472.
- Werner, A. and D. Lockington. 2006. Tidal impacts on riparian salinities near estuaries, *Journal of Hydrology* 328 (3-4), 511-522.
- Contact Information:** Gert-Jan Devriese, Ghent University, Department of Geology and Soil Science, Research Unit Groundwater Modeling, Krijgslaan 281, S8, 9000 Gent, Belgium. Phone: 09 2644664, Email: gertjan.devriese@ugent.be

Potential Consequences of Saltwater Intrusion at the German North Sea Coast for the water supply

Eley, M.¹, Howahr, M.², Schneider, A.³, Schöniger, H.M.¹, Ullmann, A.⁴, Wolf, J.² and Meon, G.¹

¹Leichtweiss Institute for Hydraulic Engineering and Water Resources, TU Braunschweig, Braunschweig, Germany

²Oldenburgisch-Ostfriesischer Wasserverband, Brake, Germany

³GRS Gesellschaft für Anlagen- und Reaktorsicherheit (GRS) mbH, Braunschweig, Germany

⁴Leibniz Institute for Applied Geophysics, Hannover, Germany

ABSTRACT

In order to assess possible impairments of the water resources at the coastal zone, an intensive analysis of possible degradation of water quantity and quality triggered by climatic and demographic change is necessary. For the coastal groundwater systems monitoring and protection of the water quality of freshwater reservoir are fundamental parts of the economic and social security and enhancements. An analysis of possible impairments helps to plan future investments in the water supply infrastructure and to guarantee a sustainable water supply for the near future.

The project NAWAK has started in 2013 and aims at examining the effects of climatic and demographic change on the coastal water supply, show impairments on both the supply and demand side of water systems for several pilot areas at the German North Sea coast in order to develop customized adaptation strategies for water supply companies. The expected project output is a planning tool based on a deterministic semi-distributed hydrological model (PANTA RHEI) coupled with a density-driven groundwater flow model (d^3f).

In the pilot areas where geophysical data are available they will be used to build up the geological model. For the modeling of the surface and groundwater hydrology the focus lies on the definition and derivation of the hydraulic and hydrologic boundaries like recharged water, drainage of wet lands and marsh and the spatial freshwater-saltwater boundary in the subsurface. Recharge of freshwater to the coastal groundwater system increase groundwater levels and hence hydraulically controls the movement of the freshwater-saltwater interface. In other words: groundwater recharge is acting as a hydraulic barrier towards saltwater intrusion. If the freshwater is drained from the area by the network of canals and ditches this barrier is impaired. This submarine groundwater discharge (SGD) is important to the coastal environment from a hydrological as well as environmental point of view. The applications of both project models shall provide the freshwater component of SGD and appropriately simulate the flow in the part of the coastal aquifer upstream of the saltwater intrusion area. In this contribution the project NAWAK is presented with focus on strategy for modeling of surface and groundwater hydrology and on possible options to mitigate sea water intrusions, e.g. by adapting groundwater withdrawal, e.g. by shifting of sensitive pumping wells, changing the delivery depth as well as increasing groundwater recharge by the means of rainwater collection basins and reduction of drainage of surface water.

1 INTRODUCTION

The development of an effective planning tool of the coastal aquifers at the German North Sea coast requires the use of two physical based hydrological models to assess present and

alternative exploitation scenarios, taking into account not only technical aspects but also economic, legal and political ones. While the d³f-code simulates the hydrodynamic and hydrochemical evolution of the regional aquifer, the semi-distributed surface hydrology program PANTA RHEI calculates the groundwater recharge from actual infiltrated precipitation water and the hydrological impacts of open drainage canal network. The dense network of drainage canal networks has been observed to have a significant quantitative effect on the fresh water balance respectively the freshwater recharge. Otherwise this network of watercourses is necessary to drain the agricultural basin. The management tool works with specified targets and options of the regional water suppliers and other stakeholders (for example the mentioned requirements on the drainage networks). These targets and options provide important inputs to the computed scenarios and generate finally the decision matrix within the planning tool.

2 METHODS

2.1 Hydrogeological modeling

The geological models introduced here were developed by processing geologists using the integrative software GSI3D[©] (since 2014: SubsurfaceViewer MX[©]). The GSI3D[©] methodology is based on the construction of close-meshed geological cross-sections and the definition of distribution boundaries for all model units found in the sections (Sobisch, 2000).

With the help of this software, all significant surface and subsurface data capable of being digitalized and geo-referenced such as boreholes, geophysical and geochemical investigations, geological (among other) maps, isoline maps and digital terrain data could be integrated in the course of iterative cross-section construction. In addition, the emerging models were complemented with old analogue hand-drawn sections and in some cases with already existing 3D data such as gOcad-TINs, ESRI-, Surfer- and GeoObject-Grids (ascii) etc. All input data are for the first time be interpreted in a three-dimensional context and tested for plausibility before being processed into the hydrogeological model.

On the basis of the constructed cross-sections and the associated layer distribution boundaries a 3D subsurface model was developed with a total area of 1,014 km². This model is based on a consistent network of 222 (so far) individual geological cross-sections for which in total more than 11,000 boreholes and geoelectric measurements were available.

2.2 Groundwater recharge

PANTA RHEI is a conceptual water balance model that describes the hydrological processes in a deterministic way. Furthermore, some sub-processes such as soil water and the snow module can be calculated physically-based. The model is the result of many years of development of hydrological models at the Institut für Wassermanagement GmbH and the Leichtweiß-Institut für Wasserbau of the TU Braunschweig (Meon et al. 2012).

PANTA RHEI is based on the assumption of nearly hydrologically similar units that result from the intersection of soil properties, land use and the surface watersheds. The meteorological input variables such as effective precipitation, solar radiation, wind and temperature are regionalized by a grid-method. The runoff generation is divided in three storages (see fig. 1). The upper two storages are influenced by root water uptake and evapotranspiration. The third storage is unaffected, so the outflow can be interpreted as groundwater recharge (Kreye et al. 2012, Eley 2013). The groundwater recharge is calculated with a time discretization of one hour for each part area and represents an essential input parameter for the groundwater model (see 2.3). In the module of runoff

concentration the temporal extending is calculated in four storages without interactions. All storages are treated as single linear reservoirs. For model calibration, the total outflow is fitted to the measured values at the basin level. In addition to runoff calibration then the model should be calibrated via a transfer function to the ground water levels.

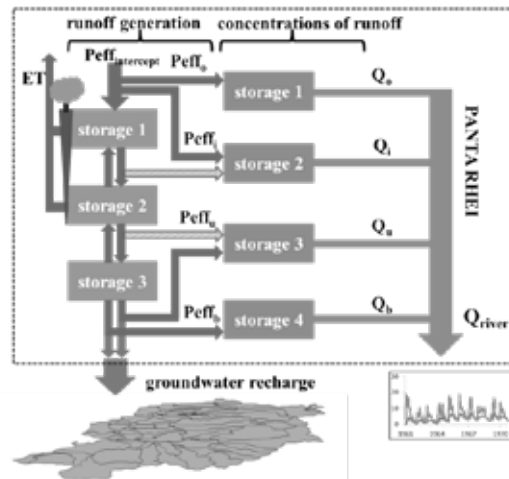


Figure 1. Structure of the conceptual model PANTA RHEI based on single linear storages with runoff generation and concentration of runoff (P_{eff} : precipitation, Q : runoff, ET: evapotranspiration) (changed according to Kreye et al. 2012).

2.3 Density-driven flow modeling

The finite volume code d³f (distributed density driven flow) has been developed with a view to the modelling of large, complex, density-influenced aquifer systems (Fein 1999, Schneider 2012). The use of cutting-edge numerical methods and their parallelisation enable simulations over long time periods with feasible computational effort.

Based on the hydrogeological model (see 2.1) a regional 3d density-driven flow model will be set up, including pumping wells of the waterworks and groundwater recharge provided by PANTA RHEI (2.2.). Scenarios to be simulated are sea-level elevation as a consequence of climate change, shifts of the seasonal distribution of precipitation and changes in the fresh water demand caused by demographic and economic factors.

For now, a 2d vertical cross section is extracted and adapted for d³f. Simulations are started with the objective of getting acquainted with the hydraulic processes in the model domain as well as testing the interaction of the various features and instruments.

2.4 Airborne electromagnetics

The geological model will be verified using geophysical data (Kirsch and Wiederhold 2014). Especially airborne electromagnetic data deliver a good database for locating the saltwater-freshwater boundary and for interpolation between boreholes. Siemon et al. (2014) give an example of clay mapping and thus mapping of low permeable layers. Deus and Elbracht (2014) show the freshwater-saltwater mapping and thus mapping of paleohydrological structures. Both works are close to the project areas of NAWAK. To overcome misinterpretations detailed data analysis and constrained inversion of the electromagnetic data is necessary and planned (Burschil et al. 2012).

3 OUTLOOK

The project NAWAK is in progress. The goal is an exactly replica of spatial and temporal dynamic of the density driven saltwater transport and the development of a planning tool

based on a generated (computed) decision matrix. Innovative is the haunted modeling concept as the kernel of the planning instrument. That is the basis for every scenarios of climate change with impact of sea-level rise and groundwater recharge. The results are adaption strategies for the regional water utilities and the water management, e.g. the relocation of wells, adaption of pumping rates, shifting of filter sections, changing of land use and adaption of drainage management.

REFERENCES

- Burschil, T., H. Wiederhold and E. Auken. 2012. Seismic results as a-priori knowledge for airborne TEM data inversion - a case study. *Journal of Applied Geophysics* 80: 121-128.
- Deus, N. and J. Elbracht. 2014. 3D-Modelling of the salt-/fresh water interface in coastal aquifers of Lower Saxony (Germany) based on airborne electromagnetic measurements (HEM). In *Proceedings of the 23rd Salt Water Intrusion Meeting*, Husum, Germany.
- Eley, M. 2013. Angewandte Kopplung zweier Prozessmodelle zur Beschreibung der wasserwirtschaftlichen Verhältnisse in einem norddeutschen Grundwassereinzugsgebiet. Masterarbeit (unveröffentlicht). TU Braunschweig. Leichtweiß-Institut für Wasserbau.
- Fein, E. and A. Schneider (eds.). d³f—Ein Programmpaket zur Modellierung von Dichteströmungen. FKZ-02 C 0465 379, final report. Gesellschaft für Anlagen- und Reaktorsicherheit (GRS) mbH, GRS-139, Braunschweig 1999.
- Kirsch, R. and H. Wiederhold. 2014. Saltwater intrusions - a challenge for geophysics. In *Proceedings of the 23rd Salt Water Intrusion Meeting*, Husum, Germany.
- Kreye, P., M. Gelleszun and G. Meon. 2012. Ein landnutzungssensitives Bodenmodell für die meso- und makroskalige Wasserhaushaltsmodellierung. In: M. Weiler (Hg.): *Wasser ohne Grenzen* (31).
- Meon, G., K. Förster, M. Gelleszun and G. Riedel. 2012. Zukünftige Entwicklung von Wasserhaushalt und Hochwasser. In: NLWKN (Hg.): *Globaler Klimawandel. Wasserwirtschaftliche Folgeabschätzungen für das Binnenland. Oberirdische Gewässer* (33).
- Schneider, A. (ed.): Enhancement of d³f und r³t (E-DuR). FKZ 02 E 10336 (BMW), final report, Gesellschaft für Anlagen- und Reaktorsicherheit (GRS) mbH, GRS-292, Braunschweig 2012.
- Siemon, B., W. Voß, J. Elbracht, N. Deus and H. Wiederhold. 2014. Airborne clay mapping at the East Frisian coast. In *Proceedings of the 23rd Salt Water Intrusion Meeting*, Husum, Germany.
- Sobisch, H.-G. 2000. Ein digitales räumliches Modell des Quartaers der GK25 Blatt 3508 Nordhorn auf der Basis vernetzter Profilschnitte. Shaker Verlag, Aachen.
- Contact Information:** Malte Eley, Technical University of Braunschweig, Leichtweiß Institute for Hydraulic and Water Resources Engineering, Dept. Hydrology, Water Management and Water Protection, Beethovenstr. 51a, Braunschweig, NI 38106 Germany, Email: m.eley@tu-braunschweig.de

Salt Water Intrusion into the Tertiary Aquifers in North Qatar Peninsula, Arabian Gulf

Elnaiem A. E.

Environmental Studies Center (ESC), Qatar University, Doha, Qatar

ABSTRACT

The State of Qatar is located in an arid zone and is surrounded by seawater from three directions North, East and West. Therefore, Qatar as a peninsula is suffering from salinization of groundwater in its coastal zone as most of the similar coastal areas in the world.

The excessive pumping and overexploitation of the limited groundwater resources resulted in a remarkable deterioration of groundwater in terms of quality and quantity due to the ingress of saline water into the two main carbonate aquifers.

This research was an effort focussed on the mitigation of groundwater problems in a farming zone in north Qatar due to saltwater intrusion. Geological, hydrogeophysical and hydrochemical investigations were conducted along two profiles more or less parallel in an area at the eastern coastal side of the country.

Special emphasis was paid to monitor saltwater intrusion phenomena in the study area, to make a historical review and comparative study to determine whether the problem is increasing or decreasing further, and to identify the influence of saltwater intrusions on the aquifers sustainability.

Contact Information: Elnaiem A. E., Environmental Studies Center (ESC), Qatar University, Doha, Qatar

Email: elnaiem@qu.edu.qa, www.qu.edu.qa

A geophysical approach for mapping and quantifying near-surface freshwater-saltwater transitions

E. Erkul¹, M. Henneberg¹, D. Wilken¹, M. Gräber², J. Scholten¹ and W. Rabbel¹

¹ Institute of Geosciences, Christian-Albrechts-Universität zu Kiel

² GeoServe Angewandte Geophysik

ABSTRACT

Geophysical prospecting of the freshwater-saltwater transition has been carried out successfully since the 1950s by mapping the spatial distribution of the specific electrical resistivity of the underground. Zones of saline or brackish groundwater could be reliably detected onshore by geoelectric depth sounding because the bulk electric resistivity of sediments is essentially determined by the electric resistivity of the pore fluid, which depends on ion concentration or salt content.

Geoelectric sounding and electrical resistivity tomography (ERT) are reliable tools for identifying zones of saltwater intrusion or groundwater discharge in a qualitative sense. In order to assess the layer resistivity in more quantitative way stratigraphic information on layer thicknesses have to be considered as additional constraints in the tomographic computations. These stratigraphic constraints can be determined by both drilling and geophysical measurements with other than geoelectrical methods. We are presenting a number of examples where additional seismic and ground-penetrating radar (GPR) measurements and stratigraphy derived from drillholes contributed to significantly improving the ERT results. Also, resistivity mapping by the electromagnetic induction (EMI) method was integrated for better areal coverage. The methodical improvement concerned basically the reliability of the determination of layer resistivity that could be converted into an estimate of pore water salinity. The results were validated by values of electric resistivity of pore water probes obtained from shallow drillholes.

Field examples from three different sites are shown demonstrating how the combination of geophysical prospecting and drilling can improve the investigation of freshwater-saltwater transition in shore areas: (1) An example of freshwater discharge that has led to a freshwater lagoon near the village of Laboe (Germany) on the Baltic Sea; the site was investigated with drillings and an amphibic geoelectric survey covering both on- and offshore profiles; (2) an example of saltwater intrusion near the village of Araxos (NW Peloponnes, Greece) where ERT, seismic and GPR were applied in order to obtain reliable quantitative results on stratigraphy and pore water salinity; (3) the shore area of a freshwater lake near Stymphalia (NW Peloponnes, Greece) where a combination of ERT, EMI and drilling was applied in order to explore the underground pore water distribution.

Managing salt water intrusion impacts in Bangladesh

M. Vogels¹, **M. Faneca Sanchez**¹, G.M.C.M. Janssen¹, and G.H.P. Oude Essink¹

¹ Department of Soil and Groundwater Systems, Deltares, Utrecht, The Netherlands

ABSTRACT

Bangladesh, being located on the Northern coast of the Bay of Bengal in South Asia, is majorly characterized by the delta of the Ganges and the Brahmaputra. Tropical monsoons, floods and cyclones occur frequently in this low-lying deltaic area. The combination of rapidly increasing anthropogenic activity and climate change increases the pressure on its coastal groundwater system and increases the magnitude of salt water intrusion. Within the BRAC WASH II (Water Sanitation and Hygiene Services) programme, the SWIBANGLA project (short name for this project) was launched. SWIBANGLA aims to update current Water Safety Plans to manage salt water intrusion impacts in Bangladesh. Part of this project is to create a 3D numerical variable-density groundwater flow and coupled solute transport model of the coastal groundwater system in Bangladesh. This model was built using SEAWAT in combination with the iMOD interface. The results of the model will be used to list key components for guidelines regarding the management of saline groundwater in the Water Safety Plans.

INTRODUCTION

In Bangladesh, saltwater intrusion is threatening drinking water resources on a large scale and is therefore confronting the population with a serious health issue (figure 1). This process has not been studied intensively in this country and has not been well recognized as a health threat yet. The guidelines used in Bangladesh to deal with drink water and sanitation technologies are incorporated in so-called Water Safety Plans (WHO, 2005, 2006, 2009, 2010). These plans mostly focus on bacterial contaminants and arsenic, and they do not take into account groundwater contamination due to salt water intrusion issues. The SWIBANGLA project aims to gather the knowledge on the groundwater system and its dynamics in order to make suggestions on the improvements of the Water Safety Plans.

Achieving the proposed project goals is a challenge that demands an integral approach. Combining technical knowledge and participative processes that increase the knowledge and awareness in the area set the framework of the project. Therefore, we developed an approach linking fact finding missions to Bangladesh, data collection, model development, monitoring workshops and participative groundwater management workshops targeting the main stakeholders.

We started with a fact finding mission to make an inventory of the main stakeholders, the available knowledge and data, and the stakeholders' main concerns and needs regarding the matter of salt water intrusion. This mission provided the project team with a basis of information and contacts that were used to analyze the groundwater system and define a conceptual model. This model was transformed into a 3D numerical variable-density groundwater flow and coupled solute transport model, used to increase the understanding of

the system, to support water resources management and to simultaneously support future research projects.

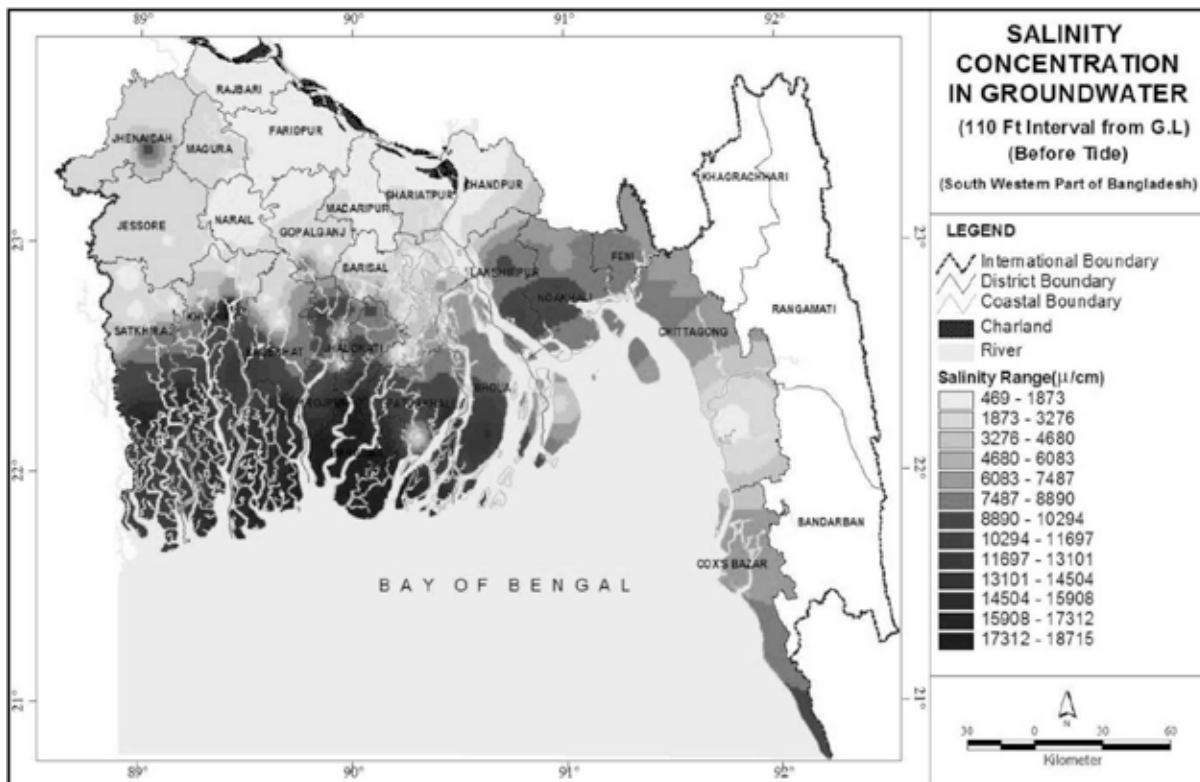


Figure 1: EC map at 35 meters depth established by the Bangladesh Agricultural Development Corporation (BADC, 2011) based on 100 observation wells with salinity measurements at a 10ft interval.

METHODS

The model was built using an adapted version of SEAWAT which supports iMOD (www.imod.nu) functionality. iMOD’s user interface and modelling philosophy both significantly simplify the model building process as well as dramatically enhance the model’s transparency and accessibility in terms of input and output, for modellers as well as for stakeholders . The integration of SEAWAT with iMOD was partly developed within this project to facilitate and stimulate the use of the model by Bangladeshi authorities in the future for groundwater resources management. The 3D model is currently under development and is being built in collaboration with the project partners in Bangladesh (BRAC, DPHE and Jahangirnagar University Dhaka).

The model study focuses on the area south of the Ganges River and borders the Indian border in the West and the Bay of Bengal in the South, see Figure 2.

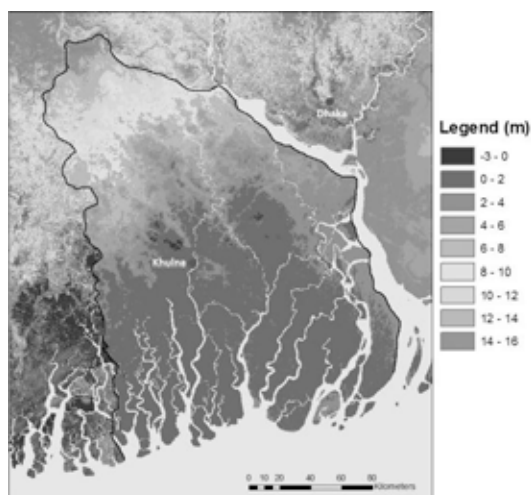


Figure 2: Illustration of total model domain and the area of interest (within black border) on a map showing the surface elevation.

The depth range of the model runs from 15m above sea level to 3000m below sea level, which is divided over 40 model layers. The horizontal model resolution is set at 1000m. The bottom of the model represents the low permeability Boka Bil formation, the first distinctive hydrogeological basis which is found at 3000m. Other boundaries are the general head boundaries at the northern and southern border of the model domain. The model's east and west borders are no-flow boundaries. The sequence of aquifers and aquitards for the model has been simplified according to the adopted profiles in previous studies (Michael, 2009). The reason behind this decision is the complex heterogeneity of the delta, which would require a complete study, not achievable within this project. The model incorporates seasonality by applying three stress periods for the surface system (rivers, precipitation and evapotranspiration), which simulates the three distinct seasons in Bangladesh: 1) a cold dry winter from November to February, 2) a humid hot summer from March to May and 3) a cool rainy monsoon season from June to October. Two stress periods are applied on part of the groundwater abstractions to simulate the differences in irrigation magnitude between the dry and the wet season.

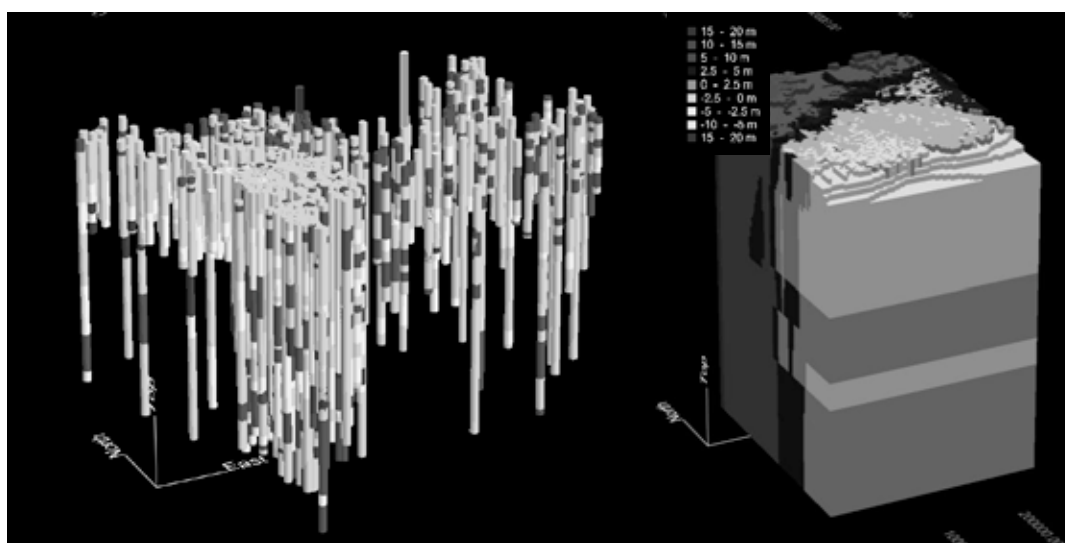


Figure 3: 3D images of the input data for the model visualized and managed with iMOD-SEAWAT. a: 3D visualization of the collected borehole dataset. b: Point water heads in a subdomain of the modeled area.

RESULTS

The current state of the model is that of fine-tuning the water balances and the fresh-salt distribution. This will be followed by performing several impact studies, for example a rising sea level scenario. Mitigation techniques will be implemented in the model and their effects and efficiency will be assessed. The model will give a better understanding in the water fluxes and solute transport of this central Bangladesh coastal groundwater system and will provide a tool to monitor the system and identify potential risks, now and in the future.

ACKNOWLEDGEMENTS

The authors wishes to thank Holly Michael of the University of Delaware, USA, for sharing data and ideas of concepts of the hydrogeological coastal system of Bangladesh.

REFERENCES

Arsenic Policy Support Unit, 2006. Experiences from pilot projects to implement water safety plans in Bangladesh. Arsenic Policy Support Unit, Dhaka, Bangladesh

BADC, 2011. Identification of Underground Salinity Front of Bangladesh.
http://www.badc.gov.bd/files/Salinity/Salinity_Front.pdf

Michael, H.A., Voss, C.I., 2009. Controls on groundwater flow in the Bengal Basin of India and Bangladesh: regional modeling analysis, Hydrogeology Journal, Vol. 17, Iss. 7, pp. 1561 – 1577.

WHO, 2005. Water Safety Plans: Managing drinking-water quality from catchment to consumer. WHO, Geneva.

WHO, 2006. Reducing salt intake in populations: report of a WHO forum and technical meeting, 5-7 October 2006, Paris, France.

WHO, 2009. Water Safety Plan Manual: Step-by-step risk management for drinking-water suppliers. WHO, Geneva.

Contact Information: Marta Faneca Sanchez, Deltares, Groundwater Management Department, 6-8 Princetonlaan 3584 CB Utrecht, The Netherlands Phone: +31 (0)88 335 7775
Fax: +31 (0)88335 7856, Email: marta.faneca@deltares.nl

MODELING OF GYPSUM DISSOLUTION DRIVEN BY VARIABLE DENSITY FLOW IN THE COASTAL KARST AQUIFER OF LESINA MARINA (SOUTHERN ITALY)

Maria D. Fidelibus¹, Claudia Campana²

¹ DICATECh, Politecnico di Bari, Bari, BA, Italy

² Autorità di Bacino della Puglia, Valenzano, BA, Italy

ABSTRACT

The application of a combined *reactive transport - density dependent flow model* to a real gypsum coastal aquifer (Lesina Marina, Southern Italy) is presented, with the aim of evaluating the potential of gypsum dissolution on sinkholes development. The area has been in fact highly susceptible to hazardous and rapid sinkhole formation since 1927, when a canal was excavated in an evaporite formation, strongly modifying groundwater flow patterns. To achieve this aim, firstly a conceptual model is defined, then a density-dependent, tide-influenced, flow model is set up and solved by means of the numerical code SEAWAT. Finally, the resulting transient flow field is used by the reactive multicomponent transport model PHT3D to estimate gypsum dissolution rate. The multi-disciplinary approach indicates that sinkhole formation in the Lesina Marina area, during the last 90 years, is scarcely connected to recent gypsum dissolution; rather, it is related to the erosion of paleo-cavities filling material (*suffosion*), caused by the new hydrodynamic conditions induced by the excavation of the canal within the evaporite formation.

INTRODUCTION

Evaporites are the most soluble rocks, which dissolve to form karst features such as those typically found in limestones, though in a shorter time. Even if the studies of Sanford and Konikow (1989) and Rezaei et al. (2005) focus on hypothetical and simplified conditions, they provide important insights into dissolution processes in carbonate coastal aquifers by using a combined geochemical-hydrodynamic modeling approach.

This study deals with the first application of a reactive transport model coupled with a variable-density groundwater flow model to a coastal gypsum aquifer, with the purpose of ascertaining time evolution of sinkholes. Numerous geochemical and hydrological data were collected both to build and validate the model. The study-site, the Lesina Marina residential area (Puglia, Southern Italy; Figure 1) is located between a lagoon and the seacoast. The Acquarotta Canal connects the Lesina lagoon to the sea: it was excavated in 1927 in an evaporite formation, changing groundwater flow patterns in the area. Since the canal was excavated, sinkholes have developed exponentially over time.

FIELD DATA INTERPRETATION

The conceptual model for the Lesina Marina study area (about 1 km²) is based on field studies carried out between 2008 and 2012 and on previous studies (Fidelibus et al., 2011). Of the 131 drillings with core recovery for stratigraphic and petrographic aims, 41 were equipped as monitoring wells for groundwater hydraulic head measure (Figure 1) and sampling. A geochemical survey along a transect (Figure 1) was completed in 2012.

Based on information from cores, the lithological succession was simplified defining only two main hydro-stratigraphic units: a sandy cover and the evaporite bedrock. Groundwater level monitoring data provide evidence that the main flow direction is towards a few breaks realized for environmental reasons in the '90s during maintenance works on the left bank cover of the canal. Indeed, the excavation of the Acquarotta Canal in the evaporite bedrock caused changes in the original groundwater flow rate and direction: the canal, working as a drain, induced an amplification of the groundwater level oscillation due to sea tide. Finally, the hydrochemical study led to evidence that gypsum dissolution is an active process influenced by concurrent processes, and that freshwater-seawater mixing enhances gypsum dissolution, moreover inducing ion-exchange, whose direction is influenced by hydrodynamic conditions.



Figure 1: Lesina Marina study area: sinkholes (last updated in March 2012) and monitoring wells locations; white dashed line shows the model transect

MODEL DEVELOPMENT

Assumptions of the conceptual model

The relevant domain chosen to represent the study-area is a 2D vertical transect (Figure 1), corresponding to a main flowline. Within the model transect there are an internal boundary (Acquarotta Canal, controlling the aquifer hydrodynamic regime with its level oscillations), and two external boundaries, landward and seaward. Both the two selected hydro-stratigraphic units can be modeled implementing the equivalent continuum model, since for the chaotic evaporite bedrock in particular, a discrete fracture network model does not seem practical: the complexity of the system “drowns” local variations so that a whole description is impossible. In coupling hydro-geochemistry and transport driven by groundwater flow, we assumed local equilibrium conditions (LEA) and isotherm conditions. As a consequence, viscosity and density dependence on temperature can be neglected. Therefore, the density equation of state assumes the form of the empirical relation developed by Baxter and Wallace (1916).

Simulation codes, temporal and spatial discretization, initial and boundary conditions, hydrogeological properties

The modeling consisted of three phases. During the first phase the aquifer was assumed to be initially filled with fresh groundwater: subsequently, a 200-yr transient simulation using SEAWAT Version 4 (Langevin et al., 2008) followed in order to define saltwater and

freshwater equilibrium as initial conditions for the following phase. The second modeling phase encompasses high temporal resolution to simulate the effects of tidal fluctuations and their propagation through the aquifer for 356 days and 19 hours. Dirichlet boundary conditions were also used for this second phase; however, the prescribed values changed in time based on observed data (hourly data for the 2010-2011 period). The transient flow field resulting from SEAWAT simulation was used as advective input for the third modeling phase of reactive transport. For this simulation, the chemical composition of groundwater and the mineral composition of the aquifer rocks were added as initial information; following this, chemical reactions, together with transport of aqueous species, were implemented by PHT3D code (Prommer et al., 2003) that couples the transport simulator MT3DMS and the geochemical modeling code PHREEQC-2.

The two-dimensional model grid consists of 332 columns (widths from 4 to 1 m) and 23 layers, each 1.29 m thick, except for the top layer: the bottom of layer 1 is set lower than the minimum expected groundwater level to avoid wetting and drying complications in the model. A type of “zone continuum model” (Langevin, 2003) was developed to define hydrogeological properties. Five discrete zones of different permeability were identified within the gypsum layer on the basis of the core data; their properties were calibrated on observed data. With the aim of introducing tidal boundary conditions, the surface water bodies (canal and sea) within the transect were explicitly simulated by using the “high-K approach” (Mulligan et al., 2011).

RESULTS

Results from the simulation steps are compared with experimental data collected at observation wells located within the model domain. For the tide-influenced model, simulated groundwater level fluctuations in observation wells were compared to monitoring data for the entire simulation period (about 1 y): observed and modeled data are in good agreement. The observed TDS concentration distribution is also satisfactorily reproduced by the model. The reactive transport model outcomes are the distributions of chemical species within the model domain, resulting from simulated water-rock interactions. For solid phases, i.e. minerals composing the geological formations, the results after the 1-y simulation of tidal effects on the coastal aquifer are interesting in terms of concentration variations between initial equilibrated and final conditions. Because of LEA and its inconsistency with precipitation kinetics, model results for the most permeable zone close to the canal should be considered highly uncertain and underrated. Apart from this zone, model results for gypsum seem to characterize the expected processes: negative deltas (gypsum dissolution) correspond to the freshwater-saltwater transition zone, towards the freshwater side.

DISCUSSION AND CONCLUSIONS

We can express the simulated gypsum dissolution rate in terms of porosity change in the adopted time unit (years). The porosity change rates within the model domain (Figure 2) suggest that the dominant evolution time of gypsum dissolution is much greater than a human lifetime. The zones where the rate is higher correspond to the transition zone: this explains the presence of paleo-cavities within the evaporite formation, linked also to eustatic sea level changes. For the convective canal surroundings, the model gives the highest rate of porosity development, together with highly underestimated values (due to gypsum precipitation).

Hence, the model results indicate that sinkhole development in the Lesina Marina area is scarcely connected to recent gypsum dissolution. Rather, it is related to *suffosion* (erosion of paleo-cavities filling material) due to changes in hydrodynamic conditions induced by the canal. On the contrary, modeling results indicate the canal surroundings as the most critical zone for gypsum dissolution: however, there the model does not reproduce real geochemical behavior as a whole, since chemical kinetics and feedback processes are not simulated.

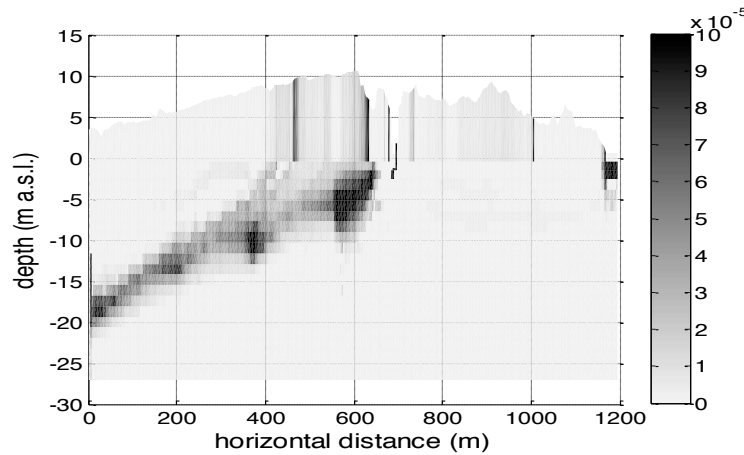


Figure 2: Porosity change in 1 year within the model transect

CITED REFERENCES

Baxter G.P. and C.C. Wallace. 1916. Changes in volume upon solution in water of halogen salts of alkali metals. II. American Chemical Society Journal 38: 70-104.

Fidelibus M.D., F. Gutierrez, and G. Spilotro. 2011. Human-induced hydrogeological changes and sinkholes in the coastal gypsum karst of Lesina Marina area (Foggia Province, Italy). Engineering Geology 118:1-19.

Langevin C.D. 2003. Stochastic Ground Water Flow Simulation with a Fracture Zone Continuum Model. Ground Water, Vol.41, No. 5: 587–601.

Langevin C.D., D. Thorne, A.M. Dausman, M.C. Sukop, and W. Guo. 2008. SEAWAT Version 4: A Computer Program for Simulation of Multi-Species Solute and Heat Transport. U.S. Geological Survey Techniques and Methods, Book 6, Chapter A22.

Mulligan A.E., C.D. Langevin, and V.E.A. Post. 2011. Tidal Boundary Conditions in SEAWAT. Ground Water, Vol. 49, No. 6: 866–879.

Prommer H., D.A. Barry, and C. Zheng. 2003. MODFLOW/MT3DMS-Based Reactive Multicomponent Transport Modeling. Ground Water, Vol. 41, No. 2: 1-11.

Rezaei M., E. Sanz, E. Raeisi, C. Ayora, E. Vázquez-Suñé, and J. Carrera. 2005. Reactive transport modeling of calcite dissolution in the fresh-salt water mixing zone. Journal of Hydrology 311: 282–298.

Sanford W.E. and L.F. Konikow. 1989. Simulation of calcite dissolution and porosity changes in saltwater mixing zones in coastal aquifers. Water Resources Research 25: 655–667.

Contact Information: Claudia Campana, Autorità di Bacino della Puglia, Str. Prov. per Casamassima, Km 3 - 70010 Valenzano, BA, Italy, Phone: 0039 080 9182224
 Fax: 0039 080 9182244, Email: claudia.campana@adb.puglia.it

Monitoring seawater intrusion by means of long-term series of EC and T logs (Salento coastal karstic aquifer, Southern Italy)

M. Dolores Fidelibus¹, L. Tulipano²

¹ DICATECh, Politecnico di Bari, Bari, Italy

² DICEA, Università Sapienza, Rome, Italy

INTRODUCTION

The objective of this work is to highlight the potentials of the Electrical Conductivity (EC) and Temperature (T) logs in seawater intrusion studies.

EC logs (though discontinuous) have been carried out during a 40 year period along wells (OWS) specifically drilled for the control of seawater intrusion in the karst coastal aquifer of Salento (Southern Italy). The OWSs belong to the Regional Monitoring Network (RMN), which was established in the nineties for the control of groundwater quantitative/qualitative status. The net is presently intended for the objectives of the FWD 2000/60/EC. All the wells of the network are accessible to multi-parametric probes and samplers. The geo-statistical elaboration of T logs gives the distribution of aquifer temperature.

EC LOGS IN OWS

The Salento peninsula, located at the SE edge of Italy, extends for about 3800 km². Miocene to Quaternary Transgressive covers overlay the largely outcropping Cretaceous limestone and dolomitic limestone basement. The coastal karst aquifer is mostly present at sea level. It is highly permeable due to fissures, fractures and karst; at regional scale it behaves as a porous aquifer. The hydraulic head varies from about 4 to less than 0.5 m AMSL (average hydraulic gradient of about 0.02 ‰). Precipitation is about 638 mm/yr, 132 mm/yr of which recharges the aquifer (yearly averages of last 50 years; Portoghese et al. 2013). Freshwater floats as a lens on saltwater of marine origin. Freshwater TDS varies between 0.2 and 0.6 g/L.

In the Salento Peninsula, groundwater demand has increased especially due to agriculture from the 1960, causing the progressive salinization of fresh groundwater: presently, ground waters with TDS>0.6 g/L are distributed in the entire coastal zone. The first research project concerning seawater intrusion in the Salento aquifer dates back to the sixties. There a net of observation wells reaching saltwater beneath freshwater was drilled and purposely equipped (Tadolini & Tulipano 1979). T-EC logs were regularly performed from 1970 up to 1986: afterward, monitoring went along with a few time gaps till 2011 under the responsibility of Puglia Regional Government.

Salento OWSs are suitable to represent the actual density stratification of groundwater: most OWSs are located in zones of horizontal flow and are screened along groundwater thickness, thus allowing the measure of the "environmental water head" (Luszczynski 1961; Post et al. 2007). In principle, timeline analysis of related EC logs allows outlining the evolution of groundwater salinization and (locally) quantifying the freshwater-saltwater equilibrium. TDS logs allow measuring freshwater thickness, position and thickness of transition zone, saltwater top and average TDS of fresh and transition thicknesses. Elevation of theoretical

sharp interface (TSI) and equivalent saltwater head (t_s) derive from density profiles (Tulipano and Fidelibus, 2002).

Till 1986 the EC-T logs were realized with different probes, prototypes of modern ones, purposely projected and designed at the time by the University research team. The EC-TDS-density conversion was followed through the measure of these parameters on a series of “standard” solutions obtained by mixing freshwater and saltwater sampled in each OWS. After 1986 the Regional Government used commercial probes. Thus, due to the large time span from the first to last monitoring survey (1970-2011), timeline analysis suffers of a few uncertainties due to variation in probes, calibrations and operators. However, if absolute values can be debatable, and notwithstanding the uncertainty in defining the real sea level elevation of reference for calculations (different from the zero topographic level), the trends over time of the TSI, the thickness of the complementary freshwater column (TFC), of the equivalent saltwater head (t_s) and the other measured and calculated parameters, provide a reliable picture of evolution of FW-SW equilibrium mostly related to the regime of exploitation and alternation of wet and dry years.

The trends of TSI and TFC (example for OWS LR, Figure 1) during the period 1974-2011, coupled with those of the annual heights of effective infiltration and irrigation (mm/yr), and with the index of groundwater stress (data from Portoghesi et al. 2013), allow highlighting the behavior of groundwater under variable climate. During 1987-1991, the GW stress index (moving average, Figure 1) increases up to 0.7 (severe stress) in 1990 in relation to the concurrence of the decrease of the effective infiltration down to a minimum of 38.2 mm/yr and the increase of irrigation up to 60.9 mm/yr (estimated through the soil moisture deficit method, with an average of about 34.1 mm/yr in the period 1950-2010, Portoghesi et al. 2013). Another peak of GW stress (moderate stress) occurs between 2000 and 2004.

Unluckily, OWS monitoring has two wide time gaps just during the periods of high GW stress: data on TSI are thus missing. However, 1995 and 1996 EC logs show that, following the first high GW stress, TSI moved upward of about 13 m with respect to the first TSI evaluation (1974). The sharp interface, despite the following increase of recharge, shows only a modest downward shift. After the second period of GW stress, TSI maintains roughly the previous elevation. In the whole monitoring period, the average TDS of the entire water column from water table up to the reference level, fixed into salt waters, obviously increases with the upwarrise of the sharp interface.

T LOGS IN THE RMN

T logs were carried out on the observation wells of RMN (location in Figure 2) each quarter during 1994-1997 and every six months between 2007 and 2012. The temperature distribution is of interest, especially in karst aquifers with low anisotropy ratio of hydraulic conductivity (k_h/k_v), for outlining preferential pathways, recharge areas and spatial extent of brackish and salt waters at regional scale (Fidelibus et al. 2011).

An example of horizontal section of the aquifer temperature (at -5 m AMSL) is shown in Figure 2: it has been obtained through a geo-statistical approach (variographical analysis and Ordinary Kriging) for the winter 1995. In the specific climatic setting, the recharge areas are identified by the lowest temperatures of thermal field (14°C); temperatures higher than 18°C signal zones of the aquifer with brackish and salt waters. The effect of the low anisotropy ratio, linked to the presence of vertical discontinuities and/or high permeability zones because of karstification, is clear from the vertical section SS' (Figure 2).

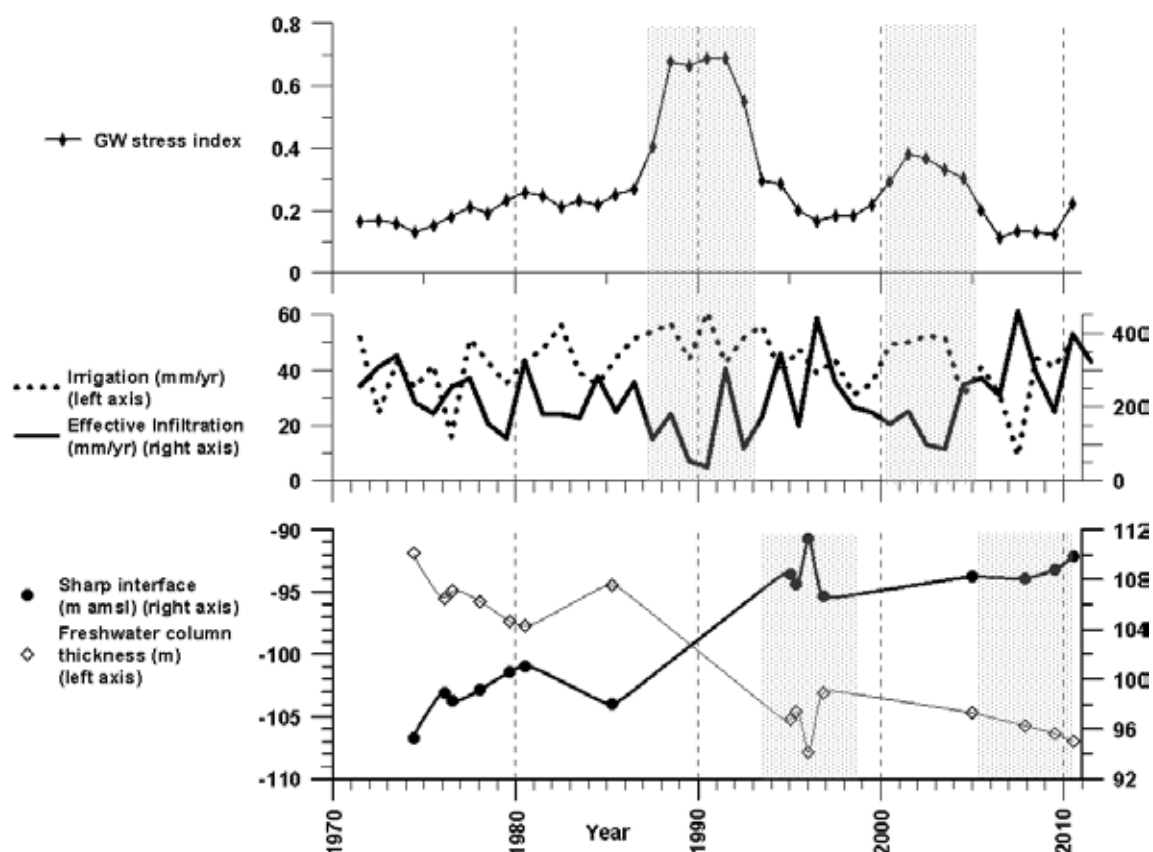


Figure 1. Groundwater Stress index (moving average), yearly irrigation and effective infiltration trends (data from Portoghese et al. 2013) compared to the tendencies of the sharp interface elevation and the freshwater column thickness during a 36 year period.

CONCLUSIONS

The timeline analysis of the trends of TSI and TFC, coupled with those referred to GW stress, irrigation and recharge, points out that, in semi-arid coastal areas with high exploitation of groundwater, the periods of low recharge (which go with drought periods and/or precipitation pattern changes) can have a decisive influence on the FW-SW equilibrium. In the selected case, even with monitoring gaps, a “critical transition” toward a new equilibrium can be observed: there are limited signs of recovery after the periods of GW stress. Human forcing and climate change do not promise any future improvement: on the light of climate change, Portoghese et al. (2013) forecast for the next 50 years even worse periods of GW stress, especially linked to the change of precipitation patterns.

A sensitivity analysis of the method of calculation of TSI shows that results are not so much affected by precise EC-TDS-density calibration or by a different reference point for calculation, how much from the “shape” of EC profiles, i.e. from the TDS distribution along the vertical of the saturated zone. This can be also demonstrated by other parameters, not shown here. Thus, a net of OWS can represent a good tool for describing the real “health” conditions of coastal groundwater. Obviously, in contexts other than that illustrated the TSI method should be tested and adjusted.

As to the temperature, it has to be emphasized that, apart from geo-statistical constraints, it represents an optimal natural proxy of the flow system, whose reconstruction is very critical in presence of variable density flow (Post et al. 2007).

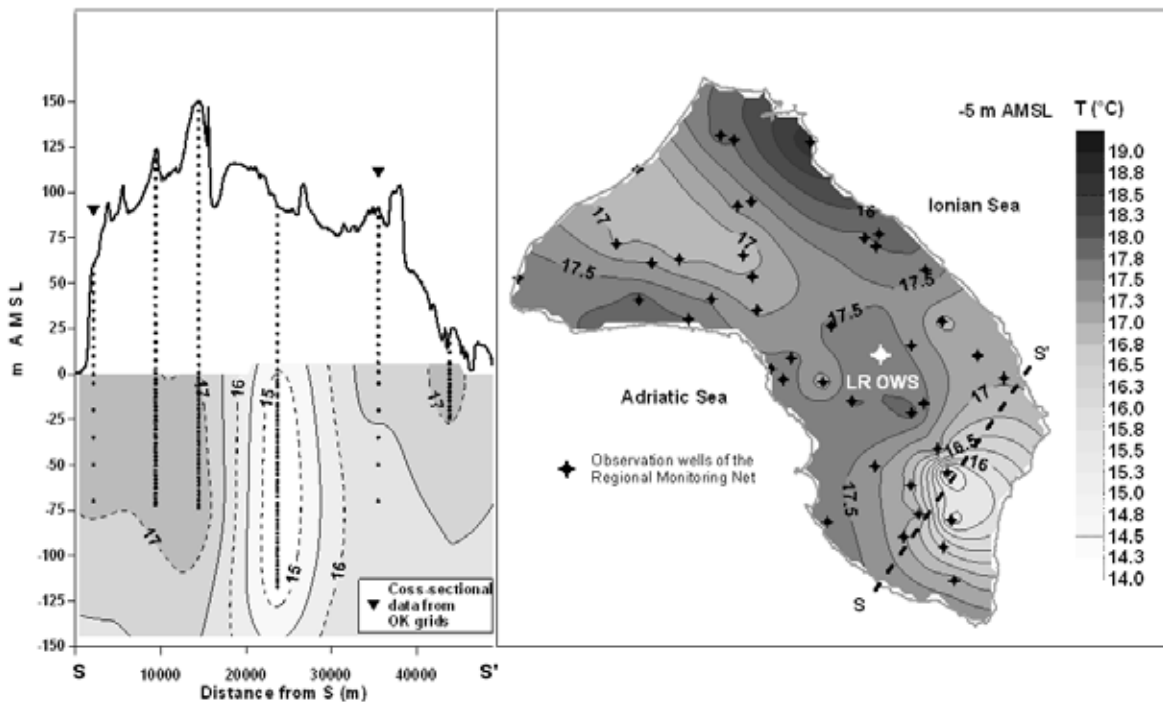


Figure 2 – Vertical section (S-S' trace) and horizontal section (-5 m AMSL) of aquifer temperature; location of Observation Wells of Regional Monitoring Net and of the LR OWS.

REFERENCES

Fidelibus M. D., Tulipano L, and P. D'Amelio. 2011. Convective thermal field reconstruction by ordinary kriging in karstic aquifers (Puglia, Italy): geostatistical analysis of anisotropy. In *Advances in Research in Karst Media*, Andreo B. et al.(Eds), Environmental Earth Series, vol. XX, 203-208, Berlin Heidelberg: Springer-Verlag, doi: 10.1007/978-3-642-12486-0_31.

Luszczynski, N.J. 1961. Head and flow of ground water of variable density. *Journal of Geophysical Research* 66, no. 12: 4247-4256.

Portoghese, I., Bruno E., Dumas P., Guyennon N., Hallegatte S., Hourcade J.C., Nassopoulos H., Pisacane G., Struglia M.V. and M. Vurro. 2013. Impacts of Climate Change on Freshwater Bodies: Quantitative Aspects. In *Regional Assessment of Climate Change in the Mediterranean*, Navarra A. and L. Tubiana (eds.), *Advances in Global Change Research* 50, Ch. 9, Springer, Dordrecht.

Post V., Kooi H. and C. Simmons. 2007. Using Hydraulic Head Measurements in Variable-Density Ground Water Flow Analyses. *Ground Water* 45, no. 6: 664–671.

Tadolini T. & L. Tulipano. 1979. The evolution of fresh water-salt water equilibrium in connection with drafts from the coastal carbonate and karst aquifer of the Salentine Peninsula (Southern Italy). 6th SWIM, Hannover (Germany).

Tulipano L. and M.D. Fidelibus. 2002. Mechanisms of groundwater salinization in a coastal karstic aquifer subject to over-exploitation. in *Procs. 17th SWIM*, Boekelman R.H. et al (Eds), 262-272, Delft (The Netherlands), 6-10 May 2002. ISBN 90-800089-8-2,

Contact Information: M. Dolores Fidelibus, Politecnico di Bari, DICATECh, 4 Via Orabona, Bari, IT 70125 Italy, Phone: +39 080 5963373, Fax: 305-555-5000, Email: mariadolores.fidelibus@poliba.it

The interrelation between multi layered aquifer and the sea, examples from Gaza and the Carmel coastal areas

Ghabayen S.¹, Weinstein Y.², Yaqubi A.¹, Herut B.³, Mushtaha, A. M.^{1,4}, Kristine Walraevens⁴, Yechieli Y.^{5,6}

1. House of Water and Environment (HWE), Gaza
2. Bar-Ilan University (BIU)
3. Israel Oceanographic and Limnological Research (IOLR)
4. Ghent University, Belgium
5. Geological Survey of Israel, Jerusalem, 95501
6. Ben Gurion University, Sede Boker

ABSTRACT

The interrelation between multi layered aquifer and the sea was studied in several locations in the coastal area of Gaza Strip (near Gaza city and near Rafah) and in the coastal area of the Carmel (Dor Bay).

In the Rafah area (southern Gaza Strip), the interface was found at very shallow depths in both upper sub-aquifers (~9 and 16 meters) at 150 m from the sea. The interface was sharp, especially in the confined unit, with the change from 20% to 90% seawater occurring within ~2 meters. Preliminary results show evidence for current seawater intrusion by the increase in the EC (Electrical Conductivity) of bottom water from 36 mS/cm to 48 mS/cm from January to June 2013, probably due to over-pumping in this area. Hydrological simulations were conducted with SEAWAT showing seawater intrusion in the different sub-aquifers in Gaza to be in 700-1100 m.

At Dor, several boreholes were drilled through three aquifer units, phreatic, semi-confined and confined (A, B and C, respectively), all within a section of 40 meters thick. In the confined units, the water level fluctuates tidally in phase with sea level, possibly indicating on good connection between the sea and the aquifers.

INTRODUCTION

The problem of salinization of coastal aquifers due to seawater intrusion is extremely severe in the east Mediterranean coastal aquifer, especially in the Gaza Strip. In several cases, the extent of the seawater intrusion reach a distance of more than 2 km (Mellol and Zeitoun, 1999) and still moving inland.

The relationship between the coastal aquifer and the sea depends on the hydraulic parameters of the aquifer and its connection to the sea, which can be studied by the response of the aquifer to tidal changes (e.g. Nielsen, 1980).

METHODS

Drilling was conducted in both regions to different depths in order to monitor the rate of seawater intrusion by tracking the location of the fresh-saline water interface in the various sub-aquifers.

The location of the interface was monitored by EC profiles. These measurements were conducted several times in order to follow the changes with time.

The effect of seawater intrusion in Gaza is farther studied by numerical simulation of different parts of the aquifer, using SEAWAT code.

The interrelation between multi layered aquifer and the sea was also studied by the effect of tide, using continuous data of water level in the Dor area (measured with divers). These data were compared to preliminary results of simulations in the different sub-aquifers using the FEFLOW code.

RESULTS

In the Rafah area (southern Gaza Strip), the interface was found at very shallow depths in both upper sub-aquifers (~9 and 16 meters) at 150 m from the sea. The interface was sharp, especially in the confined unit, with the change from 20% to 90% seawater occurring within ~2 meters (Fig. 1). Preliminary results show evidence for seawater intrusion by the increase in the EC of bottom water from 36 mS/cm to 48 mS/cm from January to June 2013. The boreholes in Gaza showed an interesting pattern of increasing nutrient concentrations (mainly nitrate) with salinity (=depth), which is the opposite trend of that anticipated and observed further north, along the Israeli coast. This should be further studied.

The simulations in Gaza were conducted for a model domain in south Gaza (Rafah and Khan Yonis; Fig. 2, 3). The transient simulation for the salinity of the shallow phreatic aquifer indicate that the seawater concentration extend to 700 meters inland while in the deep confined aquifer it extends to 1100 meters inland (Fig. 4).

At Dor, the boreholes were drilled through three aquifer units, phreatic, semi-confined and confined (A, B and C, respectively). In B, a two-step interface was found between 15-21 m and bottom water reached 60% seawater salinity. In the confined C, bottom water reached >90% seawater salinity, and the interface was sharp, at 36-38 m. In the semi confined unit (B), the water level fluctuates tidally in phase with sea level, possibly indicating on good connection between the sea and the aquifers. Interestingly, the hydraulic head in C is 50 cm higher and its tidal amplitudes are somewhat larger than in the shallower unit B. EC was also found to fluctuate in response to tide. Preliminary simulations imply good connection of the semi confined aquifer (B) according to the relatively fast response to the sea tide (Fig. 5).

DISCUSSIONS AND CONCLUSIONS

The hydrogeological relations between coastal aquifer and the sea are quite complex both in Gaza and Dor area due to the division of the aquifer into several sub-aquifers.

The increase in salinity in the Rafah area is probably due to over-pumping which is expected to enhance seawater intrusion. This needs to be farther studied to rule out seasonal effects. The simulations show intrusion to a distance of ~ 1000 meters which is expected to increase due to the extensive over pumping in Gaza Strip.

The good connection between the different sub-aquifers and the sea was exhibited in the Dor area by the relatively fast respond of the groundwater levels to the sea-tidal fluctuations. Indeed, the rocks of the semi-confined aquifer are quite permeable and are exposed very near the shoreline (~50 meters).

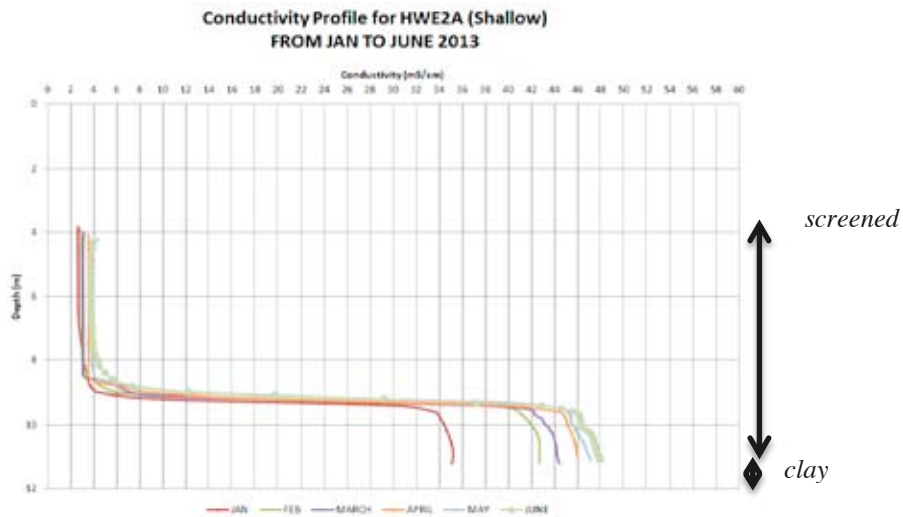


Figure 1. EC profile in well HWE2A, located at a distance of ~150 meter from the sea at Rafah area

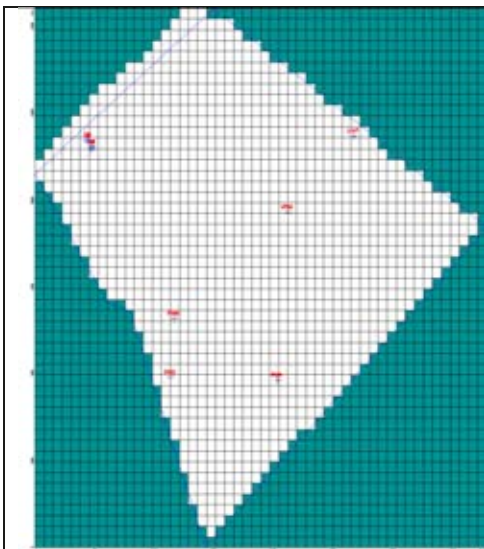


Figure 2. The model domain of the south Gaza area, of about 8 km x 12km. The wells shown in the figure are the ones used for calibration

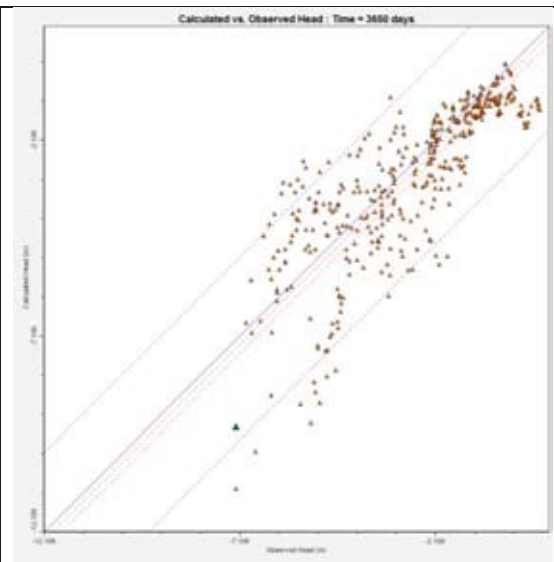


Figure 3. Steady state calibration for all the monitoring wells shown in figure 1, comparing the modeled water level and the measured water level in the aquifer. The correlation is about 85%.

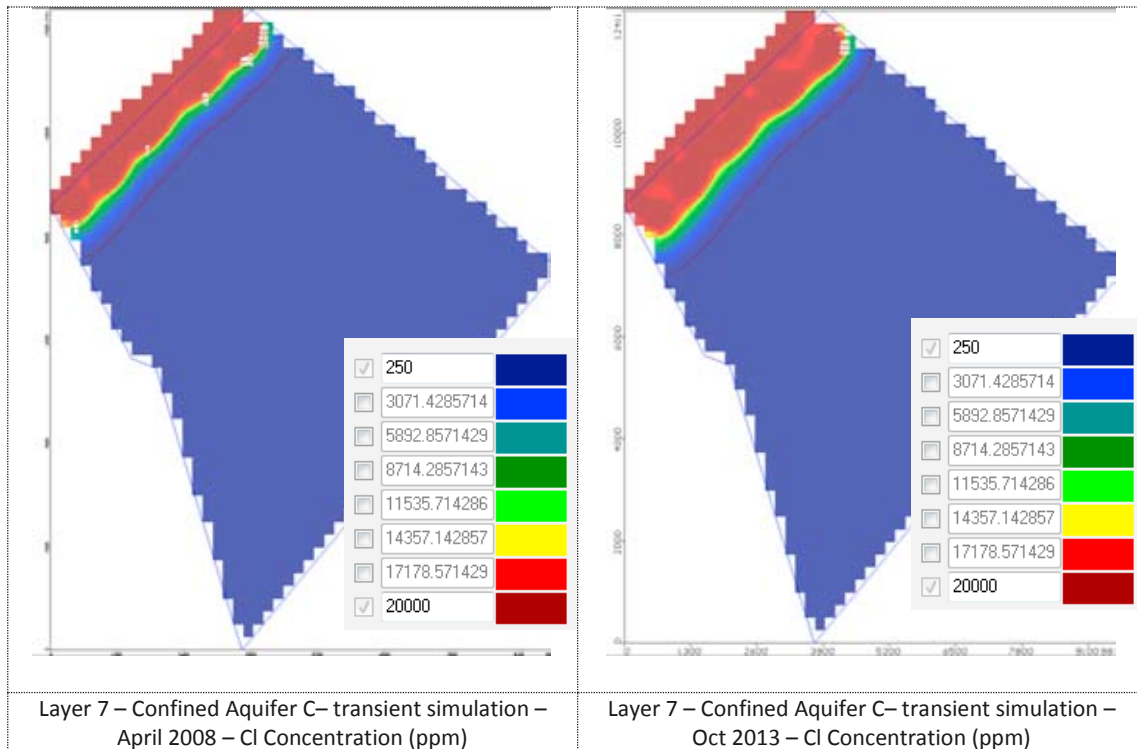


Figure 4. Transient simulation for the salinity of the deep confined aquifer C. The dark red is the seawater concentration of CL (20,000 ppm)

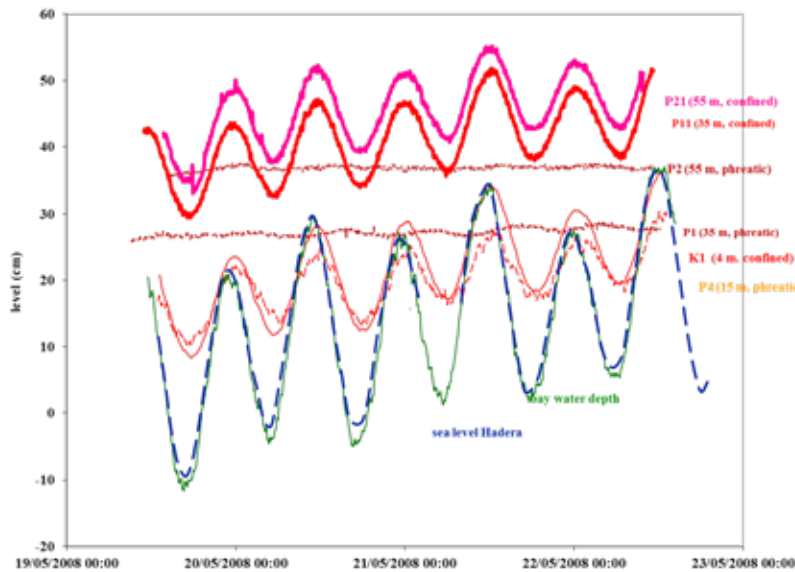


Figure 5. Water

level fluctuations in several research boreholes at different distances from the sea in both phreatic and confined sub-aquifers

REFERENCES

Nielsen, P. 1990. Tidal dynamics at water table in beaches. *Water Resources Research* 26 (2127–2134).

Mellol A.J. and Zeitoun D.G. (1999), A semi-empirical approach to intrusion monitoring in Israeli coastal aquifer, In: Bear J.et al. Eds, 1999, pp. 543-559, Kluwer Academic Publishers, Netherlands.

EFFECT OF FOREST FIRE ON COASTAL AQUIFER SALINISATION AND FRESHWATER AVAILABILITY

Beatrice M.S. Giambastiani¹, Nicolas Greggio¹, Katia Pacella¹, Andrea Iodice¹ and Marco Antonellini¹

¹CIRSA – Interdepartmental Research Centre for Environmental Sciences, University of Bologna, Italy

ABSTRACT

Forest fires have usually been studied for their impact on soil properties and consequent change in erosion hazard and runoff generation. Also the post-fire recharge and net infiltration can undergo some changes. This aspect is even more important in case of large vegetated areas growing over a coastal aquifer affected by saltwater intrusion. In the Ravenna coastal area (Italy), a dense pine forest grows on the remains of the natural coastal dune belt, overlying a sandy coastal phreatic aquifer, which is completely compromised by marine ingression. Three profiles, in different portion of the forest, were monitored (2008 and 2013) for groundwater level, physical and chemical parameters in order to highlight any change in groundwater quality, infiltration and freshwater availability occurring after a forest fire that devastated 56 hectares of the studied area in July 2012. All pre-fire groundwater parameters were similar among each other in the three monitored profiles, whereas a post-fire decrease in salinity was recorded across the burnt forest along with an increase in redox potential, infiltration and freshwater lens thickness. By applying analytical solutions, infiltration rates were calculated and comparison between all transects were made possible. The estimated infiltration rates indicated an increase in the partly and completely burnt area (219 mm/y and 511 mm/y, respectively) compared to the pristine area (73 mm/y). In the vegetated zone the aquifer recharge is generally limited to the autumn and winter season, while during spring and summer the high evapotranspiration rate exceeds the infiltration amount. This work provided an example of how fire can positively affect the quantity of fresh groundwater resources in low land coastal aquifers.

INTRODUCTION

Controlled burning has been often used in ecosystems and forests to control vegetation community structure and growth (Obrist et al. 2003). The hydrological effects of forest fire have been studied for water catchment management purpose in order to define the impacts on water balance, soil properties and consequent change in erosion hazard and runoff (Silberstein et al. 2013). However, also the post-fire recharge and net infiltration can undergo some changes (Yesertener 2005). Some recharge simulations and groundwater models (DoW 2009) have demonstrated that increasing the burn frequency and removal of pine plantations can be the only viable options for a significant increase in recharge to the groundwater system. Vegetation, in fact, plays an important role in the water cycle. In the forest environment, root uptake and canopy closure lead to an increase in evapotranspiration processes, causing a reduction of freshwater recharge into groundwater. This aspect is even more important in case of large vegetated areas growing over a sandy coastal aquifer affected by saltwater intrusion.

This work aims to define the effects of a forest fire on recharge and the changes in groundwater salinisation and freshwater availability in a salinized coastal aquifer.

Site description

In the Ravenna coastal area (NE Italy), a dense pine forest (100 hectares) grows on the remains of the natural dune belt. This non-native coastal forest was planted at the beginning of the XX century to stabilize the sand and protect inland crops from sea spray. In July 2012 a large fire devastated 56 hectares of the natural reserve and 19 hectares of the forest were completely destroyed and left with bare soil and neither pine trees nor bushes (Figure 1). This environment represents the only recharge area for the coastal aquifer, because here the aquifer becomes phreatic and rainfall can infiltrate. The coastal aquifer has a thickness ranging from 12 to 25 m and it consists of two sandy units (0-7 m and 23-25 m asl) intercalated by a fine prodelta deposit with alternations of silt, clay and sand layers (Amorosi et al. 1999). Because of low topography, high rate of natural and anthropic subsidence and a heavy drainage system, the coastal aquifer is completely compromised by marine ingression with groundwater that remains brackish to saline. Freshwater lenses have been limited in areal extent, in thickness and in time and can be found only related to dune heights (Antonellini et al. 2008). Although mean annual rainfall is 635 mm/year, annual rainfall surplus is minimal (60-150 mm/year) due to high evapotranspiration rate (800-1300 mm) and it occurs only during winter months (Mollema et al. 2013).

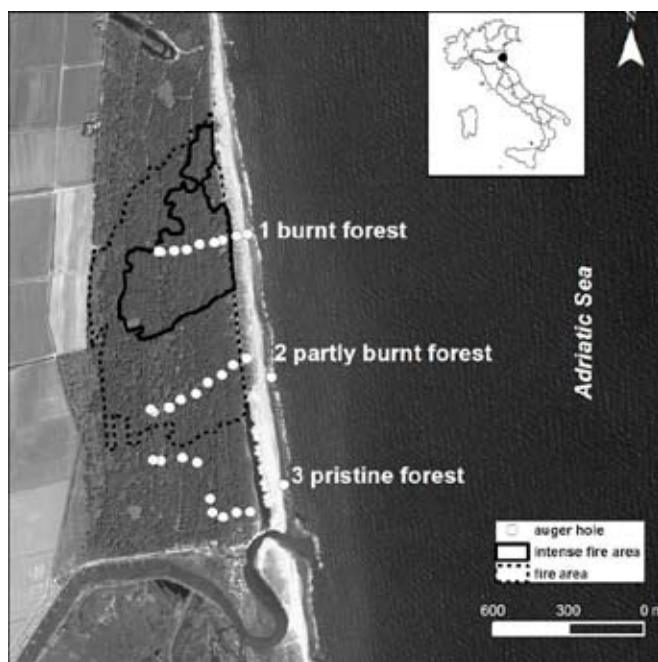


Figure 1. Location of the study area.

METHODS

Two monitoring campaigns (2008 and 2013) were carried out and used to highlight any change in groundwater quality, salinisation, and infiltration occurring after the fire. Three profiles were considered: 1) one along the completely burnt portion of the forest; 2) one in the partly (70%) burnt area, and 3) one along the pristine forest not touched by the fire (Figure 1). During every campaign 30 auger holes were drilled to monitor groundwater by water level metering, and chemical-physical parameters by a multiparameter probe.

The Darcy law and the Dupuit equations were also applied to calculate the unconfined flow and hydraulic head. In these calculations,

hydraulic gradient was measured during the monitoring, hydraulic conductivity value (30 m/day) were derived from pumping tests carried out in several piezometers located in the forest, while distance and flow length were based on the topographic profiles. Along all profiles, calculated and measured groundwater levels were compared and the infiltration rates were extrapolated with the objective of matching modelled and measured hydraulic head. The results in the burnt, partly burnt and pristine forest were compared among each other.

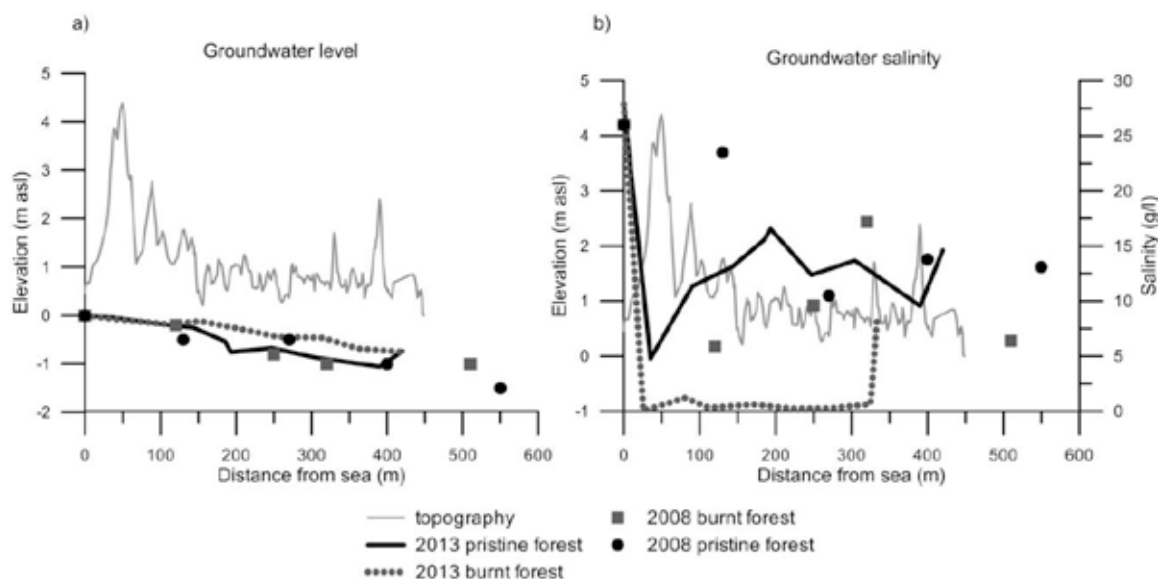


Figure 2. (a) Groundwater level and (b) groundwater salinity comparison before (2008, circled and squared symbols) and after the forest fire (2013, solid and dash lines). Shown in light grey color is also the topography. Due to limited space, only values of pristine and completely burnt forest profiles are shown.

RESULTS AND DISCUSSION

In 2008, before the fire, groundwater level and salinity were similar in all portions of the pine forest, showing from brackish to saline values and no freshwater lens along the dune system (Marconi et al. 2011). Unfortunately water level and salinity long time-series for the three profiles were not available, but our results highlighted hydraulic conditions and salinity trends, typical of all Ravenna's coastal pine forests. In fact, results of previous studies (Giambastiani et al. 2007, Antonellini et al. 2008, Vandenbohede et al. 2014) show the presence of a shallow brackish-freshwater interface with limited seasonal variations, and occasional small freshwater lenses. On the contrary, significant decrease in salinity and an increase in groundwater level were recorded in the burnt forest in 2013, one year after the fire (Figure 2). A post-fire decrease in salinity was recorded along with an increase in redox potential and the appearance of a freshwater lens (200 m long) below the dune crest.

Comparison between measured and calculated hydraulic head in the three areas had a good correlation coefficient R^2 ranging from 0.98 to 0.99 and a mean root mean square error (RMSE) of 0.10 m. The estimated infiltration rates indicated an increase in the burnt area (219 mm/y in the partly burnt and 511 mm/y in the completely burnt portion) compared to the pristine area (73 mm/y). It has to be considered that, generally, in the vegetated area the aquifer recharge is limited to the autumn and winter season while during spring and summer, the water budget is negative because the high evapotranspiration rate exceeds the infiltration (Mollema et al. 2012, Antonellini et al. 2008). Moreover, during the winter season, the water infiltrating through the aquifer is further reduced by the drainage system (several drainage ditches run along the forest), which keeps the forest dry and preserve the pine trees. Due to these reasons the infiltration amount in the full vegetated zones of the forest is generally low. Higher infiltration rate recorded in the burn area was more likely due to the reduced vegetation cover and the associated reduction in ET rather than other changes. This translated into a small increase in recharge to the watertable. Several studies (Obrist et al., 2003; Mullen et al. 2006) have demonstrated that climate variations, such as very wet or dry periods after the fire, complicate the use of fire as a restoration tool for recharging groundwater. In some cases, the positive effects on infiltration, ET, and groundwater level

can last only for a few seasons after the fire (Silberstein et al. 2013). This implicates that the recovering portion of the study area needs to be monitored longer in time.

CONCLUSIONS

This work provides an example of how fire can positively affect fresh groundwater resources quantity in low-land coastal aquifers. Pre- and post-fire groundwater quality and level were monitored in the coastal pine forest of Ravenna (NE Italy) in order to highlight the effects on groundwater salinisation and infiltration recharge in a sandy coastal aquifer compromised by saltwater intrusion. In this case study, the complete removal of vegetation cover has caused a decrease in salinity along with an increase in groundwater level, infiltration rate, freshwater lens thickness and redox potential, at least in the first year following the fire. Although the fire had a positive effect in our case, each situation is specific and needs to be monitored and evaluated in terms of post-fire climate condition, as well as soil type, type of plant cover, surface temperature, soil moisture, etc. In order to define the hydrological effects of forest fire for water catchment purposes is necessary to monitor and follow the complete recovery of the vegetation in the years following the fire, because regenerating bushes may cause a bigger water uptake nullifying the initial positive effects on freshwater availability and salinisation.

REFERENCES

- Amorosi A., M.L. Colalongo, G. Pasini, and D. Preti. 1999. Sedimentary response to late quaternary sea-level changes in the Romagna Coastal Plain (northern Italy). *Sedimentology*, no. 46: 99-121.
- Antonellini M., P. Mollema, B.M.S. Giambastiani, K. Bishop, L. Caruso, A. Minchio, L. Pellegrini, M. Sabia, E. Ulazzi, and G. Gabbianelli. 2008. Salt water intrusion in the coastal aquifer of the southern Po Plain, Italy. *Hydrogeology Journal*, no. 16:1541-1556.
- DoW. 2009. PRAMS Scenario Modelling for the Gngangara Sustainability Strategy, Hydrogeological Series, Report HG39. Department of Water, Perth, Western Australia.
- Giambastiani B.M.S., M. Antonellini, G.H.P. Oude Essink, and R.J. Stuurman. 2007. Saltwater intrusion in the unconfined coastal aquifer of Ravenna (Italy): a numerical model. *Journal of Hydrology*, no. 340: 91-104.
- Marconi V., M. Antonellini, E. Balugani, and E. Dinelli. 2011. Hydrogeochemical characterization of small coastal wetlands and forests in the Southern Po plain (Northern Italy). *Ecohydrology*, no. 4(4): 597-607.
- Mollema P. and M. Antonellini. 2013. Seasonal variation in natural recharge of coastal aquifers. *Hydrogeology Journal*, no. 21: 787-797.
- Mullen R.M., A.E. Springer, and T.E. Kolb. 2006. Complex effects of prescribed fire on restoring the soil water content in a high-elevation riparian meadow, Arizona. *Restoration Ecology*, Vol. 14, no. 2: 242-250.
- Obrist D., E.H. DeLucia, and J.A. Arnone. 2003. Consequences of wildfire on ecosystem CO₂ and water vapour fluxes in the Great Basin. *Global Change Biology*, Vol. 9, no. 4: 563-574.
- Silberstein R.P., W.R. Dawes, T.P. Bastow, J. Byrne, and N.F. Smart. 2013. Evaluation of changes in post-fire recharge under native woodland using hydrological measurements, modelling and remote sensing. *Journal of Hydrology*, no. 489: 1-15.
- Vandenbohede A., P.M. Mollema, N. Greggio, and M. Antonellini. 2014. Seasonal dynamic of a shallow freshwater lens due to irrigation in the coastal plain of Ravenna, Italy. *Hydrogeology Journal*. doi: 10.1007/s10040-014-1099-z.
- Yesertener C. 2005. Impacts of climate, land and water use on declining groundwater levels in the Gngangara groundwater Mound, Perth, Australia. *Australian Journal of Water Resources*, Vol. 8, no. 2:143-152.
- Contact Information:** Beatrice M.S. Giambastiani, CIRSA - University of Bologna, Via S. Alberto 163, 48121 Ravenna (Italy), Phone: +39 0544 937318, Fax: +39 0544 937319
Email: beatrice.giambastiani@unibo.it

Sea-level rise and seawater inundation of an atoll island, Roi-Namur, Kwajalein Atoll, Republic of the Marshall Islands

Stephen B. Gingerich¹ and Clifford I. Voss²

¹U.S. Geological Survey, Pacific Islands Water Science Center, Honolulu, HI, USA

²U.S. Geological Survey, National Research Program, Menlo Park, CA, USA

ABSTRACT

Freshwater resources on low-lying islands are vulnerable to increased frequency of seawater inundation as future sea level increases. Numerical groundwater models are useful for simulating the impacts of seawater migrating from the inundated surface downward into the freshwater lens. This study uses a groundwater model developed using hydrologic data collected during several inundation events to investigate the general processes involved as an atoll island aquifer experiences salinization and subsequent recovery. Findings from this study are useful for understanding general processes that will be experienced on low-lying islands throughout the world as recharge changes and seawater inundation events increase in frequency. A groundwater flow model of Roi-Namur Island, part of Kwajalein Atoll, Republic of the Marshall Islands (figs. 1 and 2), is being developed for the U.S. Department of Defense Strategic Environmental Research and Development Program using the U.S. Geological Survey's three-dimensional solute transport (3-D SUTRA) computer code. The groundwater model for Roi-Namur simulates freshwater, the underlying brackish-water transition zone, and saltwater in an aquifer composed of calcareous sediments overlying Pleistocene limestone. Estimates of present-day recharge, and withdrawal are used as input to the model with the current position of mean sea level as a boundary condition. The resulting freshwater-lens size and position are simulated for current conditions. The groundwater flow model is used to assess the impact of sea-level rise and storm-wave inundation on infrastructure and freshwater availability under a variety of conditions based on historic information, sea-level rise scenarios, and global climate model wind, wave, and rainfall output. In addition, various strategies to mitigate impacts are simulated. Infrequent episodes of seawater inundation during storm events (fig. 3) have severely impacted the island's freshwater resources and these events are predicted to increase in frequency as sea level rises. Estimates of future recharge are made using a daily mass-balance water budget and estimates of the potential distribution and volume of seawater that is projected to wash over the island are generated from a set of detailed oceanographic models. These estimates are applied to the 3-D groundwater model to investigate sea-level rise and climate change impacts to the freshwater lens and evaluate various strategies to mitigate the impacts. The results of these scenarios will be available to local water-system managers so that they can most effectively mitigate the impacts of sea-level rise and climate change and properly manage the groundwater resource. Moreover, the general processes illustrated with the modeling results are relevant for low-lying islands throughout the world that are vulnerable to increased seawater inundation. Preliminary results from this modeling effort will be presented.

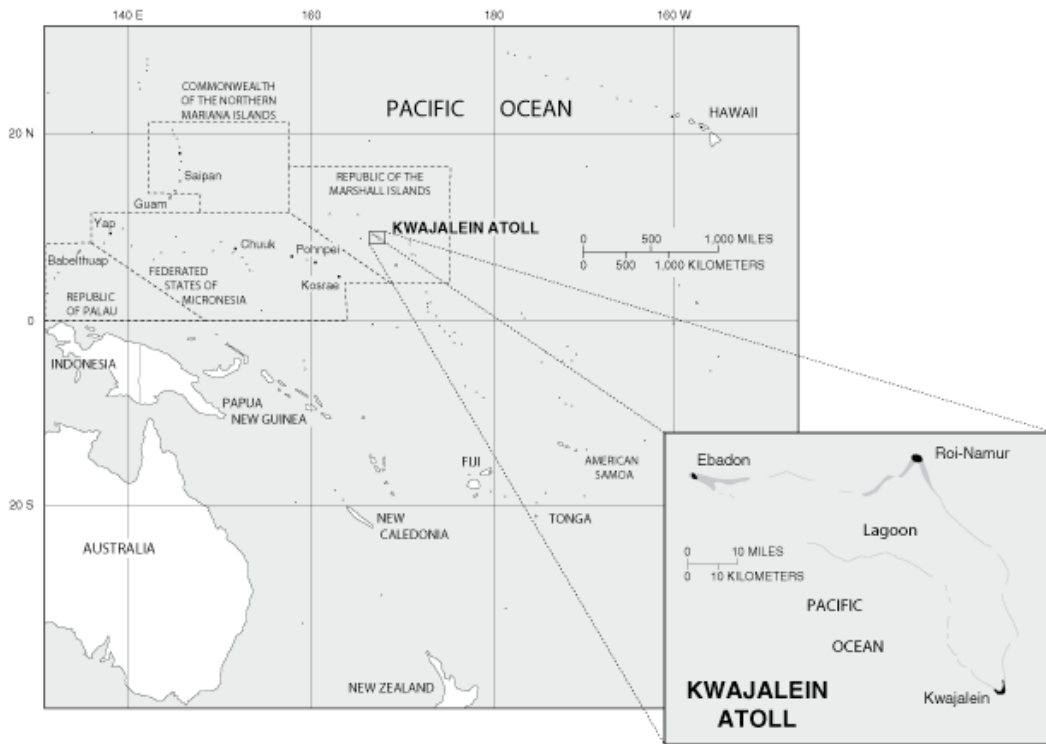


Figure 1. Kwajalein Atoll in the western Pacific Ocean.

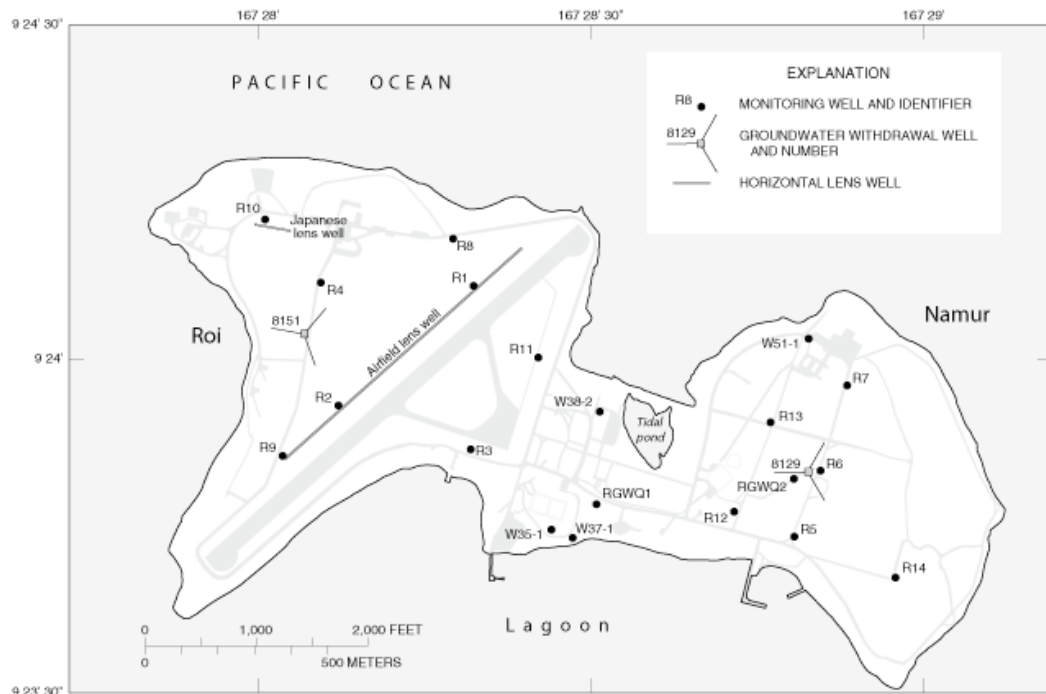


Figure 2. Groundwater withdrawal wells and monitoring wells, Roi-Namur Island.



Figure 3. Seawater inundation after several days of high sea level and surf.

Contact Information: Stephen B. Gingerich, U.S. Geological Survey, Pacific Islands Water Science Center, 677 Ala Moana Blvd, #415, Honolulu, Hawaii 96813 USA, Phone: 808-587-2411, Fax: 808-587-2401, Email: sbginger@usgs.gov

Unstable flow patterns during submarine groundwater discharge: Changing the way we look at the freshwater-seawater interface

Tania Röper¹, Janek Greskowiak¹, Gudrun Massmann¹

¹Department of Biology and Environmental Sciences, Carl von Ossietzky University of Oldenburg, D-26129 Oldenburg, Germany

ABSTRACT

The importance of submarine groundwater discharge as a material transport pathway to the ocean was already investigated by numerous studies around the world. As groundwater fluxes often contain significantly higher nutrient, metal and organic compound loads than rivers, groundwater discharge to the ocean may have crucial implications for coastal ecosystems. Moreover, discharging groundwater and recirculating seawater interact within the subterranean estuary and generate reactive zones that may alter the geochemical conditions of the water and sediment. Consequences like e.g., the eutrophication of coastal waters or the change of interstitial fauna of sandy beaches were previously reported.

However, the flow patterns in the intertidal region are still not completely understood. Contrary to today's common view of hydraulic conditions in the intertidal region, i.e., the formation of a stable upper saline plume (USP) concurrent with the existence of a so-called "freshwater discharge tube" below, which pinches out at the beach surface close to the low tide mark, this system can be extremely instable under certain conditions.

We conducted laboratory experiments supported by numerical modeling to investigate the instability of submarine groundwater discharge patterns during tidal forcing. For a gentle beach slope of 1:12, our study shows the development of a transient freshwater-seawater interface that is characterized by several migrating saltwater fingers which intrude into the aquifer. Groundwater discharge occurs in between these saltwater fingers at various locations in the intertidal region and is not limited to the low tide mark.

We suggest that a stable USP is limited to a certain range of hydrological and hydrogeological parameter values in nature and does not generally apply to all coastal environments. Especially when the beach slope falls below a critical value, the likelihood of fingering flow and an associated rather chaotic discharge pattern arise. Local sediment heterogeneities or changing recharge patterns will increase the discharge variability.

These new insights have important implications for the biogeochemistry of subterranean estuaries. If the input of nutrients, metals and organic compound is extended from the low water line to the entire intertidal area, this may lead to significant changes in species diversity and abundance of the benthic fauna as well as algae and seagrasses. Moreover, the freshwater discharge under instable conditions is likely to be highly variable over larger time periods, which must be considered when quantifying discharge rates. In case of spatially and temporally variable discharge conditions, local measurements by e.g., a seepage-meter, may lead to an underestimation of the discharge rate. It is a challenge for the future to detect and measure these flow patterns in the field.

REFERENCES

Röper, T., Greskowiak, J., Massmann, G. Instabilities of submarine groundwater discharge: Changing the way we look at the freshwater-seawater interface. *Limnology & Oceanography* (submitted).

Contact Information: Tania Röper, Department of Biology and Environmental Sciences, Carl von Ossietzky University of Oldenburg, D-26129 Oldenburg, Germany, E-Mail: Tania.roeper@uni-oldenburg.de, phone: (+49)441 – 798 3289

Measurements with an automated electrical resistivity tomography system in a freshwater/saltwater transition zone

Michael Grinat¹, Wolfgang Südekum¹, Dieter Epping¹, and Robert Meyer¹

¹Leibniz Institute for Applied Geophysics, Hannover, Germany

ABSTRACT

In order to investigate the dynamics of the freshwater/saltwater transition zone at the North Sea island Borkum two newly developed vertical electrode systems of about 20 m length were installed in the water catchment areas Waterdelle and Ostland. The systems were placed in depths between 44 m and 65 m, i.e. in the freshwater/saltwater transition zone below the water supply wells. Each of the two vertical electrode chains includes 78 stainless steel ring electrodes (spacing 0.25 m). The ongoing automated measurements are carried out using a modification of the commercial resistivity meter 4point light 10W (LGM Lippmann).

For the measurements a Wenner-alpha array is used. The data show a clear transition from (apparent) resistivities of about 80 Ωm in the upper part of the measuring section around 45 m depth to about 1-2 Ωm in the lower part around 65 m depth. Large changes occurred only within the first year of the measurements (September 2009 to September 2010); these are due to the readjustment of the local conditions (disturbed by drilling) to the undisturbed situation. Between September 2010 and February 2014 only small changes occurred in most depths, although the resistivity variations in time are different in different depths. Within the last years a very stable situation of the transition zone between freshwater and saltwater has been observed at both locations.

INTRODUCTION

At the North Sea island Borkum the required drinking water is provided by a freshwater lens. A freshwater lens, which is floating on saltwater, is influenced by tidal changes of the seawater level, seasonal changes of the groundwater level and various local and regional flow systems (Werner et al. 2013). Changes of the groundwater level can be caused by natural fluctuations of rainfall and evaporation as well as seasonal differences in groundwater use. Especially in water catchment areas up-coning of saltwater is a permanent threat. This up-coning can lead to changes of the depth and the shape of the transition zone between the freshwater lens and the underlying saltwater.

In order to investigate the dynamics of the freshwater/saltwater transition zone at Borkum in the scope of climate change two newly developed vertical electrode systems of about 20 m length were installed in the two water catchment areas Waterdelle and Ostland in September 2009. In both areas the extracted amount of freshwater is changing seasonally. The development and installation of the systems was carried out as part of the Interreg project CLIWAT (<http://cliwat.eu>). The electrode systems were installed in the boreholes CLIWAT 1 (Waterdelle) and CLIWAT 2 (Ostland) in depths between 44 m and 65 m, i.e. within the freshwater/saltwater transition zone below the water supply wells. Afterwards the boreholes were refilled according to geology. Moreover, two water gauges with filters in

different depths were installed above each of the vertical electrode systems to measure the groundwater level.

Each of the two vertical electrode chains is about 20 m long and includes 78 stainless steel ring electrodes (spacing 0.25 m). The electrodes are mounted on an isolating PVC rigid pipe normally used for groundwater observation wells. The resistivity measurements (Wenner-Alpha array) are carried out using a modification of the commercial resistivity meter 4point light 10W (LGM Lippmann). The power is supplied by batteries that are recharged by solar panels. Since end of December 2009 the data are regularly transmitted to Hannover by telemetry. A complete pseudosection with 975 single measurements (Wenner-alpha array) is measured every five hours (Wiederhold et al. 2013). The automated measurements are still ongoing. Recently, similar systems were also used by Ogilvy et al. (2009) and Poulsen et al. (2010) for monitoring of coastal aquifers.

RESULTS

For the measurements a Wenner-alpha array is used. In CLIWAT 1 only sand is found in the transition zone. The resistivity data show a clear transition from apparent resistivities of about 80 Ωm in the upper part of the measuring section around 45 m depth to about 1-2 Ωm in the lower part around 65 m depth (fig. 1). This indicates a change in water salinity from freshwater in the upper part to saltwater in the lower part of the electrode chain. Within the last years this transition zone has been very stable because several thousand measurements between September 2010 and February 2014 (all shown in fig. 1) yielded very similar results.

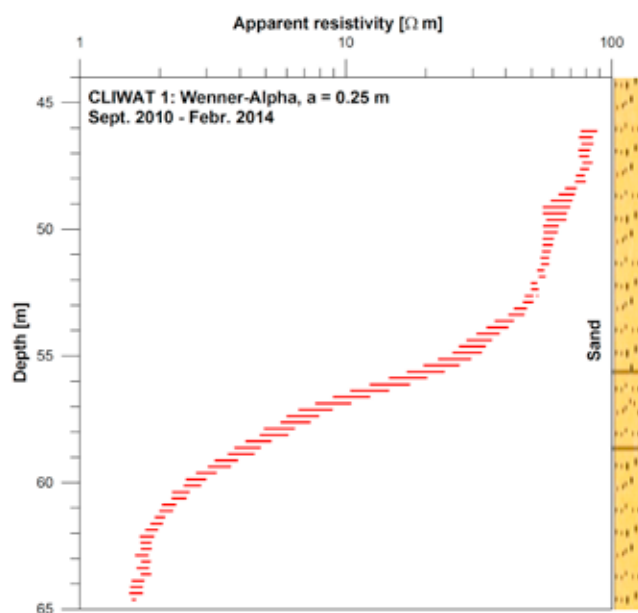


Fig. 1: Apparent resistivity measurements in CLIWAT 1 (Wenner-Alpha, spacing 0.25 m)

In the depth of the freshwater/saltwater boundary in CLIWAT 2 several layers of clay and silt were encountered within the sandy sediments (fig. 2). The different layers are clearly visible in the resistivity measurements: In the transition from resistivities of about 80 Ωm around 45 m depth to 2 Ωm around 65 m depth the sand layers show slightly higher resistivities than the clay layers. As in

CLIWAT 1 the resistivity measurements have shown only small changes within the last years.

At both locations large changes occurred only within the first year of the measurements (September 2009 to September 2010): In the first measurements after installation of the electrode systems similar resistivities were measured in all depths. The resistivities increased or decreased afterwards depending on the depth of the measurements. These changes were

caused by a readjustment of the groundwater system around the borehole to natural conditions.

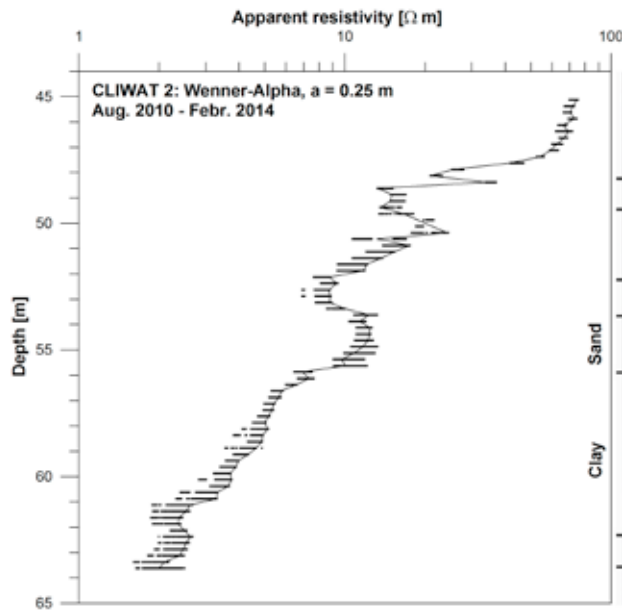


Fig. 2: Apparent resistivity measurements in CLIWAT 2 (Wenner-Alpha, spacing 0.25 m)

Since September 2010 only small changes have been observed in most depths. This indicates a very stable situation of the freshwater/saltwater transition zone at both locations. Larger time-dependent resistivity changes are observed in the sand layer between 53 m and 56 m depth in CLIWAT 2. Here a clear seasonal-dependent resistivity trend with higher resistivities between November/December and May and decreasing resistivities between May and October is visible.

Fig. 3 shows the seasonal changes in 55.1 m depth. Model calculations based on the 3D model of Sulzbacher et al. (2012) will be carried out to understand this behaviour.

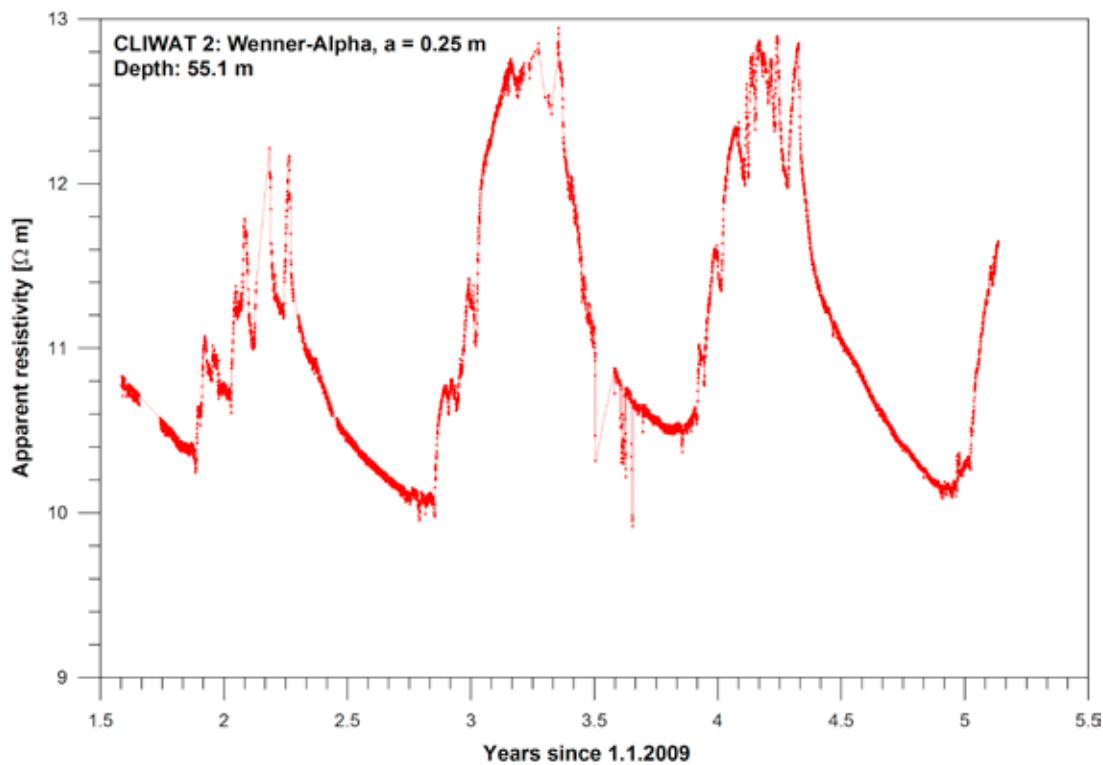


Fig. 3: Seasonal resistivity changes within the sand layer between 53 m and 56 m depth in CLIWAT 2: Apparent resistivity in 55.1 m depth.

REFERENCES

Ogilvy, R. D., P. I. Meldrum, O. Kuras, P. B. Wilkinson, J. E. Chambers, M. Sen, A. Pulido-Bosch, J. Gisbert, S. Jorreto, I. Frances, and P. Tsourlos. 2009. Automated monitoring of coastal aquifers with electrical resistivity tomography. – *Near Surface Geophysics* 7: 367–375.

Poulsen, S. E., K. R. Rasmussen, N. B. Christensen, and S. Christensen. 2010. Evaluating the salinity distribution of a shallow coastal aquifer by vertical multielectrode profiling (Denmark). – *Hydrogeology Journal* 18: 161–171.

Sulzbacher, H., H. Wiederhold, B. Siemon, M. Grinat, J. Igel, T. Burschil, T. Günther, and K. Hinsby. 2012. Numerical modelling of climate change impacts on freshwater lenses on the North Sea Island of Borkum using hydrological and geophysical methods. – *Hydrol. Earth Syst. Sci.* 16: 3621-3643; doi: 10.5194/hess-16-3621-2012.

Werner, A. D., M. Bakker, V. E. A. Post, A. Vandenbohede, C. Lu, B. Ataie-Ashtiani, C. Simmons, and D. A. Barry. 2013. Seawater intrusion processes, investigation and management: Recent advances and future challenges. – *Advances in Water Resources* 51: 3-26.

Wiederhold, H., H. Sulzbacher, M. Grinat, T. Günther, J. Igel, T. Burschil, and B. Siemon. 2013. Hydrogeophysical characterization of freshwater/saltwater systems – case study: Borkum Island, Germany. – *First Break* 31: 109-117.

Contact Information: Michael Grinat, Leibniz Institute for Applied Geophysics, Stilleweg 2, 30655 Hannover, Germany, E-Mail: michael.grinat@liag-hannover.de

Resistivity tomography, an underestimated tool for mapping fresh salt groundwater interface.

Michel Groen

Faculty of earth and life sciences, VU, de Boelelaan 1085, 1081 HV, Amsterdam, the Netherlands

ABSTRACT

Why does resistivity tomography (DC, EM) not always fulfill the (high) expectations?

For mapping the fresh and salt water interface subsurface resistivity is an important parameter because of the good contrast between sediment with salt and sediment with fresh water. Several methods can be used for measuring the earth resistivity, two methods are commonly used: Differential current systems with electrodes and EM methods which use the inductive coupling of EM fields.

All methods have their specific limitations and applications (exploration depth, resolution, noise) and the applicability depends on target depth, size, contrast and terrain conditions. At the same time, when a method is used, the configuration of the instrument itself is essential for obtaining good quality data. The data itself should be treated in the right way to generate useful inversions. And last but not least the inversion, which is a model of a resistivity distribution of the subsurface, suffers from equivalence. The problem of equivalence (one data set has more than one solution and the calculated (specific) resistivities are both influenced by water quality and lithology. Equivalence can be easily resolved with the combination of other methods.

In order to do a successful survey several essential aspects are important:

- 1) Terrain condition (topography, accessibility resistivity of the top layer, possible sources of noise.
- 2) Instrument choice, configuration and forward modeling of the expected target, checking for the best configuration.
- 3) Fieldwork, be well prepared for the unexpected.....
- 4) Interpretation and verification with other methods.

This poster will show the do's and don'ts for obtaining a successful result.

This will be illustrated by several case studies. The examples include fresh water under the sea (measured along the beach and with an underwater cable), small lenses of fresh water in agricultural fields, and CVES measurements in coastal and dune areas of the Netherlands. Also the benefits of forward modeling for testing if the target is detectable are presented.

Example
Influence of topography of the seafloor on the inversion of underwater surveys

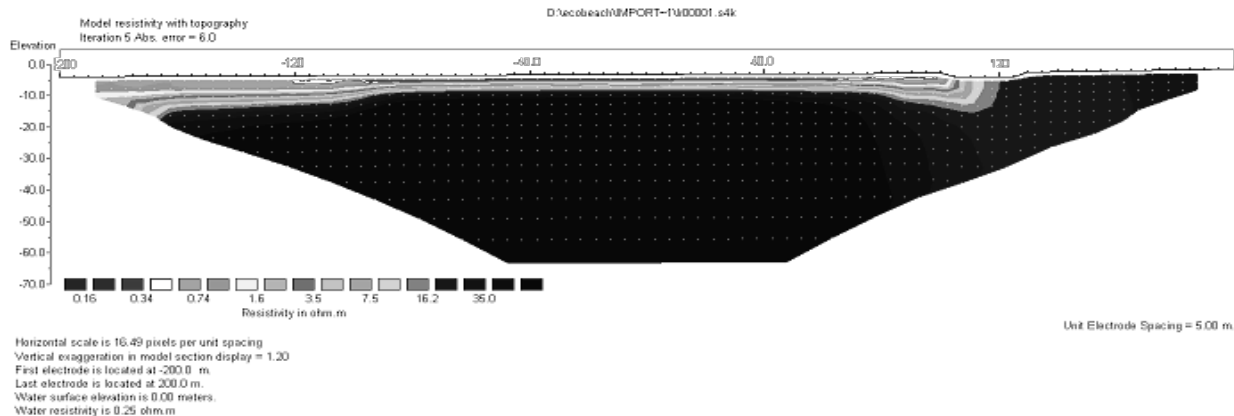


Figure 1a, CVES (Terrameter, ABEM lund), under water survey perpendicular Dutch coast, showing the influence of seafloor topography (on the right) on the inversion. (3-4 m salt water depth), light colors: sea water, dark colors: relative fresh groundwater, Wenner configuration, 64 electrodes, 5 m interval, fitting error 6%)

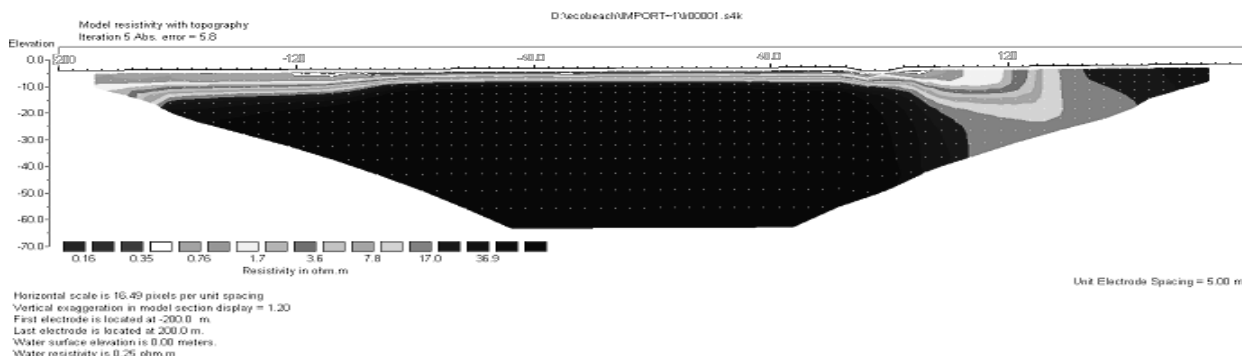


Figure 1b, the same CVES as in 1a, with slight change in seafloor topography, fitting error 5%.

Contact Information: Michel Groen, Faculty of Earth and Life Sciences VU, Department of critical zone hydrology, room D003, Email: Michel.groen@falw.vu.nl

Improvement of Water Level Measurements in Saltwater-Influenced Monitoring Wells - Application of the Base Pressure Method

Frank Skowronek¹, Jörg Grossmann¹

¹ Department K 3, HAMBURG WASSER, Billhorner Deich 2, D-20539 Hamburg, Germany

ABSTRACT

The water levels in saltwater aquifers are substantially influenced by the higher density of salt water compared to freshwater with a density close to 1 g/cm³. Without correction, the measured water level data cannot be used for hydrological purposes like groundwater level maps or groundwater modelling. Examples of the area monitored by HAMBURG WASSER illustrate the at times considerable influence of density effects on the analysis of groundwater data. Possible situations might be a density-driven shift in watershed boundaries or water level fluctuations caused by sampling of monitoring wells. Therefore, data have to be converted into corresponding freshwater heights. For this purpose, several measuring methods exist. Most important approaches are the analysis of chemical/physical profiles, geophysical logging methods and the base pressure method (subject of this article). Applicability of the base pressure method has been proved in numerous investigations by HAMBURG WASSER. Based on the pressure at the base of the monitoring well, water level and air pressure, the equivalent freshwater height is calculated. The fundamentals, application and possible sources of error of this method are presented here.

INTRODUCTION

HAMBURG WASSER performs routine measurements of the groundwater level at about 1400 monitoring wells. A small part of these monitoring wells exhibits elevated salt concentrations. The salinization of ground water results from solution processes at the edge of salt domes. If these leaching waters spread into the aquifer, normally a density-driven layering with the saltwater at the basis of the aquifer is formed.

The piezometric level of a water column depends on the air pressure as well as the density of the water and therefore on the concentration of dissolved substances and on water temperature. Under hydrostatic conditions, the pressure head of the saltwater column is lower than the appropriate freshwater column, due to the higher water density of the salt water (Figure 1). In consequence, groundwater level data from monitoring wells influenced by salt water should not be analyzed together with data from wells screened in freshwater without an appropriate correction. For hydraulic evaluations, such as the determination of the flow direction of the groundwater or the delineation of a catchment area, the water level data of the different monitoring wells have to be comparable. The groundwater level data of monitoring wells influenced by saltwater may only be used after an appropriate density correction.

Chloride concentrations, even in the range of only a few grams per liter, cause deviations of the water level up to some decimeters. In some of the deep monitoring wells of HAMBURG WATER the maximum salt concentrations reach about 60 g L⁻¹. With water column heights up to 590 m the equivalent freshwater heights lie up to about 31 m above the actually measured water height. Normalizing water level data to freshwater data requires determination of an equivalent freshwater height. If the density of freshwater ρ_f is used as a

reference, one gets the equivalent height of the freshwater column h_f as the result. The density of freshwater as reference for the groundwater zone is most suitable for most practical applications as variability in the densities in the corresponding saline waters is usually negligible. The physical relations are described amongst others by Rushton (1980) or Fetter (1994).

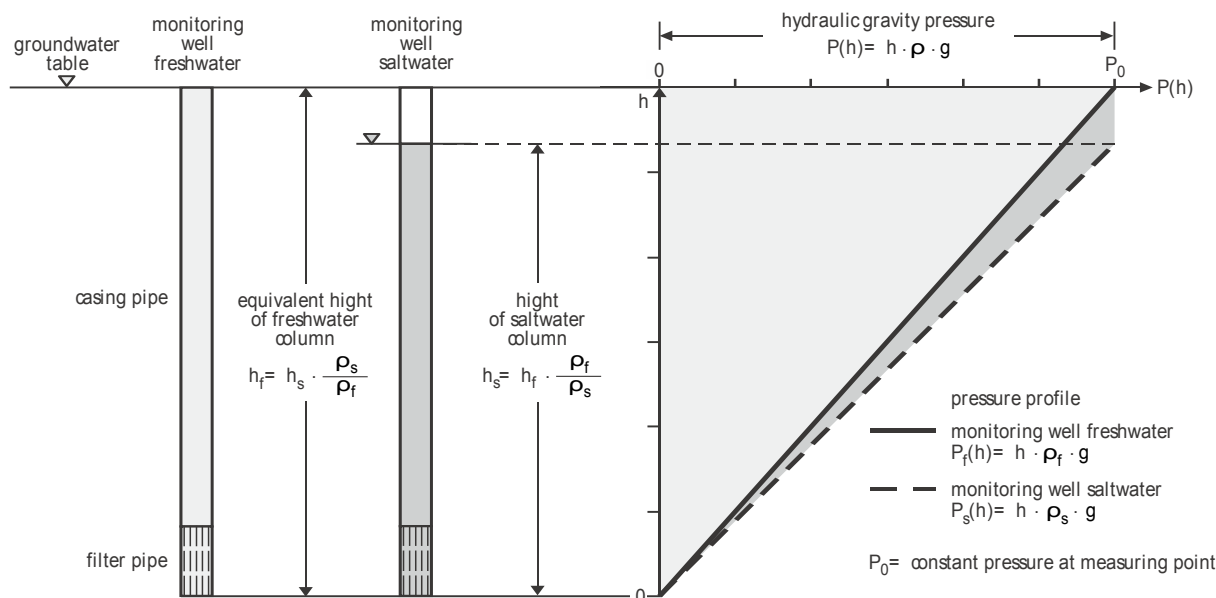


Figure 1: Visualization of the conditions in monitoring well in freshwater and saltwater

For the implementation of the corrections of water levels influenced by saltwater, base pressure measurements are used by HAMBURG WASSER. This method enables the efficient determination of the hydrostatic pressure and therefore the derivation of equivalent freshwater heights. Based on base pressure measurements from 2004 up to 2009 as well as accompanying measurement of the conductivity in the monitoring wells, the cluster of wells influenced by saltwater has been divided in two groups, one with stable and another group with variable salt concentrations. The first group of wells with stable salt concentrations usually show completely salinized water columns with small or no variations in salt concentration. The variation of density in the water columns is negligible and therefore the correction values for the transformation of the water level data are practically stable. For this group, the base pressure measurements are repeated every five years. As for the second group of monitoring wells with varying salt concentrations in the water column, variations of density have to be taken into account and detailed drift corrections are essential. For this group, the base pressure measurements are performed each year.

METHODS

With simple standard measurement methods (electrical contact gauge, data logger) only the density-influenced groundwater level can be detected. For the evaluation of the equivalent freshwater height, additional information has to be collected. Most of the existing methods focus on the determination of the average density in the saltwater column. Examples are density calculations on the base of chemical-physical parameters along depth profiles of the water column, the direct determination of the density in a depth profile by light refraction measurements, measurement of the hydrostatic uplift, of the resonance or by radiometric methods. With these measurement methods a step-by-step or a continuous density evaluation

of the water column in the monitoring well is required. Besides, these methods are time-consuming and they are influenced by methodical or systematical problems (disturbance of inhomogeneous water column by the inspection with the gauge or the sampling device, interpolation errors based on a limited number of sampling points, differences between the composition of the groundwater in the water column of the well and the aquifer).

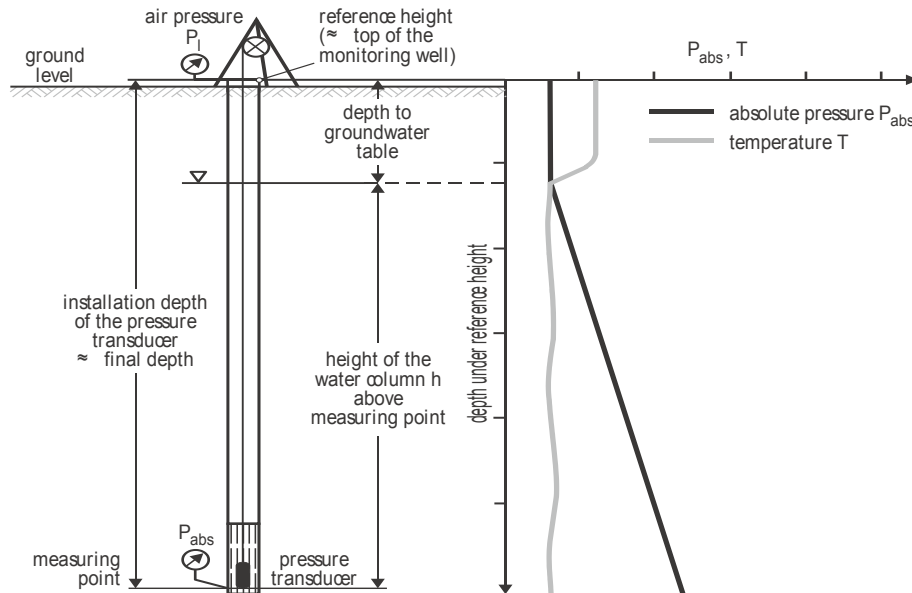


Figure 2: Principle and measured variables of the base pressure method

In contrast the base pressure method exhibits several advantages. For the determination of the hydrostatic pressure of the saltwater column at the bottom of the monitoring well as the decisive parameter, only a single direct measure is necessary and does not need to be derived from a series of interpolated values from a measuring profile. The measuring procedure and the evaluation of the data are considerably simplified as just an absolute pressure transducer has to be sunk to the final depth of the monitoring well. At the bottom of well, the absolute pressure P_{abs} , the distance between the reference height of the monitoring well and the measuring position as well as the water temperature have to be measured (Figure 2). At the same time the air pressure P_{atm} at the reference height is measured for the calculation of hydrostatic pressure P_s with the equation $P_s = P_{abs} - P_{atm}$ and the distance between water level and reference level of the monitoring well. The hydrostatic pressure P_s is inserted into the equation $h_w = P_s (\rho_f g)^{-1}$, where ρ_f is the freshwater density (Figure 1).

The only precondition for the application of the base pressure method is a monitoring well or an accessible vertical drilling with a diameter of sufficient width for the access with the pressure transducer. For precise determination of the equivalent freshwater height it is necessary to know the actual measuring depth.

DISCUSSION AND CONCLUSIONS

The essential sources of error connected with the base pressure method and the dimension of the errors are listed together with proposals for their minimization of those errors in the table below (Table 1). For the measuring equipment presently used by HAMBURG WASSER it is assumed that the total error for the calculation of the freshwater column corresponding with the absolute pressure is smaller than 0.1 % of the measuring depth, that means about +/- 0.1 m in relation to 100 m of water column height. Under these conditions the use of the

measuring method is reasonable for groundwater with a mineralization of more than 1.5 g L^{-3} or a conductivity of more than $2.000 \text{ } \mu\text{s cm}^{-1}$, respectively. For water with lower mineralization the method is suitable to detect the dimension of the equivalent freshwater column.

Table 1: Basic error sources connected with the base pressure method to determine density-corrected groundwater levels listed together with methods for the minimization of those errors

Error – Error range	Error handling, error minimization
<i>Pressure measurement (detection of the equivalent freshwater height)</i>	
Measurement error of the (base) pressure transducer – maximum 0.1 % of the measuring range	Use of a pressure transducer with improved measurement accuracy (best available class of accuracy presently is 0.05 % of the measuring range), adaption of the measuring range of the transducer to depth of the measuring point
Measurement error of barometer (measurement of air pressure) – maximum 0,1 % measuring range	Use of measurement device with improved accuracy
<i>Determination of the reference point for the correction of the water column height</i>	
Elongation of the line of the plump for the depth measure – 0,01 to 0,09 % in relation to the measuring depth	Correction of the length value assuming an elastic elongation of the line
Inaccuracy of the depth counter during metering with check marks on the rope – max. +/- 1 m reading error	Use of a calibrated depth counter or impulse generator
Deviation of well casing (borehole) from the plumb line – maximum error of the measuring depth 1.5 % at a maximum deviation of the borehole of 10° from the plumb line	Correction on the base of dip-meter logging
<i>Calculation of the equivalent freshwater height on the basis of the density of pure water at a temperature of 10° C</i>	
Local variations of the freshwater density of the non-saline groundwater in the investigation area – maximum 0,02 % of the height of water column	Calculation of the equivalent freshwater height on the basis of the average density of the non-saline groundwater in the groundwater body investigated
Deviation between reference temperature (e.g. 10° C) and temperature in the water column in the monitoring well inspected – maximum 0,11 % of the height of the water column	Correction of the calculated density of the freshwater density in the monitoring well inspected on the basis of a temperature profile of the well

REFERENCES

- Rushton, K. R. 1980. Differing positions of saline interfaces in aquifers and observation boreholes. J. Hydrology, Nr. 48, S. 185 – 189.
- Fetter, C. W. 1994. Applied Hydrogeology. Prentice Hall, New York

Contact Information: Frank Skowronek, HAMBURG WASSER, Management of Water Resources, Billhorner Deich 2, 20539 Hamburg, E-Mail: frank.skowronek@hamburgwasser.de

A Laboratory Experiment of Fingertip Splitting During Variable-Density Flow

C. R. Guevara Morel, C. Cremer, N. Goldau and T. Graf

Institute of Fluid Mechanics and Environmental Physics in Civil Engineering, Leibniz Universität Hannover, Germany

ABSTRACT

The aim of this work is to understand plume fingertip splitting in homogeneous sand. A physical experiment is conducted in order to produce data that can be used to numerically simulate and test mathematical models and to determine which mathematical approximation (Oberbeck-Boussinesq approximation, OBA) adequately reproduces plume fingertip splitting. Numerically simulating fingering during variable-density flow is challenging because the appropriate OBA level is not yet known (Kolditz et al. 1998). The numerical simulations are realized with the HydroGeoSphere (HGS) model (Therrien et al. 2004). Fluid density changes in groundwater systems can occur among others due salt water intrusion in coastal aquifers, upconing of saline waters from deep aquifers and dense plumes coming from landfills. In these cases, a denser fluid overlies a less dense fluid producing a density gradient, forcing the denser fluid to move downward through the less dense fluid. For higher density contrasts, the migration of dense plumes typically results in the formation of instabilities which manifest in the form of vertical plume fingers. This physical process is relevant because it can accelerate vertical solute transport. Therefore, the understanding of fingering in variable-density flow processes is important for the adequate management of freshwater aquifers. In this contribution, we present results from a laboratory investigation where a denser fluid overlies a less dense fluid, and where the behavior of the plume was observed. Interestingly, one finger formed initially that underwent fingertip splitting to form 3 to 5 plume fingers. The total solute mass in the system and the plume penetration depth at selected times was recorded. In continuation of existing laboratory experiments for variable-density flow (e.g. Simmons et al. 2002), the current work contributes to the understanding of these fingertip splitting, including its generation and simulation. Results suggest that a higher mathematical approximation (OBA level 3) is needed to adequately predict variable-density fingering in case of high density contrasts.

Keywords: Density-driven flow, HydroGeoSphere, fingertip splitting, physical experiment, Oberbeck-Boussinesq approximation

INTRODUCTION

The importance of variable-density flow has been reported by Kolditz et al. (1998), and Diersch and Kolditz (2002) which reviewed fundamental concepts, state equations, and physical processes involved as well as benchmark problems and relevant studies in the field of variable-density flow. Recently, an extensive evaluation of advances in variable-density flow and transport is made by Simmons et al., (2010), in which physics, modelling approaches, benchmark problems as well as future challenges involved in the numerical modeling are discussed. When numerically simulating variable-density flow, different mathematical approximations (Oberbeck-Boussinesq approximations, OBA) are used (Oberbeck 1879, Boussinesq 1903; Kolditz et al. 1998; Oswald and Kinzelbach 2004) to accurately reproduce flow and transport. Normally, numerical models are verified by comparing results with analytical solutions but due to the nonlinear nature of variable-density flow problems, analytical solutions assume a sharp interface between a dense fluid overlying a light fluid (Bear and Dagan 1964) making the testing of a variable-density flow model's

ability to simulate fingering and convective mixing a major issue (Van Reeuwijk et al. 2009). Also, multiple steady-state solutions appear in variable-density benchmark problems (e.g. the solute analog Elder (1967) problem) depending on grid discretization making model verification a problem. Recently, Van Reeuwijk et al. (2009) found that a unique solution of the Elder problem can be obtained at a Rayleigh number of $Ra < 76$. Van Reeuwijk et al. (2009) presented an analytical solution using a pseudospectral approach. The pseudospectral solution is discretization-independent and can therefore be used to verify variable-density flow models.

MATHEMATICAL MODEL

The HGS 3D numerical model describing fully-integrated variably-saturated subsurface and surface flow and variable-density solute transport was modified in order to be able to simulate the different mathematical OBA accuracies presented by Kolditz et al. (1998). The modified HGS model will then be used to reproduce the physical experiment.

LABORATORY MODEL

A laboratory experiment where a denser fluid overlies a less dense fluid is conducted. The experiment was carried out in a fully saturated sand filled glass container. A salt solution containing sodium chloride (NaCl) with a fluid density of 1200 kg m^{-3} (salt concentration of 348.61 g L^{-1} that is equivalent to 1000 % average seawater salinity) was used as the dense fluid. The fluid was stained with Eocene and introduced at the top boundary of the tank at a constant infiltration rate. Knowing the infiltration rate facilitates the calculation of the solute present in the system in time. Microscopic characteristic such as the number of fingers formed resulting from fingertip splitting as well as macroscopic characteristics such as the total solute mass in the system and the plumes penetration depth at various times were recorded.

NUMERICAL AND EXPERIMENTAL RESULTS

For model verification, the low Rayleigh number Elder problem (LREP) was simulated at different mathematical accuracies (OBA levels) using the newly modified HGS code. Numerical results were then compared with the pseudospectral solution of level OBA 1 at different times. Figure 1 shows results from the numerical simulation results of the half domain of the LREP at a $Ra = 60$ at a dimensionless time of $t = 1$ which is equivalent to 200 years in real time. The maximum fluid density in the domain is 1200 kg m^{-3} . The horizontal and vertical axes are dimensionless lengths scaled with respect to the original depth of the solute analog Elder problem. It is shown that the numerical solution depicted as red dotted line (OBA level 1) is identical to the pseudospectral solution of level OBA 1, such that the numerical model is successfully verified. Also, the green line (higher mathematical accuracy, OBA level 3) diverges from the black line (pseudospectral solution of OBA level 1), such that the more solute transport is predicted compared to the green line.

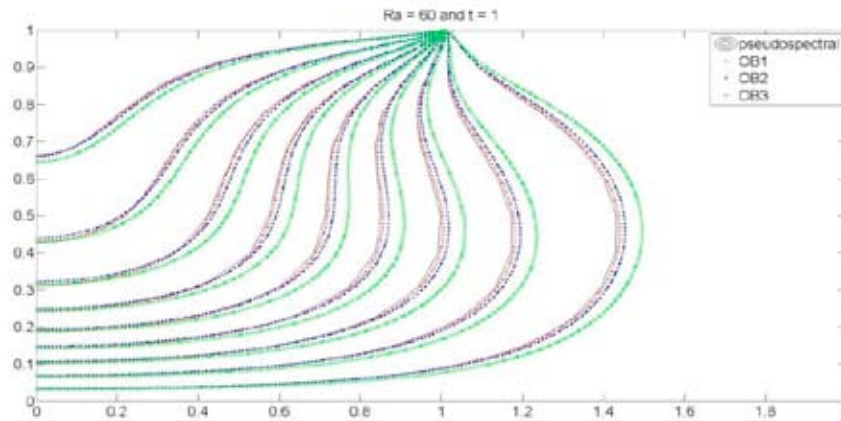


Figure 1. Results of model verification using the LREP . Black line: pseudospectral solution, red dotted line: numerical solution with low mathematical accuracy; blue dotted line: numerical solution with medium mathematical accuracy; green dotted line: numerical solution with high mathematical accuracy.

Figure 2 depicts results of the physical experiment. The source is located at the top boundary, and it is made sufficiently small in order to produce only one plume finger at early times. This is done in order try to understand fingertip splitting at later times. Solute mass present in the system, plume penetration depth and number of fingers is recorded.

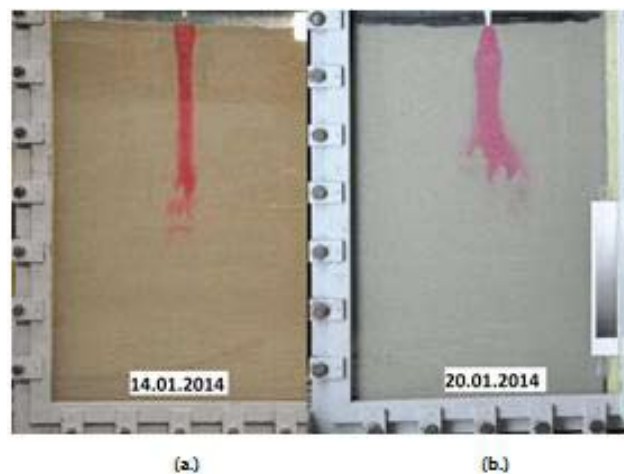


Figure 2. Results of the variable-density flow experiment at $t = 15$ min with an infiltration rate of 12.5 ml/min. The source is located (a) ca. 10 cm above the porous medium, and (b) within the porous medium

CONCLUSIONS

The numerical experiments suggest that in the case of high density contrasts, a higher mathematical accuracy is needed to simulate variable-density flow. This finding may be an indicator that solute transport is underestimated when lower accuracies are used in case of the existence of high density gradients. Nevertheless the question of which mathematical reproduces nature more accurately is still not completely solved. The need of physical experiments in order to test numerical models and corroborate numerical results is evident. The developed model will be used to test appropriateness of the Oberbeck-Boussinesq assumptions in the simulation of fingertip splitting.

REFERENCES

- Bear J., Dagan G. 1964. Some exact solutions of interface problems by means of the hodograph method. *J. Geophys. Res.* 69: 1563-1572.
- Boussinesq V.J. 1903. *Theorie analytique de la chaleur*, vol. 2. Paris, France: Gauthier-Villars; [chapter 2.3].
- Diersch H.-J.G., Kolditz O. 2002. Variable-density flow and transport in porous media: approaches and challenges. *Adv Water Resour* 25(10): 899-944.
- Elder J.W. 1967. Transient convection in a porous medium. *J Fluid Mech* 27(3): 609-23.
- Kolditz O., Ratke R., Zielke W., Diersch H.-J.G. 1995. Coupled physical modelling for the analysis of groundwater systems. In *Notes on Numerical Fluid Mechanics*, Vol. 51, Vieweg, Braunschweig-Wiesbaden.
- Oberbeck A. 1879. Ueber die Wärmeleitung der Flüssigkeiten bei Berücksichtigung der Strömung infolge von Temperaturdifferenzen. *Ann Phys Chem* 7:271-92.
- Oswald S.E., Kinzelbach W. 2004. Three-dimensional physical benchmark experiments to test variable-density flow models. *J Hydrol* 290(5):22-42.
- Prasad A., Simmons C.T. 2005. Using quantitative indicators to evaluate results from variable-density groundwater flow models. *Hydrogeol J* 13(10):905-14.
- Simmons C.T., Bauer-Gottwein P., Graf T., Kinzelbach W., Kooi H., Li L., Post V., Prommer H., Therrien R., Voss C.I., Ward J., Werner A. 2010. Variable density groundwater flow: from modelling to applications. In Wheater H.S., Mathias S.A., Xin Li, eds. *Groundwater Modelling in Arid and Semi-Arid Areas*. 1st ed Cambridge: Cambridge University Press 7:87-117.
- Simmons C.T., Pierini M.L., Hutson J.L. 2002. Laboratory investigation of variable density flow and solute transport in unsaturated-saturated porous media. *Transp Porous Media* 47(2):215-44.
- Therrien R., McLaren R.G., Sudicky E.A., Panday S.M. 2004. *Hydrogeosphere: a three-dimensional numerical model describing fully-integrated subsurface and surface flow and solute transport*. Université Laval, University of Waterloo 275 pp.
- van Reeuwijk M., Mathias S., Simmons C., Wards J. 2009. Insights from a Pseudospectral approach to the Elder problem. *Water Resour Res* 45,28 W04416, doi:10.1029/2008WR007421.
- Contact Information:** Carlos R. Guevara Morel, Leibniz Universität Hannover, Institute of Fluid Mechanics and Environmental Physics in Civil Engineering, Appelstrasse 9A 30167, Hannover, Germany, Phone: +49 511762 - 3710, Email: guevara@hydromech.uni-hannover.de

On the development of instabilities under density-driven flow conditions in saturated porous media: physical and numerical experiments

C. Cremer , C. R. Guevara Morel, N. Goldau and T. Graf

Institute of Fluid Mechanics and Environmental Physics in Civil Engineering, Leibniz Universität Hannover, Germany

ABSTRACT

Density driven flow occurs frequently in nature, e.g. in geothermal reservoirs, at waste disposal sites or due to saltwater intrusions. If a dense fluid is spilled and infiltrates through the soil it eventually reaches a prevailing freshwater (groundwater) table, leading to a situation where the dense fluid overlies a less dense. Due to buoyancy, the denser fluid moves through the less dense fluid. Typically, this results in the formation of dense plume fingers which are known to have an influence on the propagation of the plume in space and time. While the dense fingers flow direction is downward, it is counterbalanced by upward flow of freshwater between the fingers. The formation of those dense fingers is commonly attributed to material heterogeneity in heterogeneous porous media. However, the formation of fingers also occurs in media that are considered homogeneous on the lab scale (porous media where all grains have the same diameter). In homogeneous sand, the formation of dense fingers can be attributed to either i) the different arrangement of grains (e.g. in tetrahedrons or hexahedrons) inducing pore-scale heterogeneity, or ii) random variations in solute concentration causing varying buoyancy effects where both i) and ii) finally result in different average flow velocities. The adequate reproduction of those two effects in numerical models however remains a challenging task.

Building on previous work we try to mimic pore-scale heterogeneity in numerical models by applying perturbations to trigger the onset of instabilities. Such artificially generated perturbations have already been utilized with success previously by Schincariol et al. 1997, Simmons et al. 1999 and Weatherill 2004. We present results from a physical sand-tank experiment as well as results from numerical simulations of it. For the physical experiment a highly dense solution of NaCl (fluid density of 1200 kg m^{-3}) is stained with 0.3 g l^{-1} Eocine and injected with a constant infiltration rate on top of a domain filled with fully saturated coarse sand. This creates a situation where the dense stained solute overlies the less dense freshwater. Aim of the physical experiment is to have a benchmark to verify variable-density flow models.

The physical experiment is then implemented as a numerical model. Different trigger methods are implemented in the numerical model and by comparison to results of the physical experiment examined for their capability to realistically reproduce nature. Results indicate that the application of an artificial perturbation is necessary to create dense plume fingers and a propagation of the plume matching the propagation in the physical experiment.

REFERENCES

Schincariol R.A., Schwartz F.W., Mendoza C.A. 1997. Instabilities in variable density flows: Stability and sensitivity analyses for homogeneous and heterogeneous media. *Water Resour. Res.* 33(1), 31-41.

Simmons C.T., Narayan K.A., Wooding R.A. 1999. On a test case for density-dependent groundwater flow and solute transport models: The salt lake problem *Water Resour. Res.*, 35(12), 3607-3620

Weatherill D., Simmons C.T., Robinson N.I. 2004. Testing density-dependent groundwater models: two-dimensional steady state unstable convection in infinite, finite and inclined porous layers. *Adv Water Resour.* 27, 547-562.

Contact Information: Clemens Cremer, Leibniz Universität Hannover, Institute of Fluid Mechanics and Environmental Physics in Civil Engineering, Appelstrasse 9A 30167, Hannover, Germany, Phone: +49 511762 - 3709, Email: cremer@hydromech.uni-hannover.de

Contribution of Nuclear Magnetic Resonance for supporting hydraulic model generation

T. Günther¹, R. Dlugosch¹, M.-Müller-Petke¹ and S. Costabel²

¹Leibniz Institute for Applied Geophysics (LIAG), Hannover, Germany

²Federal Institute for Geosciences and Resources, Berlin, Germany

INTRODUCTION

In order to understand the dynamics of saltwater/freshwater interfaces and to predict future processes in a changing climate, density-driven groundwater modeling (e.g., Sulzbacher et al. 2012) becomes an inevitable tool. Realistic hydraulic models must include the three-dimensional distribution of lithological units and their hydraulic properties in the subsurface. Boreholes do often not provide the sufficient spatial density to describe the typical heterogeneity of glacial sedimentary settings, and borehole logs can hardly provide the needed quantities. The most important parameter in groundwater models is the hydraulic conductivity K , but also porosity and specific storage. In density-driven models, as often used in saltwater intrusion problems, additionally the groundwater salinity of the current state is needed. Geophysical measurements can help to close the gaps between boreholes and to derive these parameters. Particularly electrical and electromagnetic (EM) methods are successfully applied since the electrical conductivity is sensitive to both clay content and fluid salinity (e.g. Wiederhold et al. 2013). However, the inversion proves to be ambiguous, i.e. a variety of models can fit the data. Furthermore, the main problem for the interpretation of results is to distinguish whether a good conductor indicates clay/silt or increased salinity.

Data from nuclear magnetic resonance (NMR) - applied at the laboratory, in boreholes or from the surface - directly reveal the water content of the investigated unit. Furthermore, the measured relaxation time T of the signal is proportional to medium pore size. Main disadvantage of surface NMR is its sensitivity to noise and its inability to detect fast-decaying signals from very small pores, e.g. clay, due to instrumental dead times. In the last years, instrumentation, measurement schemes, and data analysis methods have developed rapidly and made it applicable in a wide range of settings to characterize sediments from gravel to silt. Recently, Dlugosch et al. (2013) found a new model for computing K of clay-free sediments from porosity Φ and T providing better calibration and an upper limit for K .

Surface NMR, as one-dimensional method also called magnetic resonance sounding (MRS), is applied by deploying an increasing current through a transmit loop and measuring signals from the precessing protons in a receiver. While first inversion routines used only the initial amplitudes, a simultaneous inversion of the whole data space, i.e., inversion including T , is state-of-the-art now. Model discretization is either blocky (a limited number of layers with variable thickness, water content and T) or fixed with smoothness constraints on both quantities. As the resistivity distribution in the subsurface is needed to calculate the MRS sensitivity, the inversion of resistivity measurements is either done before (Vouillamoz et al. 2012) or jointly with MRS (Günther and Müller-Petke 2012). A simultaneous two-dimensional inversion of Φ and K was recently presented by Dlugosch et al. (2014).

EXAMPLES

Case 1: Investigation of a freshwater lens

Within the EU funded project CLIWAT (CLImate and WATer) the dynamics of the freshwater lens beneath the North Sea Island Borkum was investigated. The whole island was covered by an helicopter electromagnetic (HEM) survey accompanied by several methods: seismics, vertical electric sounding (VES), ground penetrating radar (GPR), direct push, borehole measurements and fluid probes (Wiederhold et al. 2012). Four MRS were conducted in the eastern part of the island with good to excellent noise conditions.

In order to decrease ambiguity and to improve accuracy of the results, the soundings were jointly inverted with neighboring VES using a block model of common layer boundaries (Günther and Müller-Petke, 2012). This procedure improved the accuracy of the resulting three primary properties water content, T and resistivity significantly compared to two separate inversions. The parameters and their uncertainties were used to calculate the secondary (target) parameters Φ , K and salinity and their uncertainties (Figure 1). For the latter, fluid and direct push measurements were used to fit a modified Archie equation. For hydraulic conductivity we used the model of Dlugosch et al. (2013). The necessary calibration was achieved using a pumping test in one of the boreholes (Sulzbacher et al., 2012) and a collocated sounding.

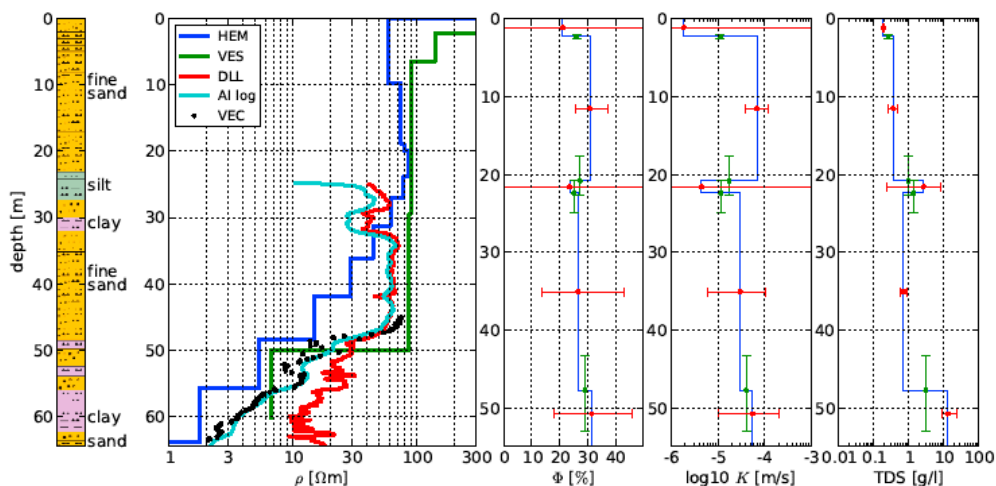


Figure 1. Geophysical results at the borehole CLIWAT 2 in Borkum: lithology (left), resistivity from different borehole and surface measurements (middle), and hydraulic parameters (Φ , K and salinity) derived from MRS/VES joint inversion results (after Günther and Müller-Petke, 2012, and Wiederhold et al., 2013).

The sounding presented in Figure 1 is used for verification since a research borehole was drilled there, logged with borehole tools and equipped with a buried electrode chain. The inversion results can be very well attributed to the present lithology. Furthermore, the derived hydraulic parameters show realistic values with moderate uncertainty due to the pumping activity that influenced the measurements. Soundings at other locations show even lower error bars and parameters with reliability comparable to standard hydrology methods. Of course, the number of locations was too small for generating a hydraulic model, but the model parameters of Sulzbacher et al. (2012) could be confirmed and adjusted.

Example 2: Two dimensional characterization of a shallow glacial channel

While initially only one-dimensional soundings were conducted, experiments with several overlapping loops lead to two-dimensional subsurface images, however firstly only of water content. Dlugosch et al. (2014) presented a scheme that inverts for both water content and relaxation time with results from the investigation site Eddelsdorf, where a shallow glacial channel of silty sediments is embedded in a sandy aquifer. These lithological setting was reconstructed (Figure 2) by jointly interpreting the images with the two parameters from surface NMR and with the resistivity from an electric resistivity tomography (ERT).

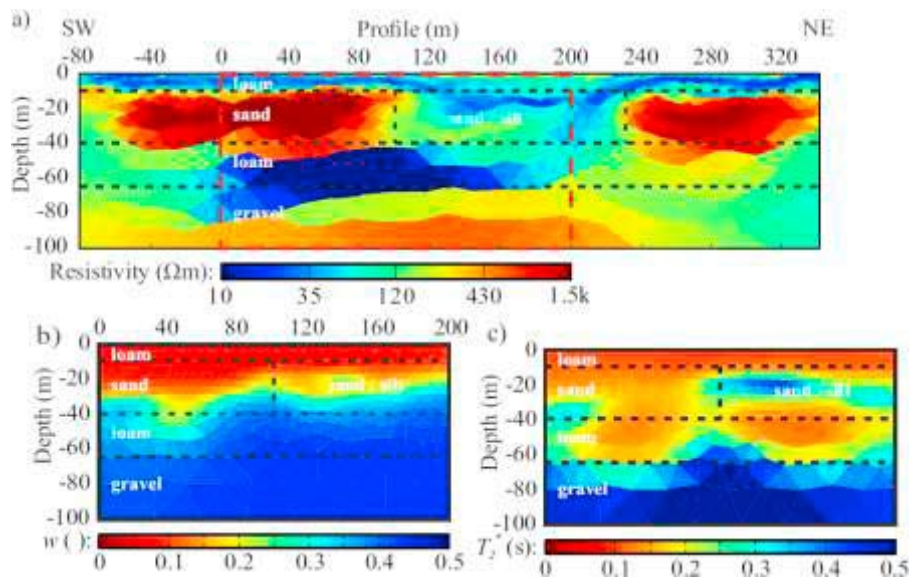


Figure 2: Resistivity (a), water content (b) and relaxation time (c) from 2D ERT and surface NMR experiments, respectively, at Eddelstorf (after Dlugosch et al., 2014).

Example 3: Vadose Zone characterization

The soil physical parameters of the vadose zone are of importance for quantifying groundwater recharge of aquifers and their protection against contaminants. MRS with small loops is in principle able to image the capillary fringe above a shallow water table. However, subsequent inversion and fitting of the water content leads to unreliable values. Costabel and Günther (2014) inverted MRS amplitude data directly for water retention (WR) parameters using three different WR models and show that reliable values for saturated water content, fringe height and pore distribution index are obtained for a sandy soil (Figure 3).

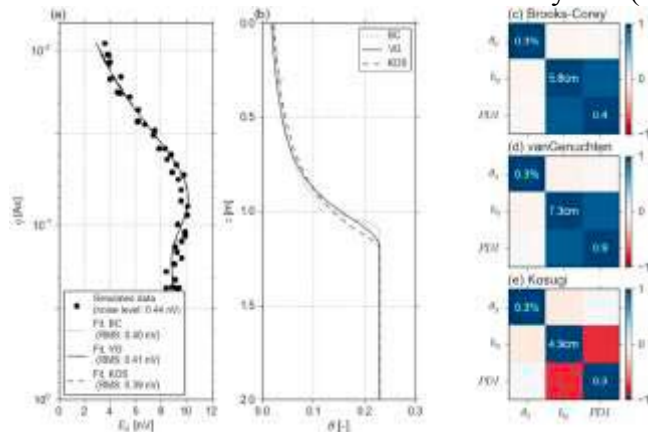


Figure 3: Data and model response (a) of inversion results using three different water retention models for describing the capillary fringe (b), uncertainty and covariance of parameters (c-e) for the Barnewitz/Nauen site (from Costabel and Günther, 2014).

DISCUSSION AND CONCLUSIONS

The application of surface NMR measurements can provide valuable information that helps to feed hydraulic models. This is particularly important in the context of salt-water problems where a differentiation between lithology and salinity must be made. It requires the knowledge of electrical conductivity, which can be obtained using electrical or electromagnetic measurements. A joint inversion of all data decreases ambiguity in the interpretation, and reduces the uncertainty of the obtained parameters.

However, surface NMR is mostly applied in form of soundings or relatively short profiles as its use becomes extensive, particularly in case of significant electromagnetic noise. Therefore it is not straightforward to create three-dimensional models in the catchment scale. Only spatial HEM or fast ground EM methods can provide line or areal data in limited time. Methods need to be developed which interweave point-wise information from combined soundings or boreholes with spatially dense data.

Calibration is needed and can typically be obtained by using pumping tests or samples in the laboratory. However, the developed petrophysical relations allow for narrowing the limits of the final quantities which in turn improves the reliability of the groundwater models.

REFERENCES

- Costabel, S. and T. Günther. 2014. Non-invasive estimation of water retention parameters by observing the capillary fringe with magnetic resonance sounding. *Vadose Zone Journal*, in press.
- Dlugosch, R., T. Günther, M. Müller-Petke and U. Yaramanci. 2014. Two-dimensional distribution of relaxation time and water content from surface NMR. *Near Surface Geophysics*, early online, doi:10.3997/1873-0604.2013062.
- Dlugosch, R., T. Günther, M. Müller-Petke and U. Yaramanci. 2013. A general model for predicting hydraulic conductivity of unconsolidated material using nuclear magnetic resonance. - *Geophysics*, 78(4), EN55-EN64.
- Günther, T. and M. Müller-Petke. 2012. Hydraulic properties at the North Sea island of Borkum derived from joint inversion of magnetic resonance and electrical resistivity soundings. - *Hydrol. Earth Syst. Sci.*, 16 (9), 3279-3291, doi:10.5194/hess-16-3279-2012.
- Sulzbacher, H., H. Wiederhold B. Siemon, M. Grinat, J. Igel, T. Burschil, T. Günther, and K. Hinsby. 2012. A modelling study of the freshwater lens of the North Sea Island of Borkum. - *Hydrol. Earth Syst. Sci.*, 16, 3621-3643, doi:10.5194/hessd-9-3473-2012.
- Vouillamoz, J.-M., J. Hoareau, M. Grammare, D. Caron, L. Nandagiri, and A. Legchenko. 2012. Quantifying aquifer properties and freshwater resource in coastal barriers: a hydrogeophysical approach applied at Sasihithlu (Karnataka state, India): *Hydrol. Earth Syst. Sci.*, 16, 4387-4400.
- Wiederhold, H., H. Sulzbacher, M. Grinat, T. Günther, J. Igel, T. Burschil and B. Siemon. 2013 : Hydrogeophysical characterization of freshwater/saltwater systems - case study: Borkum Island, Germany. *First Break*, 31(8), 109-117.

Contact Information: Thomas Günther, Leibniz Institute for Applied Geophysics, Stilleweg 2, 30655 Hannover, Germany, Phone: +49-511-643-3494, Email: Thomas.Guenther@liag-hannover.de

Hydrogeochemical characterization of groundwater in Soc Trang Province, southern Vietnam

Hoang Thi Hanh¹, Hoang Dai Phuc¹, Pham Thi Thu¹, Christian Glaeser^{1,2}, Jens Boehme^{1,2}

¹ Project “Improvement of groundwater protection in Vietnam” (IGPVN)

National Center for Water Resources Planning and Investigation (NAWAPI), Hanoi, Vietnam

² Federal Institute for Geosciences and Natural Resources (BGR), Hannover, Germany

ABSTRACT

Environmental isotope techniques were applied to study the hydrogeochemical characteristics of groundwater in Soc Trang Province, southern Vietnam in frame of the project Improvement of Groundwater Protection in Vietnam (IGPVN). Water samples were collected from both monitoring wells, private tube wells and production wells (at the Water Treatment Plant). Surface water samples were collected from a number of river, pond or channel. Major ions and stable isotope data of both groundwater and surface water samples in dry season showed no hydraulic connection between surface water and groundwater in Soc Trang Province. Some aquifers may be located in previously occurring salty areas. Salt water intrusion during the dry season occurs to some extent on Hau River, but did not affect the target aquifer. ³H analytical results differentiated two categories of groundwater: recharged with submodern water (prior to 1953) that includes qh, qp, qp₂₋₃ and n₂² aquifers and mixture of pre- and post- 1953 water that includes qh and qp aquifers. The mean transit velocity in the qp₂₋₃ aquifer located in Soc Trang Province was in a range between 2.3 – 7.8 m/yr. The pump rate at the two WTPs (My Xuyen and Long Phu districts) were exceeding the maximum sustainable yield of the aquifer and contamination from surface water may eventually occur.

INTRODUCTION

Lower Pleistocene (qp₁) and middle-upper Pleistocene (qp₂₋₃) aquifers are dominantly used for various purposes among seven porous aquifers in Soc Trang Province which locates in a coastal area in the Mekong Delta of southern Vietnam. The fresh water-bearing aquifer qp₂₋₃ was reported to be widely saline. The qp₁ aquifer is of high water bearing capacity and not fully understood. Since 1985, groundwater resource in Soc Trang Province was investigated. Recently, in 2010, aquifer storativity as well as groundwater hydrochemical characteristics were fully reported in frame of the planning for groundwater exploitation, utilization and protection in Soc Trang Province. However, the connection between groundwater and surface water, the origin of groundwater and groundwater flow processes were not clearly studied. Moreover, application of environmental isotope hydrology in hydrogeochemical study to manage and protect groundwater system in Soc Trang Province in particular and in the south of Vietnam in general was not fully concerned.

MATERIALS AND METHODS

The project Improvement of Groundwater Protection in Vietnam (IGPVN) constructed a groundwater monitoring network in Soc Trang Province, including five monitoring wells located in different districts, up to 150 m deep and provided access to the qp aquifer. In

2013, the IGPVN conducted two field surveys in dry season (4/2013) and rainy season (11/2013) to collect water samples from all the five monitoring wells and three other private tube wells and four surface water samples for chemical analysis as well as stable isotope (^2H and ^{18}O) determination. Another sampling for ^{14}C , stable isotopes and ^3H determination were conducted in June, 2013, during which, groundwater samples were collected from monitoring wells (5 monitoring wells of the National Monitoring Network and 1 monitoring well of IGPVN project), production wells (at the water treatment plants in 5 districts in Soc Trang Province) and surface water samples were collected from the pond or channel nearby. Chemical analysis and stable isotope determination were done at the Water Laboratory in the Federal Institute for Geosciences and Natural Resources (BGR). ^3H and ^{14}C determination were conducted by the Institute for Nuclear Science and Technology, Vietnam. Field data and laboratory analytical data were processed using relevant software (AquaChem, SigmaPlot, ArcGIS).

RESULTS AND DISCUSSION

Major ions

Field survey data in dry season 2013 showed low Na/Cl ratio (0.55) together with high Cl content (4910 mg/L) in river water sample collected far from the coastal line that may indicate salt water intrusion. However, this is not the case for other river water samples as well as groundwater samples. Most of the groundwater samples displayed high Na/Cl ratios and low Cl contents indicating desalination process in which freshwater is dominant, or both low Na/Cl ratios and low Cl contents indicating mixed processes. Analytical results for surface water sample collected in rainy season did not show any high Cl content, maximum value was only 35.7 mg/L. No salt water intrusion process was inferred from rainy season data.

Groundwater samples collected from the target aquifer (qp₂₋₃) are mainly of Na-HCO₃-SO₄, Na-Mg-Ca-HCO₃ and Na-Mg-HCO₃-SO₄ types in which, SO₄ was believed to originate from pyrite oxidation process or gypsum dissolution. Heavy metals and trace elements were not detected or were observed at low concentrations.

There was no difference in major ion contents of groundwater samples (both private tube wells and IGPVN monitoring wells) between dry season and rainy season. However, among four surface water sampling locations investigated, three locations (SW1, SW2 and SW3) showed significant variations in major ion contents from dry season to rainy season. Accordingly, those water samples shifted from Na-Cl type in dry season to mixed water type or bicarbonate Ca-Na-Mg type in rainy season.

Stable isotopes

The stable isotopic compositions $\delta^2\text{H}$ and $\delta^{18}\text{O}$ (in permil (‰) difference in $^2\text{H}/^1\text{H}$ and $^{18}\text{O}/^{16}\text{O}$ ratios between the samples and the Vienna Standard Mean Ocean Water (VSMOW)) were determined for water samples from Soc Trang Province.

The $\delta^2\text{H}$ and $\delta^{18}\text{O}$ values of the groundwater ranged from -47.7 to -34.7 ‰ and from -6.82 to -3.77 ‰, respectively; and those of the surface water ranged from -54.5 to -14.5 ‰ and from -7.11 to -0.44 ‰, respectively.

Stable isotope data are not available for local meteoric water in Soc Trang Province, therefore, IAEA/WMO Global Network for Isotopes in Precipitation (GNIP) data set for Bangkok was adapted.

Basing on the location of the water sample points on the scatter plot, some possible interpretations are as follows:

SW1 was shifted far towards the direction of less negative $\delta^{18}\text{O}$ values, displaying a strong enrichment in ^{18}O that may indicate a strong evaporation effect and an intrusion of seawater. SW2 was enriched in ^{18}O because of the mixing between river water and seawater at the estuary. SW3 and SW4 were depleted in stable isotope contents comparing to SW2 that may indicate a dilution effect. However, samples were collected at the end of the dry season and it was complicated to explain this dilution effect, if existing.

ST1, ST11 and GW1 located close to the GMWL might be recharged from surface water bodies during the rainy season. ST7 and GW3 showed little enrichment effects and therefore, their recharge from surface water, if existing, might occur in the beginning of the dry season when evaporation process starts to occur. However, the differences between SW1 and ST7 and between SW4 and GW3 on stable isotope contents despite their nearby locations may indicate no hydraulic connection between those river waters and the corresponding groundwaters. Similar results can be inferred from the differences between SW2 and ST4 as well as between SW3 and ST3.

The enrichment of ^{18}O in the ST4 and GW2 samples at higher degree than in the SW2 sample suggest that ST4 and GW2 are located in previously occurring salty area. Salt water intrusion enhanced by tributaries during dry season may cause insignificant effect in stable isotope content of the target aquifer.

Tritium

The T concentrations ranged from below the detection limit of 0.46 TU to 1.05 TU and from 1.14 TU to 1.53 TU for groundwater and surface water, respectively. The 7 samples with T contents below the detection limit were most likely recharged with water prior to 1953, or older than 70 years. The 4 samples with T contents from 0.6 – 1.05 TU are a mixture of pre- and post-1953 water. The T contents of surface water samples were quite low indicating exchange process of surface water with groundwater which has lower T contents.

¹⁴C dating

Carbon-14 ages ranged from 10,700 years to 22,500 years for groundwater from qp aquifer, and from 15,300 years to over 40,000 years for groundwater from n aquifer. The age of groundwater sample from the National monitoring well Q59804T (n^2_2) was so young possibly because the well was not perfectly sealed off so that younger water from upper aquifers could leak down into the well.

Among the seven groundwater samples from qp_{2,3} aquifer, the two samples collected from the WTPs (My Xuyen and Long Phu) showed younger ages than the others, indicating that younger (ground)water from the upper layers may be drawn down as a result of over exploitation at those WTPs and that contamination from surface water may eventually occur. This may imply that the pump rate at those sites were exceeding the maximum sustainable

yield of the aquifer. However, this should be confirmed by annually monitoring data for ^{14}C to clarify if there is a progressively declining ^{14}C dates in those wells. Other 3 production wells did not show abnormally younger ages at least indicating that the aquifers are completely confined, and there was no hydrogeological window and therefore, no way for the overlying younger water to leak down. Still no information about pump rate can be inferred from these dating results.

Among three national monitoring wells of n aquifer, the well Q59804T (n_2^2) showed much younger age (15,300 years) than the other 2 wells, probably because the well was not perfectly sealed off and younger water from overlying aquifers could leak down into the well, or the casing could be cracked. It might also be possible that this well is part of different aquifer.

Static water level monitoring data from a number of the National monitoring wells in Soc Trang Province provided by DWRPIS was selected to input to ArcGIS and draw a contour map. Basing on the ^{14}C dating data of the qp₂₋₃ aquifer and the apparent groundwater flow direction, three wells (LP, VC and MX) were used to determine the aquifer transit velocity. The mean transit velocity in the qp₂₋₃ aquifer located in Soc Trang Province was in a range between 2.3 – 7.8 m/yr. Those values were obtained by considering the distances between LP – VC and MX – VC wells and the differences between the ^{14}C ages of the water samples there.

CONCLUSIONS

Major ions and stable isotope data of both groundwater and surface water samples in dry season showed no hydraulic connection between the rivers and the corresponding aquifer in Soc Trang Province. Any recharge from surface water to aquifers in Soc Trang should occur outside the vicinity of Soc Trang Province. Some groundwater sampling points are located in previously occurring salty area. Salt water intrusion during the dry season occurs to some extent on Hau River, but did not affect the target aquifer.

^3H analytical results differentiated two categories of groundwater: recharged with submodern water (prior to 1953) that includes qh, qp, qp₂₋₃ and n_2^2 aquifers and mixture of pre- and post-1953 water that includes qh and qp aquifers.

The pump rate at the two WTPs (My Xuyen and Long Phu districts) were exceeding the maximum sustainable yield of the aquifer and contamination from surface water may eventually occur. It is necessary to control the pump rate at these WTPs to prevent any possible contamination.

Tidal, spring-neap, and seasonal dynamics of a saltwater-freshwater mixing zone in a beach aquifer

James W. Heiss¹ and Holly A. Michael^{1,2}

¹Department of Geological Sciences, University of Delaware, Newark, DE, USA

²Department of Civil and Environmental Engineering, University of Delaware, Newark, DE USA

ABSTRACT

The fate of chemicals discharging to the marine environment through submarine groundwater discharge may be influenced by physical flow and transport processes in the beach aquifer. A more comprehensive understanding of beach hydrodynamics over a range of time scales will thus aid in more accurately estimating chemical fluxes to coastal surface waters. The combined effects of tidal stage, tidal amplitude, and seasonal upland water table oscillations on the salinity distribution and flow dynamics in a tide-dominated sandy beach were investigated over one year using field measurements and variable-density numerical modeling. Measurements and simulations revealed an intertidal saline circulation cell with a structure and cross-sectional mixing zone area that varied over tidal, spring-neap, and seasonal time scales. Seasonal upland water table oscillations were the most important factor controlling the size of the mixing zone, followed by tidal amplitude and tidal stage. The size of the circulation cell expanded as the upland water table declined. The expansion of the cell displaced the fresh discharge zone and offshore interface seaward. The saltwater circulation cell shifted from below the upper beachface to the low tide mark in response to a change in tidal amplitude over a spring-neap cycle. Tidal stage had minimal effect on the salinity distribution in the intertidal zone over a semidiurnal tidal cycle. Seasonal variation of mean sea level did not appear to influence intertidal salinity. Salinity measurements one day following Hurricane Sandy suggest that the beach aquifer adjusted quickly after a moderate storm surge and enhanced terrestrial fresh groundwater inflow from rainfall. The highly transient nature of beach aquifer salinity over multiple time scales may have important implications for the types and rates of chemical transformations that occur in groundwater prior to discharge to the ocean.

INTRODUCTION

The intertidal and nearshore zones of beach aquifers host a significant proportion of total SGD [Li et al., 1999] and a biogeochemically active mixing zone [Charette and Sholkovitz, 2002]. These reactive environments can affect the fate of land-derived chemicals discharging to the nearshore zone. [see review in Slomp et al., 2004]. Since biogeochemical reactivity in the intertidal zone may be linked to subsurface salinity [e.g. Ullman et al., 2003], a better understanding of physical flow and transport processes in the beach aquifer will aid in more accurately predicting chemical fluxes to the coastal ocean.

A brackish to saline circulation cell forms beneath the intertidal zone as waves and tides drive seawater into the beach aquifer [Lebbe, 1999; Michael et al., 2005; Robinson et al.,

2006]. The resulting hydraulic head gradients cause seawater to circulate, initially downward and then seaward above a region of terrestrial fresh groundwater that discharges at the base of the beach. A freshwater-saltwater mixing zone forms along the perimeter of the circulation cell due to hydrodynamic dispersion. Field and numerical modeling studies demonstrate that the circulation cell can respond to tidal stage [e.g. Befus et al., 2013], tidal amplitude [Robinson et al., 2007; Abarca et al., 2013] and precipitation, however the importance of seasonal oscillations in terrestrial fresh groundwater inflow have not been investigated in the field. Further, the combined affects of these driving mechanisms (tidal stage, tidal amplitude, and seasonal terrestrial freshwater gradients) have not yet been combined into a continuous variable-density numerical model.

METHODS

Field measurements were combined with a variable-density numerical to identify the physical forcing conditions and time scales that are most important for affecting intertidal salinities. The study was conducted in the intertidal zone of a tide-dominated sandy beach at Cape Henlopen, USA. Pore water was sampled for salinity in the intertidal zone over one continuous year to obtain profiles over a tidal cycle (n=7), spring-neap cycle (n=7), seasonal cycle (n=14), and one day following the landfall of Hurricane Sandy (n=1). Water table elevation 33 m behind the dune was recorded every 15 minutes over the one year timeframe. Tide levels were taken from a nearby (<1 km) tide gauge station (NOS tidal station 8557830, Lewes, Delaware). The variable-density groundwater flow and solute transport code SEAWAT (Langevin et al., 2008) was combined with the Periodic Boundary Condition package [Post, 2011] to simulate flow and transport in the beach aquifer. The boundary conditions of the cross-sectional model were a time-varying head boundary along the landward boundary to represent seasonal water table fluctuations, and a 5-constituent tidal signal along the aquifer-ocean interface (bottom panel; Figure 1). Aquifer parameters and the amplitude of the head fluctuation at the landward boundary was adjusted until simulated heads and concentrations over the year timeframe, and groundwater velocities at the time of the tracer test reasonably matched field measurements. The aquifer-ocean interface was set as zero-concentration gradient for outflow and a constant concentration (28) for inflow. The landward boundary was a constant concentration (0).

RESULTS

Hydraulic heads and salinities in the coastal aquifer varied over tidal, spring-neap and seasonal time scales. The water table behind the dune fluctuated between 5 and 10 cm over a tidal cycle, 10-25 cm over a spring-neap cycle, and 30 cm seasonally (top panel; Figure 1). The cross-sectional area of the saltwater-freshwater mixing zone along the perimeter of the circulation cell also varied over the three time scales. Over a tidal cycle, the area fluctuated up to 3 m² and was generally largest 3-4 hours after high tide (Figure 2a). The area fluctuated by about 10 m² over 14 day spring-neap cycles, with a 4-5.5 day lag between spring tide and the largest area (Figure 2b). The area varied the most in response to seasonal inland water table oscillations, varying up to 115 m³. The area at this time scale varied inversely with the water table behind the dune; the area was largest when the water table was at its yearly maximum, and largest when the water table was at its yearly minimum (Figure 2c). These results, which show the importance of seasonality on saltwater-freshwater mixing in beach aquifers, were qualitatively supported by the field observations.

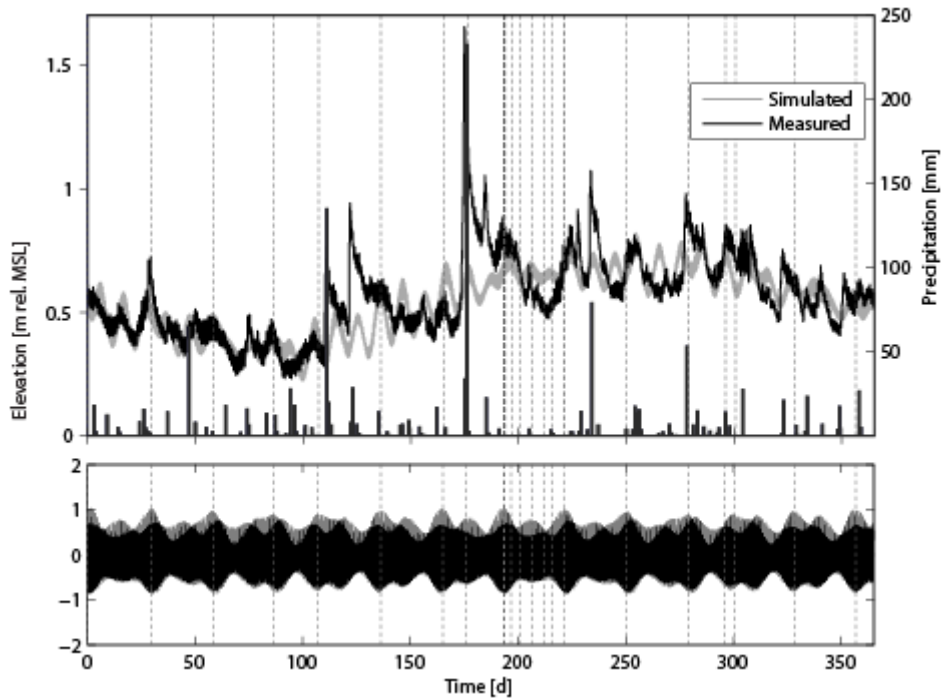


Figure 1. Measured and simulated head 33 behind the dune with precipitation (top panel). Tidal signal used in the model (bottom panel).

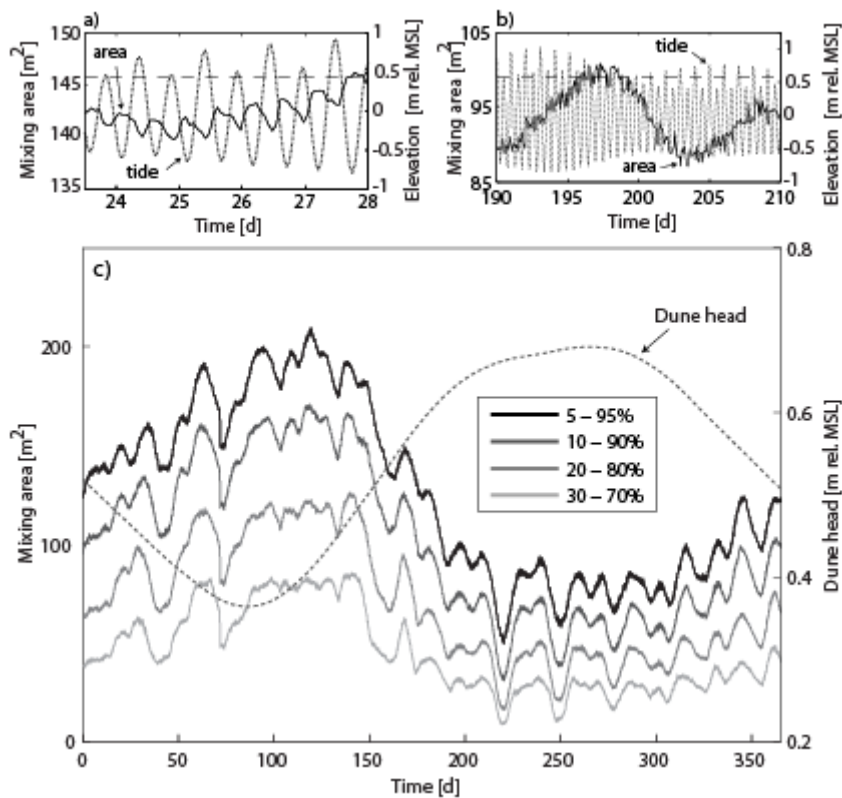


Figure 2. Area of mixing zone over a) tidal cycles; b) spring-neap cycle for the 5 -95% saltwater contours; c) mixing zone area over the one year simulation period for a range of salinity contours.

REFERENCES

- Abarca, E., H. Karam, H. F. Hemond, and C. F. Harvey. 2013. Transient groundwater dynamics in a coastal aquifer: The effects of tides, the lunar cycle, and the beach profile, *Water Resources Research* 49, 1–16, doi:10.1002/wrcr.20075.
- Befus, K. M., M. B. Cardenas, D. V. Erler, I. R. Santos, and B. D. Eyre. 2013. Heat transport dynamics at a sandy intertidal zone. *Water Resources Research* 49(6): 3770–3786. doi:10.1002/wrcr.20325.
- Charette, M. A., and E. R. Sholkovitz. 2002. Oxidative precipitation of groundwater-derived ferrous iron in the subterranean estuary of a coastal bay, *Geophysical Research Letters* 29(10): 1444, doi:10.1029/2001GL014512.
- Langevin, C. D., D. T. Thorne Jr, A. M. Dausman, M. C. Sukop, and W. Guo. 2008. SEAWAT version 4: A computer program for simulation of multi-species solute and heat transport, Technical Report, in U.S. Geological Survey Techniques and Methods Book 6, Chapter A22, 39 pp.
- Lebbe, L. 1999. Parameter identification in fresh-saltwater flow based on borehole resistivities and freshwater head data, *Advances in Water Resources* 22(8):791–806.
- Li, L., D. A. Barry, F. Stagnitti, and J. Y. Parlange. 1999., Submarine groundwater discharge and associated chemical input to the coastal sea, *Water Resources Research* 35(11), 3253-3259.
- Michael, H. A., Mulligan, A. E., and C. F. Harvey. 2005. Seasonal oscillations in water exchange between aquifers and the coastal ocean. *Nature* 436: 1145–1148.
- Post, V. E. 2011. A new package for simulating periodic boundary conditions in MODFLOW and SEAWAT, *Computers and Geosciences* 37(11): 1843–1849.
- Robinson, C., B. Gibbes, and L. Li. 2006. Driving mechanisms for groundwater flow and salt transport in a subterranean estuary, *Geophysical Research Letters* 33: L03402. doi:10.1029/2005GL025247.
- Robinson, C., B. Gibbes, H. Carey, and L. Li. 2007. Salt-freshwater dynamics in a subterranean estuary over a spring-neap tidal cycle, *Journal of Geophysical Research* 112(C9): 1–15. doi:10.1029/2006JC003888.
- Slomp, C. P., and P. Van Cappellen. 2004. Nutrient inputs to the coastal ocean through submarine groundwater discharge: controls and potential impact. *Journal of Hydrology* 295: 64–86. doi:10.1016/j.jhydrol.2004.02.018.
- Ullman, W. J., B. Chang, D. C. Miller, and J. A. Madsen. 2003. Groundwater mixing, nutrient diagenesis, and discharges across a sandy beachface, Cape Henlopen, Delaware (USA). *Estuarine, Coastal Shelf Science* 57: 539-52.

Contact Information: Holly. A. Michael; 302-831-4197; hmichael@udel.edu

Calibration of a seawater intrusion model with surrogate simulations

Daan Herckenrath^{1,2}, Leanne K. Morgan^{1,2} and Adrian D. Werner^{1,2}

¹National Centre for Groundwater Research and Training, Adelaide, Australia

²School of the Environment, Flinders University, Adelaide, Australia

ABSTRACT

In both local and global optimization literature, surrogate models are increasingly used to optimize parameters for models that require significant computational resources. In this study, calibration is undertaken for a computationally demanding seawater intrusion model using simpler, more computationally efficient surrogate models. The “complex” model comprises a heterogeneous SEAWAT-model that employs a computationally demanding solver for advective transport. Less computationally demanding surrogate models that are subsequently used are comprised of a SEAWAT-model with a more efficient advective transport solver and a model applying MODFLOW’s SWI-package. Both types of surrogate models provide only an abstract image of the “true” complex model due to numerical diffusion and a sharp interface assumption. However, it is assumed that such surrogate models mimic the physical behaviour of the complex model, which suggests their use to infer parameter sensitivities that can be used to calibrate and perform uncertainty analyses for the complex model with less computational effort. Results of this study compare parameter estimates that are obtained with a standard calibration approach of the complex model versus a calibration approach with simpler surrogate models. Furthermore, uncertainty measures and structural model error is analysed together with the computational gains when surrogate models are employed for model calibration.

Keywords: Surrogate Model, Inversion, SWI-package, SEAWAT

Contact Information: Daan Herckenrath, National Centre for Groundwater Research and Training, Adelaide, SA 5001, Australia.

Email: daan.herckenrath@flinders.edu.au

Hydrogeophysical inversion techniques for seawater intrusion models

Daan Herckenrath^{1,2}

¹National Centre for Groundwater Research and Training, Adelaide, SA 5001, Australia

²School of the Environment, Flinders University, GPO Box 2100, Adelaide, SA 5001, Australia

ABSTRACT

High-resolution geophysical data is commonly used for the development of seawater intrusion models. Typically, geophysical data is processed and inverted separately, after which seawater intrusion models are provided with hydrostratigraphy and salinity distributions that are inferred from the inverted geophysical images. Increased use of airborne geophysical surveys and advancements in inversion algorithms developed for both groundwater and geophysical methods provide the opportunity to extract information in a more intuitive fashion, in which geophysical and hydrogeological models are used in a single inversion framework. The main advantage of such framework is the definition of a hydrogeological interpretation of a geophysical dataset that can be tested in an inverse modelling exercise which would otherwise be absent. In this presentation two examples are given of hydrogeophysical inversion strategies, including a joint and coupled inversion. In the joint inversion study, parameters of a groundwater model are simultaneously estimated with those pertaining to an electromagnetic sounding. A second study is presented in which parameters of a seawater intrusion model are estimated by fitting observed geophysical signals. This presentation concludes with a summary of how hydrogeological inversion strategies can be applied to use seawater intrusion models and geophysical models in a more integrated way.

Keywords: Inversion, Geophysics, Modelling, Hydrogeophysics

Assessing managed aquifer recharge (MAR) for coastal aquifer management in Asia, South America and Europe in a changing climate

K. Hinsby¹, Z. Ma², J.C. Wu³, H.W. Liu², S. Montenegro⁴, G. C. da Silva Jr.⁵, D. Postma¹, A.R. Johnsen¹, C.S. Jacobsen¹, and S.R. Sørensen¹.

¹Geological Survey of Denmark and Greenland,

²China Geological Survey,

³Nanjing university,

⁴Federal University of Pernambuco,

⁵Federal University of Rio de Janeiro.

ABSTRACT

Population growth in coastal regions, climate change and sea level rise pose increasing challenges to the sustainable management of coastal aquifers and ecosystems and the conjunctive use of groundwater and surface water globally. The project Water4Coasts, which includes partners from Brazil, China and Denmark, seeks to develop and apply new innovative monitoring, data handling, modeling and management solutions, and share experiences on sustainable management of coastal water resources and ecosystems in a changing climate. In this paper we present selected preliminary results and conclusions from the case study sites in Recife (Brazil), Laizhou Bay (China) and the Island of Falster (Denmark).

INTRODUCTION

Sustainable management of coastal water resources and ecosystems face increasing problems globally (Wu *et al.* 1993, 2008, da Silva Jr. *et al.*, 2010, Hinsby *et al.*, 2011, 2012, 2013 Montenegro *et al.*, 2012, Sonnenborg *et al.* 2012, Rasmussen *et al.*, 2013). The main objectives of the project Water4Coasts, from the “ecoinnovation” program of the Danish Ministry of Environment, are to evaluate and promote innovative solutions within: 1) Techniques for controlling saltwater intrusion and land subsidence; 2) Efficient methods for early warning and flood risk reduction from streams and canals; 3) Methods for reducing nutrient loadings to surface waters and 4) New efficient monitoring, data handling and visualization techniques. The study focuses on investigations in three coastal aquifers at Laizhou Bay, China; Recife, Brazil and Marielyst/Falster, Denmark. The three study sites are located in very different climatological and hydro(geo)logical settings in the northern and southern hemisphere, with annual precipitation ranging from around 600 mm (evaporation greater than 1600 mm and drought conditions in Laizhou, China) up to more than 2000 mm (Recife, Brazil), and at three different seas: The Pacific ocean, the Atlantic ocean and the Baltic Sea.

METHODS

In Water4Coasts evaluation of different methods for controlling saltwater intrusion are considered, such as managed aquifer recharge of rainwater and/or recycled water for development of positive

hydraulic barriers to control saltwater intrusion. Such systems have been in operation in, for instance, California (e.g. Reichard and Johnson, 2005) and Northern Spain (Ortuño *et al.* 2012) for decades, while managed aquifer recharge in coastal dunes is well known from the Netherlands (Karlsen *et al.*, 2012). Rainwater harvesting and injection is a relevant option for the Recife site with annual precipitation of up to more than three meters in wetter years, but it may also be a relevant option at both of the other sites. For the Danish site at the Baltic Sea, regional climate models have estimated that the current winter precipitation may increase by about 50% in this century. Rainwater harvesting, storage and injection in aquifers may be an option both for controlling saltwater intrusion and for flood risk reduction. Likewise, direct injection of recycled water to coastal aquifers (managed aquifer recharge) is considered to be a realistic option to control saltwater intrusion in all three investigated sites, in order not only to control saltwater intrusion and reduce flooding risks, but also to further reduce nutrient loadings to coastal waters and, in some cases, mitigate or reduce the risk of land subsidence. The Water4Coasts project considers different options for all three study sites and compares experiences for monitoring and controlling saltwater intrusion gained at the three study sites in Brazil, China and Denmark.

RESULTS

Results from the three study sites presented here include: 1) Initial assessment of the feasibility of rainwater harvesting and MAR in Recife, Brazil; 2) Monitoring, local and regional modelling of current saltwater intrusion from seawater and old marine sediments in Laizhou Bay area, China; and 3) Assessment of the chemical and microbiological quality of drain water potentially used for injection in possibly horizontal saltwater barrier wells on the Island of Falster, Denmark.

Recife, Pernambuco State, Brazil

Recife Coastal Plain multi-aquifer system consists of two deep semi-confined aquifers, Cabo and Beberibe, covered by a phreatic aquifer, Boa Viagem. The excessive drawdown of the potentiometric heads in the deep aquifers due to overexploitation is aggravated by the high urbanization level, which highly decreases the chance of natural recharge of the system. Thus, the importance of evaluating the potential of managed aquifer recharge using rainfall as an alternative for recovering the potentiometric heads in the confined aquifers is increasing. In this context, an artificial recharge experiment simulating the use of rainfall volume storage was performed. The experiments were carried out in a region where the highest drawdowns in Cabo aquifer have been observed, in order to verify the artificial recharge results. Different scenarios were analyzed with numerical analysis by the finite element program CODE_BRIGHT (Olivella, 1995). The results suggest that managed aquifer recharge by injection wells in the site studied is feasible. Nevertheless, experiments with long-term injection and analysis should be carried out to further evaluate the potentiometric head variations caused by long-term managed aquifer recharge.

Laizhou Bay, Shandong Province, China

Different scenarios including change in abstraction (reducing water exploitation 30% and increasing brine-water mining 30%), sea level rise (rise of 0.3 m) and managed aquifer recharge along the “Yellow River to Qingdao canal” (injection volume is $1.8 \times 10^5 \text{ m}^3/\text{d}$) are currently being modeled at two scales. The modeled areas, located between Weifang city and the southern coastline of Laizhou Bay are shown in Figure 1.

Two density-dependent groundwater flow models have been established for the Chinese study area between The City of Weifang and the coastline of Laizhou Bay 1) A regional model covering all of the area shown in Figure 1 is set up in SEAWAT (Langevin *et al.*, 2007) and 2) A smaller more

detailed model is established about 1020 km² in northwestern part of the area. The model is set up in FEMWATER (Lin *et al.*, 1997). The models are established by China Geological Survey and Nanjing University. Based on the data of groundwater level, chloride and TDS concentration, regional scale and small scale models are identified and validated.

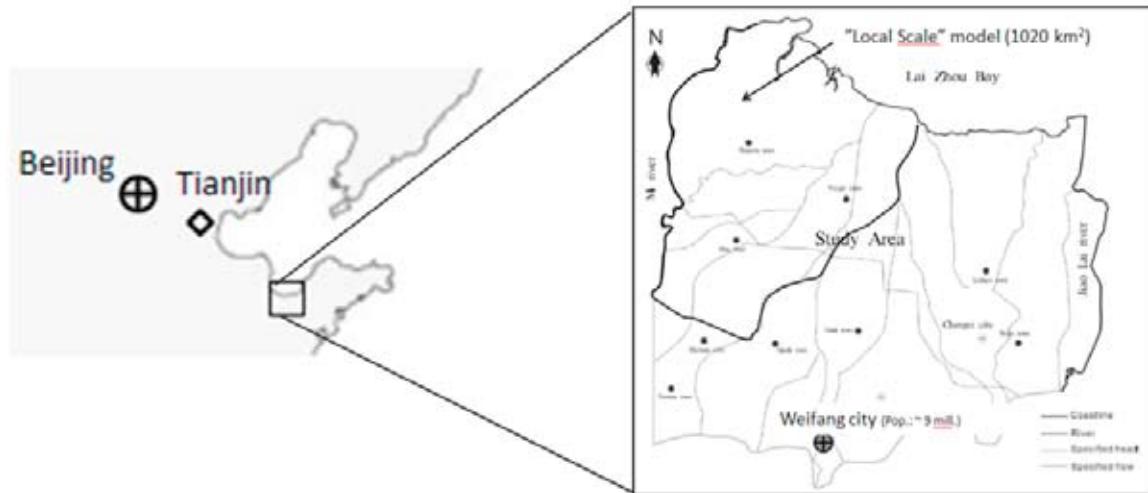


Figure 1. Laizhou Bay study area in China.

The migration of the saltwater intrusion interface was analyzed in a variety of modelling schemes in order to assess the impact of different scenarios. According to the modeling results, the seawater intrusion speed is about 450 m/a during the 1980s and 1990s, and then it slows down to 50 m/a or less in recent years. In addition, they show that the intrusion speed will increase by approximately 5% and 18% as having 50% more pumping and 0.3m sea level rising, respectively. Additional results show that the sea level rise has relatively little effect on the interface under current conditions. However, changes in aquifer recharge and abstraction have a conspicuous effect on the seawater intrusion interface, and can significantly affect the seawater intrusion interface migrating southwards. Consequently, change in abstraction scheme is the simplest and more practical way to avert seawater intrusion, because the Municipal Government is able to implement effective management quickly, while managed aquifer recharge may be the best way to prevent saltwater intrusion. However, the feasibility of such actions must be further identified according to hydrogeological conditions, drilling technology and injection water quality.

Marielyst, Falster, Denmark

Saltwater intrusion and the impact of climate change and sea level rise has been modelled with SEAWAT (Rasmussen *et al.*, 2013). Currently the model is improved and recalibrated and prepared for the evaluation of different design of saltwater intrusion barriers, which may include both vertical and horizontal barrier wells (Rasmussen *et al.*, this volume). Results from parallel studies on the organic, inorganic and microbiological quality of water from drainage canals in the study area, which potentially may be used for managed aquifer recharge in injection barrier wells, show that a rather high number of different types of pharmaceuticals (e.g. cardiovascular medicine, psychopharmica, anti-inflammatory painkillers and antibiotics) and some pathogens are currently present in drain waters, and that these therefore would need efficient pre-treatment before injection. Finally, geochemical modelling demonstrates that the evolution of groundwater chemistry and the significance of redox processes may differ significantly between single and dual porosity media.

DISCUSSION AND CONCLUSIONS

The preliminary results and assessments demonstrate that MAR may contribute to control and mitigate salt water intrusion problems in the investigated aquifers, as has also been demonstrated in several MAR systems successfully operating mainly in the U.S. and Europe. However, the studies also demonstrate that MAR requires strict control with the quality of the recharged waters and efficient treatment before recharge/injection, especially to ensure efficient removal of e.g. pathogens and potential emerging contaminants (e.g. pharmaceuticals) from sewage systems and agricultural practices etc. In addition, injection of oxic surface water into anoxic groundwater environments may mobilize trace elements such as As and Ni, e.g. from oxidation of pyrite, and create other severe groundwater quality or well clogging problems. Hence, required pretreatment, subsurface hydraulics, chemical processes and solute transport, as well as transport and fate of contaminants and naturally occurring trace elements in groundwater, need to be carefully assessed before designing and installing full scale operating MAR systems.

REFERENCES

- Hinsby, K., Ma, Z., Wu, J.C., Montenegro, S., Silva G. C. da et al. Managing coastal aquifers in Asia, South America and Europe in a changing climate – exchanging experiences and recommendations. 3rd Asia-Pacific Coastal Aquifer Management Meeting, October 21-24, Beijing, China, 2013.
- Hinsby, K., Markager, S., Kronvang, B., Windolf, J., Sonnenborg, T. O., and Thorling, L. 2012. Threshold values and management options for nutrients in a catchment of a temperate estuary with poor ecological status, *Hydrol. Earth Syst. Sci.*, 16, 2663-2683.
- Hinsby, K., E. Auken, G. H. P. Oude Essink, P. de Louw, F. Jørgensen, B. Siemon, T. O. Sonnenborg, A. Vandenbohede, H. Wiederhold, A. Guadagnini, and J. Carrera. 2011. Assessing the impact of climate change for adaptive water management in coastal regions. *Hydrol. Earth Syst. Sci.*, 149, special issue.
- Karlsen, R.H., F.J.C. Smits, P.J. Stuyfzand, T.N. Olsthoorn, B.M. van Breukelen. 2012. A post audit and inverse modeling in reactive transport: 50 years of artificial recharge in the Amsterdam Water Supply Dunes. *J. Hydrol.*, 454-455, 7-25.
- Langevin, C.D., Thorne, D.T., Dausman, A.M., Sukop, M.C. and Guo, W. 2007. SEAWAT Version 4: a computer program for simulation of multi-species solute and heat transport. US Geological Survey, Techniques and methods, Book 6, Chapter A22, US Geol. Survey, Reston, VA.
- Lin, H.C.J, Richards, D.R., Talbot, C.A. *et al.* FEMWATER. 1997. A Three-Dimensional Finite Element Computer Model for Simulating Density-Dependent Flow and Transport in Variably Saturated Media. U.S. Army Corps of Engineers etc, Technical Report CHL-97-12.
- Montenegro, S., and Ragab, R.: Impact of possible climate and land use changes in the semi-arid regions. 2012. A case study from North Eastern Brazil, *J. Hydrol.*, 434, 55-68.
- Olivella, S., 1995 Nonisothermal Multiphase Flow of Brine and Gas Thorough Saline Media. Tesis Doctoral, Universitat Politècnica de Catalunya, Departament D'Enginyeria del Terreny i Cartogràfica.
- Ortuño, F., Molinero, J., Garrido, T., and Custodio, E.. 2012. Saltwater injection barrier recharge with advanced reclaimed water at Llobregat delta aquifer (Spain), *Water Sci. Techn.* 66, 2083-2089.
- Rasmussen, P., Sonnenborg, T. O., Gonciar, G., and Hinsby, K.. 2013. Assessing impacts of climate change, sea level rise, and drainage canals on saltwater intrusion to coastal aquifer, *Hydrol. Earth Syst. Sci.*, 17, 421-443.
- Rasmussen, P., Sonnenborg, T.O. and Hinsby, K. Evaluating hydraulic barriers for reducing and controlling saltwater intrusion in a changing climate. SWIM23, pp. ??, this volume.
- Reichard, E.G. and Johnson, T.A. 2005. Assessment of Regional Management Strategies for Controlling Seawater Intrusion. *Journal of Water Resources Planning and Management*, 131(4):280-291.
- Silva Jr., G. C., Bocanegra, E., Custodio, E., Manzano, M., and Montenegro, S. 2010. State of knowledge and management of Iberoamerican coastal aquifers with different geo-hydrological settings, *Episodes*, 33, 91-101.
- Sonnenborg, T. O., Hinsby, K., van Roosmalen, L., and Stisen, S. 2012. Assessment of climate change impacts on the quantity and quality of a coastal catchment using a coupled groundwater-surface water model, *Clim. Change*, 113.
- Wu, J. C., Meng, F. H., Wang, X. W., and Wang, D.. 2008. The development and control of the saltwater intrusion in the eastern coastal of Laizhou Bay, China, *Environ. Geol.*, 54, 1763-1770.
- Wu, J.C., Xue, Y., Liu, P., Wang, J., Jiang, Q. and Shi, H. 1993. Sea-Water Intrusion in the Coastal Area of Laizhou Bay, China .2. Sea-Water Intrusion Monitoring, *Ground Water*, 31, 740-745.

Contact information: Klaus Hinsby, Geological Survey of Denmark and Greenland, Department of Hydrology, O. Voldgade 10, 1350 Copenhagen, Denmark, tel.: +45 91 333 618, e-mail: khi@geus.dk

Responses to Climate Change and Development Stressors on Small Oceanic Islands

Shannon T. Holding¹ and Diana M. Allen¹

¹Department of Earth Sciences, Simon Fraser University, Burnaby, BC, Canada

ABSTRACT

The freshwater lenses of small islands are vulnerable to stressors from climate change and development, in particular: sea level rise, storm surge inundation, changes to groundwater recharge, and increased pumping. This study evaluates the freshwater lens response to stressors on a low-lying limestone island as a case study representative of islands with similar hydrogeological setting. Recharge was modeled using the HELP hydrologic model, and then used as input to a density-dependent flow and solute transport model constructed using SEAWAT. The SEAWAT model was used to simulate altered recharge states, sea level rise and increased pumping. Ongoing work focuses on the lens response to storm surge. Stressors were modeled using scenarios of gradual and instantaneous change to determine the effect of the rate of change of the applied stressor on the magnitude and timing of the lens response. The modeling results were interpreted with geospatial analyses to quantify area and volume of the simulated lens, allowing quantitative comparison of lens morphology between different stressor scenarios. By the 2090s, sea level is expected to rise by 0.6 m and recharge is projected to decrease by up to 15% relative to baseline values. When applied instantaneously to the model, these stressors resulted in a reduction of the FWL volume by up to 42%. If stressors were applied gradually, the overall magnitude of impact to the FWL was reduced, suggesting that solver time stepping may be a factor. Upconing of the underlying saltwater was observed at all wellfield locations under increased pumping, but when climate change was included, the magnitude of upconing increased for all wells.

Keywords: Freshwater Lens, Small Islands, Numerical Modeling, Climate Change, Pumping

INTRODUCTION

The freshwater resources of small islands primarily comprise fresh water lenses (FWLs). The extent and morphology of the FWL is controlled by many factors, including the size, shape, topography, and geology of the island (Falkland 1991; Robins and Lawrence 2000). Groundwater recharge is the primary source of freshwater to the lens, and therefore, factors affecting the amount of recharge to the lens, such as precipitation and evapotranspiration, also have a significant impact on the FWL morphology (Ayers and Vacher 1986). The many factors controlling FWL morphology demonstrate that the freshwater resources of small islands rely on a delicately balanced hydrogeological system. Since the island hydrogeological system is self-contained and the FWLs are limited in size (due to the nature of small islands), there is a low capacity to buffer stresses when imbalances in the system occur. Therefore, the freshwater resources of small islands may be particularly vulnerable to degradation exacerbated by climate change and human activities.

This study evaluates the spatial and temporal response of an island FWL to major stressors including changes to recharge, sea level rise, and increased pumping. The research is based on Andros Island, The Bahamas, which represents a typical low-lying limestone island with a thin FWL, as is common throughout the Caribbean and South Pacific regions (Falkland 1991). Andros Island is comprised of several smaller islands and cays (Figure 1) and is relatively undeveloped, but has the largest FWL in The Bahamas. Groundwater is exploited via municipal wellfields located in 11 communities as well as a limited number of private wells. The southern regions of Andros Island receive approximately 39% less rainfall than the northern regions.

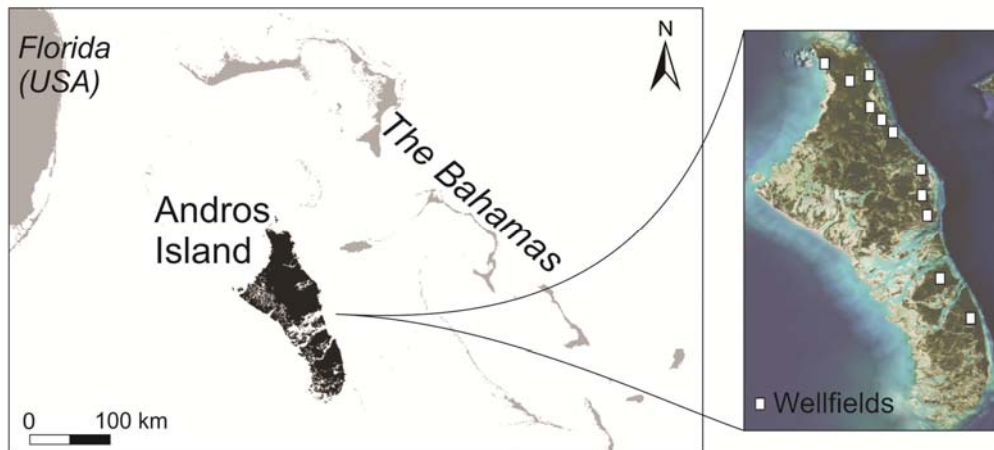


Figure 1. Andros Island with municipal wellfields indicated

METHODS

Recharge Modeling (HELP)

Recharge was modeled using the software HELP (Schroeder et al., 1994), which accounts for components of the water budget such as soil moisture storage, runoff, interception and evapotranspiration. A 100 year baseline climate data series, generated using a stochastic weather generator, was used as input to a vertical percolation column representative of the island. Recharge was then modeled for the 2090s using published climate change predictions for The Bahamas (McSweeney et al. 2010).

Numerical Modeling (SEAWAT)

A three-dimensional density-dependent numerical groundwater flow and solute transport model was developed using SEAWAT to simulate the FWL on Andros Island. The island was divided into a northern and southern model to allow for refined grid resolution and to optimize computational efficiency. The baseline model was calibrated to available field data.

Climate change scenarios were simulated by increasing sea level by 0.6 m and altering recharge to represent the projected climate state for the 2090s. Scenarios of increased pumping were simulated by raising the pumping rate of the wellfields incrementally by up to 10 times the current rate and observing recovery of the lens after pumping was stopped. These stressors were applied to the model both gradually and instantaneously to determine the effect of the rate of change of the applied stressor on the magnitude and timing of the lens response.

RESULTS

The simulation of the FWL in the baseline model provides a snapshot of the average annual FWL morphology (Figure 2a). The northern region of Andros Island has a large FWL, whereas the southern region has several smaller lenses. By the 2090s, recharge will decrease by 11% in the north and decrease by 15% in the south relative to baseline values. SEAWAT simulations of future climate conditions (reduced recharge and sea level rise) result in reduction of FWL areal extent and volume (Figure 2b). Simulations of reduced recharge alone result in the majority of FWL reduction, with sea level rise contributing a smaller proportion of lens reduction. This is likely due to the hydrogeological system on Andros Island being recharge-limited and thus able to accommodate changes in water table elevation (Werner and Simmons 2009; Michael et al. 2013).

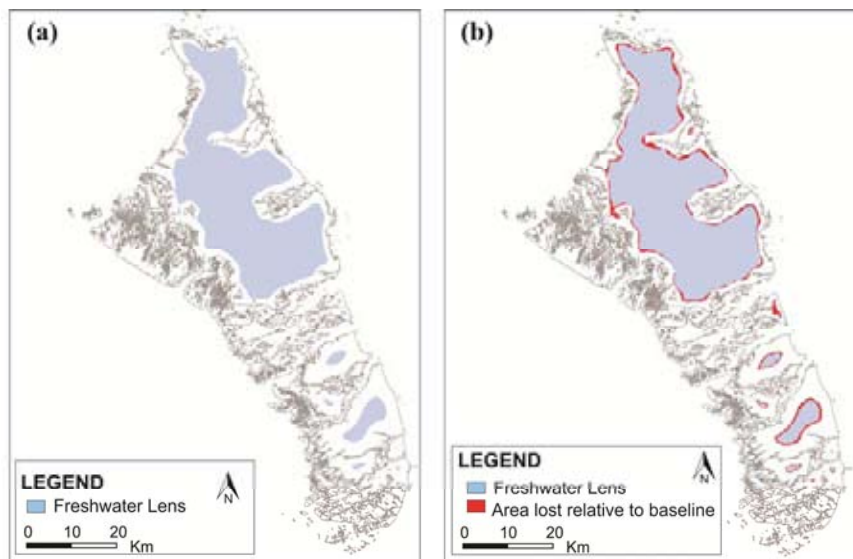


Figure 2. a) baseline FWL; b) climate change FWL (instantaneous shift model)

The gradual shift model had less FWL loss than the instantaneous shift model (Table 1), although the difference in area/volume change was significantly smaller in the northern model due to the larger lens size. In both the northern and southern models, the rate of change in concentration was higher near the periphery of the FWL than in the center of the lens as expected, because here the lens is thinner.

Upconing of the underlying saltwater was observed at all wellfield locations under increased pumping. However, when pumping was simulated under climate change conditions, the magnitude of upconing increased for all wells. In addition, the residual upconing after pumping stopped was larger under climate change conditions, and simulations of the southern model indicated that the FWL was highly degraded with saltwater.

Table 1. Percent change in freshwater lens morphology relative to baseline model

Modeled Region	Model Type	% Change Area	% Change Volume
Northern	Gradual	-4.1	-5.9
	Instantaneous	-4.5	-6.1
Southern	Gradual	-16.8	-24.2
	Instantaneous	-25.3	-42.1

CONCLUSIONS

Changes in the area and volume of the FWL were significant for the southern model, given that the baseline FWLs are small and thus more susceptible to change. The greatest impacts to lens morphology occurred along the periphery of the lens, where most settlements on Andros are located. Therefore, even small changes to the FWL can have significant implications for resource sustainability.

The response of the FWL was found to be sensitive to how the stressors were applied to the model. If applied gradually, the cumulative impact to the FWL was less than when the stressors were applied instantaneously. Model time stepping may be a determining factor. This result has important implications for how climate change stressors are applied to models because most modeling studies use instantaneously applied stressors.

The effect of multiple stressors, demonstrated in this study by simulating pumping and climate change together, also reduce the ability of the FWL to respond to and recover from stressors. Therefore, future studies should evaluate the cumulative impacts of stressors and interactions of various factors affecting the FWL. The approach used to characterize the FWL response on Andros Island is transferrable to other low-lying islands with similar hydrogeological setting.

Ongoing work evaluates the spatial and temporal response of the FWL to storm surge inundation and compares the results to the stressors evaluated in this study.

REFERENCES

- Ayers, J.F., and H.L. Vacher. 1986. Hydrogeology of an atoll island: A conceptual model from detailed study of a Micronesian example, *Ground Water* 24: 185-198.
- Falkland, A. ed. 1991. *Hydrology and water resources of small island: a practical guide*, United Nations Educational, Scientific, and Cultural Organization (UNESCO), Paris.
- McSweeney, C., M. New, G. Lizcano and X. Lu. 2010. The UNDP Climate Change Country Profiles, *Bulletin of the American Meteorological Society* 91, 157-166.
- Michael, H.A., C.J. Russoniello and L.A. Byron. 2013. Global assessment of vulnerability to sea-level rise in topography-limited and recharge-limited coastal groundwater systems, *Water Resources Research*, 49 (4): 2228-2240.
- Robins, N., and A. Lawrence. 2000. Some hydrogeological problems peculiar to various types of small islands, *Water and Environmental Management Journal*, 14 (5):341-346.
- Schroeder, P.R., T.S. Dozier, P.A. Zappi, B.M. McEnroe, J.W. Sjostrom and R.L. Peyton. 1994. *The Hydrologic Evaluation of Landfill Performance (HELP) model: Engineering documentation for Version 3*, Rep. EPA/600/R-94/168b, U.S. Environmental Protection Agency, Washington, D.C.
- Werner, A.D., and C.T. Simmons. 2009. Impact of sea-level rise on sea water intrusion in coastal aquifers, *Ground Water*, 47, 197-204.

Contact Information: Shannon T. Holding, Simon Fraser University, Department of Earth Sciences, 8888 University Drive, Burnaby, BC, V5A1S6, Email: sholding@sfu.ca

Freshwater lenses as archives for climate history - insights from depth-specific age dating and stable water isotope analysis, Langeoog Island, Germany

Georg J. Houben¹, Paul Koeniger¹ and Jürgen Sültenfuß²

¹Federal Institute for Geosciences and Natural Resources (BGR), Hannover, Germany

²Institute for Environmental Physics, University of Bremen, Bremen, Germany

ABSTRACT

The age stratification of groundwater contained in a freshwater lens of Langeoog Island, Germany, was reconstructed based on depth-specific sampling and the tritium helium dating method. The vertical distribution of groundwater ages is spatially strongly variable. This is an effect of the variable land use and the resulting differences in groundwater recharge. Dune valleys contribute significantly more groundwater recharge per area than dune tops and up to four times more than other land uses such as forests and urban areas. The fresh groundwater shows a distinct decrease of stable isotope ratios with increasing depths. This mirrors an evolution of the climatic conditions at the time of recharge. Combined with dating of groundwater, this pattern could be matched to observed climate data, which show a distinct air temperature increase during the last 50 years.

INTRODUCTION

Langeoog is a barrier island of about 20 km² size, located off the North German coast, in the intertidal Wadden Sea. Water supply for population and tourists relies on the extraction of groundwater from one of three freshwater lenses. The lenses are recharged only by rainfall.

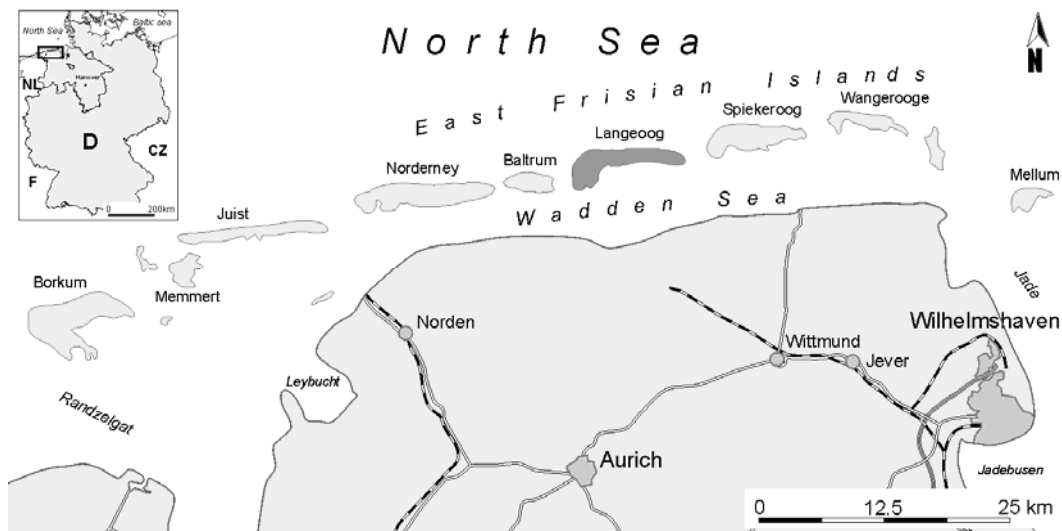


Figure 1. Location map.

METHODS

Several multi-level observation wells with short (1 to 2 m) screens allowed the depth-specific sampling of groundwater. Stable water isotope ratios $\delta^2\text{H}$ and $\delta^{18}\text{O}$ were analyzed after vaporization on a PICARRO L2120-i laser cavity ring-down apparatus against Vienna Standard Mean Ocean Water (VSMOW). Tritium and dissolved noble gases were analyzed at the Institute for Environmental Physics at Bremen University (Sültenfuß et al., 2009).

RESULTS

The freshwater lens as climate archive

The fresh groundwater samples generally show a decrease of stable water isotope ratios with increasing depths. Groundwater ages also increase with depth (Fig. 2). These patterns mirror an evolution of the climatic conditions over time. The freshwater column contains a climate archive which reflects e.g. temperature changes during the last decades. Combined with age dating of groundwater, this pattern could be matched successfully to air temperature records from the neighboring island of Spiekeroog (Fig. 3).

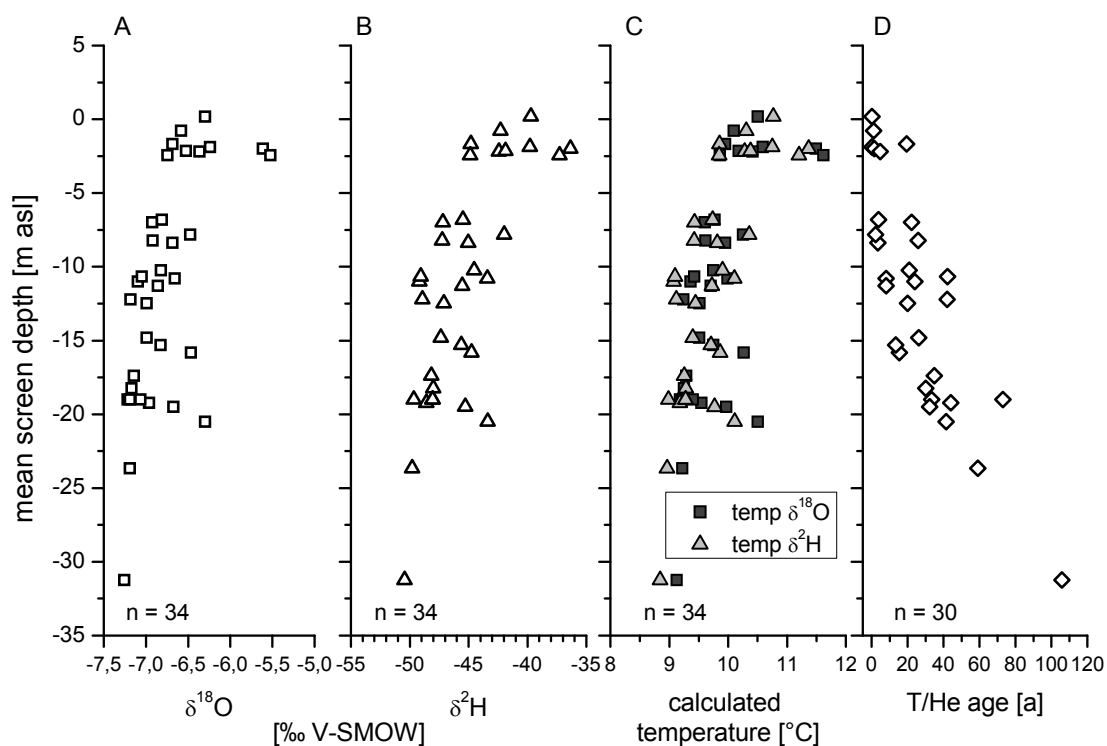


Figure 2. Stable water isotope ratios (A) $\delta^{18}\text{O}$, (B) $\delta^2\text{H}$, (C) recharge temperatures after Dansgaard (1964), and (D) tritium helium age, as a function of screen depth.

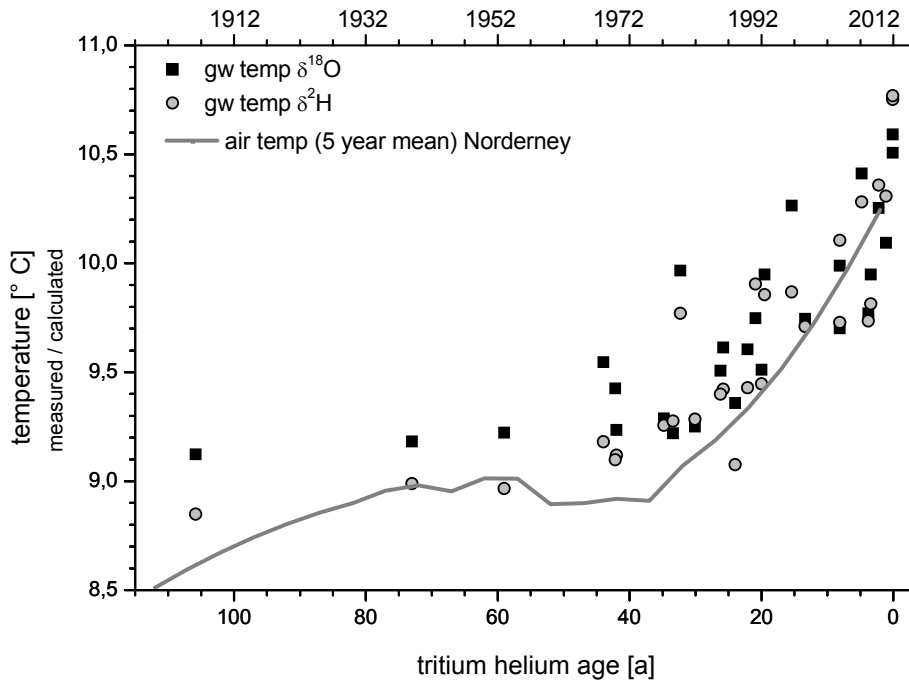


Figure 3. Comparison of measured air temperatures from Norderney and groundwater temperatures from Langeoog calculated after Dansgaard (1964).

Age stratification as indicator of spatially inhomogeneous groundwater recharge

The age stratification of the freshwater lenses currently in use was investigated using depth-specific sampling and tritium helium age dating (Fig. 4). It shows an increase of age with depth, with age layers successively becoming thinner due to ongoing exfiltration at the sides.

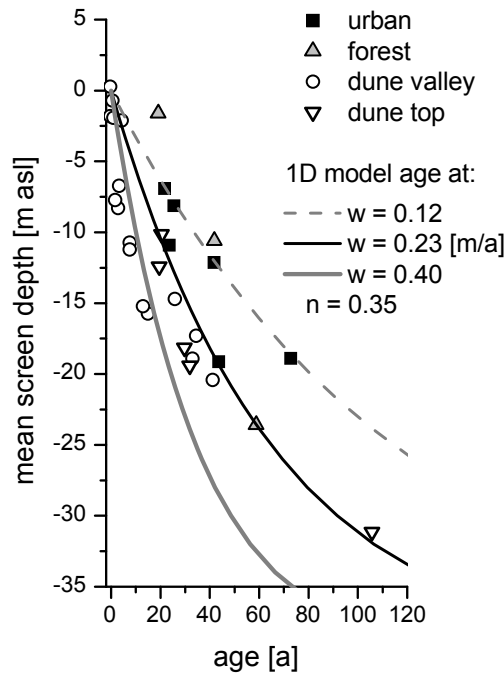


Figure 4. Measured tritium helium groundwater ages as function of mean screen depth compared to 1D age models after Vogel (1967, 1970). w = recharge rate, n = porosity.

The observed stratification is strongly affected by variations in land use and the resulting differences in recharge rates. Dune valleys contribute almost twice as much groundwater recharge per area than urban zones and forests. Infiltration at dune tops is significantly lower than in the valleys, probably due to repellency of the dry sand. Not only is the thickness of the individual age layers thinner under areas receiving less recharge compared to dune valleys but this might also affect the total thickness (or interface depth) of the freshwater lens. If the area of an individual type of land use is sufficiently large, the thickness (or interface depth) may differ from an adjacent area of different land use and recharge rate.

DISCUSSION AND CONCLUSIONS

The combination of depth-specific age-dating of groundwater with hydrochemical and stable water isotope analysis gives a good insight into the internal dynamics of freshwater lenses. The age stratification is a function of the groundwater recharge rate which is strongly influenced by the type of land use. Dune valleys act as collectors of groundwater recharge and contribute more than any other type of land use. Two dimensional analytical models of age stratification which assume a homogeneous recharge (e.g. Greskowiak et al. 2013) cannot explain the age distributions encountered on Langeoog.

Variations of the stable isotope ratios of groundwater over depth can indicate changing climatic conditions over time. Freshwater lenses may thus preserve a climate archive. Islands are especially useful as climate archives, since the proximity to the ocean dampens the influence of temperature extremes, altitude effects are absent, and the system size is small. The reach of this approach is limited by the diminishing thickness of age layers with depth and the range of the chosen dating technique.

REFERENCES

- Dansgaard, W. 1964. Stable isotopes in precipitation. *Tellus*, 16, 436-468.
- Greskowiak, J., T. Röper, V.E.A. Post. 2013. Closed-Form approximations for two-dimensional groundwater age patterns in a fresh water lens. *Ground Water*, 51(4), 629-634.
- Sültenfuß, J., W. Roether, and M. Rhein. 2009. The Bremen mass spectrometric facility for the measurement of helium isotopes, neon, and tritium in water. *Isotopes in Environmental and Health Studies*, 45(2), 83-95.
- Vogel, J.C. 1967. Investigation of Groundwater Flow with Radiocarbon. International Atomic Energy Agency, Proceedings Series, 355-368, Vienna.
- Vogel, J.C. 1970. Carbon-14 dating of groundwater. International Atomic Energy Agency, Proceedings. Series, 225-239, Vienna.

Contact Information: G.J. Houben, Federal Institute for Geosciences and Natural Resources (BGR), Stilleweg 2, 30655 Hannover, Germany, Phone: 0049-511-643-2373, Email: georg.houben@bgr.de

Hydrogeological features of freshwater lenses on volcanic islands - physical and numerical modeling

Katrina Mariner^{1,2}, **Georg J. Houben**³, Leonard Stoeckl^{2,3} and Martin Thullner⁴

^{1,2}Samoa Water Authority (SWA), Apia, Samoa

²Leibniz University, Hannover, Germany, Germany

³Federal Institute for Geosciences and Natural Resources (BGR), Hannover, Germany

⁴Helmholtz Centre for Environmental Research (UFZ), Leipzig, Germany

ABSTRACT

We conducted sandtank experiments and numerical model simulations of three typical hydrogeological features of freshwater lenses found on volcanic islands of the Hawaiian type. We investigated the effects of impermeable sheet intrusions (dikes), fringing reefs, and saltwater overwash during storms. The sandtank experiments of the first two cases could be modeled successfully using a 2D numerical model. Although our sandtank is only 5 cm wide, the overwash case showed strong 3D effects, which could not be recreated by the 2D model.

INTRODUCTION

The hydrogeology of volcanic islands is strongly influenced by the presence of lava tubes, volcanic layers of strongly variable hydraulic conductivity (e.g. porous cinder layers vs. fractured Aa lava flows), fringing reefs, and dikes.

We conducted sandtank experiments, followed by numerical models, of three typical hydrogeological features of freshwater lenses, oriented on the Island of Savai'i, Samoa:

- (A) Impermeable volcanic dike: secondary sheeted vertical intrusions (dikes) may separate the aquifer into several compartments. Head differences across dikes can be large.
- (B) Fringing reef: coral reefs often rim volcanic islands. While the reef material can be quite permeable, the hydraulic conductivity of the basalt may be even larger. The fringing reef may therefore act as a local confining layer.
- (C) Saltwater overwash: during storm events, seawater may be infiltrated through the soil to the top of freshwater aquifers.

METHODS

The set-up of the sandtank experiments is based on Stoeckl and Houben (2012). Experiments were carried out using an acrylic glass box (2.0 m length, 0.5 m height and 0.05 m width). The freshwater and saltwater densities were 1.000 and 1.025 g/cm³. To visualize the interaction of saltwater and freshwater, tracer colorants were added at a concentration of 0.3 g tracer per liter. For Cases A and B, the aquifer was initially saturated with saltwater (red) and freshwater recharge was applied from the top of the model by drippers (yellow and blue). Several recharge rates were applied consecutively.

For numerical modeling, the finite element model FEFLOW 6.1 (Diersch 2005) was used for Cases A and B, and the simulation model Crunch for Case C.

Case A: The impermeable dyke feature was constructed with plasticine and was installed into the model prior to infilling the model with medium sand, the latter representing the basaltic aquifer (Fig. 1).

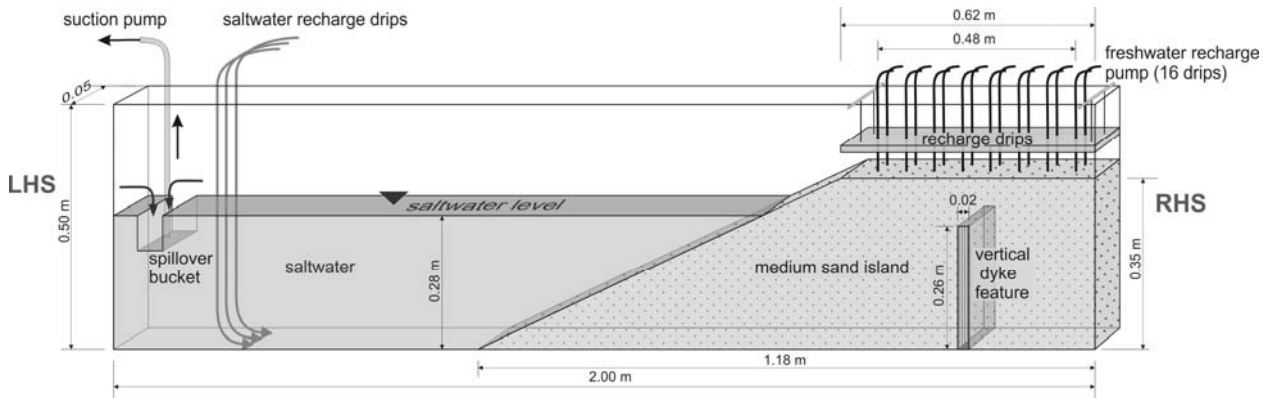


Figure 1. Physical model setup for Case A.

Case B: For the fringing reef case, the sandbox was filled with coarse sand, representing the basaltic aquifer. Fine sand, representing the fringing reef, was added at the coast (Fig. 2).

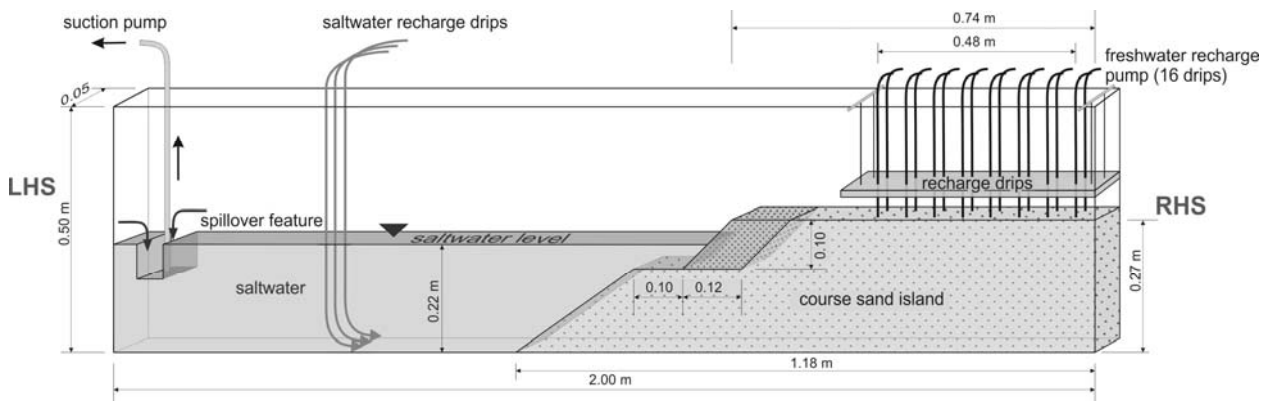


Figure 2. Physical model setup for Case B.

Case C: The tank was completely filled with sand and initially saturated with freshwater. Recharge was applied from the right side to create horizontal flow. Overwash was simulated by injecting saltwater into the upper half of the recharge valves (Fig. 3).

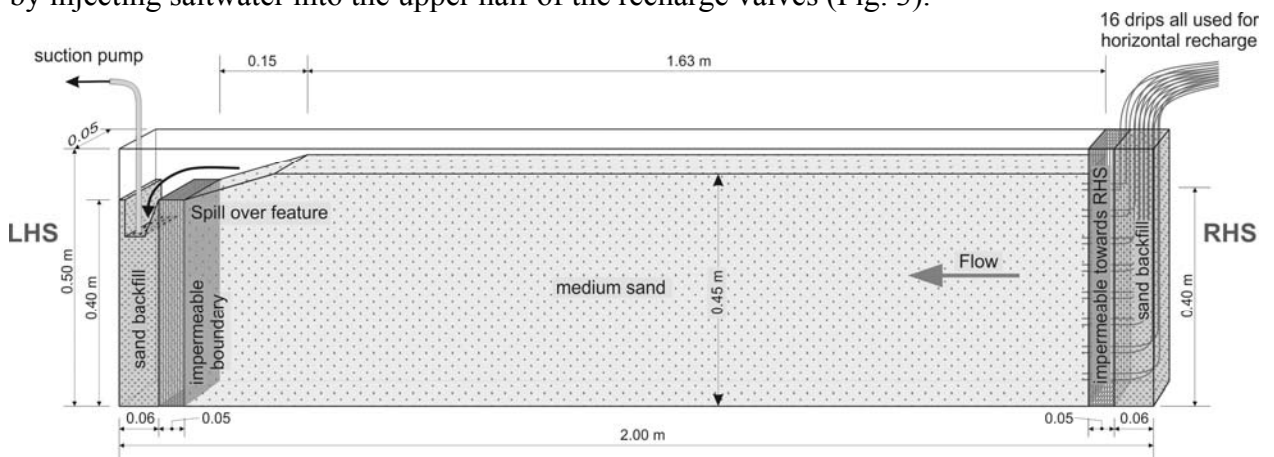


Figure 3. Physical model setup for Case C.

RESULTS

Case A. Impermeable vertical dike

The effects of an impermeable dikes became clearly visible, especially the vertical flow components. The resulting interface geometry, for a set of four recharge rates, was successfully recreated with a 2D numerical model (Fig. 4). The slight differences between the physical and numerical results can be attributed to limited observational accuracy.

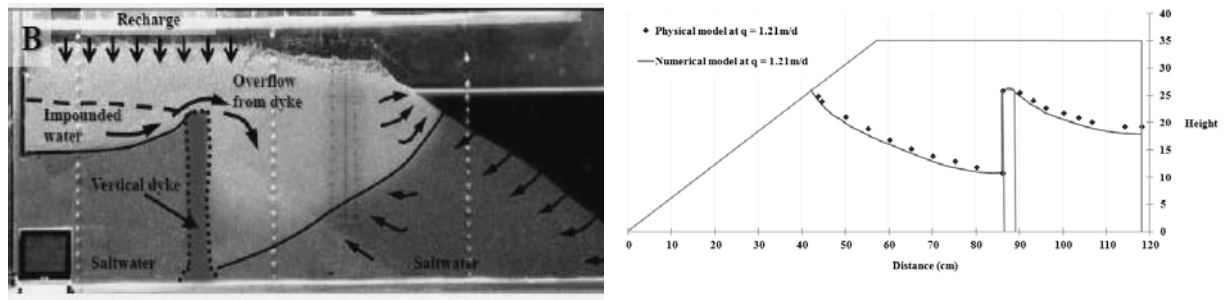


Figure 4. Left: Interface geometry at equilibrium (recharge rate: 1.21 m/d). Right: Comparison of experimental results and numerical model (flipped).

Case B. Fringing reef

A large proportion of the outflowing freshwater passes underneath the less permeable reef and forms submarine springs, a feature also common in Samoa. The comparison between numerical and physical models yielded a good fit for all recharge rates studied (Fig 5).

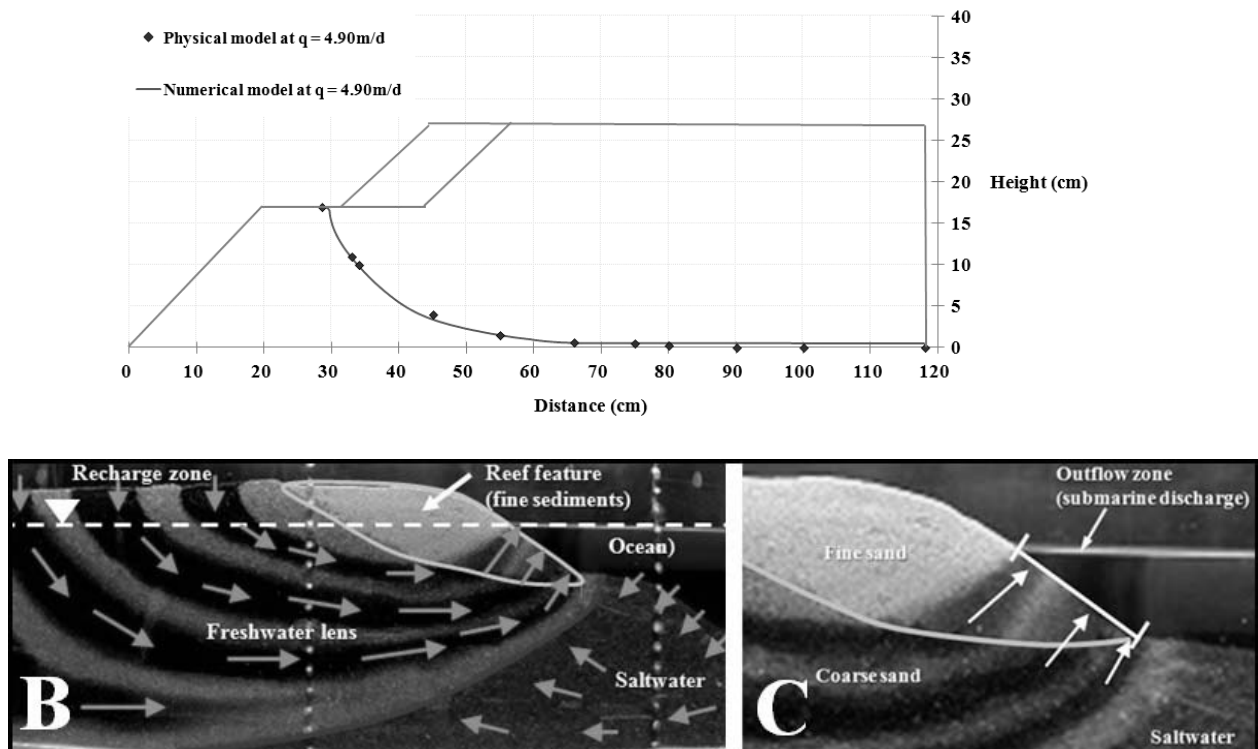


Figure 5. Top: Comparison of experimental results and numerical model (flipped). Below: flow paths at equilibrium (recharge rate: 4.90 m/d).

Case C. Saltwater overwash onto horizontally flowing freshwater

Although the sandtank is only five centimeters wide, strong 3D effects occurred. Saline water flowed downwards on one side of the model, while freshwater rose on the opposite side (Fig. 6). This phenomenon occurred in several experimental runs, using different flow rates and salinity contrasts. Transient fingering was also visible. A 2D numerical model was therefore not able to simulate the outcome of the experiments. Clearly, a 3D approach would be needed.

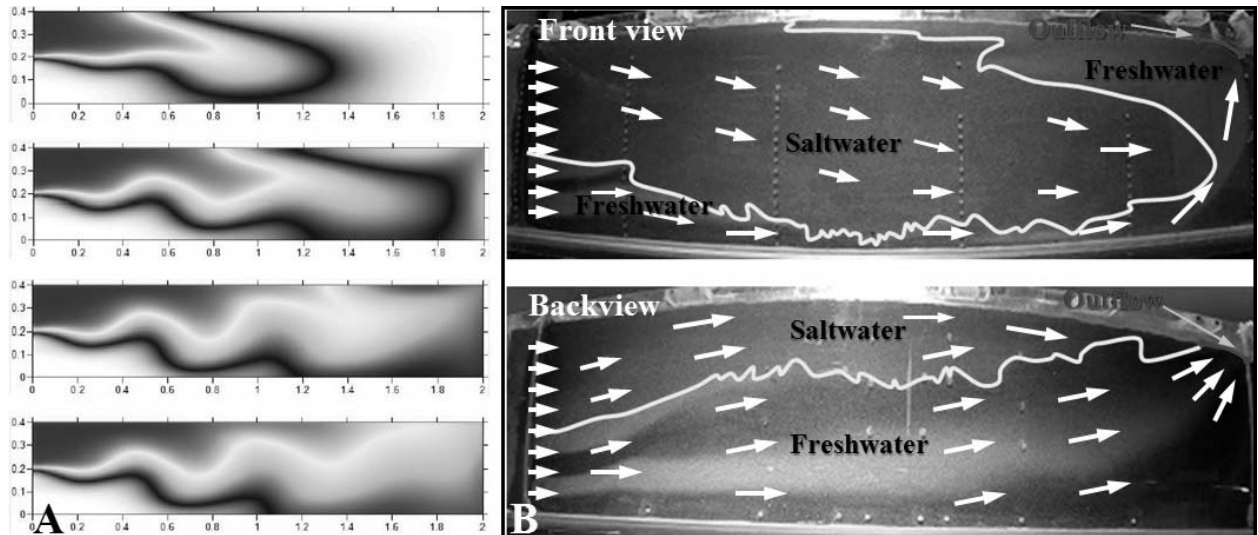


Figure 6. (A) Numerical 2D model, (B) front view, and (C) back view of sandtank experiment. Total recharge: 1.94 m/d.

DISCUSSION AND CONCLUSIONS

Sandtank experiments and numerical models of three typical hydrogeological features of freshwater lenses on volcanic islands were compared. While the results of the sandtank experiments on impermeable sheet intrusions (dikes) and fringing reefs could be modeled successfully using a 2D FEFLOW model, the saltwater overwash case showed strong 3D effects, even in our sandtank of only 5 cm width, and the numerical 2D model was unable to recreate the experimental results.

REFERENCES

Diersch, H.J.G. 2005. FEFLOW: Finite Element Subsurface Flow and Transport Simulation System. WASY GmbH Institute for Water Resources Planning and Systems Research, Berlin. pp.292.

Stoeckl, L., and G.J. Houben. 2012. Flow dynamics and age stratification of freshwater lenses: experiments and modeling. *Journal of Hydrology*, 458-459, 9-15.

Contact Information: G.J. Houben, Federal Institute for Geosciences and Natural Resources (BGR), Stilleweg 2, 30655 Hannover, Germany, Phone: 0049-511-643-2373, Email: georg.houben@bgr.de

Impact of tourism on groundwater extraction on the island of Langeoog, Germany

Georg J. Houben¹

¹Federal Institute for Geosciences and Natural Resources (BGR), Hannover, Germany

ABSTRACT

The economy of the Northern German Island of Langeoog is largely dominated by tourism. Water supply depends on the extraction of groundwater from a freshwater lens. Almost three quarters of the groundwater extraction can be attributed directly to tourism. Water demand shows a strong seasonality which mirrors the holiday seasons. The introduction of water-saving household appliances in the 1990s has significantly reduced the water demand. The tendency towards more frequent but shorter vacations may increase water demand again somewhat. So far, extraction has remained sustainable, as stable groundwater levels show.

INTRODUCTION

The island of Langeoog, a barrier island of about 20 km² size, is situated in the Wadden Sea off the North German coast. Water supply depends on the extraction of groundwater from one of three freshwater lenses.

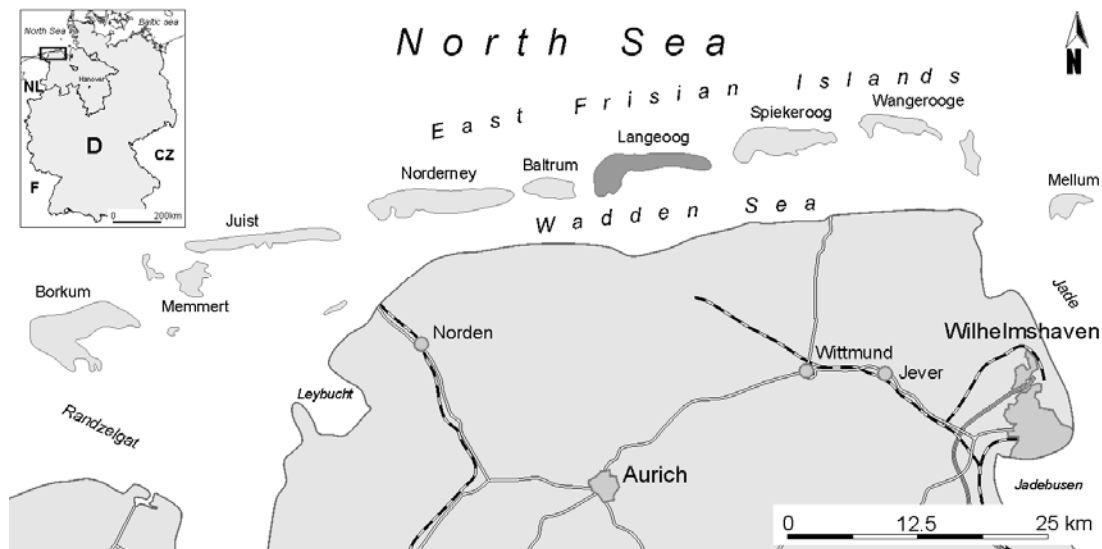


Figure 1. Location map.

Historically, the small population (1885: 202 people) obtained its water from the collection of rain water and from shallow dug wells. Many of the latter were affected by a severe storm flood in 1905. This, and increasing tourism, created demand for a more stable and less vulnerable water supply. In 1909 three wells, 14 to 18 m deep, were drilled in the western freshwater lens, close to the village. They had to be abandoned in 1989 due to microbiological quality problems. Several new wells were drilled from 1938, extracting water from the eastern part of the western lens. In order to prevent upconing of saline water,

extraction today is distributed over 20 small wells, screened from 10 to 18 m below sea level. Pumping is done intermittently at low rates of 10 m³/h per well.

RESULTS

Prior to World War II, water consumption increased due to state-sponsored tourism and construction workers who worked on military installations. Tourism ceased during the war years and consumption leveled off. Immediately after the war, the tourist infrastructure was used to accommodate large numbers of refugees, resulting in a jump in water demand. The post-war network suffered from large losses due to bomb damage, as shown by the difference between extraction and accounted-for consumption (1951 to 1969 data only), but this problem was eliminated until the 1960s (Fig. 2).

Today, Langeoog's economy is almost exclusively dominated by tourism. In 2011 around 1,540,000 overnight stays and 124,000 day visitors were counted. Numbers have remained more or less on this level for the last 20 years, after a steady increase from the 1950s (Fig. 2). The permanent population on the island is about 2,000, with 150 additional seasonal workers during the summer months. Water demand continuously increased until the 1980s, closely following the trend of increasing tourism (Fig. 2). With the implementation of water-saving household appliances (e.g. washing machines, dishwashers) and toilets, which started in the 1990s, consumption significantly decreased. In 2011, extraction was 333,000 m³/a. This is about a quarter less than the peak demand of 452,000 m³/a recorded in 1983, although the number of overnight stays has remained more or less the same since 1990 (Fig. 2).

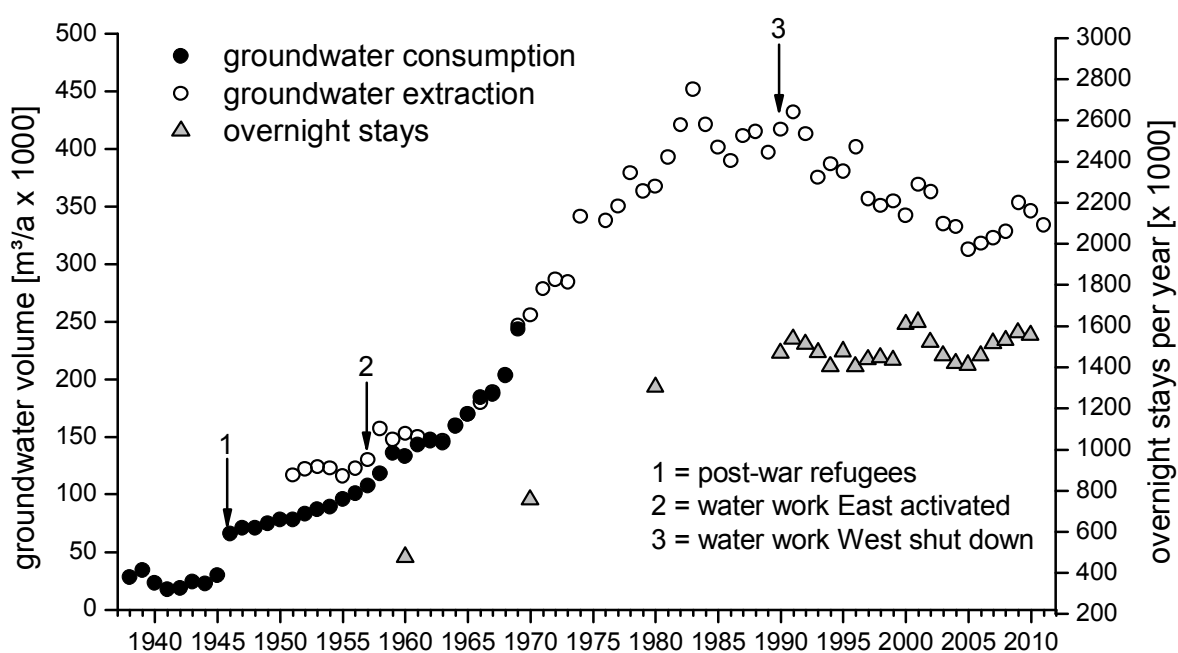


Figure 2. Historical development of groundwater extraction on the island of Langeoog compared to overnight stays (data provided by the water supply company OOWV).

Groundwater levels showed no negative trend during the 1980s when the extraction was at its peak (Fig. 3). With today's lower water demand the system remains stable. Levels reach their minimum during the summer when demand is highest and no recharge occurs but recover during the winter. Groundwater extraction can thus be assumed to be sustainable.

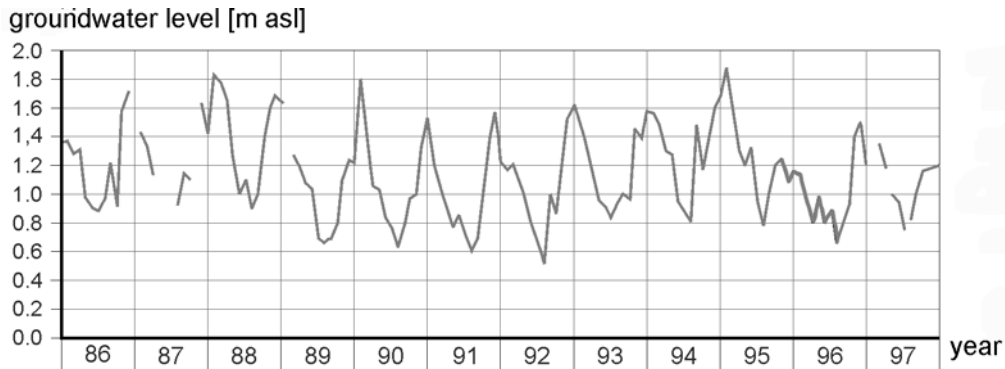


Figure 3. Groundwater levels in an observation borehole on Langeoog (data: OOWV).

Average water consumption in Germany is about 125 liters per day and person, including small businesses. The consumption of the 2000 permanent inhabitants thus amounts to 92,000 m³/a. Subtracting this number from the total consumption in 2011, the remainder of 242,000 m³/a, equivalent to about 72 % of the total, can be attributed directly to tourism. Disregarding the day visitors, one overnight stay corresponds to a consumption of 157 l/d*p. This above average number reflects the need to clean apartments, wash linen/ towels and take showers after a beach day. In the coming years, water saving may partially be compensated by the tendency towards more frequent but shorter vacations (Fig. 4). While a tourist would stay around two weeks in the 1980s, vacations have become significantly shorter, and today guests stay about one week. Since the number of overnight stays has remained more or less constant, this means, that the shorter duration of stay is compensated by more visits (Fig. 4). More frequent changes of guest apartments of course increases the frequency of cleaning apartments and of washing linen and towels.

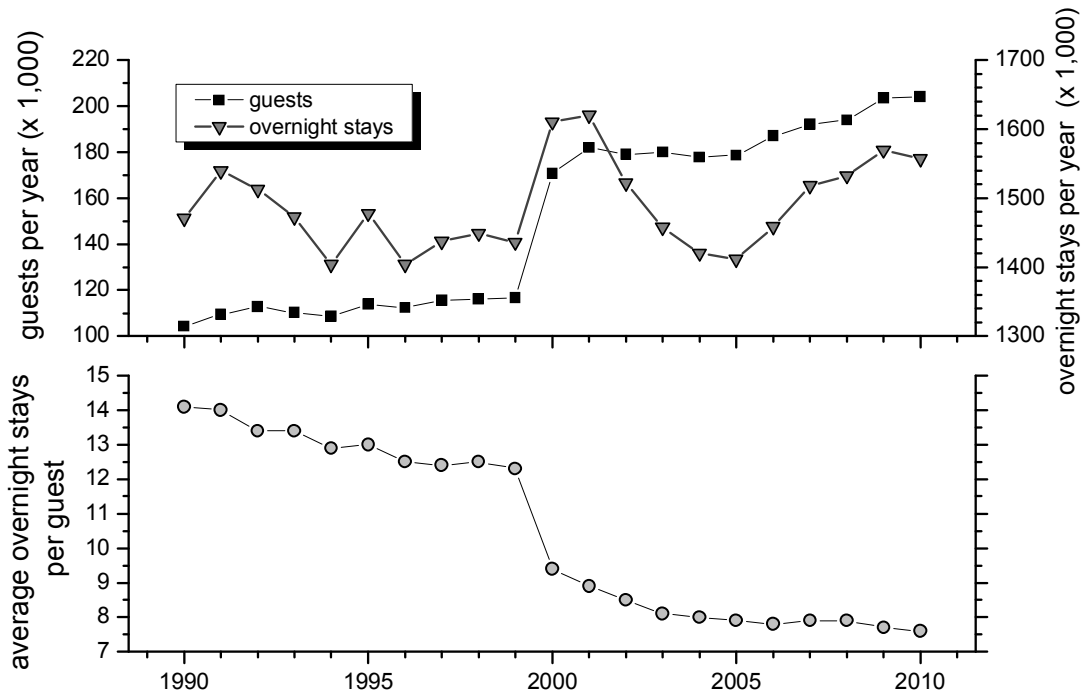


Figure 4. Development of tourism on Langeoog 1990 to 2010. The conspicuous “jump” in the curve around the year 2000 is related to the introduction of a digital tourist card, which replaced a previous analog tracking system (data: Langeoog municipality).

Individual vacation seasons, public holidays and weekends can easily be identified in the consumption curve (Fig. 5). The lowest water demand on Langeoog during the winter season of 2011 was 238 m³/d, while the maximum during the Easter holidays was 1,894 m³/d, a factor of eight between maximum and minimum! The highest demand in summer corresponds to the season of lowest or no groundwater recharge. The smaller neighboring island of Spiekeroog shows the same pattern (Fig. 5).

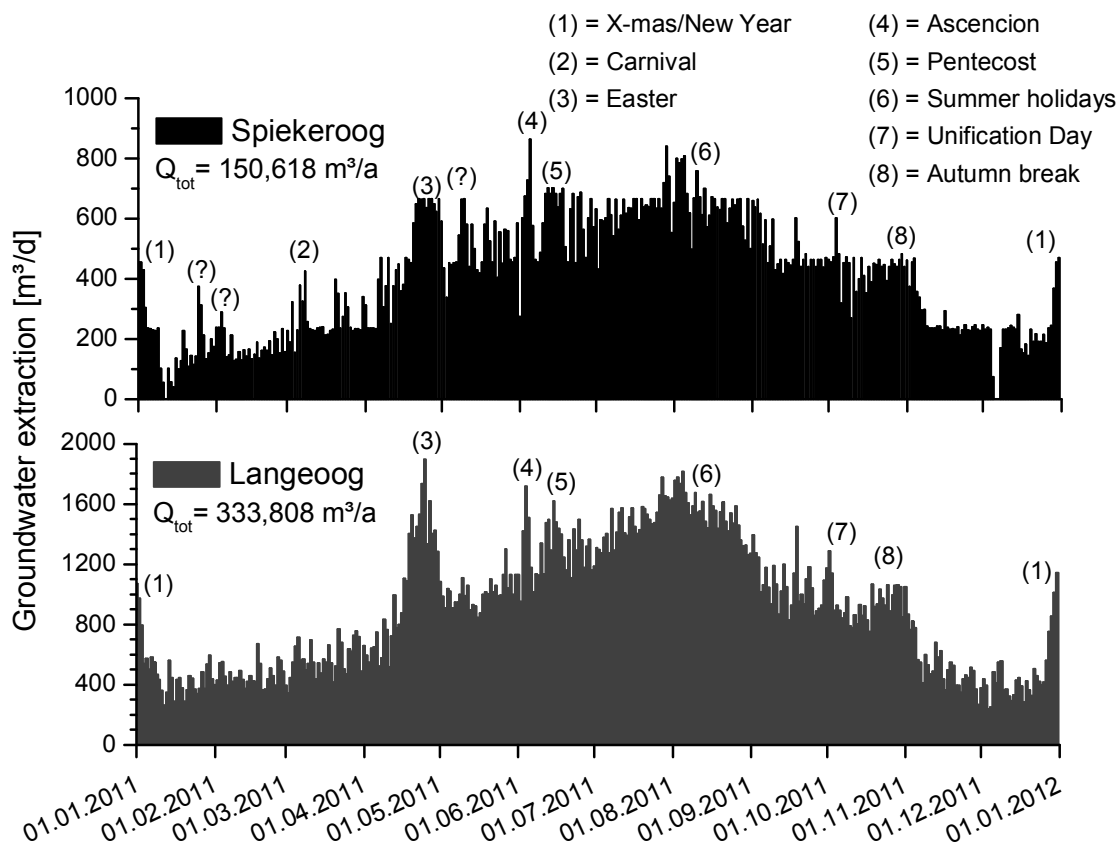


Figure 5. Groundwater extraction in 2011 on the islands of Spiekeroog and Langeoog (data provided by the water supply company OOWV).

DISCUSSION AND CONCLUSIONS

The temporal development of water consumption on the island of Langeoog closely reflects the history of tourism, both on the decadal and annual scale. The increase of tourism in the decades following World War II is mirrored by an increase in water demand. Overnight stays reached a plateau around the early 1990s but water demand decreased due to the implementation of water saving schemes. The impact of the latter effect seems to level off in the last years, so that water demand will probably reach a plateau at the current level of consumption. Groundwater levels show that the extraction is sustainable.

Contact Information: G.J. Houben, Federal Institute for Geosciences and Natural Resources (BGR), Stilleweg 2, 30655 Hannover, Germany, Phone: 0049-511-643-2373, Email: georg.houben@bgr.de

Use of high-resolution tidal data and highly-parameterized inversion for model calibration in managed coastal aquifers

Joseph D. Hughes¹, Jeremy T. White² and Christian D. Langevin³

¹U.S. Geological Survey, Florida Water Science Center, Lutz, Florida, USA

²U.S. Geological Survey, Texas Water Science Center, Austin, Texas, USA

³U.S. Geological Survey, National Center, Reston, Virginia, USA

ABSTRACT

High-frequency water-level data for an 11-day period were used to calibrate a refined three-dimensional groundwater model of the coastal Biscayne aquifer in Florida, USA. The Biscayne aquifer in the study area is karstic and highly permeable and is intersected by a canal system managed to control flooding, provide recharge to municipal well fields, and control saltwater intrusion. The groundwater model was dynamically coupled to a hydrodynamic model of the canal system that uses a diffusive wave approximation of the Saint Venant equations and gate opening data for surface-water control structures in the study area. Initial model parameters and onshore external boundaries were derived from an existing model of the Biscayne aquifer. High-resolution tidal data were used to define water-levels in Biscayne Bay and at the downstream end of canals discharging to Biscayne Bay.

Aquifer water-level data exhibited periodic fluctuations caused by tides in Biscayne Bay, and were decomposed into the eight largest harmonic constituents present in the tidal data. A combination of raw water-level data and processed tidal efficiency data at specific frequencies were used with highly parameterized inversion methods to calibrate values of aquifer hydraulic diffusivity and canal leakance. The interference patterns produced by the tidal signal and its propagation through the canal system provide sufficient information to justify use of a highly parameterized calibration approach. Inclusion of the surface-water system in the model and use of surface-water data improved model calibration. This, in turn, provided important new insight regarding the complex interaction of the surface-water and groundwater systems to tidal forcing.

Contact Information: Joseph D. Hughes, U.S. Geological Survey, Florida Water Science Center, Lutz, Florida, 33559, USA, Phone: 813-498-5029, Fax: 813-498-5002, Email: jdhughes@usgs.gov

Integrating improved conceptual knowledge into a 3-D variable density numerical model for a heavily exploited coastal aquifer with submarine spring discharge in South Portugal

Rui T. Hugman¹, Tibor Stigter² and Jose Paulo Monteiro¹

¹CTA, Universidade do Algarve, Faro, Portugal

²UNESCO-IHE, Dept. of Water Science and Engineering, Delft, Netherlands

ABSTRACT

The *Albufeira-Ribeira de Quarteira* aquifer system on the south coast of Portugal is an important source of groundwater for agriculture and tourism, as well as contributing to significant freshwater discharge along the coast in the form of inter- and sub-tidal springs, and maintaining groundwater dependent ecosystems along the Quarteira stream. During the last period of heavy abstraction in the late 1990s, water quality deteriorated significantly. This has alerted to a need to better understand the system, both in terms of quantifying available freshwater and the behavior of the fresh/saltwater interface. Towards this end, a variable density model that accurately represents the complex 3D geologic structure of the aquifer system is under development. The configuration and extent of the aquifer system is still subject to a certain amount of uncertainty. In an initial phase, several hypotheses of the system's structure are tested with a numerical 2D profile model to simplify 3D model development. Results support a conceptual model that includes a connection between the various layers of the aquifer system and confirms the potential for an extensive freshwater lens several km offshore.

INTRODUCTION

The study area is in the Algarve, a Mediterranean region in the south of Portugal, where several uses already compete for groundwater resources, including coastal groundwater dependent ecosystems. At the beginning of the 21st century, surface water replaced groundwater for public supply and currently all publicly owned boreholes are either inoperative or held in reserve in case of emergency. The limitations of this single source strategy, demonstrated during the drought in 2004-05, have induced a move towards including groundwater as part of a more complex concept of integrated water resource management (Stigter et al. 2009). This requires quantifying and understanding available resources to avoid repeating the past mistakes of overexploitation. This paper focuses on the initial phase in the development of a 3D numerical model of the *Albufeira-Ribeira de Quarteira* (ARQ) aquifer system. The end goal for this model is to serve as one of several tools under development to aid in the efficient and effective management of groundwater resources in the region.

Hydrogeological Background

The ARQ aquifer system is described in Almeida et al. (2000). These last authors defined the limit of the ARQ, as shown in Figure 1, with the aim to define inventory and management units. The aquifer systems develop mostly within lithologies dating from the Miocene and Jurassic, believed to be occasionally separated by low permeability Cretaceous formations. Dolomites and occasionally limestones, karstified to a certain degree and depth, make up the

Jurassic formations, reaching up to 700m thickness. In both aquifer systems, these formations crop out in the north, with a Miocene and Cretaceous cover to the south. The Miocene formation is composed of sands and fossiliferous sandy limestones (occasionally karstified), almost entirely covered by low permeability clayey consolidated sand and gravel deposits of the Plio-Quaternary, which can reach 40m thickness.

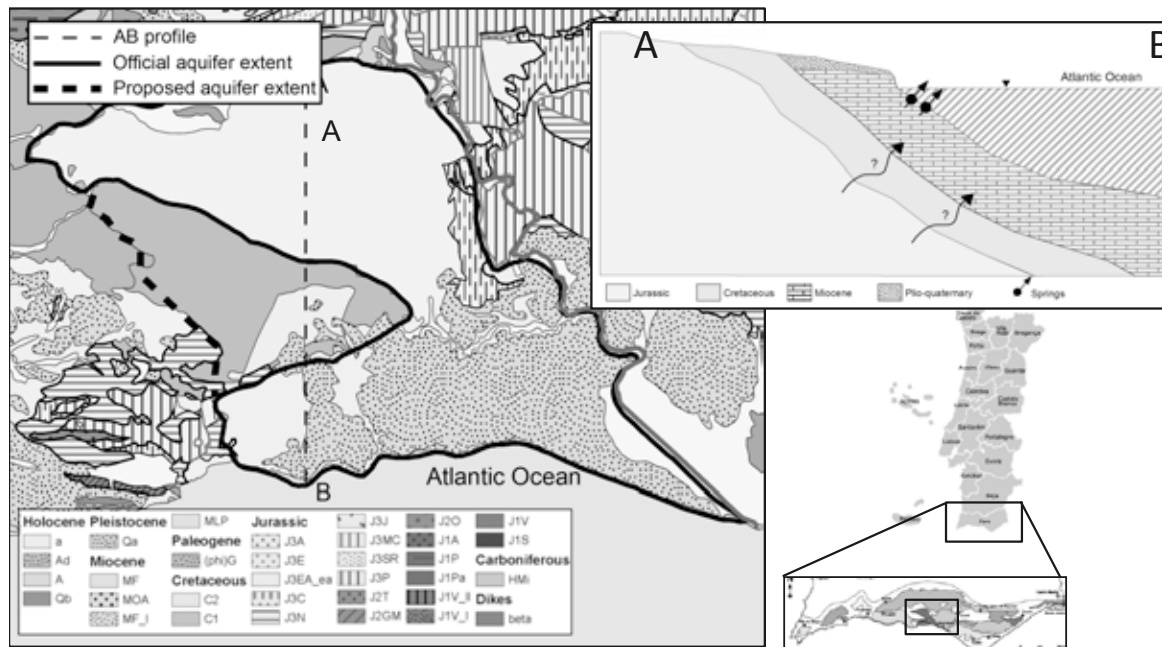


Figure 1. Location and geological map of the study area (adapted from Manupella, 1992).

We have previously applied geophysical methods to update the current hydrogeological conceptual model, along with an analysis of available borehole logs and water level and quality data (Francés et al. 2014). This new data points to the need to increase the extent of the current conceptual model of the system to include the (area marked by thick dotted line in Figure 1). The outcropping formation in this area is the low permeability Cretaceous, however the underlying Jurassic formation connects the northern and southern parts of the system. Results also verify the existence of the confining cretaceous formation in the south; however, we were unable to confirm explicitly the connection between Jurassic and Miocene formations in this part of the system. Furthermore, during several offshore field campaigns submarine springs and indications of freshwater discharge were found a couple of kilometers from the shoreline.

This paper presents a modeling exercise that aims to determine whether a connection is reasonable, taking into account realistic values of hydrogeological parameters. At the same time, the potential extent of offshore freshwater discharge is analyzed. Results will serve to define how far a future 3D model must be extended beyond the shoreline.

METHODS

Existing borehole log data was complemented with new data from the geophysical methods to determine the depths and thicknesses of the various formations. Constant head boundary conditions were set along the top of the Miocene layer, coinciding with the sea floor. Prior to introducing transport and density effects into the models, conductivity (k) values of the

Cretaceous formations (k_{Cret}) was varied over several orders of magnitude ($1e^{-6}$ m.d⁻¹ to 1 m.d⁻¹). Results from each variant are then compared against measured values of k for the Miocene (k_{mio}) and Jurassic (k_{jur}) to constrain the range of acceptable values of k_{Cret} . The calibration process was carried out using the parameter estimation software PEST (Doherty, 2002). Post calibration, mass transport was included. Hydrogeological parameters for the area, reported in the literature were assigned (Almeida et al. 2000). Longitudinal and transversal dispersivity were defined as 5 m and 0.5 m respectively, according to the empirical relationship suggested by Neuman (2005). The models were constructed with the FEFLOW code (Diersch & Kolditz, 2002), and run until reaching quasi-steady state conditions.

PRELIMINARY RESULTS

Sensitivity of the flow model to k_{Cret} is relatively low, and allows for a range of values over several orders of magnitude (0.001 m.d⁻¹ to 0.1 m.d⁻¹) before values in the other two formations are forced beyond an acceptable range. The k values that gave the best fit at each end of the range were applied to the variable density transport model. Figure 2 shows the salinity distribution obtained from the model variant with the $k_{Cret} = 0.001$ m.d⁻¹. Results from other end of the k_{Cret} range are similar, however the freshwater lens extends significantly less offshore.

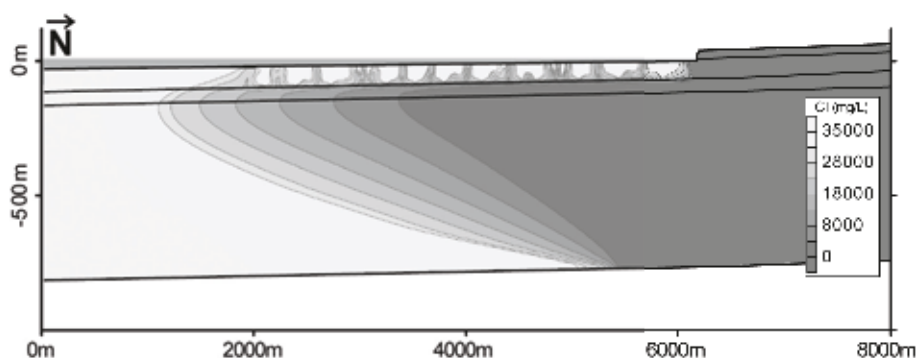


Figure 2. Example of Cl distribution ($k_{Cret} 0.001$ m.d⁻¹).

Depth and extent of the salt-water toe in the upper-Miocene layer are similar to results from geophysical profiles taken perpendicular to the beach (Figure 3). The Miocene formations with seawater are characterized by low resistivity <15 ohm.m, and by 30-50 ohm.m when saturated with freshwater (Francés et al. 2014). The presence of low resistivities further inland than simulation results can be explained by tidal and wave pumping effects. Data on the salinities in the deep Jurassic layers are unavailable, however model results confirm the potential for brackish discharge over 4 km from the shore.

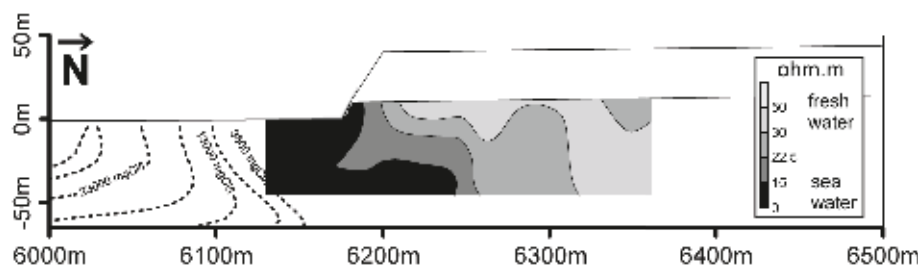


Figure 3. Comparison between model results and FDEM resistivity profile.

DISCUSSION AND CONCLUSIONS

Simulation results are far from being a definitive representation of the ARQ system, however they do give us first look at how the system might work. Despite the model results not giving a conclusive answer in regards to the connection between the Jurassic and Miocene, they do point to the affirmative. The question remains of how well connected they are. These preliminary results indicate that the chosen parameter values are within an acceptable range to represent the aquifer system, confirmed by both an adequate fit with measured hydraulic head and distribution of the saline groundwater wedge. These preliminary simulations also explain the occurrence of submarine freshwater discharge up to 4 km offshore. Together with the presence of fractures or karstified conduits, this can explain the occurrence of freshwater discharge several kilometers from the shore found during the field-campaigns. Confirming the existence of this potential storage of freshwater would be of interest from a management perspective, as it could represent a significant volume available at less risk from saltwater intrusion.

ACKNOWLEDGMENTS

The first author wishes to thank the FCT for the PhD grant SFRH/BD/80149/2011.

REFERENCES

- Almeida, C., Mendonça, J.J.L., Jesus, M.R., Gomes, A.J. 2000. *Sistemas Aquíferos de Portugal Continental*. INAG, Lisbon
- Diersch, H.-J. G., & Kolditz, O.. 2002. Variable-density flow and transport in porous media: approaches and challenges. *Advances in Water Resources*, 25(8-12), 899–944.
- Doherty, J. 2002. *Model-Independent Parameter Estimation*, 4th ed. Watermark Numer Comput 279.
- Francés, A P, Ramalho, E., Fernandes, J., Groen, M., De Plaen, J., Hugman, R., Mohamed A Khalil, Monteiro Santos, F A.. 2014. Hydrogeophysics contribution to the development of hydrogeological conceptual model of coastal aquifers – Albufeira-Ribeira de Quarteira aquifer case study. In proceedings of: 8^a Assembleia Luso Espanhola de Geodesia e Geofísica, Jan 2014, Evora, Portugal.
- Manuppella, G., 1992. *Carta Geológica da Região do Algarve (1:100000)*. Serviços Geológicos de Portugal, Lisbon.
- Stigter, T.Y., Monteiro, J.P., Nunes, L.M., Vieira, J., Cunha, M. C., Ribeiro, L., Nascimento, J., and Lucas, H.. 2009. Screening of sustainable groundwater sources for integration into a regional drought-prone water supply system. *Hydrol Earth Syst Sci Discuss* 6:85–120. doi: 10.5194/hessd-6-85-2009.
- Contact Information:** Rui T. Hugman, Universidade do Algarve, Faculdade de Ciência e Tecnologia, Campus de Gambelas, 8005-139 Faro, Portugal, Email: rui.hugman@ist.utl.pt

Paper on Salt Water Intrusion

S. Huizer^{1,2}, M.F.P. Bierkens^{1,2} and G.H.P. Oude Essink²

¹Department Physical Geography, Utrecht University, Utrecht, Netherlands

²Unit Subsurface and Groundwater Systems, Deltares, Utrecht, Netherlands

ABSTRACT

In many coastal regions around the world climate change will lead to a sea level rise and an increase in extreme weather conditions. This prospect has resulted in a new focus on coastal protection in the Netherlands, resulting in the initiation of an innovative coastal defence project called the Sand Motor. In this project a large body of sand or so-called mega-nourishment has been constructed along the Dutch coast. This body of sand will be distributed slowly along the coastline by wind, waves and currents. Keeping the coastal defence structures in place and creating a unique, dynamic environment with changing morphology over time.



Because of the large size of the body of sand (21.5 million m³) and the position at the coastline and near coastal dunes, the Sand Motor might cause a substantial increase of the fresh water availability by increasing the volume fresh water lens underneath the dunes. This creates an opportunity to combine coastal protection with an increase of fresh water resources in coastal regions.



With a three dimensional, density dependent, groundwater model the effects of changing morphology over time and the potential increase in fresh water availability have been studied. The groundwater model encompasses a region of 11.5 by 6 km around the Sand Motor, including the nearby coastal dunes and low lying polder systems. The presentation will elaborate on the challenges in the modelling of a dynamic coastal system with changing boundary conditions and the potential increase of fresh water resources by the Sand Motor.



Contact Information: Sebastian Huizer, Utrecht University, Department Physical Geography, Heidelberglaan 2, Utrecht, 3583 CS Netherlands, Phone: + 31 030 2532367, Email: s.huizer@uu.nl

Cost-Effective Management of Sea Water Intrusion in Shallow Unconfined Aquifers

M. S. Hussain¹, A. A. Javadi¹

¹Engineering Department, University of Exeter, Exeter, UK

ABSTRACT

The cost efficiency aspects of different hydraulic barriers to control seawater intrusion (SWI) in shallow unconfined aquifer are investigated using the direct integration of simulation model with multi objective optimization tool. Positive barrier by recharging the water into aquifer using subsurface pond, negative barrier by abstraction of saline water and combination of these two are the three scenarios that are optimally assessed in this study. In the descriptive case study considered, the results indicate that application of treated waste water (TWW) as source of recharge increases the efficiency and the practical value of combined management scenario to control SWI.

INTRODUCTION

The SWI is one of the most challenging environmental problems which threaten the quality and availability of freshwater in coastal aquifer, especially, in arid and semi-arid zones of the world. The anthropogenic factors of the modern world such as unplanned exploitation of groundwater intensify the negative impacts of SWI. As a result, groundwater resources should be protected from saltwater intrusion using appropriate measures. Bruington (1972) and Todd (1974) list different methodologies that attempt to control SWI in aquifers. These include reduction of pumping rates, relocation of pumping wells, installations of subsurface barriers, deep recharge using a line of injection wells along the coast, pumping of saline water along the seacoast and combination techniques. The efficiencies of some of these control methods have been investigated by integrating the simulation models with optimization tools to address long-term planning of groundwater management problems. Ataie-Ashtiani and Ketabchi (2011) present a review of the previous research works carried out on the simulation-optimization (S/O) modelling for control of SWI.

The present study investigates the efficiencies of different management methods to control SWI in unconfined aquifers using S/O technique. In addition, by utilizing the unsaturated flow in vadose zone and by focusing on the use of TWW as a more economic source of water for recharging the aquifer, a new combined methodology is introduced for SWI that includes Abstraction, Desalination and Recharge by TWW (ADRTWW)). In the S/O process, Non-dominated sorting genetic algorithm (NSGA-II) is integrated with SUTRA (Voss and Provost, 2010) to assess three different management scenarios of SWI control: (i) Recharge only, (ii) abstraction only and (iii) combined abstraction and recharge. The S/O process is aimed to find the optimal solutions for these three approaches in an hypothetical case study in vertical section. The objectives of the optimization process include minimizing the total construction and operation cost of management scenarios, minimizing the total mass of salt in the aquifer.

MODEL DESCRIPTION

The descriptive model of unconfined aquifer considers a 2D domain with dimensions 200*100 m. As future plan the system will require one production well to pump fresh water

with constant rate of 26 m³/day at location of 40m from inland boundary and at depth 30 m below ground surface. Figure 1, shows the location of this production well and the resulted salinity in the aquifer under steady state condition before and after pumping. The total calculated mass of solute in the aquifer would be raised from 27 tons prior the pumping to 98 tons after pumping. Accordingly, and as it illustrated from Figure 1 the system and a designed production well are threaten by SWI. In order to alleviate this problem the management action required to be taken to comply with the planned demands of water while protecting the system against SWI.

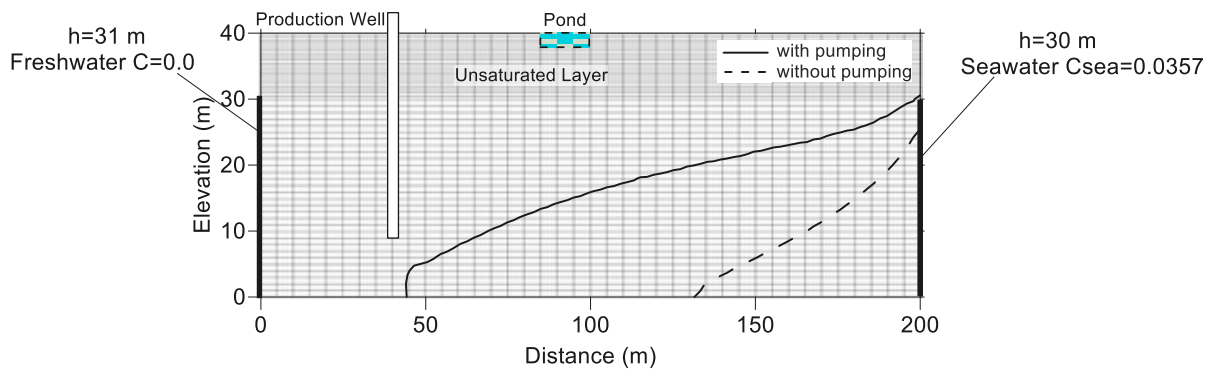


Figure 1. Pre and post-pumping distribution of salinity (0.5 isochlors).

FORMULATION OF OPTIMIZATION MODELS

Three management models (recharge only, abstraction only and combination of abstraction and recharge) are proposed as hydraulic barriers to restrict the negative aspects of the intruded saline wedge during the pumping of freshwater from production well. The S/O model is developed by direct linking of the numerical model with the NSGA-II. The S/O process aims to minimize the total mass of salt (f_1) in the aquifer as well as minimizing the costs (f_2) of construction and operation of the management process. Based on available parameters in each scenario, the objective functions and the set of used constraints are expressed mathematically as follows:

$$\min f_1 = \sum_{i=1}^N C_i v_i \quad (1)$$

Management Model 1: Recharge by TWW (Recharge only Scenario)

$$\min f_2 = QR * (CR + MPTW) * \Delta t + CP + CPM \quad (2)$$

Management Model 2: Abstraction followed by desalination (Abstraction only Scenario)

$$\min f_2 = DA * CD + QA * (CA + CT) * \Delta t - r * QA * MPT * \Delta t \quad (3)$$

Management Model 3a: ADR (Combined Scenario)

$$\min f_2 = QR * CR * \Delta t + DA * CD + QA * (CA + CT) * \Delta t - (r * QA - QR) * MPT * \Delta t + CP + CPM \quad (4)$$

Management Model 3b: ADR TWW (Combined Scenario)

$$\min f_2 = QR * (CR + MPTW) * \Delta t + DA * CD + QA * (CA + CT) * \Delta t - r * QA * MPT * \Delta t + CP + CPM \quad (5)$$

Subject to: $0.0 < QA(m^3/day) < 52.0$; $0.0 < LA(m) < 200.0$; $10.0 < DA(m) < 40.0$; $0.0 < LR(m) < 200.0$; Concentration at abstraction location $> 0.5 C_{sea}$; and total mass of salt (f_1 or Total C) < 27.0 tons (total C for no management condition before designing the production well).
Where:

$f_{1,2}$:management objective functions	CR	:cost of artificial recharge (\$0.12/m ³)
N	:total number of nodes in the domain	CA	:cost of abstraction (\$0.42/m ³)
C_i	solute concentration at node i	CT	:cost of desalination (\$0.6/m ³)
v_i	:cell volume at node i	CD	:cost of installation/drilling of well (\$200 /m)
QA	: abstraction rate (m ³ /sec)	CP	: cost of pond construction (\$350)
QR	: recharge rate (m ³ /sec)	MPT	: market prices of desalinated water (\$1.5/m ³)
LR	: horizontal distances of the recharge pond from the left boundary	MPTW	: market prices of TWW (\$0.25/m ³)
LA	: horizontal distances of the abstraction well from the left boundary	CPM	: annual cost of maintenance and cleaning of pond (assumed to be 10% of CP)
Δt	: duration of management process (10 years)	r	: recovery ratio of desalination plant (60%)

Appropriate cost values are taken from literature (Javadi et al, 2012). In the management model 1 the TWW with total dissolved solids (TDS) of 1300 mg/l (0.0013 kg_s/kg_f) is artificially recharged by defining a subsurface pond with 15.0 m long and 2.0 m deep to replenish 2.0 m constant head of water in aquifer (Figure 1). The average rate of recharge which is calculated by SUTRA directly under pond is 0.35 m/day. As illustrated in Equation 2, this model has a fixed cost function (f_2) corresponding to this constant rate of recharge. This results in reducing the number of objective functions of the management model 1 to one (only f_1). Also, the location of pond (LR) is the only decision variable in recharge scenario; therefore the optimal value of f_1 can be readily obtained through parametric study instead of optimization. In this case trade-off of pond location against total solute mass in system (f_1) is found by changing the pond locations along the length of the domain (Figure 2). The location of pond at (110.0-140.0) m from the landside is recommended as the environmentally friendly outcomes of the recharge scenario.

In the abstraction only scenario (Model 2) the brackish water is continuously abstracted from the saline zone followed by the desalinization process to serve the human and irrigation demands. Therefore, the benefit earned from selling of this desalinated water is included with negative sign in its cost function. And finally in the third scenario the efficiency of the management models 1 and 2 in controlling of the SWI are combined. The two different schemes are considered and assessed in combined scenario: i) Abstraction of saline water followed by desalination and recharging the aquifer with the same desalinated water (ADR), and ii) Abstraction of saline water followed by desalination and recharging the aquifer with external and cheap source of water such as treated waste water (ADRTWW). Based on optimal results for location of pond (110.0 m to 140.0 m) obtained in management models 1, the location of recharge basin (LR) in combined scenarios are considered fixed at distance 120m from left boundary in order to guarantee the maximum efficiency from the pond. The first scheme (ADR) is proposed by Javadi et al (2012) as effective and economic method for controlling SWI.

RESULTS

The results of the recharge scenario show that the associated cost of artificial recharge by TWW is 7386 \$ for the considered period of time ($\Delta t=10$ years). The recharge basin is failed to satisfy the efficiency requirements of the management process or to control salinity levels under 27 tons which is obtained from pre-pumping condition. However, it maintains the total mass of solute in the system lower than the level resulted by steady state condition of post-pumping. The later positive aspect of recharge scenario simultaneously with conclusive outcome of abstraction scenario would enhance the efficiency of the management process in combined scenario. The Pareto fronts (the optimal solutions) obtained from S/O process in the management models 2 and 3 are illustrated in Figure 3. The both scenarios successfully

prevent the intrusion of salt water. The second scheme of the combined scenarios (ADRTWW) shows a significantly greater efficiency in terms of minimizing the total cost and concentration than all other strategies. Application of the all produced water from desalination plant directly to meet the consumption needs; and also the relatively low cost of the TWW itself are the responsible factors for the positive progression of the ADRTWW scheme than other scenarios. Consequently, the ADRTWW management methodology is recommended to control the SWI trend in unconfined aquifer systems with small thickness.

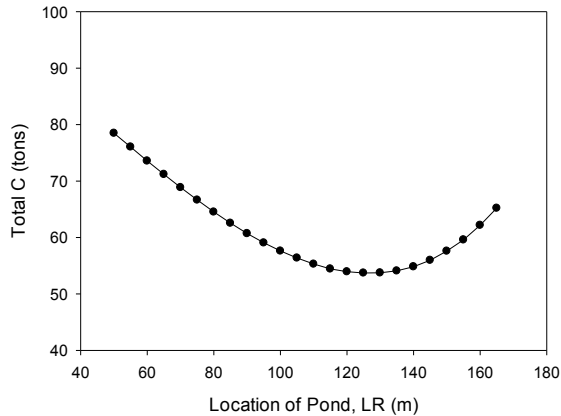


Figure 2. Total concentration vs. the pond locations in recharge scenario.

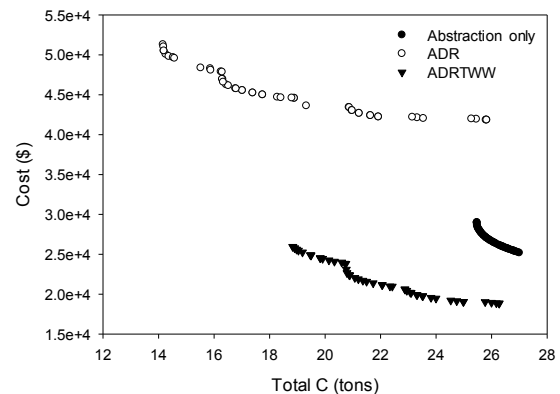


Figure 3. Pareto fronts of Abstraction and combined scenarios.

DISCUSSION AND CONCLUSIONS

The response of an unconfined aquifer to different management scenarios of controlling SWI was investigated using S/O process. A new integrated methodology ADRTWW was proposed to control SWI in unconfined aquifers. The main distinguishing feature of ADRTWW is to collect TWW in percolation ponds and use it as the source of recharge instead of deep injection. The results show that for the case study considered, the proposed methodology controls SWI with the least cost and least salt concentration.

REFERENCES

- Ataie-Ashtiani, B. and Ketabchi, H. 2011. Elitist Continuous Ant Colony Optimization Algorithm for Optimal Management of Coastal Aquifers. *Water Resources Management* 25, 165-190.
- Bruington, A. 1972. Saltwater intrusion into aquifers. *JAWRA Journal of the American Water Resources Association* 8, 150-160.
- Javadi, A. A., Abd-Elhamid, H. F. and Farmani, R. 2012. A simulation-optimization model to control seawater intrusion in coastal aquifers using abstraction/recharge wells. *International Journal for Numerical and Analytical Methods in Geomechanics* 36, 1757-1779.
- Todd, D. K. 1974. Salt-water intrusion and its control. *Water technology/ resources Journal of American Water Works Association* 66, 180-187.
- Voss, C. I. and Provost, A. M., 2010. SUTRA-A model for saturated-unsaturated variable-density ground-water flow with solute or energy transport. The U.S. Geological Survey (USGS), Water Resource Investigation, Open-File Report 02-4231, 300 pp.

Contact Information: Mohammed S. Hussain, University of Exeter, Engineering Department, Harrison Building, North Park Road, Exeter, EX4 4QF UK, Phone: +44-1392-723909, Email: msh218@exeter.ac.uk

Investigating freshwater lenses with ground-penetrating radar (GPR): capabilities, limitations and perspectives

Jan Igel¹, Thomas Günther¹, Moritz Kuntzer², Hans Sulzbacher¹ and Helga Wiederhold¹

¹Leibniz Institute for Applied Geophysics, Hannover, Germany

²Institute for Soil Science, Leibniz University Hannover, Germany

INTRODUCTION

Ground-penetrating radar (GPR) is a geophysical tool that is commonly used for near-surface investigation. GPR uses electromagnetic waves in the MHz-GHz frequency range that are emitted by a transmitting antenna at the ground surface. When propagating through the subsurface, a part of the waves is reflected at each interface or object, where the electrical properties (conductivity and dielectric permittivity) change. These reflected waves can be recorded at the ground surface by a receiving antenna and provide information of the subsurface structure. As water content has a major influence on dielectric permittivity of porous materials, high contrasts as at the groundwater table cause strong radar reflections. On the other hand, the radar-wave velocity is linked to the dielectric permittivity and thus can be used to deduce soil moisture or porosity of aquifers.

The aim of our presentation is to evaluate the capabilities of GPR for investigating a freshwater lens. We demonstrate the capability using field data from Borkum island, which is the largest and westernmost island of the East Frisian islands chain along the German North Sea coast. It is located 10 km north of the mainland and is a typical barrier island with dunes at the northern open sea side and a low marshland at the southern land side. The island is one of the pilot areas intensely investigated in the CLIWAT project (www.cliwat.eu). In addition to classical hydrological exploration techniques, various geophysical methods were developed and used in order to deduce a realistic groundwater model of the whole island. This model was used as the basis for groundwater modelling of climate-change impacts on the freshwater lens (Sulzbacher et al. 2012, Wiederhold et al. 2013).

GPR INVESTIGATION

Measurements

To determine electromagnetic wave velocities and to characterise the sediments, common midpoint (CMP) soundings and vertical radar profiling (VRP) in groundwater observation wells were performed (Igel et al. 2013). Velocity distribution was similar all over the investigated area and was used to deduce the porosity of the near-surface sandy sediments. In addition, 20 km of constant offset were measured in the central and eastern part of the island in order to map the groundwater table and reveal the stratigraphy of the near surface sediments. We used GSSI equipment with 80 MHz unshielded and 200 MHz shielded antennas for the CMP and constant offset measurements together with a RTKGPS to measure the topography, which is important for further processing of the data. The VRP measurements in the observation wells were done with a Mala Geosciences 100 MHz borehole antenna. GPR performance showed to be good in the sandy dune areas with investigation depths of more than 10 m, whereas it was very poor at the beach and in the lower marshland areas due to the high attenuation of GPR waves caused by the salt water.

GPR velocities and hydraulic properties

The electromagnetic wave velocities were determined by CMP soundings at different locations on the island as well as by vertical radar soundings in several observation wells. Both methods yielded similar results for the sandy sediments with 0.124 m/ns and 0.065 m/ns for the vadose zone and saturated sediments below the water table, respectively (Igel et al. 2013). Variation within the island showed to be very small which is attributed to the homogeneity of the aeolian and marine sediment deposition. From the radar-wave velocities below the groundwater table, the porosity of the sand was deduced to 35.6 vol% using the complex refractive index method (CRIM) and assuming full saturation. From the velocity within the vadose zone and assuming the same porosity as in the saturated zone, the mean water content for the unsaturated zone was determined to 8 vol%, which is close to the field capacity of the fine to medium grained sands.

Sedimentological structures

GPR yielded a detailed image of the upper 10 m of sediments (Figure 1). In order to assign the radar reflections to sedimentological interfaces, some auger and core drillings were driven on the profile. The upper sediments showed to be well-sorted aeolian dune sands with interspersed paleosol and peat layers. In the GPR section these sediments show typical structures as dune foresets and cross bedding. At greater depth, the fine to medium grained sand is loaded with shell detritus overlying a 0.2–0.6 m thick layer of silt loam with high organic matter content. This layer shows a strong reflection in the GPR section at about 0 m asl and is interpreted as former tidal flat surface before the island was build. The layer can be observed in the GPR data on wide areas in the western part of the island. A detailed look at this reflector shows discontinuities that are interpreted as erosion channels of the former tideways. These structures are a few decimetres to meters wide and up to 40 cm deep so that the layer is likely to show some leakage to water flow. This finding is confirmed by pumping tests (Sulzbacher et al. 2012). They show that this layer separates the upper unconfined aquifer from a lower confined aquifer, but in some areas there is leakage.

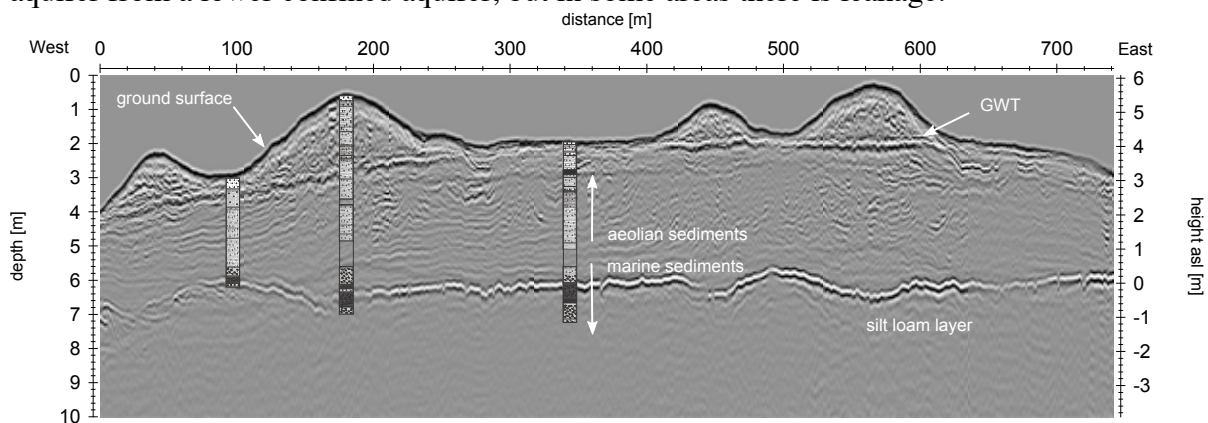


Figure 1. Migrated GPR section across a dune area in the central island with lithology from hand drillings (GWT=groundwater table). Note the high vertical exaggeration factor of 25.

Groundwater table

The groundwater table could be identified in most GPR sections as a distinct reflection. Before interpreting this reflection, one has to take into consideration that GPR – as other geophysical methods used for groundwater investigation – is sensitive to in-situ water

content and not to pressure heads as readings in observation wells are. Thus, one has to correct the GPR groundwater tables for the capillary rise height and the transition zone above that influences the traveltime of the reflected waves. The GPR groundwater reflection showed to be 45 cm above the pressure heads in observation wells in the vicinity of the GPR profiles and were corrected by this value. Figure 2 shows the interpolated groundwater table based on observation wells, open waters and GPR data. The elevation varies from about 0 m (mean sea level) at the coast and in the marshland to about 3.5 m asl in the dune areas and shows some local depressions in the vicinity of the production wells of the local water supplier. In the central area of the island, the observation-well density is low and information from GPR enhances data coverage in this region. The benefit of such geophysical investigation that provides high data density is illustrated in the two insets where interpolation without and with additional GPR information is depicted. If no information of GPR was available, a significantly smaller extension of the freshwater lens in this region would be obtained. The insets also show the GWT in two wells that had been installed after generating the contour plot. They demonstrate an improper GWT map if only relying on the observation wells and open water information (1.5 m deviation at the verification wells) and support the findings of GPR investigation: a much larger freshwater lens in the centre of the island.

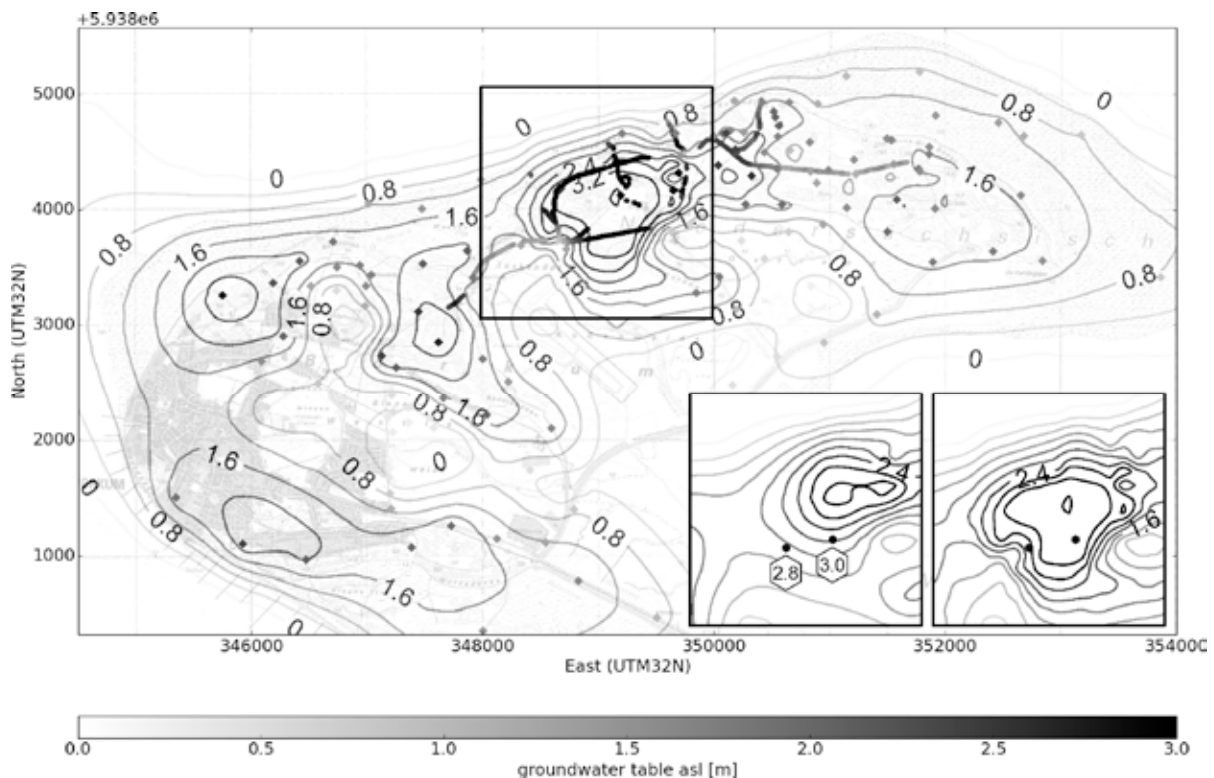


Figure 2. GWT map (contours) of Borkum island derived from observation wells and open water readings (diamonds) and GPR (lines). The inset shows how the contour lines change when including GPR data (left hand side: without GPR, right hand side: including GPR) and show the water tables of two wells that were installed afterwards for verification of the map (hexagons).

CONCLUSIONS AND OUTLOOK

GPR has shown to be a valuable tool for investigating freshwater lenses within coastal environments and provides additional information to standard hydrological investigation. As

it is a fast and non-destructive tool, it can be used to map groundwater tables on large areas and is therefore useful to extrapolate the exact, but only sparsely available information of monitoring wells and hand drillings. GPR also reveals the stratigraphy of the near-surface aquifer and may be used to distinguish highly permeable sediments from aquitards and provides hydraulic properties as porosity and water content.

GPR is limited to environments with low attenuation of electromagnetic waves, i.e., environments with relatively low electrical conductivity. For clayey soils or saltwater, attenuation is commonly high and the depth of investigation might be very small, and GPR can completely fail in extreme cases. On the other hand, dry areas, solid rocks and sandy sediments with freshwater are promising and GPR may provide information up to a depth of 10 m and more. Care has to be taken when interpreting the GWT reflections. The capillary fringe and the transition zone have to be corrected in order to obtain pressure heads from GPR data, which are commonly used by hydrologists. A critical step is the transformation of traveltimes of the reflected GPR signals into depths by migration and time-depth conversion. For this process, a good velocity model is indispensable, which should be calibrated at locations of monitoring wells or hand drillings.

Besides the capabilities demonstrated above, there are promising approaches to extract further information from GPR data. Some observed weak reflections from below the GWT are not yet fully understood, but seem to correlate with former GWT fluctuations. Investigating the origin of these reflections might provide information on the recent – as well as the former – GWT from one single measurement only. Since the signal of the GWT reflection is a function of the emitted source wavelet and the shape of the transition zone, it might be used to deduce the water retention function of the sediment/soil without the need for direct access or sampling of the sediments. This will be valuable additional information that is not available from observation wells. CMP measurements with successively separated transmitting and receiving antenna are relatively time consuming and thus limited to some individual soundings in an area. Multi-offset measurements with antenna arrays provide continuous CMP data along profiles and may provide information on water content distribution on wide areas in the future. As GPR is a fast tool, repeatedly mapping the GWT on large areas can efficiently give information about seasonal variations of freshwater lenses.

REFERENCES

Igel, J., Günther, T. and Kuntzer, M. 2013. Ground-penetrating radar insight into a coastal aquifer: the freshwater lens of Borkum Island. - *Hydrology and Earth System Sciences*, 17, 519–531, doi:10.5194/hess-17-519-2013.

Sulzbacher, H., Wiederhold, H., Siemon, B., Grinat, M., Igel, J., Burschil, T., Günther, T. & Hinsby, K. 2012. Numerical modelling of climate change impacts on freshwater lenses on the North Sea Island of Borkum using hydrological and geophysical methods. – *Hydrology and Earth System Sciences*, 16, 3621–3643, doi:10.5194/hess-16-3621-2012.

Wiederhold, H., Sulzbacher, H., Grinat, M., Günther, T., Igel, J., Burschil, T. & Siemon, B. 2013. Hydrogeophysical characterization of freshwater/saltwater systems – case study: Borkum Island, Germany. - *First Break*, 31, 109-117.

Contact Information: Jan Igel, Leibniz Institute for Applied Geophysics, Stilleweg 2, 30655 Hannover, Germany. Phone: +49-511-6432770, Fax: +49-511-6433665, Email: jan.igel@liag-hannover.de.

Saltwater upconing zone of influence

D. Jakovović^{1,2}, A.D. Werner^{1,2}, V.E.A. Post^{1,2} and P.G.B. de Louw³

¹ National Centre for Groundwater Research and Training, Flinders University, GPO Box 2100, Adelaide, SA 5001, Australia

² School of the Environment, Flinders University, GPO Box 2100, Adelaide, SA 5001, Australia

³ Deltares, Department of Soil and Groundwater, P.O. Box 85467, 3508 AL, Utrecht, The Netherlands

ABSTRACT

In this study, we define and characterize the saltwater upconing zone of influence (SUZI), which is the extent of impact in terms of saltwater rise attributed to pumping. While the zone of influence of a pumping well can be clearly defined in terms of hydraulics (e.g. drawdown), the zone of influence in terms of upconing has received considerably less attention. In coastal areas where a threat of saltwater intrusion and upconing exists, characterization of the salinity zone of influence of a pumping well would provide an improved basis for coastal aquifer management decision-making, e.g. relating to the salinity implications of pumping well operations. Both radial and three-dimensional numerical modelling of saltwater upconing at the field scale were undertaken. The extent of impact in terms of saltwater rise was found to be dependent on the relative magnitudes of the pumping rate and the lateral flow. The three-dimensional coastal setting simulations revealed an asymmetrical shape of the lateral extent of the SUZI, i.e. the SUZI is largest in the direction parallel to the coast. This occurs because the specified head boundary condition at the ocean limits the drawdown near the coast. Also, the inland extent of seawater in the aquifer further limits the propagation of the SUZI perpendicular to the coast, thereby compressing the SUZI in this direction. The steady-state simulations were also compared to the predictions by the Ghyben-Herzberg approximation, including in cases where sloping interfaces occur and where solute dispersion is significant. This provided a reasonable first-order insight into the nature of the magnitude of the SUZI. Observations from this study offer an insight into the formation and extent of the SUZI below pumping bores. Furthermore, the extent of saltwater upconing impact was found to be highly influenced by the lateral flow, implying that lateral flow should be considered in the saltwater upconing studies. Further simulations are needed to explore the effects of multiple-bore pumping as well as transient effects due to intermittent pumping.

Contact Information: D. Jakovović, National Centre for Groundwater Research and Training, Flinders University, GPO Box 2100, Adelaide, SA 5001, Australia, Email: danica.jakovovic@flinders.edu.au

The salinization of useful Cenozoic aquifers by ascending Mesozoic brines – characterization on the basis of hydrochemical data from northern and central Poland

Dorota Kaczor–Kurzawa

Polish Geological Institute – National Research Institute, Kielce, Poland

ABSTRACT

Synthesis of hydrochemical data, concerning 12 000 chemical analyses from HYDRO Bank Database of Polish Hydrogeological Survey, was used to formulate a quantitative estimation of groundwater salinization process which occurs within Cenozoic aquifers as a result of the ascent of diluted brines from Mesozoic formations. The data allowed to forecast the potential salinization hazard of Major Groundwater Basins and major groundwater intakes.

INTRODUCTION

The ascent of diluted brines from Mesozoic formations to Cenozoic useful aquifers leads to groundwater salinization which causes a real threat to groundwater quality and disposable reserves on substantial areas in northwestern and central Poland.

The aim of this paper is to discuss the origin of geogenic groundwater salinization within the Cenozoic aquifers, and to present the forecast of salinization hazard to Major Groundwater Basins and major groundwater intakes. The study area (40 000 km²) corresponds to the area of well developed salt tectonics forms within the Permian-Mesozoic complex (Figure 1).

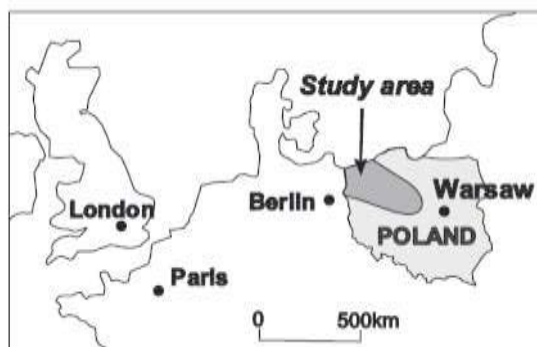


Figure 1. Location of the study area

METHODS

The characterization of groundwater salinity in Cenozoic deposits is based on over 12 000 chemical analyses collected in HYDRO Bank Database of Polish Hydrogeological Survey (Polish Geological Institute). The assessment of reliability of water data for individual Cenozoic aquifers relied on elimination of those results of analyses which could indicate that water salinity was caused either by Baltic seawater intrusions or by anthropogenic pollution. Particular attention was paid to the results of analyses of groundwater extracted for public use in cities where the probability of anthropogenic pollution of groundwater is high. The basic indicator of anthropogenic origin of chlorides in groundwater is an increased concentration of sulphates and nitrogen. Measurements showing the amount of nitrates in water of $>0.1 \text{ mg/dm}^3$, and that of sulphates of $>40 \text{ mg/dm}^3$ in confined aquifers, and 75 mg/dm^3 in unconfined ones, were rejected.

The variation in salinity displayed by groundwaters from Cenozoic layers was compared against the background of the tectonic setting of Permian-Mesozoic formations, and a scheme of groundwater circulation system in Cenozoic deposits. Chemical analyses, measurements of stable oxygen and hydrogen isotope ratios were done for groundwater samples collected in areas above selected fault zones and salt tectonic structures, which allow for upward migration of brines under pressure along the tectonically produced pathways.

RESULTS

Synthesis of hydrochemical data conducted for the best recognized part of the study area, in NW Poland (26 000 km²), allowed a quantitative estimation of groundwater salinization process occurring within Cenozoic aquifers (Kaczor 2006). Similar data synthesis is currently being prepared for the central Poland area. The resultant „Maps of distribution of increased chlorides concentrations in Quaternary, Paleogene and Neogene aquifers” present the distribution of groundwater salinization zones within Cenozoic aquifers (Kaczor 2006).

A groundwater salinization zone within a Cenozoic aquifer is defined by a group of wells with concentration of chloride ion in water exceeding ($> 60 \text{ mg/dm}^3$ – for Quaternary, and $> 70 \text{ mg/dm}^3$ – for Neogene and Paleogene aquifers) upper limits of hydrogeochemical background values. In the described part of NW Poland, such increased concentrations of chlorides were recorded in almost 800 wells, and the total area of confirmed salinity is 8600 km², i.e. 33% of the whole area of interest.

According to presented forecast, the upward migration of brines is hazardous to groundwater quality of 4 out of 20 Major Groundwater Basins, and to 16 among 31 major groundwater intakes yielding more than 100 m³/h of water, located in the investigated area of NW Poland. The described regional synthesis of hydrochemical data helps to choose suitable areas and to project research concerning salinization problems affecting some specific intakes.

Szubin communal intake (yield 1000 m³/d), located in Kujavian region in Central Poland, can serve as an example (Figure 2, 3).

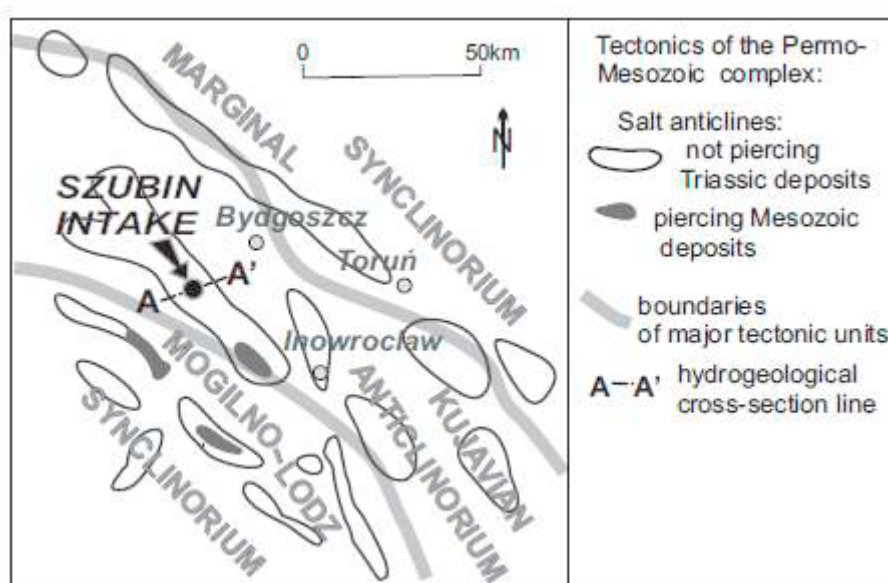


Figure 2. Location and tectonic situation of Szubin intake

Groundwater of this intake is characterized by the chlorides content exceeding accepted norms for drinking water (250 Cl mg/l). The maximal chlorides content was examined in wells nr 4 (510 mg Cl/l) and 6 (540 mg Cl/l).

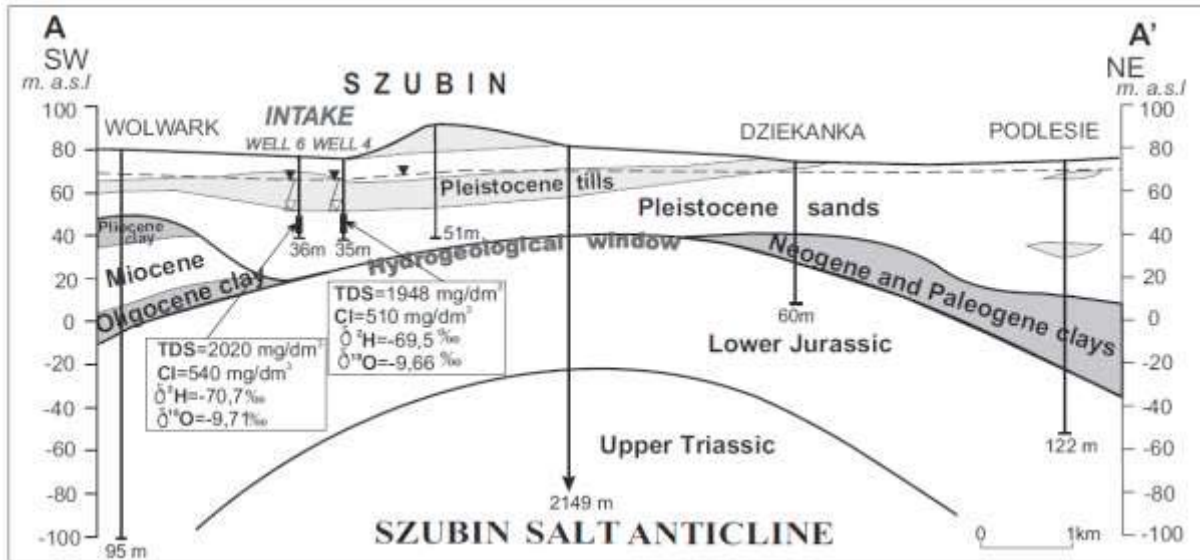


Figure 3. Hydrogeological cross-section and tectonic situation in vicinity of Szubin intake

This groundwater is mixed with groundwater of better quality, coming from other wells, before the introduction to the communal water-pipeline. The salinization of groundwater at this intake was caused by upward migration of saline water from the Mesozoic complex. Such conclusion is supported by the results of measurements of stable oxygen and hydrogen isotope ratios (Figure 4), suggesting that the examined groundwater contains an admixture of “older” waters, which have migrated from the Mesozoic rocks.

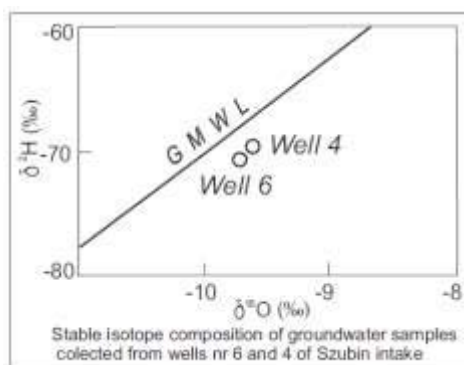


Figure 4. Stable isotope composition of investigated waters

The hydrogeological window, existing on the crest of Szubin salt anticline (Figure 2, 3), allows an ascent of saline waters from Jurassic towards the Cenozoic aquifer.

DISCUSSION AND CONCLUSIONS

The saline waters within the Mesozoic formation are under pressure, which enables their upward migration through a system of fractures and faults towards the Cenozoic aquifers (Dowgiałło et al. 1990). This process is most intense in hydrogeological windows developed in areas of erosional reduction of the overlying Paleogene and Neogene clays on uplifted tectonic blocks and salt-cored anticlines. Such hydrogeological windows are considered the main zones of brine ascent in northern Germany (Grube et al. 2000).

The extent of groundwater salinity zones in Cenozoic aquifers is dependent on flow directions of groundwaters which dilute the brines migrating upwards from Mesozoic rocks. That is why the areas of confirmed salinity are not always coincident with the groundwater ascent zones.

Salinity of groundwaters in the described Cenozoic aquifers is not a result of the currently ongoing process of dissolution of the Zechstein salt bodies, because they are mostly isolated from the groundwater active circulation system. This observation does not correspond to numerous examples of dissolution of salt diapirs during the Holocene reported at northern Germany (Grube et al. 2000). Only a few cases of Zechstein salt structures leaching, during the Cenozoic period, have been confirmed in Polish Lowland, and concern several diapirs piercing through the Mesozoic rocks. The role of salt structures in the process of groundwater salinization relies primarily on the fact that areas of reduced thickness of clays, isolating saline groundwaters from fresh groundwaters, occur above the crests of salt core anticlines.

REFERENCES

- Dowgiałło, J., Nowicki, Z., Beer, J., Bonani, G., Suter, M., Synal, H. A. & Wölfli W. 1990. ^{36}Cl in groundwater of the Mazowsze basin (Poland). *Journal of Hydrology*, 118: 373-385.
- Grube, A., Wichmann, K., Hahn, J. & Nachtigall, K., H. 2000. Geogene Grundwasser versalzung in den Lockergesteins-grundwasserleitern Norddeutschlands und ihre Bedeutung für die Wasserwirtschaft. *Technologiezentrum Wasser Karlsruhe*, 9: 1-203.
- Kaczor, D. 2006. The salinity of groundwater in Mesozoic and Cenozoic aquifers of NW Poland - origin and evolution. *Studia Geologica Polonica*, 126:5-76. (www.sgp.pan.pl/126tom.html)

Contact Information: Dorota Kaczor–Kurzawa, Polish Geological Institute-National Research Institute, ul. Zgoda 21, 25-953 Kielce, Email: dorota.kaczor-kurzawa@pgi.gov.pl

Assessment of Saltwater intrusion in the aquifer of Tripoli Lebanon

O. Kalaoun^{1,2}, A. Al Bitar¹ and M. Jazar²

¹CESBIO, Université de Paul Sabatier, Toulouse, France

²LaMA, Université Libanaise, Tripoli, Liban

ABSTRACT

The aquifer of Tripoli is located in the north of Lebanon and includes the city of Tripoli which is the second largest city with 600, 000 inhabitants. Fresh water supplies for Tripoli are provided from rivers surrounding the city and large pumping wells extracting water from the aquifer. In the last decade water demand increased drastically due to demographic development. Extensive pumping from municipality and personal wells has induced a decrease in the groundwater table and an aggravation of the saltwater intrusion phenomena. Measurements of water conductivity in selected wells have been done in 2008 and 2009 to assess the water quality.

In this study we develop a mathematical model for saltwater intrusion. The model is based on the 2D Boussinesq approximation considering two non-miscible fluids (fresh water and saltwater). We obtain a system of two equations with two unknowns. Considering the sharp interface approximation we reduce our system to one non-linear differential equation with one unknown: the fresh water head. We implemented the finite element method to solve the differential equation. The model is then applied to the Tripoli aquifer.

INTRODUCTION

The studied zone is a part of Tripoli that is on the Mediterranean Sea, its total area is 17.66 km², with Mediterranean climate whose temperature oscillates between 5 C and 30°C. Like many coastal cities, Tripoli is impacted by the saltwater intrusion phenomena, this natural process is aggravated by the over - exploitation of fresh underground water. In this study we implement a 2D saltwater intrusion model based on the Boussinesq equations coupled to the Ghyben - Herzberg approximation.

Background

Based on (Jazar & al., 2012) and (Bear,1979), we use mathematical transformation, perform numerical algorithm, then a tricky reconstruction that allow us to obtain numerical simulations of the two interfaces dry soil/ fresh water and fresh/ salter water of Tripoli basin.

METHODS

Geometric of the domain and boundary conditions

The figure 1 shows a schematic representation of a coastal aquifer subject to saltwater intrusion. Tripoli is divided into lower and upper zones. The altitude in the lower zone varies between 4 and 15 meters. We restrict our study on the lower zone of Tripoli. This

zone rests on a horizontal substratum of Tripoli's aquifer at constant altitude 200 m below the sea level. The boundary of the studied zone is devised into two parts: Γ_1 which represents the shore and Γ_2 which is the boundary between the lower zone and the upper zone of Tripoli city.

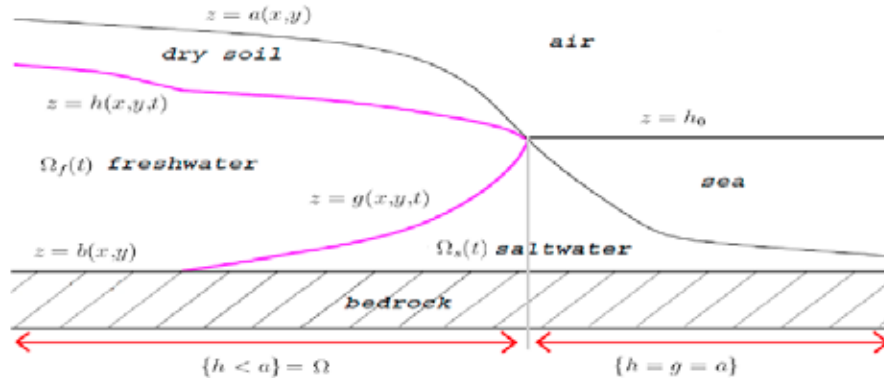


Figure 1: Schematic representation of the computational domain

Mathematical Model

We assume that we are in permanent regime. Indeed, the two interfaces $z=h$ and $z=g$ move very slowly. Moreover, we assume that $b=cte$ since the substratum of the aquifer has a small variation. The two interfaces h and g are calculated using the following system (Jazar & al 2012) and (Bear, 1979):

$$\begin{cases} 0 = \text{div}((h-g)\nabla(1-\varepsilon_0)h) & \text{in } \{h < a\} \\ 0 = \text{div}((g-b)\nabla((1-\varepsilon_0)h + \varepsilon_0g)) & \text{in } \{g < a\} \end{cases} \quad (1)$$

$\varepsilon_0 = (\rho_s - \rho_f) / \rho_s$ where ρ_s and ρ_f are the mass density of the salt and fresh water respectively. In permanent regime and considering a hydrostatic saltwater zone, the couple (h, g) satisfies the "Ghyben - Herzberg" relation (Bear, 1979):

$$(1 - \varepsilon_0)h + \varepsilon_0g = h_0 \quad (2)$$

Where h_0 is the sea level, assumed to be constant independent of time. The second equation of the system (1) is then trivial and the system (1) can be reduced to the first equation.

Setting $\Omega_1 = \{g > b\}$ and $\Omega_2 = \{g = b\}$ then the function (3) satisfies

$$-\Delta u = 0 \quad \text{in } \Omega \quad (4)$$

where $\Omega = \Omega_1 \cup \Omega_2$ and

$$u = u(h) := \begin{cases} (h-b)^2 & \text{in } \{g=b\} \\ \left(\frac{h-h_0}{\varepsilon_0}\right)^2 & \text{in } \{g>b\} \end{cases} \quad (3)$$

Algorithm of the numerical implementation

The numerical computation of u as defined in (4) is easy. However, our concern is to determine the interface g , that is equivalent to the determination of the internal boundary between Ω_1 and Ω_2 . We can write:

$$\Omega_1 = \left\{ u < \left(\frac{h_0 - b}{1 - \varepsilon_0} \right)^2 \right\} \quad \text{and} \quad \Omega_2 = \left\{ u > \left(\frac{h_0 - b}{1 - \varepsilon_0} \right)^2 \right\} \quad (5)$$

Indeed,

$$F(h) = (h - h_0)^2 - \varepsilon_0^2 (h - h_0)^2 = (h(1 - \varepsilon_0) - h_0 + \varepsilon_0 b)(h - h_0 + \varepsilon_0(h - b))$$

Then,

$$\{F(h) < 0\} = \{h < h_1\} \text{ since in } \Omega_1, u = \left(\frac{h - h_0}{\varepsilon_0}\right)^2, \text{ then, } \Omega_1 = \left\{u < \left(\frac{h_1 - h_0}{\varepsilon_0}\right)^2 = \left(\frac{h_0 - b}{1 - \varepsilon_0}\right)^2\right\},$$

where $h_1 = \frac{h_0 - \varepsilon_0 b}{1 - \varepsilon_0}$. Similarly for Ω_2 .

To summarize, the algorithm is as follows:

1. Numerical computation of u using equations (3) and (4).
2. Determination of the two domains Ω_1 and Ω_2 using equation (5).
3. Computation of the interface h as follows:

$$h = \begin{cases} h_0 + \varepsilon_0 \sqrt{u} & \text{in } \Omega_1 \\ b + \sqrt{u} & \text{in } \Omega_2 \end{cases} \quad (6)$$

4. Using Ghyben - Herzberg relation (2), we compute the interface g as follows:

$$g = \begin{cases} \frac{(h_0 - (1 - \varepsilon_0)h)}{\varepsilon_0} & \text{in } \Omega_1 \\ b & \text{in } \Omega_2 \end{cases} \quad (7)$$

RESULTS

The numerical simulations have been implemented in a rectangle of 6 km length and 2 km width by using the finite elements method. We use the software Freefem ++ to simulate the equation (4) (Hecht F., 2012). The substratum is considered as reference level: $b = 0$ m and $h_0 = 200$ m. Concerning the boundary conditions, we have $h = h_0$ on Γ_1 (the shore), on (Γ_2) we know that the interface h is at 7 m up to the level sea, then using (4) we have

$$u = \begin{cases} 0 & \text{on } \Gamma_1 \\ (207 - 0)^2 & \text{on } \Gamma_2 \end{cases}.$$

Finally, we have the following system:

$$\begin{cases} -\Delta u = 0 & \text{in } \Omega \\ u = 0 & \text{on } \Gamma_1 \\ u = 42849 & \text{on } \Gamma_2 \end{cases} \quad (8).$$

The "FreeSWIM" method is validated using numerical software called "BFSWIM" that is a computational fluid dynamics for porous media flow and hydrological systems, taking into account 3D heterogeneity, anisotropy, and various couplings (Ababou R., 1993) and (Al - Bitar, A, and Ababou, R., 2005). The analytical solution introduced by (Bear, 1979) and Ghyben – Herzberg is also calculated in order to validate our method. Figure 2 shows that the interface g calculated by the "FreeSWIM" method is close to that calculated by the "BFSWIM" software and the analytical solution. Then, we implement this method on an aerial photo of the lower zone of Tripoli city, and the interface g is detected as shown in figure 3.

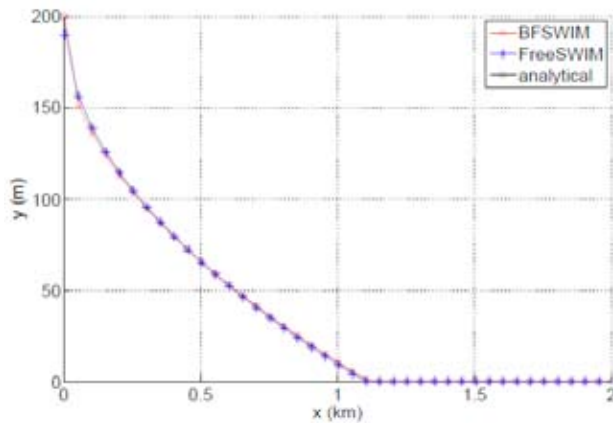


Figure 2: Comparison between analytic and numerical solutions

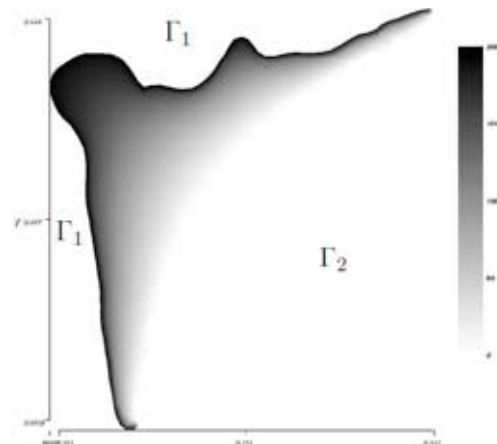


Figure 3: Freshwater/ saltwater interface in Tripoli

DISCUSSION AND CONCLUSIONS

To summarize, we introduced a new method that combines mathematical transformations, simple numerical computations and tricky computations that enable us to compute numerically the interface fresh / salt water. We qualitatively compare numerical simulations in steady state with the analytical solution and with the BFSWIM model, and then we implement the simulations on the lower zone of Tripoli city. Currently a model taking into consideration well pumping and transient state simulations is being implemented. More thorough and quantitative comparison with benchmark models and validation against wells measurements in the Tripoli aquifer will be done.

REFERENCES

Jazar M. & al. 2012. Derivation of seawater intrusion models by formal asymptotic. accepted for publication SIAM Journal on Applied Mathematics (SIAP).

Ababou R. Bagtzoglou.1993. A.C., Bigflow: A Numerical Code for Simulating Flow in Variably Saturated, Heterogeneous Geologic Media Theory and User's Manual. Version 1.1, NUREG/ CR- 6028. USA.

Hecht, F. 2012. Freefem ++ is a partial differential equation Solver. Journal of Numerical Mathematics.

J. Bear.1979. Hydraulics of Groundwater, Mc Graw - Hill, New York.

Al - Bitar, A., Ababou, R. 2005. Random field approach to seawater intrusion in heterogeneous coastal aquifers: unconditional simulations and statistical analysis. In Geostatistics for Environmental Applications .pp 233-248. Springer Berlin Heidelberg.

Contact Information: O. Kalaoun, Lebanese University, laboratoire de mathématique et applications (LaMA - Liban), Tripoli, Lebanon, B. O. Box 37, Phone: 009616446632, Fax: 009616446056, Email: omar.kalawoun@hotmail.com.

Characteristics of real time variations of freshwater-saltwater interface using a new monitoring method at Jeju island, South Korea

Yongcheol Kim¹, Heesung Yoon¹ and Gipyoo Kim²

¹ Korea Institute of Geoscience and Mineral Resources (KIGAM), South Korea

² Jeju Water Resources Headquarter, South Korea

ABSTRACT

In the present study, a new method using an interface-floating device to monitor the time series change of the freshwater-saltwater interface is developed and has been applied Handong-1, a sea water intrusion monitoring station of Jeju island, South Korea. The cross-correlation analysis using 21-days time series data in August, 2013, shows that the lag times of the freshwater level and the interface compared to tide were calculated to be 80 minutes and 195 minutes, respectively. Monitoring data from September to November indicates that the groundwater and interface level fluctuations are highly affected by the tide level. The interface level shows the rising tendency reducing the size of the freshwater lens. The floating device can be applied to sea water intrusion warning system if it is combined with a wireless submersible distance measuring device and remote communication technology.

INTRODUCTION

Most of the coastal monitoring wells are equipped with a single sensor at specific depth for water pressure, temperature and/or electrical conductivity. However, single depth method can give us only the information that the freshwater-saltwater interface is up or down from the sensor. Multi-depth method which is equipped with several sensors at different depth can be used to monitor the interface. The method, however, has blind zone between the sensors and economic problems to get high resolution vertical profile data. Geophysical logging can be used to monitor the interface, but it gives us a vertical location of the interface only at a specific time instead of time series data.

In the present study, a new method using an interface-floating device to monitor the time series change of the freshwater-saltwater interface is developed and has been applied Handong-1, a sea water intrusion monitoring station of Jeju island, South .

METHODS

A new method using a interface-floating device to monitor the time series change of the freshwater-saltwater interface is developed. The floating device can move up and down along with movement of the interface because it has intermediate density between freshwater and saltwater. Although in case that there is more or less wide transition zone, it can give us a real time location of the upper or lower boundary or a certain density within the transition zone. It has been applied to Handong-1, a sea water intrusion monitoring station of Jeju island, South Korea with a depth-fixed pressure sensor. Figure 1 shows the location of Handong-1, tide level monitoring station and weather station.



Figure 1. Location of study site

RESULTS AND DISCUSSIONS

The device was a success in obtaining time series data of the groundwater and interface levels (Figure 2).

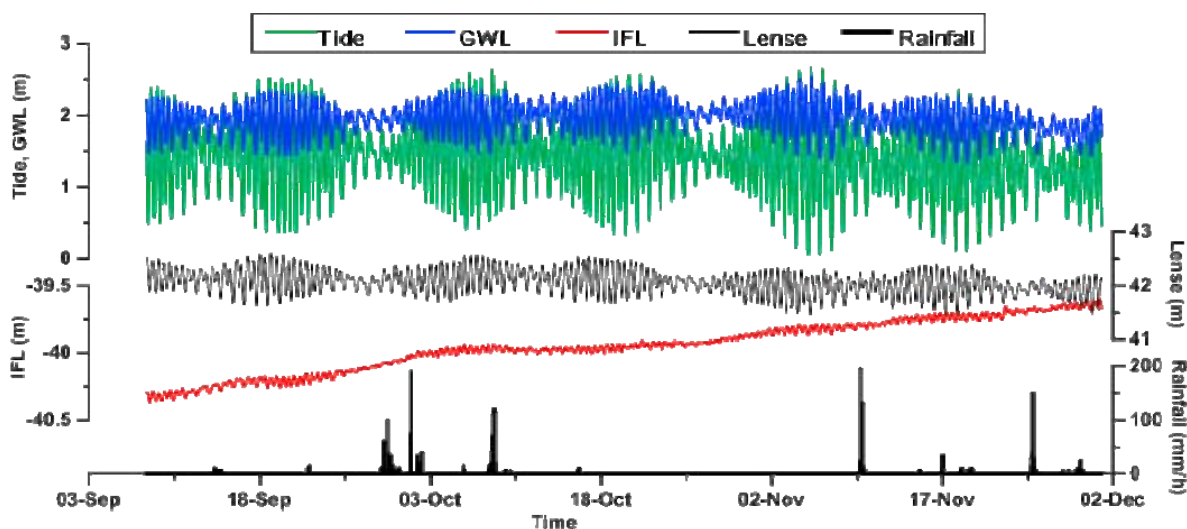


Figure 2. Time series data of groundwater and interface levels

Based on the 21-days time series data in August, 2013, it is found out that maximum amplitude of the freshwater level and the interface are damped down to 1.1m and 0.14m, respectively, compared to tide of which maximum amplitude was 2.6m. The lag times of the freshwater level and the interface compared to tide were calculated to be 80 minutes and 195 minutes, respectively. According to vertical EC profiles obtained from 32 times well logging from April 2001 to August 2011, the average depth of the upper and lower boundary is -34.6m and -44.8m from the mean sea level, respectively. The upper and lower boundary of the transition zone has EC values of about $2,000\mu\text{S}/\text{cm}$ and ranging 47,000 to $51,000\mu\text{S}/\text{cm}$,

respectively. The device was estimated to move up and down following the brackish water of about 8,000 μ S/cm in this site.

Monitoring data from September to November indicates that the groundwater and interface level fluctuations are highly affected by the tide level (Figure 2). The interface level shows the rising tendency reducing the size of the freshwater lens. A long-term data will be obtained and analyzed to find out the effect of rainfall on interface fluctuations and the cause of upward trend of the interface level.

The floating device can be applied to sea water intrusion warning system if it is combined with a wireless submersible distance measuring device and remote communication technology.

ACKNOWLEDGMENT

This work was supported by the Basic Research Project (14-3211-2) of the Korea Institute of Geoscience and Mineral Resources (KIGAM) funded by the Ministry of Science, ICT and Future Planning.

Contact Information: Yongcheol Kim, Korea Institute of Geoscience and Mineral Resources, 124 Gwahang-no, Yuseong-gu, Daejeon 305-350, Korea, Email: yckim@kigam.re.kr

Salt Water Intrusions – a Challenge for Geophysics

Reinhard Kirsch¹, Helga Wiederhold²

¹Agency for Agriculture, Environment and Rural Areas Schleswig-Holstein, Flintbek, Germany

²Leibniz Institute for Applied Geophysics, Hannover, Germany

ABSTRACT

The use of geophysical techniques for the mapping of saltwater intrusions has a long tradition. Today, the focus of interest is shifted from mapping to modeling of saltwater intrusions to predict the behavior while enhanced groundwater extraction or climate change take place. This leads to challenges for geophysics, e.g.

- discrimination between saline aquifer and clays, both with high electrical conductivity
- imaging of subsurface structures leading to pathways for salt- or freshwater
- assessment of hydraulic conductivity from geophysical data

A variety of geophysical techniques are available to meet these challenges. Saline aquifer material and clay, although both being highly conductive, show distinct differences in NMR (nuclear magnetic resonance) decay time and can so be differentiated. NMR measurements as well as resistivity mapping enable an approach to permeability estimation. Finally, a clear picture of the aquifer structure can be obtained with seismic reflection measurements.

INTRODUCTION

Even small concentrations of salt in water strongly reduce the resistivity of water (Figure 1). The salinity of North Sea water (34 – 35 g/l) leads to a electrical resistivity of less than 1 Ωm (ohm x meter). If this water fills the pore space of an aquifer and a porosity of 35% is assumed, the electrical resistivity will be in the range of 1 – 2 Ωm . The electrical resistivity of a freshwater aquifer is in the range of 80 – 200 Ωm . Therefore, saltwater and freshwater aquifers are clearly distinguishable using geophysical resistivity techniques, if the aquifer material is clay free.

For the modelling of the saltwater affected groundwater systems not only the course of the freshwater-saltwater boundary is of interest. Input from geophysical measurements can be the structure of water permeable and impermeable layers including pathways for saltwater intrusions. Here it is important to distinguish between saltwater filled aquifers and clay layers, both with very low electrical resistivity. Finally an assessment of hydraulic parameter like porosity or hydraulic conductivity from geophysical measurements would be welcomed by modeller, but here a lot of future research work is required.

MAPPING THE FRESHWATER SALTWATER BOUNDARY

The basic resistivity technique is vertical electrical sounding (VES) leading to the 1D resistivity distribution beneath the sounding point. Figure 2a shows 3 VES carried out behind the dyke of the Island of Föhr where a dipping low resistivity layer identified as saltwater bearing aquifer is detected. The dip of this layer is in accordance with the dip of the freshwater saltwater boundary after the Ghyben-Herzberg relation. Large scale mapping of the freshwater saltwater boundary using airborne techniques like SkyTEM is time and cost effective (Fig. 2c). In Figure 3 results of a SkyTEM survey are shown where low resistivities in the Northern part of the island indicate saltwater influence, while high resistivities in the Southern part show the freshwater lens.

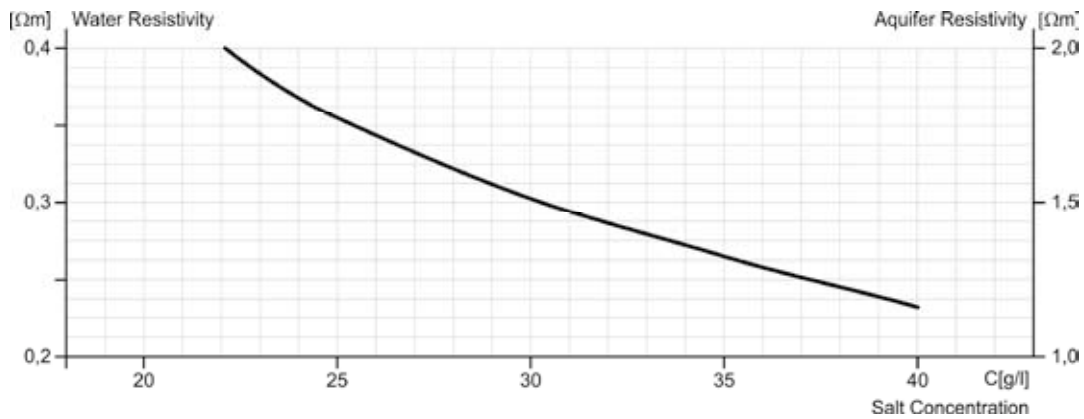


Figure 1. Influence of salt concentration on the electrical resistivity of water and aquifer for temperature of 10°C (after Kaye & Laby 2004).

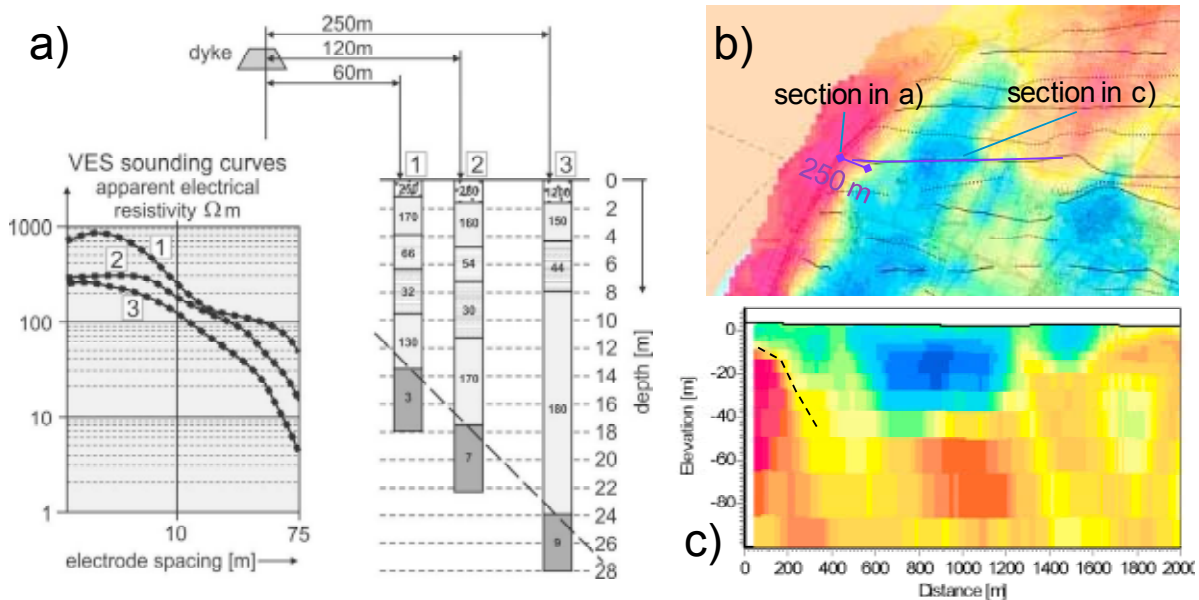


Figure 2. a) Freshwater saltwater boundary from VES at the shoreline of the island of Föhr (Ketelsen and Kirsch 2006); b) resistivity map -10 - -20 m msl from SkyTEM survey; c) fresh-/saltwater boundary in resistivity cross-section from SkyTEM survey.

Submarine groundwater discharge can be of importance for the aquatic ecosystem and for the future water supply. In case of freshwater discharge, high resistivity spots in a low resistivity environment must be detected. (e.g. Swarzenski et al. 2006). Marine electromagnetic systems enable the detection of submarine groundwater discharge apart from the shoreline (Goldman et al. 2005).

Both saltwater saturated sand and clay show low electrical resistivities and are not distinguishable by resistivity methods. Laboratory results of NMR (nuclear magnetic resonance) decay time of sand with different clay content and salinity of pore water show that the decay time strongly depends on clay content, but only to a minor degree on pore water salinity (Elali 2011). So, NMR measurements, normally used for water content determination and hydraulic conductivity assessment, might offer a method for a unique identification of saline groundwater.

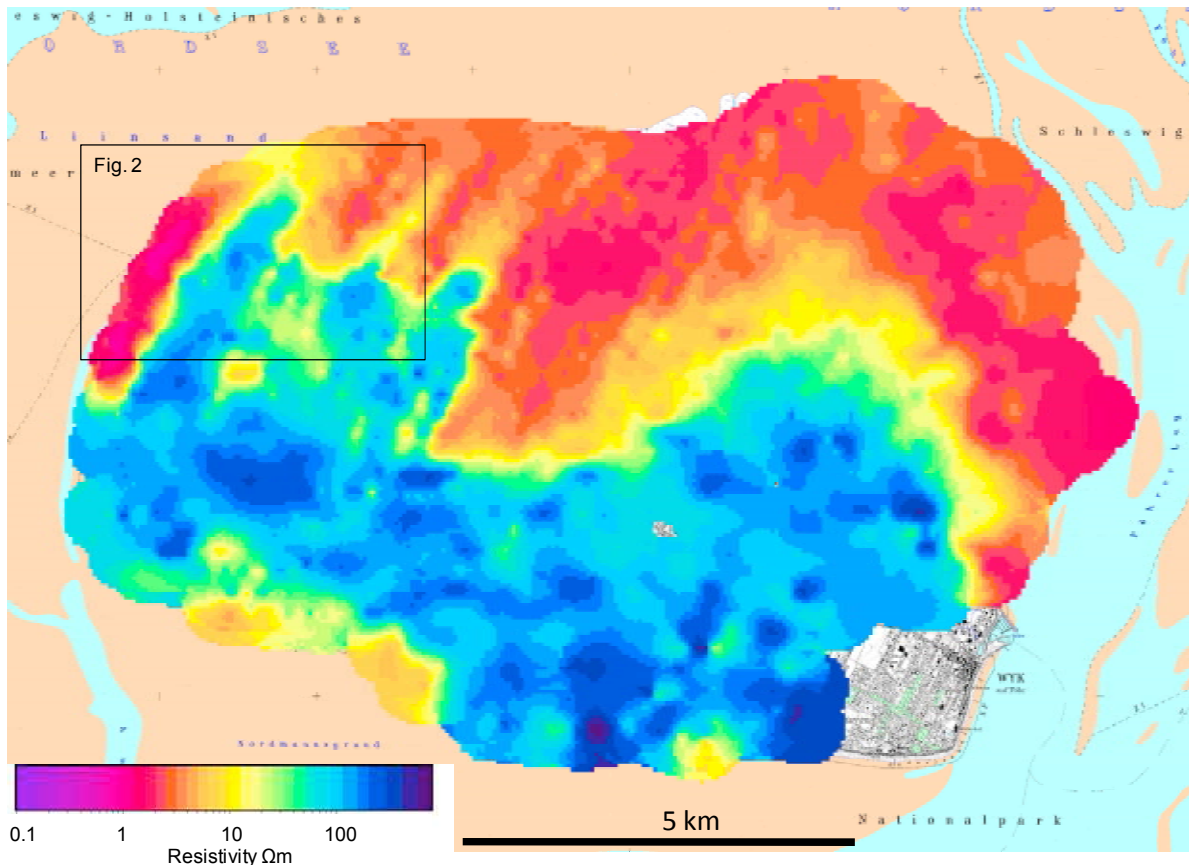


Figure 3. Results of a SkyTEM survey: resistivities in the depth range -10 – -20 m msl, saltwater intrusion in the Northern part of the island (Wiederhold et al. 2010).

INPUT PARAMETER FOR GROUNDWATER MODELLING

Aquifer geometry:

The depth structure of groundwater permeable (sand, gravel) and impermeable (till, clay) layer in the model region can be obtained by reflection seismic measurements. In a seismic section as shown in Figure 4 layer boundaries can be clearly detected and traced. This is important for the imaging of underground structures with influence of the groundwater flow conditions like glacial thrust faulting (see Figure 4) or buried glacial valleys. However, for a clear identification of groundwater permeable or impermeable layers additional information like drilling results or resistivity surveys are required. To obtain a detailed image of the near surface layers radar (GPR) techniques can be applied. However, due to the high absorption of the radar signal in low resistivity layers saltwater bearing sand or clay cannot be imaged by GPR.

Hydraulic conductivity:

A direct determination of hydraulic conductivities with geophysical methods is not possible. An indirect approach uses the dependence of the NMR decay time of the effective porosity (mobile water content) of the aquifer (e.g. Dlugosch et al. 2011). If a relation between electrical resistivity and hydraulic conductivity can be found, airborne electromagnetic data can be used to identify lateral variations of hydraulic conductivities on a local scale.

The hydraulic conductivity of the unsaturated zone strongly depends on the water content. The propagation speed of the radar signal also depends on the water content of the

underground and can be used for a rough assessment of the hydraulic conductivity. The use of NMR for the unsaturated zone is in development (Costabel and Yaramanci 2011).

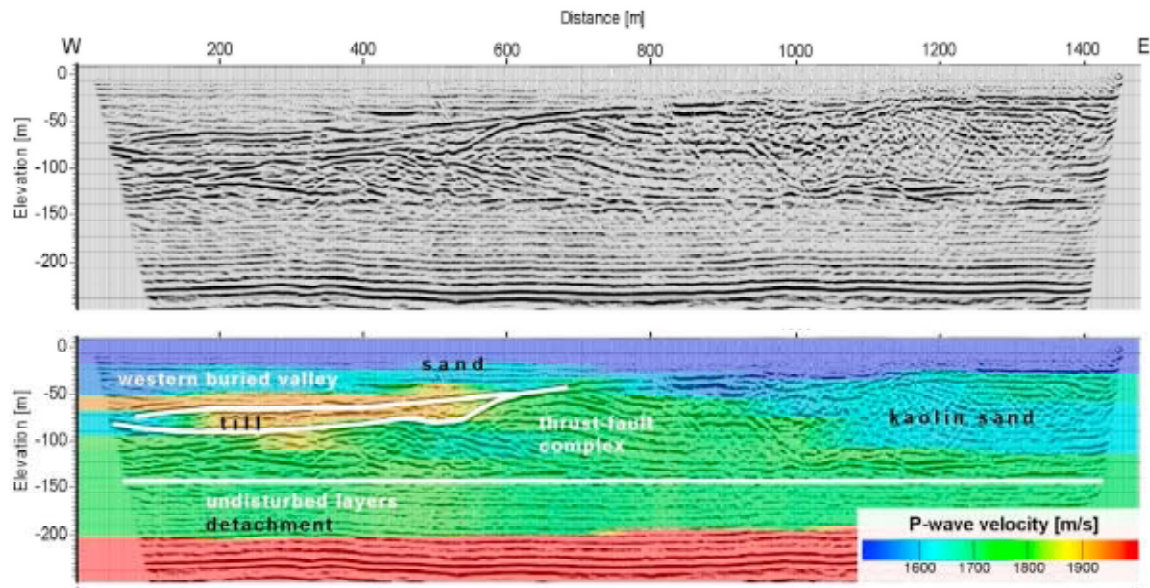


Figure 4. Reflection seismic section showing glacial thrust faulting of near surface aquifers and impermeable layers (Burschil et al. 2012).

REFERENCES

- Burschil, T., Scheer, W., Kirsch, R., and H. Wiederhold. 2012. Compiling geophysical and geological information into a 3-D model of the glacially-affected island of Föhr. - *Hydrol. Earth Syst. Sci.*, 16, 3485-3498. <http://www.hydrol-earth-syst-sci.net/16/3485/2012/hess-16-3485-2012.html>
- Costabel, C. and U. Yaramanci. 2011. Relative hydraulic conductivity in the vadose zone from magnetic resonance sounding. *Geophysics*, 61-71.
- Dlugosch, R., Müller-Petke, M., Günther, T., Ronczka, M. and U. Yaramanci. 2011. An extended model for predicting hydraulic conductivity from NMR measurements. 17th European Meeting of Environmental and Engineering Geophysics of the Near Surface Geoscience Division of EAGE, 12.-14.09.2011, Leicester UK.
- Elali, F. 2011. The Influence of Porosity, Saturation Degree, Clay Content and Pore Water Conductivity on NMR and SIP Parameters. PhD thesis, Technische Universität Berlin, Berlin, GE.
- Goldman, M., Gvirtzman, H., Meju, M. and V. Shtivelman. 2005. Hydrogeophysical case studies at the regional scale. In: Rubin, Y. and S. Hubbard (eds.) *Hydrogeophysics*, 361-389, Springer.
- Kaye, G.W.C. and T.H. Laby. 2004. *Tables of Physical & Chemical Constants* NPL National Physical Laboratory UK, web edition.
- Ketelsen, R. and R. Kirsch. 2004. Zur geophysikalischen Erkundung von Versalzungs zonen im Grundwasser. *Meyniana* 56: 21-4.
- Swarzenski, P.W., Burnett, W.C., Greenwood, W.J., Herut, B., Petersen, R., Dimova, N., Shalem, Y., Yechieli, Y. and Y. Weinstein. 2006. Combined time-series resistivity and geochemical tracer techniques to examine submarine groundwater discharge at Dor Beach, Israel. *Geophysical Research Letters* 33.
- Wiederhold, H., Siemon, B., Steuer, A., Schaumann, G., Meyer, U., Binot, F. and K. Kühne 2010. Coastal aquifers and saltwater intrusions in focus of airborne electromagnetic surveys in Northern Germany. Ext. abstract, 21. Salt Water Intrusion Meeting, Ponta Delgada/Azores, Portugal.

Contact Information: Reinhard Kirsch, State Agency of Agriculture, Environment and Rural Areas Schleswig-Holstein, Geological Survey, Hamburger Chaussee 25, D-24220 Flintbek, Germany, Phone: 0049-4347-704-534, Fax: 0049-4347-704-502, Email: reinhard.kirsch@llur.landsh.de

Quantifying the relative contribution of climatic and pumping impacts to coastal aquifer depletion using a highly parameterised groundwater model: Uley South Basin (South Australia)

Matthew J. Knowling, Adrian D. Werner and Daan Herckenrath
National Centre for Groundwater Research and Training, School of the Environment,
Flinders University, GPO Box 2100, Adelaide, SA 5001, Australia

ABSTRACT

Coastal aquifer depletion is becoming increasingly widespread given the growing demand for freshwater globally. Understanding the extent to which aquifer depletion is caused by groundwater pumping, as opposed to natural factors such as climatic variability (e.g., recharge patterns, land use change), is essential for effective groundwater management. Despite this, the relative contribution of climatic and pumping impacts on groundwater response is rarely quantified. The relative contribution of these impacts can be assessed by comparing calibration-constrained model predictions of natural groundwater level time series (i.e., in the absence of groundwater pumping) and observed groundwater level time series. Previous studies that adopt this approach employ lumped-parameter models, and thus only offer preliminary insight into specific causes of aquifer depletion given that the model's ability to represent complex spatially distributed system responses is limited. In this study, we build on previous modelling strategies for distinguishing between climatic and pumping impacts by using a highly parameterised, regional groundwater model to investigate the relative spatial and temporal contributions of climatic and pumping impacts to aquifer depletion in a regional setting. The analysis is applied using a groundwater model of the Uley South Basin (USB), South Australia, where there is conjecture surrounding the cause of declining groundwater levels. Results show that the relative impact of climate variability and pumping is highly variable spatially. Preliminary findings demonstrate that the relative contribution of pumping impacts to groundwater decline is greater than that of climate variability over the majority of USB. A representative groundwater level time series is given in Figure 1. The magnitude of these impacts is shown to be dependent on (1) proximity to the coastal boundary condition, (2) hydraulic property estimates (achieved ultimately through model calibration), and (3) effects of aquifer desaturation. Results also show that historical groundwater level variation in the coastal zone of USB is controlled to an approximately equal extent by climatic and pumping impacts, which is an important outcome for informing groundwater management given the risk of seawater intrusion. This study demonstrates the ability of state-of-the-art groundwater (and seawater intrusion) models to provide unique insight into climate-versus-pumping-induced aquifer impacts.

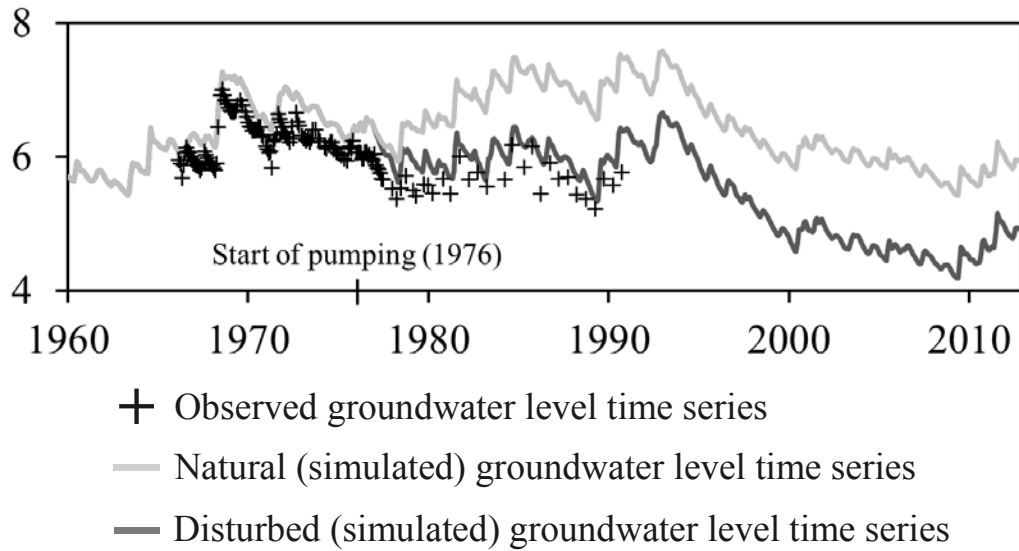


Figure 1: Natural and disturbed (i.e., pumped) groundwater level time series (in m AHD) at observation well ULE136.

Author contact information: Matthew J. Knowling, National Centre for Groundwater Research and Training, School of the Environment, Flinders University, GPO Box 2100, Adelaide, SA 5001, Australia. E-mail: matthew.knowling@flinders.edu.au

Application of airborne electromagnetics for groundwater investigations in the vicinity of salt structures

F. Krause¹, A. Ogroske², M. Popp² and S. Schäfer¹

¹K+S Aktiengesellschaft, Kassel, Germany

²Fugro Consult GmbH, Berlin, Germany

ABSTRACT

To map and monitor the occurrence of mineralized groundwater surrounding several salt structures in Germany, extensive hydrogeological exploration programs were executed. Numerous airborne electromagnetic surveys (AEM) were performed between 1996 and 2013, with frequency-domain helicopter borne electromagnetic (HEM) systems (Barnasch & Beer, 2012; Siemon et al., 2011; Siemon et al., 2010), or time-domain helicopter borne (HTEM) systems, respectively.

After interpolation of the 1D inversion results, an analysis of observed resistivity profile maps identified the general hydrogeological system and large-scale geological structures (e.g. salt domes) in the investigated areas. The interpretation of AEM data under consideration of further hydrological and geological information led to the identification of distinctive areas of mineralized groundwater and transition zones between fresh and saline waters. In this context, AEM applications are a powerful tool to support monitoring networks, geological mapping and groundwater models.

The process of complementing knowledge from AEM surveys with information from wells, boreholes, geophysical borehole logs, surface geophysics, groundwater samples and 3D subsurface models is illustrated by means of case studies, improving hydrogeological and geological interpretations. Advantages and constraints of the chosen method are shown.

REFERENCES

Barnasch, J., & Beer, W. W. 2012. Aerogeophysikalische Messungen im Werra-Kaligebiet. Kali und Steinsalz, 1/2012.

Siemon, B., Steuer, A., Ullmann, A., Vasterling, M., & Voß, W. 2011. Application of frequency-domain helicopter borne electromagnetics for groundwater exploration in urban areas. *Physics and Chemistry of the Earth*, 36: 1373-1385.

Siemon, B., Ullmann, A., Vasterling, M., Meyer, U., Beer, W. W., & Plümacher, J. 2010. Airborne Electromagnetic Survey of the Groundwater Mineralisation in the Potash Mining District of The Werra River, GER, Near Surface 2010– 16th European Meeting of Environmental and Engineering Geophysics. Zurich, Switzerland.

Contact Information: Florian Krause, K+S Aktiengesellschaft, Bertha-von-Suttner-Straße 7, 34131 Kassel, Germany, Email: florian.krause@k-plus-s.com

Recent Updates to the SEAWAT Computer Program

Christian D. Langevin¹

¹United States Geological Survey, Reston, Virginia, USA

ABSTRACT

The SEAWAT computer program, based on MODFLOW and MT3DMS, is developed and released by the U.S. Geological Survey. The program has been continuously updated and improved since it was first released in 2002. An updated version of SEAWAT is presently under development. This updated version is based on the latest MODFLOW version (MODFLOW 2005 Version 1.11). As part of this update, the underlying program is being redesigned to optionally allow conservation of fluid volume for situations where density variations are moderate. This is an alternative to solving the full, extended Oberbeck-Boussinesq form of the mass conservation equations. For most saltwater intrusion applications, the extended Oberbeck-Boussinesq terms can be excluded due to the slight density variation of only about 2.5 percent between freshwater and seawater. In these situations, the updated version can be used with additional MODFLOW packages that were not supported in previous SEAWAT versions. These packages include the Stream (STR) Package, Version 2 of the Multi-Node Well (MNW2) Package, Segmented Evapotranspiration (ETS) Package, Drains with Return Flow (DRT) Package, and the Surface Water Routing (SWR) Process. The updated version also contains several other enhancements, including new flexibility for entering solute concentrations through MODFLOW package auxiliary variables, better design of MODFLOW and MT3DMS flow and transport time steps, an alternative storage formulation that improves convergence characteristics for wetting and drying problems, and improved numerical approximations for water table conditions. These enhancements will extend usage of SEAWAT to a wider variety of complex groundwater flow problems.

Contact Information: Christian D. Langevin, U.S. Geological Survey, 411 National Center, Reston, VA 20192, USA. Email: langevin@usgs.gov

Palaeo-climatic and Hydraulic control on Saline Groundwater in Holocene Delta Plains

Flemming Larsen¹, Long Vu Tran², Hoan Hoang², Luu Thi Tran², and Nhan Quy Pham²

¹Geological Survey of Denmark and Greenland (GEUS),

²Hanoi University of Mining and Geology

Abstract

Eustatic sea-level changes during the Quaternary period, with water levels drops down to 130 m below current during periods with glaciations, have had a paramount impact on the sedimentological development of geologically young delta systems and the distribution of fresh and salty groundwater in their aquifers. In delta systems, gravels, sands, silts and clays are deposited and form multi-aquifer systems, but early studies of the Mississippi delta have documented erosion of deep entrenched valley systems in these systems during low sea-level stages. These erosional structures are subsequently filled up with low-permeable clay-rich formations during high sea-level, and these geological units appear to control the distribution of palaeo saltwater in the delta systems. We have conducted a study focused on the past climatic and hydraulic controls on the presence of palaeo saltwater in the Red River delta plain (RRDP) in Vietnam. Saltwater in aquifers in the RRDP was studied using: field geophysical methods, including TEM and borehole logging, measurements of saltwater intrusion in the Red River, exploratory drilling, groundwater sampling and determination of major ions and water stable isotope content, hydraulic laboratory experiments, chemical analysis of interstitial clay pore water, and groundwater flow modelling with the SEAWAT code.

The geophysical result reveals that remains of palaeo saltwater is present in deep, incised valleys, filled up with fine grained, marine deposits during Holocene transgressions. The controlling mechanisms of the leaching of the trapped marine pore water are the thickness and permeability of the marine sediments and the leaching time of the pore water. In sediments with a permeability below 10^{-14} m^2 ($K < 10^{-7} \text{ m/s}$), transport of marine pore water is controlled by diffusion, and in a sequence of sediments with a thickness of 60 m, leaching of salty water takes more than 10.000 years. With larger permeability of the sediments, transport of salty pore will be controlled by a faster, density driven process, and palaeo saltwater is leached out within few hundred years. Similar results, with so-called inverted saltwater profiles, with dense, salty groundwater overlying less dense fresh groundwater, has been reported by others in the literature, and we therefore suggest that these findings have a general application in the understanding of the occurrence of palaeo saltwater in Holocene delta plains worldwide.

Contact information: Flemming Larsen, Geological Survey of Denmark and Greenland, Department of Geochemistry, O. Voldgade 10, 1350 Copenhagen, Denmark, tel.: +45 91 333 561, e-mail: flar@geus.dk

Historic and projected saltwater distribution at the left bank of the river Scheldt near the port of Antwerp, Belgium.

Gert-Jan Devriese¹, Jasper Claus¹ and **Luc Lebbe**¹

¹Department of Geology and Soil Science, Ghent University, Ghent, Belgium

ABSTRACT

To investigate the influence of the planned changes (e.g. the construction of the Saeftinghedock and the Deurganckdock sluice, the creation of several nature compensation areas, changes in the management of streams, etc.) at the left bank of the Scheldt near the port of Antwerp, a 3D density dependent groundwater model has been developed. The developed model starts in 1976. This date has been chosen as it coincides with the earliest developments at the 'Waasland' harbor. Additionally, it allowed us to use the salinization map of De Breuck et al. (1974) for the initial saltwater distribution. From the situation in 1976, the current situation has been obtained by changing the boundary conditions of the model every few years to the new developments in and around the 'Waasland' harbor. As such a good fit between the simulated and the observed hydraulic heads and saltwater concentrations for the current situation was obtained. From the current situation on, three development phases have been distinguished. The first one focusses on the development of nature reserves as a compensation for the deepening of the lower sea Scheldt while the second and third phase focus on the expansion of the 'Waasland' harbor as well as on the development of additional (optional) nature reserves. The results of the model indicate that the hydraulic heads and saltwater concentrations in large parts of the left bank of the Scheldt are going to rise due to the creation of new (controlled) tidal areas. This will also induce salinization in some of the neighboring areas as well as in an area that is specially conducted for the creation of salt meadows. In the harbor itself the hydraulic heads will rise in all newly developed areas (sluice, tidal dock and newly heightened areas). The saltwater will raise at the location of the new tidal dock and sluice, while near the newly heightened areas the salt water will significantly lower in only a few years. Additionally the developed 3D density dependent groundwater model revealed the leakage of brackish water from the docks from the 'Waasland' harbor to the largest waterways in the neighborhood of the harbor.

INTRODUCTION

In the next 10 to 15 years the view of the 'Waasland' harbor and the surrounding areas will drastically change due to a series of planned developments. The foreseen developments have two reasons, the first one is the expansion of the port of Antwerp and includes e.g. the construction of the Saeftinghedock, the construction of the Deuckganckdock sluice to connect the Deurganckdock with the 'Waasland' harbor and the heightening of new terrains. The second reason is nature development. As compensation for the loss of valuable nature by dredging parts of the sea Scheldt new nature reserves have to be created. These new nature reserves include two tidal areas, a controlled tidal area, salt meadows and adaptations to the current water management of several waterways in order to optimize the nature along them. To investigate the influence of all the foreseen developments on the hydraulic heads and salt water distribution at the left bank of the Scheldt a 3D density dependent groundwater model has been constructed. For this model the MOCDENS3D code (Lebbe and Oude Essink 1999) was used. Visual MOCDENS3D (Vandenbohede 2007) was used as a postprocessor.

METHOD

The developed model starts in 1976, this coincides with the earliest developments at the left bank of the river Scheldt. Additionally, it allowed us to use the salinization map of De Breuck et al. 1974 for the initial saltwater distribution of the area. From 1976 on, the current situation has been reached by working in 5 discrete time steps. At the end of each time step the boundary conditions of the model were changed according to the planned developments in and around the ‘Waasland’ harbor. By doing so a good fit between the observed and modeled hydraulic heads and salt water concentrations was possible. For the modeling of the future changes at the left bank of the Scheldt, the foreseen developments have been divided into three development phases each corresponding with a foreseen development horizon (2016, 2020 and 2025). Again, the boundary conditions have been changed at each of these horizons including the new developments in and around the ‘Waasland’ harbor. After the last horizon the model has been continued for 50 more years to see the evolutions in the long term.

RESULTS

Figure 1 shows some of the results of the conducted 3D density dependent groundwater flow model. On this figure, the saltwater distribution near the water table is given for four periods. The upper left figure, gives the salinity distribution in 1976. This distribution is derived from the salinity map of De Breuck et al. (1974) and was used for the initial concentrations. From this figure it seems that the area closest to the Scheldt (at the right of the figure) is saline with the occurrence of 3 fresh water lenses within the area. Furthermore, brackish water can be observed locally near the largest waterways. The upper right figure shows the salinity distribution in 2013. In the upper part of the figure the draining channels are clearly coming forward as places with higher salinities while the intermediate areas are subject to limited freshening. In the ‘Waasland’ harbor there is a clear freshening near the heightened terrains while the different docks are clearly visible as places with a higher saltwater concentration. Furthermore, an outflow of brackish water from the most southern docks towards the largest waterways can be observed. The figure in the lower left corner shows the simulated saltwater distribution in 2030. This is 5 years after the last development horizon. On this figure the concentrations in the northern part of the model area are clearly raised due to the construction of new (controlled) tidal areas. In these new areas the water of the Scheldt can again (freely) flow leading to the infiltration of brackish water. Additionally the construction of the Saeftinghedock just south of these new tidal areas also led to the increase of salt concentrations near the dock. For the rest the same elements are visible as in the current situation: a freshening at the heightened terrains, a salinization near the docks and an outflow of brackish water from the southern docks towards the main waterways. The last figure (at the lower right) shows the situation in 2075. This is the situation 50 years after the last changes. This figure shows the evolutions in the long term. As can be seen the earlier discussed processes have continued leading to a complete freshening of the groundwater reservoir under the heightened terrains, while the docks are clearly distinctive due to their higher concentrations. The outflow from the southern docks continued leading to a clear salinization at the most important waterways around the heightened terrains of the ‘Waasland’ harbor. Furthermore, the salinization in the new tidal areas continued leading to similar saltwater concentrations as in the Scheldt.

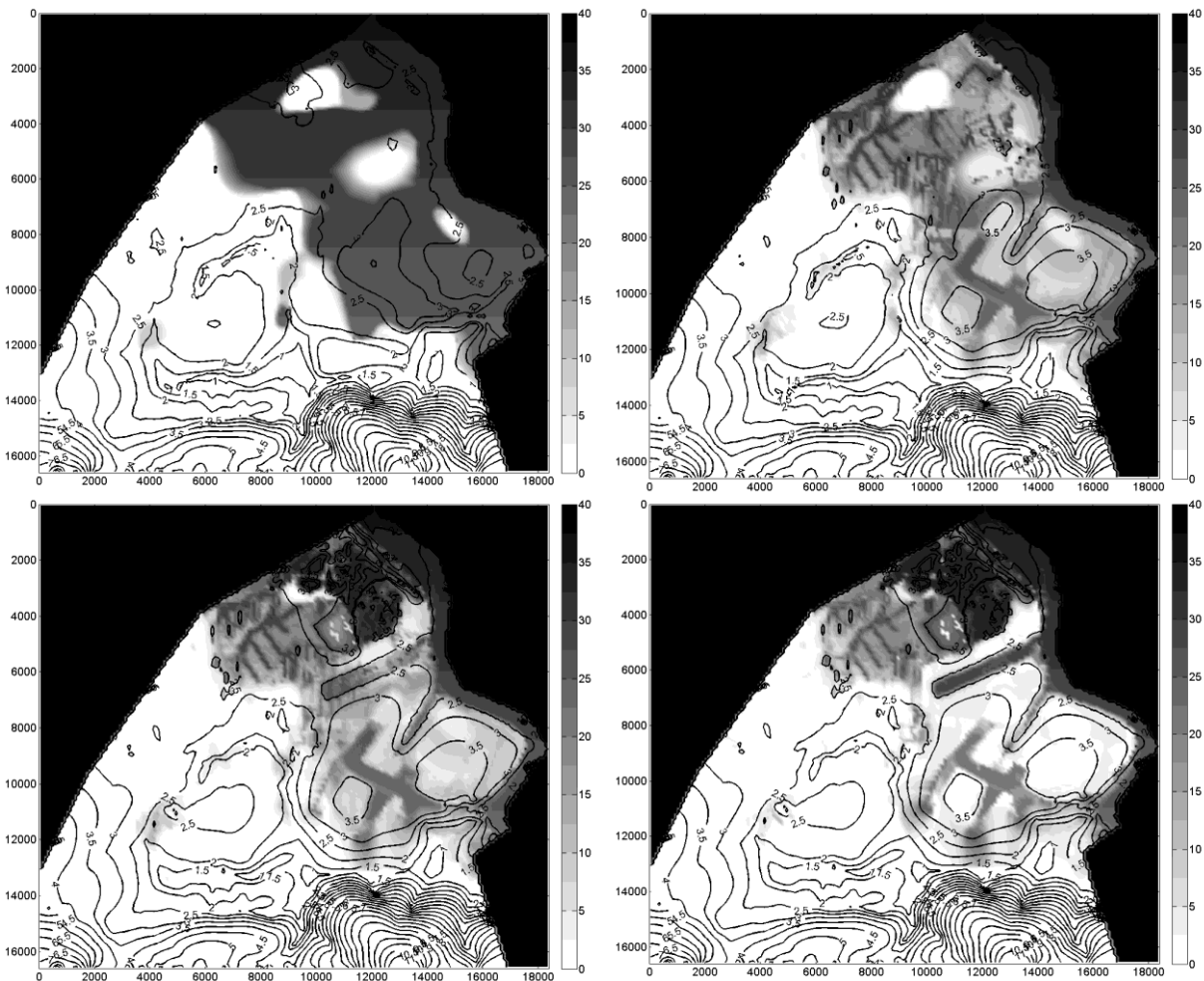


Figure 1. Saltwater distribution near the water table (upper left: 1976, upper right: 2013, lower left: 2030 and lower right: 2075). (Colour scale gives the saltwater percentages, black: 40% salt relative to North Sea water, white: 0% salt relative to North Sea water; black lines give the contourlines of the hydraulic heads.)

CONCLUSIONS

The historic, current and projected saltwater distributions and hydraulic heads at the left bank of the river Scheldt in and around the ‘Waasland’ harbor are modeled well by changing the reigning boundary conditions every few years according to the planned changes in and around the ‘Waasland’ harbor. The results show a clear increase in the saltwater concentrations at the newly constructed tidal docks and (controlled) tidal areas, whereas there is a clear freshening at the newly heightened terrains. Furthermore the currently present higher saltwater concentrations near the draining channels remain just as the lower concentrations in the intermediate areas between the draining channels. At last the model showed the outflow of brackish water from the southern docks in the direction of the largest waterways around the heightened terrains of the ‘Waasland’ harbor.

REFERENCES

De Breuck, W., G. De Moor, R. Marechal and R. Tavernier. 1974. Depth of the fresh-salt water interface in the unconfined aquifer of the Belgian coastal plain. Proc. 4th Salt Water Intrusion Meeting, Gent, map.

Lebbe, L., and G. Oude Essink. 1999. Section 12.11. MOC DENSITY / MOCDENS3D-code. 434-439, in Chapter 12. Survey of Computer codes and Case Histories.. Eds. Sorek, S. & Pinder, G.F. in: Seawater Intrusion in Coastal Aquifers, Concepts, Methods and Practices. Eds. Bear, J., Cheng, H-D, Herrera, I., Sorek, S. and Ouazar D. Kluwers Academic Publishers.

Vandenbohede, A. 2007. Visual MOCDENS3D: visualization and processing software for MOCDENS3D, a 3D density dependent groundwater flow and solute transport model. User Manual. Research Unit Groundwater Modeling, Ghent University.

Contact Information: Gert-Jan Devriese, Ghent University, Department of Geology and Soil Science, Research Unit Groundwater Modeling, Krijgslaan 281, S8, 9000 Gent, Belgium. Phone: 09 2644664, Email: gertjan.devriese@ugent.be

The effects of sea tides on fresh-saline water interface fluctuations at coastal aquifers - preliminary results of field data and laboratory experiments

Levanon Elad^{1,2}, Yechieli Yoseph², Shalev Eyal² and Gvirtzman Haim¹

¹ Institute of Earth Sciences, Hebrew University of Jerusalem, Jerusalem, Israel

² Geological Survey of Israel, Jerusalem, Israel

ABSTRACT

This study deals with the effects of sea-tides on groundwater level and fresh-saline water interface (FSI) fluctuations, in order to understand the dynamics of the coastal groundwater system influenced by tide fluctuations.

Monitoring of groundwater levels and Electrical Conductivity (EC) in several observation boreholes at the coastal aquifer of Israel shows that sea-tide induces fluctuations of groundwater level with the same wave periodicity, but with decreasing amplitude as the groundwater pressure wave propagates inland. In a similar way, the interface between the fresh groundwater and the saline seawater fluctuates with the same periodicity as well.

Time series analysis of field data measured in observation boreholes located up to 70 meter from the shoreline, showed a dramatic time-lag between the fluctuations of the hydraulic heads and those of the salinity. While the response of groundwater level to sea-tide was relatively fast (around 1.5 hours), the response of the FSI was much slower (around 12 hours).

In order to understand this phenomenon we conducted a laboratory experiments in a two-dimensional flow tank, which enabling simulation of sea-tide and high-resolution monitoring in time and space of groundwater level and EC. Preliminary results from the laboratory experiments show the same phenomenon observed in the field, namely a significant time-lag between the fluctuations of the groundwater level and those of the FSI.

Both field data and the laboratory results indicate that the propagation of the pressure wave into the aquifer is much faster than the salinity changes. It seems that the sea-tide fluctuations induce a pressure wave that triggers much slower salinity advection.

INTRODUCTION

Understanding the processes and mechanisms taking place at the FSI at coastal aquifers has become an important issue for basic hydrology research and for water management as well. Many researchers dealt with the effect of sea-tide on the induced groundwater-table fluctuations in the vicinity of the shoreline (e.g. Ataie-Ashtiani et al. 1999; Nielsen 1990) and on the resulted fluctuations of the FSI by field monitoring (Kim et al. 2006, Levanon et al. 2013) or laboratory experiments (Kuan et al. 2012).

METHODS

Time series analysis- Field data

Groundwater and FSI fluctuations were measured in nine observation boreholes located up to 70 m from the shoreline at the coastal aquifer of Israel, and the Mediterranean Sea level was measured at the same time. These field data was analyzed using Cross-Correlation (CC) analysis, in order to determine the correlation and the time-lag between the different time series and to understand the dynamics of the coastal groundwater system influenced by tide fluctuations.

Laboratory experiments

The laboratory experiments were conducted in a two-dimensional rectangular flow tank, filled with granular material and saturated with water, simulating a homogenous and phreatic coastal aquifer (Fig. 1).

The flow tank is divided into three distinct chambers: a central flow chamber representing the aquifer, and two side chambers, which formed the boundary conditions during the experiment. The left chamber represents the seawater boundary and the right one represents the inland boundary of the regional fresh groundwater. At the back of the flow tank 168 electrodes were introduced in order to measure voltage in-situ and 6 piezometers in order to measure groundwater level along the cross-section. An engine, controlled by a computer, is connected to the outflow in the left boundary, enables changing the 'seawater' level in this boundary according to the experiment progression. The different water levels are controlled by a system of elevators, pipes and pumps.

The experiments included 2 water bodies: fresh water with density of 0.997 g cm^{-3} , and saline water, colored by red food color, with density of 1.028 g cm^{-3} similar to the density of the Mediterranean Sea.

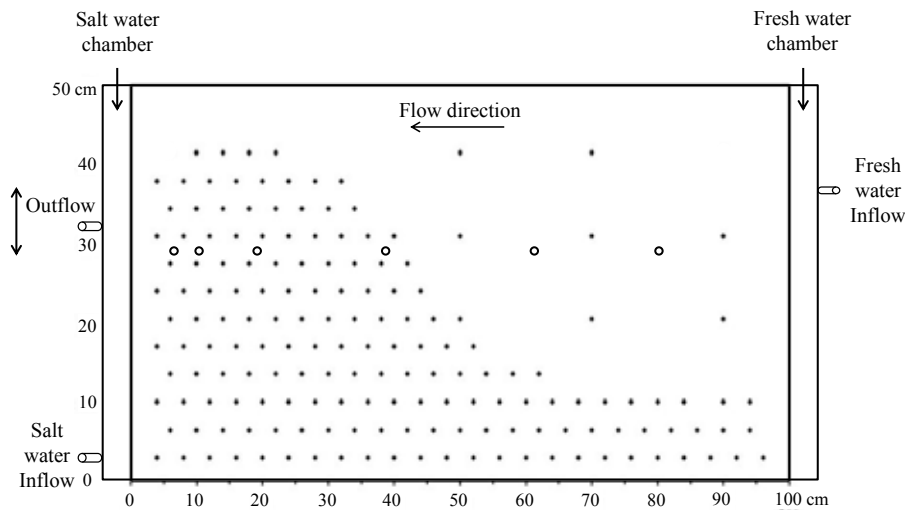


Figure 1. A schematic figure of the laboratory system. The black dots represent the location of the electrodes and the circles represent the location of the piezometers.

In the first stage of the experiment the porous medium was saturated with fresh water and the hydraulic gradient was the average hydraulic gradient between high and low tide. Then, the red saline water was inserted into the left chamber and penetrated into the porous medium creating FSI. After getting a static equilibration of the FSI the second stage of the experiment started, when the outflow and the saline water level in the left boundary fluctuated by the engine to create 'tide-like' fluctuations.

Tidal amplitude in the experiment was 2 cm (the hydraulic gradient was 1-3%), and the time difference between two high tides was half an hour.

RESULTS

Both groundwater level and the FSI, which were measured in the coastal aquifer, were influenced by sea-tide and fluctuated at the same periodicity as sea-tide periodicity (Levanon et al. 2013). The CC analysis produced unexpected results, namely a time-lag of about 10 hours between the head and salinity oscillations, both measured at the same borehole located 70 m from shoreline. While the response of groundwater level to sea-tide was relatively fast (around 1.5 hours), the response of the FSI was much slower (around 12 hours).

Preliminary results from the laboratory experiments showed the same phenomenon as observed in the field. While the induced 'sea-tide' wavelength in the laboratory was 30 minutes (compared to 12 hours in the field) and its amplitude was 2 cm (compared to 10-40 cm in the field), the results of the laboratory experiments showed a significance time lag between groundwater level and FSI fluctuations (Fig. 2).

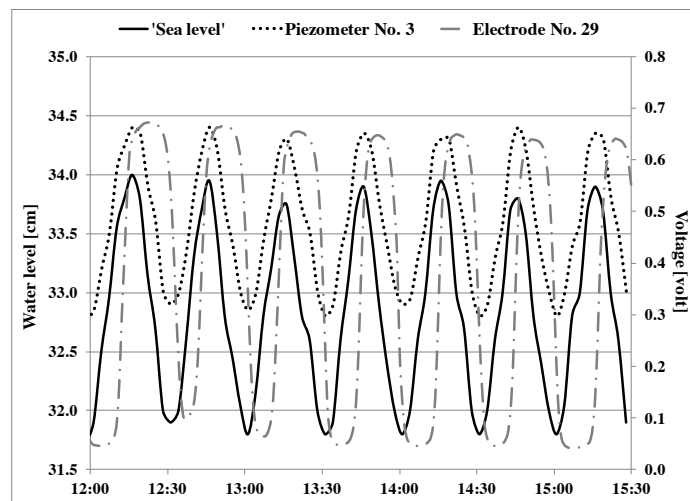


Figure 2. Preliminary results from the laboratory experiment. The groundwater level (dotted line) reacts immediately to 'sea level' fluctuations (solid line), while the FSI (grey dashed line) has a significance time-lag.

DISCUSSIONS AND CONCLUSIONS

Groundwater monitoring at the coastal aquifer of Israel indicates a significance time lag between groundwater level and the FSI fluctuations caused by sea-tide. This phenomenon was also observed in the preliminary laboratory experiments, despite the different scales (time and dimensions) between the field and the laboratory. It seems that the sea-tide fluctuations induce a relatively fast pressure wave which causes groundwater level oscillations, and later triggers much slower salinity advection which influences the FSI.

REFERENCES

- Ataie-Ashtiani, B., R. E. Volker, and D. A. Lockington. 1999. Tidal effects on sea water intrusion in unconfined aquifers. *Journal of Hydrology* 216 (1-2):17-31.
- Kim, K. Y., H. Seong, T. Kim, K. H. Park, N. C. Woo, Y. S. Park, G. W. Koh, and W. B. Park. 2006. Tidal effects on variations of fresh-saltwater interface and groundwater flow in a multilayered coastal aquifer on a volcanic island (Jeju Island, Korea). *Journal of Hydrology* 330 (3-4):525-542.
- Kuan, W. K., G. Jin, P. Xin, C. Robinson, B. Gibbes, and L. Li. 2012. Tidal influence on seawater intrusion in unconfined coastal aquifers, *Water Resour. Res.*, 48, W02502, doi:10.1029/2011WR010678.
- Levanon, E., Yechieli, Y., Shalev, E., Friedman, V., Gvirtzman, H. 2013. Reliable Monitoring of the transition zone between fresh and saline waters in Coastal Aquifers. *Groundwater monitoring & remediation* 33 (3): 101-110.
- Nielsen, P. 1990. Tidal dynamics at water table in beaches. *Water Resources Research* 26 (2127–2134).

Quantify the Influence of the Ocean Current on the Submarine Groundwater Discharge

Wei-Ci Li¹, I-Hsien Lee¹ and Chuen-Fa Ni¹

¹ Graduate Institute of Applied Geology, National Central University, Taiwan

ABSTRACT

In recent years, submarine groundwater discharge (SGD) is one of the important processes in the hydrological cycles. Previous investigations have recognized that many factors, such as the shoreline slopes, aquifer hydraulic conductivity, and tidal amplitudes might significantly control the SGD rates for an interested site. Ocean currents are common phenomena around the world that typically occur near coastal lines. The ocean currents may create pressure changes due to the current flows pass through interfaces of aquifers and seawater. This study employed HYDROGEOCHEM (Hydrologic Transport and Geochemical Reactions Model) numerical model to quantify the influences of ocean currents on output fluxes of SGD. A synthetic two-dimensional profile model is considered for illustration purpose. Based on the energy conservation equation (Bernolli's equation) for groundwater flow, the velocity heads influenced by ocean currents are not negligible in this study because the velocities of ocean currents are several orders of magnitudes greater than that of groundwater. With a variety of ocean current velocity values (from 0.2 m/s to 1.5 m/s) applied in the numerical model, we found that the ocean current leads to the increase the SGD rate up from 2.6 m/d to 6.3 m/d when the ocean current velocity was increased from 0.1 to 1.5 m/s. Such results suggest that the influences of ocean currents on SGD rates are significant, especially for coastal lines with high ocean current velocities.

INTRODUCTION

Submarine groundwater discharge (SGD) is defined as any upward flux of water from seabed sediment into the overlying marine water column (Smith 2004). Previous studies show that various factors impacts SGD, including terrestrial geometry (e.g., Konikow et al. 2013), tides (e.g., Li et al. 2009), waves (e.g., Nielsen 1990), density convection (e.g., Taniguchi et al. 2002), and seasonal recharge (e.g., Michael et al. 2005).

Despite of those factors impact on the SGD, interactions between aquifer surfaces have also studied for years (e.g., Cardenas and Wilson 2006). However, they often focused on the particle erosion or small scale relationship, little attention is paid for larger scale, such as the flux changed of SGD and the interaction between ocean current and aquifer.

This study went to employ HYDROGEOCHEM 4.0 to simulate SGD in two-dimensional unconfined coastal aquifer. Base on the measured velocity 92cm/s of Kuroshio around east coastline of Taiwan (Zhu et al. 2006). The influence of ocean current on SGD will be quantified with five velocities of ocean current 0.1, 0.5, 1.0, 1.5 m/s.

METHODS

HYDROGEOCHEM 4.0

HYDROGEOCHEM4.0 is a two dimensional numerical model coupled of water flow, thermal transport, solute transport, and mixed geochemical kinetic/ equilibrium reactions in a saturated/unsaturated porous media. This model is designed for a generic application to reactive transport problems controlled by both kinetic and equilibrium reactions in

subsurface media (Yeh et al., 2004). HYDROGEOCHEM 4.0 was employed to simulate SGD in two-dimensional unconfined coastal aquifer in this study. Five velocities of ocean current 0.1, 0.5, 1.0, 1.5 m/s will flow through the aquifer in seaside, the current velocity result in pressure head reduced on seawater boundary due to Bernoulli's equation. The influence of ocean current on SGD can be quantified finally.

Flow equation

The flow equation of HYDROGEOCHEM is modified Richard equation that describes density dependent fluid flow in variably saturated media. It can be derived based on continuity of fluid continuity of solid, Darcy's law, consolidation of the media, and compressibility of water (Yeh et al., 2004):

$$\frac{\rho}{\rho_0} F \frac{\partial h}{\partial t} = \nabla \cdot \left[K \cdot \left(\nabla h + \frac{\rho}{\rho_0} \nabla z \right) \right] + \frac{\rho^*}{\rho_0} q \quad (1)$$

in which F is the generalized storage coefficient (1/L), K is the hydraulic conductivity tensor (L/T):

$$F = \alpha' \frac{\theta}{n_e} + \beta' \theta + n_e \frac{\partial S}{\partial h} \quad (2)$$

$$K = \frac{\rho g}{\mu} k = \frac{\left(\frac{\rho}{\rho_0}\right)}{\left(\frac{\mu}{\mu_0}\right)} K_{so} K_r \quad (3)$$

where ρ is the fluid density (M/L³), ρ_0 is the referenced fluid density (M/L³), h is the pressure head (L), t is the time (T), z is the potential head (L), ρ^* is the fluid density of either injection or with draw ($=\rho$) (M/L³) and q represent the source or sink representing the artificial injection or withdraw of fluid [(L³/L³)/T]. In equation (2), α' is the modified compressibility of the media (1/L), θ is the effective moisture content (L³/L³), n_e is the effective porosity (L³/L³), β' is the modified compressibility of the liquid (1/L) and S means the degree of saturation of water (dimensionless). For equation (3), μ_0 is the fluid dynamic viscosity at zero chemical concentration [M/(LT)], μ means the fluid dynamic viscosity [M/(LT)], K_{so} is the referenced saturated hydraulic conductivity tensor (L/T) and $k_r = k/k_s$ represent the relative permeability or conductivity (dimensionless).

Transport Equation

The transport equation for species i consider advection, dispersion, diffusion, source/sink, radioactive decay and biogeochemical reaction. The equation was derived based on the continuity of mass and Fick's laws (Yeh et al., 2004):

$$\frac{\partial \theta C_i}{\partial t} + \left(\theta \alpha' \frac{\partial h}{\partial t} + \frac{\partial \theta}{\partial t} \right) C_i = (\mathcal{L}(C_i) - Q C_i) + M_i + \theta r_i|_R, i \in \{N\} \quad (4)$$

in which \mathcal{L} is the advection-dispersion operator denoting:

$$\mathcal{L}(C_i) = -V \cdot C_i + \nabla \cdot (\theta D \cdot \nabla C_i) \quad (5)$$

$r_i|_R$ denotes production rate r_i due to R reactions, which is described by:

$$r_i|_R = \sum_{i=0}^R (v_{ik} - \mu_{ik}) R_K \quad (6)$$

where $\{N\} = \{1, 2, \dots, N\}$ in which N is the number of species. In equation (4), C_i is the concentration of the i -th species in units of chemical mass per water volume [M/L³] and M_i means the external source/ sink rate of the i -th per unit medium volume [(M or L³)/T]. For

equation (5), V means the Darcy's velocity [L/T] and D represent the dispersion coefficient tensor [L²/T]. In equation (6), v_{ik} and μ_{ik} are the reaction stoichiometry of the i -th species in the k -th reaction associated with the products and reactants respectively.

Since seawater intrusion is often considered as density-dependent problem, in HYDROGEOCHEM, the density of groundwater is a function of chemical concentration as (Cheng, 1995) :

$$\rho = \rho_w + \sum_{i=1}^{M_a} c_i m_i \left(1 - \frac{\rho_w}{\rho_i}\right) \quad (7)$$

In this study, the temperature is considered as a constant 25 °C , and the activity coefficient of ion is neglected.

Conceptual model

The conceptual model is shown in Figure 1. The left hand side of the domain is land boundary, and right hand side is sea boundary. The length of the simulation domain is 200 m, and the depth is 33 m. Beach slope 10 % started from distance 120m to 180m from land boundary. In simulation domain, it contains 1573 nodes and 3000 elements.

The tide waveform used in the sea boundaries with amplitude 1 m, and the frequency is 2 times per day. It was divided in 64 equal stress periods to capture the tide above the beach face during simulation time 8 days.

Constant head 31 m is used for the land side flow boundary conditions, and sea boundaries is sets as no flow. This study considers seawater as a density-dependent liquid with constant concentration 0.59 mole/L, mean sea level locates with $Z=30$ m. Following Robinson et al. (2007), longitudinal dispersivity is sets as 0.5m, the transverse dispersivity is 0.05 m, the porosity of the aquifer is set 0.25, and diffusion coefficient is 6.6E-2 m²/day. Note that the aquifer is assumed homogeneous and isotropic, which the hydraulic conductivity is 10 m/day.

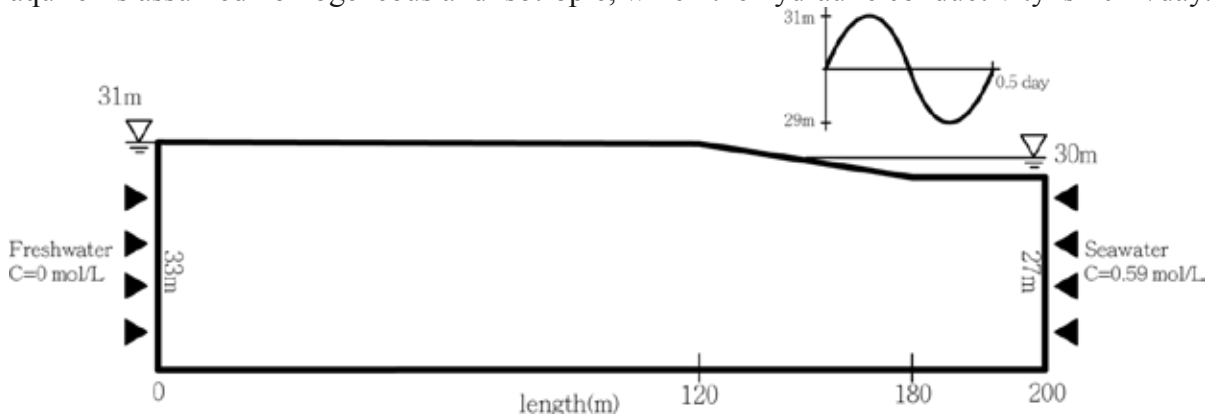


Figure 1. The conceptual model of simulation domain

To simply the situation when ocean current flows upon the aquifer, this study assumed seawater is constant concentration and frictionless, considered the Bernoulli's equation, which is:

$$\frac{P}{\rho g} + \frac{V^2}{2g} + z = H \quad (8)$$

where P is pressure [F/L²], H is total head in aquifer[L], z means height of considered point [L]. g is gravitational acceleration [L/T²], V is velocity of ocean current [L/T], which is often

neglected in groundwater problems. Following Bernoulli's equation, the ocean current will reduce the pressure gradient in aquifer with $\frac{V^2}{2g}$.

RESULTS AND DISCUSSION

Figure 2 illustrates the saline concentration distribution with and without ocean current in simulation time 8 days. In Figure 2, except the seawater freshwater interface, similar to previous studies, tide fluctuation makes an upper saline plume (USP) on the beach slope. Figure 2b shows that due to pressure head decreased by ocean current, the seawater/freshwater interface moved more closed to seaside than the situation without ocean current. However, ocean current also increase the influences of tide on beach slope, it makes the range of USP bigger. Figure 3 shows that freshwater in aquifer discharged into ocean due to ebb tide, which is one of physical processes in seawater circulation (Santos et al., 2012). Compare to Figure 2a and 2 b, ocean current increases hydraulic from land to sea, it makes more freshwater discharge to the sea.

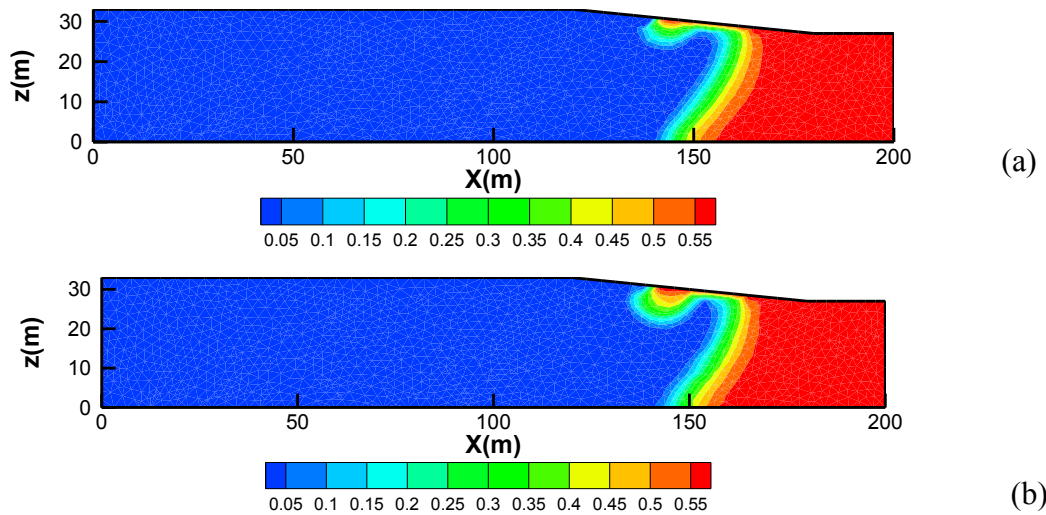


Figure 2. Saline concentration distribution at ebb tide in time=8 day (a) without ocean current and with ocean current V=1.5m/s (mole/L)

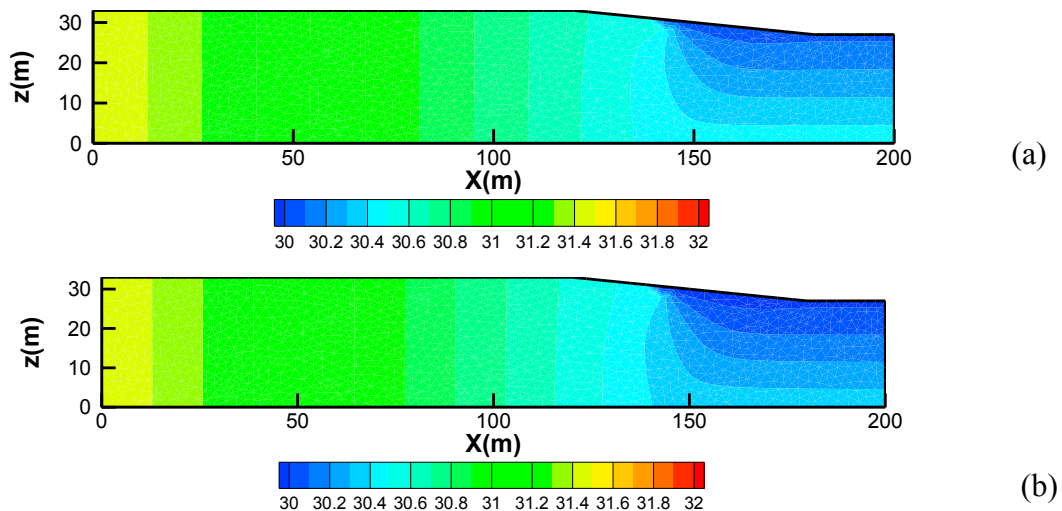


Figure 3. Total head at ebb tide in time=8 day (a) without ocean current and with ocean current V=1.5m/s (mole/L)

Freshwater discharge velocity on beach slope was employed to quantify the influences of ocean current in this study. In Figure 4, it shows that ocean current have significant effect on the discharge velocity, in $V=1.5$ m/s case, the output velocity can increase from 2.6m/d to 6.3m/d when the ocean current velocity was increased from 0.2 to 1.5 m/s.

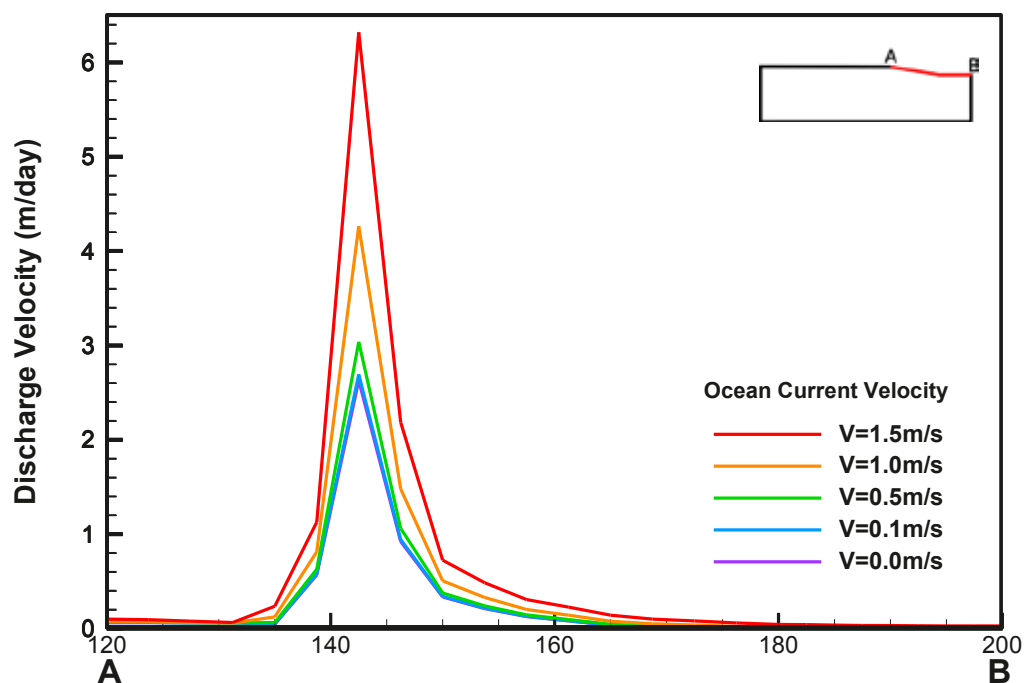


Figure 4. Freshwater discharge velocity on the beach slope

CONCLUSIONS

This study simulated the influence of ocean current on beach slope by using Bernoulli's equation, simulation results show that the ocean current effect will: (1) reduce the penetrate distance of seawater/freshwater interface; (2) increase the range of upper saline plume. Moreover, ocean current makes more freshwater discharge into to the sea, the output velocity can increase from 2.6m/d to 6.3m/d when the ocean current velocity was increased from 0.2 to 1.5 m/s.

REFERENCES

- Cardenas, M. B., and J. L. Wilson. 2006. The influence of ambient groundwater discharge on hyperheic zones induced by current-bedform interactions. *Journal of Hydrology*, no. 331: 103–109.
- Cheng, H. P. 1195. Development and application of a three-dimensional finite element model of subsurface flow, heat transfer, and reactive chemical transport. Ph.D. Dissertation, Department of Civil and Environment Engineering, the Pennsylvania State University, University Park, PA 16802.
- Konikow, L. F., M. Akhavan, C. D. Langevin, H. A. Michael, and A. H. Sawyer. 2013. Seawater circulation in sediments driven by interactions between seabed topography and fluid density. *Water Resources Research* 49, no. 3: 1386–1399.
- Li, X., B. X. Hu, W. C. Burnett, I. R. Santos, and J. P. Chanton. 2009. Submarine groundwater discharge driven by tidal pumping in a heterogeneous aquifer. *Groundwater* 47, no. 4: 558-568.

Michael, H. A., A. E. Mulligan, C. F. Harvey. 2005. Seasonal oscillations in water exchange between aquifer and the coastal ocean. *Nature*, no. 436: 1145-1148.

Nielsen, P. 1990. Tidal dynamics of the water table in beaches. *Water Resource Research*, no. 26: 2127–2134.

Robinson, C., L. Li, and D. A. Barry 2007. Effect of tidal forcing on a subterranean estuary. *Advances in Water Resources*, no. 30, 851-865.

Santos, I. R., Eyre, B. D., and M. Huettel 2012. The driving forces of porewater and groundwater flow in permeable coastal sediments : A review. *Estuarine, Coastal and Shelf science*, no. 98, 1-15.

Smith, A. J. 2004. Mixed convection and density-dependent seawater circulation in coastal aquifers. *Water Resource Research*, no. 40, W08309.

Taniguchi, M., W. C. Burnett, J. E. Cable, and J. V. Turner. 2002. Investigation of submarine groundwater discharge. *Hydrology Processes*, no.16: 2115–2129.

Yeh, G. T., Y. Li, P. M. Jardine, W. D. Burgos, Y. Fang, M. H. Li, M. D. Siegel. 2004. HYDROGEOCHEM 4.0: A Coupled Model of Fluid Flow, Thermal Transport and HYDROGEOCHEMical Transport through Saturated-Unsaturated Media: Version 4.0.

Zhu, X. H., J. H. Park, I. Kaneko. 2006. Velocity structure and transports of the Kuroshio and the Ryukyu current during fall of 2000 estimated by an inverse technique. *Journal of Oceanography*, no.62: 587-596.

Contact Information: Chuen-Fa Ni, Graduate Institute of Applied Geology, National Central University, Chungli City, Taoyuan 32001, Taiwan, Phone: 886-3-4227151 ext. 65874, Fax: 886-3-4263127, Email: nichuenfa@geo.ncu.edu.tw

The coastal springs along the Taranto Gulf (South Italy)

Zuffianò L.E., Limoni P.P., Barnaba F., Basso A., Casarano D., Dragone V., Santaloia F., Polemio M.,
Istituto di Ricerca per la Protezione Idrogeologica – CNR, Bari, Italy,

ABSTRACT

The Mar Piccolo (literally “small sea”), a sea internal basin which is part of the Taranto Gulf, located along the Ionian coast in southern Italy (Apulia region), represents a peculiar and sensitive environmental area and a social emergency due to the level of sea water pollution coming from the close industrial area of Taranto.

The paper describes the preliminary results to define a conceptualization of the aquifer as main support to characterize the hydrological balance of the internal sea, the geochemistry of groundwater, and the effect on the ecological equilibrium of the coastal environment.

INTRODUCTION

The aquifer occurring in the carbonate sequence of the Murgia plateau feeds numerous coastal springs and constitutes the main local source of pure fresh groundwater.

Galeso, Battentieri and Riso are the main subaerial springs located along the coast of Mar Piccolo, not far from the town of Taranto (respectively point 2, 3 and 4 in Figure 1). This area is also characterized by several submarine springs, locally called “Citri” (Cerruti, 1938, Cotecchia et al., 1990).

Submarine freshwater discharge plays an important role in the hydrogeological equilibrium of the system.

GEOLOGICAL AND HYDROGEOLOGICAL SETTING

The area, located between the southern part of the Murgia plateau and the Ionian sea, is geologically characterized by a sequence of Mesozoic limestone (the Apulian carbonate platform) constituting the foreland of the southern Apennines chain.

The main geological units outcropping in the study area are represented by a carbonate sequence constituted by Cretaceous limestones; a Middle Pliocene-Lower Pleistocene calcarenite; a Lower Pleistocene clay; a Middle and Upper Pleistocene calcarenite and sand; a Holocene alluvial deposits and coastal deposits (Figure 1).

In the area, hydrogeological situation is characterized by a deep aquifer located in the carbonate rocks. The Mesozoic sequence is intensely fissured and karstified, and forms an important groundwater reservoir. In the sediments of Pleistocene sequence, local shallow aquifers of limited extension occur. They are located at topographically depressed areas, where Quaternary deposits, constituted by sands and calcarenites, overlie impermeable clays formations.

The base level of groundwater corresponds to the sea level. The piezometric heads (Figure 1) drop rapidly from value above 10 m a.s.l. in the inner areas, to values close to 1 m a.s.l. near the shoreline. The variations of the piezometric surface are related to the permeability of the rocks. In particular, the evolution of the piezometric surface shows that the main directions of groundwater outflows are primarily focused towards Mar Piccolo, to the draining effect that coastal springs (subaerial and submarine).

The flow rate of the Galeso Spring is about 500 l/s, that of the Battentieri spring is less than 200 l/s, whereas that of the Riso spring is about di 100 l/s (Polemio et al., 2014).

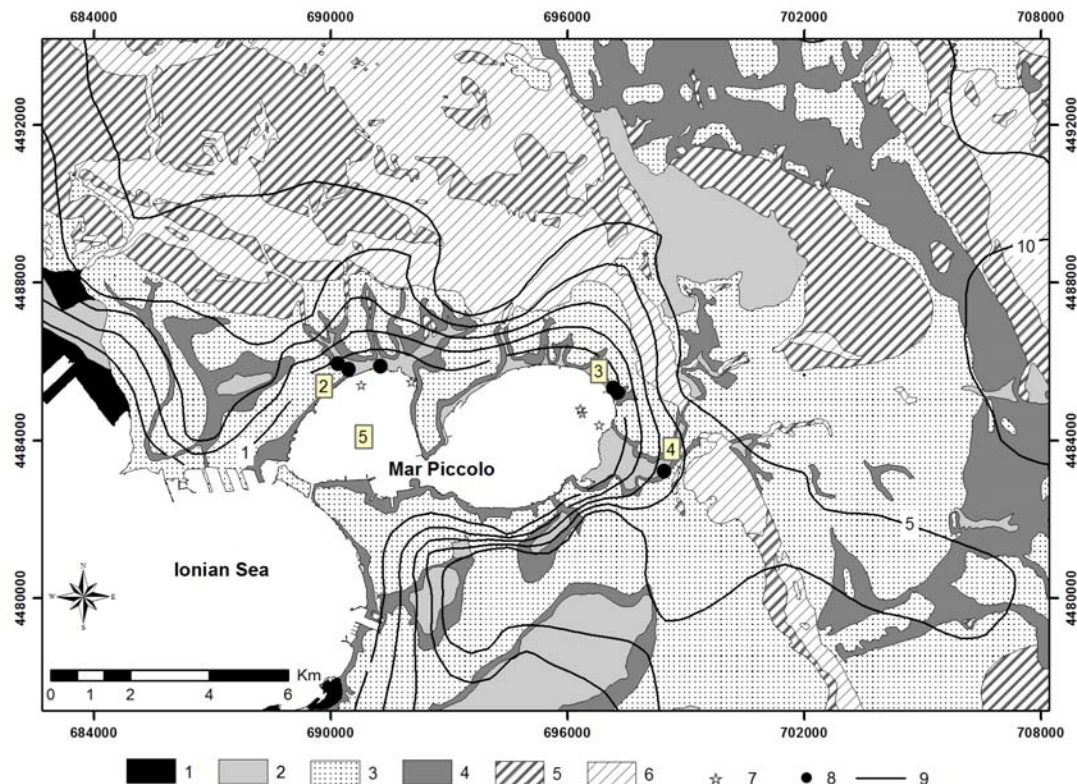


Figure 1. Simplified geological and hydrogeological map. Legend: 1) coastal deposits, 2) alluvial deposits, 3) terraced marine deposits, 4) subappennine clay, 5) gravina calcarenites, 6) altamura limestone, 7) submarine spring, 8) subaerial spring, 9) piezometric line.

CHEMICAL ANALYSES OF WATER AND INTERPRETATION

Determination of the main constituents of waters was performed by means of ion chromatography methods, for separation of both cations and anions, with conductometric detection. Ion chromatography analyses results are shown in Table 1.

Total alkalinity values of the samples were determined by titration with 0.1N HCl, to a pH=4.5 endpoint. The location of sampling points is shown in Figure 1.

Sample	Name	pH	E.C.	Li ⁺	Na ⁺	K ⁺	Mg ²⁺	Ca ²⁺	F ⁻	Cl ⁻	Br ⁻	NO ₃ ⁻	HCO ₃ ²⁻	SO ₄ ²⁻
1	Carbonate aquifer	7,75	0,51	<0,05	12,5	3,19	24,2	57,9	0,27	12,9	0,05	23,7	281	7,48
2	Galeso Spring	6,98	3,83	0,03	569,0	17,64	75,0	123,0	3,68	1060,5	4,22	16,8	354	160,6
3	Battentieri Spring	7,05	5,30	0,04	824,5	30,13	98,0	141,7	3,67	1638,7	5,99	13,7	372	222,6
4	Riso Spring	7,02	3,91	0,02	575,9	22,03	77,8	125,0	2,89	1068,7	4,20	22,5	366	156,2
5	Seawater	7,33	48,3	0,15	11160	337,1	1297	408,7		21024	69,4		171	2458

Table 1. Electrical Conductivity (E.C.) in mS/cm; Concentration in mg/L

The ground water of carbonate aquifers is generally characterized by a predominance of calcium and bicarbonate ions, as a result of dissolution of the minerals calcite and dolomite. The process of dissolution and precipitation of calcite can be schematized with the following reaction:

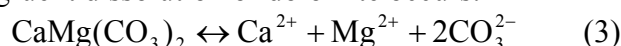


Saturation with respect to calcite is expressed by the saturation index:

$$SI_{\text{calcite}} = \log \frac{[Ca^{2+}][CO_3^{2-}]}{K_{\text{calcite}}} = \log \frac{IAP_{\text{calcite}}}{K_{\text{calcite}}} \quad (2)$$

where $[Ca^{2+}]$ and $[CO_3^{2-}]$ are the activities of ions, calculated from the analyses; IAP_{calcite} is the ion activity product for calcite.

Dolomite is a very poor soluble mineral, if compared with calcite. In a system containing calcite, dissolution of dolomite may be congruent or incongruent, depending on the concentration of calcium derived from calcite (Wigley, 1973b). If water is subsaturated with respect to calcite, congruent dissolution of dolomite occurs:



Saturation with respect to dolomite is expressed by the saturation index:

$$SI_{\text{dolomite}} = \frac{[Ca^{2+}][Mg^{2+}][CO_3^{2-}]^2}{K_{\text{dolomite}}} = \log \frac{IAP_{\text{dolomite}}}{K_{\text{dolomite}}} \quad (4)$$

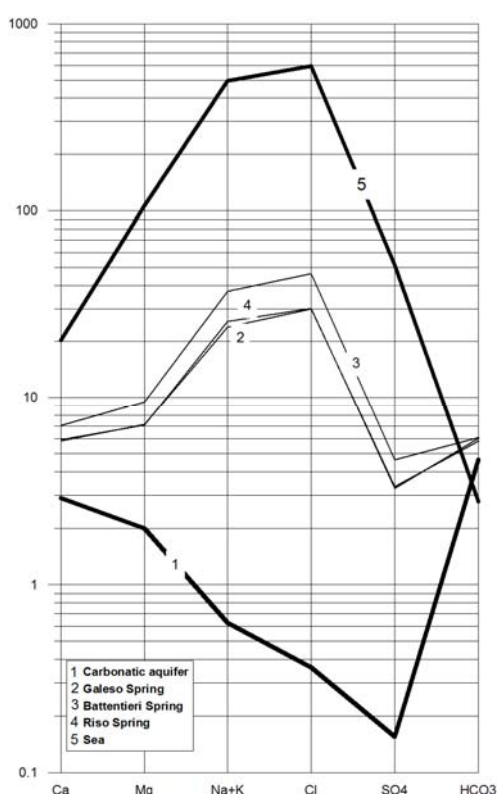


Figure 2. Schoeller diagramm

The sample of coastal springs are subsaturation with respect to calcite and respect to dolomite (Table 2).

These waters are characterized by rather high values of electrical conductivity, high concentrations of alkaline ions (Na^+ and K^+) and chloride ion. This water shows the chemical characteristics of fresh groundwater contaminated by seawater intrusion.

The geochemical composition of the samples (Figure 2) can be considered between that of seawater (sample 5) and the water of carbonate aquifer when not affected by the seawater intrusion (sample 1). The freshest groundwater sample was collected from an irrigation well and it is representative of local fresh groundwater.

The fraction of seawater (f_{sea}) of each sample is calculated from the concentration of the chloride ion, considered as conservative ion in the mixing process (Appelo and Postma, 2005):

$$f_{\text{sea}} = \frac{m_{Cl^-, \text{sample}} - m_{Cl^-, \text{fresh}}}{m_{Cl^-, \text{sea}} - m_{Cl^-, \text{fresh}}} \quad (5)$$

The results are shown in Table 2. In particular, the water show a mixing ratio of fresh water and sea water between 5% and 8%.

The expected concentration of the different ions ($m_{i, \text{mix}}$), resulting from mixing between fresh water and salt water, is calculated by:

$$m_{i, \text{mix}} = f_{\text{sea}} \cdot m_{i, \text{sea}} + (1 - f_{\text{sea}}) \cdot m_{i, \text{fresh}} \quad (6)$$

where $m_{i, \text{sea}}$ e $m_{i, \text{fresh}}$ are the concentration in seawater and freshwater of the species i .

The enrichment or depletion ($m_{i, \text{react}}$) of the species i is then obtained by:

$$m_{i, \text{react}} = m_{i, \text{sample}} - m_{i, \text{mix}} \quad (7)$$

where $m_{i,react}$ may take both positive and negative value, or be equal to zero (only mixing). Table 2 shows the results of calculations. The change of the concentration of the ions, calculated from the concentration determined by analytical means, indicates the presence of additional geochemical processes that modify the water hydrochemistry compared to the composition resulting from the simple mixing.

Sample	SI _{calcite}	SI _{dolomite}	f %	Ca ²⁺ _{mix}	Ca ²⁺ _{react}	Mg ²⁺ _{mix}	Mg ²⁺ _{react}	HCO ₃ ²⁻ _{mix}	HCO ₃ ²⁻ _{react}
1			0						
2	-0,3	-0,30	5,0	1,9	1,2	3,6	-0,6	4,4	1,4
3	-0,2	-0,08	5,0	2,1	1,4	4,8	-0,8	4,4	1,7
4	-0,3	-0,17	7,2	1,9	1,2	3,7	-0,5	4,4	1,6
5			100						

Table 2. Saturation indexes for calcite and dolomite; fraction of seawater; mixing; reacting.

Water samples show an enrichment of calcium and depletion of magnesium ion. These effects could be related to the dolomitization of the limestone induced by seawater intrusion, as suggested by Hanshaw et al. (1971).

ACKNOWLEDGEMENTS

The research is part of RITMARE Project (The Italian research for the Sea), coordinated by the National Research Council and funded by the Ministry of Education, University and Research.

REFERENCES

- Appelo C. A. J. and Postma D. Geochemistry, Groundwater and Pollution 2nd edition, Rotterdam, Balkema, 2005, 649 pp.
- Cerruti A. 1938. Le sorgenti sottomarine (Citri) del Mar Grande e Mar Piccolo di Taranto. Ann. Istit. Sup. Nav. Di Napoli, VII, Napoli.
- Cotecchia, F., Lollino, G., Pagliarulo, R., Stefanon, A., Tadolini, T., and Trizzino, R. 1990. Hydrogeological conditions and field monitoring of Galeso submarine spring in the Mar Piccolo of Taranto (southern Italy), 11th Proceeding of Salt water intrusion meeting: Gdansk, 171-208.
- Hanshaw B.B., Back W. Deike R. G. 1971. A geochemical hypothesis for dolomitization by groundwater. Economic Geology, 66, 710 – 724.
- Polemio M., Barnaba F., Basso A., Casarano D., Dragone V., Limoni P.P., Santaloia F. Zuffianò L.E. 2014. Progetto Ritmare (la Ricerca Italiana per il Mare). Rapporto sul modello concettuale relativo alle principali sorgenti censite. 1 – 39.
- Wigley T.M.L. 1973 (b). Geochimica et Cosmochimica Acta, 37, 1397 – 1402.

Contact Information: Maurizio Polemio, Istituto di Ricerca per la Protezione Idrogeologica – CNR, Bari, Italy, Email: m.polemio@ba.irpi.cnr.it

Self-potential (SP) response to seawater intrusion in coastal aquifers

D.J. MacAllister^{1,2}, M.D. Jackson¹, A.P. Butler² and J. Vinogradov¹

¹Department of Earth Science and Engineering, Imperial College London, SW7 6AS

²Department of Civil and Environmental Engineering, Imperial College London, SW7 6AS

ABSTRACT

Seawater intrusion is a major threat to the sustainability of coastal water supplies. Long-term self-potential (SP) monitoring has been conducted on the South-Coast of the UK in the chalk aquifer, in order to test its application for remote detection of the saline front. Tidal SP fluctuations of c. 2mV have been observed. We attribute tidal SP fluctuations to the exclusion potential, caused by the salinity gradient and the movement of the saline front in the chalk matrix. Furthermore we observe a systematic increase in SP beginning 5 days prior to saline breakthrough; with a maximum magnitude of 300 μ V at the base of the borehole. We attribute this to the diffusion potential, generated by the local movement of saline water through a fracture logged close to the location of the maximum SP change. These results suggest, for the first time, that SP can provide early warning of seawater intrusion.

INTRODUCTION

Management of abstraction from coastal aquifers is of critical importance to ensure sufficient and sustainable water supplies in coastal areas, but remains a significant challenge. A key reason is that monitoring data, required for such management, are limited (Post, 2005). The most common monitoring strategy is to measure the fluid electrical conductivity (FEC) of the water in monitoring and/or abstraction boreholes. However, spatial resolution is limited by the number and distribution of monitoring boreholes. Measurements at abstraction boreholes can detect the saline front only when it arrives. Therefore monitoring techniques are required that are cheap and non-intrusive, but allow remote detection of saline intrusion.

The self-potential (SP) method comprises the passive measurement of electrical potential at the ground surface and in boreholes. The SP arises to maintain overall electro-neutrality when a separation of electrical charge occurs in response to natural or induced gradients in thermodynamic potential, such as fluid potential (head), and chemical potential (concentration) (Revil, 1999). SP signals are therefore likely in coastal aquifers because gradients in head and concentration are both present. There is evidence from oil and gas reservoir studies that an encroaching saline front may generate a measurable SP signal at an abstraction borehole prior to breakthrough (e.g. Jackson et al., 2012). We test this by conducting a 6 month monitoring program in a borehole located in the coastal UK Chalk aquifer, supplemented by laboratory experiments. We investigate SP signals associated with natural variations in head, and in the location of the saline wedge.

METHOD

Field site

The field site was located near Brighton on the south coast of the UK. The data were acquired from the Saltdean monitoring borehole approximately 1.7km from the coast. This borehole is known to experience seasonally elevated salinity levels to c. 15,000 μ S/cm (Jones

and Robins, 1999). The aquifer unit penetrated by the borehole is the Upper Cretaceous Seaford Chalk, which is the main regional aquifer. The Chalk is a dual porosity aquifer, with matrix porosity in the range 35-47%, but with fractures acting as the primary flowpaths, yielding transmissivities of about 500m²/day (MacDonald and Allen, 2001).

Borehole data acquisition

The Saltdean borehole has a water column of c. 30m, is c. 60m deep, has a diameter of c. 1m and is open hole below 15mAOD. The ground level is 30.19mAOD. The borehole monitoring tool, logged with a 5 minute sampling rate, comprised 14 non-polarising electrodes with 2m spacing. The water table fluctuates around 1.01mAOD depending on the tide and in-land freshwater head. The shallowest electrode is located at -0.81mAOD and the deepest electrode is located at -26.81mAOD. Three probes measuring conductivity (FEC), temperature (T) and pressure (P) were also installed at -2.81mAOD, -8.81mAOD and -26.81mAOD. An additional electrode was installed at the surface as a reference electrode.

RESULTS

Borehole monitoring data - referenced against the surface electrode

The head gradually decreased during the monitoring period, and there are fluctuations of varying frequencies around the long-term trend (Fig 1a). Analysis of the head data in the frequency domain using a Fast Fourier Transform (FFT) reveals that the data has semi-diurnal, diurnal and fortnightly frequencies. Consequently, the head data are consistent with semi-diurnal, diurnal, and spring-neap tidal cycles, superimposed on a gradual decrease in head caused by low rainfall during the monitoring period. The variation in head over a semi-diurnal tidal cycle is typically c. 50cm. The FEC in the borehole (Fig 1a) remains low throughout the first three months of the monitoring program, although fluctuating with tides around a mean value of 630 μ S/cm. Saline water was observed to enter the borehole in late August 2013, reaching a maximum conductivity of 4,000 μ S/cm by mid-September.

The SP data (Fig 1b) shows no obvious long-term trend, but there are fluctuations of varying frequencies, similar to the head data. A FFT of the SP data reveals semi-diurnal and diurnal frequencies. The SP is therefore recording the tidal signature. The variation in SP over a tidal cycle is c. 2mV, and is anti-correlated with head. The SP also becomes less positive with depth, with a range of c. 5mV from the top to the base of the borehole (Fig 1b).

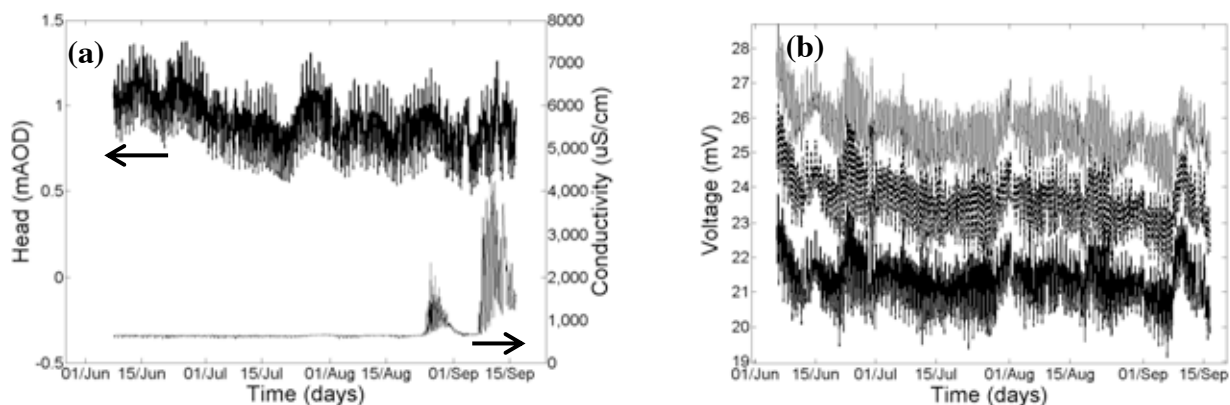


Figure 1 (a) Head and conductivity measured in the borehole. (b) The voltage measured in the borehole at -26.81mAOD, -14.81mAOD and -2.81mAOD. There is a gradient with depth with the voltage decreasing at the shallower electrodes.

Borehole electrode response to temperature and salinity variations

The SP clearly exhibits a tidal signature. However, the borehole FEC and temperature also display tidal signatures, and variations in both of these can affect the electrode response. Temperature fluctuations contribute a maximum of c. $150\mu\text{V}$. Conductivity fluctuation induce a voltage change of c. $50\mu\text{V}$. Hence it is clear that the conductivity and temperature variations in the borehole do not significantly affect the performance of the electrodes, suggesting that the tidal SP response is caused by sources within the aquifer.

Borehole monitoring data - referenced against a borehole electrode

The SP referenced against the surface electrode does not yield any obvious long-term trend, so we analysed the difference in voltages measured in the borehole to examine if there is evidence of the SP responding to the long-term movement of the saline water in the aquifer prior to breakthrough (Fig 2). To do this, we reference the borehole electrode voltages against the borehole electrode at -2.81mAOD which remained in a stable low conductivity environment throughout the monitoring period (Fig 2a). After filtering out the semi-diurnal SP we observe a systematic increase in the SP starting c. 5 days before breakthrough (Fig 2b). This is observed throughout the array, but the magnitude decreases up the borehole, from c. $300\mu\text{V}$ at -26.81mAOD (Fig 2b) to c. $50\mu\text{V}$ at -4.81mAOD .

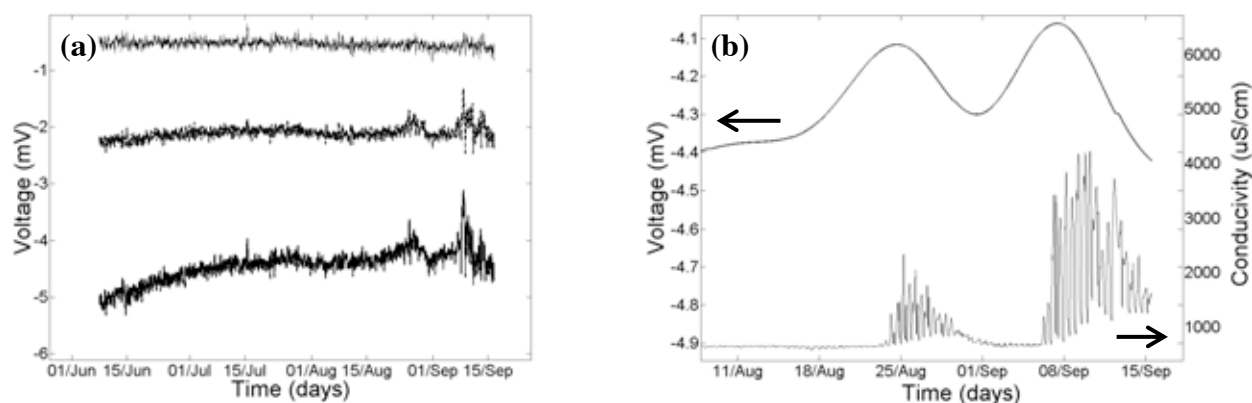


Figure 2 (a) Voltage at -26.81mAOD , -14.81mAOD and -4.81mAOD and referenced against the electrode at -2.81mAOD . (b) Filtered voltage and FEC at -26.81mAOD showing an increase in voltage prior to breakthrough of saline water.

DISCUSSION

Tidal SP and vertical gradient

There are two likely SP source mechanisms for the c. 2mV tidal response. The first is the streaming potential, which arises as a result of head gradients. The second is the exclusion-diffusion potential arising as a result of the concentration gradient (e.g. Revil, 1999).

Laboratory measurements of the streaming potential coupling coefficient (Jaafar et al., 2009) yield values of $-521\mu\text{V}/\text{mH}_2\text{O}$ and $-17\mu\text{V}/\text{mH}_2\text{O}$ for samples of Seaford Chalk saturated with groundwater and seawater, respectively. Consequently, we conclude that a streaming potential source cannot be solely responsible for observed tidal SP response. Indeed, the laboratory value of the streaming potential coupling coefficient suggests that the c. 50cm tidal head variations contribute only c. $260\mu\text{V}$ of the observed 2mV SP response. The exclusion potential arising in response to the concentration gradient associated with saline intrusion is the most likely SP source mechanism. To date, no measurements are available of the exclusion potential in chalk. However, the negative surface charge interpreted from streaming potential measurements is consistent with exclusion of negative ions from the

rock pore space and an excess of positive charge migrating down the concentration gradient (Revil, 1999). Thus, on a regional scale the movement of the saline water through the matrix generates an exclusion potential. The SP becomes less positive as the saline front approaches the monitoring location, which explains why the SP is anti-correlated with head, and may also explain the 5mV gradient: the saline front is closer to the base of the borehole.

Seasonal SP variations with borehole electrode referencing

The SP is observed to become more positive c. 5 days prior to saline breakthrough, when referenced against the borehole electrode. There is evidence that the saline water enters the borehole through a fracture at the base (Jones and Robins, 1999). We suggest that the diffusion potential (opposite sign to the exclusion potential) is the dominant SP source within the fractures on a local scale. This explains the positive change in voltage observed prior to saline breakthrough. This suggests that the change in voltage is related to the position of the saline front. However further work, most likely constrained inversion, is required to estimate the position of the front relative to the borehole and how changes in voltage are related to its position over time. It is clear, however, that SP appears to systematically change pre-breakthrough providing early (c. 5 days) warning of saline intrusion.

CONCLUSIONS

A 6 month program to measure SP in a monitoring borehole in the UK south-coast Chalk aquifer has revealed a c. 2mV tidal signature, consistent with the observed variations in head. The magnitude of the tidal SP response cannot be explained solely by streaming potentials. Instead, we argue that the SP measured at the borehole primarily reflects the exclusion potential established across the salinity front in the matrix. Furthermore a systematic increase in SP prior to saline breakthrough appears to be consistent with a local diffusion potential in the fractures. The increase in SP appears to provide early warning of the advancing saline front c. 5 days before breakthrough. Our results provide the first field evidence that borehole SP measurements can be used to remotely monitor saline intrusion.

REFERENCES

- Jaafar, M.Z., Vinogradov, J. and Jackson, M.D., 2009. Measurement of streaming potential coupling coefficient in sandstones saturated with high salinity NaCl brine. *Geophysical Research Letters*, 36, L21306, doi:10.1029/2009GL040549.
- Jackson, M.D., Gulamali, M.Y., Leinov, E., Saunders, J.H. and Vinogradov, J., 2012. Spontaneous Potentials in Hydrocarbon Reservoirs During Waterflooding: Application to Water-Front Monitoring. *SPE Journal*, 17, 53-69.
- Jones, H.K. and Robins, N.S., 1999. The Chalk Aquifer of the South Downs. *British Geological Survey*, Keyworth, Nottingham.
- MacDonald, A.M. and Allen, D.J., 2001. Aquifer properties of the Chalk of England. *Quarterly Journal of Engineering Geology and Hydrogeology*, 34, 371-384.
- Post, V.E.A., 2005. Fresh and saline groundwater interaction in coastal aquifers: Is our technology ready for the problems ahead? *Hydrogeology Journal*, 13, 120-123.
- Revil, A., 1999. Ionic Diffusivity Electrical Conductivity Membrane and Thermoelectric Potentials in Colloids and Granular Porous Media: A Unified Model. *Journal of Colloid and Interface Science*, 212, 503-522.
- Contact Information:** Donald John MacAllister, Department of Earth Science and Engineering, Imperial College London, SW7 2AZ, United Kingdom. E-mail: d.macallister11@imperial.ac.uk

Geologic and hydrodynamic effects on shallow groundwater-surface water exchange and chemical fluxes to an estuary

Audrey H. Sawyer^{1,2}, **Holly A. Michael**^{1,3}, Kevin Kroeger⁴, Olesya Lazareva⁵, Kyle Crespo², Christopher Russoniello¹, Fengyan Shi², James Kirby², Clara S. Chan¹, Thomas Stieglitz⁶

¹Department of Geological Sciences, University of Delaware, Newark, DE, USA

²Department of Earth and Environmental Sciences, University of Kentucky, Lexington, KY USA

³Department of Civil and Environmental Engineering, University of Delaware, Newark, DE, USA

⁴USGS Woods Hole Coastal & Marine Science Center, Woods Hole, Massachusetts

⁵Delaware Environmental Institute, University of Delaware, Newark, DE, USA

⁶Europole Mer, Institut Universitaire Européen de la Mer, Plouzané, France

ABSTRACT

Fluxes of nutrients and other chemicals from aquifers to coastal waters can have adverse impacts on ecosystems. While solute concentrations may change along groundwater flowpaths toward the sea, they can also be modulated near the point of discharge in the shallow benthic zone below the sediment-water interface. This benthic reactivity depends on the supply of reactants from both groundwater and surface water and the duration of contact in the mixing zone. These factors are closely tied to physical processes: fluxes from above and below, as well as mixing and residence time in the benthic zone. We characterized heterogeneity in benthic exchange and associated solutes in the Delaware Inland Bays (USA), which are impacted by severe eutrophication. The spatial and temporal variability in benthic fluxes resulting from surface water hydrodynamics and sediment heterogeneity was simulated by linking hydrodynamic circulation models with mathematical solutions for benthic exchange forced by current-bedform interactions, tides, and waves (Figure 1). Total fluxes driven by the three mechanisms were similar, but mechanisms were dominant at different locations and times. Storms were an important factor, increasing wave-driven exchange by orders of magnitude. The spatial distribution of permeability, including near-surface sediments and larger-scale geologic features (paleochannels), also strongly controlled submarine groundwater discharge and benthic exchange rates. High-resolution measurements from a hand resistivity probe, groundwater sampling, and measurements of biogeochemical parameters in transects across paleochannel features and interfluves within the estuary were used to characterize stratigraphic effects on both the nature of the physical exchange processes and solute concentrations and fluxes. By modifying patterns of groundwater flow, discharge, and mixing between fresh groundwater and saline surface water, stratigraphic features influence the geochemistry in the subsurface and near the sediment-water interface, affecting rates and patterns of chemical fluxes to coastal waters. For example, at this site, more than 99% of the groundwater-borne nitrate flux to the Delaware Inland Bays occurs within interfluve portions of coastline, and more than 50% of the ammonium flux occurs at the paleovalley margin (Figure 2).

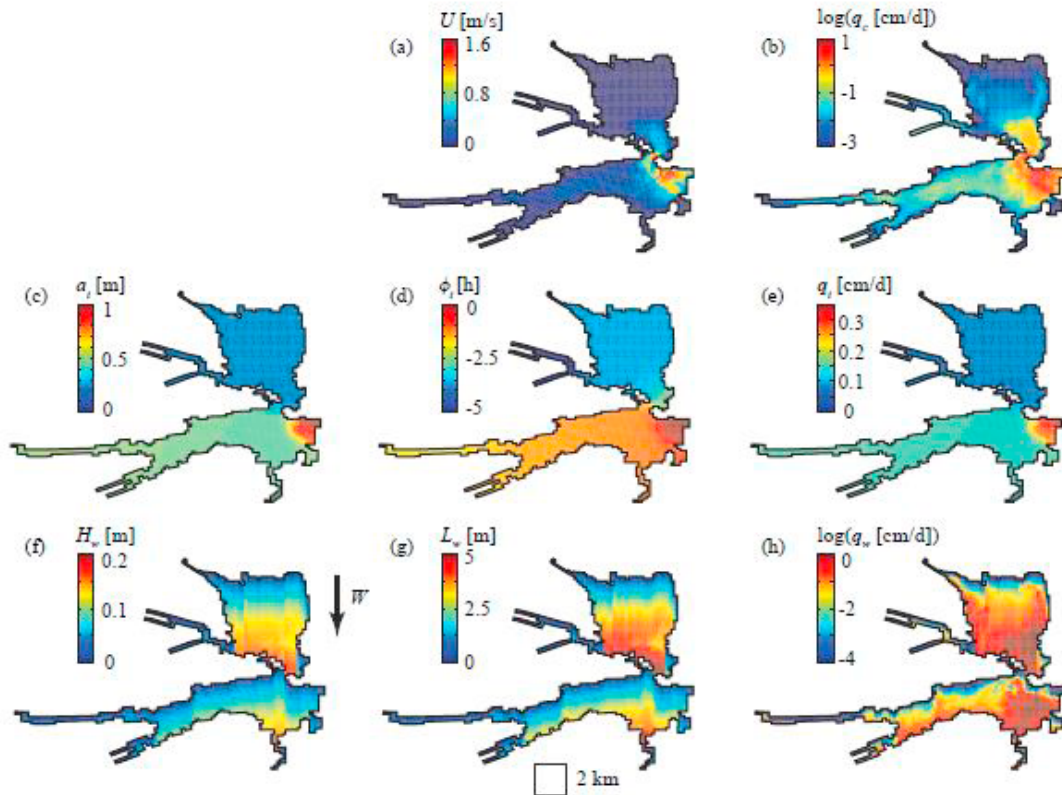


Figure 1. Simulated surface water hydrodynamics and benthic fluxes with constant M2 tide and steady uniform wind of 5 m/s from the North. Averages are taken over one tidal cycle. a. Current speed. b. Benthic flux due to current-bedform interactions, where bedform wavelength is 50 cm and height is 2 cm throughout the estuary. c. Tidal amplitude. d. Phase of tide relative to open ocean (negative values indicate a phase lag). e. Benthic flux due to tidal pumping. f. Significant wave height. g. Wavelength. h. Benthic flux due to wave pumping. From Sawyer et al. (2013)

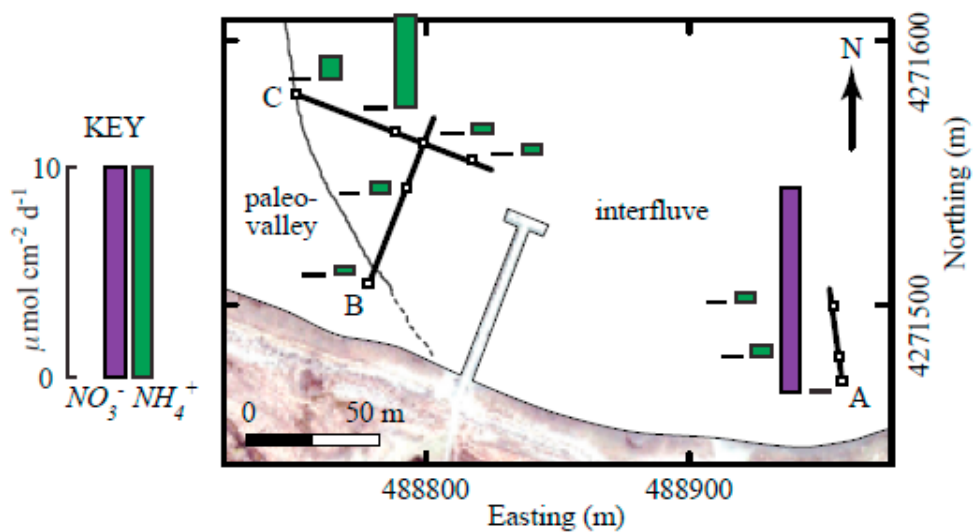


Figure 2. Calculated NO_3^- and NH_4^+ fluxes across the sediment-water interface. Scale bar is shown at left. Fluxes were calculated based on 1-D advection and dispersion calculated from seepage meter measurements and fitted dispersion coefficients for salinity profiles along transects A-A', B-B', and C-C'. From Sawyer et al., in press.

Contact Information: Holly Michael, University of Delaware Department of Geological Sciences,
255 Academy Street, Newark, DE, 19716 USA, Phone: +1 302-831-4197
Email: hmichael@udel.edu

REFERENCES

- Sawyer, A.H., F. Shi, J. Kirby, and H.A. Michael. 2013. Dynamic response of surface water-groundwater exchange to currents, tides, and waves in a shallow estuary, *Journal of Geophysical Research – Oceans* 118, doi: 10.1002/jgrc.20154.
- Sawyer, A.H., O. Lazareva, K.D. Kroeger, K. Crespo, C.S. Chan, T. Stieglitz, H.A. Michael. Stratigraphic controls on fluid and solute fluxes across the sediment-water interface of an estuary, *Limnology & Oceanography*, in press.

Combining numerical modelling and field-based methods to obtain spatially and temporally variable recharge to a semi-arid coastal aquifer: Uley South Basin, South Australia

Carlos M. Ordens^{1,2,3}, Adrian D. Werner^{1,2}, Vincent E. A. Post^{1,2}, John L. Hutson², Matthew J. Knowling^{1,2}

1. National Centre for Groundwater Research and Training, Flinders University, GPO Box 2100, Adelaide, SA 5001, Australia.
2. School of the Environment, Flinders University, GPO Box 2100, Adelaide, SA 5001, Australia.
3. CVRM, Geo-Systems Centre, Instituto Superior Técnico, Lisbon, Portugal.

ABSTRACT

This study explores the recharge processes within the coastal, semi-arid Uley South Basin (USB), South Australia, and attempts to quantify the spatial and temporal variability in recharge fluxes to the system. This aquifer presents significant management challenges, because it supplies around 70% of the Eyre Peninsula's water demand, and yet there have been historical declines in groundwater levels approaching mean sea level in places. USB has been managed entirely based on recharge estimates, and reliable recharge estimates remain central to the sustainable allocation of pumping from the basin. A predictive tool capable of simulating recharge across the basin is required, partly for direct management applications, but also to underpin proposed groundwater models of USB.

Field-based estimates of recharge are often inadequate for assessing groundwater management options at the basin scale, due to the need to account for spatial and temporal variability in recharge in devising water-use strategies. One-dimensional (1D) unsaturated zone models are commonly advocated to provide temporally and spatially fine resolutions of recharge. Although 1D models are associated with large uncertainties in recharge quantification, they are rarely validated with independent field-based estimates. In this study, field-based methods are combined with numerical modelling to estimate basin-scale recharge to USB. The 1D LEACHM code was adopted in an integrated-GIS framework to simulate recharge according to depth to water table, topographical slope, substrate characteristics and vegetation type. Variations to the conceptual model that reflect uncertainties associated with complex recharge processes are considered. Results show that selected combinations of unsaturated zone lithologies and representations of preferential flow produce spatially and temporally averaged recharge rates that fall within the range estimated using the chloride mass balance method, and recharge timing consistent with the water-table fluctuation method. Because very little unsaturated zone data are available to parameterise and validate

the 1D model, the field-based methods proved to be vital to validate the recharge model's predictions.

The effect of saline gravel pit lakes (Ravenna, Italy) on ground water chemistry.

Pauline N. Mollema^{1,2}, Antonellini M.¹, Stuyfzand P.J.^{2,3}

1 University of Bologna, Laboratory "Renzo Sartori" Ravenna Campus, Via San Alberto 163, 48123 Ravenna, Italy.

2 VU University Amsterdam, Faculty of Earth and Life Sciences, De Boelelaan 1085, 1081 HV Amsterdam, The Netherlands

3 KWR Watercycle Research Institute, Groningehaven 7, PO Box 1072, 3430 BB Nieuwegein, The Netherlands

ABSTRACT

The hydrochemistry of gravel pit lakes excavated into Holocene beach gravel deposits near the Adriatic Coast of Emilia Romagna (Italy) was studied to determine the influence of these lakes on water and chemical budgets of the aquifer.

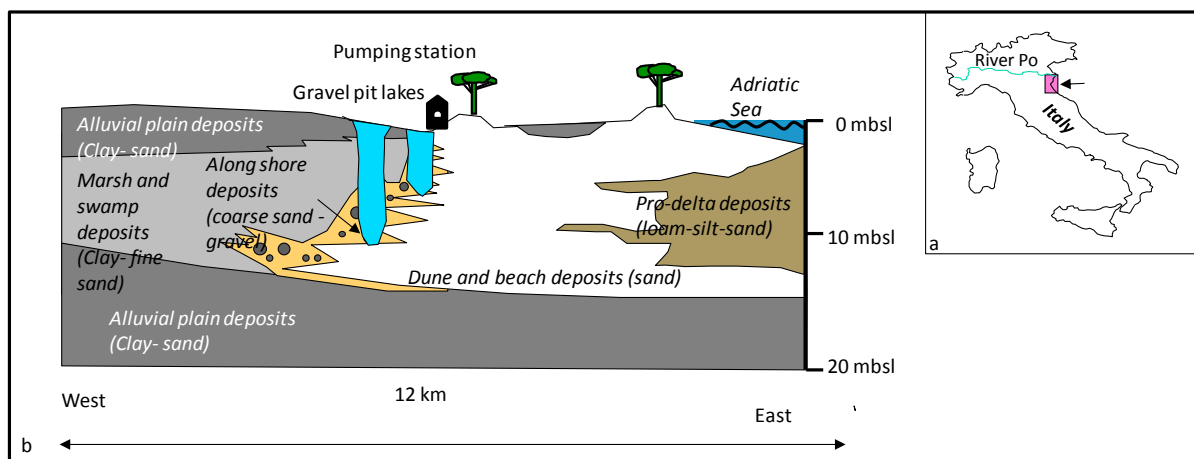


Fig 1. a: Location of study area in Italy and b: Geologic profile perpendicular to the coast with location of gravel pit lakes.

INTRODUCTION

Italy is the top gravel and sand producer after the United States with $14 \cdot 10^6$ metric tons per year. Where gravel pits are dug below the water table in coastal zones, they may fill up with brackish/saline groundwater and become artificial lakes. Gravel pit lakes have a positive effect on water quality where they reduce the concentration of phosphates and nitrates, but they may also have a negative effect on water quality by allowing the mobilization of soil-bound elements like arsenic (this study; Muelleger et al. 2013). A large part of the study area, the coastal region near Ravenna on the Adriatic Sea (Italy), is below sea level and hydraulic gradients are typically directed inland. The unconfined aquifer is mostly brackish/saline, in part due to trapped Holocene transgression water (Mollema et al. 2013) and this affects soil quality and vegetation species diversity in the wetlands, pine forests and natural areas (Antonellini and Mollema, 2010). Small freshwater lenses form only near irrigation ditches (Vandenbohede et al. 2014; this volume). Surface water net evaporation rates are as high as 894 mm/year in the Mediterranean climate (Mollema et al. 2013). The water that leaves the lakes by evaporation and also by the intense land drainage is replaced by in-flowing ground water, making the lakes flow-through reservoirs. After excavation is

terminated, the gravel pit lakes near Ravenna are used for water sports including fishing, canoeing and swimming. At first sight the water may seem suitable for these activities. This study, however, shows that the water is not as clean as it seems.

METHODS

In total 40 ground and surface water samples were analyzed. All water samples were filtered in the field through a 0.45 μm filter and analyzed for major and trace elements by VU University Amsterdam and ACME Canada laboratories using conventional analytical methods (ICP-OES on acidified subsamples, IC for anions). Multi-Parameter Ground water Monitoring Dataloggers (Acquatroll™ and Divers) were used to log temperature and electrical conductivity changes with depth in the gravel pit lakes.

RESULTS

The results of the hydrochemical analysis are presented along a profile perpendicular to the coast (Fig. 1). The pH of the gravel pit lakes is on average 8.5 and this is higher than the pH of ground water near the gravel pit lakes (7.4), seawater (8.3) or river water (8.4). In general, the concentration of most cations, anions and chemical (trace) elements increases towards the coast (Fig. 2a). Water in gravel pit lake EMS is depleted in comparison with the average groundwater composition, regarding Al, Ca, Fe, Mn, Cr, Co, Cu, Ni and Zn and enriched in As, Ba, Cl, Mg, Mo, Sb, and pH (Fig. 2a, not all shown). The shallow groundwater below the paleo and coastal dunes is depleted in many elements with respect to the deeper groundwater. NO_3^- occurs in small amounts in the Apennine Rivers and in well EMS1, and only in P5S there is a high concentration of NO_3^- (56 mg/L).

DISCUSSION AND CONCLUSIONS

Creating gravel pit lakes, where there used to be a soil layer on top of an unconfined aquifer, brings about many changes, especially if there are many gravel pit lakes close to one another. For example, the lakes create an environment where many more algae, plant and animal species may thrive than in groundwater. This sets in motion a whole sequence of biochemical processes. These plus the typical chemical processes of coastal aquifers (cation exchange, calcite dissolution and redox reactions, (e.g. Stuyfzand 1989; Stuyfzand et al. 1999) and lake processes such as precipitation of calcite, metal (hydro)oxides and other minerals determine the hydrochemistry of the gravel pit lakes and aquifer downgradient (Fig. 2). Low-pH ground water rich in dissolved metals released by redox reactions flows into the gravel pit lakes where pH and oxygen content are higher. This chemical environment causes the precipitation of metal oxides and calcite to the bottom of the lake. Some elements such as As remain partly in solution. The lake water lost to net evaporation and to drainage is continuously replaced by new brackish saline groundwater. The salinity of the lake, therefore, may increase over time. The presence of the lakes implies the absence of soil and the unsaturated zone over a large surface (7% of the Quinto Bacino Watershed). The precipitation that falls on top of the lakes is mixed immediately with the brackish water of the lakes and thereby does not contribute to the formation of fresh groundwater lenses. The particular salinity range of the coastal gravel pit lakes and the lack of stratification make them less sensitive to eutrophication than freshwater gravel pit lakes (Bleich et al. 2011). As a consequence, there is less neoforming organic material available to fix (trace) metals to the lake bottom sediments. This may in part explain the relatively high concentration of for example As.

For gravel pit lakes in general and for the ones studied here in particular, the water quality needs to be monitored carefully for dissolved metals and trace elements to be able to use them safely after excavation.

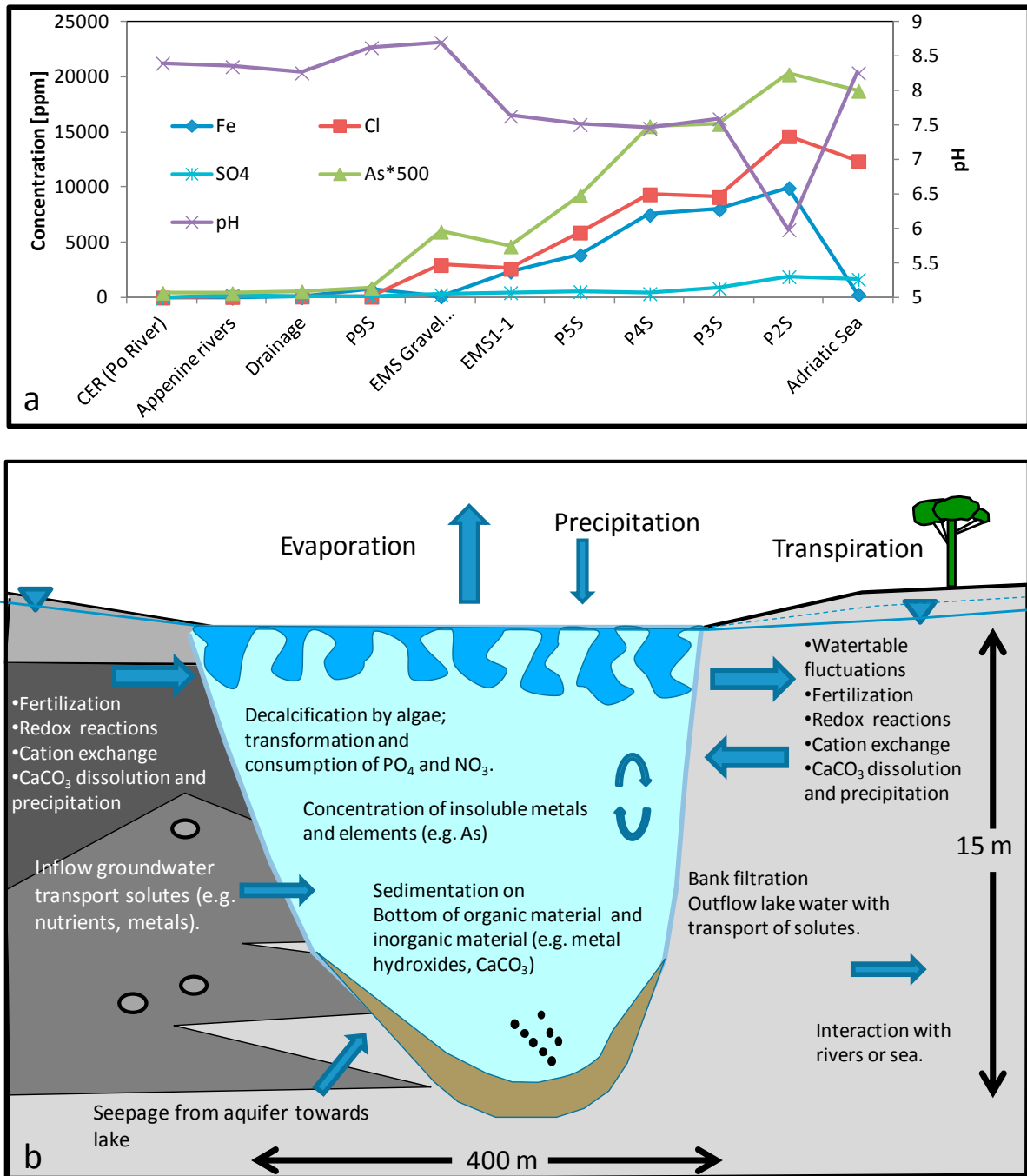


Fig 2. a. Concentrations averaged for observation wells and a gravel pit lake in a profile perpendicular to the Adriatic coast. P2S, P3S, P4S, P5S, EMS1 and P9S are the names of groundwater monitoring wells, CER is the name of the channel that brings water from the Po River to Ravenna. Surface water composition is shown for comparison. b. Hydrochemical processes occurring in and around coastal gravel pit lakes.

Acknowledgements: Thanks to the students of IGRG at the University of Bologna for help in the field.

REFERENCES

Antonellini M. and Mollema P. 2010. Impact of groundwater salinity on vegetation species richness in the coastal Pine forests and wetlands of Ravenna, Italy. *Ecological Engineering* 36: 1201-1211.

Bleich S., Powilleit M., Seifert T., Graf G., 2011. β -diversity as a measure of species turnover along the salinity gradient in the Baltic Sea, and its consistency with the Venice System Marine Ecology Progress Series 436: 101–118.

Mollema P.N., Antonellini M., Dinelli E., Gabbianelli G., Greggio N, Stuyfzand P.J. 2013. Hydrochemical and physical processes influencing salinization and freshening in Mediterranean low-lying coastal environments. *Applied Geochemistry* 34:207-221.

Muellegger C., Weilhartner A., Battin T.J., Hofmann T. 2013. Positive and negative impacts of five Austrian gravel pit lakes on groundwater quality. *Science of the Total Environment* 443: 14–23.

Stuyfzand P. J. 1999. Patterns in groundwater chemistry resulting from groundwater flow. *Hydrogeology Journal* 7:15–27 .

Stuyfzand, P.J. 1989. Factors controlling trace element levels in ground water in The Netherlands. Proc. Sixth Int. Symp. Water Rock Interaction, Malvern (UK), August 3-8 1989, D.L. Miles (ed), Balkema Rotterdam, 655-659.

Vandenbohede A, Mollema PN, Antonellini M, Greggio N. 2014. Seasonal dynamics of a shallow freshwater lens due to irrigation in the coastal plain of Ravenna, Italy. On-line by *Hydrogeology Journal* .

Contact Information: Pauline N. Mollema. University of Bologna (Italy) / VU University Amsterdam (The Netherlands). Email: pmollema@gmail.com

Biogeochemical Consequences of Seawater Intrusion into Coastal Aquifers

Willard S. Moore, Department of Earth and Ocean Sciences, University of South Carolina, Columbia, South Carolina, USA

EXTENDED ABSTRACT

Coastal populations are expanding rapidly, while potable coastal water supplies are decreasing due to sea water intrusion into coastal aquifers. This is a global problem that affects almost all coastlines of the world. Although over-pumping of coastal aquifers is the primary cause of sea water intrusion, several other factors must also be considered. Sea level rise, drainage of coastal wetlands, replacement of permeable surfaces with hard surfaces (roads, parking lots, buildings, etc.), dam construction, breaches of confining layers by coastal dredging and pilings all contribute to sea water intrusion.

This talk is not about potable water supplies. Instead I will focus on some of the biogeochemical consequences of sea water intrusion into coastal aquifers. I will discuss how replacing fresh water with sea water in coastal aquifers changes the biogeochemical reactions that occur within these systems. Finally I will show that these aquifers, which we call subterranean estuaries, exchange reaction products with the coastal ocean. The flow into the ocean is called submarine groundwater discharge (SGD).

During the past 15 years there has been considerable new research on SGD (e.g. Moore 2010). Investigators in this field recognize that SGD is not simply fresh groundwater flowing into the ocean, but represents mixing of salt water and freshwater in coastal aquifers, accompanied by biogeochemical reactions. To emphasize the processes of salt water-freshwater mixing and reactions with aquifer solids, these coastal aquifers are called subterranean estuaries (Moore 1999). Fluids in subterranean estuaries are enriched in the products of these biogeochemical reactions, including nutrients, carbon, and metals (Moore 2010). Thus, SGD transports these products to surface estuaries and the coastal ocean. There are over 100 studies of the role of SGD in supplying nutrients, carbon, and metals to coastal waters; most conclude that SGD is a more important source of these materials than local rivers (Moore 2010).

As salt water intrudes into coastal aquifers, the subterranean estuary expands inland. For example in the early 1900's there was a 100-500 m zone of brackish water at the base of the Biscayne aquifer in southern Florida (Barlow and Reichard 2010). By 1946 canals had been installed to drain the coastal wetlands. The zone of brackish water in the aquifer moved inland 2-16 km, primarily beneath the canals, increasing the size of the subterranean estuary along this 25 km coastline from ~20 to over 120 km² (Barlow and Reichard 2010). Subsequent canal construction through 1995 did little to change the

extent of seawater intrusion because the early canals removed most of the standing water. This example has been repeated along coastlines worldwide.

Replacement of permeable sediments with hard surfaces has a similar effect to wetland drainage. To control the water that accumulates on such surfaces, storm drains are required to channel the water. As surface water is directed to storm drains and to the ocean, surface water infiltration is reduced and groundwater levels decrease, leading to sea water intrusion.

Industrial use of groundwater places a major demand on coastal aquifers. For example prior to October 1962, the Upper Floridan aquifer below the city of Brunswick, GA, had a head of +3 to +5 m. In 1963 a paper mill began pumping about $1.4 \times 10^5 \text{ m}^3$ freshwater day^{-1} from the aquifer. Within 14 months the head in the aquifer had dropped to -3 m (Wait and Gregg 1973). Within 30 years a 5 km^2 subterranean estuary developed beneath the city, rendering the city wells non-potable due to 1-2.5 g/L chloride concentrations (Joiner 1991).

Depletion of groundwater has accelerated during the past 50 years. For example prior to 1950 less than $1 \text{ km}^3 \text{ yr}^{-1}$ of groundwater was pumped from the U.S. Gulf and Atlantic coastal plains; by 2008 this had increased to almost $9 \text{ km}^3 \text{ yr}^{-1}$ (Konikow 2011).

Salt water intrusion along the coastline of the Laizhou Gulf in Shandong, China, covered a total area of 16 km^2 in 1979; by 1989, the salt water intrusion area became a continuous zone covering an area of 238 km^2 (Xue et al. 1993). By 2009 the extent of salt water in the aquifer reached 4200 km^2 (Cao 2012). During the past century these examples have been repeated with similar consequences along most populated coastlines of the world. There is no doubt that the subterranean estuary is rapidly expanding inland as freshwater in the aquifer is replaced by salt water.

The subterranean estuary is a distinct coastal environment. It contains a mixture of sea water and fresh water out of contact with the atmosphere, but in intimate contact with aquifer solids. These solids often contain organic carbon, both ancient and recent. During sea water intrusion, solids that have not been exposed to sea water for thousands of years are inundated with salt water. The immediate consequence is the desorption of surface-bound ions into the fluid phase. Such things as phosphate, ammonia, barium, radium, cesium, and others are displaced from the solids by the major ions in seawater. A longer term consequence is the oxidation of organic carbon. The most powerful oxidizing agent in most natural systems is oxygen. However its oxidizing capacity is limited by its solubility in water, a maximum about 0.28 mmol per liter in most near-surface waters. Once oxygen is depleted, a number of chemical species can serve as electron acceptors to facilitate carbon oxidation. Among these, sulfate ion is the most prominent as its concentration in sea water is about 29 mmol per liter. As SO_4^{2-} is converted to H_2S , S gains 8 electrons; as O_2 is converted to CO_2 , it only gains 4 electrons. Thus a liter of sea water has potentially 50 times more oxidizing capacity than a liter of fresh water.

The reaction products of sulfate oxidation of organic matter include both inorganic and organic forms of dissolved N, P, and C as well as sulfide. The ensuing reducing conditions in the aquifer lead to reduction of iron and manganese oxides. This results in increased concentrations of Fe^{2+} and Mn^{2+} as well as other metals, plus the release of ions that were attached to the oxides. As this chemically-altered fluid exchanges into coastal waters, it carries high dissolved concentrations of nutrients, carbon, and metals.

Continued over utilization of fresh water in coastal aquifers and other anthropogenic changes will lead to greater inland expansions of subterranean estuaries. Although sea water intrusion may reduce fluxes of fresh groundwater through SGD, the biogeochemical reactions of the fluids and aquifer solids may increase concentrations of the desorption and oxidation reaction products. Thus, the expansion of the subterranean estuary may lead to greater total SGD fluxes of nutrients, carbon, and metals because the biogeochemical reactions that affect their concentrations may operate over larger spatial scales and affect aquifers that have not been in contact with seawater for thousands of years.

References

- Barlow, P.M. and E.G. Reichard. 2010. Saltwater intrusion in coastal regions of North America. *Hydrogeology Journal* 18: 247–260.
- Cao, Jianrong. 2012. Status, characteristics and risk assessment for seawater intrusion in typical coastal region in China. *International Symposium on Climate Change and Human Activities: Coastal Consequences and Responses*, East China Normal University, Shanghai.
- Joiner, C.N. 1991. Chloride concentrations in the upper water-bearing zone of the Upper Floridan aquifer in the Brunswick area, Georgia, October-November 1990. U.S. Geological Survey Open-File Report 91-174.
- Konikow, L.F. 2011. Contribution of global groundwater depletion since 1900 to sea-level rise. *Geophysical Research Letters* 38: L17401.
- Moore, W.S. 1999. The subterranean estuary: a reaction zone of ground water and sea water. *Marine Chemistry* 65: 111-126.
- Moore, W.S. 2010. The effect of submarine groundwater discharge on the ocean. *Annual Reviews of Marine Science* 2: 345-374.
- Wait, R.L. and D.O. Gregg. 1973. Hydrology and chloride contamination of the principal artesian aquifer in Glynn County, GA. *GA Geologic Survey Hydrologic Report 1* Atlanta, GA.
- Xue, Yuqun, et al. 1993. A study on sea-water intrusion in the coastal area of Laizhou Bay, China: Distribution of sea-water intrusion and its hydrochemical characteristics. *Ground Water* 31: 532-537.

Contact information: Willard S. Moore. Dept. Earth & Ocean Sciences, Univ. South Carolina, Columbia, SC, 29208 USA, Phone 803-777-2262, Fax 803-777-6610, Email moore@geol.sc.edu.

Seawater intrusion vulnerability indicators for freshwater lenses in strip islands

Leanne K. Morgan^{1,2}, Adrian D. Werner^{1,2}

¹National Centre for Groundwater Research and Training, Flinders University, GPO Box 2100, Adelaide, SA 5001, Australia.

²School of the Environment, Flinders University, GPO Box 2100, Adelaide, SA 5001, Australia.

ABSTRACT

Freshwater lenses on small islands have been described as some of the most vulnerable aquifer systems in the world. However, there is little guidance on methods for rapidly assessing the vulnerability of freshwater lenses to the potential effects of climate change. We address this gap using a simple steady-state analytic modelling approach to develop seawater intrusion (SWI) vulnerability indicator equations. The vulnerability indicator equations quantify the propensity for SWI to occur in strip islands due to recharge change and sea-level rise (SLR) (incorporating the effect of land surface inundation (LSI)). Freshwater lenses are conceptualised as either flux-controlled or head controlled. A number of inferences about SWI vulnerability in freshwater lenses can be made from the analysis: (1) SWI vulnerability indicators for SLR (under flux-controlled conditions) are proportional to lens thickness (or volume) and the rate of LSI and inversely proportional to island width; (2) SWI vulnerability indicators for recharge change (under flux-controlled conditions) are proportional to lens thickness (or volume) and inversely proportional to recharge; (3) SLR has greater impact under head-controlled conditions rather than flux-controlled conditions, whereas the opposite is the case for LSI and recharge change. Example applications to several case studies illustrate use of the method for rapidly ranking lenses according to vulnerability, thereby allowing for prioritisation of areas where further and more detailed SWI investigations may be required.

Contact Information:

Leanne K. Morgan: leanne.morgan@flinders.edu.au

Adrian D. Werner: adrian.werner@flinders.edu.au

Seawater intrusion overshoot – possible occurrence and cause

Leanne K. Morgan^{1,2}, Mark Bakker³, Adrian D. Werner^{1,2}

¹National Centre for Groundwater Research and Training, Flinders University, Adelaide, Australia

²School of the Environment, Flinders University, Adelaide, Australia

³Water Resources Section, Faculty of Civil Engineering and GeoSciences, Delft University of Technology, Delft, The Netherlands

ABSTRACT

A number of numerical modelling studies of transient sea-level rise and seawater intrusion have reported an overshoot phenomenon, whereby the freshwater-saltwater interface temporarily extends further inland than the eventual steady-state position (Watson et al., 2010; Chang et al., 2010). Recently, Morgan et al. (2013) used physical sand tank modelling to confirm that seawater intrusion overshoot is a physical process. As previous studies considered only instantaneous sea-level rise scenarios, in this study we assess whether seawater intrusion overshoot could occur under gradual sea-level rise scenarios commensurate with those predicted by the Intergovernmental Panel for Climate Change (IPCC, 2007). In addition, the cause of seawater intrusion overshoot is explored. Modelling is carried out using the MODFLOW Seawater Intrusion (SWI2) Package (Bakker et al., 2013) and SEAWAT (Guo and Langevin, 2002).

Keywords: Seawater intrusion, sea-level rise, sharp interface, density-dependent modelling

REFERENCES

Bakker M, Schaars F, Hughes JD, Langevin CD, Dausman AM, 2013, Documentation of the seawater intrusion (SWI2) package for MODFLOW: U.S. Geological Survey Techniques and Methods, book 6, chap. A46, 47 p., <http://pubs.usgs.gov/tm/6a46/>.

Chang SW, Clement TP, Simpson MJ, Lee KK, 2011, Does sea-level rise have an impact on saltwater intrusion?, *Advances in Water Resources*, 34(10), 1283-1291, doi:10.1016/j.advwatres.2011.06.006.

Guo W, Langevin C, 2002, User's guide to SEAWAT: A computer program for the simulation of three-dimensional variable-density ground-water flow: USGS Techniques of Water Resources Investigations, Book 6, Chapter A7.

Intergovernmental Panel on Climate Change (IPCC), 2007, *Climate Change 2007: Working group I: The physical science basis. Projections of future changes in climate*, http://ipcc.ch/publications_and_data/ar4/wg1/en/spmssp-projections-of.html. Accessed 29 April 2011.

Morgan LK, Stoeckl L, Werner AD, Post VEA, 2013, Assessment of seawater intrusion overshoot using physical and numerical modelling, *Water Resources Research* 49, 6522- 6526. doi:10.1002/wrcr.20526.

Watson TA, Werner AD, Simmons CT, 2010, Transience of seawater intrusion in response to sea-level rise, *Water Resources Research*, 46, W12533, doi:10.1029/2010WR009564.

Contact Information: Leanne K. Morgan, National Centre for Groundwater Research and Training, Flinders University, GPO Box 2100, Adelaide, SA 5001, Australia
Email: leanne.morgan@flinders.edu.au

Coastal Water Resources Vulnerable to Climatic Change by Sea Level Rise (Gaza Strip Coastal Aquifer Case Study)

Ashraf M. Mushtaha^{1,2} & Kristine Walraevens²

¹Director of Environmental and MIS Department, CMWU, Gaza Strip - Palestine

²Laboratory for Applied Geology and Hydrogeology, Ghent University, Krijgslaan 281-S8, 9000 Gent, Belgium

ABSTRACT

Gaza Strip will be exposed to the global climate change effects the same as the other countries. According to the survey and primary findings of UNDP-PAPP Report 2009, agriculture and water resources are the most vulnerable to climate change and are expected to be exposed to direct effects of temperature, precipitation change and sea level rise, but still the potential impact of global climate change is one of the least addressed factors in water resources planning in developing countries. Moreover, the potential impacts of climate change have not been quantified at local level yet. This paper aims to evaluate the groundwater resource under sea level rise scenarios for Gaza Strip. To evaluate the potential impact of sea level rise as an impact of climate change on Gaza water resources, a 3D groundwater model is used after calibrating the developed model versus the existing situation. The results show that all the groundwater along the coastal line will be directly affected and around 66 Km² of the aquifer will be invaded by sea water in a very short time.

KEYWORDS

Gaza Strip, Groundwater Modeling, Climate Change, Sea Level Rise, MODFLOW

BACKGROUND

Gaza Strip is a coastal area along the Eastern Mediterranean Sea. The total area of the Gaza Strip is about 365 km². The Gaza Strip forms a transition zone between the semi-humid coastal zone in the North, the semi-arid zone in the East, and the Sinai desert in Egypt in the South. The population of the Gaza Strip reaches more than 1.7 Million inhabitants (PCBS, 2012). The population is expected to be around 2 Million inhabitants in the year 2015 and about 2.9 Million inhabitants by the year 2025 (CMWU, 2010).

Groundwater is the main water resource in the Gaza Strip. Gaza aquifer is a saline coastal aquifer with freshwater lenses floating above saline water, both near the coast and inland. The thickness of the aquifer ranges from few meters in the South East to about 180m in the North West of the Gaza Strip. The general groundwater flow pattern is from inland areas to the sea. Gaza aquifer is classified as unconfined aquifer and therefore is susceptible to all sources of pollution. The aquifer comprises tertiary and quaternary formations. The bottom of the aquifer consists of shallow marine clays, shales and marls called Saqiya Formation. The aquifer itself consists of consolidated quartz sands with calcareous material called Kurkar Formation. The aquifer has high permeability and porosity values.

Amnesty International (annual report, 2009) states that only 10% of the Gaza Coast Aquifer has fresh water suitable for drinking. Water situation in the Gaza Strip has been deteriorating in both quantitative and qualitative aspects. Increasing temperatures in the area will lead to an increase of water demand for drinking, other human usage and crops, which shall not only threaten the food security but also the economic stability and all life aspects.

According to the reports of the National Communication Arab Countries, a rise of one degree in temperature will increase the value of evapotranspiration by 2.3% in Saudi Arabia (UNFCC, 2011). The expected increase in water requirements for agriculture will be about 6% by 2020 in Lebanon and 7 to 12% in the Kingdom of Morocco.

INTRODUCTION

The coastal aquifer in the Gaza Strip is the only natural source of water supply for all activities (domestic, irrigation and industrial supply). The groundwater is being pumped through more than 5,000 wells all over the Gaza Strip. The latest published figure for groundwater abstraction was around 169 Million Cubic Meter (MCM) for the year 2011 (CMWU, 2012). More than 50% of the abstracted groundwater was for domestic water supply (89 MCM). Groundwater recharge from different components (i.e. rainfall, agricultural return flow, water and waste water network losses, and waste water collection lagoons) is around an average of 100 – 110 MCM yearly (Mushtaha, 2010). Yearly groundwater balance difference is around 50 to 60 MCM, which is being pumped out from the groundwater, causing seawater intrusion and/or groundwater level decline in areas that are far away from the coast. Both have a common result which is groundwater quality deterioration. Existing stresses to the Gaza Coastal Aquifer from both heavy abstraction and low recharge quantities have led to groundwater quantity and quality deterioration. Another major stress is threatening the aquifer as a result of global climatic change effects as sea water level rise.

The most significant environmental effects of climatic change for the people of occupied Palestinian territories (oPT), over the course of this century, are projected to be a decrease in precipitation and significant warming. Annual precipitation rates are deemed likely to fall in the Eastern Mediterranean decreasing 10% by 2020 and 20% by 2050, with an increased risk of summer droughts (UNDP-PAPP, 2009). The impact of climatic change on the water resource will strongly affect livelihood in the area in the future. This will lead to adaptation focusing at the regional and local level on water insecurity and food insecurity. The climatic change impacts in Gaza are further compounded by the Israeli occupation and siege imposed on Gaza Strip since long years. A higher variability in precipitation translates into reduced yields for rainfed agriculture, and could also mean greater frequency of flash floods. Reduced amounts of precipitation will mean greater strain on the deteriorating quality of the groundwater resource. Increased temperatures will also lead to abstracting more water from the only source (groundwater), and also temperature increase will lead to desertification, particularly in the South. Finally, sea level rise will contaminate the coastal soil and increase the saline intrusion already experienced throughout Gaza Strip. The Palestinian National Authority (PNA) recommends to adopt a Climate Change Adaptation Strategy for the oPT as the most effective means by which the PNA can enhance the capacity of the Palestinians to cope with current and future climate hazards. This is the first study in the Gaza Strip showing the sea level rise effects to the only groundwater resource.

OBJECTIVES

This paper will discuss the sea level rise scenarios on the Gaza Coastal Aquifer, by analyzing different cases as: sea level rise by 25cm and by 100cm. The study uses full 3D groundwater model MODFLOW v.4.2 to predict the effects of sea level rise to the coastal aquifer in the Gaza Strip.

GROUNDWATER MODEL DEVELOPMENT

Model Description

The model active area is 1,162.5 km² (figure1). The model boundary extends beyond the Gaza Strip political boundaries towards the North where a no flow boundary is adopted (parallel groundwater elevation contour lines), towards the East where the coastal aquifer pinches out (no flow boundary), towards the South in Egypt, where data do not exist and a no flow boundary is assumed, and finally towards the West where the Mediterranean Sea is located (head fixed to zero).

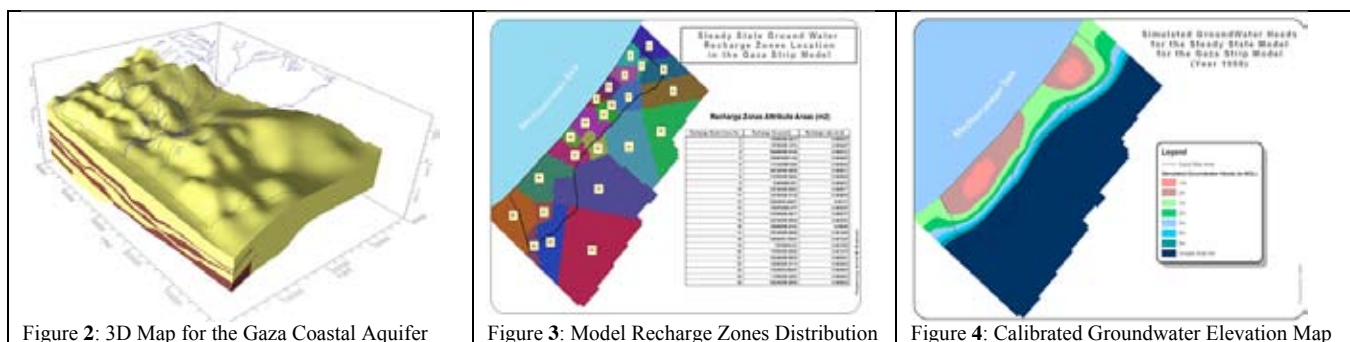


Figure1: Regional Groundwater Boundaries Map

Visual Modflow v4.2 is a 3D model with finite difference method used to generate the model grid which divided into 500m X 500m cells. The vertical discretization is used to present the nature of the aquifer

where clay layers are separating the unconfined aquifer from the semi-confined aquifer along the coastal zone and extend around 2Km inland towards the East as shown in the 3D map in figure2. Hence eleven layers have been used to present this complicated discretization of the Gaza aquifer.

The model was run for steady state simulation for year 1998, where figure 3 and 4 represent the calibrated recharge values and calibrated groundwater elevation respectively. Afterwards transient model simulation and calibration has been performed from year 2000 to year 2004, in which a verification simulation has been carried out from year 2005 till year 2010.



SEA LEVEL RISE SCENARIOS

The model will be capable to simulate the groundwater flow under different sea level rise scenarios (25cm, and 100cm). The main objectives of the numerical model will be to show the impact of sea level rise on the Gaza Coastal Aquifer for 10 years after sea level rise event.

25cm Sea Level Rise

The model was run on a monthly basis for 10 years. The results show that the seawater will reach about 2Km in the Gaza Coastal Aquifer, especially in the South within the first 5 years of simulation, while at 10 years of simulation the seawater will reach more than 2.5Km in the Gaza Coastal Aquifer in the South. Table 1 shows the seawater invasion of the different areas after 5 and 10 years of simulations.

Table 1: Sea Water Invasion Distance from the shoreline (25cm sea level rise effects)

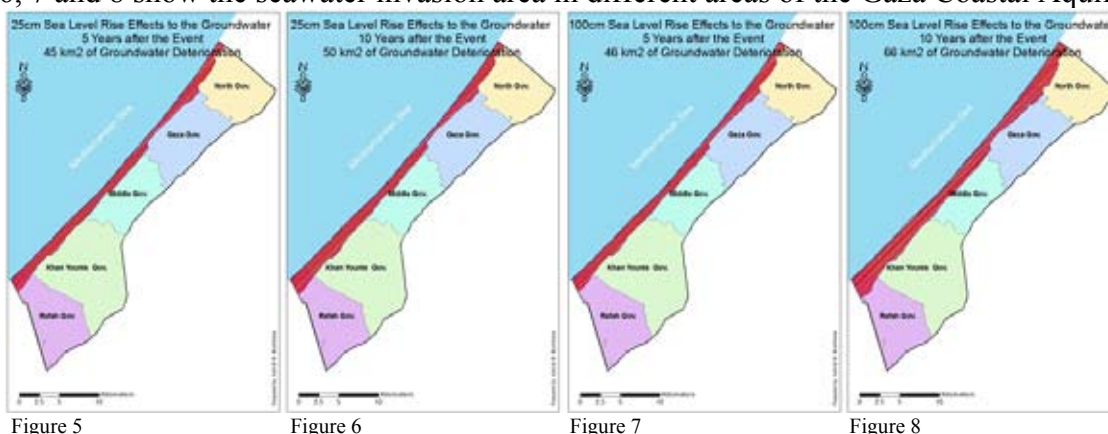
Governorate	Simulation Time	
	5 years	10 years
North	1.0 Km	1.3 Km
Gaza	1.5 Km	1.6 Km
Middle	1.0 Km	1.3 Km
Khan Younis	1.5 Km	2.0 Km
Rafah	2.0 Km	2.6 Km
Total Area of seawater intrusion	44 Km ²	50 Km ²

100cm Sea Level Rise

The model was run on a monthly basis for 10 years. The results show that the seawater will reach about 2Km in the Gaza Coastal Aquifer, especially in the South within the first 5 years of simulation, while at 10 years of simulation the seawater will reach more than 2.8Km in the Gaza Coastal Aquifer in the South. Table 2 shows the seawater invasion of the different areas after 5 and 10 years of simulation; where figure 5, 6, 7 and 8 show the seawater invasion area in different areas of the Gaza Coastal Aquifer.

Table 2: Sea Water Invasion Distance from the shoreline (100cm sea level rise effects)

Governorate	Simulation Time	
	5 years	10 years
North	1.2 Km	2.0 Km
Gaza	1.5 Km	2.2 Km
Middle	1.2 Km	1.6 Km
Khan Younis	1.5 Km	2.2 Km
Rafah	2.0 Km	2.8 Km
Total Area of seawater intrusion	45 Km ²	66 Km ²



DISCUSSION AND ANALYSIS OF THE RESULTS

The model results show that the most affected areas are those where domestic wells are concentrated (within 2 km from the shoreline). Those wells are located in sand dune areas in the North Gaza and Western Rafah Governorates. Added to that an acceleration of seawater intrusion occurs in the North and South of the Gaza Strip where the water level is below mean sea level. The model shows that the two applied scenarios have the same trend but one is faster than the other.

Each five years of simulation, a map has been generated to show the extent of sea water intruding in the aquifer underneath Gaza Strip, and based on that an area calculation has been done to show the destroyed aquifer from the sea level rise action. Most destruction occurs at the early stage of the event, while afterwards it will be mainly depending on the aquifer abstraction regime. The area calculated shows that around 45km² of the Gaza aquifer will be intruded by seawater, whereby the groundwater will be no more suitable for drinking.

CONCLUSIONS:

1. There is a major impact of a sea level rise to the Gaza Coastal Aquifer.
2. The groundwater resource in the Gaza Strip will be polluted by saltwater.
3. The seawater will replace 45Km² of freshwater in the Gaza Coastal Aquifer after 5 years in both scenarios'.
4. The seawater will replace 50Km² and 66Km² of the Gaza Coastal Aquifer after 10 years with 25cm and 100cm of sea level rise respectively.
5. The 1.7 million inhabitants living in the Gaza Strip will have insufficient and unacceptable water resources.

RECOMMENDATIONS:

1. The related Palestinian institutions should look for new water resources (i.e. seawater desalination) to secure suitable drinking water to the Gaza Strip people.
2. Minimizing the abstraction rate especially in the West of North and Rafah Governorates may decrease the damage of seawater intrusion in case of sea level rise.
3. Create a positive pressure zones inland will minimize the sea water intrusion movement towards the negative pressure zones (inland) by creating a recharge areas in the Western area and along the Mediterranean coast.

REFERENCES

- Mushtaha. 2010. Water Resource Status, CMWU
UNDP-PAPP. 2009. Analysis of the climatic change in the oPt
Amnesty International. 2009. Annual Report
Palestinian Central Bureau of Statistics (PCBS). 2012. Census Final Results Population Report
UNFCCC. 2011. Second National Communication
IPCC. 2007. Intergovernmental Panel on Climate Change (2007) Climate Change and Water, Technical Paper IV, Geneva

Contact Information: Ashraf M. Mushtaha, Coastal Municipalities Water Utility, Gaza Strip, State of Palestine and PhD Student, Geology and Hydrogeology Department, Ghent University, Belgium, Phone: 972-599-487742, Fax: 972-8-2822896, Email: amushtaha@cmwu.ps or ashraf3@hotmail.com

Saltwater intrusion in the Crau coastal aquifer (South of France): validation of variable density modeling using geophysical and geochemical data

Bach Thao Nguyen, Olivier Banton, Adriano Mayer, Konstantinos Chalikakis and Michel Daniel
Université d'Avignon et des Pays de Vaucluse – UMR 1114 EMMAH, 84000 Avignon, France

ABSTRACT

The research focus on the effect of variable groundwater density on the modeling of seawater intrusion in coastal aquifers. In this setting, the concomitant presence of freshwater and saltwater alters flow patterns typically represented by the Darcy equation. Models of ground water subjects to density changes suffer of several difficulties: 1) The change on the aquifer permeability due to the one of salinity is difficult to take into account during simulation and generates instability. 2) Influences of heterogeneity in this context are more important than in other setting having constant density. 3) Data set must be detailed in order to get a reliable model results. 4) In general, the results of modeling are less robust.

To address and discuss these problems, we set up a variable density groundwater model using FEFLOW. The studied area is the Crau aquifer, in the Mediterranean region of Southern France. It has been chosen because of the long term records of hydrogeological and climatic data (salinity, piezometric levels, water geochemistry, rainfall, irrigation seepages and exploitation).

The first results indicate that the interface between freshwater and saltwater is very influenced by the heterogeneities in aquifer properties and the effects of irrigation and groundwater withdrawal. To better constraint the data set for the variable-density flow model, geophysical acquisitions have been carried out using Electrical Resistivity Tomography (ERT) and Electromagnetic surveys (EM). This has provided subsurface information on vertical salinity and lithology distribution. Furthermore, Radon-222 activity in groundwater has been used to estimate independently the groundwater velocity following the method of Schubert et al 2011. Radon-based groundwater velocity results of the same order of magnitude as the velocity estimated with FEFLOW. Groundwater discharges into ponds surrounding the Crau area, will also be assessed during the course of this study by using Radon mass balance between ponds and groundwater, as well as salinity data.

Keywords: saltwater intrusion, Crau aquifer, FEFLOW, EM-34, ERT, Radon-222

A Flexible Predictive Tool for Salt Water Intrusion in the Red River Delta

Duc H. Nguyen^{1,2} and Keisuke Nakayama²

¹Department of Hydrology and Water Resources, Water Resources University, Hanoi, Vietnam

²Department of Civil and Environmental Engineering, Kitami Institute of Technology, Hokkaido, Japan

SUMMARY

For the management of estuarine water resources, it is necessary to have an instrument to determine the salinity concentration for any given location on the basis of directly measurable parameters such as geometry, river flow, and tide. Such an instrument is called a predictive tool. This can be used to simulate a case, in which one or more of the input parameters are subjected to change.

To date, numerous models for salt intrusion have become available. They are often used to make predictions of changes in salinity distribution under various boundary conditions. It is often implicitly supposed that if a model has been calibrated to reproduce measurements, then it will have some levels of predictive capability (Carter et al. 2006; Gallagher and Doherty 2007). However, this hypothesis is not always reasonable. It appears that a model developed for a specific condition of climate, geology, and hydrology does not represent the physical processes realistically and suitably in different environments (Beven 2000). In other words, the predictability of a model may only be fully achievable for a specific condition at which the model is calibrated, but it may be uncertain to some extent.

In many studies involving real world situations, a predominant disadvantage of the models is that they require a large number of measured data before the calibration and prediction can take place. The input data for boundary and initial conditions, such as topography, freshwater discharge, hydraulic conductivity, tidal velocity, and dispersion coefficient are extremely difficult to measure in reality that constrains the accurate modeling of the salt water intrusion.

While the modeling theory seems to favor simple, characterized by a few components and a restricted set of parameters, practical applications often require detailed representation of processes, and predictive models have to address complex environmental problems (Fenicia et al. 2009). However, a predictive model must have complex simulation capabilities, and that model should be supported by the available large datasets (Hunt et al. 2007). As data availability may be much different from one location to another, establishment of model complexity is not always desirable. This requires flexible model structures that can adapt well to different requirements of specific applications. Predictive models should be developed in a way to strike a balance between model complexity and data availability, by keeping models as simple as possible, but complex enough to justify the dynamics of the data (Fenicia et al. 2008; Savenije 2009).

The analytical salt intrusion model of Savenije (2005) is a good example of a flexible modeling approach. This model was originally developed for use in single channel estuaries considering the channel shape under tidally averaged conditions. The model involves two calibration coefficients that can be determined on the basis of an extensive salinity intrusion survey. It also contains some semi-empirical formulas that allow the prediction of the salt intrusion for a wide range of estuaries. However, there is no definitive answer to the question of whether the tidally averaged salt intrusion model can be applied to predict the future

salinity distribution in complicated geometrically estuaries, in which the estuary shape significantly varies as a function of tidal amplitudes. Such estuaries exhibit a narrow and nearly prismatic shape at low tide, but at high tide, they are very broad, and the banks strongly converge upstream.

In this paper, we present a predictive solution for salt intrusion based on the work of Savenije (2005). The proposed method was developed based on the premise that a calibrated model can be used for making predictions of future system behavior if the information content of the calibration data is sufficiently enough to constrain the model parameters. Hence, the parameterizations estimated through calibration for different geometric and hydrologic conditions can ensure the model to reproduce the reality that it is designed to represent. This strategy allows us to utilize the model at a level of complexity that sufficiently represents all processes at which a prediction of interest depends. The method was extended to establish empirical relations for the model parameters as a function of directly measurable parameters such as geometry, freshwater flow, and tide. Thus, changes in boundary conditions and their influences on the salinity distribution can be predicted.

The developed method was adapted for use in the Red River Delta (RRD) in North Vietnam. This delta comprises four estuary branches: Tra Ly, Red River, Ninh Co, and Day (Figure 1). Existing topography, salinity, and tidal data during a month in the dry season of 2006 were used to calibrate the model parameters. Predicted results of longitudinal salt intrusion profile were compared with field datasets in 2008 and 2009 to validate the method. A relatively good agreement was found between the model calibrated parameters and those computed from the empirical relations (Figure 2). We also found that the predicted salt intrusion profiles agree well with the measured data. These findings provide a key for the further investigation of salt water intrusion in estuaries.

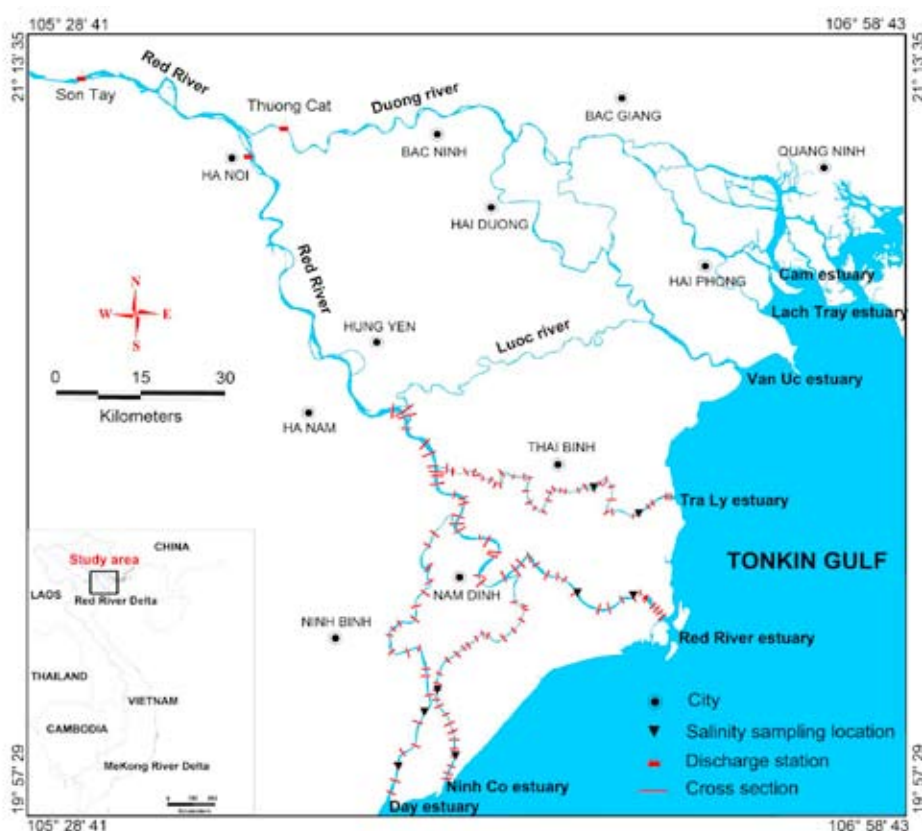


Figure 1. The study area.

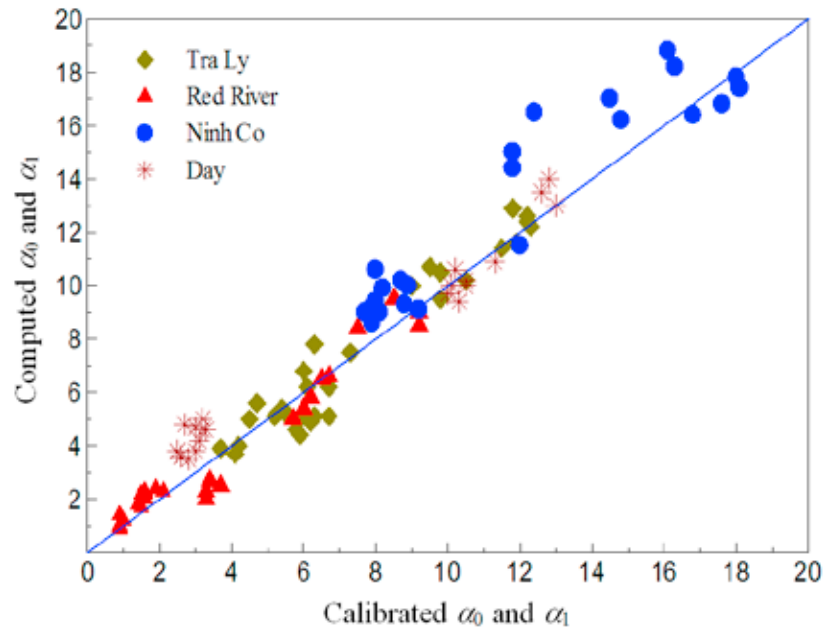


Figure 2. Comparison between the calibrated mixing coefficients and the computed values obtained from the empirical relations.

REFERENCES

- Beven, K.J. 2000. Uniqueness of place and the representation of hydrological processes. *Hydrology and Earth System Science*, Vol.4 (2), 203–213.
- Carter, J.N., Ballester, P.J., Tavassoli, Z., and King, P.R. 2006. Our calibrated model has poor predictive value: An example from the petroleum industry. *Reliability Engineering and System Safety*, Vol.91, 1373–1381.
- Fenicia, F., Savenije, H.H.G., Matgen, P., and Pfister, L. 2008. Understanding catchment behavior through stepwise model concept improvement. *Water Resources Research*, Vol.44, W01402, 1–13, doi:10.1029/2006WR005563.
- Fenicia, F., Savenije, H.H.G., and Avdeeva, Y. 2009. Anomaly in the rainfall-runoff behaviour of the Meuse catchment. Climate, land use, or land use management? *Hydrology and Earth System Science*, Vol.13, 1727–1737, doi:10.5194/hess-13-1727-2009.
- Gallagher, M. and J. Doherty. 2007. Predictive error analysis for a water resource management model. *Journal of Hydrology*, Vol.34 (3–4), 513–533.
- Hunt, R.J., Doherty, J.E., and Tonkin, M.J. 2007. Are models too simple? Arguments for increased parameterization. *Ground Water*, Vol.45 (3), 254–262.
- Savenije, H.H.G. 2005. *Salinity and Tides in Alluvial Estuaries*. Elsevier, Amsterdam, 197 pp.
- Savenije, H.H.G. 2009. The art of hydrology. *Hydrology and Earth System Sciences*, Vol.13, 157–161.

Contact Information: Duc Hoang NGUYEN, Water Resources University, 175 Tay Son str., Dong Da dis., Hanoi, Vietnam. Phone: +84-90-471-6969, Email: ducnh@wru.edu.vn

Hydrological history of Amsterdam Water Supply Dunes simulated with a 2D cross-section model

Philip Nienhuis¹, Theo Olsthoorn^{1,2} and Pierre Kamps¹

¹Waternet (Amsterdam Water Supply), Amsterdam, The Netherlands

²Faculty CITG (Civ. Eng. & Geosc.), Delft Technical University Delft, The Netherlands

ABSTRACT

To allow sufficiently reliable inference of feasibility of future seasonal storage of fresh water in the aquifers below the Amsterdam Water Supply Dunes (AWD), the entire hydrological history of the drinking water production in the Amsterdam Water Supply Dunes since 1853 has been simulated with a 2D cross-section groundwater model. The 2D model was extracted from the existing 3D groundwater model and its calibration was exclusively based on that of its parent 3D model. As the 2D model yielded semi-quantitative insights until then unavailable with the 3D model, additional calibration and validation was started, in turn yielding information on the sensitivity of the present-day situation for early historical hydrological situations.

INTRODUCTION

In the course of modeling of seasonal storage of fresh water in fresh or saline aquifers below the Amsterdam Water Supply Dunes (AWD; location see Figure 1), it proved unavoidable to model the entire history of the drinking water supply abstraction since the mid-19th century including the dynamics of the fresh groundwater lens (Nienhuis and Olsthoorn, 2012, 2013). Even though that history was only modeled in a 2D cross-section, it yielded already an unintended but welcome byproduct, viz. an improved and comprehensive insight in the large-scale behavior of the fresh water lens. The overall hydrological history was already

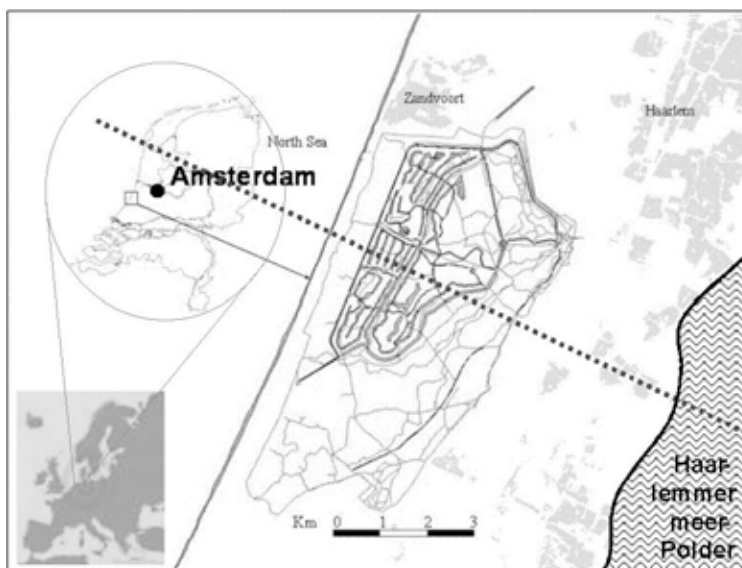


Figure 1. Location of Amsterdam Water Supply Dunes

qualitatively known and had even partly been simulated and –to some extent- validated with a transient 3D-groundwater model (Kamps et al, 2006). Recent simulations of the hydrological history yielded for the first time semi-quantitative indications on relative contributions to, and effects on, the fresh groundwater lens by various historical events and on the validity of our groundwater models as regards the fresh/saline groundwater distribution under and around the AWD.

MODEL BUILD-UP

The 2D-cross-section model was extracted from the 3D AMWADU groundwater model (Kamps, 2006). The cross-section lies perpendicular to the coast, parallel to the predominant groundwater flow direction, and extends from 3 km into the North Sea to 12 km inland (Figure 1). The movements of the fresh/saline groundwater interface (FSI) in AMWADU is based on the SWI package. As that SWI version doesn't allow the FSI to move through aquitards, nor allows generation of brackish water, the 2D cross-section model has been based on Seawat. Mflab (Olsthoorn, 2010) was used for all model manipulations.

Initially the model assumed fully saline aquifers in the entire coastal area, with only a shallow (~5 m thickness) fresh groundwater layer under the historical lake Haarlemmermeer in the East. To obtain an acceptable starting position of the fresh/saline interface under the AWD, we modeled a theoretical build-up of the freshwater lens out of precipitation starting in 1500 AD. The modeled period 1500-1850 proved sufficient (in the model) to obtain a freshwater lens in dynamic equilibrium with precipitation and other boundary conditions. From 1850 on the hydrological history was entered in the model as far as we could reconstruct it from historical data and -information.

Preliminary calibration and verification

AMWADU has extensively been calibrated as far as possible within technical and practical limitations. Historical movements of the FSI have been validated for the period 1904-2004 (Kamps et al, 2006). AMWADU's calibration was inherited as a start for the 2D cross-sectional model. We only verified the 2D-model in terms of the depth of the FSI under the AWD. It was concluded that the FSI position was simulated about 10 % too shallow (see also Nienhuis et al, 2012). At the time, this state of the calibration was found acceptable for the original purpose of the 2D model, i.e., a pre-feasibility study of future seasonal fresh water storage in and under the freshwater lens. For that purpose a much more important requirement was that the simulated FSI at the start of the simulated seasonal storage was in point equilibrium with past stresses, to mitigate model artefacts caused by the model seeking equilibrium from possibly incorrectly entered starting positions of the FSI. It would be virtually impossible to distinguish such artefacts from the simulated effects of seasonal storage we were after.

Additional results

The simulations clearly show the rise of the FSI under the AWD due to overexploitation of the freshwater lens in the first half of the 20th century by wells tapping the deeper aquifers, and the recuperation of the freshwater lens after the start of infiltration of pre-purified Rhine water around 1957. The 2D model allowed for the first time semi-quantitative insights in hydrological phenomena that couldn't be inferred from the existing 3D model. Examples are that (1) the reclaimed lake Haarlemmermeer, where in 1850 the hydraulic potential was lowered by more than 6 meters, induced a large-scale groundwater flow system transporting saline North Sea water, beneath the freshwater lens system under the AWD, to the present-day Haarlemmermeerpolder, and (2) this saline groundwater flow system has significantly dragged the freshwater lens in eastward direction. The 2D model simulations show that because of this drag, the future equilibrium position of the FSI near the coast is significantly shallower than in 1850, hitherto rendering full recuperation of the local freshwater lens thickness to historical values unattainable. Reclamation of lake Haarlemmermeer in 1850 proved to be the dominating factor influencing groundwater flow and distribution of fresh and saline groundwater in a wide area, much more than the drinking water supply in the AWD itself, and this situation will continue a long time into the future.

CONTINUED SIMULATION STEPS

The abovementioned insights motivated further simulation steps aimed at getting a better quantitative understanding of the groundwater systems in and around the AWD.

A first attempt to calibrate the 2D model is based on comparing the simulated historical positions and movements of the FSI with historical positions inferred from chloride- and GEM-cable (“geohm cable”) measurements (Kamps, 2011). Starting from the very late 19th century some scarce quantitative data are available. The data intensity grew slowly until the 1950’s. From the period since 1960 a fair amount of quantitative data is available.

Based on Delsman et al (2013) the historical FSI under former lake Haarlemmermeer (before 1850) was assumed to lie at about 50-60 m below datum level. To that end the build-up of the freshwater lens from scratch was replaced by a theoretical FSI position in 1500 AD, with the FSI at the sea bottom some 200 m from the water line, from there gradually descending under the AWD to about 60 m depth, and extending horizontally at that depth to the east of the 2D model cross-section.

RESULTS

Initial calibrations runs show that the FSI position in the first half of the 20th century is not very well simulated in the AWD. However, simulated and measured FSI positions match better starting from the 1960s onward (Figure 2). With a thicker initial fresh part of the aquifer under lake Haarlemmermeer the simulated freshwater lens under the AWD reaches greater depths.

Because the fresh groundwater initially input under former lake Haarlemmermeer in the east is hydraulically connected with the North Sea, the fresh groundwater is pushed up in the period 1500-1850. Higher potentials in lake Haarlemmermeer can be used to mitigate this effect but we have yet insufficient data to support this.

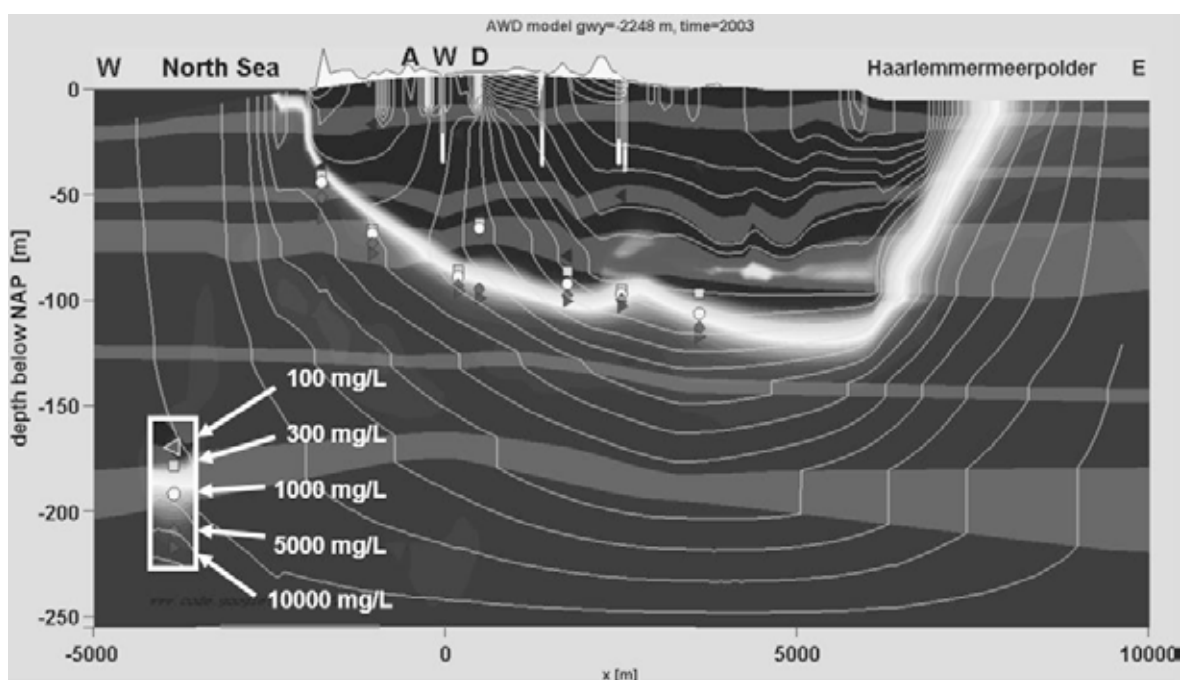


Figure 2. Simulated FSI position in 2003

DISCUSSION AND CONCLUSIONS

The strong influence of assumed FSI positions from before 1850 on the simulated present-day situation implies that the model results should be interpreted with due caution. This is not unexpected, given the long response time of the freshwater lens to changing external stresses; the response time is probably much longer than the 160+ years since 1850. On the one hand this sensitivity suggests that some imaginable historical hydrological situations are more probable than others; on the other hand there are insufficient data to validate the early hydrological history.

In spite of the great uncertainties about the exact paleo-hydrological conditions, the simulated FSI position at the end of the simulated period is reasonably in accordance with the salinity distribution inferred from chloride and GEM-cable measurements.

It seems the best we can do is concentrate on the movements and positions of the FSI in fairly recent decades, taking advantage of the fact that the earlier in history a hydrological stress occurred, the less influence it has on the current and future hydrological situations.

REFERENCES

- Delsman, J.R., K.R.M. Hu-a.ng, P.C.Vos, P.G.B. de Louw, G.H.P. Oude Essink, P.J.Stuyfzand and M.F.P.Bierkens 2013. Paleo-modeling of coastal salt water intrusion during the Holocene: an application to the Netherlands. *Hydrol. Earth Syst. Sci* 10, 13707-13742
- Kamps, P.T.W.J., 2011. Methoden van kartering van zoet, brak en zout grondwater in de Amsterdamse Waterleidingduinen (Methods for mapping fresh, brackish and saline groundwater in the Amsterdam Water Supply Dunes). Internal report (in Dutch) Waternet, Amsterdam, 33pp
- Nienhuis, P.R., T.N. Olsthoorn and P.T.W.J. Kamps 2012. Modelling AS(T)R in the Amsterdam Water Supply Dunes to explore options to cope with future intake water shortages caused by climate change. In: *Proceedings of 22nd Salt Water ntrusion Meeting SWIM 2012, Armação dos Búzios, June 17-22, p.138-139*
- Nienhuis, P., Kamps, P., and T.N. Olsthoorn 2013. 160 Years of History of the Amsterdam Water Supply Dune Area Modeled with Variable Density, Outlook into the Future, in: *Proceedings of MODFLOW and More 2013: Translating Science Into Practice*, edited by: Maxwell, R., Hill, M., Zheng, C., and Tonkin, M., Golden, CO, USA, 2013.
- Nienhuis, P.R., P.T.W.J. Kamps and F.W. Schaars 2006. Historical Field Data 1904-2004 Used to Validate 100 Years Movement of Salt/Fresh Interface Simulated with the SWI-Package. Paper presented at the 1st SWIM-SWICA Joint Salt Water Intrusion Meeting, Cagliari-Chia Laguna
- Olsthoorn, T.N. 2010. <http://code.google.com/p/mflab>

Contact Information: Philip Nienhuis, Waternet, Hydrology and Ecology Dept., Vogelenzangseweg 21, 2114 BA VOGELENZANG, The Netherlands. Email: philip.nienhuis@waternet.nl

Large scale salt water behavior in the Pakistani Punjab

Theo Olsthoorn^{1,2}, Naveed Alam¹

¹Faculty CITG (Civ. Eng. & Geosc.), Delft University of Technology, The Netherlands

²Waternet (Amsterdam Water Supply), Amsterdam, The Netherlands

Abstract

The distribution of the salt in the center of the doabs between the large and infiltrating Punjabi rivers in Pakistan till large-scale irrigation perturbed the groundwater hydrology is likely due to accumulation and density flow caused by evaporation triggered by deep rooting trees. The situation is dynamic because the rivers have always irregularly and often drastically altered their course on time scales that are of the same order as the time required to reach a new salt equilibrium after a change of the course of a major river. Both this accumulation and the impact of shifting river courses make the subsurface salinity distribution highly dynamic on the time scales of centuries to millennia, the development of which is highly disrupted due to recent human impact in the water cycle, including groundwater.

Introduction

There are still large-scale riddles to be solved with respect to subsurface distribution of salt water (Bennett et al, 1967). One of the them is that in the Pakistani Punjab as it existed before the onset of the large-scale irrigation in the late 1900s. This irrigation has massively been developed and intensively used since and has totally perturbed the groundwater situation in the area. The groundwater has been dominated for millennia by the mighty Indus River and its five large tributary rivers Jhelum, Chenab, Ravi, Beas, Sutlej, all emanating from the Himalayas through which they have been deepening their canyons to keep pace with the rise of this young mountain range. The Punjab and Sind alluvial plains were formed by the thousands of meters thick sediments of these rivers, deposited since the onset of the collision of the Indian and Eurasia plates, while the more easterly Himalayan Rivers mainly formed the alluvial basins of India (Bender and Raza, 1995).

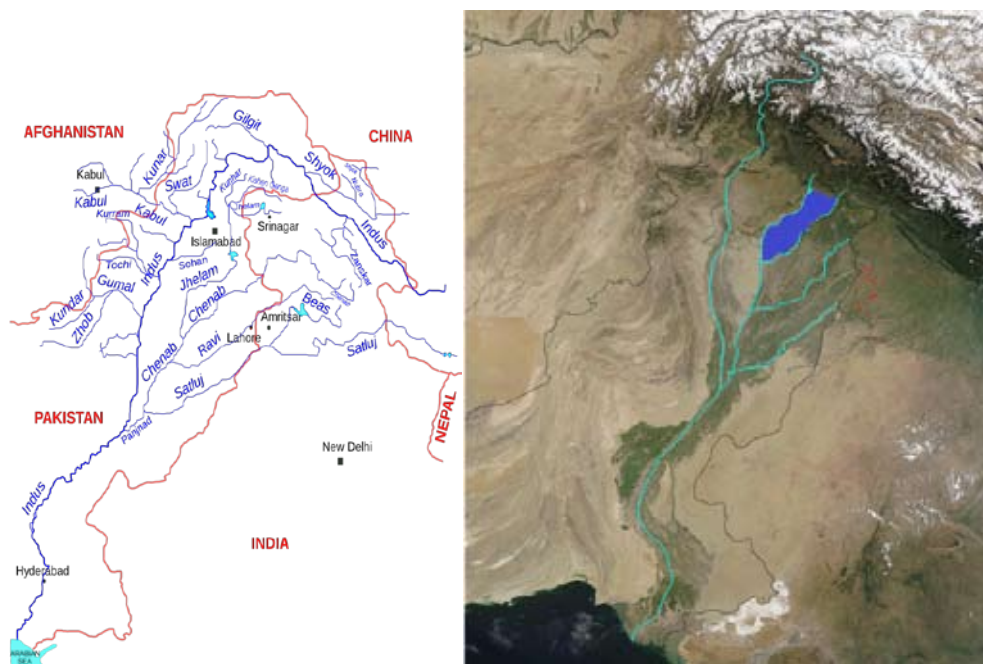


Figure 1: Punjabi rivers overview left and in their Himalayan context right, with one of the doabs, i.e. the Chaj doab indicated in blue.

The alluvial planes at the foot of the Himalayas can be regarded as a set of elongated islands, called doabs, lying between these large rivers being essentially deserts until irrigation commenced (Eggemont 1993).

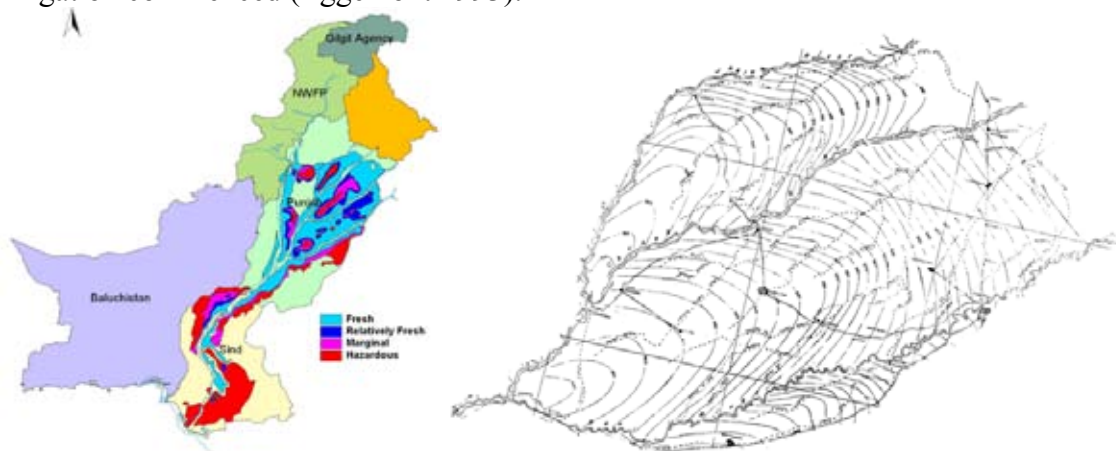


Figure 2: Salinity within the doabs (left). Right: Chaj and Ravi doabs with groundwater contours showing flow dominant flow from the rivers to the doab interiors, based on groundwater data before irrigation.

Mechanisms determining salt distribution in the Punjab

Originally, the Punjabi Rivers have been mainly infiltrating, as was evidenced by the bowl-shaped groundwater surface between them measured in the early period of irrigation development (Bennett et al, 1967). Clearly, evapotranspiration must have been the major force driving groundwater from the rivers towards the center of the doabs in between. This flow caused salt water to mound towards the center of these doabs. Indeed,

the groundwater in the doabs away from the rivers is generally saline while the flood plains along the rivers are fresh over large depths.

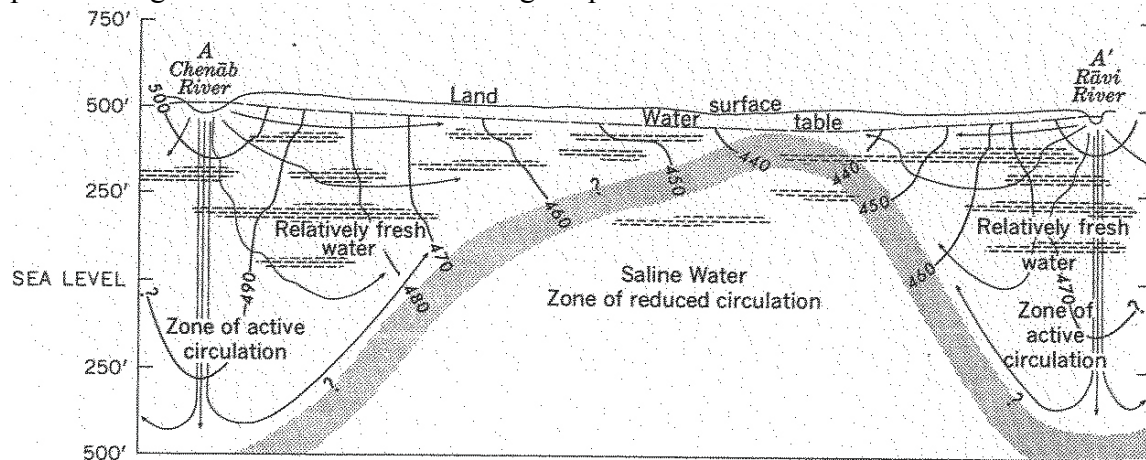


Figure 3 Fresh- and saltwater distribution in the doab between the Chenab and Ravi Rivers (USGS, 1967)

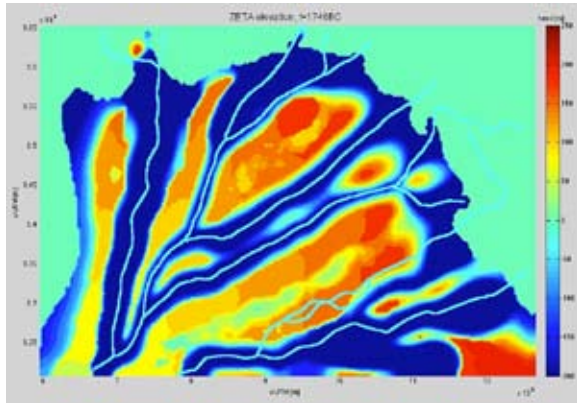


Figure 4: Punjabi rivers with simulated salt distribution, situation ca. 1500BC

It is hard to imagine a sink for this salt water, which naturally accumulates inside the doabs. The large masses of salt required to match evapotranspiration over millennia cannot be stored in the unsaturated zone. A large-scale deep groundwater flow towards the Arabian Sea some 1000 km further south may provide an unresolved contribution to the solution, but is hard to quantify. At least such a flow at an average gradient of 0.175 m/km is unable to prevent accumulation of salt water within the doabs where flow is dominated by the gradient from the rivers to the groundwater depression in the interior of the doabs. Therefore, downstream transport of salt water to the Arabian Sea by the mentioned natural groundwater gradient cannot provide a substantial discharge of salt water from the Punjab.

A third mechanism might be recirculation of salt caused by density flow triggered by the increase of salinity under evapotranspiration from the phreatic zone (Bauer et al, 2006). The bowl-shaped groundwater depression between the rivers (fig. 2) that existed before irrigation started is indicative of such evapotranspiration. However, the deep position of the phreatic surface, which near the center of the doabs reached depths in the order of 20 m relative to the rivers as well as to ground surface, requires special mechanisms for this evapotranspiration to be possible.

British botanists or geographers have in the nineteenth century registered native plant species of the doabs. Among the species abundantly present before the recent irrigation development, was *Prosopis cineraria*, or Ghaf tree, an evergreen and worshipped tree that develops taproots up to several tens of meters length (Canadell et al. 1996), thus capable of reaching the groundwater anywhere within the doabs. These trees can also withstand salinities up to half of that of seawater, while their bean-like fruits are edible by both cattle and humans. These fruits have saved people fleeing the fertile flood planes into the desert central doabs during wars, which is probably the reason for worshipping the tree (Eggemont, 1993). We suspect that the Ghaf tree has been the major cause of evapotranspiration of groundwater within and throughout the doabs in their natural setting and, through this, dominating the entire natural groundwater distribution and salinity of the Punjab.

It is not likely or even impossible for such trees to be large-scale salt sinks. The fruits of these trees are fresh as are the leaves. A major mechanism of the tree to prevent salt stress is by a continuous and dynamic formation of new fresh roots with abandonment of old roots having become salty. However, large-scale salt accumulation in the Punjabi unsaturated zones is not known. We, therefore, adopt that there exists a mechanism that returns salt into the saturated zone. It could be flushing after wetter periods or a more complex feedback mechanism involves tap and shallow roots in combination with so-called hydraulic lift (Canadell et al. 1996). Although such mechanisms are known to exist they have still not been intensively studied in practice.

A major mechanism, that incidentally alters the groundwater situation and, in its wake, the saltwater distribution are shifts of the course of big rivers, which has taken place numerous times in the long and recent past. Of course, shifting river courses are at the basis of the filling of whole sinking basin with thousands of meters of sediment. Wilhelmy (1969) has mapped courses of the Punjabi rivers over the last four thousand years, based among others on archeological sites and historic settlements. Geologists have more recently mapped the tectonic lifting of the Punjab and shown this as a major cause of a general westward shift of the Punjabi rivers to the west of the Sutley River. A shift of a river course, which may be and often has been a sudden event, changes the groundwater flow within the system. New freshwater is formed below the new river course and the freshwater along its old course gradually disappears, while the water table rises below the new river bed and declines under the abandoned riverbed towards its new equilibrium. Time to reach a new equilibrium is in the order of 1500 years, based on our cross sectional models, which is within the time in which river shifting has taken place. As a consequence of these time sales the saltwater distribution in the Punjab is never in equilibrium.

Due to flow from the rivers towards the center of the doabs salt groundwater is transported from great depths towards the water table. The evaporation from the doabs easily lifts an initial saltwater interface elevation at sea level to the current water table at 175 m above sea level. From this mechanism, it is clear that the current distribution of salt and fresh water is ruled much more by current groundwater flow patterns than by the elevation of the sea.

Return of saltwater due to accumulation under evapotranspiration as a major mechanism

One of the more challenging mechanisms is the return of salt water to the deeper zones caused by the density flow occurring near the water table under the influence of evapotranspiration in which plants leave salt water behind while extracting groundwater as has been demonstrated for the Okavango Delta in Botswana (Bauer et al, 2006).

This mechanism can be shown to work at least in theory, by demonstrating it in a density driven groundwater model. However, the exact mechanism cannot be understood in detail due to limitations of our models on the one hand and the lack of supporting field evidence on the other. One reason why unstable downward flow of saline water above fresher water cannot be accurately modeled is that adequate modeling requires a much smaller Rayleigh number than can be achieved in a more wide-scale model necessary to study regional phenomena (Post, 2004). This does not mean that such convective flows cannot occur in a general density driven groundwater model, but the time and spatial scales in which such convective flows occur may be quite dependent on the model and therefore deviate from the real world. This means that at most the mechanism can be illustrated, without relevance to the scales at which these mechanisms play in the real case.

Application of spatial and cross sectional density driven models for the Punjab has been a challenge. The use of the new MODFLOW 2005 with SWI (Bakker et al, 2013) will reveal the overall distribution of the salinity initially, but also discharges saltwater along with the evapotranspiration, which will not occur in reality. Of course the same happens in SEAWAT (Langevin et al. 2006) when a negative recharge is applied to simulate evapotranspiration. This will not happen when simulating evapotranspiration using the EVT or ETS packages in MODFLOW, which allow extracting water while leaving salt behind, thus causing accumulation of salt, due to which unstable downward transport of accumulated salt does take place under the increase of density.

With such a mechanism, recycling of salt occurs, implying that over time, the salt in the system will be a mixture of salt of marine origin, originally in place, and of salt infiltrated with the river water and concentrated under the influence of evapotranspiration; hence the rivers themselves will be a source of salt on the long run when no escape of salt from the system is possible.

The presentation will concentrate around the simulation of the diverse mechanisms in an attempt to illustrate the origin of the saltwater in the Punjab. Especially the redistribution of the salt in the subsurface caused by the documented shifts of the Punjabi Rivers over the last four thousand years will be illustrated together with their time scales and consequences for the current situation.

References

Alam, N. (2014) Sustainable conjunctive use of groundwater for additional irrigation. Draft PhD Thesis, TUDelft.

Bakker, Mark, Schaars, Frans, Hughes, J.D., Langevin, C.D., and Dausman, A.M., 2013, Documentation of the seawater intrusion (SWI2) package for MODFLOW: U.S. Geological Survey Techniques and Methods, book 6, chap. A46, 47 p., <http://pubs.usgs.gov/tm/6a46/>.

Bauer, P, Supper, R, Zimmermann, S. Kinzelbach, W. (2006) Geoelectrical imaging of groundwater salinization in the Okavango Delta, Botswana. *Journal of Applied Geophysics* 60, 126-141.

Bender F.K. and H.A. Raza (1995) *Geology of Pakistan. Beiträge zur regionalen Geologie der Erde. Gebrüder Brontraeger. ISBN 978-3-443-11025-3. 414p, 140 figs, 38 tables.*

Bennett, G.D, Rehman, A-U, Sheikh, I.A. Sabir, A. (1967) *Analysis of aquifer tests in the Punjab Region of West Pakistan. USGS, Geological Survey Water Supply Paper, 1608-8G.*

Canadell, J., Jackson, R.B., Ehleringer J.R. Mooney, H.A. Sala, O.E. and Schulze, E.D. (1996) Maximum rooting depth of vegetation types at the global scale. *Oecologia*. 108:583-595

Eggemont, P.H.L. (1993) *Alexander's campaign in Southern Punjab. Orientalia Loveniensi Analecta 54. Uitgeverij Peeters en Departement Oriëntalistiek, Leuven. ISBN 90-6831-499-8, 162pp.*

Greenman, D.W, Swarzenski W.V. and Bennett G.D. (1967) *Groundwater hydrology of the Punjab, West Pakistan, with emphasis on problems caused by canal irrigations. USGS Water Supply Paper 1608-H.*

Langevin, C.D., Thorne, D.T., Jr., Dausman, A.M., Sukop, M.C., and Guo, Weixing, 2007, *SEAWAT Version 4: A Computer Program for Simulation of Multi-Species Solute and Heat Transport: U.S. Geological Survey Techniques and Methods Book 6, Chapter A22, 39 p.*

Olsthoorn, T.N. (2014) <http://www.google.code.com/p/mflab>

Post, C.E.A. (2004) *Groundwater salinization processes in the coastal area of the Netherlands due to transgressions during the Holocene. PhD Thesis. Free University Amsterdam, ISBN 90-9017404-4. 137pp.*

Wilhelmy, Herbert (1967) 'The Shifting River: Studies in the History of the Indus Valley', *Universitas*, Vol. 10, No. 1, pp.53-68

Contact Information: Theo Olsthoorn, TU-Delft, Stevinweg 1, 2628 CN Delft. Email: T.N.Olsthoorn@tudelft.nl, mobile: +31-6-20440256

Global Quick Scan of the Vulnerability of Groundwater systems to Tsunamis

D. Zamrsky^{1,2}, M. Faneca Sanchez¹, G.H.P. Oude Essink¹

¹ Deltares, Unit of Subsurface and Groundwater Systems, Utrecht, The Netherlands

² Wageningen University, Wageningen, The Netherlands

ABSTRACT

Major tsunami events have struck the coasts around the world with fatal consequences in terms of human casualties and material damage. While effects of a tsunami are clearly visible and well documented on the surface, little is known about the impacts on groundwater resources in the inundated areas. This study focuses on finding the most vulnerable areas to groundwater salinization caused by tsunami inundation. In our study, we present a Global Quick Scan of the vulnerability of the deltaic fresh groundwater resources to tsunamis. Two major steps were taken. As a first step, a vulnerability index is constructed. It is calculated using different types of topographical data. Regions with income below poverty line (1\$/day per capita) are picked as the most vulnerable ones, due to no availability of alternative freshwater resources. Once these areas are selected, a search for parameter statistics is performed using a method of raster masking (overlay). Parameter statistics help to create ranges of values for relevant model parameters such as soil type and precipitation, which are then used in the second step. This step is a modeling process of salinization of fresh groundwater aquifers due to tsunami inundation. The severity of salinization is quantified as time necessary for a specific area to restore a freshwater concentration in more than 90% of its original extent.

INTRODUCTION

Fresh groundwater resources in deltaic areas are used for domestic, agricultural and industrial purposes. These resources in the coastal zone are threatened by salinization of the aquifers due to global change (increase of groundwater extraction due to population growth), climate change (including sea level rise), as well as natural disasters such as floods and tsunamis. Studies of how the coastal fresh groundwater resources are affected by the latter phenomena are often done a posteriori, especially the studies related to tsunami effects (e.g. the 2003 Sumatra Tsunami, Illangasekare, *et al.*, 2006). Then it is often too late to take appropriated measures to counteract the negative effects (e.g. on drinking water supply). These complex studies are time consuming, and need data which might not be available at the time of the disaster when a fast reaction of the water authorities is needed, e.g. to facilitate a quick and easy access to a fresh water supply system.

METHODS

We created a global database of relevant vulnerability indicators and model parameters. We collected SRTM90m data (Digital Elevation Model of the world), soil maps, gross domestic product and population density (step 1). We generated clustered data sets and used those to generate fast and simple variable-density groundwater flow and coupled solute transport models to simulate the salinization of groundwater systems in the coastal zone (step 2). These quantifications could give water managers a first approximation of the effects that a tsunami would have on the salinization of the fresh groundwater. The data collected in this database and the results of the models have been used to generate a map showing the areas with coastal groundwater systems vulnerable to tsunami effects and the magnitude of the

possible impact of a tsunami. Python 2.7 scripts were used to transform the input data step by step, to extract parameter statistics (e.g. soil types), and to find the most vulnerable areas.

METHOD STEP 1 Vulnerability index

Information from the SRTM90m dataset is used to assess topographical parameters such as elevation, topographic slope and distance to coast (using GDAL and python scripts). The following equation is used to determine the vulnerability:

$$vulnerability\ index = 4 * ID_{elev} + ID_{dist} + ID_{slope} \quad (1)$$

where *elev* is topographic elevation, *dist* is distance to coast and *slope* is topographic slope. This formula is based on Rao *et al.* (2008) and has been tested in the northwestern coast of Japan (flood plains (Sendai and Minamisoma), V-shaped bays (Myiako, Rikuzentakata, Kesenuma) and a river estuary (Kitakami River), using historical 2011 data) and Spain (Murcia, Mallorca, being similar to the Japanese coastal zone). However, the threat of tsunamis is not the same throughout the world, and therefore, we selected only the areas with a high risk of tsunamis. For that, the global tsunami hazard study by Løvholt *et al.* (2012) was used to choose only areas with potential high risk of tsunami. In addition, regions with income below poverty line (1\$/day per capita (Chen and Ravallion, 2007)) are picked as the most vulnerable ones, due to no availability of alternative freshwater resources.

METHOD STEP 2 Variable-density groundwater flow modeling

SEAWAT (Langevin *et al.*, 2007) is used for the numerical simulations of variable-density groundwater flow and coupled solute transport. An adapted Henry concept is chosen to represent the impact of a tsunami on a coastal aquifer system, introducing constant head boundaries and recharge fluxes. SRTM90m data has been used to determine the different values of the inland constant head boundary. The conceptual 2D model is created with total length of 5km and depth of 50m; each model simulation has a unique combination of parameter values, see table 1. Number of columns and model layers are 5002 and 53, resp. The top soil layer has 4 model layers of each 0.25m thickness; longitudinal dispersivity is 1m ($\alpha_T/\alpha_L=0.1$); the MOC solver is used. The tsunami is conceptualized as follows; figure 1 shows the three different phases within such a disastrous event:

1. Phase 1: 500 years to determine the shape of the salt water wedge;
2. Phase 2: tsunami implemented as a head over the inundated area for a short duration;
3. Phase 3: the top layer of 1 m over 2 km length ($X=2-4$ km) is fully saturated with sea water (in terms of salt concentration) due to either a porous unsaturated medium, present top system (agriculture, ditches etc.) and/or local depressions where the sea water can stay after the wave retreat.

An important conceptual choice in the modeling process is the following: the severity of tsunami impacts in terms of head and thickness of the saturated top soil layer after wave retreat is the same for all 2D models. This is to be able to compare the response of different hydrogeological systems on a global scale, focusing on a-priori in-situ hydrogeological parameters. Basically, this means the initial starting concentration of phase 3 over $X=2-4$ km in the top soil layer of 1m thickness is saline. As such, this 1m saline saturated thickness can be considered as a worst case scenario. We are aware that phase 2 has its effects (e.g. an unsaturated zone is probably present where the salt water could infiltrate) but in our vulnerability assessment this issue is assumed to be beyond our scope, for now. In addition, the direction of the tsunami hitting the coastline, the distance from the source (epicenter) and bathymetry are also not implemented in our approach).

These 2D models simulate among others the loss in fresh groundwater volume of the system after the tsunami. We have chosen for the zone below the inundated area of depth 7m (being a zone where often shallow groundwater is extracted in underdeveloped areas). In addition, the characteristic time of a groundwater system in the same zone is determined before it recovers 90% of the fresh groundwater that was available previous to the tsunami event.

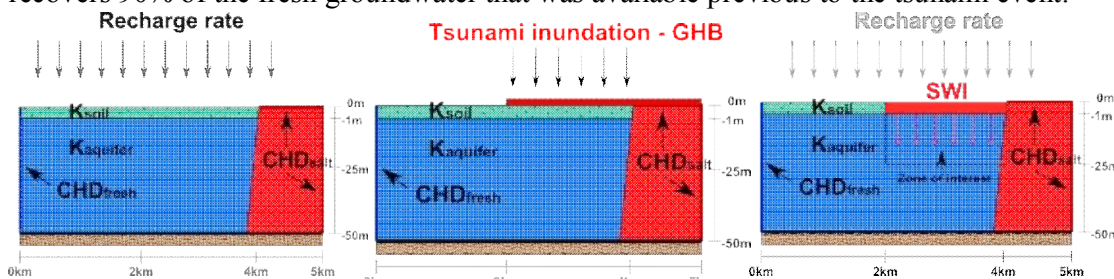


Figure 1: Schematisation of the conceptual model: three phases but basically only the phases 1 and 3 are modeled.

Variable parameters	Value			
	A	B	C	D
Recharge (fresh) (m/d)	0.0001	0.001	0.0025	0.005
CHD fresh (m)	1.0	5.0	15.0	-
K soil (m/d)	0.005	0.05	5.0	50.0
K aquifer (m/d)	1.0	100.0	-	-

Table 1: Variable hydrogeological parameters (4*3*4*2=96 model combinations).

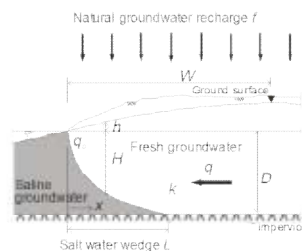
RESULTS

With the 2D models, two different times are characterized:

1. **Characteristic time** – time of zone recovery till 90% as before tsunami, and
2. **Reach time** – time necessary for the salt front to reach the deep zone (at least 10% of salt in the zone). This time determines how long it takes before deeper groundwater extraction wells could be contaminated with saline groundwater.

Figure 2 shows the 96 default ‘Henry’ salt water wedges (the end of phase 1). After modeling phase 3, differences in (fingered) plumes are detected, which are caused by difference in recharge rates, the constant head boundary at the hill site, and the hydraulic conductivities in the top soil aquifer of 1 m and the aquifer below it. Some characteristics are (keeping the traditional equation in mind):

$$L = -\frac{q_0}{f} - \sqrt{-\left(\frac{q_0}{f}\right)^2 - \frac{k}{f} D^2 (1 + \alpha) \alpha}$$



- the salt water intrusion wedge largely depends on the outflow flux; a large outflow flux reduce the length of the wedge,
- a low hydraulic conductivity in the aquifer reduces the length of the wedge,
- an increase in groundwater recharge can reduce the wedge length significantly.

On top, the characteristics of the tsunami event are:

- fingers do occur in most hydrogeological systems,
- high hydraulic conductivities in the aquifer fastens the flow of intruded seawater out of the drinking water zone,

- a large outflux from the inland area reduces the deep outflow of intruded seawater,
- a large groundwater recharge causes a deeper outflow of intruded seawater.

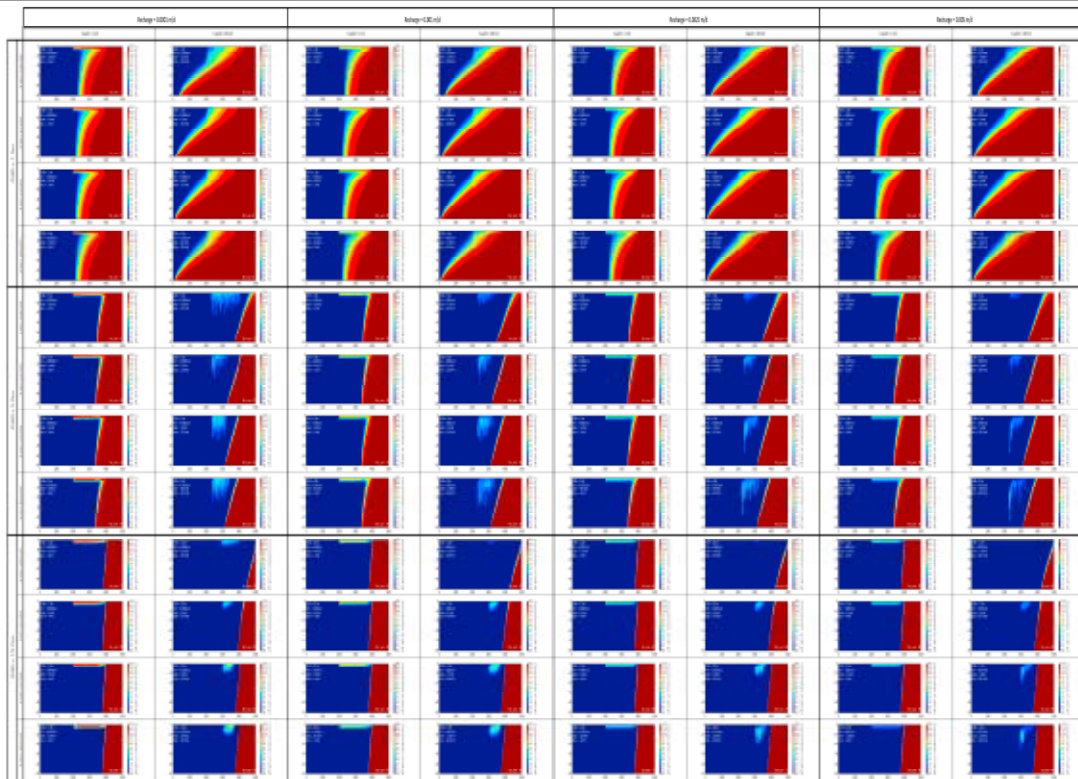


Figure 2: 2D profiles of all 96 adapted Henry cases, 2.5 yrs after tsunami event.

The method proposed in this study sets a framework for vulnerability assessments to different types of hazards of the groundwater system on a global scale. A similar approach could be adopted for assessing the effect of sea level rise and future increased groundwater extractions on vulnerable coastal groundwater systems worldwide.

REFERENCES

- Chen, S. and Ravallion, M. 2007. Absolute poverty measures for the developing world 1981 -2004. PNAS 104: 16757-16762.
- Illangasekare, T., et al. 2006. Impacts of the 2004 tsunami on groundwater resources in Sri Lanka, Water Resour. Res., 42, W05201, doi:10.1029/2006WR004876.
- Langevin, C. D., Thorne, D. T., Dausman, A. M., Sukop, M. C., Guo, W., 2007. SEAWAT Version 4: A Computer Program for Simulation of Multi-Species Solute and Heat Transport: U.S. Geological Survey Techniques and Methods Book 6, Chapter A22.
- Løvholt, F., S. Glimsdal, et al. (2012). Tsunami hazard and exposure on the global scale. Earth-Science Reviews 110(1-4): 58-73.
- Michael, H. A., C. J. Russoniello, and L. A. Byron (2013), Global assessment of vulnerability to sea-level rise in topography-limited and recharge-limited coastal groundwater systems, Water Resour. Res., 49, 2228–2240, doi:10.1002/wrcr.20213.
- Rao, K. N., P. Subraelu, et al. (2008). "Sea-level rise and coastal vulnerability: an assessment of Andhra Pradesh coast, India through remote sensing and GIS." Journal of Coastal Conservation 12(4): 195-207.

Contact Information: Gualbert Oude Essink, Deltares, Unit Subsurface and Groundwater Systems, 6-8 Princetonlaan 3584 CB Utrecht, The Netherlands. Phone: +31 (0)6 30550408, Email: gualbert.oudeessink@deltares.nl

Saline water circulation beneath the fresh-saline interface: results of laboratory experiments and numerical modeling

I. Oz^{1,2}, E. Shalev¹, Y. Yechieli¹, I. Gavrieli¹, H. Gvirtzman²

¹Geological Survey of Israel

²Institute of Earth Sciences, Hebrew University of Jerusalem

ABSTRACT

In this study we examined the interface configuration and the circulation flow of saltwater within coastal homogenous aquifers adjacent to a saltwater body with a long term stratified water column. Such systems consist of three different water types: the regional fresh groundwater and the low and high salinity brines forming the upper and lower water layers of the saltwater body, respectively. High density difference, which is expected to be developed between the two water layers of the Dead Sea during the operation of the "Seas Canal" project, makes it an ideal case study for studying such systems.

The groundwater interface configuration and the density-driven circulation flows that develop in the aquifer are examined using laboratory experiments and numerical modeling at the same scale. The laboratory experiments were conducted in a two-dimensional rectangular flow tank, filled with granular material, simulating a homogenous and phreatic coastal aquifer. For the numerical modeling we used RST2D computer code and COMSOL Multiphysics (FEMLAB 3.5a) in order to quantitatively evaluate the coupled fluid and solute transport equations.

The results of both numerical simulations and the laboratory experiments show that the steady-state configuration of the fresh-saline interface is more complicated than those which developed within a coastal aquifer adjacent to a non-stratified saltwater body, as three interfaces between the three different water types are developed. The numerical model, which is calibrated against the salinity distribution and groundwater discharge rate in the laboratory experiments, allows the quantification of the flow rates and flow patterns. These flow patterns, which cannot be derived from laboratory experiments, show the development of three circulation cells which are confined between the three interfaces. We found that these unique configuration and flow patterns are sensitive to the model parameters (using dimensionless parameters), meaning that the creation of three-circulation-cells is limited to a certain range of values of each parameter. Outside of this range, only a single circulation cell develops, either by the two saltwater bodies, or by the high salinity brine solely. The threshold values for the transformation between these different flow configurations were also determined.

As mentioned above, the creation of three circulation cells in this hydrological system is predicted by numerical simulations solely. In order to validate these calculated flow patterns we have been conducting laboratory experiments, in which we expose the aquifer to brines with the exact same concentrations (density of 1100 kg/m³). By using this method we are able to monitor the progress of the dye color front over time and to calculate the flow velocities and the flow directions within the different levels of the saline wedge. At first we applied this method to the simple system of a single interface. Such systems consist of two different water types: the regional fresh groundwater and the saline water from the saltwater body. At the next stage, we will apply this method to the complex system of three interfaces and three circulation cells.

As expected, adjacent to a non-stratified saltwater body, a single circulation cell of the saline water forms beneath the interface. We examined the nature of the flow regime and the

sensitivity to changes in the parameters. The results show that the flow velocities in the saline area are increasing with depth (i.e.; when moving towards the lower boundary). The flow velocities also increased with distance (i.e.; when moving away from the saltwater boundary), although this trend is shifting next to the interface where the flow velocities decrease. The flow direction of the saline water beneath the fresh-saline interface is mostly sub-horizontal (parallel to the lower boundary), with a minor component downward. Preliminary result of parametric analysis shows that the magnitude of the downward component is mostly sensitive to changes in the transversal dispersivity.

Controlled level drainage, a feasible measure to increase a fresh water lens in creek deposits

Pieter S. Pauw¹, E.S. van Baaren¹, M. Visser¹, P.G.B. de Louw¹ and G.H.P. Oude Essink¹
1 Department of Groundwater Management, Deltares, Utrecht, The Netherlands

ABSTRACT

A new artificial recharge measure to expand a fresh water lens in creek ridge deposits is presented. Creek ridges are common in the southwestern part of the Netherlands, and the freshwater lenses are used intensively here for irrigation. The measure is based on a controlled level drainage system, which is used to infiltrate fresh surface water in the creek ridge and at the same time keeping the groundwater level as high as possible. Field measurements in combination with numerical modelling were used to study the feasibility of the measure just north of the village Serooskerke.

INTRODUCTION

The south-western part of the Netherlands is a deltaic area where large areas lie at or below mean sea level. The shallow hydrogeological system in these areas can be characterized by a 1 – 5 m thick semi-confining layer overlying a 10 - 40 m thick aquifer (Goes et al. 2009, De Louw et al. 2011). The semi-confining layer consists of fine sand, clay and peat deposits and is incised by tidal channel and gully deposits (Figure 1). The tidal channel and gully deposits appear as elevated ridges in the landscape, and are referred to as ‘creek ridges’.

Beneath the creek ridges, a fresh water lens is present with a maximum thickness between 5 and 30 meters. The lens is important for irrigation in the area, as the majority of the groundwater and the surface waters are saline and there is little transport of fresh water from other areas (De Louw et al. 2011). The amount and rate of fresh water extraction is regulated by the authorities to prevent excessive drawdown and to prevent saltwater upconing. As a consequence, the irrigation demand exceeds the extraction limits in long dry periods, which leads to crop damage. This problem is expected to increase in the future due to the anticipated sea level rise, climate change and land subsidence (Oude Essink et al. 2010). Therefore, countermeasures are likely needed to assure a sustainable and robust fresh water supply.

In this paper, a new measure is presented to expand the fresh water lens in a creek ridge, just north of the village Serooskerke (Figure 1). The measure is based on controlled level drainage, which is used to infiltrate fresh surface water and at the same time keeping the groundwater level as high as possible. The feasibility of the measure is studied using field measurements and numerical modelling.

METHODS

A controlled level drainage system (Figure 1) was installed in April 2013. Various measurement techniques were used to determine the hydraulic head variation and groundwater salinity distribution at site, prior to the installation of the measure. Since April 2013, geophysical measurements and chemical sampling are used to study the effect of the controlled level drainage on the fresh water lens.

In addition to the field measurements, a numerical model was constructed using SEAWAT (Langevin et al., 2008). The purpose of this model was to determine the long-term effects of the measure on the freshwater lens.

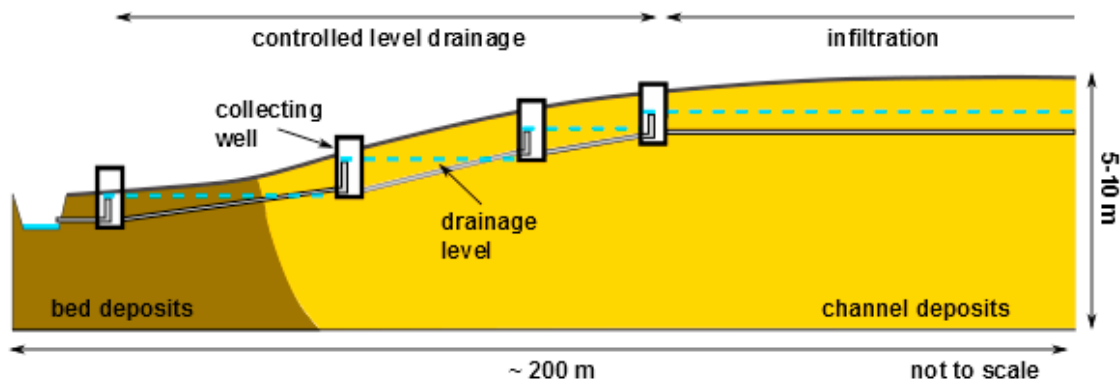


Figure 1: concept of controlled level drainage in a creek ridge.

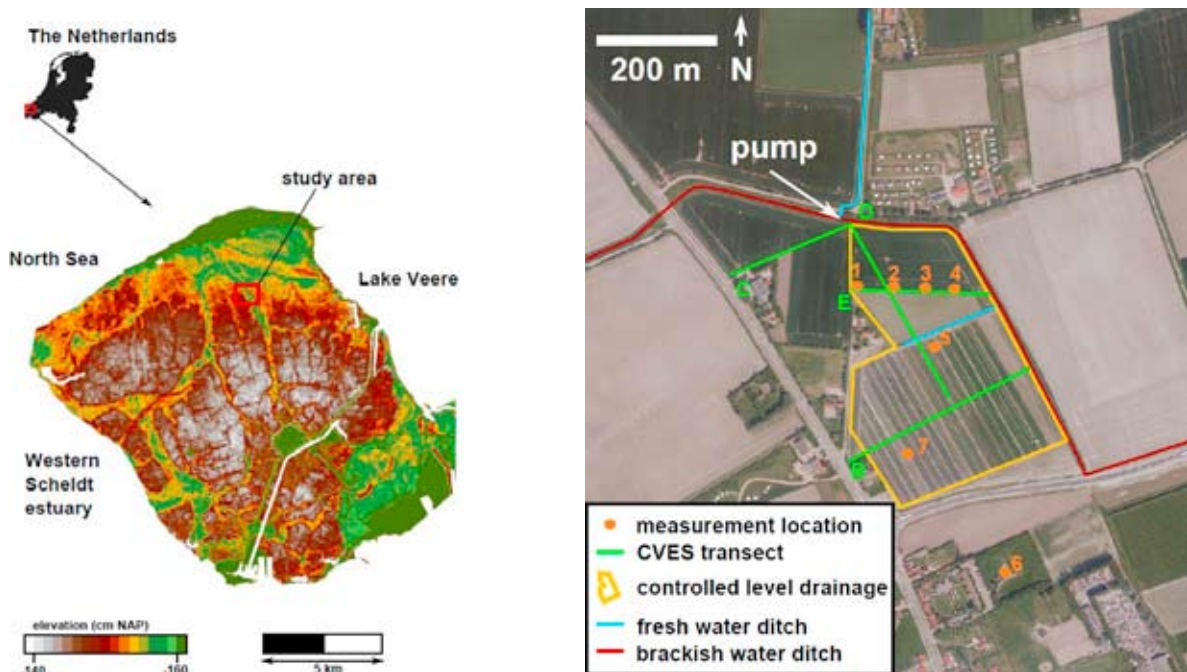


Figure 2: Left: Study area where the controlled level drainage has been installed. Right: Overview of the controlled level drainage area, the most relevant brackish and fresh water ditches and the measurement locations.

RESULTS

For brevity of this paper, only the results of the sampling are given here. Six piezometers using 40 cm screens at several depths were used to sample the groundwater at measurement location 1 (Figure 2). Figure 3 shows the electrical conductivity (EC) of the groundwater in September 2013 (prior to the infiltration) and February 2014 (during the infiltration). The data shows a decrease of the fresh-saline transition zone of about 1.5 m. A reference measurement at a location where the controlled level drainage was not installed, showed a decrease of the fresh water lens of about 0.1 m during this period.

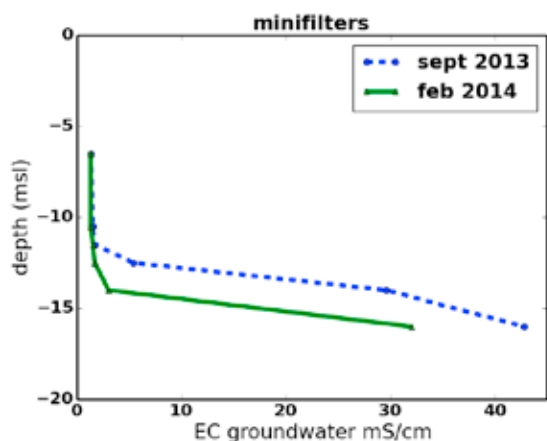


Figure 3: Results of the groundwater sampling at measurement location 1 (Figure 2).

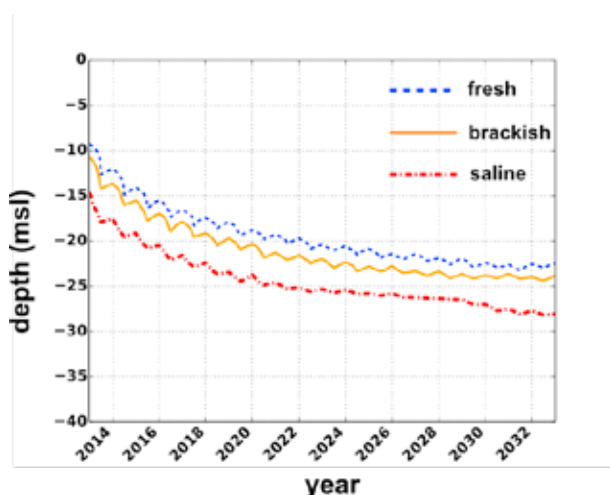


Figure 4: Result of the numerical model which was used to estimate the long-term effect of the measure. The blue, orange and red lines indicate the 1000, 5000 and 10000 mg l^{-1} Chloride contour. Chloride is used as a representative proxy and varies between 0 (fresh water) and 18630 mg l^{-1} (sea water).

The numerical model indicates that the measure leads to a significant expansion of the fresh water lens in the creek ridge on the long term. During the infiltration period (half a year) the transition zone lowers. During the following dry period, the transition zone depth recovers only a slightly. The net result over the year is an expansion of the fresh water lens.

DISCUSSION AND CONCLUSIONS

The controlled level drainage system is intended to be used as a relatively easy and cheap measure to increase the fresh water lens in creek ridge deposits. The advantage of the method is that the expansion of the lens does not occur locally, but along the total area where the groundwater level is increased by controlled level drainage. The disadvantage is that it takes a relatively long time before the expansion of the lens is realized. The expansion of the fresh water lens contributes to a larger freshwater (safe) yield from the lens, but this was not further quantified.

REFERENCES

De Louw, P.G.B., Eeman, S., Siemon, B., Voortman, B.R., Gunnink, J., Van Baaren, S.E., Oude Essink, G.H.P., 2011. Shallow rainwater lenses in deltaic areas with saline seepage. *Hydrol. Earth Syst. Sci.* 15, 3659–3678

Goes, B. J. M., Oude Essink, G. H. P., Vernes, R. W., and Sergi, F., 2009: Estimating the depth of fresh and brackish groundwater in a predominantly saline region using geophysical and hydrological methods, Zeeland, the Netherlands, *Near Surf. Geophys.*, 7, 401– 412,

Langevin, C.D., Thorne, D.T., Dausman, A.M., Sukop, M.C., Guo, W., 2008. SEAWAT Version 4: a computer program for simulation of multi-species solute and heat transport: U.S. Geological Survey Techniques and Methods. Book 6, 39pp (Chapter A22).

Oude Essink, G. H. P., Baaren, E. S., and de Louw, P. G. B., 2010: Effects of climate change on coastal groundwater systems: A modeling study in the Netherlands, *Water Resour. Res.*, 46,

Contact Information: Pieter S. Pauw, Deltares en Wageningen University and Research. Department of Groundwater Management. Utrecht, The Netherlands. Email: pieter.pauw@deltares.nl

Groundwater salinity patterns at the land-ocean boundary of the Netherlands

Pieter S. Pauw⁵, M.M.A. Groen¹, J. Groen^{1,2}, K.J. van der Made³ and V.E.A Post⁴

¹ Critical Zone Hydrology Group, VU University, Amsterdam, The Netherlands

² Acacia Water, Gouda, The Netherlands

³ Wiertsema & Partners, Tolbert, The Netherlands

⁴ School of the Environment, Flinders University, Adelaide, Australia

⁵ Department of Groundwater Management, Deltares, Utrecht, The Netherlands

INTRODUCTION

Understanding the land-ocean boundary of coastal aquifers is of key importance to investigate submarine groundwater discharge and salt water intrusion. The characterization and specification of boundary conditions at the coast is also a critical step in constructing groundwater flow models. While many previous studies have significantly improved our understanding of the land-ocean boundary of unconfined aquifers, relatively few studies have focused on confined systems. For confined aquifers, the land-ocean boundary essentially differs from a phreatic aquifer, as fresh groundwater flow continues below the seabed instead of terminating at the shore (Figure 1).

Because direct observation in the offshore more difficult, more expensive and considered less relevant compared to onshore investigations, much less is known about the interaction between groundwater and coastal waters in confined systems than in unconfined systems. In particular, relatively little documented cases of these systems have been described in literature.

The objective of our study was to expand the number of documented cases of confined aquifer systems with data from the Netherlands. We have investigated groundwater salinity patterns at the land-ocean boundary along the North Sea coast using electrical resistivity cone penetration test (ER-CPT) measurements. With this method, a probe with a conical tip is pushed into the ground which measures penetration resistance, friction, pore water pressure and the electrical resistivity of the subsurface. In this paper, we illustrate two ER-CPT measurements that were taken in the intertidal area.

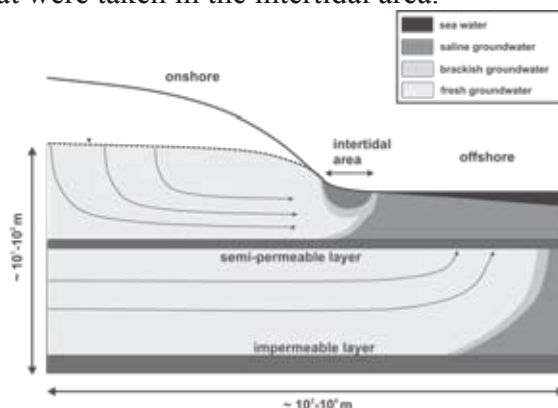


Figure 1. Concept of a confined coastal aquifer. Note that this figure is not at scale and that the freshwater tongue may extend much further below the seabed.

METHODS

During an electrical resistivity cone penetration test (ER-CPT), a 3.6 – 4.4 cm diameter probe is pushed into the subsurface by a heavy truck (Figure 2). The tip of the probe consists of a cone where the cone resistance (qc) is measured. Just after the cone, at the sides of the probe, the sleeve friction (fs) is measured. The ratio of qc and fs , the friction ratio (R_f), is often used to in combination with qc to estimate the lithology:

$$(1) \quad R_f = \frac{fs}{qc} \cdot 100\%$$

High values of R_f in combination with low values of qc indicate fine grained and clayey materials, whereas the opposite combination is characteristic for sands (Lunne, 1997). In addition to the cone resistance and the sleeve friction, the pore water pressure (u) can be measured. In low-permeable sediments u is usually different than in aquifers. More detailed information about the measurement of qc , fs and u , including soil classification based upon these data, can be found in Lunne (1997).

Within a few decimeters from the cone, the electrical resistivity of the subsurface (ρ_s) is measured using two or four electrodes. In clay-free sediments, ρ_s can be related to the electrical resistivity of the fluid (ρ_f) using Archie's Law (Archie, 1942). ρ_f can be used to estimate the salinity.



Figure 2. ER-CPT measurement in the intertidal area.

RESULTS

Figure 3 shows the results of two ER-CPTs. 73H was taken in the higher part of the intertidal area. The Rf and u values indicate multiple low-permeable layers. The ρ_s values indicate that fresh groundwater is present until -40 m mean sea level (msl). 71H was taken in the lower part of the intertidal area (i.e., below msl). Here, the Rf and u values also indicate multiple low-permeable layers. The ρ_s values indicate that from the surface to -17 m msl, the groundwater is saline to brackish. Fresh groundwater is present between -17 to -30 m msl, and is likely confined by a low-permeable layer. Below -30 m msl the groundwater salinity increases again.

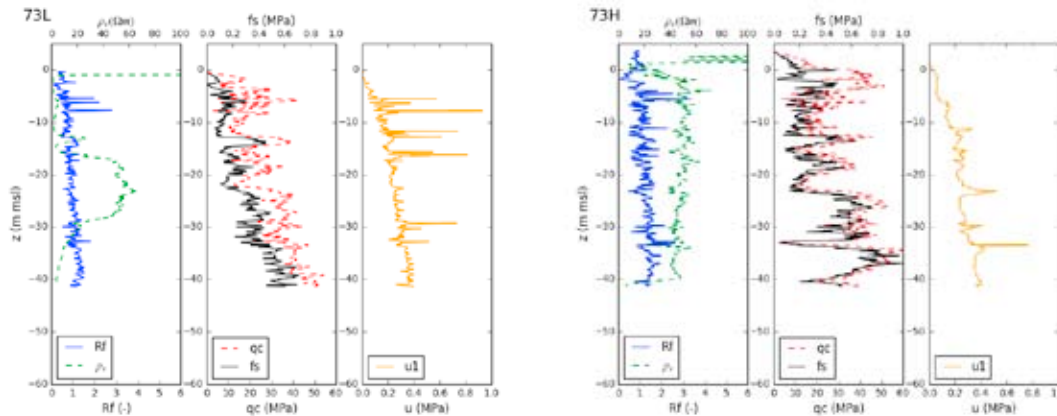


Figure 3: ER-CPT measurements in the intertidal area near Zandvoort.

These observations illustrate the complex heterogeneity and salinity patterns below the intertidal area near Zandvoort aan Zee, which raises questions about the governing groundwater flow processes but also gives valuable information for constructing a groundwater flow model. The section of fresh groundwater indicated in 73L may be part of an offshore discharge component of the fresh coastal dune groundwater flow system, or paleowater (i.e., not the result of the current hydrological boundary conditions). In all other ER-CPT measurements that were taken along the coast of the Netherlands in this study (not shown here), we observed a fresh water tongue in the lower part of the intertidal area. This suggests that in similar heterogeneous aquifer systems, fresh water tongues extending some distance below the seabed are rule rather than exception.

REFERENCES

- Archie, G.E. 1942. The electrical resistivity log as an aid in determining some reservoir characteristics. Transactions of the American Institute of Mining and Metallurgical Engineers 146: 54–61.
- Lunne, T., Robertson, P.K. and Powell, J.J.M. 1997. Cone Penetration Testing in Geotechnical Practice. –Blackie Academic & Professional, London, 312 pp.

Salt Water Intrusion Monitoring in Coastal Aquifers from High Frequency Downhole Hydrogeophysical Observatories

P.A. Pezard^{1,4}, P. Gouze¹, H. Perroud^{1,2}, J. Lofi¹, N. Denchik¹, G. Henry^{1,4}, M. Geeraert¹, D. Neyens³, J.-P. Bellot³, A. Levannier⁴

¹Géosciences Montpellier, Université de Montpellier, France (ppezard@gulliver.fr)

²Université de Pau et des Pays de l'Adour, Pau, France

³imaGeau, Cap Alpha, Clapiers, France

⁴Schlumberger, Montpellier, France

ABSTRACT

In a context of rapidly growing demography, increasing industrial and agricultural pressure and global climatic warming, coastal aquifers are increasingly subjected to overexploitation and associated sea water intrusion. This phenomenon is particularly acute in semi-arid region such as mediterranean countries and islands, where most coastal aquifers are exposed, especially in the vicinity of metropolitan areas. In order to protect and preserve the long term heritage constituted by this groundwater resource, new aquifer monitoring technologies have been designed and tested in France over the past ten years.

Initially as part of the EC-funded *ALIANCE* project (FP5-2002/2005), a new kind of near-field, high frequency downhole hydrogeophysical observatory was designed, constructed and set-up at a series of coastal sites chosen as representative of typical geological contexts, hydrological regimes and human impact. These new downhole methods were conceived for long-term *in-situ* monitoring and prevention of sea water and brine intrusions in coastal aquifers. The principle of this now called *Subsurface Monitoring Device* (or else "SMD") observatory designed to last over several years is based on the high-frequency (such as daily) probing of the formation electrical resistivity, temperature, pressure and fluid chemistry around a borehole or nearby boreholes. For so-called "real-time" subsurface management, this device is aimed at producing accurate near-field boundary conditions to reduce uncertainties in models, and thereby contribute to the decision-making process for endangered aquifer management. At present, the system is being applied to groundwater management, risk management in the context of salt water intrusion in coastal aquifers or fresh water storage and recovery in shallow brackish aquifers.

Over the past few years, this approach has produced downhole time-depth images extending now over more than two years, revealing details of subsurface dynamics in the context of salt water intrusion in exploited coastal aquifers (Maguelone, Hossegor, Coutières, Barcarès and Marana, France) or the storage of fresh water in shallow saline aquifers (Serooskerke, Holland). These resistivity images, once converted into pore fluid conductivity or salinity not only reveal the details of aquifer quality changes over depth and time, but also provide access to the maximum amount of fresh water that might be extracted over time, yielding a novel way to exploit coastal aquifers and, in the end, reach an increased sustainability of this often essential and sometimes endangered coastal resource.

Keywords: hydrogeophysical observatories, electrical properties, downhole monitoring, coastal aquifer, salt water intrusion.

INTRODUCTION

Over 50 % of the accessible water at or near the Earth surface is over-exploited due to human activities. Groundwater is particularly at risk in urban or semi-arid areas, with the maximum danger in coastal zones where more than 60% of the world population is concentrated. As the main source of drinking water, this strategic but vulnerable resource is of utmost importance. While the physical processes associated with salt-water intrusion are still being discussed, more field data are needed to assess the predictive models developed for management and vulnerability assessment of groundwater resources in coastal environments.

For this, a set of new hydrogeophysical tools, methods and scientific approaches was developed, and tested as part of the ALIANCE research project to obtain an improved description of aquifer and fluid parameters in the subsurface. In particular, a new permanent downhole method was designed for long-term (over several years) *in-situ* monitoring and prevention of brine intrusion in coastal aquifers. The principle of the observatory is based on the high-frequency (such as daily and at meter-scale) probing of the aquifer electrical resistivity around a borehole. The objective was to improve groundwater sustainability and quality in coastal and semi-arid environments. In particular, the slow renewal of groundwater enhances the need for long-term management tools. Precise monitoring is thus also needed to develop, test and validate new models needed to assess and plan ahead aquifer vulnerability, thereby linking exploration, monitoring, modelling and management facilities.

Finally, the cornerstone of the ALIANCE project was the setting-up of field in-situ facilities for experimentation and long-term monitoring. At Maguelone located 10 km south of Montpellier (France) along the mediterranean shoreline, one of the three new ALIANCE coastal experimental sites was developed for instrumental purposes. Limited to the north by the Prevost coastal lagoon and to the south by the Mediterranean shore, this site offers a natural laboratory to study clastic and clay-rich coastal reservoirs saturated with saline fluids.

After the deployment of a first prototype in 2004 as part of ALIANCE, the field experiments at Maguelone expanded to test at shallow depth new electrical instruments designed by IMAGEAU for deeper deployment in the context of CO₂ geological storage projects. Among 5 new holes drilled for this at Maguelone, two of them were fully cored for geological and petrophysical studies. Together with downhole geophysical logs, these measurements are the basis of a calibration of resistivity data into pore fluid salinity data.

METHODS

Inversion of electrical resistivity in terms of "NaCl equivalent" pore fluid salinity

The electrical resistivity R_o of a porous media can be written as a simple product of the electrical formation factor F by the resistivity R_w of the pore fluid (in $\Omega.m$). After Archie (1942), the electrical formation factor F is related to porosity by :

$$F = \emptyset^{-m} \quad (1)$$

with \emptyset for porosity and m as a connectivity term for porosity depending on pore shape, and varying from about 1.3 to 2.5. A mean value of $m=2.0$ is often used in the absence of sufficient core measurements. In terms of conductivity, we have to the first order :

$$\frac{1}{R_o} = C_o = \frac{C_w}{F} \quad (2)$$

with C_o for porous media conductivity and C_w for pore fluid conductivity (both in mS/m). When surface conduction cannot be neglected with respect that of the electrolytic conduction term (with clays, in particular), a more complete model (Waxman & Smits, 1968) integrating surface conductivity term (C_s) is needed with :

$$C_o = C_w / F + C_s \quad (3)$$

The surface conductivity term (C_s) is related to the circulation of cations within the double or "Gouy" layer in relation the cation exchange capacity (CEC) of the minerals. The CEC equates to the number of mobile cations in the pore space per unit mass, expressed in meq/100 g (or cmole/kg). Per unit volume, the CEC is called Q_v (expressed in eq/L = 96 320 C), with:

$$Q_v = \frac{(1 - \emptyset)}{\emptyset} \cdot \rho_m \cdot CEC \quad (4)$$

where \emptyset is porosity and ρ_m is grain density (in kg/m³). The surface electrical conductivity becomes then, after *Revil et Glover (1998)* :

$$C_s = \frac{2}{3} \cdot \rho_m \cdot \beta_s \cdot CEC \quad (5)$$

where β_s accounts for cations mobility in the external part of the double layer and is equal to $0,51 \cdot 10^{-8} \text{ m}^2 \cdot \text{s}^{-1} \cdot \text{V}^{-1}$ for a NaCl solution. If the surface conductivity is measured on core and compared to potassium (K) amount used here as an empirical proxy for clay content in the sediment, a regression relating the two can be derived with, for the Maguelone site :

$$C_s = (0.48) K - (31.7) \quad (6)$$

leading to the possibility to derive a continuous downhole log for the surface conductivity C_s from the potassium profile derived from spectral natural gamma radioactivity. Once F computed on the basis of any porosity log such as that obtained from P-wave velocities (*Wyllie et al., 1956*), the pore fluid conductivity C_w is obtained from :

$$C_w = (C_o - C_s) \cdot F \quad (7)$$

and the pore fluid salinity can be derived for a NaCl solution after *Guéguen et Palciauska (1992)* from :

$$\text{Ln}(s) = (0.97) \text{Ln}(C_w) - 4.88 \quad (8)$$

RESULTS

At Maguelone (France), the resistivity data inversion in terms of downhole pore fluid salinity reveals the presence of salt water intruding into a 3 m-thick permeable aquifer at about 15 m depth with, below that, a diffusion profile in mostly clay-rich sediments with rare sandy and permeable layers saturated with fresh water. In the absence of m values for pore connectivity, two profiles are presented ($m=1.5$ and 1.8 ; *Figure 1*), almost overlapping which underlines the low impact of m on the inversion, generally is in good agreement with pore fluid samples taken from a multi-packer Westbay completion from Schlumberger (*Figure 1*).

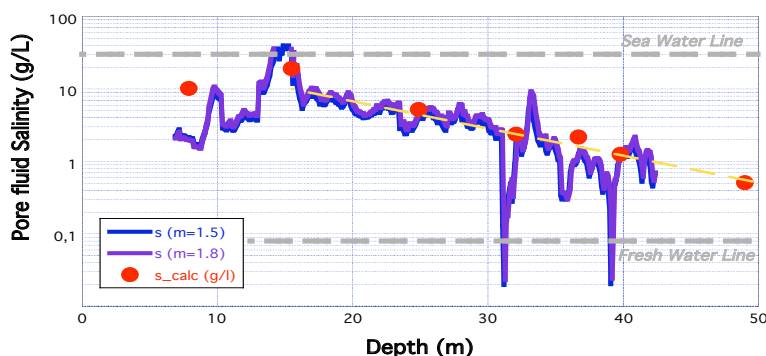


Figure 1. Pore fluid salinity profiles derived from downhole electrical resistivity data inverted after calibration from cores and logs, and compared to salinities measured from downhole fluid samples.

DISCUSSION AND CONCLUSIONS

In summary, this new hydrogeophysical approach provides a high resolution means to follow at decimeter to meter scale the changes over time in pore fluid composition along a downhole section. This constitutes the basis to set-up a permanent monitoring strategy from in-situ, high frequency, autonomous observatories such as that of imaGeau (*Figure 2*).

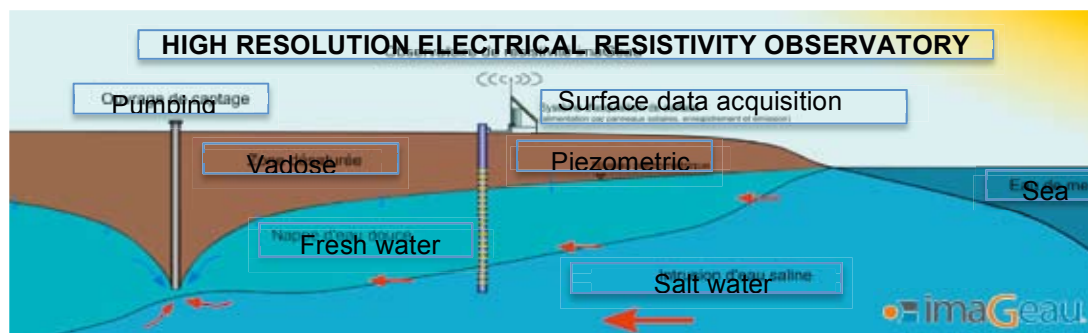


Figure 2. Salt-water intrusion high-frequency field monitoring set-up and principle from SMD downhole electrical resistivity observatory (sketch provided by imaGeau).

Over the past few years, this approach has produced downhole time-depth images extending now over more almost a year (Figure 3), revealing details of subsurface dynamics in the context of salt water intrusion in exploited coastal aquifers (Hossegor, Coutières, Barcarès and Marana; France) or the storage of fresh water in shallow saline aquifers (Serooskerke; Holland). These resistivity images, once converted into pore fluid conductivity or salinity not only reveal the details of aquifer quality changes over depth and time, but also provide access to the maximum amount of fresh water that might be extracted over time, yielding a novel way to manage coastal aquifers and, in the end, reach an increased sustainability of this often essential and sometimes endangered coastal resource.

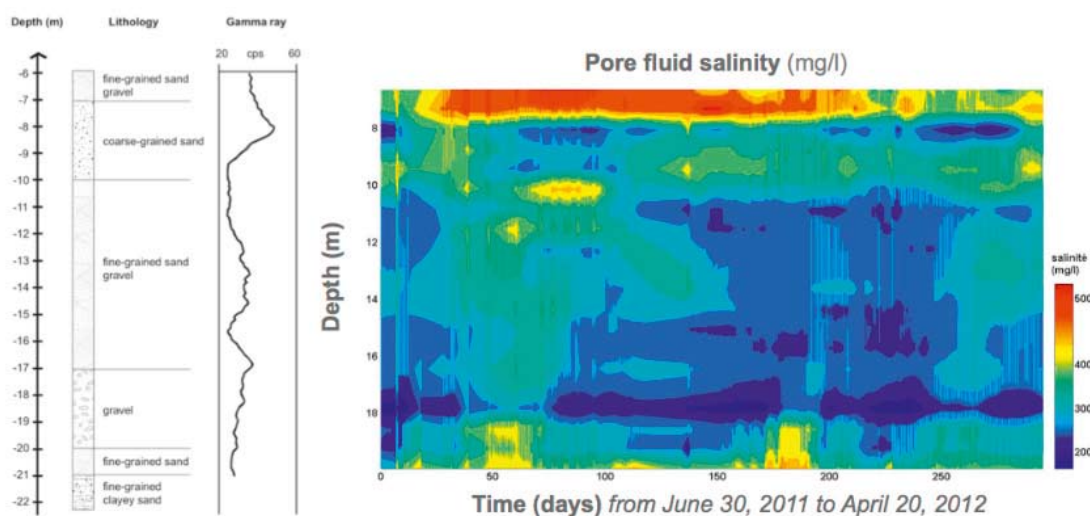


Figure 3. Time-depth image of pore water salinity at Hossegor (SW France) for 300 days. Brackish water is detected above 8 m and isolated from the city aquifer by a clay layer (below). The high-frequency SMD monitoring data reveal not only seasonal changes in water quality but also, with vertical stripes, the impact of city pumping from a nearby well located 6 m from the SMD.

REFERENCES

- Archie, G.E. (1942). "The electrical resistivity log as an aid in determining some reservoir characteristics". *Petroleum Transactions of AIME* **146**: 54–62.
- Guéguen et Palciauska, 1992. Introduction à la physique des roches, pp. 192.
- Revil et Glover, 1998. Nature of surface electrical conductivity in natural sands, sandstones, and clays, *Geophysical Research Letters*, 25, 5, 691–694.
- Waxman, M.H. and Smits, L.J.M. (1968). "Electrical conductivities in oil-bearing shaly sands". *SPE Journal* **8** (2): 107–122.
- Wyllie, M.R.J., Gregory, A. R., and Gardner, L. W., 1956. Elastic wave velocities in heterogeneous and porous media. *Geophysics*, 21, 41–70.

Technical aspect relating to salt groundwater intrusion problem in coastal provinces in IGPVN project

Hoang Dai Phuc

IGPVN Project

National Center for water resources Planning and Investigation

85 Nguyen Chi Thanh street, Dong Da District, Ha Noi capital, Viet Nam

ABSTRACT

This article presents the technical work related to the research, forecasting, assessing salt groundwater intrusion in aquifers through operating monitoring networks in coastal provinces, Nam Dinh, Quang Ngai and Soc Trang in IGPVN project. The monitoring networks were designed in accordance with geological, hydrogeological features and groundwater extraction status in each province to monitor the variation in the quality and quantity of groundwater over time. The salt groundwater intrusion in these provinces were monitored by CTD-Diver that can measured electrical conductivity (EC) installed in monitoring wells located nearby salty boundaries of aquifers. The increase or decrease of EC values in these monitoring wells allow us to access about dynamic and movement speed of salty boundaries over time. The sampling task in monitoring wells were performed two times a year to identify changes in groundwater quality, in addition C_{14} and isotopic samples were taken also to determine the age of groundwater and relationship between groundwater and surface water. Initial monitoring results had reflected the relationship between groundwater and surface water, the influence of factors such as rainfall, groundwater extraction on the dynamic of groundwater in general and the movement of salty boundaries in particular.

INTRODUCTION

The recent growth of both population and economy in Viet Nam is based on the extensive exploitation of available water resources. Since surface water is vulnerable and increasingly affected by climate change, untreated sewage water and industrial waste water, freshwater aquifers will become the major resource for the future water supply of Viet Nam. Sustainable management of this finite resource is essential to life, development and environment. Against this background, Improvement of Groundwater Protection is essential for social and economic development of Viet Nam and, therefore, the major objective of the IGPVN project. Initially, the activities are focused on the coastal provinces in Viet Nam. One of the topics is defined to be of major concern for Viet Nam is Groundwater sanitization by seawater intrusion that was studied by different technical activities in each province. These technical activities had been executed in building process of monitoring networks and in monitoring process, as follows:

Groundwater monitoring Networks

Nam Dinh, Quang Ngai and Soc Trang are coastal provinces in IGPVN project that were installed groundwater monitoring networks. The locations of the monitoring wells have been chosen by the IGPVN Project based on geological and hydrogeological characteristics of provinces, following the criteria listed below:

Hydrogeological: access aquifers most relevant for water supply, complement existing monitoring sites with respect to spatial heterogeneity of aquifers.

Logistical: availability of public land, accessibility by heavy vehicle (drilling, sampling, pumping test), absent groundwater extraction in vicinity.

Economical: available budget limits the density of the monitoring network.

Monitoring wells were drilled by rotary drilling method and PVC pipe/casing, the screen slot width is 0.3 mm.

The monitoring wells were equipped with Mini-Divers, Cera-Divers and CTD-Divers to measure water level automatically.

CTD-Diver is capable of measuring the electrical conductivity of the water and it is usually installed in the fresh-salt boundary of aquifer to track water quality change.

Cera-Diver is commonly used in water with TDS from 0,8 to 1 g/l.

Mini-Diver often used in fresh water wells.

Monitoring wells and divers are usually checked every three months; the broken divers are to be replaced with the new divers right away. The salty intrusion in aquifer will be monitored by the changing of EC value that measured by CTD divers. This thing is very helpful for groundwater management in controlling groundwater quality.

Well logging

Geophysical well logging has been carried out in IGPVN monitoring wells and especially the induction well logging data provide further insight to this issue. The well logging was done before casing to determine the best position for screen, this process also determine the salinity of groundwater in formation so we can decide install the well or not. Otherwise the induction well logging has been carried out in Nam Dinh in 03/2010 after casing and the results were showed the difference of formation conductivity in depth.

Other activities

Beside the technical activities in drilling process, the groundwater sampling campaigns are also organized two times a year (March and November) to collect the groundwater samples in monitoring wells to assess the groundwater quality over time.

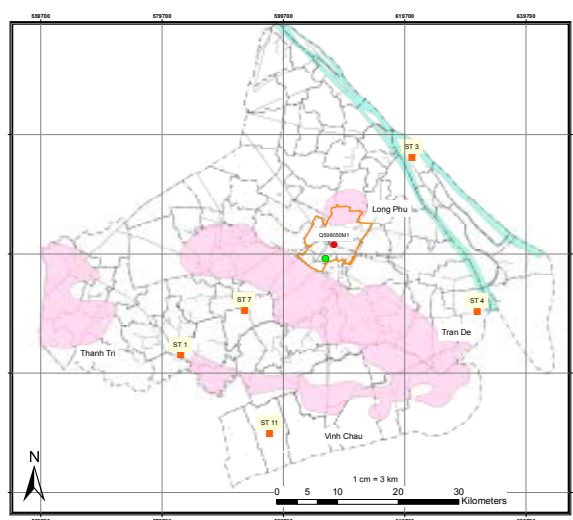


Figure 1. Monitoring wells and fresh - salt boundary in Soc Trang province.

RESULTS

Monitoring data in province has show the changing of EC value but these changes are different in each province because of the different in groundwater dynamic. In Quang Ngai, EC value of groundwater has the inverse trend in comparison with groundwater level, when

groundwater level come down, the EC value of it come up. It is can be explained by the good relationship between groundwater and surface water or even sea water.

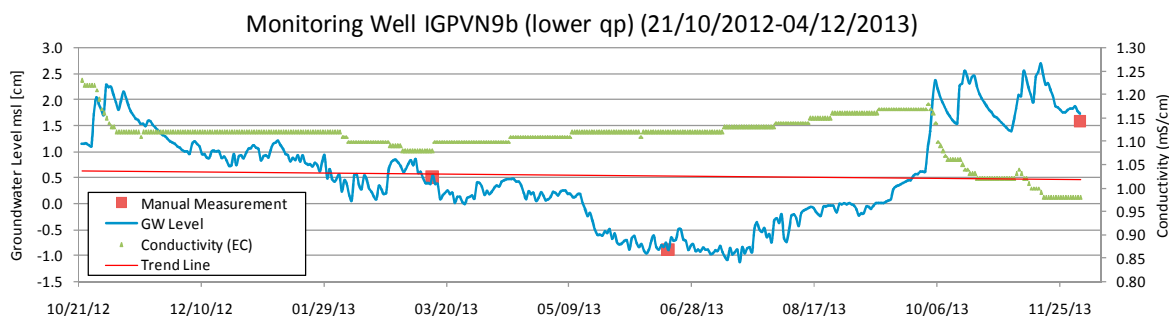


Figure 2. Graph of monitoring data in monitoring well IGPVN9b (Quang Ngai province).

In Nam Dinh province, the map about salinity groundwater was establish based on archive data from field survey of domestic household wells during rainy and dry season 1999 and 2000, collected by Hoang Duc Nghia 2008, together with data of IGPVN project from May 2010 and the salinity boundary determined in frame of the hydrogeological mapping (Do 1996b) and by geomagnetic and georadar studies in 2009 (Nguyen Van Dan et al. 2009).

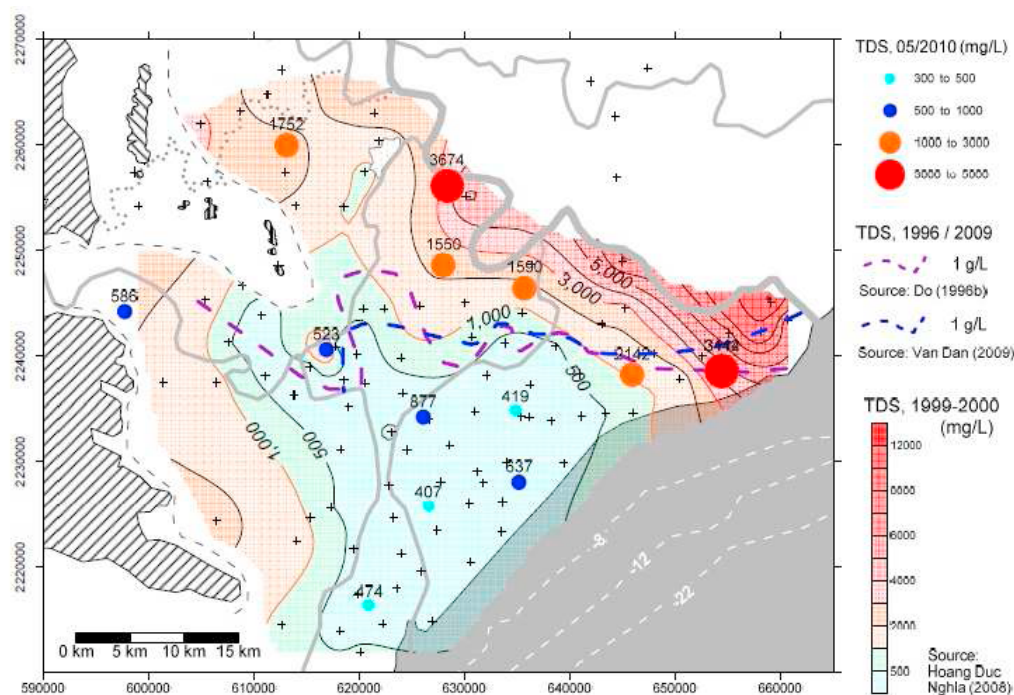


Figure 3. Salinity distribution map (TDS) in qp pore water, based on data from IGPVN monitoring wells in May 2010 (colour symbols, TDS in mg/L).

Indicate locally increasing salinity, such as in E boundary of the freshwater lens . Observations do not confirm brackish qp pore waters in W Nam Dinh suggested by archive data however, old as well as new data are limited in that area. The study of Nguyen Van Dan et al 2009 concludes in the mapping of the 1 g/l salinity boundary in qp aquifer based on geomagnetic and georadar studies. This boundary matches well old and new hydrochemical data in the central part, but does not in E as well as in W central area of Nam Dinh.

However, even when these geophysical methods are generally applied for shallow aquifers (< 40 m bgl), the applied modifications and the accuracy of the results are not discussed here. Generally, the transition between fresh and brackish pore waters is assumed to be quite sharp. Therefore, continuous monitoring of the transition area is necessary to quantify the movement of the salinity boundary.

Also in Nam Dinh, the results from induction logging were used to make cross sections. Figure 4 shows section crossing qp and n aquifer with fresh pore water in SW part up to brackish pore water in the NE. Four formation conductivity depth profiles are plotted for stations Q228, Q227, Q226 and Q225, derived from induction logging data. The plots are interpreted here to represent salinity profiles. Even in low saline formations changing clay content, indicated by natural gamma and confirmed by lithological description, shows only minor impact to the formation conductivity. Consequently, high conductive Holocene formations indicate the existence of high saline pore waters in the Holocene Thai Binh and Hai Hung formations. These formations mainly consist of marine fine grained sediments with high silt and clay content, occasionally intercalated with sandy layers.

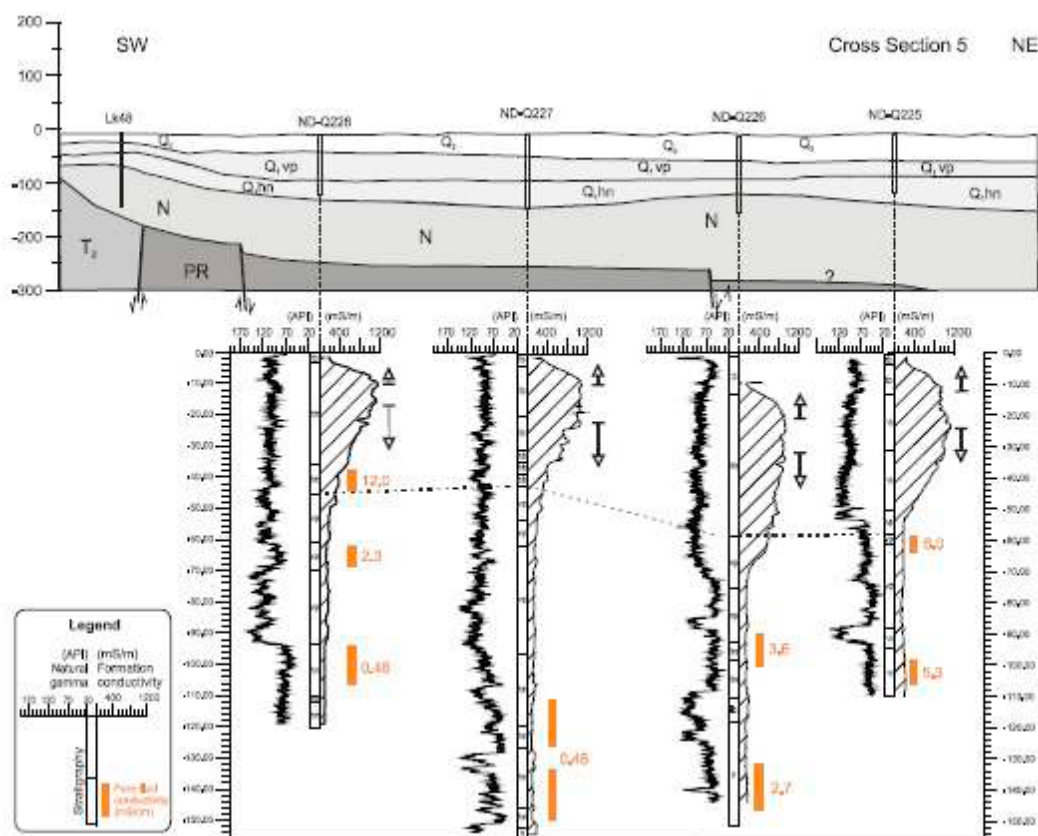


Figure 4. Cross section in Nam Dinh province showing depth profiles of natural gamma (API) and the formation conductivity (mS/m) measured by induction logging.

The shape of the formation conductivity profiles provide further insight into vertical movement of saline pore waters when interpreted as typical diffusion profiles. Since advection may be neglected in fine grained sediments, diffusive transport is the dominant transport process driven by the specific concentration gradient. Diffusion profile with asymmetrical shape and a long slope downwards is found in Q228 and Q227 representing a high concentration gradient to the underlying pore waters. The more symmetrical shape in Q225 stands for a lower salinity gradient of the pore waters from Holocene to Pleistocene

formations. Since diffusive transport in clay formations requires a stable concentration gradient in a long term, very low saline pore water in qp (and n) unit in SW Nam Dinh already must have existed during the Holocene marine transgression time if not much earlier. Thus, downward and, in a lesser extent, upward diffusion is believed to be the main driver of salinity (Na-Cl) transport, indicated by arrows. This explains the existence of brackish aquifers not only in qh1 and qh2 but also in deeper qp and n aquifers. The fresh water aquifer in S and W Nam Dinh only exists due to the continuous side flow of fresh groundwater flushing saline waters to the East as well as coastward. Thus, increasing groundwater abstraction threatens to interrupt or even inverse the flushing process.

DISCUSSION AND CONCLUSIONS

- Groundwater monitoring networks were operated quite well in three years in Nam Dinh province and nearby one year in Quang Ngai and Soc Trang provinces, monitoring data have shown the status about groundwater resource in aquifers in which include salty intrusion based on the data of CTD divers.
- The relationship between the changing of EC value and groundwater level is different in different area, it reflects the relationship between groundwater and surface water especially in shallow coastal aquifers.
- CTD divers in monitoring wells nearby salt-fresh boundary played an important role in monitoring the salty intrusion in aquifers.
- The results from induction logging is very important in groundwater exploration, at the same time these conductivity data of formations will be used to calculate the conductivity of groundwater in aquifers. The resulting pore water salinity profile has to be taken with care in the diffusion model helps to understand and quantify sanitization processes in Nam Dinh as a basis for future numerical modeling of salinity intrusion processes.

REFERENCES

- Frank Wagner, Dang Tran Trung, Hoang Dai Phuc and Faulk Lindenmaier. 2011. Assessment of Groundwater Resources in Nam Dinh province, Final technical report. No
- Hoang Dai Phuc, Pham Thi Thu. 2013. Technical report 31, Checking monitoring wells and downloading data from Diver in Quang Ngai province.

Hydrogeological model of a complex coastal aquifers: the case of Sibari Plain (Southern Italy)

De Rosa R.¹, Romanazzi A.², Apollaro C.¹, Cianflone G.¹, Dominici R.¹, Vespasiano G.¹, Molinari P.³, Polemio M.²

1. DiBEST, Univesità della Calabria, Rende (CS) - Italy

2. CNR-IRPI, Bari (BA) – Italy - m.polemio@ba.irpi.cnr.it

3. Agriconsulting, Roma - Italy

ABSTRACT

The increasing overexploitation of water resources is observed on a global scale in the previous decades; this trend involves the coastal regions of Mediterranean Basin (Van Beynen et al., 2012). As an effect of increasing groundwater withdrawals from coastal aquifers, the phenomenon of seawater intrusion is becoming a serious problem for most of the coastal aquifers, especially in the Mediterranean area. The aim of this paper is to present the modeling of a coastal porous aquifer located in the plain of Sibari (Southern Italy). The model was implemented using piezometric historical data to establish the effect of seawater intrusion, since the well discharge was negligible (natural conditions) to the anthropogenic modification in subsequent decades, to be used for forecasting purpose and for evaluate the evolution of groundwater resource.

GEOLOGICAL AND HYDROGEOLOGICAL CONTEXT

The Sibari Plain is located in Northeastern Calabria Region and represents the most recent and northern sector of the Crati Basin (N-S tectonic valley controlled since Middle Pleistocene by normal faults). The evolution of Sibari Plain is controlled by NW-SE left strike-slip fault system active since Middle Miocene to Middle Pleistocene (Van Dijk et al., 2000).



Figure 1. Geologic map of Sibari plain and study area.

The Tortonian-Messinian sediments represents the infilling of the Corigliano Basin, a wedge-top depozone located above thrust-sheet of the Calabrian Arc and southern Appennines terranes; it's composed by siliciclastic and evaporitic units passing upward to Pliocenic clays and marls with maximum thickness of 400m. The Pleistocene-Holocene succession, 1000-1500m thick, covers along a discordance surface the previous deposits and it is composed by alternation of sandy-gravelly and marly-clayey deposits. The Miocenic and Pliocenic sedimentary succession shows a lateral variability in thickness due to sin-sedimentary tectonic (Spina et al., 2011). The Holocenic evolution of the middle sector of the Sibari Plain is closely connected to building of the actual Crati Delta started about 6ky BP, which caused the coastal line advancing from the archeological site of Favella della Corte to the actual position covering about 7 km with the development of continental, paralic and coastal environments Study area is about 365 km² for a coastline of about 35 km (Figure 1). The area can be conceptualized into three hydrogeological complexes (from the top): Sand and Clay, Clay and Silt, Sand and Conglomerate, this last constituting the deep confined aquifer, the bottom of which is not well-defined. Shallow aquifer is predominantly fed by direct rainwater infiltration. In fact this aquifer exchanges water with drainage network but the total effect is groundwater feeds the river system of the plain (mainly the Coscile and Crati Rivers). Deep aquifer is fed by outflows of the mountainous aquifers as the case of limestone aquifer of Pollino Mount, and of shallow granitic aquifer of the Sila massif. The maximum piezometric levels of the deep aquifer are equivalent to approximately 40 m a.s.l., so in some areas it presents artesian feature. Water exchanges between the two aquifers are concentrated in the western or inland area, where the thickness of clay complex is lower. Both aquifers are used for irrigation discharge since seventies. On the base of these data conceptual model was achieved (Figure 2).

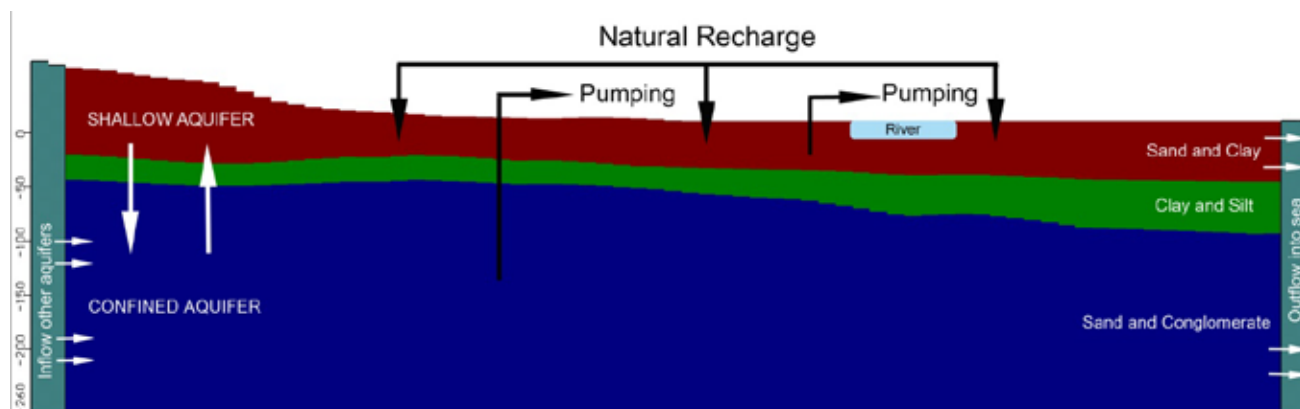


Figure 2. Conceptual model of Sibari plain. Schematic hydrogeological section W-E.

MODEL DEFINITION AND CALIBRATION

The computer codes selected for numerical groundwater modelling were MODFLOW and SEAWAT. The modeled aquifer area was uniformly discretized into a finite difference grid of 97,735 cells of 240 m x 350 m. For the vertical discretization, model was divided into five layers of variable thicknesses, defined on the basis of a multi-methodological geological survey. Climatic, hydrological, and agricultural data were processed to define inputs for the numerical model. As boundary condition CHD cells (Constant Head Boundary) for the coastline and for the west border of Pollino Mount and Sila Massif were used. Modflow River Condition (RIV) was used to simulate Crati and Coscile rivers. The riverbed altitude and the river water height of the main rivers were obtained through on-site surveys. The hydrological assessment of net rainfall and infiltration, using monthly and annual average precipitation and temperature data for the period 1930-1975,

was realized (Polemio et al., 2004; Petrucci and Polemio, 2007; Polemio et al., 2013). Data of 13 rain gauges, three of which were thermometric, were used (Polemio and Casarano, 2004). The rainfall and temperature were determined in each cell using a multiple linear regression as function of altitude. The mean annual rainfall ranges from 620 to 690 mm/y; the mean annual temperature ranges from 14.2 to 17.3°C. Evapotranspiration was determined using Turc method and ranges from 550 to 590 mm/y. Infiltration was calculated using an infiltration coefficient (IC) for each hydrogeological complex. The mean annual recharge, equal to 20 mm/y. Model was calibrated with PEST code with a correlation coefficient equal to 0.91, a RMS equal to 10 and is being validated with nineties years piezometric and concentration datas.

RESULTS AND CONCLUSION

The water balance of both aquifers in natural condition was calculated (Table 1).

<i>Shallow aquifer</i>			
<i>In or recharge</i>	<i>10⁶ m³/y</i>	<i>Output or discharge</i>	<i>10⁶ m³/y</i>
<i>rainfall infiltration</i>	<i>11.6</i>	<i>archaeological area</i>	<i>2.5</i>
<i>leakage from rivers</i>	<i>16.5</i>	<i>discharge for irrigation/drinking</i>	<i>13.1</i>
<i>Inflow from deep aquifer</i>	<i>3.23</i>	<i>outflow into rivers</i>	<i>15.5</i>
		<i>outflow into sea</i>	<i>0.17</i>
<i>Deep aquifer</i>			
<i>In or recharge</i>	<i>10⁶ m³/y</i>	<i>Output or discharge</i>	<i>10⁶ m³/y</i>
<i>Inflow from upward aquifers</i>	<i>71.0</i>	<i>discharge for irrigation/drinking</i>	<i>-</i>
<i>Inflow from shallow aquifer</i>	<i>0.97</i>	<i>outflow into sea</i>	<i>68.69</i>
		<i>outflow to shallow aquifer</i>	<i>3.35</i>

Table 1. Main in/out of the shallow and deep aquifer determined by steady conditions of modeling.

Preliminary results of steady or (almost) natural flow conditions together with the spatial domain of groundwater salinity are now available as the modification up to seventies. A relevant decrease of piezometric surface and increasing effects of seawater intrusion were observed in the shallow aquifer (Figure 3). Low modification of piezometric levels and salinity were observed in the deep aquifer. These preliminary results and next result scenarios will be used together with on-going survey data to assess trend of future groundwater availability and quality.

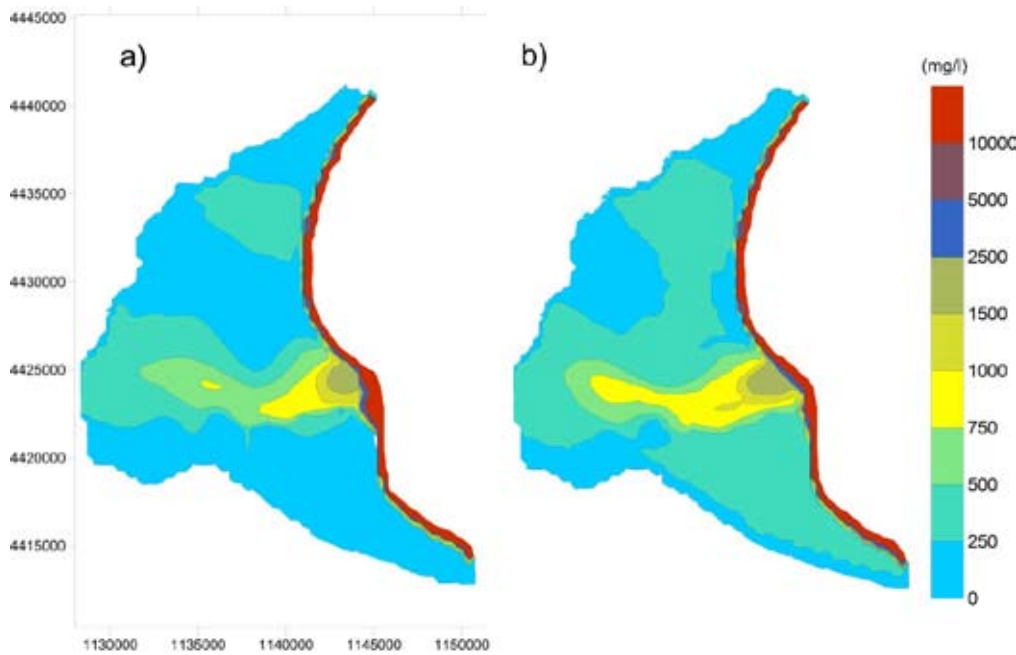


Figure 3. Maps of salinity intrusion of shallow aquifer (historical scenarios) (a) Steady-state simulation (1930s); (b) results of the last year of transient simulation of 1970-79.

ACKNOWLEDGEMENTS

This work is a contribution to the PON Amicus 01_02818 project - "Study of the reduction of pollution and the protection of the coastal environment in selected areas of Calabria".

REFERENCES

- Petrucci, O. and Polemio M. 2007. Flood risk mitigation and anthropogenic modifications of a coastal plain in southern Italy: combined effects over the past 150 years, *Nat. Hazards Earth Syst. Sci.*, 7(3), 361-373.
- Polemio, M. and Casarano D. 2004. Rainfall and drought in southern Italy (1821-2001), in *The Basis of Civilization - Water Science?*, edited by J. C. Rodda and L. Ubertini, IAHS, Roma, Italy. pp. 217-227.
- Polemio, M., Petrucci O. and Gatto L. 2004. Suscettività alla siccità in Calabria ed effetti sulle acque sotterranee, *Atti dei Convegni Lincei*, 204, 245-250.
- Polemio, M., Dragone, V. and Romanazzi, A. 2013. La risorsa idrica. Sfruttamento, depauperamento dei serbatoi sotterranei e utilizzo razionale nel caso della Calabria, in Dramis, F., and Mottana, A., eds., *L'acqua in Calabria: risorsa o problema?: Accademia Nazionale delle Scienze - Scritti e Documenti: Roma, Aracne*, p. 2-29.
- Spina V., Tondi E. and Mazzoli S. 2011. Complex basin development in a wrench-dominated back-arc area: Tectonic evolution of the Crati Basin, Calabria, Italy. *Journal of Geodynamics* 51, 90–109.
- Van Beynen P.E., Niedzielski M.A., Bialkowska-Jelinska E. and Matusick Alsharif, J. K. 2012. Comparative study of specific groundwater vulnerability of a karst aquifer in central Florida, *Applied Geography*, 32, 868-877.
- Van Dijk J.P., Bello M., Brancaleoni G.P., Cantarella G., Costa V., Frixia A., Golfetto F., Merlini F., Riva M., Torricelli S., Toscano C. and Zerilli A. 2000. A regional structural model for the northern sector of the Calabrian Arc (southern Italy). *Tectonophysics* 324, 23–60.

A peculiar case of coastal springs and geogenic saline groundwater

Polemio M.⁽¹⁾, Limoni P.P.⁽¹⁾, Liotta D.⁽²⁾, Palladino G.⁽¹⁾, Zuffianò L.E.⁽¹⁾, Santaloia F.⁽¹⁾

⁽¹⁾ Istituto di Ricerca per la Protezione Idrogeologica – CNR, Bari, Italy,

⁽²⁾ Dipartimento di Scienze della Terra e Geoambientali, Università di Bari.

ABSTRACT

The coastal carbonate Apulian aquifers, located in southern Italy, feed numerous coastal cold springs and constitute the main local source of high quality water. The group of Santa Cesarea Terme springs constitutes the unique occurrence of thermal groundwater outflow, observed in partially submerged coastal caves. The spring water is rich of hydrogen sulfide and the water temperature ranges from 22 to 33 °C.

Geological and hydrogeological surveys including chemical and isotopic analyses of both groundwater and seawater have been carried out. Stable isotopes $\delta^{18}\text{O}$, δD were used to define the origin of the thermal waters and the recharge mechanism of the geothermal systems while the unstable isotope ^3H was determined for estimating the age of the thermal waters and to define the conceptual model of this low temperature geothermal resource.

It was demonstrated that the spring groundwater of Santa Cesarea, which has been used for spa from several decades, is due to mixing of three components: a thermal saline fluid rich in sulphur, saline water due to seawater intrusion and fresh water that derives from meteoric infiltration in the carbonate outcrops.

INTRODUCTION

These springs are known from ancient times (Aristotele in III century BC) and the physical-chemical features of their thermal waters resulted to be partly influenced by the sea level variations. Some hypotheses about the origin of these warm waters have been proposed up to now by some researchers (Zezza, 1980, Calò et al., 1991, Maggiore and Pagliarulo, 2004) but some uncertainties existed. For this reason, the area was selected in order to define the conceptual model of the geothermal resources related to the thermal springs and, as a consequence, the origin of the thermal springs (pilot site of the Vigor Project).

GEOLOGICAL AND HYDROGEOLOGICAL SETTING

The Santa Cesarea Terme area is located along the south-eastern coast of the Salento peninsula, a carbonate plateau defined by a wide, WNW–ESE trending, antiform structure, dissected by a series of extensional and strike-slip faults (Tozzi, 1993). Starting from the Early Triassic, the area was part of the Apulia platform palaeo-domain, characterized by shallow-water carbonate sedimentation (Mostardini and Merlini, 1986). Since Cretaceous times, the Salento peninsula experienced a series of alternating transgression and regression phases, giving rise to a succession characterized by lacunae and unconformities. In particular, during the Middle Pleistocene, the area underwent a severe regional uplift (Doglioni et al., 1994). As shown in the geological map of Figure 1, the Altamura Limestone (Upper Cretaceous) represents the calcareous bedrock at Santa Cesarea Terme, consisting in well-bedded, peritidal dolomitic limestone. This Cretaceous formation is overlaid, through a marked angular unconformity, by coral reef limestone belonging to the Castro Limestone (Late Eocene-Early Oligocene; Bosellini et al., 1999; Bossio et al., 2005).

Locally, both Altamura Limestone and Castro Limestone are unconformably overlain by the bentonic foraminifer-bearing Oligocene calcarenite (Porto Badisco Calcarenites) and by the Messinian poorly bedded white calcarenite (Andrano Calcarenites). The younger formations cropping out at Santa Cesarea Terme are the Uggiano La Chiesa Formation (Middle Pliocene-Lower Pleistocene) and the Salento Calcarenites (Pleistocene). The first is mainly made of yellow calcarenites while the latter consists of massive to poorly bedded, weakly cemented calcarenites, related to a slope environment, as testified by the presence of slumpings and submarine slides. The offshore equivalent of the Salento Calcarenites are well imaged in the seismic lines and form a series of prograding units settled during a forced regression (Aiello and Budillon, 2004).

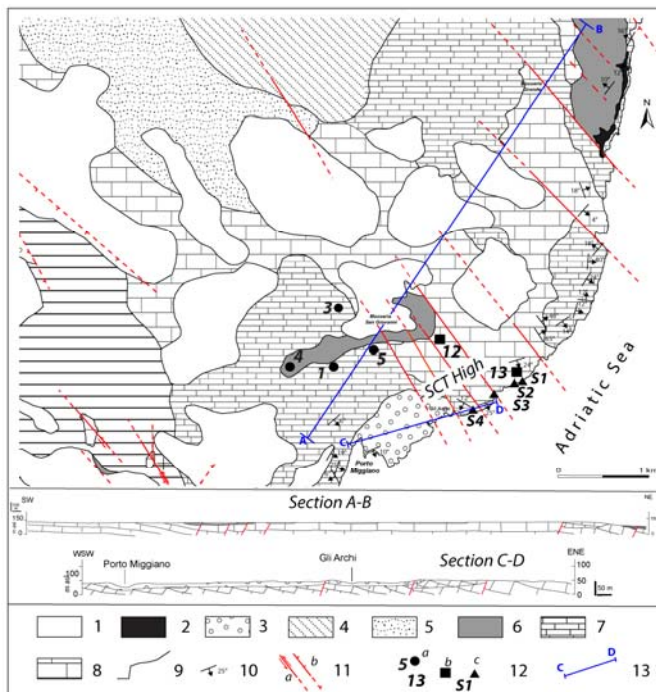


Figure 1: Simplified geological map of the studied area. Legend: 1) red clays, 2) talus deposits, 3) Salento Calcarenites, 4) Uggiano La Chiesa Formation, 5) Andrano Calcarenites, 6) Porto Badisco Calcarenites, 7) Castro Limestone, 8) Altamura Limestone, 9) stratigraphic contact, 10) strata attitude, 11) fault (a-transtensional, b-normal, dashed when inferred), 12) water sampling sites (a-cold well, b-thermal well, c-thermal spring), 13) trace of the geological sections.

limited extension, are located within the Neogene deposits. Usually they occur in topographically depressed areas, where Quaternary sands and calcarenites overlie impermeable clay formations.

Belonging to a coastal area, the deep groundwater, which top is located almost at the sea level, is involved in saltwater intrusion, with the salt-fresh water interface at some meters below the sea level moving inland. Therefore the deep fresh groundwater has been intercepted only some meters above the sea level. Locally, where the thermal wells are, the piezometric level has been measured at some meters above the ground level.

CHEMICAL ANALYSES OF WATERS

Temperature, electrical conductivity, dissolved oxygen, redox potential, pH, alkalinity of waters have been determined in the field. Cations (Li^+ , Na^+ , K^+ , Ca^{2+} , Mg^{2+} , Sr^{2+}) and anions (F^- , Cl^- , Br^- , NO_3^- , SO_4^{2-}) were analyzed by means of ion chromatography (IC) methods.

Minor and trace elements were determined by inductively coupled plasma mass spectrometry. Values for $\delta^{18}\text{O}$, δD and ^3H were obtained by mass spectrometry. Location of the sampling points is shown in Figure 1.

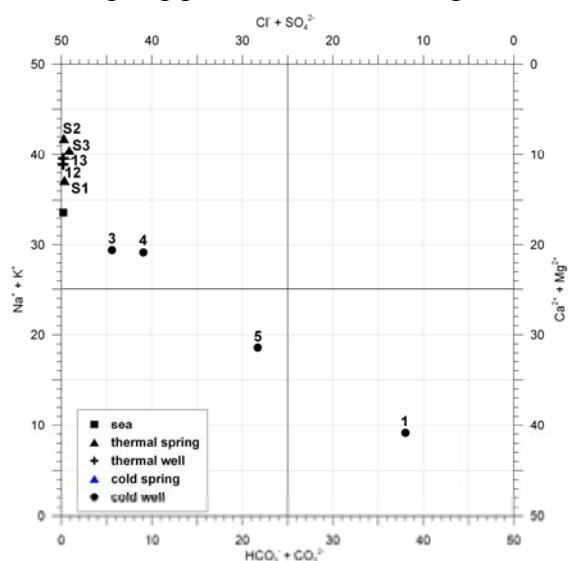


Figure 2: Langelier-Ludwig diagram of some of the analyzed groundwater samples.

chloride ion. High contents of alkali earth metal ions (Ca^{2+} - Mg^{2+}) have been found for the fresh groundwater (sample 1), which displays the typical composition of the groundwater flowing within the deep aquifer within the Salento peninsula (Fidelibus and Tulipano, 1986). The other cold-water samples (5, 3, 4) are a mixture of fresh groundwater and seawater.

As concerns the secondary constituents, the thermal waters are marked by higher concentration of Li^+ , Sr^{2+} , F^- and Br^- respect to those measured for the cold-water samples. Lithium is considered as a reliable indicator for the residence time of groundwater in the aquifer (Edmunds and Smedley, 2000). Most of the trace element concentrations are related to the redox environment of thermal waters. As a matter of fact, the measured redox potential values range from negative to slightly positive (-300 mV to 30 mV).

The D/H isotopic ratios suggest that the cold water samples (1, 5, 4, 3) have a meteoric origin. The thermal waters sampled at both wells (12, 13, 14) and springs (S1, S2, S3, S4) have an enrichment in oxygen $\delta^{18}\text{O}$. This enrichment could be interpreted as due to evaporation of deep fluids (Panichi, 1982). The thermal waters sampled at the wells (12 and 13) record a low tritium content while higher contents, up to almost 5 TU, occur for the cold water samples. These results suggest that the thermal waters should be recharged by groundwater characterized by a relatively long residence time (greater than 55 years), connected to a deep groundwater circulation system. In addition, the data for the cold-water samples provide evidence of recent recharge.

CONCLUSION

The thermal system of Santa Cesarea, which has been used for spa from several decades, seems essentially due to three water types or components: 1) pure fresh groundwater from meteoric infiltration in the carbonate rocks, 2) saline water due to seawater intrusion, 3) a thermal saline fluid rich in sulphur. The resulting mixture is undersaturated with respect to calcite, thus aggressive enough to enhance the karst processes in the area.

In this narrow area, the source of geogenic salinization of spring groundwater was referred to ascending very deep groundwater, more saline than current sea water.

The highest temperatures (22°-33° C) of the waters have been measured in some wells (thermal wells in Figure 1) located in a narrow area not far from the coastal sector where the thermal springs develop. Some meters from these thermal wells, the groundwater temperature decreases reaching the typical values of the deep Salento aquifer, that is about 18-19°. The thermal groundwater has higher total dissolved solids (e.g. 58000 mg/L) with respect to the fresh groundwater (generally up to 500 mg/L).

The major constituents are plotted in the Langelier-Ludwig diagram shown in Figure 2. The thermal waters are characterised by high values of alkaline ions (Na^+ - K^+), higher than those measured for the seawater.

Moreover, they show high content of

The geochemical composition and the physical features of the sampled waters suggest that thermal waters should be moving from ancient seawaters subjected to intense evaporation processes, infiltrated at great depth within the seabed substratum. Afterwards, these thermal fluids should flow up through the almost vertical structures, related to the transtensional structures, identified within a narrow sector of the studied territory. Thermal waters are five times older than the deep aquifer (Santaloia et al. in print).

ACKNOWLEDGEMENTS

VIGOR Project is part of the Interregional Programme “Renewable Energies and Energy Savings FESR 2007-2013 – Axes I Activity line 1.4 “Experimental Actions in Geothermal Energy”, funded by MiSE-DGENRE.

REFERENCES

- Aiello, G. and Budillon, F. 2004. Lowstand prograding wedges as 4th order glacio-eustatic cycles in the Pleistocene continental shelf of Apulia. SEPM Special Publication n. 81, “Cyclostratigraphy: Approaches and Case Histories” (D’Argenio B., Fisher A.W., Premoli, Silva I., Weissert H., Ferreri V., Eds.), 215-230.
- Bosellini, A., Bosellini, F.R., Colalongo, M. L., Parente, M., Russo, A. and Vescogni, A. 1999. Stratigraphic architecture of the Salento coast from Capo d’Otranto to Santa Maria di Leuca (Apulia, southern Italy). Riv. Ital. Paleont. Strat., 105 (3), 397-416.
- Bossio, A., Mazzei, R., Monteforti, B. and Salvatorini, G. 2005. Stratigrafia del Neogene e Quaternario del Salento sud-orientale (con rilevamento geologico alla scala 1:25.000). Geologica Romana, 38, 31 – 60.
- Calò, G. and Tinelli, R. 1995. Systematic hydrogeological study of a hypothermal spring (S. Cesarea Terme, Apulia), Italy, Journal of Hydrology, 165, 185 – 205.
- Dogliani, C., Mongelli, F. and Pieri, P. 1994. The Puglia uplift (SE-Italy): an anomaly in the foreland of the Apenninic subduction due to buckling of a thick continental lithosphere. Tectonics, 13 (5), 1309-1321.
- Edmunds W.M. and Smedley P.L. 2000. Residence time indicators in groundwater: the East Midlands Triassic sandstone aquifer, Applied Geochemistry 15, 737–752.
- Fidelibus M. D. and Tulipano L. 1986. Mixing phenomena owing to sea water intrusion for the interpretation of chemical and isotopic data of discharge waters in the Apulian coastal carbonate aquifer (Southern Italy). 9^o Salt Water Intrusion Meeting, The Netherlands.
- Maggiore, M. and Pagliarulo, P. 2004. Circolazione idrica ed equilibri idrogeologici negli acquiferi della Puglia. Geologi e territorio, n. 1, 13-35.
- Mostardini, F. and Merlini, S. 1986. Appennino centro meridionale. Sezioni geologiche e proposta di modello strutturale. Memorie della Società Geologica Italiana, 35, 177-202.
- Panichi, C.:Aspetti geochimici delle acque termali. 1982. In: C.N.R. (Italian Council for Research Ed.). Il graben di Siena, PFE-SPEG-RF-9, Rome, Italy, 61–72.
- Tozzi M. 1993. Assetto tettonico dell’avampaese apulo meridionale (Murge meridionali-Salento) sulla base dei dati strutturali. Geologica Romana, 29, 95 - 111.
- Zeza F. 1980. Le sorgenti ipotermali solfuree di Santa Cesarea Terme. Azienda di cura e soggiorno e turismo Santa Cesarea Terme. Estratto dalla rivista quadrimestrale di cultura e civiltà salentina “Salentum” - Anno III nn. 1–2 – edita dall’E.p.t. di Lecce.

Contact Information: Maurizio Polemio, Istituto di Ricerca per la Protezione Idrogeologica – CNR, Bari, Italy, Email: m.polemio@ba.irpi.cnr.it

Hydrogeological modeling for sustainable groundwater management under climate change effects for a karstic coastal aquifer (Southern Italy)

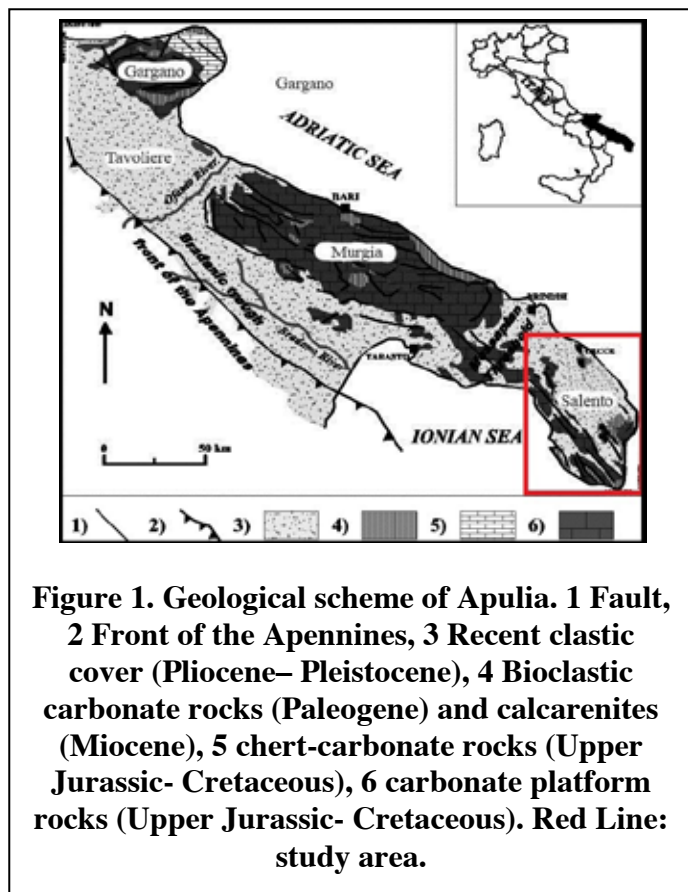
Polemio M., Romanazzi A.
CNR-IRPI, Bari, Italy - m.polemio@ba.irpi.cnr.it

ABSTRACT

Seawater intrusion is a pervasive problem affecting coastal aquifer, where the concentration of population and the increasing water demand creates risks of overexploitation, especially in those areas where is the only resource of drinking and irrigation water. We focus attention on a karst coastal groundwater system effect of an intensive agricultural use. The general purpose of this paper is to prove the capability of numerical models in management of groundwater. In particular for achieve forecast scenarios to evaluate the impacts of climate change on groundwater resources. A large-scale approach was chosen. Qualitative and quantitative groundwater trends from 1930 to 2060 was so defined. Results show an important piezometric decrease and an increment of seawater intrusion and so a deterioration of groundwater resource. For these use requirements different scenarios of pumping are considered for management and mitigation of seawater intrusion effects.

GEOLOGICAL AND HYDROGEOLOGICAL CONTEXT

The Apulian region, with its 800 km of coastline, is the largest coastal karstic aquifer in Italy. In particular, the region is composed of three karst structural domains: Gargano, Murgia and Salento (Figure 1). The Murgia and Salento Mesozoic rocks form a lithological, geological and groundwater continuum but have a different hydrogeological behavior due to different lithofacies, the different degree of fracturing and karst, and to very different boundary conditions (Polemio et al., 2009). From an hydrogeological point of view Salento can be subdivided into five hydrogeological complexes (from the bottom): Limestones, Andrano Calcarenites, Gravina Calcarenites, sub-Apennine clays and Sands. The piezometric gradient is generally low (0.3-0.5% as mean value), with maximum height values lower than 5 m a.s.l.. Deep aquifer is exclusively fed by rainwater infiltration because of scarcity of superficial stream and for the



presence of extended surface karst areas that create direct link between rainwater and the deep karst system. Natural discharge is both diffused and concentrated. There are numerous springs located along coastline. A distributed flow along Salento coast was estimated about 56,7 l/s*km (Romanazzi and Polemio, 2013). On the base of these datas conceptual model was achieved (Figure 2).

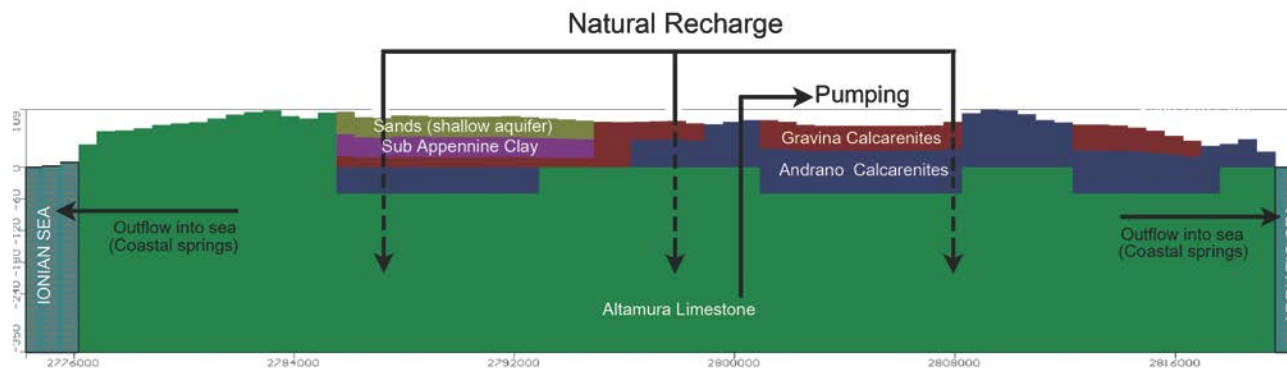


Figure 2. Conceptual model of Salento model area. Generic schematic section W-E.

MODEL DEFINITION, CALIBRATION AND PREDICT SCENARIOS

The numerical codes used were MODFLOW (McDonald and Harbaugh, 1988) and SEAWAT (Guo and Langevin, 2002). The active domain of the study area (active cells) covered approximately 2,300 km² with 45,925 cells. Vertically, the area was divided into 12 layers, from 214 to -350 m a.s.l., to allow a good lithological and hydrogeological discretization. Thickness and geometry of layers were defined on the 3D knowledge of hydrogeological complexes. As input, natural recharge, considering the climate change, from 1930 to 2000, was calculated in addition to geological and hydrogeological datas. Trends of agricultural activity, available from 1971 to 2000, by the National Institute of Statistics Data, ISTAT, were evaluated to take account of human activity on the territory, whose vocation for tourism and agriculture accounts for approximately 70% of groundwater resources. A first model representing the natural steady-state condition at thirties years was made and later model was validated with two transient scenarios using 1989 and 2000 experimental datas. The purposes of these implementations are, besides validated model, to supervise and to evaluate the development of groundwater resource in the area, in the last seventy years, or in the period from 1930-2000. The results emphasizes an essential decrease of piezometric level and a development of the intrusion phenomenon of seawater into aquifer (Polemio and Romanazzi, 2012; Romanazzi and Polemio, 2013). Three forecast transient scenarios, referred to 2000-2020, 2020-2040 and 2040-2060, were implemented, on the basis of this calibrated and validated model, with the aim to predicting the evolution of piezometric level and seawater intrusion. We referred for forecast datas of precipitation and temperature to the Giorgi and Lionello model, in relation to the defined "A1B scenario" (Giorgi and Lionello, 2008). This climate forecast model give temperature and precipitation predictions, in reference to 1961-1980, for the period 2001-2100. An average increase of temperature equal to +0.9 ° C was so considered for decade 2001-2020 and equal to +2.4 ° C in the interval 2041-2060. Precipitations, instead, shows a negative change in percentage, compared to the period 1960-80, equal to -3.9%, -5.9% and -9% respectively for 2001-2020, 2021-2040 and 2041-2060. These datas are in agreement with other climate change models presents in literature (Garcia- Ruiz et al., 2011). A new water budget was elaborated for the years 2020, 2040 and 2060. Since in not possible to predict future irrigation discharges, these were

left constant and equal to those of the years 2000. The scenarios results shows a general decrease of the piezometric head and a deterioration of water quality caused by seawater intrusion (Romanazzi et al., 2013) (Figure 3).

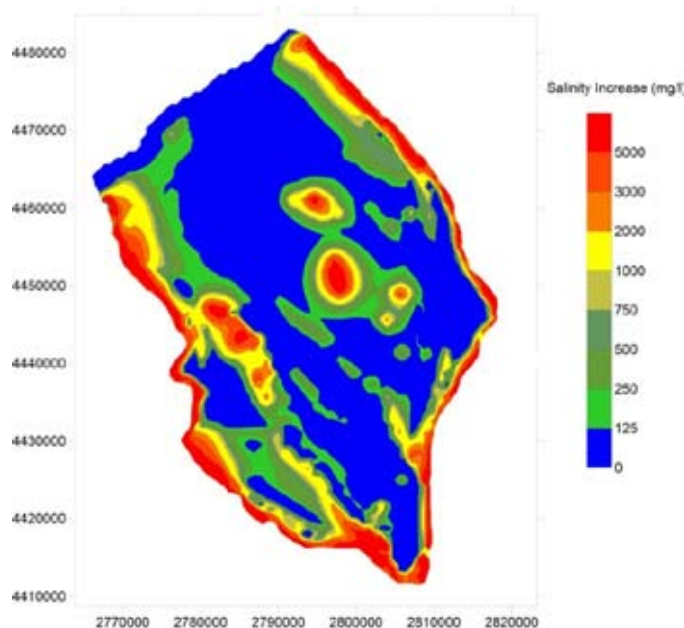


Figure 3. Salinity increase (mg/l) between 1930 and 2060.

MANAGEMENT CRITERIA AND CONCLUSION

That being so, new management tools are essentials. Apulian regional laws tried to regulated groundwater abstraction until 1984. First Regional Water Recovery Plan, called PRA, tried to define a groundwater quality zonation in the Region (Apulia Region, 1982). In this plan new discharges was forbidden in which areas where water quality was lowest due high salinity, especially along coastline. In 2007 Regional Administration promoted the new Water Protection Plan, called PTA (Apulia Region, 2009), on the base of advice of Water Framework Directive, WFD 2000/60 (European Community, 2000). Plan defined two zones for Salento karst aquifer. In the first, located along coast, where is a low quality water, new discharges was forbidden. In the second zone, defined “qualitative and quantitative protection zones”, new authorizations are permitted but regulate by some parameters as the depth of well and piezometric and chloride limits values. However both plans do not explain in detail the hydrogeological criteria used to define zones. Based on international (LaMoreaux, 2010; Jiménez-Madrid, 2010) and local studies (Polemio et al., 2009, Polemio et al., 2010) a new management criterion was implemented into the model. To define the zone boundary, a very simple criterion was used: threshold equal to 0.5 g/l between pure fresh groundwater and any type of mixing between fresh and saline groundwater (Polemio et al., 2010). Three zones are so defined. In the first, coinciding with the coastal zone, salinity is always above the threshold, in the second, a transition zone, salinity is function of more parameters, and the third, in the inner area, where salinity value is permanently below the threshold. These three zones was implemented in the model and, keep constant the discharges quantity of 2000 years but with no discharge from coastal zone. In others words, the same pumping was redistributed in the three different areas. A new piezometric and salinity distribution had permitted to study the reaction of the aquifer. This simple proposal show as large

scale numerical model can be used for support the management of groundwater resources and subsequent applied for predictive scenarios, especially in those areas where policy of groundwater resource scientifically based is absent.

REFERENCE

- Apulia Region 1982. Regional Water Recovery Plan (PRA), Water Protection Service, General Report.
- Apulia Region 2009. Regional Water Protection Plan (PTA), Water Protection Service, General Report Area.
- European Community (EC) 2000. Directive 2000/60/EC of the European parliament and of the council of 23 October 2000 establishing a framework for community action in the field of water policy. Official Journal of the European Communities L327, pp. 1–72.
- Garcia-Riuz J., Lopez-Moreno J.I., Vicente-Serrano S.M., Lasanta-Martinez T., and Begueria S. 2011. Mediterranean water resources in a global change scenario, *Earth Science Reviews*, 105, 121-139.
- Giorgi, F. and Lionello, P. 2008. Climate change projections for the Mediterranean region. *Global and Planetary Change* 63, 90–104.
- Guo W. and Langevin C.D. 2002. User's Guide to SEAWAT: A Computer Program for Simulation of Three-Dimensional Variable-Density Ground-Water Flow, U.S. Geological Survey Open-File Report 01-4340.
- Jiménez-Madrid, Carrasco F. and Martínez C. 2010. The Protection of Groundwaters Destined for Human Consumption in Karstic Aquifers. *Advances Towards Safeguard Zones* Springer Heidelberg Dordrecht London New York.
- La Moreaux, J.W. 2010. Sustainable Water Resources with Case Studies in Historic Areas in Egypt and Syria, *Advances in Research in Karst Media*, Springer Heidelberg Dordrecht London New York.
- McDonald M.G. and Harbaugh A.W. 1988. A modular three-dimensional finite-difference ground-water flow model, *Techniques of Water-Resources Investigations of the United States Geological Survey*, book 6.
- Polemio, M., Dragone, V. and Limoni, P.P. 2009. Monitoring and methods to analyse the groundwater quality degradation risk in coastal karstic aquifers (Apulia, Southern Italy). *Environmental Geology*, 58, 299-312.
- Polemio M., Casarano D. and Limoni P.P. 2010. Apulian coastal aquifers and management criteria, SWIM - 21 - 26, June, St. Miguel, Azores, Portugal.
- Polemio M. and Romanazzi A. 2012. Modelling and groundwater management of a karstic coastal aquifer: the case of Salento (South Italy), SWIM, 17-22 June, Armacao dos Buzios, Brazil.
- Romanazzi A., Gentile F., Trisorio Liuzzi G., and Polemio M. 2013. The sustainability of groundwater exploitation for agriculture in the case of a wide coastal karstic aquifer (Salento), 1 CIGR – Inter – Regional Conference on Land and Water Challenges, 10-14 Sept., Bari.
- Romanazzi A. and Polemio M. 2013. Modelling of coastal karst aquifers for management support: Study of Salento (Apulia, Italy), *Italian Journal of Engineering Geology and Environment*, 13, 1, pp. 65-83.

The impact of tides on mixing and spreading in heterogeneous coastal aquifers.

M. Pool¹, V. Post¹ and C. Simmons¹

¹ National Centre for Groundwater Research and Training, Faculty of Science and Engineering, Flinders University, Adelaide, Australia.

ABSTRACT

Understanding the effects of heterogeneity in the hydraulic conductivity field and tidal oscillations on the 3D dynamics of seawater intrusion in coastal aquifers is fundamental for the design of water-resources management schemes in coastal aquifers. Proper accounting of mixing is relevant not only in determining sustainable management policies but also in analyzing reactions that result from mixing. However, in most applications, the medium and thus the flow field are highly heterogeneous and mixing is strongly influenced by spatial heterogeneity and temporal flow fluctuations. Therefore, evaluating and dealing with seawater intrusion problems remains a challenge due to the complexity, spatial and temporal variability, and uncertainty inherent to natural flow and transport systems. The objective of this study is to identify the controls of tidally driven dynamics in heterogeneous coastal aquifers, with emphasis on the quantification of tidal impacts on solute mixing and spreading. Several sets of heterogeneous hydraulic conductivity realizations were generated, and for each realization, three-dimensional numerical simulations of density dependent flow and solute transport were conducted. The simulations show that heterogeneity produces an inland movement of the toe location along with a widening of the mixing zone. Tidal fluctuations have a similar effect on the seawater intrusion dynamics but the increase of the width of the mixing zone can be much larger than due to heterogeneity alone. The parametric analysis revealed that the key dimensionless parameter controlling the tidally mixing behavior is the wave number (n_w) which depends on the tidal amplitude and the aquifer's tidal propagation parameter. We find that tidal impacts become significant for $n_w \leq 600$. These insights critically underpin quantitative guidance on the inclusion and exclusion of tidal effects in the analysis of seawater intrusion for achieving ground-water sustainability in coastal aquifers.

Contact Information: Maria Pool, National Centre for Groundwater Research and Training, Flinders University, GPO Box 2100, Adelaide, SA, 5001, Phone: +61 8 8201 2193, Fax: +61 8 8201 7906, Email: mpoolr@gmail.com

The use of multi-level pressure and salinity data to understand freshwater-lens dynamics

Vincent E.A. Post¹, Jean Marçais², Maarten J. Waterloo³, Michel M.A. Groen³ and M. Teresa Condesso de Melo⁴

¹Flinders University, School of the Environment / National Centre for Groundwater Research and Training, Adelaide, Australia

²Ecole polytechnique, Programme d'approfondissement Sciences pour les défis de l'environnement, Palaiseau, France

³VU University, Faculty of Earth and Life Sciences, Amsterdam, The Netherlands

⁴CVRM - Geo-Systems Centre, Instituto Superior Técnico, Lisboa, Portugal

ABSTRACT

In this contribution we present the results of field measurements made using a multi-level sampling device to characterise the vertical variation of groundwater pressure and salinity in a siliciclastic aquifer below a tiny island in the Ria de Aveiro lagoon in Portugal. The setup and installation of the system are described, and the results of an experiment where pressure and salinity were measured at regular time intervals during a tidal cycle will be presented. The dual nature of the vertical pressure gradients suggests that there is a distinct two-layer behaviour, with gradients being much higher at shallow depths (up to 4 metres below the ground surface) than at deeper depths (more than 4 metres below the ground surface). The hydraulic conductivity is estimated using the vertical displacement of the groundwater, which is inferred from the variations of the salinity with time, in combination with the measured pressure gradients. Finally, the implications of the layered nature of the aquifer for the conceptual and numerical model of the island aquifer are discussed.

Contact Information: Vincent E.A. Post, Flinders University, Faculty of Science and Engineering, School of the Environment / National Centre for Groundwater Research and Training, GPO Box 2100, Adelaide, SA 5001, Australia, Phone: +61(0)8 82015077, Email: vincent.post@flinders.edu.au

Saltwater Intrusion in karst aquifers along the Eastern Mediterranean

Mutasem El-Fadel, **Grace Rachid**, Ibrahim Alameddine and Majdi Abu Najm
Department of Civil & Environmental Engineering, American University of Beirut, Lebanon

ABSTRACT

The scale and magnitude of saltwater intrusion in the karst aquifer of the coastal city of Beirut-Lebanon, a densely populated area that is heavily dependent on groundwater for domestic purposes, was quantified. The city suffers from saltwater intrusion primarily from the wide proliferation of building wells and over-extraction. A monitoring program was developed and implemented to characterize groundwater quality and investigate the severity of saltwater intrusion. Multiple physical, chemical and microbiological parameters were analyzed. Additionally, socioeconomic indicators were collected in an attempt to correlate salinity levels with these factors. Groundwater chemistry, ionic relationships, hydro-chemical diagrams and groundwater quality indices (GQI) were also used to delineate saltwater intrusion hotspots. Concentration data exhibited large spatial variability in salinity levels across districts with Total Dissolved Solids (TDS) levels ranging from a low of 400 to as high as 29,000 ppm. The results can help assess the extent and intensity of saltwater intrusion and improve existing policy planning and management tools for coastal aquifers.

INTRODUCTION

The vulnerability of coastal groundwater aquifers to saltwater intrusion (SWI) is increasing globally due to high water demands in densely populated coastal regions that are increasing their reliance on groundwater resources. SWI in such systems is expected to further increase with projected population growth and urbanization. Moreover, the potential sea level rise, associated with climate change, is also expected to exacerbate the problem (Barazzuoli *et al.* 2008; Kumar *et al.* 2007). Despite widespread studies of SWI, its investigation in karst aquifers remains limited, particularly in view of the multiple challenges in understanding, characterization, as well as modeling of karst aquifers. This study quantifies SWI along the Eastern Mediterranean coastline, known for its fractured and karst nature, through examining a case study that looks at groundwater salinity in the city of Beirut, Lebanon.

Municipal Beirut lays on a 20km² triangular shaped-peninsula that extends westward into the Mediterranean Sea. The city has a 9km shoreline (Figure 1). It is highly urbanized and hosts a population of 400,000 (CAS 2008), inhabiting various districts with varying densities, land uses, and socioeconomic conditions. Cenomanian limestone (C4) underlies the study area, with quaternary sediments mainly overlying it (alluvium, soils or moving dunes) (50% of the area) with some Miocene beds forming a single saturated zone with an estimated thickness of 700m (Khair 1992). The resulting aquifer is heavily exploited, with an estimated 4000 small building scale wells tapping into it (SOER 2011).

Being heavily jointed and faulted (Ukayli 1971) coupled with its proximity to the sea, makes Beirut's underlying aquifer susceptible to SWI. The telltale signs of SWI were observed as early as 1969, through geo-electrical processing that confirmed SWI through tectonic fractures (FAO 1997). Chloride concentrations in the aquifer have continued to increase with time to reach more than 4,200 mg/l in 2005 (Khair 1992; Saadeh 2008).

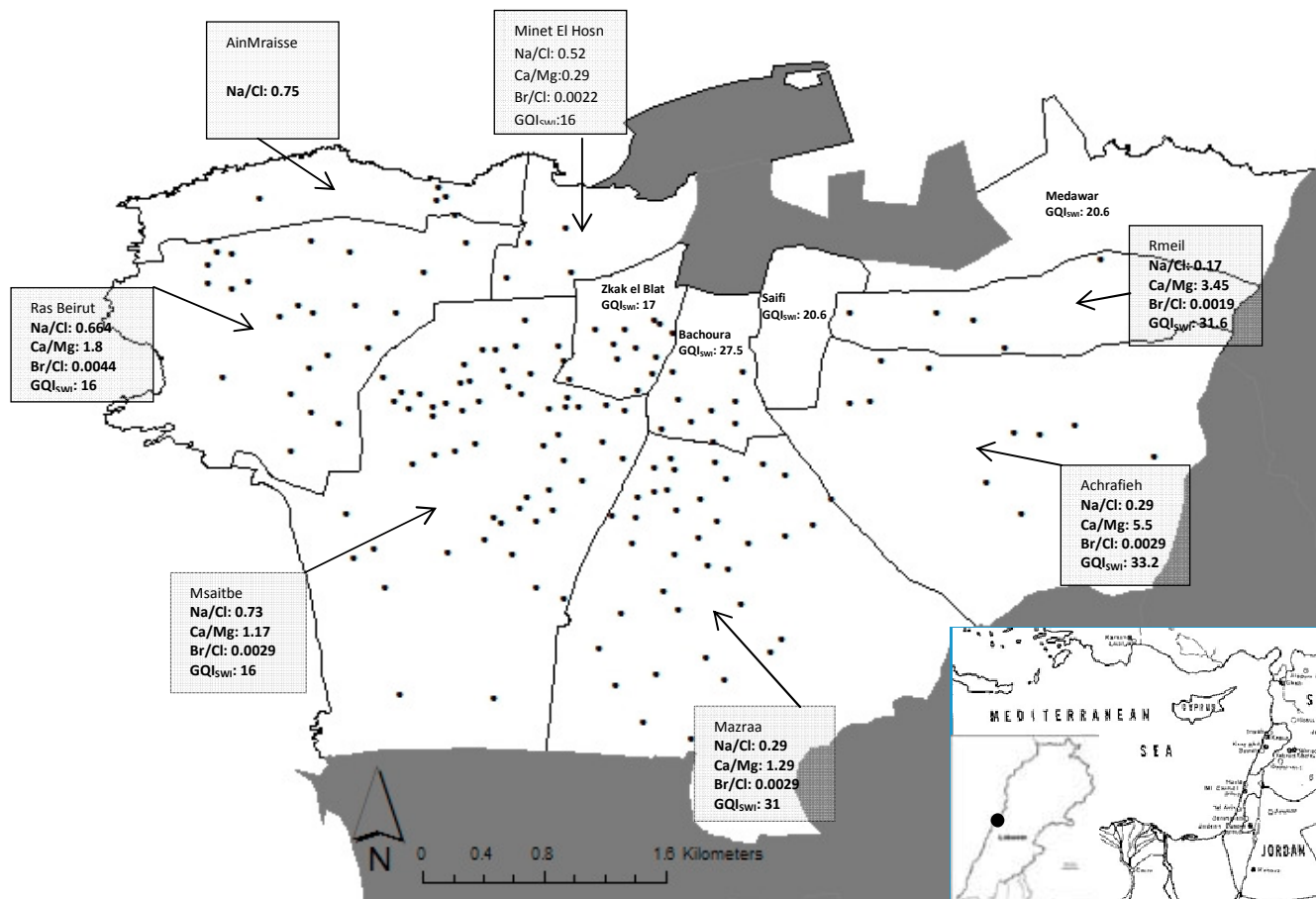


Figure 1. Study area with distribution of groundwater wells and ionic ratios per district

Methods

A monitoring program was developed to characterize the groundwater quality and examine the extent of saltwater intrusion. Sampling was initiated in the early summer of 2013 (June), whereby samples were collected from 165 groundwater wells in residential districts. A stratified sampling approach was used, whereby the density of sampled wells in each district was based on the corresponding population density. Parameters analyzed included TDS, hardness, HCO_3^- , CO_3^{2-} , NO_3^- , SO_4^{2-} , Ca^{2+} , Mg^{2+} , Cl^- , Br^- , Na^+ and K^+ ions, along with microbiology. Analyses were undertaken in accordance with Standard Methods for the Examination of Water and Wastewater (APHA/AWWA/WEF, 2005). Ionic ratios, specifically Na^+/Cl^- , $\text{Ca}^{2+}/\text{Mg}^{2+}$, Br^-/Cl^- , $\text{SO}_4^{2-}/\text{Cl}^-$ and $\text{Ca}^{2+}/(\text{SO}_4^{2-} + \text{HCO}_3^-)$, were used to assess the geochemical state of groundwater. The hydro-chemical Piper diagram was also generated in order to analyze and characterize water type and quality. Groundwater quality indices (GQI) were calculated based on Babiker et al. (2007), who developed a generalized GQI, and on El-Fadel et al. (2013), who developed SWI

specific GQI (GQI_{SWI}). Based on hydrogeochemical processes associated with saltwater intrusion, GQI_{SWI} indicates the contribution of freshwater and ranges from 0 (seawater) to 100 (freshwater). Information about socioeconomic indicators, including household size, education level, employment and income were collected to correlate with measured salinity levels.

Results and Discussion

Concentration data exhibited large spatial variability across and within districts particularly manifested in TDS and Cl^- values. Elevated TDS concentrations with an average of 4,061 mg/l were recorded, and exceeding 20,000 mg/l at several locations. As expected, Cl^- values correlated well with TDS ($R^2 = 0.913$). The Cl^- mean concentration over Beirut was 1,898 mg/l; yet some areas had concentrations >10,000 mg/l suggesting strong SWI. This spatial heterogeneity could be attributed, primarily, to the karstic nature of the geology in the area. Overall, the study area exhibited a low Na^+/Cl^- (0.5 – 0.82 meq/l) and a high Ca^{2+}/Mg^{2+} (1.1 – 5.5 meq/l), both typical signs of saltwater intrusion. The Br^-/Cl^- ratio averaged 0.0033 (Figure 1). Average SO_4^{2-}/Cl^- ratio of 0.1 meq/l was observed for all districts except for Mazraa (1.4 meq/l). Similarly, the average $Ca^{2+}/(SO_4^{2-} + HCO_3^-)$ ratio was high (> 1) for all districts. Accordingly, ionic ratios in the early summer (i.e. before the water table drops with the dry summer) indicate that SWI is well developed in most districts: Zkak el Blat, Msaitbe, Ain Mraisse and Minet el Hosn (Figure 1). Other districts are showing evident signs of SWI.

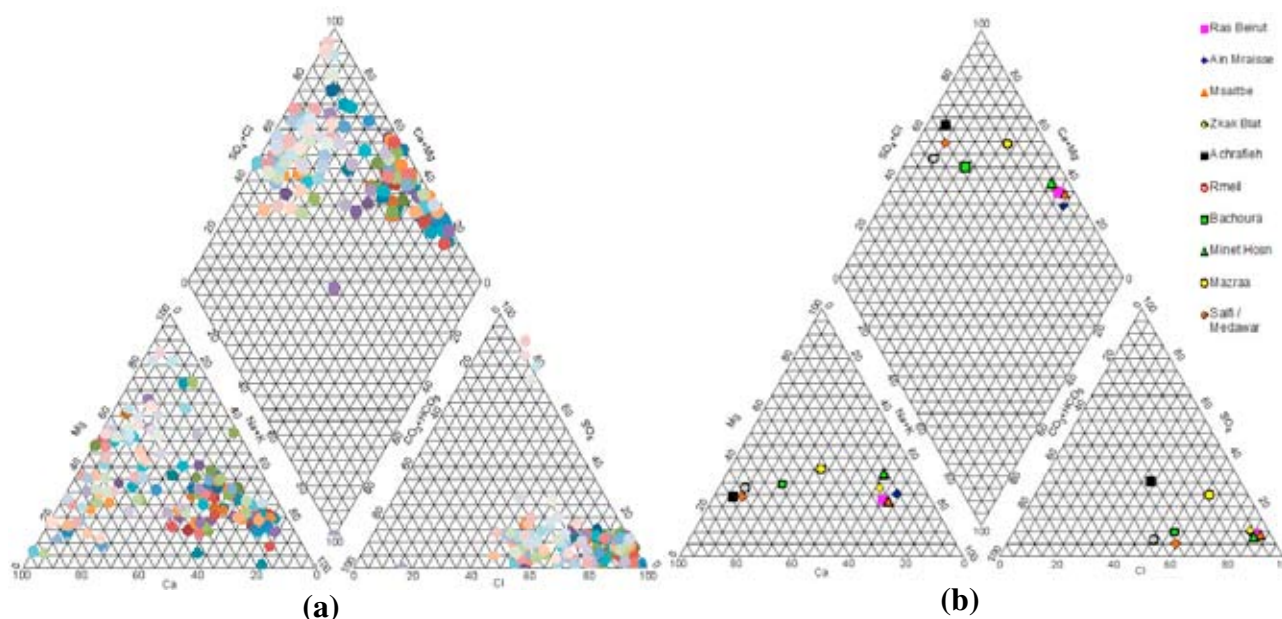


Figure 2 Piper diagram representing Beirut's groundwater quality in early summer (June 2013) (a) at the well level; (b) at the individual districts level (averaged across wells)

The generated piper diagrams (Figure 2) reveal the major hydro-geochemical facies of ($Ca^{2+} - Mg^{2+} - Cl^- - SO_4^{2-}$) and ($Na - Cl$) in the study area. The diagrams point towards SWI together with dolomitization. The generalized GQI for Beirut, which includes various parameters (Ca^{2+} , Mg^{2+} , Na^+ , Cl^- , NO_3^- , SO_4^{2-} , TDS, FC, TC), was 59.67 reflecting a very poor water quality. Recalculating GQI without the nitrates and coliforms so as to directly capture the effects of

salinization, the GQI increased to 69.3, a value that still reflects poor water quality. For the specific GQI_{SWI} , the study area had a mean value of 21 reconfirming the severity of SWI. In an effort to characterize individual districts, mean concentrations were calculated for each. Groundwater in the Zkak el Blat, Msaitbe, Ain Mraisse, Minet el Hosn, and Ras Beirut districts was found to be primary saline ($Na^+ - K^+ - Cl^-$), whereas other districts had secondary saline ($Ca^{2+} - Cl^-$) waters. The GQI for Zkak el Blat (56.5), Msaitbe (58.35), Ain Mraisse (62) and Ras Beirut (60) confirmed high salinization; whereas the districts of Achrafieh, Rmeil, Saifi and Medawar had $GQI > 86$, indicating relatively good water quality. For the specific GQI_{SWI} , all individual districts reported an average $GQI_{SWI} < 33$, with the lowest value reported in Ain Mraisse ($GQI_{SWI} = 14$).

Conclusions

Hydro-chemical analyses and groundwater quality ratios and indices confirmed the scale and quantified the magnitude of groundwater salinization in much of municipal Beirut. While proximity to shoreline, population and water demand induces variability, the spatial heterogeneity in Beirut could be greatly attributed to the karstic nature of the area's geology. Further groundwater mixing and salinization is expected to occur later in the dry season as the water table level drops. The monitoring program and socio-economic indicators' analysis is ongoing to further understand the drivers, extent, intensity and impact of saltwater intrusion in the area to better inform policy planning and management of coastal aquifers.

References

- APHA/AWWA/WEF. 2005. Standard Methods for the Examination of Water and Wastewater, 21st ed. American Public Health Association/American Water Works Association/ Water Environment Federation, Washington, DC.
- Babiker, I. S., Mohamed, M. A. and Hiyama, T. 2007. Assessing groundwater quality using GIS. *Water Resources Management*, 21, 699–715
- Barazzuoli, P., M. Nocchi, R. Rigati, and M. Salleolini. 2008. A conceptual and numerical model for groundwater management: a case study on a coastal aquifer in southern Tuscany, Italy. *Hydrogeology Journal* 16 (8):1557-1576.
- CAS 2008. Statistical Yearbook 2007. Central Administration for Statistics.
- El-Fadel, M., Tomaszkiwicz, M. and Abu Najm, M. 2013. Sustainable Aquifer Management in urban areas: the role of groundwater quality indices. In Conference Proceedings: 4th Global Forum on Urban Resilience and Adaptation, 31 May – 2 June, 2013, Bonn, Germany
- FAO 1997. Seawater Intrusion in Coastal Aquifers: Guidelines for Study, Monitoring and Control, pp. 119-122. Food and Agriculture Organization of the United Nations Rome .
- Kumar C. P., Chacahadi A. G., Purandara B. K., Kumar S., and Juyal R. 2007. Modelling of Seawater Intrusion in Coastal Area of North Goa. *Water Digest* 2 (3):80-83.
- Khair, K. 1992. The Effects of Overexploitation on Coastal Aquifers in Lebanon, *International Association of Hydrogeologists*, 3, 349-362.
- Saadeh, M. 2008. Influence of overexploitation and seawater intrusion on the quality of groundwater in Greater Beirut. Masters of Science Thesis. RWTH Aachen, Germany
- SOER 2011. State of the Environment Report 2010. MOE/UNDP/ ECODIT
- Ukayli, M. 1971. Hydrogeology of Beirut and Vicinity, Master of Science Thesis, American University of Beirut, Lebanon
- Contact Information:** Mutasem El-Fadel, American University of Beirut, Civil and Environmental Engineering Department, Beirut, Lebanon, Email: mfadel@aub.edu.lb

Requirements of modeling the freshwater lens of the Island of Sylt

Kai Radmann, Sören Kathmann, Caroline Schlegel, Johannes Michaelsen
CONSULAQUA Hamburg, Germany

ABSTRACT

Many islands face the problem of limited fresh water resources. Fresh water lenses are often the only available water reservoirs for the production of drinking water. Those reservoirs are limited and threatened by salt water intrusion. Salt water intrusion will be enforced when the balance between fresh and salt water is disturbed for instance by high abstraction rates.

The Northern German island of Sylt faces the problem of an increasing seasonal drinking water demand and limited water resources. High abstraction rates and other utilizations of the aquifer lead to a hazardous situation. These threats require a sustainable management of the different utilization in order to avoid irreversible damages to the freshwater reservoir. A 3D density dependent groundwater model represents a valuable tool for this task. For this reason the management of the two water companies on the island decided to assign CONSULAQUA to set up, calibrate and test a 3D groundwater model.

The numerical groundwater model is based on a hydrogeological model which is shown in the schematic cross section in Figure 1. The model contains 21 slices respectively 20 layers.

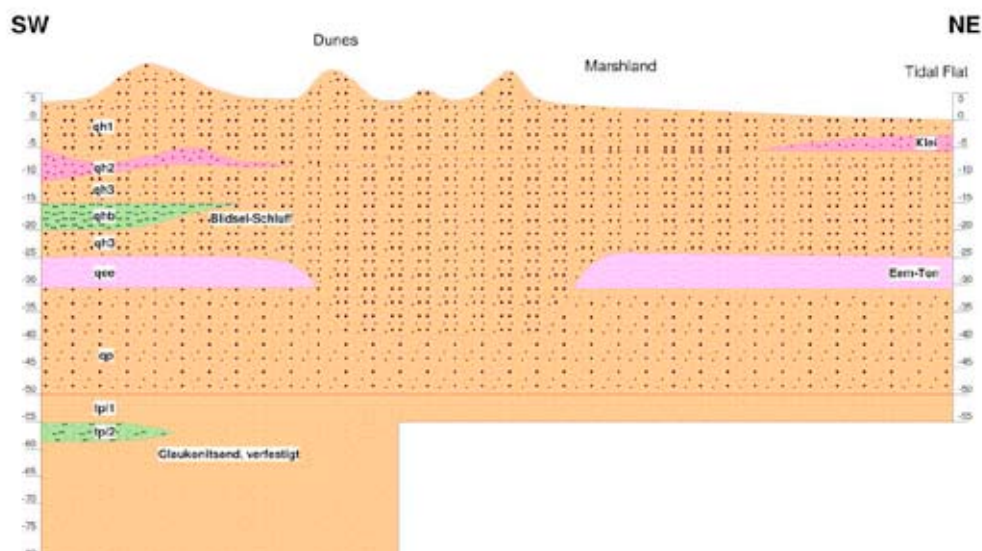


Figure 1: Hydrogeological model for the area under investigation.

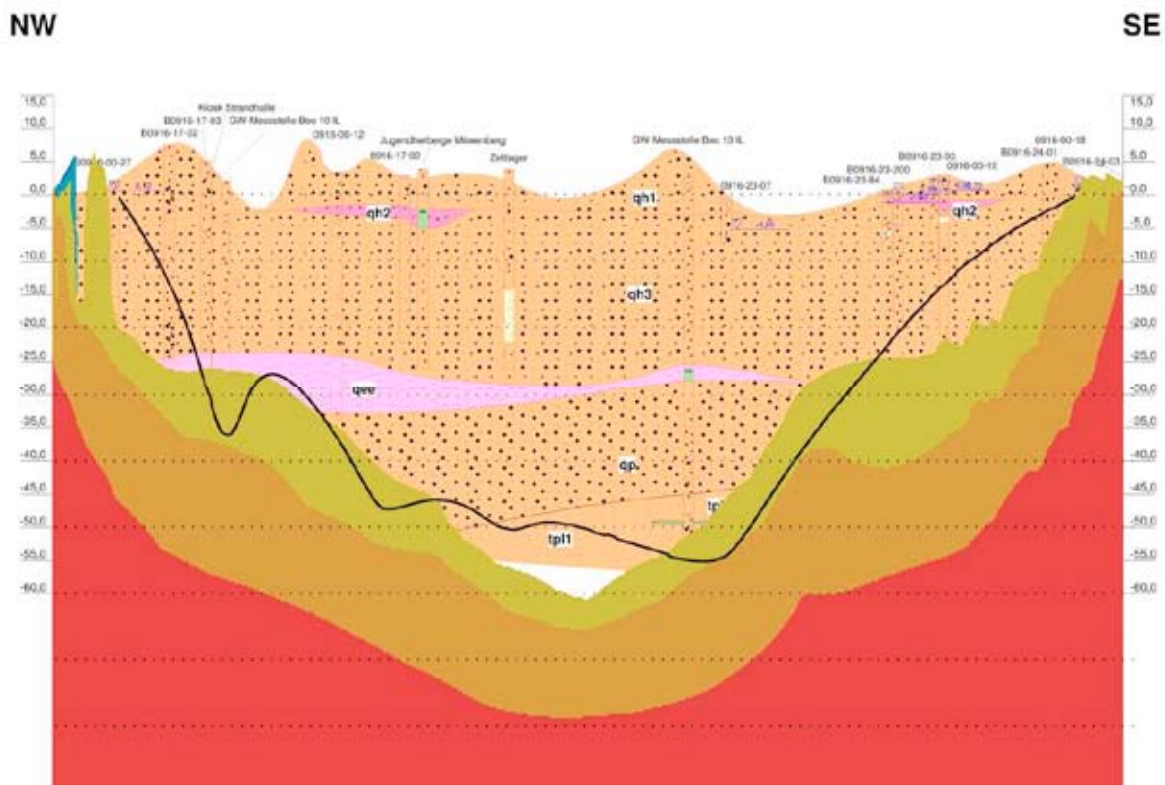


Figure 2: Comparison of the calculated (colored area) and measured (black line) fresh/salt water distribution.

In order to simulate exchange between salt and freshwater in the area of the North Sea in an adequate way, a buffer zone of 1.000 m has been implemented (Figure 3), which does not belong to the mainland, e.g. the Königshafen offshore Listland, and the Ellenbogen spit. The buffer zone enables the freshwater lines to propagate even below seafloor which has been recently observed at freshwater sources on the tidal flats of the Königshafen.

At the outer border of the model area a saltwater piezometric head with 0 mNN (Constant hydraulic head (1st) boundary condition) and a constant mass boundary (Constant mass (1st) boundary condition) with a salt concentration of 35 g/l were assigned to all slices. Additional to the outline mass boundary a constant mass boundary with 35 g/l was applied on the buffer area (North Sea) only on slice 1 (Figure 3). Groundwater recharge was only applied to the core area.

Simulating groundwater of the Wadden Sea islands faces the challenge to find appropriate starting conditions regarding the state of freshwater / saltwater interface development. The question to be answered: Has the aquifer already reached equilibrium conditions.

About 1000 years ago the area of Sylt was still part of the mainland. After several storm floods and other climatic influences the island was separated from the mainland. In this state, it is assumed that the groundwater in the island consisted entirely of fresh water. The intrusion of saltwater into the island's aquifer system started at this point. Therefore the calibration had been done within two steps:

First the process of saltwater intrusion has been modeled for 1000 years (Figure 4). We assume that a quasi-equilibrium state has been reached.

The long term calculation generated the starting condition for the second step of calibration: 50 years under pumping conditions.

Calibration succeeded to reach a good adaption between calculated and measured hydraulic heads respectively saltwater concentrations (Figure 2).

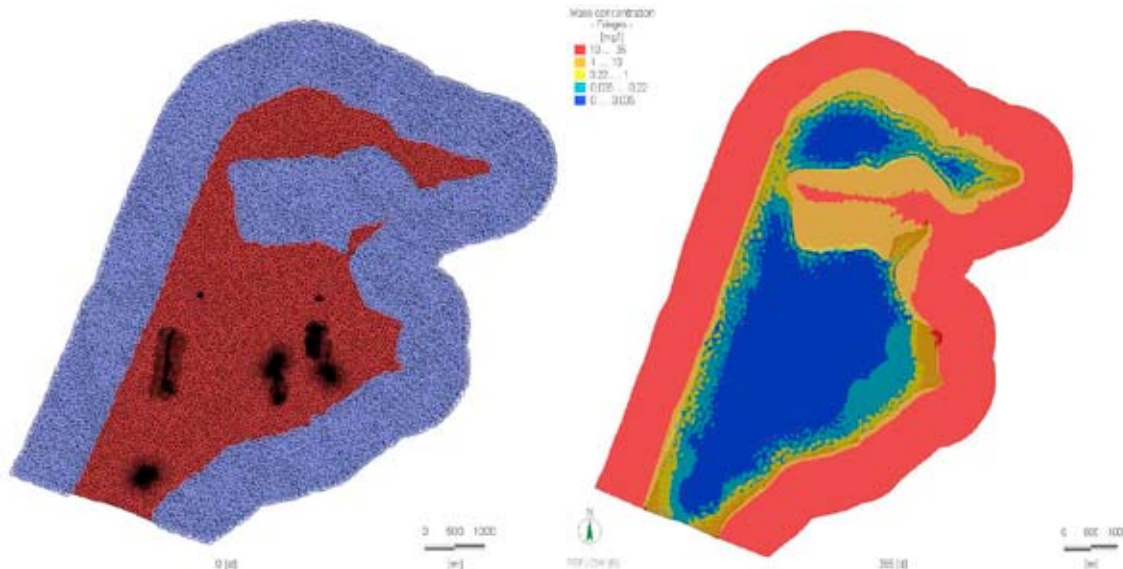


Figure 3: Model area, discretization and constant mass boundary conditions.

Figure 4: Calibrated fresh and saltwater distribution.

After the successful calibration, a transient model test was performed. For the testing of the model, we used piezometric heads from 05/01/2010 to 05/01/2011 recorded at observation points spread over the island. Two piezometers were installed at each observation point in order to record the level of surface water heads as well as groundwater heads. Data of some water gauges revealed a linear correlation between groundwater dynamics and fluctuation of surface water level. For the transient calculation the varying groundwater recharge was calculated after Grossmann using the daily rainfall statistic from the German Weather Service for the station “List” and the evaporation by Haude. By varying the specific storage coefficients in the upper layers a good match between measured and calculated hydrographs could not be achieved. These discrepancies have been detected for all observation wells and occurred only in during winter.

The winter 2010/2011 was characterized by snowfall events and periods with soil temperatures below freezing point. In the days with snowfall and low soil temperatures no groundwater recharge could occur. After the freezing period, the snow melted and infiltrated into the aquifer. The ‘frozen water’ (snow) and the low soil temperature lead to a delay of recharge. After ordering and analyzing the records of the German Weather Service for measured snowfall and temperature the recharge was adapted to the new situation. Every 10 cm of snow were converted in equivalent recharge values and applied to the recharge value of the following day, when temperatures rose above zero degrees. With this adaption it was possible to reproduce the measured hydrographs (Figure 5, Figure 6).

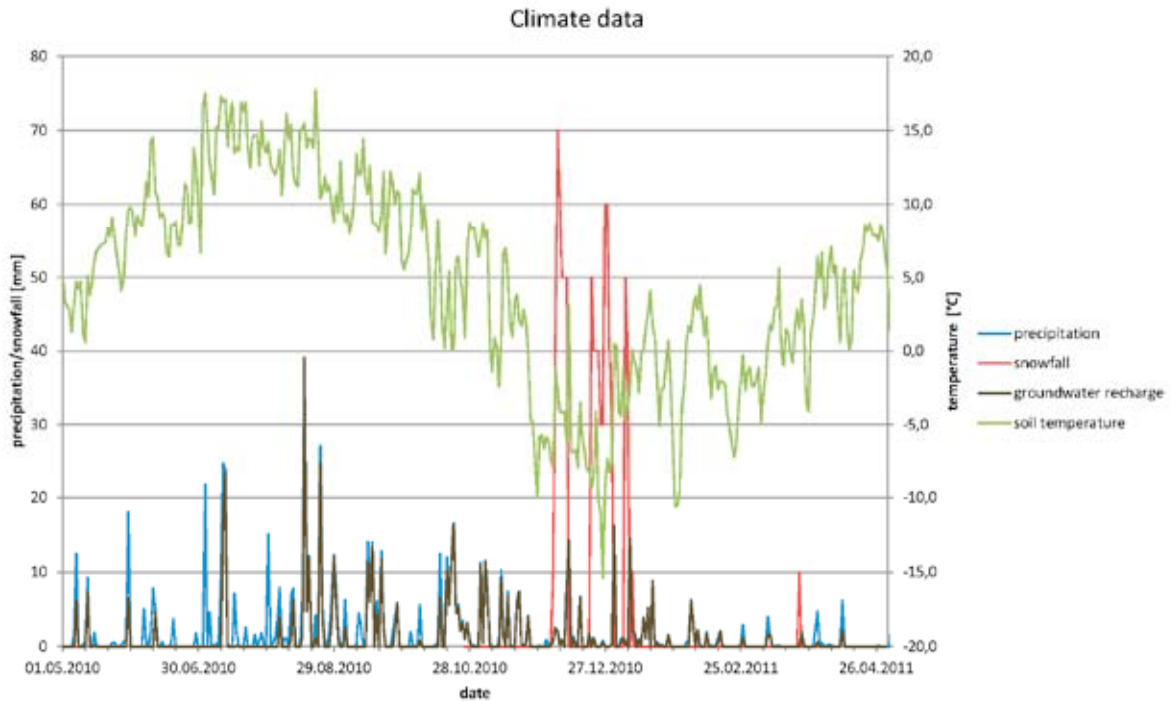


Figure 5: Climate data of the climate station "List" for the year 05/2010 - 05/2011.

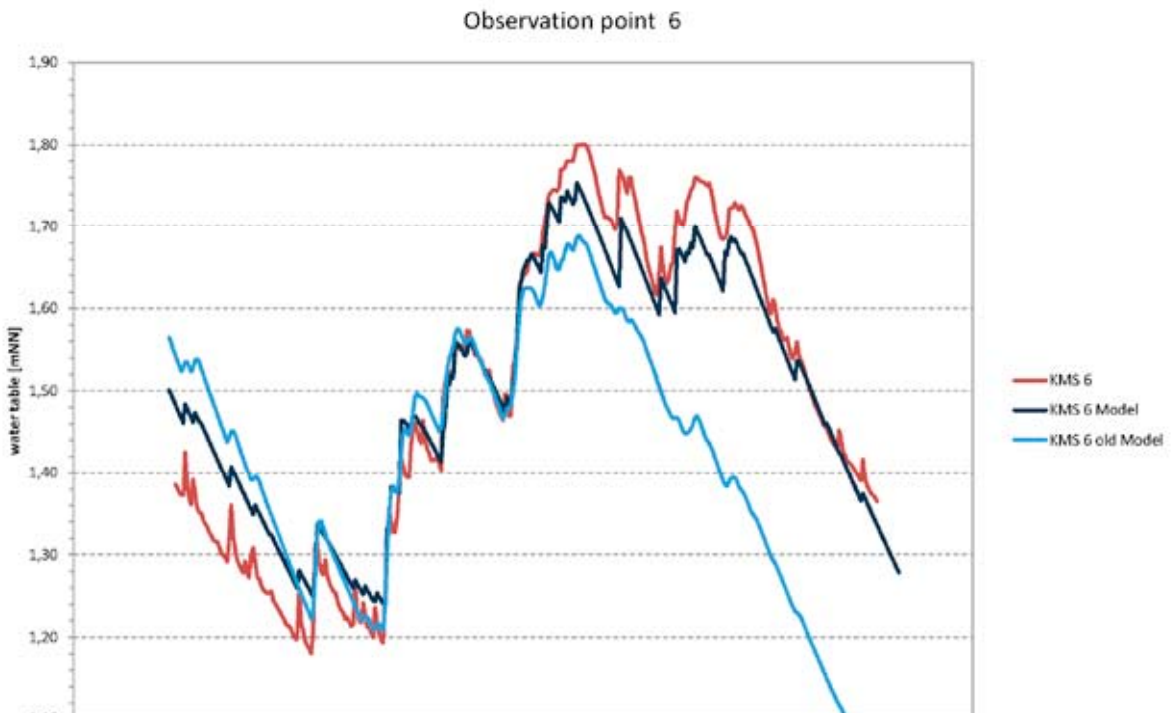


Figure 6: Groundwater hydrographs of observation point 6 (red = measured; black = calibration; blue = before adaption of recharge).

Contact Information: Kai Radmann, CONSULAQUA Hamburg, Ausschlaeger Elbdeich 2, 20539 Hamburg, Germany, Email: kRadmann@consulaqua.de

Evaluating hydraulic barriers for reducing and controlling saltwater intrusion in a changing climate

Per Rasmussen¹, Torben O. Sonnenborg¹ and Klaus Hinsby¹

¹Dept. of Hydrology, Geol. Survey of Denmark and Greenland, Copenhagen, Denmark.

ABSTRACT

Groundwater abstraction from coastal aquifers is vulnerable to sea level rise, increasing groundwater abstraction and drainage because they may potentially impact saltwater intrusion and hence groundwater quality depending on the hydrogeological setting. In the present study the impacts of sea level rise, drainage systems and changes in groundwater abstraction are quantified for an island located in the Western Baltic Sea using the modeling packages MODFLOW/MT3DMS/SEAWAT. Increasing chloride concentrations have been observed in several abstraction wells indicating that saltwater intrusion is ongoing. The water resources on the island are abstracted from a confined chalk aquifer. In order to prevent saltwater intrusion a hydraulic barrier is established. The effectiveness of the barrier consisting of injection wells is examined for a projected climate change scenario using variable density modeling.

INTRODUCTION

Groundwater abstracted from coastal aquifers is at risk of increased saltwater intrusion as an effect of the projected climate changes. This problem is studied for an area located in the southeastern part of Denmark on the island of Falster in the Baltic Sea (Figure 1). The local waterworks abstract groundwater from a shallow chalk aquifer. Part of the aquifer is located near the coast where an increasing chloride concentration has been monitored in groundwater abstraction wells over the last decades (Rasmussen et al. 2013).

In some coastal areas where saltwater intrusion has been threatening groundwater well fields, injection wells have been installed to generate a hydraulic barrier that prevents further saltwater intrusion, e.g. in Spain and USA. Climate changes might cause, among other things, sea level rise and changes in groundwater recharge. The objective of the present study is to conduct a model analysis of the effect of injecting freshwater into the groundwater aquifer to act as a hydraulic barrier to prevent further saltwater intrusion in a climate change scenario with increasing sea level and reduced groundwater recharge.

METHODS

The groundwater abstraction wells in focus are located on a barrier island between the Baltic Sea to the east and a low laying drained area to the west (Figure 1). A previous model study has examined possibly effects of increasing sea level, changes groundwater recharge, and canal stage on groundwater quality (Rasmussen et al. 2013). The model area of 44km² is discretized using a grid size of 50m by 50m, and 32 model layers varying in thickness from 2m to 12m down to a depth of -200m.a.s.l. The main aquifer consists of fractured and crushed chalk overlain by up to 45m of clayey till and sand.

In order to model the historical changes the study area has undergone from an area with saltwater lagoon and barrier islands to reclaimed and drained land with groundwater abstraction, a modeling period of more than 3000 years were carried out in order to reach a steady-state situation for the freshwater-saltwater distribution. From 1960 groundwater abstraction was implemented in the model. The modeling packages MODFLOW/MT3DMS/SEAWAT were used for the variable density modeling.

Eight combinations of sea level rise (0.5m, 0,75m, and 1m), changed groundwater recharge (decrease of 15%, increase of 15%), and changed canal stage (-30cm, +30cm) were analyzed. The climate change effects of sea level rise and changed recharge was gradually implemented in the model form 2010 to 2100. The model simulations were continued for additionally 200 years to year 2300.

It was found that the most severe scenario concerning the chloride concentration in groundwater abstraction wells were the scenario with a 0.75m sea level rise and a decrease in groundwater recharge of 15%. This “worst case” scenario has been used for the present study.

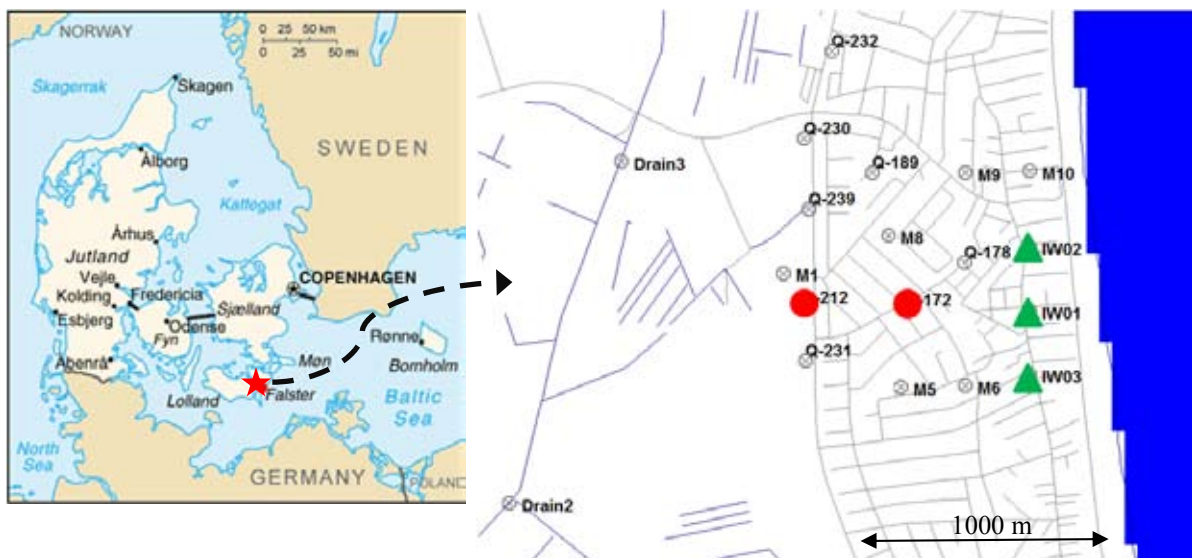


Figure 1. Location of study area (red star on left panel). Right panel shows part of the study area with two abstraction wells (red dots) and three injection wells (green triangles).

Three injection wells were added in the area between the well field and the coast line (Figure 1). The injection wells were located so far from the coast that they were not penetrating the saltwater wedge. The wells were screened in the upper fractured chalk from an elevation of -12m to -30m. The injection rates were the same as the average abstraction rates for the waterworks wells, 68 m³/d. The injection wells are located 300m from the coast with spacing of 250m. The abstraction wells of interest for this study, Q-172 and Q-212, are located 750m and 1150m, respectively, from the coastline (Figure 1).

The injection of water in the three injection wells was started in year 2300 and the simulation was continued for additional 100 years. The salinity concentrations were monitored in the two abstraction wells, Q-172 and Q-212 (Figure 1).

RESULTS

100 years of freshwater injection has a significant effect on the extension of the freshwater lens in both horizontal and vertical direction. Figure 2 upper panels show the freshwater-saltwater distribution in the year 2300 before start of the injection. Figure 2 lower panels show the freshwater-saltwater distribution after 100 years of freshwater injection.

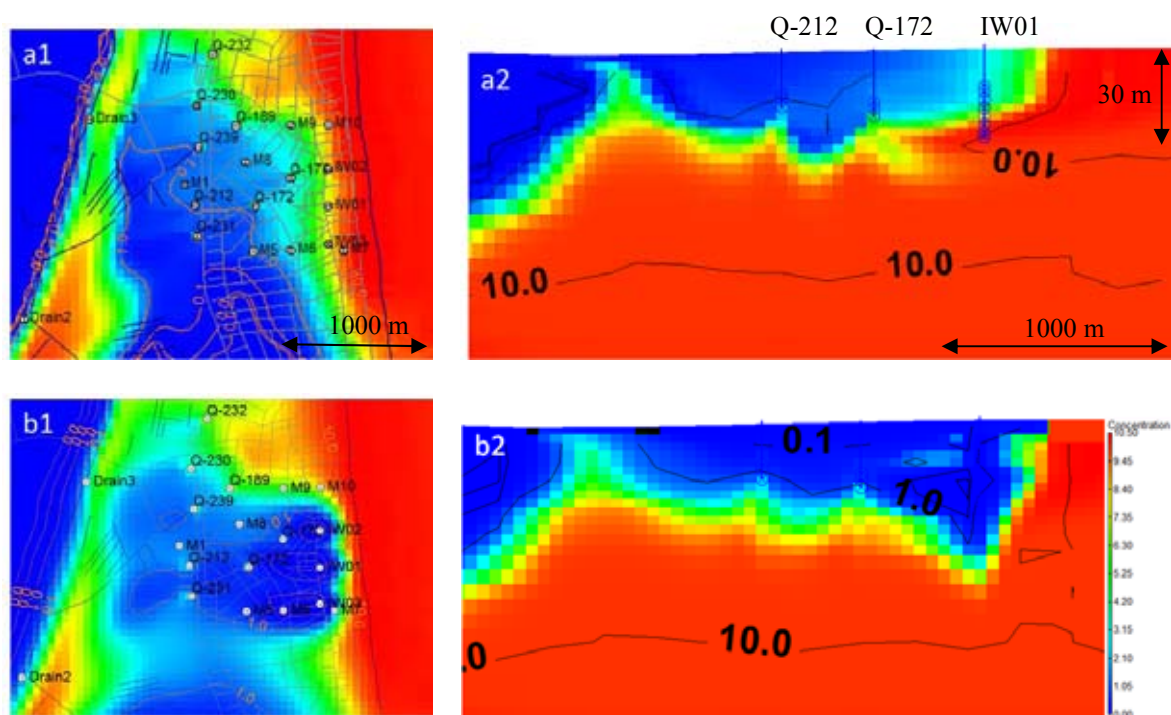


Figure 2. Saltwater distribution, plan view and cross section. Plan view: model layer 8, elevation -22m. Cross sections through wells Q-212, Q-172, and IW01. Panel a1 and a2: before injection. Panel b1 and b2: after 100 years injection. Contours: TDS (g/l).

The spacing between the three injection wells is seen to be sufficiently close to preventing saltwater intrusion between the injection wells.

Figure 3 shows the effect of the freshwater injection on TDS concentration in the two abstraction wells, Q-172 and Q-212. In the left panel the effects of the climate scenario implemented from year 2011 to 2300 is shown. The right panel shows the effect on TDS concentrations during 100 years of water injection starting in the year 2300. The effect of the injection well is first observed in the abstraction well closest to the injection wells and the coast, Q-172, after 25 years. In the abstraction well located further from the injection wells and the coast, Q-212, the effect is seen after 50 years. In well Q-172 a significant reduction in TDS concentration is found through the rest of the injection period. After 100 years of injection, the TDS concentrations are reduced to a level that is close to the concentrations found before the effects of the climate changes commenced.

However, the negative effects of climate changes could have been avoided if the injection wells had been installed before the onset of sea level rise and reduction in groundwater recharge.

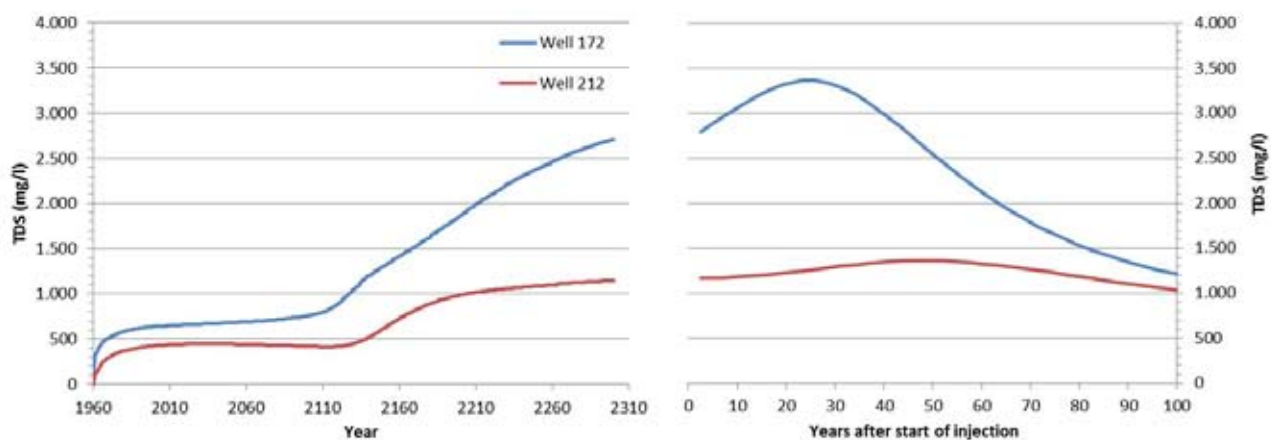


Figure 3. Effect of injection wells on TDS concentration in two groundwater abstraction wells. Location of wells, see figure 1. Left panel shows effects of a climate scenario implemented from year 2011. Right panel shows effect on TDS concentrations of 100 years water injection starting in the year 2300.

DISCUSSION AND CONCLUSIONS

Injection wells are tested as a hydraulic barrier to alleviate increased saltwater intrusion into coastal aquifers due to effects of projected climate change effects. Variable density modeling studies shows that fresh water injected into a coastal aquifer can prevent further increase in chloride concentrations in abstracted groundwater. The effectiveness of the hydraulic barrier in reversing the increasing trend in chloride concentrations in groundwater abstraction wells depends among other things on the timing of the injection scheme installation relative to the timing of climate changes.

Further studies in the area are planned to characterize the variation in hydraulic conductivity by calibrating the variable density model against available data on hydraulic head and chloride concentration using the pilot points method. Results from an airborne electromagnetic survey (SkyTEM) will be used to estimate the chloride concentration in the aquifers and it will be tested if these data can be used as targets in the calibration process. Also different designs of the hydraulic barrier including the number of injection wells, the injection rate and the location and orientation of the wells will be examined.

REFERENCES

P. Rasmussen, T. O. Sonnenborg, and K. Hinsby. 2013. Assessing impacts of climate change, sea level rise, and drainage canals on saltwater intrusion to coastal aquifer. *Hydrol. Earth Syst. Sci.*, 17, 421–443, 2013. www.hydrol-earth-syst-sci.net/17/421/2013/. doi:10.5194/hess-17-421-2013.

Contact Information: Per Rasmussen. Geological Survey of Denmark and Greenland (GEUS), Department of Hydrology. Øster Voldgade 10, DK-1350 Copenhagen K. Phone: +45 91 33 36 33, E-mail: pr@geus.dk.

Experimental Investigation of Transient Saltwater Intrusion in Heterogeneous Porous Media

G. Robinson¹, G. Hamill¹ and A. Ahmed¹

¹EERC, Queen's University, Belfast, Northern Ireland, UK

ABSTRACT

A 2D sandbox style experiment was developed to compare the results of numerical modelling to physical testing for saltwater intrusion in homogeneous and heterogeneous aquifers. The sandbox consisted of a thin central viewing chamber filled with glass beads of varying diameters (780 μm , 1090 μm and 1325 μm) under fully saturated conditions. Dyed saltwater (SW) was introduced at the side boundary and a head difference imposed across the porous media. Images of the SW wedge were recorded at intervals in order to assess the suitability of the numerical models predictions of transient SW intrusion. Numerical modelling of the experimental cases were simulated using SUTRA. Two main parameters were chosen to express the condition of the intruding SW wedge at each recorded time step; the toe penetration length (TL) and the width of the mixing zone (WMZ). The WMZ was larger under transient conditions in the heterogeneous case, while the TL was longer for the homogeneous case. The increased variability in the flow field for the heterogeneous case resulted in increased dispersion, and thus, increased WMZ.

INTRODUCTION

Image analysis has been widely used to track the migration of contaminants in groundwater flow using sandbox style experiments (Schincariol & Schwartz, 1990; Goswami & Clement, 2007; Chang & Clement, 2013). Laboratory scale saltwater (SW) intrusion may not be capable of reproducing exactly the conditions found in real world aquifers, but the increased level of control does allow for validation of numerical methods. This paper briefly outlines the implementation of image analysis techniques to heterogeneous aquifers and presents a comparison of TL and WMZ from the physical tests with numerical simulations using SUTRA (Voss & Provost, 2010).

METHODS

Sandbox Experimental Setup

The sandbox (0.38m x 0.128m x 0.01m) consisted of a narrow viewing chamber filled with glass beads packed in a variety of arrangements. Two tanks were located at either side of the viewing chamber and were separated from the chamber by a fine screen. One of the side tanks was filled with clear deionised fresh water (FW) while the other contained a SW solution (density = 1025kg/m³) dyed with food colouring. The water levels in these tanks provided constant head FW and SW boundaries using a variable overflow system similar to Goswami & Clement (2007). By imposing a difference in water level (dH) between the side tanks a hydraulic gradient was created across the porous media and a SW wedge intruded into the central viewing chamber. Ultrasonic sensors, with an accuracy of 0.1mm, were used to measure the water level in both side tanks. Two LED lights provided transmissive illumination of the SW wedge progression through the clear porous media. Initially, the aquifer was totally flushed with FW and $dH=6\text{mm}$ was imposed. Images of the dyed SW wedge were recorded every 5 minutes until a steady state condition was reached (50 minutes). The head difference was then decreased to $dH=4\text{mm}$ and the advancing

movements of the wedge were captured. After a steady state condition was achieved, the receding SW wedge dynamics were analysed by finally increasing $dH=5\text{mm}$. An 8-bit 1280 x 1024 resolution high speed IDT Vision camera was used to capture the images. Initially, 3 diameters of beads ($780\mu\text{m}$, $1090\mu\text{m}$ and $1325\mu\text{m}$) were tested under homogeneous conditions. A series of tests using horizontal layered and hand packed block-wise bead arrangements followed the homogeneous experiments. The results from the homogeneous $1090\mu\text{m}$ tests and hand packed block-wise experiment, which included all 3 bead diameters, are discussed further in this paper. An intrinsic test based on Darcy's law was conducted to determine the permeability for each bead arrangement and was used in the numerical model.

Calibration

In order to calculate the salt concentration field from the light intensities captured in the images a calibration was required. The calibration involved flushing the aquifer with known concentrations of dyed SW solution and recording the change in light intensity. For this experiment 8 concentrations were used: 0, 0.05, 0.10, 0.20, 0.30, 0.50, 0.70, 1.00, where 0 equates to undyed FW and 1.00 equates to fully dyed 1025kg/m^3 SW. A power curve was chosen to describe the relationship between concentration and light intensity, and a least squares regression analysis was used to determine suitable values for the curve coefficients.

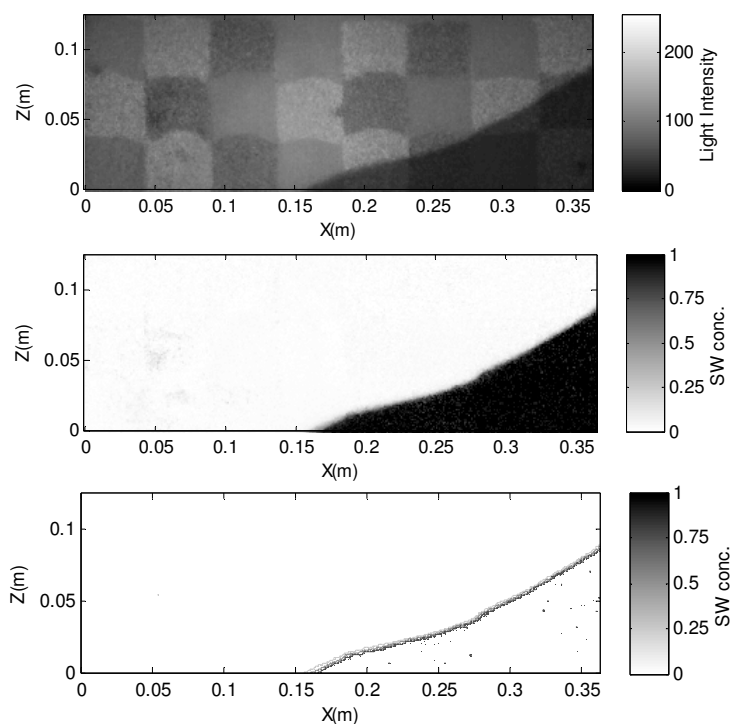


Figure 1. Analysis area of image (top), colour map of SW concentration (middle) and contour plot of concentration isolines [0.25 0.50 0.75] (bottom)

Figure 1 shows an image of the block-wise aquifer and a contour plot of the 0.25, 0.50 and 0.75 concentration isolines. The top plot in Figure 1 shows large discrepancies in lighting uniformity, which complicates the calibration step as average image light intensity is no longer a suitable parameter to use in the regression analysis. This prompted the use of a pixel-wise calibration method, where a least squares regression analysis was carried out for every pixel in the image. Each individual pixel locations calibration relationship was then applied to the test data, with the results shown in the middle and bottom plots of Figure 1. The pixel-wise calibration method is capable of producing concentration fields in highly non-uniform lighting conditions with small error.

RESULTS

Transient toe length (TL)

The transient experimental and numerical TL for the blocked heterogeneous case is shown in Figure 2 (top left). Generally the numerical results compare fairly well to the physical tests, as shown in the steady state 0.5 concentration isolines in Figure 2 (bottom left). However, the numerical model over predicts the steady state TL at $dH=6\text{mm}$, but under predicts the TL at $dH=4\text{mm}$. This change from over prediction to under prediction is hypothesized as being due to packing issues, where the porous media at the bottom is being compressed more due to the load of the media situated above it. The homogeneous TL results (not shown) have very similar trends to the blocked heterogeneous but are slightly larger at steady state conditions. The range of bead size did not provide a large enough permeability variation for a significant change in the steady state TL. Figure 2 shows a lag in TL movement when the head difference increases from $dH=4\text{mm}$ to $dH=5\text{mm}$. The SW wedge should be receding under these conditions but has been delayed. After it begins to move the receding TL reaches a steady state condition quicker than the advancing wedge. This is in agreement with Chang & Clement (2013) who reasoned that the flow field changes from the SW opposing the FW while the SW wedge is advancing, to a unidirectional flow field while the SW wedge is receding. This would also explain the delay in wedge movement when dH is increased as the flow field has to reorientate.

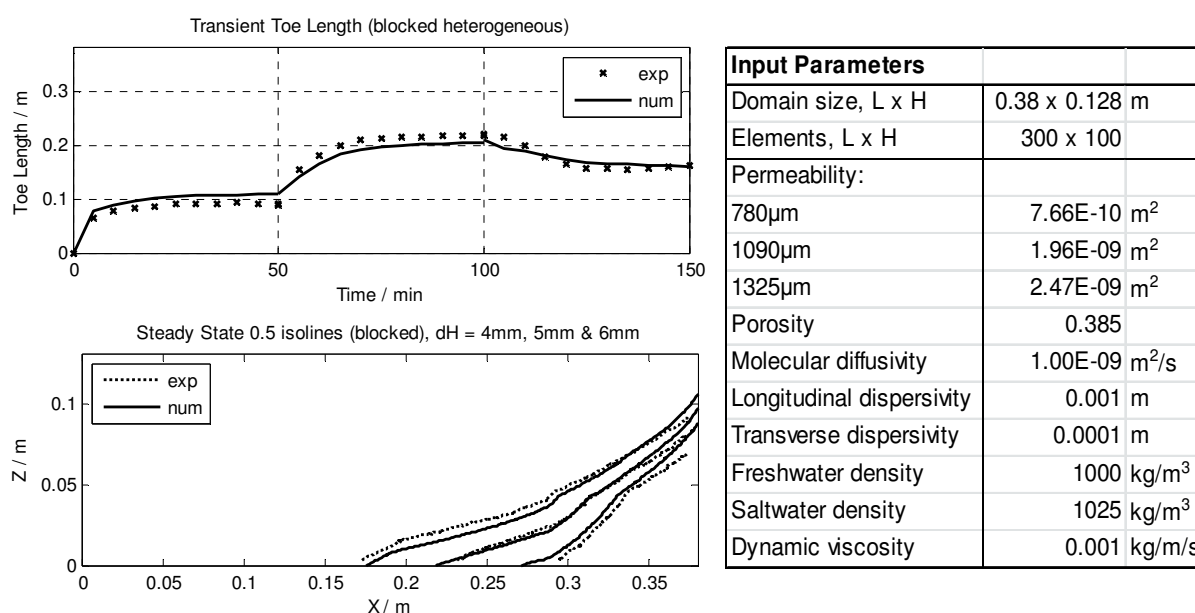


Figure 2. Transient TL, 0-50min $dH=6\text{mm}$, 50-100min $dH=4\text{mm}$, 100-150min $dH=5\text{mm}$ (top left), steady state 0.5 conc. isolines (bottom left) and numerical model input parameters (right)

Transient width of mixing zone (WMZ)

The transient experimental and numerical WMZ for the homogeneous and blocked heterogeneous case is shown in Figure 3. The size of the mixing zone in both the homogeneous and heterogeneous case is very small, around 5mm. The experimental results show much greater variation in WMZ to the numerical, particularly when the head difference across the aquifer is changed. This is attributed to small scale heterogeneities induced in the packing process and from slight variations in bead size. The WMZ shows a similar response to the TL when increasing from $dH=4\text{mm}$ to $dH=5\text{mm}$. However, the lag response and

magnitude of WMZ increase are smaller for the homogeneous case because the higher uniformity of the permeability field allows the switch in flow field to establish faster. The size of the WMZ change is much greater when the wedge is receding. This can be explained by the increased velocities the unidirectional flow field creates which increases dispersion.

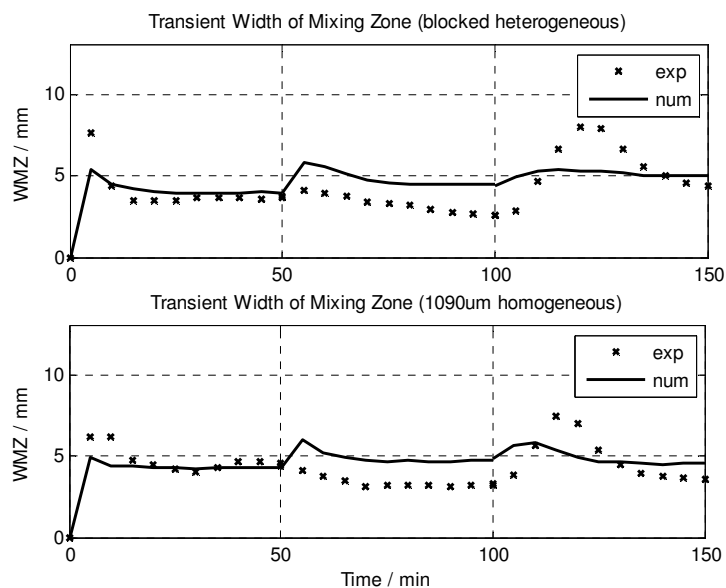


Figure 3. Transient WMZ, heterogeneous (top) and homogeneous (bot)

CONCLUSION

An experimental system was developed and calibrated, and a study conducted to determine the effects of heterogeneity on a transient SW wedge, in terms of toe length (TL) and width of mixing zone (WMZ), for a homogeneous and block-wise heterogeneous case. The homogeneous results were similar to the heterogeneous cases in terms of TL and WMZ. Larger WMZs were observed in the heterogeneous case under transient conditions while the TLs were slightly longer in the homogeneous case. There was an increase in WMZ when the head difference was changed, but the response was greater for receding wedges when compared to advancing wedges. The WMZ response was in agreement with the hypothesis of changing flow field direction within the SW wedge discussed in Chang & Clement (2013) for receding TL.

REFERENCES

Chang, S.W. & Clement, T. P., 2012. "Experimental and numerical investigation of saltwater intrusion dynamics influx-controlled groundwater systems", *Water Resour. Res.*, 48, W09527, doi:10.1029/2012WR012134.

Goswami, R.R. & Clement, T.P., 2007. "Laboratory-scale investigation of saltwater intrusion dynamics", *Water Resources Research*, vol. 43, no. 4, pp. W04418.

Schincariol, R.A. & Schwartz, F.W., 1990. "An experimental investigation of variable density flow and mixing in homogeneous and heterogeneous media", *Water Resour. Res.* 26 Z10., 2317_2329.

Voss, C.I. & Provost, A.M., 2010. "SUTRA: A model for saturated-unsaturated, variable-density ground-water flow with solute or energy transport", 2.2nd edn, USGS, Virginia.

Contact Information: Gareth Robinson, Queen's University Belfast, Environmental Engineering Research Centre, SPACE David Keir Building, Stranmillis Road, Belfast, UK, BT9 5AG, Phone: 028 90974751, Fax: 305-555-5000, Email: grobinson18@qub.ac.uk

Stochastic Analysis of Saltwater Intrusion in Heterogeneous Aquifers using Local Average Subdivision

G. Robinson¹, A. Ahmed¹ and G. Hamill¹

¹EERC, Queen's University, Belfast, Northern Ireland, UK

ABSTRACT

This study investigates the effects of ground heterogeneity, considering permeability as a random variable, on an intruding SW wedge using Monte Carlo simulations. Random permeability fields were generated, using the method of Local Average Subdivision (LAS), based on a lognormal probability density function. The LAS method allows the creation of spatially correlated random fields, generated using coefficients of variation (COV) and horizontal and vertical scales of fluctuation (SOF). The numerical modelling code SUTRA was employed to solve the coupled flow and transport problem. The well-defined 2D dispersive Henry problem was used as the test case for the method. The intruding SW wedge is defined by two key parameters, the toe penetration length (TL) and the width of mixing zone (WMZ). These parameters were compared to the results of a homogeneous case simulated using effective permeability values. The simulation results revealed: (1) an increase in COV resulted in a seaward movement of TL; (2) the WMZ extended with increasing COV; (3) a general increase in horizontal and vertical SOF produced a seaward movement of TL, with the WMZ increasing slightly; (4) as the anisotropic ratio increased the TL intruded further inland and the WMZ reduced in size. The results show that for large values of COV, effective permeability parameters are inadequate at reproducing the effects of heterogeneity on SW intrusion.

INTRODUCTION

It has been well established that heterogeneity, in the form of variable conductivity fields, has a significant effect on flow through a porous media (Held et al. 2005; Abarca, 2006; Ahmed, 2009; Kerrou & Renard, 2010). A popular method of representing heterogeneity is to use probabilistic methods. It has become so popular that Eurocode 7 recommends probabilistic methods as an option to consider when determining characteristic properties of porous media, as they take account of spatial variability (Hicks & Samy, 2002). This study seeks to comprehensively investigate the effects of heterogeneity by simulating a broader range of cases not reported in other works. The additional simulations provide results at the extremities of the known trends and solidify the findings of previous studies.

Background

Numerous investigations into heterogeneous saltwater intrusion have used a stochastic approach to account for the spatial variation in conductivity (Held et al. 2005; Abarca, 2006; Kerrou & Renard, 2010). Held et al. (2005) studied the effects of heterogeneity on an intruding saltwater wedge for the benchmark Henry problem. The objective of Held et al. (2005) was to determine whether results from heterogeneous stochastic simulations could be reproduced using simple effective parameters simulated homogeneously, thus neglecting the long computational time required for stochastic processes. Abarca (2006) recognised the limitations of the Henry problem and hypothesized a purely dispersive version that would better represent the salinity profiles seen in reality. The dispersive problem uses the same boundary conditions as the Henry problem but saltwater-freshwater mixing is assumed to be due to advection and velocity dependent dispersion, instead of diffusion. Kerrou & Renard

(2010) simulated this 2D dispersive Henry problem for isotropic and anisotropic cases and also extended the problem to the third dimension. This paper extends the 2D simulations of the dispersive Henry problem carried out by Abarca (2006) and Kerrou & Renard (2010) for cases of varying scales of fluctuation (SOF), coefficients of variation (COV) and anisotropic ratios (ξ), by combining the computer code SUTRA (Voss & Provost, 2010) with random field generation using local average subdivision (LAS) (Fenton, 1990).

METHODS

Random field generation using local average subdivision (LAS)

A lognormal distribution is used to describe the random permeability field $K(x)$ that has a mean (μ_k) and standard deviation (σ_k). Therefore $\ln(K)$ will have a Gaussian distribution where the respective mean ($\mu_{\ln k}$) and standard deviation ($\sigma_{\ln k}$) are determined from transformations (Fenton, 1990; Ahmed, 2009). The spatial correlation of the random fields takes the form of a Gauss-Markov exponentially decaying function, and is determined by the SOF (θ). The LAS algorithm creates a field of elements by dividing a global average value into 4 sub-fields whose local average is equal to the value of the global average (Fenton, 1990). This step continues recursively until the number of elements required in the field is achieved. Initially, LAS is used to construct a Gaussian random field, $G(x)$, with zero mean, unit variance and spatial correlation. The random permeability of each element is then assigned using the transformation:

$$K_i = \exp[\mu_{\ln k} + \sigma_{\ln k}G(x_i)] \tag{1}$$

where x_i is the centre of the i th element. Random fields in this study are defined by the scale of fluctuation (SOF, θ), coefficient of variation (COV = σ_k/μ_k) and anisotropic ratios ($\xi = \theta_h/\theta_v$, where θ_h and θ_v are the horizontal and vertical SOF).

Dispersive Henry problem

The dispersive Henry problem consists of a confined aquifer with a hydrostatic saltwater pressure boundary at one side and a freshwater flux boundary at the other. Figure 1 shows the numerical domain and simulation inputs with visual representations of the TL and WMZ.

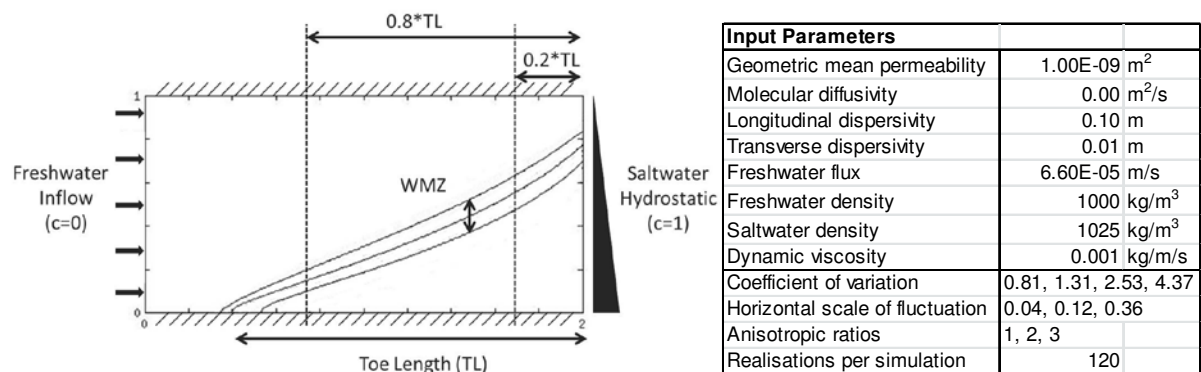


Figure 1. Dispersive Henry problem simulation domain and input parameters

The TL is defined as the distance between the saltwater boundary and where the 50% saltwater isoline intersects the bottom boundary. The WMZ is the average of the vertical distances between the 25% and 75% saltwater isolines within the range 0.2*TL and 0.8*TL. The TL and WMZ are determined for each realization and then averaged to give the values reported in this paper.

RESULTS

Effect of Coefficient of Variation (COV)

Results from a selection of the stochastic simulations are presented in Figure 2. When compared to the effective permeability simulations, an increase in COV resulted in a reduction of TL and an increase in WMZ for the heterogeneous simulations.

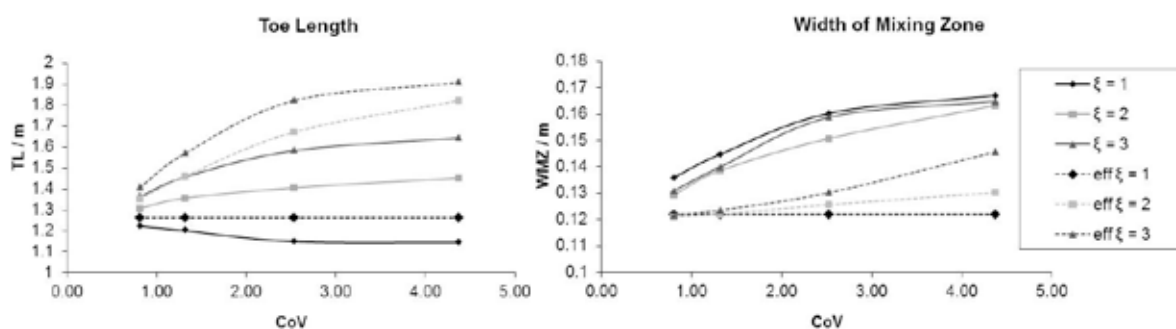


Figure 2. TL and WMZ for changing CoV and ξ for stochastic (line) and effective homogeneous (dashed) simulations

This was typical for all anisotropic ratios. The increase in WMZ can be explained by the greater longitudinal and transverse dispersions observed in heterogeneous media, which become greater with increasing COV. The effect of heterogeneity on TL can also be explained by the increase in dispersion. The increased dispersion acted to spread the salt further, reducing the sharpness of the density difference within the wedge. As a result the slope of the wedge became more linear than the curved shape observed in the homogeneous cases. The overall result was a reduction in TL with increasing COV. These results are in agreement with Abarca (2006) and Kerrou & Renard (2010).

Effect of Anisotropic Ratio (ξ)

As ξ increased the TL became larger, due to the flow pathways tending to align in the horizontal direction, forming channels of correlated permeability spanning the length of the domain. The chances of encountering a region of low permeability become smaller as the field becomes increasingly more correlated in the horizontal direction. This is observed most notably in the isotropic case ($\xi = 1$), where the TL decreased with increasing COV while it increased for anisotropic cases ($\xi > 1$). However both isotropic and anisotropic cases show a reduction in TL when compared to their effective homogeneous counterparts. The WMZ generally increased with increasing COV and only a slight decrease in width was observed with increasing ξ . This is because the WMZ is predominately determined by the dispersion, which will increase when there is more variability along the concentration gradient. However, dispersion also increases with higher fluid velocities which are observed in larger ξ in the horizontal direction. Therefore the change in WMZ with increasing ξ is small due to the balancing of dispersive mechanisms with regards to spatial variability and fluid velocity.

Effect of Scale of Fluctuation (θ)

In general, an increase in SOF resulted in a seaward movement of the TL, as is shown in Figure 3. For the smallest value of SOF shown ($\theta=0.04$) the TL has intruded the furthest. This is contrary to what would normally be expected. An increase in SOF would imply an increase in dispersion, therefore resulting in a reduction of TL. However this trend can be explained in terms of the number of permeability flow channels available in the domain. As

the SOF decreases, the porous media contains a larger frequency of high and low permeability zones. Whenever the flow encounters a low permeability zone, there is a higher chance that nearby a large permeability channel will exist and the flow will not have to deviate as much to continue moving further inland. Similar to the effect of changing ξ , the WMZ was not significantly affected by changes in SOF but was dominated by COV.

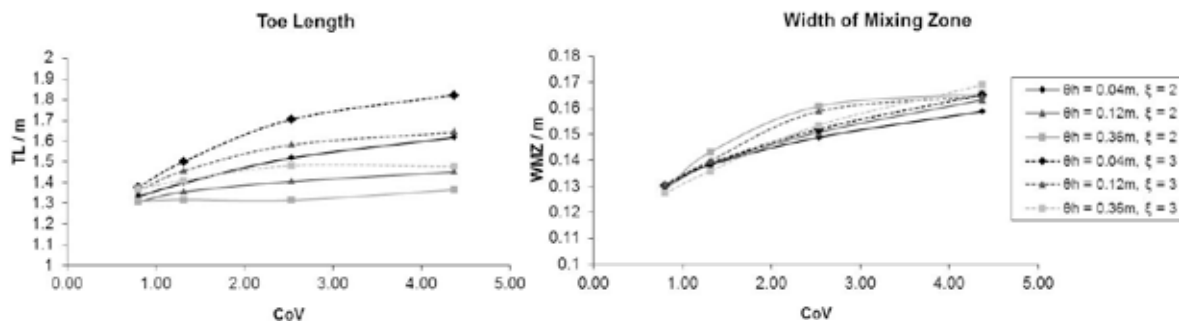


Figure 3. TL and WMZ for changing CoV, SoF and ξ

CONCLUSIONS

This paper has briefly described the effect of varying scales of heterogeneity on an intruding saltwater wedge. The scale of heterogeneity was represented by coefficients of variation (COV), scales of fluctuation (SOF) and anisotropic ratios (ξ). Simulations have shown that increases in COV dominated the changes in the width of the mixing zone, while the toe length movements were also dependent on ξ and SOF. An increase in ξ produced a landward movement of the toe, while an increase in SOF resulted in a seaward movement. Increases in COV resulted in enhancing the effects of these trends. The ability to apply an effective homogeneous permeability value to represent aquifer heterogeneity is useful as it negates the need for a computationally intense and time consuming stochastic process. However for large values of COV and SOF effective permeability values do not adequately portray the intrusion of a saltwater wedge in terms of toe penetration length and width of mixing zone.

REFERENCES

- Abarca, E., 2006. "Seawater intrusion in complex geological environments", Department of Geotechnical Engineering and Geo-Sciences (ETCG) Technical University of Catalonia, UPC.
- Ahmed A., A., 2009. "Stochastic analysis of free surface flow through earth dams", Computers and Geotechnics, vol. 36, no. 7, pp. 1186-1190.
- Fenton, G., 1990. "Simulation and Analysis of Random Fields", Princeton University.
- Held, R., Attinger, S., Kinzelbach, W., 2005. "Homogenization and effective parameters for the Henry problem in heterogeneous formations", Water Resources, 41:1-14. doi:10.1029/2004WR003674
- Hicks MA, Samy K., 2002. "Reliability-based characteristic values: a stochastic approach to Euro code 7", Ground Eng 35(12):30-4.
- Kerrou, J., Renard, P., 2010. "A numerical analysis of dimensionality and heterogeneity effects on advective dispersive seawater intrusion processes", Journal of Hydrology 18 (1), 55-72.
- Voss, C.I. & Provost, A.M., 2010. "SUTRA: A model for saturated-unsaturated, variable-density ground-water flow with solute or energy transport", 2.2nd edn, USGS, Virginia.

Contact Information: Gareth Robinson, Queen's University Belfast, Environmental Engineering Research Centre, SPACE David Keir Building, Stranmillis Road, Belfast, UK, BT9 5AG, Phone: 028 90974751, Fax: 305-555-5000, Email: grobinson18@qub.ac.uk

Geoelectrical monitoring of freshwater-saltwater interaction in physical model experiments

Mathias Ronczka¹, Leonard Stoeckl² and Thomas Günther¹

¹Leibniz Institute for Applied Geophysics (LIAG), Hannover, Germany

²Federal Institute for Geosciences and Natural Resources (BGR), Hannover, Germany

INTRODUCTION

The availability of freshwater in coastal aquifers is endangered by saltwater intrusion (e.g. over-pumping, sea level rise, storm surge). As differences in the mineralization of groundwater affect the electrical conductivity, geoelectrical measurements are suitable for imaging saltwater distribution in aquifers. Monitoring the geoelectrical resistivity comes into widespread use for the characterization of the subsurface and reveals general information about the pore fluid and its temporal variability.

Typically, saltwater intrusion is the movement of the saltwater wedge into a coastal freshwater aquifer. The position of this wedge depends mainly on groundwater recharge rates and geological characteristics of the subsurface. The dynamics and rates of saltwater intrusion are further affected by climate change. In order to make quantitative predictions, we simulate a coastal aquifer in the laboratory using a transparent model tank and change recharge rate and sea level. Furthermore, saltwater inundation is simulated by short temporary slopover. Geo-electrical surface measurements are conducted during these experiments and time-lapse inversion of the data is done, revealing fluid conductivity and thus salt concentration.

EXPERIMENTS

A two dimensional physical experiment was conducted within a 200 cm long, 50 cm high and 5 cm wide acrylic tank. Using filter gravel ($d \sim 0.7$ to 1.2 mm), a cross-section of a coastal aquifer was simulated. After saturating the model with saltwater (density of $1025 \text{ kg}\cdot\text{m}^{-3}$ and electrical conductivity of about $6 \text{ S}\cdot\text{m}^{-1}$) to a height of 30 cm, three different experiments were conducted:

1. Freshwater (density of $1000 \text{ kg}\cdot\text{m}^{-3}$) was recharged to the onshore part of the model by drippers until equilibrium was reached and the saltwater-freshwater interface was in steady-state, forming a typical wedge.
2. The freshwater recharge rate was reduced causing a movement of the saltwater-freshwater interface into the aquifer.
3. The sea level was temporary increased slightly above the top of the aquifer for about 5 min, simulating saltwater inundation. After the saltwater front had moved through the aquifer steady-state was reached again.

By coloring the fresh- and saltwater with different tracer dyes (Uranin and Eosin), movements could be visualized and compared to hydraulic modeling and geophysical inversion results.

For geoelectrical measurements, 32 electrodes were distributed equidistantly with spacing of 6 cm. To enhance the resolution at the saltwater wedge, 7 electrodes were placed at the

sloping beach face within the saltwater. We used the RESECS equipment with a Schlumberger configuration providing 225 measurements for each time in about 3 minutes each. In total 948 time frames were measured in a total experiment time of 2 days.

The electrical fields are three-dimensional and disturbed by the final dimensions of the tank. But the measurement scheme only allows for reconstructing a two-dimensional resistivity distribution. Therefore, a hybrid 2D/3D approach was used for data inversion: First a 2D triangle mesh was constructed using the dimensions of the tank, the shore and the sea level. The 3D mesh consists of triangle prism elements aligned across the y-axis. All cells belonging to one triangle face form a region with only one unknown and smoothness constrains between each other. Furthermore, all cells belonging to seawater were combined into one inversion region, which is decoupled from the aquifer and is represented by only one resistivity. The BERT package (Günther et al. 2006) was used for inversion. Forward modeling was achieved using a refined finite element mesh.

RESULTS

Experiment 1

The inversion result of the initial steady-state reveal resistivities of 0.76 and 0.16 Ωm for the aquifer and the sea, respectively. The latter agrees well with sampling. The homogeneous initial state allows to derive a formation factor of $F = 5$ that is used to compute fluid conductivity from the determined bulk resistivity using $\sigma_w = F/r$. The inversion results (right-hand-side column) and corresponding photos are depicted in Figure 1.

Shortly after starting the artificial precipitation, the freshwater starts to displace the saltwater in the aquifer. The process successively slows down since freshwater starts to discharge at the shoreline. However, as the freshwater is on top, it immediately leaves the tank and thus the sea resistivity remains constant.

The resulting conductivity images agree very well with the photographs at the same time. However the interface is blurred indicating the limited resolution. After about 12 hours there is only a thin layer of saltwater at the bottom of the tank, but in the inversion result it appears thicker. The final steady-state is again very well reproduced.

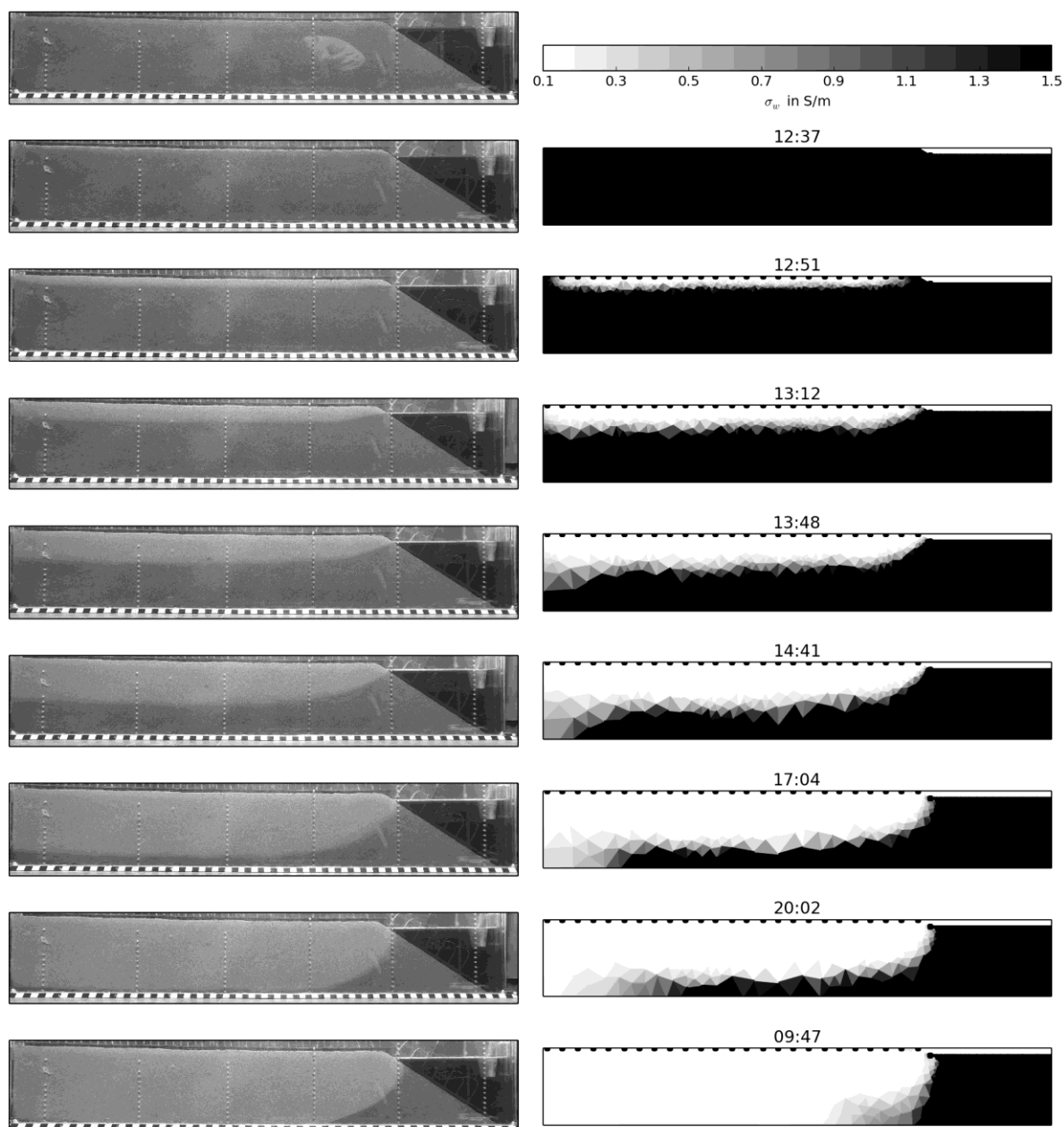


Figure 1. Photographs (left) and retrieved fluid conductivity distribution for experiment 1 (displacement of saltwater by freshwater recharge).

Experiment 2

Starting at steady-state after the first experiment, the flow rate of freshwater was reduced. Within approximately four hours the saltwater wedge was moving about 50 cm in onshore direction. As the movement of the wedge is quite slow, only four different time-steps are depicted in Figure 2. Compared to the photos taken, the movement is generally observable in the inversion result. However, the coarse mesh at the bottom of the tank does not allow a better localization of the wedge. Still, these small resistivity changes are resolvable.

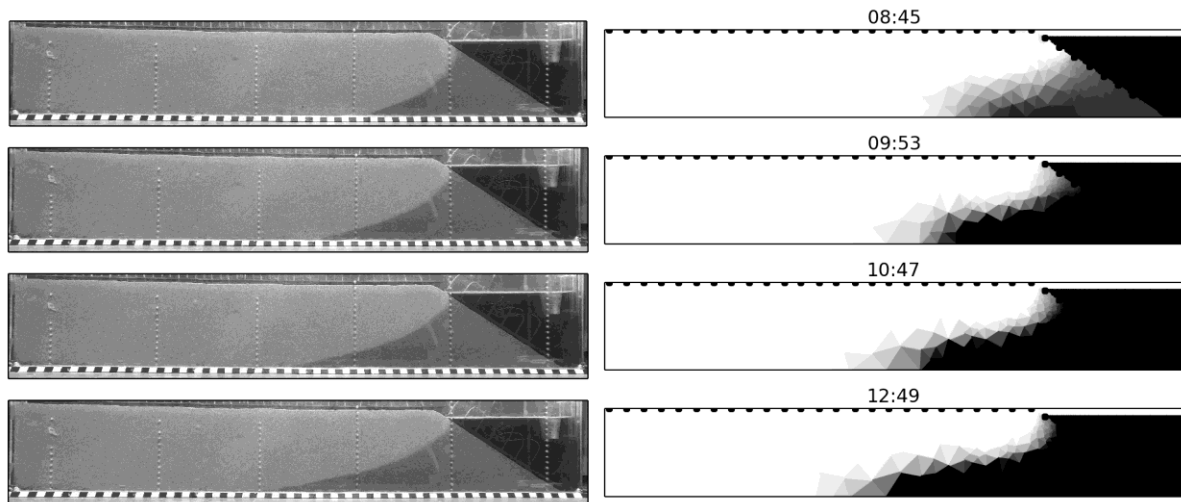


Figure 2. Photographs (left) and retrieved fluid conductivity distribution for experiment 3 (increased recharge rate and interface movement).

DISCUSSION AND CONCLUSIONS

Using a hybrid 2D/3D inversion for geoelectric data on a laboratory scale was mostly successful. The third experiment (sea water inundation) could not be fitted correctly, because of the changing model-geometry at the beginning of the experiment. This leads to artifacts that influence the whole time-lapse inversion. By using the predecessor-model as base line model these artifacts can be removed for later time-steps.

The position of the freshwater-saltwater interface in the aquifer could be determined by electrical resistivity tomography (ERT) based on surface measurements. It images the dynamics of the interface with high temporal resolution. The spatial resolution decreases with depth. The reconstructed fluid conductivity agrees well with the photographs of the dye tracer. Up to this point artifacts near the slope could not be removed. The possibility of removing affected electrodes is under investigation. Sometimes there is a slight discrepancy that might be within the equivalency of models. Moreover, there might be a separation between dye and saltwater due to dispersion.

REFERENCES

Günther, T., Rücker, C. & Spitzer, K. (2006): 3-d modeling and inversion of DC resistivity data incorporating topography - Part II: Inversion. *Geophys. J. Int.*, 166 (2), 506-517.

Contact Information: Mathias Ronczka, Leibniz Institute for Applied Geophysics (LIAG), Stilleweg 2, 30655 Hannover, Germany, Phone: +49-511-643-3491, Fax: +49-511-643-3665, Email: Mathias.Ronczka@liag-hannover.de

Monitoring inland salt-water intrusion with long-electrode ERT

M. Ronczka, T. Günther and F. Oppermann

Leibniz Institute for Applied Geophysics, Hannover, Germany

INTRODUCTION

In coastal regions, but also inland, fresh water supply is threatened by saltwater intrusions. The support of water plants to ensure water supply is of main interest. As the electrical resistivity is mainly influenced by the pore fluid, it is a key parameter for detecting and monitoring saltwater. Results of 2D or 3D electromagnetic surveys or electric resistivity tomography (ERT) give insight into the lithological and hydrological properties of the subsurface. However, most methods show limited investigation depths or are cost-intensive for investigating an area in the catchment scale. As an alternative to classic multi-electrode surveys, long-electrode ERT (LE-ERT) can provide three-dimensional imaging if a sufficient amount of metal-cased boreholes is available. Hence, a cost efficient monitoring is possible as non-recurring costs appear only for the installation procedure.

As the usual point approximation of electrodes is not accurate enough, we use the complete electrode model (CEM) for numerical simulation of the electric field propagation. With this it is possible to model electrodes of arbitrary shape by including two additional equations into the finite element solution of the forward problem, (Rücker and Günther 2011). Changing contact impedances along one electrode does not change the electrical fields significantly. Sensitivity distributions reflect the change of the measured apparent resistivity, if the resistivity of the subsurface is modified. The sensitivity distributions in Figure 1 verify the fact that the patterns are shifted into deeper regions leading to a greater investigation depth caused by the electrode length. The most critical disadvantage is the loss of vertical resolution in the depth range of the boreholes and thus the information content in the near surface region. By mixing surface electrodes with long electrodes an improvement of the resolution can be achieved as shown by a synthetic study (Ronczka et al. 2013).

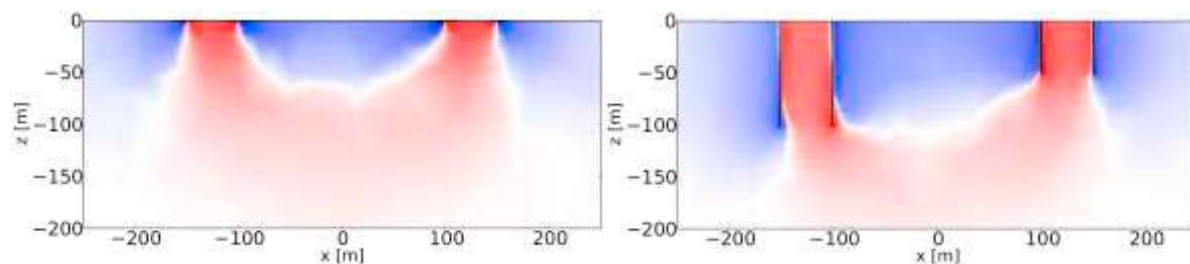


Fig. 1: Sensitivity distributions a for dipole-dipole measurements using surface (left) and long electrodes of different length (right)

TEST SITES

Measurements were conducted on two test sites in south-eastern Brandenburg. A major fault zone and glacial valleys exists that possibly enables vertical fluid transport from salt-domes to surface aquifers. Although it is not completely clear which sources and processes are dominant, a salt water intrusion is present on both locations. First test site is a medium-scale (500x500m) area near Müllrose with 13 boreholes, to which we added 6 point electrodes, and a nearly one-dimensional geological structure. The 40 m thick top layer consists of Pleistocene sands and gravels followed by an approximately 50 m thick Miocene brown coal and silt layer (Voss et al. 2013). The baseline inversion result (Figure 2) shows the main geology and agrees with 2D ERT results. The blue coloured zone indicates conductive parts at a depth of about 35 m. Fluid conductivities (see Figure 1 right side) taken from a multiply filtered ground water well show saline water at about 30 – 40 m depth. The triangle marked curve, taken from the LE-ERT inversion result, at the borehole position agrees well with the fluid samples (circle markers).

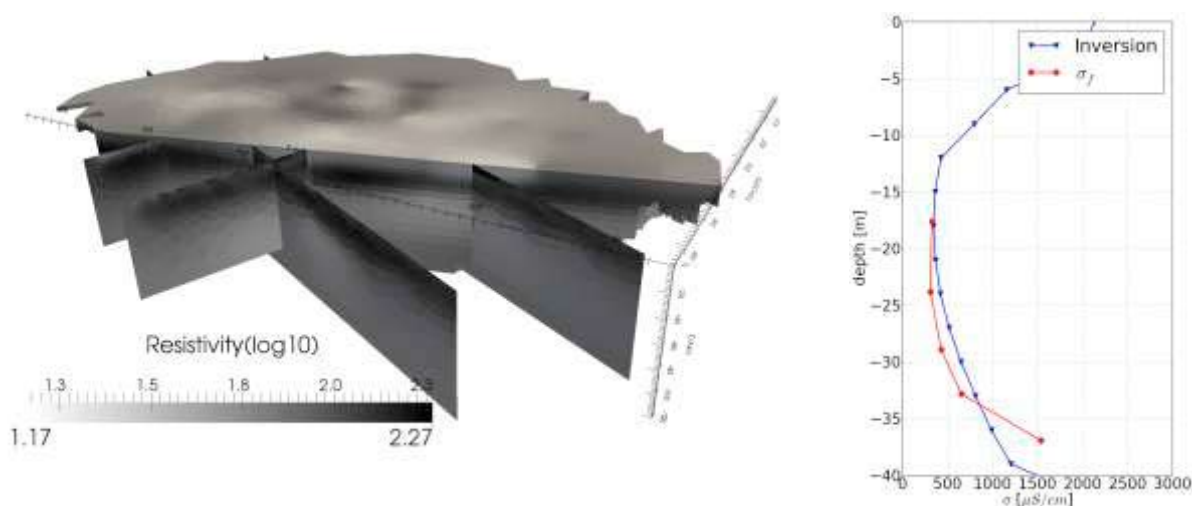


Fig. 2: 3D inversion result of test site Müllrose together with 2D ERT results (left) and measured fluid conductivities together with fluid conductivities derived from the LE-ERT result using a fitted Waxman-Smiths equation.

A subsequent permanent installation on this test site allows regular monitoring measurements. As the geology remains constant, resistivity changes are only caused by changes in the pore fluid. Nevertheless, a good baseline model is needed for a successful time-lapse inversion. Four repeated measurements have been carried out within six months. Fluid conductivities were taken from different water wells for every time step. The difference of measurements in June and September is shown in Figure 3. Here, a decreasing resistivity is indicated by the mesh with edges, i.e. increasing fluid salinity and an increasing by the mesh without edges. As expected, the greatest changes can be found near the surface. Although LE-ERT is not that sensitive at shallow depth, these can be interpreted as a dry-out in the unsaturated zone. Nevertheless, interpretations concerning the near surface region had to be treated carefully. More significantly, the increasing resistivity at the bottom of the near-surface aquifer indicates that the before observed increased salinization seems to vanish slightly in time.

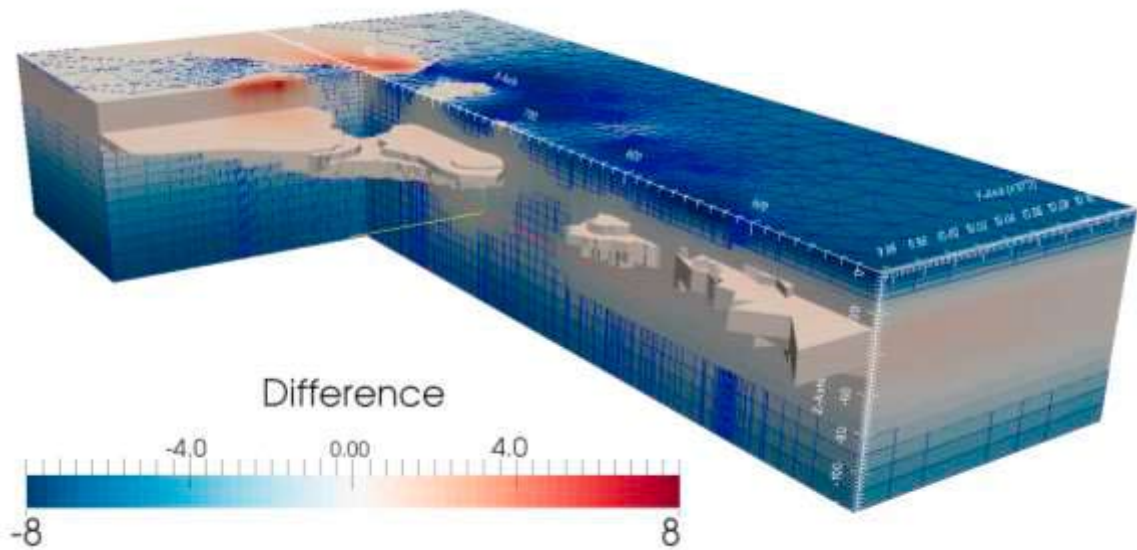


Fig. 3: Difference (in per cent) between two time steps (June and September) from monitoring measurements of the test site Müllrose. Cells with edges indicate decreasing resistivity and the cells without edges denote increasing resistivity.

The second test site (Briesen water works) is an area of 4x3km in the catchment of a water supplier where artificial recharge with river water is done. Borehole measurements lead to the conclusion that an extensive use of the water plant lead to a salt water intrusion into a shallow aquifer. Some water wells were contaminated by saltwater and had to be disabled. A two-week field campaign was conducted with a high-voltage transmitter and eight self-developed data loggers using 28 boreholes and two additional surface electrodes at regions of low coverage. Prior to the field measurements we used resolution analysis methods optimizing the survey to find out which measurements provide the best information content of the subsurface. With this optimized measurements we conducted a 3D long electrode ERT survey (LEERT) in order to locate possible saltwater intrusions. Readings from 40 current injections generated a data set of about 700 data points. A first inversion result is shown in Figure 4. The transition to a highly conductive zone at about 200 m depth is associated with a saltwater contamination as supported by resistivity logs in several boreholes. The highly resistive layer at about 70 m depth can be seen in some borehole logs as well. As the hydrogeological situation seems to be quite complicated, a further interpretation has to be done including ground water flow information to verify where the salinization comes from and which layers are affected. Even the borehole logs are very heterogeneous in this region.

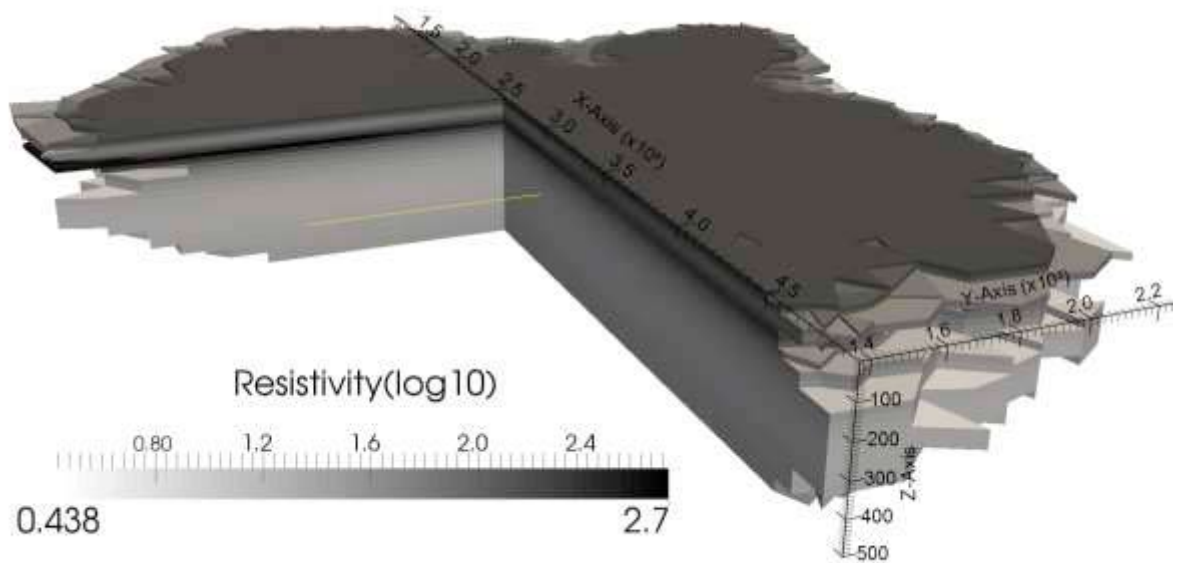


Fig. 4: Inversion result of the LE-ERT survey at the second test site (Briesen).

CONCLUSIONS

It could be shown that LE-ERT provides reasonable resistivity distributions compared to electro-logs from borehole measurements and surface ERT measurements. Furthermore, comparison with fluid samples demonstrates that salinity can be reliably retrieved. As real 3D measurements these surveys can cover large areas about several square kilometers, assuming a sufficient borehole density. Thus it represents a low-cost method for monitoring saltwater intrusion in the catchment scale.

REFERENCES

- Rücker C. and T. Günther. 2011. The simulation of finite ERT electrodes using the complete electrode model. In *Geophysics*, 76 (4), F227
- Ronzka M., T. Günther and C. Rücker. 2013. Long Electrode ERT for salt water monitoring: Modeling, Sensitivity and Resolution. In *Proceedings of 19th EAGE Near Surface Geoscience conference*, Bochum
- Voss T., M. Ronzka and T. Günther. 2013. Saltwater monitoring with long-electrode electrical resistivity tomography. *Biuletyn Panstwowego Instytutu Geologicznego Hydrogeologia*, 456, 621-626.

Tide cleaning of heads in unconfined coastal aquifers via processing of signal wave components

J.P. Sánchez-Úbeda ¹, M.L. Calvache ¹, M. López-Chicano ¹ and C. Duque ¹⁻².

¹Department of Geodynamics, University of Granada, Granada, Spain.

²Department of Geosciences, University of Oslo, Oslo, Norway.

ABSTRACT

An effective method to remove the tide effects from head data at different depths has been developed. The method has been applied in the discharge zone of Motril-Salobreña coastal aquifer (South Eastern Spain) for two time intervals (one month and one year). It consists in handling the groundwater head like a wave, which is defined in terms of amplitude, frequency and phase. These significant tide components are extracted from the original tide-perturbed head by low and high pass filters of frequency applying software tools of signal processing. The obtained signal represents the non-perturbed head level, which allows to delve into the non-tide water head affections that can be detected in the discharge zone of coastal aquifers.

INTRODUCTION

Tidal perturbation in groundwater head measurements near the coastline is, in principle, an issue with two principal faces. It is possible to create analytical and numerical models to derive aquifer parameters via relationships between tide and groundwater head. Secondly, the tide oscillation and consequent the gradient variability at discharge zone produce an enhanced of mixing zone due to an increase in local dispersivity values (**Cirpka and Atting 2003; Guarracino et al. 2012**). The changes in groundwater heads associated with changes in recharge, pumping and modifications of the aquifer conditions would represent a third face that can be achieved through the study of the groundwater head without tidal oscillation. The present study has the aim of obtaining a simple but efficient method for filtering data of tidal oscillation considering only the principal tide components detected on monitoring groundwater. Then, the method will be applied in two different time intervals of data and at two different depths

Background

Several studies proposed different equations to eliminate the tide oscillation in monitoring wells close to the sea, but they only accounted mathematics approximations of head fluctuation with higher or lower accuracy. **Nielsen (1990)** developed a mathematical model based on Boussinesq's equation and different analytical solutions, and the comparison of these with measurements presented greatest discrepancies mainly due to seepage face formation. **Erskine (1991)** derived transmissivity/storage ratio based on time lag and tidal efficiency factor values and performed a filtering of groundwater head data using these two factors, and the results showed imperfections owing to non-tidal effects. **Trefry and Johnston (1998)** applied least-square techniques to eliminate tidal oscillation from a pumping test data, but applied on more than one day period the results do not show a good fit or completely clean up. In any case, these methods are applied to a time interval comprising no more than several days or one month, and always in relatively shallow aquifers (tens of meters) and specific coastal morphologies or multi aquifer systems. **Li and**

Jiao (2003), Zhou et al. (2013) and Bye and Narayan (2009) proposed methods focused on the effects of tide on the saltwater-freshwater interface configuration and water table predictions, but not on cleaning groundwater head measurements.

METHODS

The study is based on the processing signal via frequency and amplitude detection of the different harmonics components of the tide observed in the measured groundwater head. Tide data with hourly time resolution has been used from *Puertos del Estado (Spanish Ministry of Development)*. Head data were monitored with hourly resolution in two piezometers (P1 and P2) 300 meters from coastline and screened at -128 m and -34 m in depth respectively (relative to mean sea level). They are closed one to each other (3 m) so we can treat them as a single point where the groundwater head is recorded in two different depths.

First step of the filtering process consist to calculate principal harmonic components in terms of frequency, amplitude and phase in tide and head data in both points, which allows recognizing all the tidal components that affect to the latter. It has been carried out by applying a modified script based on T_TIDE (**Pawlowicz et al., 2002**). The outputs are frequency, amplitude, phase and *snr* factor (“*signal to noise ratio*”), indicating the most significant tidal constituents from the analyzed signal (when *snr* > 2).

Next steps consist to isolate those constituents by filtering the original groundwater head signal through the application of low and high pass filters, based on the *Fourier Series Development*. Density spectral analysis for both groundwater head signals is used to confirm the principal tidal frequencies on that, compared with T_TIDE output frequencies. These harmonics of different frequencies are removed from the original data by filters based in different wavelets families. The derived signals represent the non-tide perturbed groundwater head.

RESULTS AND DISCUSSION

Principal results have been obtained for two different time intervals (a month and a year). The adjustment of the significant tidal components was performed on the largest time interval, with the aim to obtain all possible or detectable harmonics of tide. Filtering of data and cleaned up the signals was performed separately viewing thus the possible inconsistencies due to the selected time interval.

TIDE								P1						
Tide ID	F (h ⁻¹)	P (h)	A (m)	A_Err (m)	Pha (°)	snr		Tide ID	F (h ⁻¹)	P (h)	A (m)	A_Err (m)	Pha (°)	snr
SA	0.0001	8764.24	0.0594	0.013	359.38	22		SSA	0.0002	4382.12	0.0636	0.03	119.17	4.5
SSA	0.0002	4382.12	0.0192	0.012	40.41	2.5		K1	0.0418	23.93	0.012	0.001	182.02	150
MF	0.0031	327.86	0.0059	0.009	352.96	0.4		N2	0.0790	12.66	0.0109	0.001	118.63	160
O1	0.0387	25.82	0.0199	0.001	121.98	210		M2	0.0805	12.42	0.0529	0.001	122.42	4000
P1	0.0416	24.07	0.0115	0.001	151.07	89		S2	0.0833	12.00	0.0163	0.001	105.54	340
K1	0.0418	23.93	0.0324	0.001	155.94	610		P2						
N2	0.0790	12.66	0.032	0.002	31.87	230		Tide ID	F (h ⁻¹)	P (h)	A (m)	A_Err (m)	Pha (°)	snr
M2	0.0805	12.42	0.1573	0.002	48.62	410		SSA	0.0002	4382.12	0.052	0.023	121.14	5.2
S2	0.0833	12.00	0.0619	0.002	73.97	860		K1	0.0418	23.93	0.0035	0.001	180.42	23
K2	0.0836	11.97	0.0172	0.003	69.61	32		N2	0.0790	12.66	0.004	0.001	115.71	56
M4	0.1610	6.21	0.0166	0.001	160.39	310		M2	0.0805	12.42	0.0194	0.001	121.16	1400
MS4	0.1638	6.10	0.0117	0.001	226.45	120		S2	0.0833	12.00	0.005	0.001	49.68	77

Table 1. Principal harmonic components of tide and piezometers P1 and P2.

Table 1 show the significant components of tide, P1 and P2 (T_TIDE outputs), where the columns indicate (left to right) *tide identification*, *frequency*, *period*, *amplitude*, *amplitude's error*, *phase* and *snr*. The adjusted components in P1 and P2 are consistent with the obtained

tidal frequencies, including the semiannual tide component (*SSA: Solar Semi Annual*), with a period of 4382 hours. As it shown in figure 1, the most notable tidal frequencies are the semidiurnal and diurnal for a month time interval (*K1, N2, M2* and *S2* for P1 and P2 in table 1), corroborated by spectral density analysis. The semimonthly tide has not been detected due to the minimum affection on the amplitude of groundwater head signals, if it is compared to the high influence of semidiurnal tide (meanly *M2*), so maybe string and neap tides are masked.

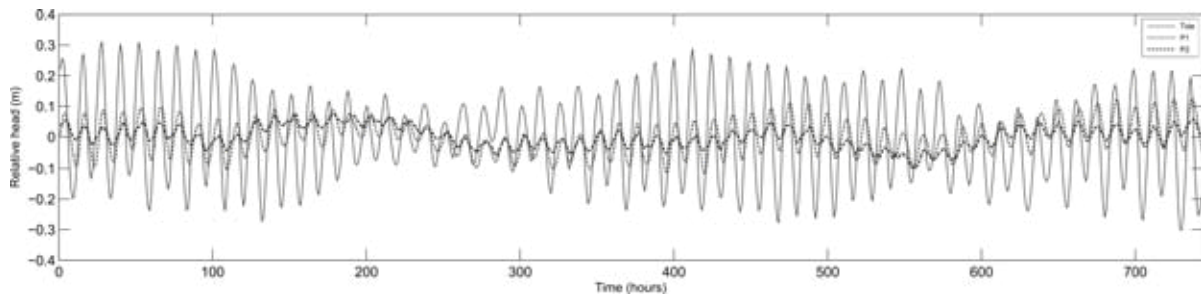


Figure 1. Relative levels of Tide and piezometers P1 and P2 in August 2012.

Figure 2 shows the obtained filtered signals for P1 and P2, together with the original groundwater head data in each case for all the monitoring year.

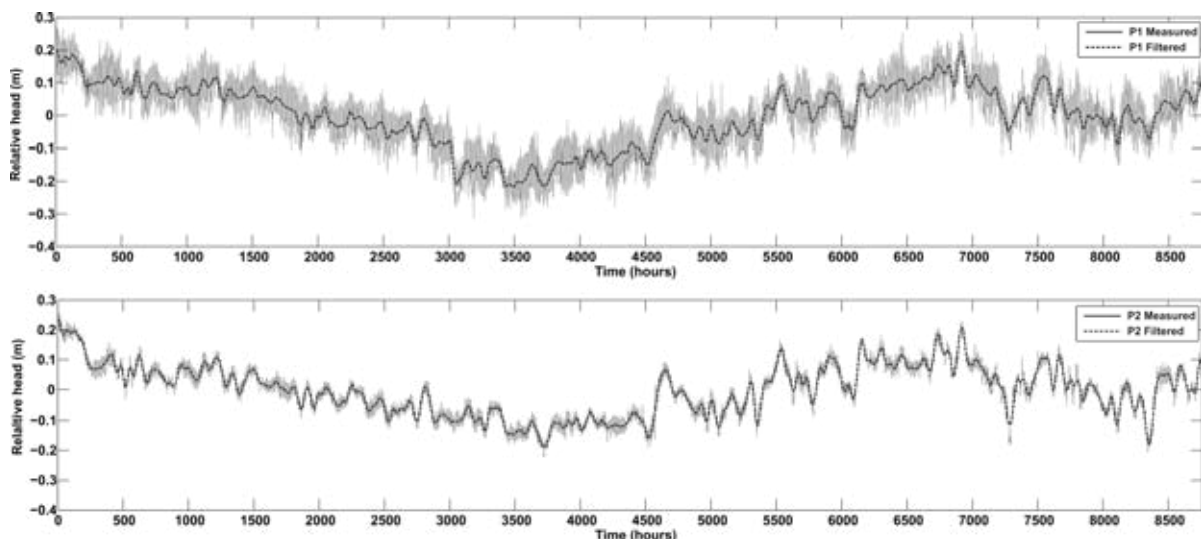


Figure 2. Original and filtered levels in piezometers P1 (upper) and P2 (lower) from 21/03/2012 to 21/03/2013.

The general annual trend is similar in both points, but differences between P1 and P2 regarding to their depths can be detected. The mean amplitude value for tide is around 0.6 m, and it induces amplitude on the groundwater head ranging from 0.1 to 0.3 m depending on the depth of measurement. Thus, P1 measured signal presents an important noise component and high tidal affection, meanwhile in P2 is more damped. The applied filters clean up the original signal at different levels of frequency, remaining non-tidal lower frequencies.

It can be observed differences between the filtering of both time intervals (a month and a year) that involves the treatment of the annual signal at lower frequencies than monthly signal. Nevertheless the method results in a congruent fit between the monthly signal and the same month within the annual signal.

CONCLUSIONS

Tide and groundwater head data have been differentiated by signal processing tools. This allowed to distinguish the affection of tide on wells close to the coast by filtering the groundwater head signals. The changes in the results at different depths confirmed the higher affection deeper in the aquifer. The treatment of different time intervals has showed that the method is accurate regardless of the time interval and pass filters used. The results finally enable to quantify and remove the tidal oscillations from groundwater levels that will lead to a better knowledge of the inland processes and changes in the discharge zone as well as their affections in the settings of the salt wedge.

Acknowledges

This study was performed by the project research CGL2012-32892 funded by the *Ministry of Science and Innovation* and the research group of the *Junta de Andalucía RNM-369*. Also thanks to *Puertos del Estado (Spanish Ministry of Development)* to have proportioned tidal data and coauthors by their corrections.

REFERENCES

- Cirpka, O. A. and Attinger, S. 2003. Effective dispersion in heterogeneous media under random transient flow conditions. *Water Resources Research*, 39 no. 9: 1257.
- Erskine, A. D. 1991. The effect of tidal fluctuation on a coastal aquifer in the U. K. *Ground Water* 29, no. 4: 556-562.
- L. Guarracino, J. Carrera and E. Vázquez-Suñé. 2012. Analytical study of hydraulic and mechanical effects on tide-induced head fluctuation in a coastal aquifer system that extends under the sea. *Journal of Hydrology* 450–451, 150–158.
- John, A.T., Bye and Kumar A., Narayan. 2009. Groundwater response to the tide in wetlands: Observations from the Gillman Marshes, South Australia. *Estuarine, Coastal and Shelf Science* 84, 219–226.
- Li H. and J. J. Jiao. 2003. Influence of the tide on the mean watertable in an unconfined, anisotropic, inhomogeneous coastal aquifer. *Adv. Water Resources* 26, no. 1: 9-16.
- Nielsen, P. 1990. Tidal dynamics of the water table in beaches. *Water Resources Research* 26, no. 9: 2127-2134.
- R. Pawlowicz, B. Beardsley and S. Lentz. 2002. Classical Tidal Harmonic Analysis Including Error Estimates in MATLAB using T_TIDE. *Computers and Geosciences* 28, 929-937.
- Trefry, M. G. and C. D. Johnston. 1998. Pumping test analysis for a tidally forced aquifer. *Ground Water* 36, no. 3: 427-433.
- Zhou, P., Li, G., Lu, Y., and Li, M. 2013. Numerical modeling of the effects of beach slope on water-table fluctuation in the unconfined aquifer of Donghai Island, China. *Hydrogeology Journal* 22, no. 2: 383-396.

Contact Information: Juan Pedro Sánchez Úbeda, University of Granada, Geodynamics Department, Science Faculty. Av. Fuentenueva s/n, 18071, Granada, Spain, Email: juampesu@ugr.es

Hydrodynamic effects in the discharge zone of the Motril-Salobreña coastal aquifer due to the drilling of artesian wells

J.P. Sánchez-Úbeda,¹ C. Duque^{1,2}, J. M. Gómez Fontalva¹, M.L. Calvache¹, M. López-Chicano¹ and B. de la Torre¹.

¹Department of Geodynamics, University of Granada, Granada, Spain.

²Department of Geosciences, University of Oslo, Oslo, Norway.

ABSTRACT

Flow patterns with vertical upward components are commonly present in discharge zones of coastal unconfined aquifers. Motril-Salobreña aquifer (Granada, south eastern Spain) shows this flow configuration confirmed by artesian wells, 300 m from the coast. The principal objective of this study is to explore how to simulate the observed flow patterns at the vicinity of these wells considering the uncertainties in the hydrogeological parameter values and the aquifer structure in the study area. A synthetic cross section with a numerical 3D density-dependent model has been developed in order to achieve the following: (a) find the optimal boundary conditions to represent the artesian wells located in the discharge zone either with drains or pumping wells, (b) explain the changes in saltwater-freshwater contact position and submarine groundwater discharge when wells are drilled in this location and (c) determine the modification of the flow pattern and salinity distribution in the discharge zone due to anisotropy, multilayer aquifer and configuration of the wells cased (distribution of the screened sections).

The model has been constructed with SEAWAT representing the artesian wells as pumping wells and also as a localized drainage point. The results were compared then with field observations considering a simple isotropic aquifer to a multilayered one and under different initial conditions, anisotropy ratios or cased configurations throughout the saturated thickness.

The results show that a drain boundary condition is representing more accurately the observations in the artesian well than a pumping well and the distribution of the screened sections has only a local affection on the dynamic of the flow. Higher anisotropy and hydraulic conductivity lead to higher vertical flow and a displacement seawards of the salt water intrusion. Hence, the consideration of a multilayer system with different hydraulic properties results in better adjustment between salinity observations and model data that indicates that Motril-Salobreña aquifer is layered in the proximity of the shore.

Acknowledges

This study was performed by the project research CGL2012-32892 funded by the *Ministry of Science and Innovation* and the research group of the *Junta de Andalucía RNM-369*. Also thanks to coauthors by their corrections as the reviewers for their hints.

Contact Information: Juan Pedro Sánchez Úbeda, University of Granada, Geodynamics Department, Science Faculty. Av. Fuentenueva s/n, 18071, Granada, Spain, Email: juampesu@ugr.es

Climate change effect on seawater intrusion evolution in Dar Es Salaam coastal plain, Tanzania

G. Sappa¹, M.T. Coviello¹, and G. Luciani¹

DICEA, Department of Civil, Building and Environmental Engineering - Sapienza - University of Rome, Rome, Italy

Keywords: climate change, seawater intrusion, groundwater exploitation, Dar Es Salaam

ABSTRACT

This paper presents some of the results from the ACC Dar Project, an EU cofunded project, leaded by Sapienza, University of Rome in partnership with Ardhi University of Dar Es Salaam (Tanzania). The aim of the project was to improve the effectiveness of municipal initiatives for supporting coastal peri-urban populations in their efforts to adapt to Climate Change (CC) impacts, thus contributing to the implementation of the National Adaptation Programme of Action (NAPA) of the United Republic of Tanzania. The overall objective of this part of the project was to explore the current degree of seawater intrusion into Dar es Salaam's coastal aquifer, and its relationships with climatic conditions and urbanization processes, in order to identify the areas of the city with the highest priority for adaptation action implementation. Subsequently, saltwater intrusion of coastal aquifers will accelerate due to the reduction of groundwater recharge. The objective of this study is (i) to explore the current degree of seawater intrusion into Dar es Salaam's coastal aquifer, and its relationships with climatic conditions and urbanization processes, (ii) to identify the relationships with environmental parameters, related to climate variability, and anthropogenic factors, related to changes in land cover and the population's water demand. Starting from the analysis of a database of more than 400 monitoring boreholes physical – chemical analysis results, referred to the period 2001-2010, in 2012 two large specific monitoring campaigns have been driven on about 80 monitoring wells, where samples have been taken to make laboratory analysis, and three in situ monitoring campaigns on about 35 boreholes have been carried on to build an updated assessment of seawater intrusion in the area under study. Here are presented the results of the elaborations and the interpretation.

INTRODUCTION

The use of groundwater resources is increasing due to population rise, economic growth, intensified agricultural development, and the loss of surface water due to contamination. Climate change impacts the water supply management and groundwater quality in the coastal aquifers (Essink et al., 2010). The influence of climate changes on groundwater levels and salinity due to sea level rise and changes in precipitation and temperature (Kundzewicz et al., 2008). Since saltwater intrusion is directly related to the recharge rate of the groundwater, this allows for other factors that may contribute to the encroachment of seawater into the freshwater aquifers. The ACC Dar Project aims to improve the effectiveness of municipal initiatives for supporting coastal peri-urban populations in their efforts to adapt to Climate Change (CC) impacts, thus contributing to the implementation of the National Adaptation Programme of Action (NAPA) of the United Republic of Tanzania. Starting from a database of physical – chemical analysis results referred to more than 400 monitoring boreholes, investigated between 2001-2010, in 2012 two large specific monitoring campaigns have been driven on about 80 monitoring wells, where samples have been taken to make laboratory analysis, and three in situ monitoring campaigns on about 35 boreholes have been carried on to build an updated assessment of seawater intrusion in the area under study, which has a surface of approximately 260 km², 40 km stretch along the

coastline to the north of the City centre and is bordered to the east by the Indian Ocean. The western boundary is the Dar es Salaam Plateau, which rises west of the Ocean along the entire study area up to the Pugu Hills. The hydrogeological boundaries are the Mzinga River to the South and the Nyakasangwe River to the North.

METHODS

On the basis of the information gathered during a preliminary phase of recognition of historical information, a data collection methodology was defined. That methodology consisted of two main activities: collection of historical data from a variety of existing sources, and the execution of groundwater monitoring campaigns (June 2012 - January 2013), in order to compile a set of historical and current data that will be useful when evaluating the evolution of seawater intrusion.

Groundwater monitoring activity

Given the morphological and geological characteristics of the Dar es Salaam Region, the first step was the assessment of the study area in order to design a borehole monitoring network. That network includes the coastal sandy plain (Mjema 2007), progressing from the Indian Ocean towards inland, and including the entire metropolitan area as well as some peri-urban areas (not located in the plateau) within the Kinondoni, Ilala and Temeke districts.

A subset of boreholes located in the study area was chosen for the monitoring network from the database of 400 georeferenced boreholes, with consideration for uniformity of spatial distribution: the network consists of 79 boreholes, uniformly distributed with a frequency of about 1 borehole per 3 km².

The study area and the boreholes monitoring network are shown in Fig. 1. The monitoring procedures consisted in a variety of survey activities depending on temporal scale (long-term and monthly surveys) and the type of data to be collected (in situ and laboratory measures).

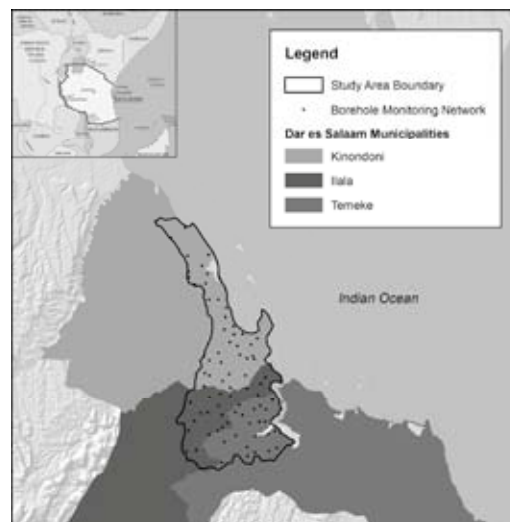


Figure 1 – The study area and the monitoring boreholes network

The monitoring campaigns were performed following the scheme in Table 1. In order to manage the large quantity of data collected during the monitoring campaigns and to assure its consistency and maintenance over time, a specific relational database for the ACC-Dar Borehole Monitoring Network Storage was built in MS Access (ACC-Dar BMD) (http://www.planning4adaptation.eu/042_Maps.aspx).

Monitoring campaigns	Frequency	Data collected
Long-term monitoring activity involving the entire borehole network (79 boreholes)	Twice in 6 months: - June 2012 (after the “long rainy season”) - November 2012 (before the “short rainy season”)	SWL measure (using contact meters) Physical parameters in situ measure (using multiparametric probes): T, pH, EC, TDS Chemical parameters lab measure (laboratory analysis of collected water sample): Ca ⁺⁺ , Mg ⁺⁺ , Na ⁺ , K ⁺ , HCO ₃ ⁻ , SO ₄ ⁻ , Cl ⁻ , NO ₃ ⁻⁻ , F ⁻ , NH ₄ ⁺
Monthly monitoring activity involving a sub-group of the borehole network (33 boreholes, mainly located in the area close to the coastline)	Monthly: - September 2012 - October 2012	SWL measure (using contact meters) Physical parameters in situ measure (using multiparametric probes): T, pH, EC, TDS

Table 1 – Scheme of the monitoring campaign driven in 2012

Data Analysis Methods

In the aim of evaluating the seawater intrusion and its evolution in the last ten years, the study has proceeded according to the following steps:

- Elaboration of distribution maps for various parameters (TDS, Cl, SO₄, and EC);
- Graphical representation in the form of a Piper diagram, in order to distinguish water types and identify the most significant groups;
- Data analysis using Cl-Y diagrams (cross plots) related to the theoretical freshwater-seawater dilution line;
- Hydrochemical facies analysis by Stuyfzand (1986, 1993) classification.

The joint use of these methods allows for the comparison of water samples according to two end members (a freshwater and a salt one), involved in the mixing represented by a line. The Δ ionics, which overlap simple mixing between fresh water and salt water and recognise the presence of other salt sources, were calculated in order to qualitatively and quantitatively study the processes.

Once the chemical composition of the two presumptive end-members of mix are defined, the cross plots of each constituent vs. chloride will allow comparison of the data with the theoretical mixing line.

RESULTS

Geological and hydrogeological settings

The geological setting of the Tanzanian coastal area can be divided into different regions, depending on their distinctive tectonic development (Kent et al. 1971).

In the area of concern, two main geological units are recognized: Quaternary and Neogene.



Figure 2 - A geological cross section of the study area (Msindai, 1988)

Neogene sandstone formations, interbedded with siltstones and mudstones, occupy the upland zone south and west of the city centre. Within Neogene formations, several distinct varieties are recognizable. Various types of sandstone occupy over three-quarters of the region (Msindai 2002). The Quaternary: an upper unconfined sand aquifer and a lower semi-confined sand aquifer, separated by a clay aquitard. The sediment type for both aquifers consists of Quaternary deposits from Pleistocene to the recent age. The recent hydrogeological assessment of this area (Mjema 2007) reports that the groundwater active recharge of the aquifer is produced, in large part, by coastal plain infiltration.

Present assessment

First of all, to identify the facies of Dar es Salaam's coastal groundwater, all samples related to the June 2013 campaign have been plotted in a Piper diagram and, generally, all the waters are located in the areas corresponding to chlorinate or sulphated facies. The distribution of the representative points of the samples on the anionic triangle, facilitated differentiation of three groups, corresponding almost exactly to the three districts in the study area: Kinondoni, Ilala, and Temeke.

To understand the relative importance of chlorinated and sulphated facies on overall salt content, the respective relationships between these parameters are shown below. In Figure 3, TDS is compared with the sum of chlorides and sulphates, revealing a strong linearity among the samples represented. It therefore appears that the salinity of a majority of the samples depends mainly on Cl and SO₄ ions. Despite the possibility that aquifer waters reflect a mixing process between three water types, the present hydrochemical study assumed that the principal process occurring in the aquifer is the mixing of intruding seawater and freshwater that feeds laterally. The main process that takes place in detrital aquifers is the ionic exchange, which implicates mostly the major cations Ca, Mg, Na, and K.

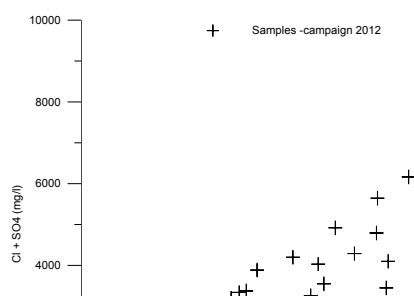


Figure 3 – TDS vs Cl+SO₄ in samples collected in 2012

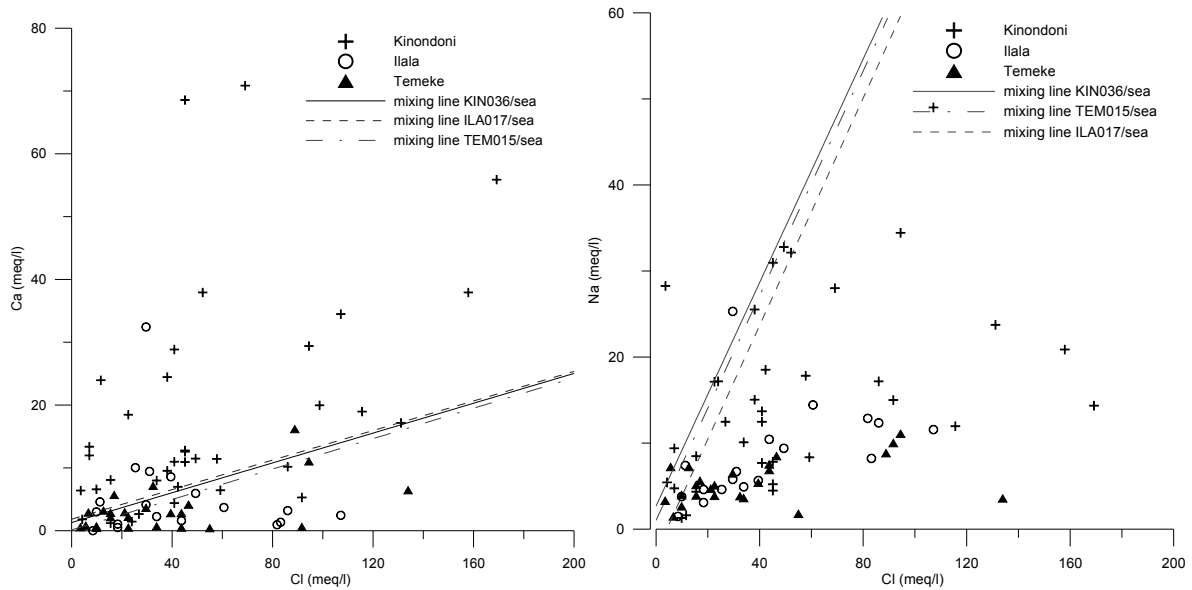


Figure 4 – Ca and Na vs Cl concentration, distinguished by districts

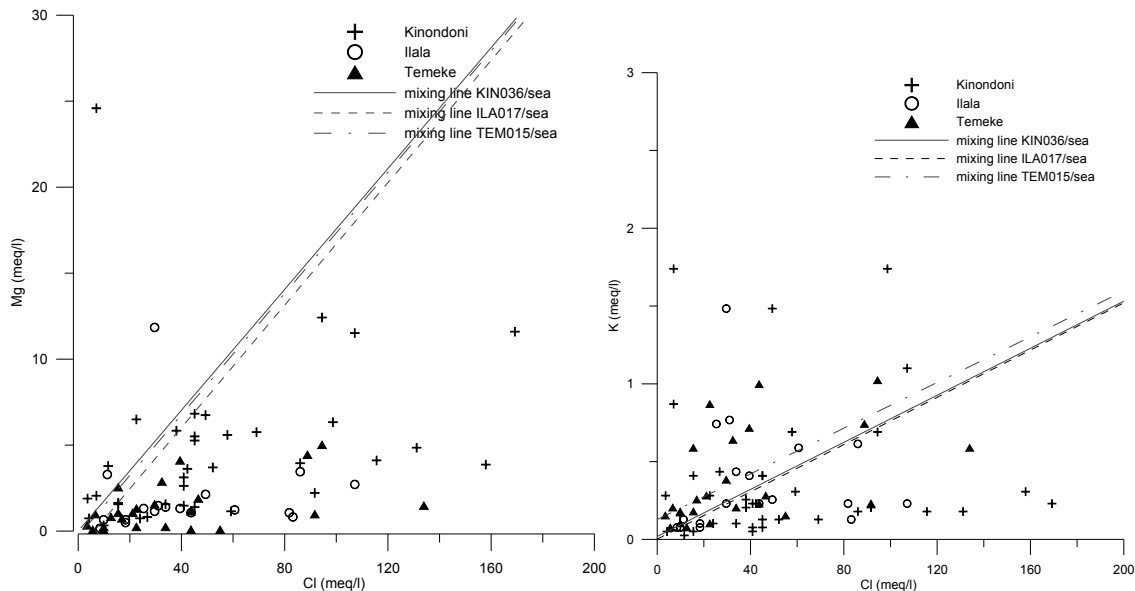


Figure 5 – Mg and K vs Cl concentration, distinguished by districts

DISCUSSION AND CONCLUSIONS

The analysis of the distribution of the samples shows that a small group of them follows the conservative mixing line, instead, an important group, taken mainly in the Kinondoni district, highlights an enrichment of calcium ions and a depletion of Na, K, and Mg, typical of an inverse cation exchange. By plotting the same ratio for single districts, specific sectors of the study area can be identified. The Kinondoni group reflects behavior attributable to inverse ionic exchange for the following boreholes: KIN01, KIN02, KIN09, KIN010, KIN011, in the NE sector; KIN033, KIN037, KIN038, and KIN039 for the SW sector, and KIN023 in the SE sector. Sectors affected by seawater intrusion appear to be fewer in Ilala and Temeke: samples from ILA002, ILA004, ILA017, ILA009, and ILA011 for the former and TEM06, TEM008, TEM009, TEM011 and TEM025 for the latter. For these two groups,

it is interesting to observe that the first follows the phenomenon observed in Kinondoni, while Temeke shows intrusion only along the coast. All sectors affected by seawater intrusion are highlighted in the map shown in Figure 6.



Figure 6 – Sectors affected by seawater intrusion

REFERENCES

- Essink, O., van Baaren, E. S., de Louw, P. G. B., 2010. Effects of climate change on coastal groundwater systems: A modeling study in the Netherlands. *Water Resources Research*, Vol. 46, Is. 10
- Kent, P.E., Hunt, J.A. and D.W. Johnstone, 1971. *The Geology and Geophysics of Coastal Tanzania*. Geophysical Paper No. 6, National Environment Research Council, Institute of Geological Sciences, London, 101pp.
- Kundzewicz, Z. W., Mata, L. J., Arnell, N. W., Döll, P., Jimenez, B., Miller, K., Oki, T., Şen, Z. and Shiklomanov, I., 2008. The implications of projected climate change for freshwater resources and their management. *Hydrol. Sci. J.* 53(1), 3-10.
- Mjemah, I.C., 2007. *Hydrogeological and Hydrogeochemical Investigation of a Coastal Aquifer in Dar es Salaam, Tanzania*. Ph.D. Thesis, Ghent University, Ghent, 222 pp.
- Msindai, K., 2002. *Engineering geological mapping of Dar Es Salaam City, Tanzania*. *Tanz. J. Sci.* Vol. 28(2).
- Sappa, G., Trotta, A., Vitale, S., 2014. *Climate Change Impacts on Groundwater Active Recharge in Coastal Plain of Dar es Salaam (Tanzania)*. *Proceedings of IAEG Congress*. Turin (Italy).
- Stuyfzand, P.J. 1989. A new hydrochemical classification of water types. *J. Regional Characterization of Water Quality*, *Proceedings of the Baltimore Symposium*, IAHS Publ. no. 182.
- Contact Information:** Giuseppe Sappa, DICEA, Department of Civil, Building and Environmental Engineering - Sapienza - University of Rome, Via Eudossiana, 18, 00186, Rome, Italy, Email: giuseppe.sappa@uniroma1.it, Tel. 0039-3452808882 Fax. 0039-06233239345

Simulation of seawater intrusion with standard groundwater codes

Frans Schaars¹, Mark Bakker²

¹ Artesia BV, Schoonhoven, Netherlands

² Water Resources Section, Faculty of Civil Engineering and Geosciences,, Delft University of Technology, Delft, Netherlands

ABSTRACT

We developed a method to simulate steady interface flow in multi-layer coastal aquifers with regular groundwater codes such as standard MODFLOW. The main step is a simple transformation of the hydraulic conductivities and thicknesses of the aquifers. Standard groundwater codes may be applied to compute the head distribution in the aquifer using the transformed parameters. For example, for flow in a single unconfined aquifer, the hydraulic conductivity needs to be multiplied with 41 and the base of the aquifer needs to be set to mean sea level (for a relative seawater density of 1.025). Once the head distribution is obtained, the Ghijben-Herzberg relationship is applied to compute the depth of the interface. The method may be applied to quite general settings, including spatially variable aquifer properties. Any standard groundwater code may be used, as long as it can simulate unconfined flow where the transmissivity is a linear function of the head. The proposed method is benchmarked successfully against a number of analytic and numerical solutions. The method is based on the analogy of interface flow and unconfined flow. We will show the consequences of using different methods for calculating the intercell conductance, and different approaches for drying and wetting cells, including the methods used in MODFLOW-NWT.

INTRODUCTION

Seawater intrusion in coastal aquifers may be simulated with computer codes that combine groundwater flow, contaminant transport, and density effects, such as SEAWAT (Langevin et al. 2008), SUTRA (Voss and Provost 2010), and FEFLOW (Diersch and Kolditz 2002). Alternatively, seawater intrusion may be simulated with the SWI package for MODFLOW (Bakker and Schaars 2005) SWI does not require a vertical discretization of an aquifer, as it applies the Dupuit approximation for flow within an aquifer. As a result, SWI simulations require much less computational effort, typically at least three orders of magnitude less than the codes that solve the combined flow and transport equations (Bakker et al. 2003; Dausman et al. 2010).

Final steady-state conditions are of interest in large regional models that include a coastal boundary in order to estimate pre-development conditions in an aquifer, to design well fields in coastal aquifers, or to evaluate proposed designs to limit seawater intrusion. For such simulations, it is often sufficient to simulate flow in an aquifer as interface flow (e.g., Cheng et al. 2000; Mantoglou 2003). SWI is better suited to compute the steady position of the interface, but it is inconvenient as it requires specification of the initial interface position as well as some algorithm-specific parameters. In addition, it may take a significant simulation time before steady state is reached.

The steady position of an interface between fresh and salt water may be computed from the head with the well-known Ghyben-Herzberg equation (e.g., Bear 1972; Strack 1989; Fitts 2002). Application of the potential introduced by Strack (1976) is a common approach for

the simulation of steady interface flow in a single aquifer. The Strack potential is implemented in the analytic element codes Gflow (www.haitjema.com) and AnAqSym (www.fittsgeosolutions.com). Strack's potential is applicable to aquifers with piecewise homogeneous properties. Although it is in theory applicable to multi-aquifer systems, it is inconvenient as it leads to a system of linked, non-linear differential equations (Sikkema and Van Dam 1982; Bakker 2006).

For simulation of steady interface flow in multi-aquifer systems with variable properties, it seems necessary to apply a numerical solution technique.

The objective of this paper is to present an approach to simulate the steady-state position of the interface in a heterogeneous multi-aquifer system with a standard single-density groundwater code. At steady-state, the saltwater is stagnant and the saltwater head is constant everywhere in the saltwater zone. No sinks or sources may be present in the saltwater. The simplest case of unconfined interface flow is discussed here, for more complicated examples, including multi aquifer flow we refer to Bakker & Schaars (2013) The example is solved using MODFLOW (Harbaugh et al.2000; Harbaugh 2005).

STEADY UNCONFINED INTERFACE FLOW

Consider steady unconfined interface flow in a deep aquifer so that the interface doesn't touch the bottom of the aquifer anywhere, as illustrated in Fig. 1a. The saltwater is at rest. The Dupuit approximation is adopted so that the depth D of the steady interface below sea level may be computed with the standard Ghyben-Herzberg equation as (e.g., Bear 1972; Strack 1989; Fitts 2002)

$$D = \alpha(h - z_s) \quad (1)$$

where h is the freshwater head defined as (e.g. Post et al., 2007)

$$h = \frac{p}{\rho_f g} + z \quad (2)$$

where p is the pressure in the water. The factor α is defined as

$$\alpha = \frac{\rho_f}{\rho_s - \rho_f} \quad (3)$$

As the saltwater is stagnant, the pressure is hydrostatic and the freshwater head increases with depth as:

$$h(z) = z_s + (z_s - z)/\alpha \quad (4)$$

The thickness of the freshwater zone may be computed as

$$H = D + (h - z_s) = (\alpha + 1)(h - z_s) \quad (5)$$

So that the transmissivity becomes

$$T = (\alpha + 1)k(h - z_s) \quad (6)$$

where k is the hydraulic conductivity.

This linear relationship between head and transmissivity may be simulated with a single-density groundwater code that is able to simulate unconfined flow where the transmissivity is a linear function of the head, provided the hydraulic conductivity and bottom of the aquifer are transformed as

$$\begin{aligned}\tilde{k} &= (\alpha + 1)k \\ \tilde{z}_b &= z_s\end{aligned}\quad (7)$$

In Figure 1 the example is displayed for the problem of a circular island with a radius of 1000 m, a hydraulic conductivity of 10 m/d and areal infiltration of 0.001 m/d. The head is equal to h_0 along the coast. The sealevel z_s equals zero and $\alpha = 40$.

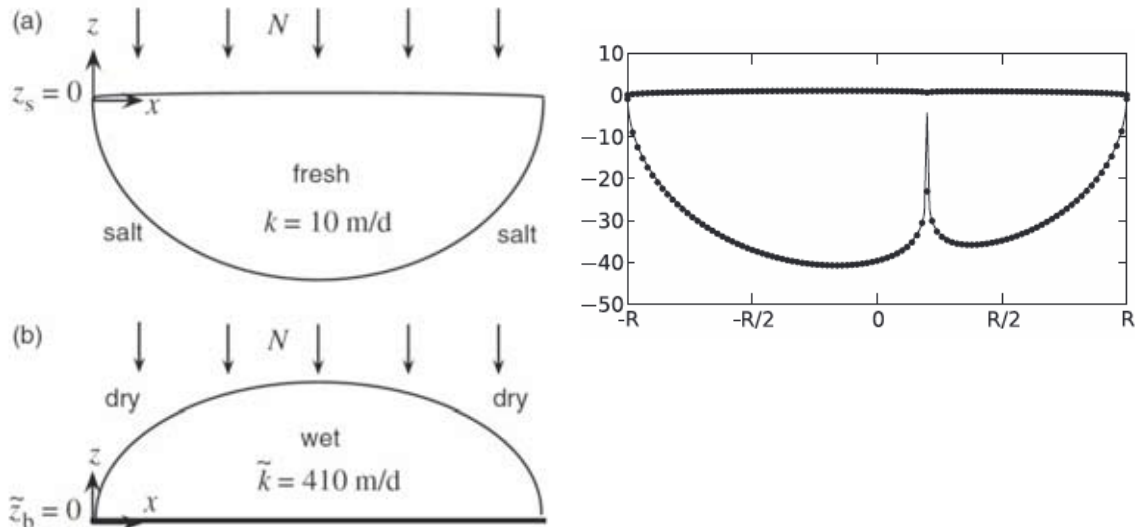


Figure 1. (a) Cross section of unconfined interface flow on a circular island, (b) equivalent unconfined flow problem in transformed model domain (vertical exaggeration much larger in bottom figure than in top figure). On the right: comparison of Strack solution (line) with MODFLOW (dots) for the simulation with a pumping well (200 m from center island, radius 0.3 m and discharge 200m³/d).

DISCUSSION AND CONCLUSIONS

An approach was presented to simulate steady Dupuit interface flow in heterogeneous multi-aquifer systems with standard single-density groundwater codes. Such cases cannot be solved with codes that implement the more elegant Strack potential, which is applicable to piecewise homogeneous aquifers only. Accuracy of the approach was demonstrated through comparison with exact interface flow solutions for homogeneous aquifers obtained with Strack's potential. The basic idea of the approach presented in this paper is to transform the domain such that it is identical to an unconfined flow problem.

REFERENCES

- Bakker, M. 2003. A Dupuit formulation for modeling seawater intrusion in regional aquifer systems. *Water Resources Research* 39, no. 5: 1131-1140.
- Bakker, M., G.H.P. Oude Essink, and C.D. Langevin. 2004. The rotating movement of three immiscible fluids -- a benchmark problem. *Journal of Hydrology* 278: 270-278.
- Bakker, M., and F. Schaars. 2005. The Sea Water Intrusion (SWI) package manual part I. Theory, user manual, and examples version 1.2. www.modflowswi.googlecode.com.

Bakker, M. 2006. Analytic solutions for interface flow in combined confined and semi-confined, coastal aquifers. *Advances in Water Resources* 29, no. 3: 417-425.

Bakker, M., and F. Schaars. 2013. Modeling Steady Sea Water Intrusion with Single-Density Groundwater Codes. *Ground Water* Vol 51 no. 1. 135-144

Bear, J. 1972. *Dynamics of fluids in porous media*. Dover, New York, NY.

Cheng, A.H.D., D. Halhal, A. Naji, and D. Ouazar. 2000. Pumping optimization in saltwater-intruded coastal aquifers. *Water Resour. Res.* 36, no. 8: 2155-2165

Dausman, A.M., C.D. Langevin, M. Bakker, and F. Schaars. 2010. A comparison between SWI and SEAWAT -- the importance of dispersion, inversion and vertical anisotropy. In *Proceedings of the 21st Salt Water Intrusion Meeting, Azores, Portugal, June 21-26, 2010*. [\url{www.swim-site.org}](http://www.swim-site.org).

Diersch, H.J.G., and O. Kolditz. 2002. Variable-density flow and transport in porous media: approaches and challenges. *White Papers Vol. II*. [\url{http://www.feflow.info/manuals.html}](http://www.feflow.info/manuals.html).

Fitts, C.R. 2002. *Groundwater Science*, Academic, San Diego, CA.

Harbaugh, A.W., E.R. Banta, M.C. Hill, and M.G. McDonald. 2000. MODFLOW-2000, The US Geological Survey modular ground-water model -- user guide to modularization concepts and the ground-water flow process. *US Geol. Surv., Open-File Report 00-92*.

Harbaugh, A.W., 2005. MODFLOW-2005, the US Geological Survey modular ground-water model - the ground-water flow process: U.S. Geol. Surv. *Techniques and Methods*, vol. 6-A16 (variously paginated).

Langevin, C.D., D.T. Thorne Jr., A.M. Dausman, M.C. Sukop, and W. Guo. 2008. SEAWAT Version 4: A Computer Program for Simulation of Multi-Species Solute and Heat Transport. *U.S. Geol. Surv. Techniques and Methods Book 6, Chapter A22*, 39 p.

Mantoglou, A. .2003. Pumping management of coastal aquifers using analytical models of saltwater intrusion. *Water Resour. Res.* 39, no. 12: 1335, doi:10.1029/2002WR001891.

Post, V., H. Kooi, and C. Simmons. 2007. Using hydraulic head measurements in variable-density ground water flow analyses. *Ground Water* 45, no. 6: 664-671.

Sikkema, P.C., and J.C. van Dam. 1982. Analytical formulas for the shape of the interface in a semi-confined aquifer. *Journal of Hydrology* 56, no. 3-4: 201-220.

Strack O.D.L. 1976. A single-potential solution for regional interface problems in coastal aquifers. *Water Resources Research* 12, no. 6: 1165-1174.

Strack, O.D.L. 1989. *Groundwater mechanics*. Prentice Hall, Englewood Cliffs, NJ. Available from: www.strackconsulting.com

Voss, C. I., and A. Provost. 2010. SUTRA, a model for saturated-unsaturated variable-density ground-water flow with solute or energy transport. *U.S. Geol. Surv. Water Resour. Invest. Rep.*, 02-4231, Version of September 22, 2010 (SUTRA Version 2.2).

Contact Information: Frans Schaars, Artesia BV, korte weistraat 12, 2871BP Schoonhoven, the Netherlands, Email: f.schaars@artesia-water.nl

The fresh-saltwater distribution on the Island of Föhr – assembling of a data base for the assessment of climate change impact

Wolfgang Scheer¹, Bernd König¹ and Broder Nommensen¹

¹Agency for Agriculture, Environment and Rural Areas Schleswig-Holstein, Flintbek, GE

ABSTRACT

The North Frisian island of Föhr was a pilot area of the European INTERREG IVB project CliWat which was focussed on the development of adaptation strategies to meet the ground water situation in a future climate. Due to a rising sea level and increasing ground water recharge in the North Sea region, significant changes of the fresh-salt water distribution are expected leading to the demand of a future adaptation of the management of ground and surface water in these areas.

A combination of hydrogeological surveys and geophysical measurements, like airborne TEM (SkyTEM) and reflection seismic, was used to map the hydrogeological structure and the present state of the fresh-salt water distribution of the island. The results of these investigations were merged in a geological 3D-model which was used as data base for a geohydrological model with future climate scenarios as input parameter.

As a result of the model, areas of the island were identified that are expected to react most sensible to the impacts of future climate change and sea level rise. To verify the geometry and the (present) hydraulic conditions of the model, additional surveys, like drillings, cone penetration tests (CPT), direct push conductivity probe and ground water analyses were carried out at several locations of the island including offshore drillings and measurements during the low tide. The main focus thereby was put on the distribution pattern of salt water in the marsh area of the island and on the survey of the range of fresh water discharge to the Wadden Sea.

INTRODUCTION

Föhr is the second largest German North Sea island. It's landscape can roughly be divided into two main areas. The Southern and South-western parts are dominated by sand and moraine deposits of Saalian age (Geest), which reach terrain heights up to 12 m above sea level. The lowlands in the Northern and North-eastern parts of the island (Marsh) are covered by fine grained Holocene sediments (Figure 1). The underground of the island shows a heterogeneous geological set-up with an alternating sequence of sandy and clayey sediments that have been thrust-faulted by glaciotectonic processes.

Caused by favourable ground water recharge rates in the moraine areas, a more than 80 m deep reaching fresh water lens exists which is the resource for the drinking water supply to the population of the island. The distribution of fresh and salt water on the island and the dimension of the fresh water lens have been investigated by a SkyTEM survey that also delivered a good overview of the ground water discharge from the moraine areas towards the Wadden Sea in the Southern and Western parts of the island as well as in the northern direction to the marsh lands.

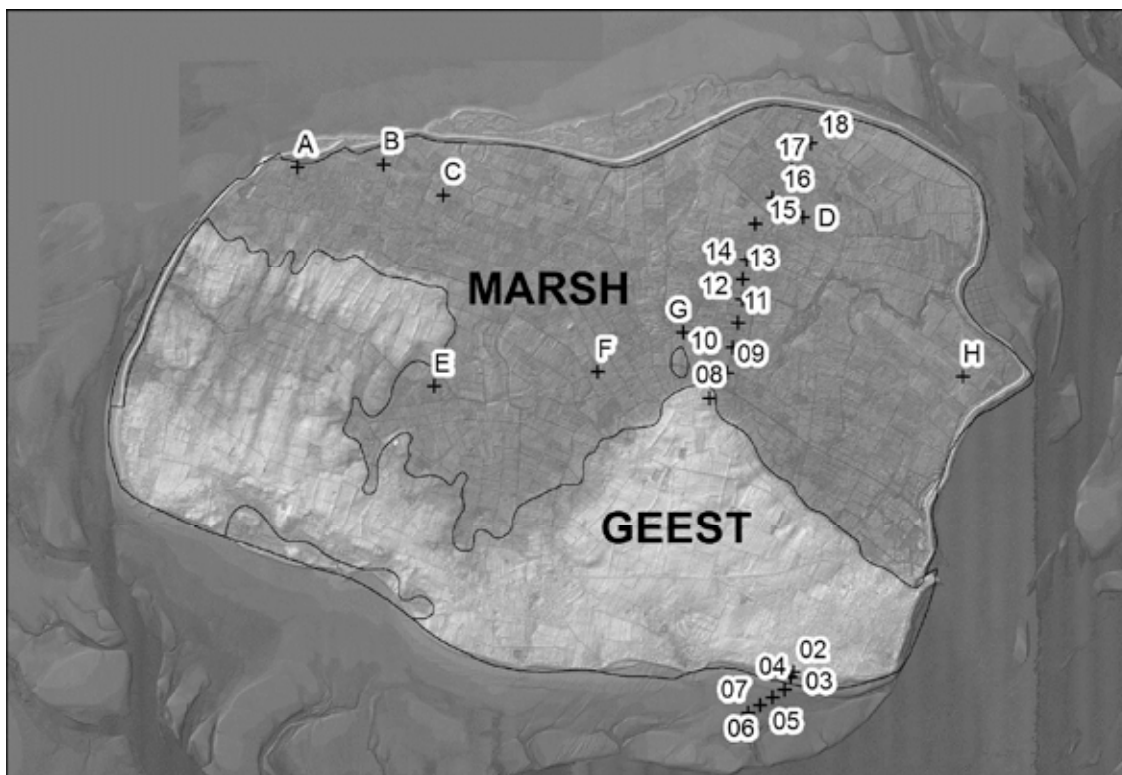


Figure 1. Terrain model, locations of drillings, CPT and direct push measurements Section 1 (loc. 2 – 7) tidal flat; Section 2 (loc. 8 – 18) marsh; (loc. A – H) marsh

MAPPING OF THE FRESH/SALT WATER DISTRIBUTION

At 24 locations a combination of drillings, direct push conductivity and CPT measurements have been carried out, completed by sampling for chemical analyses in all relevant layers (Figure 1).

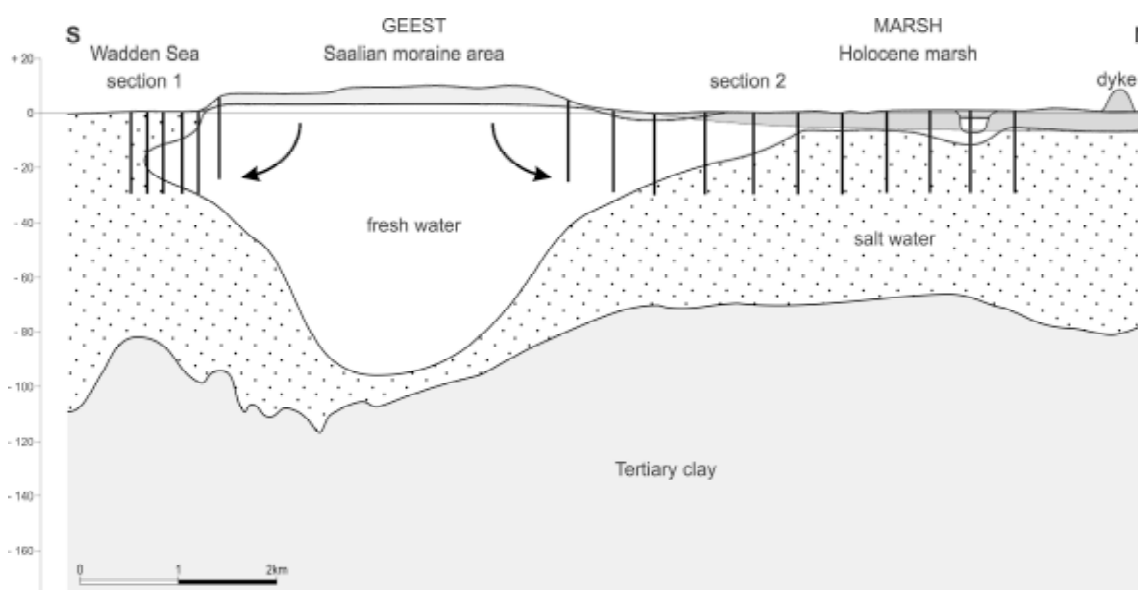


Figure 2. A cross section showing the extend of the fresh water lens, derived from SkyTEM data, direct push measurements and chemical sampling Section 1 (loc. 2 – 7); Section 2 (loc. 8 – 18)

RESULTS

The compiled information from the new investigation shows a good conformance with the existing data. Figures 3 and 4 give some examples of the findings in details.

Cross section from the shore to the Wadden Sea.

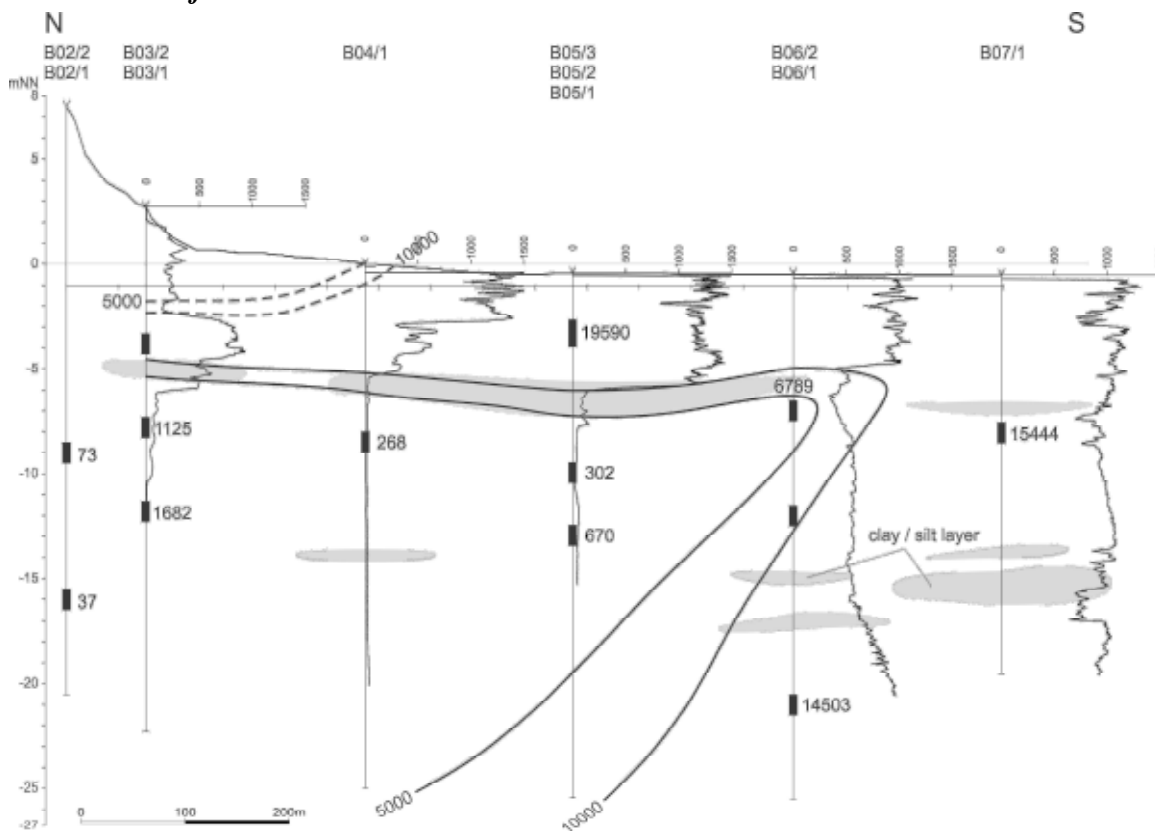


Figure 3. cross section 1 with measured and interpolated distribution of Chloride (mg/l) and logs of the electrical conductivity (mS/m) in the Wadden Sea, Section 1 (loc. 2 – 7)

The SkyTEM data as well as the results of the ground water model indicate a significant ground water discharge towards the Wadden Sea at the South-Eastern coast of the island. The new field measurements and samples along cross section 1 proved that the discharge of fresh water extends to a range of more than 600 m offshore. At this part of the coast a layer of clayey and silty material prevents the discharging fresh water largely from mixing with the overlaying salt water (Figure 3).

Cross section from the Geest to the Marsh

The wide lowland of the Marsh is covered by clayey and silty sediments that mostly were deposited in the Holocene before the first dykes were built some 500 years ago. Due to the low permeability of the Holocene clay and the abstraction of fresh water via the system of drainage ditches, recharge of ground water generally is poor. So the aquifers in large parts of the marsh contain brackish or salty water. A discharge of fresh water from the Geest into the aquifers of the marsh, as it clearly could be seen in the SkyTEM data, was proved by the new field measurements and samples (Figure 4). The sediments of an ancient tidal creek were found in the northern part of the section, causing a local infiltration of fresh water. A system of ancient tidal creeks, covering the whole marsh area, can be identified by laser scan measurements of the relief heights. These tidal creeks are relicts of the times when the area was daily flooded by the tide. Today the creeks which were refilled with sandy or clayey

material, cause local inhomogeneity in permeability of the covering layer of the aquifers in the marsh area, with influence on the distribution of salt and fresh water.

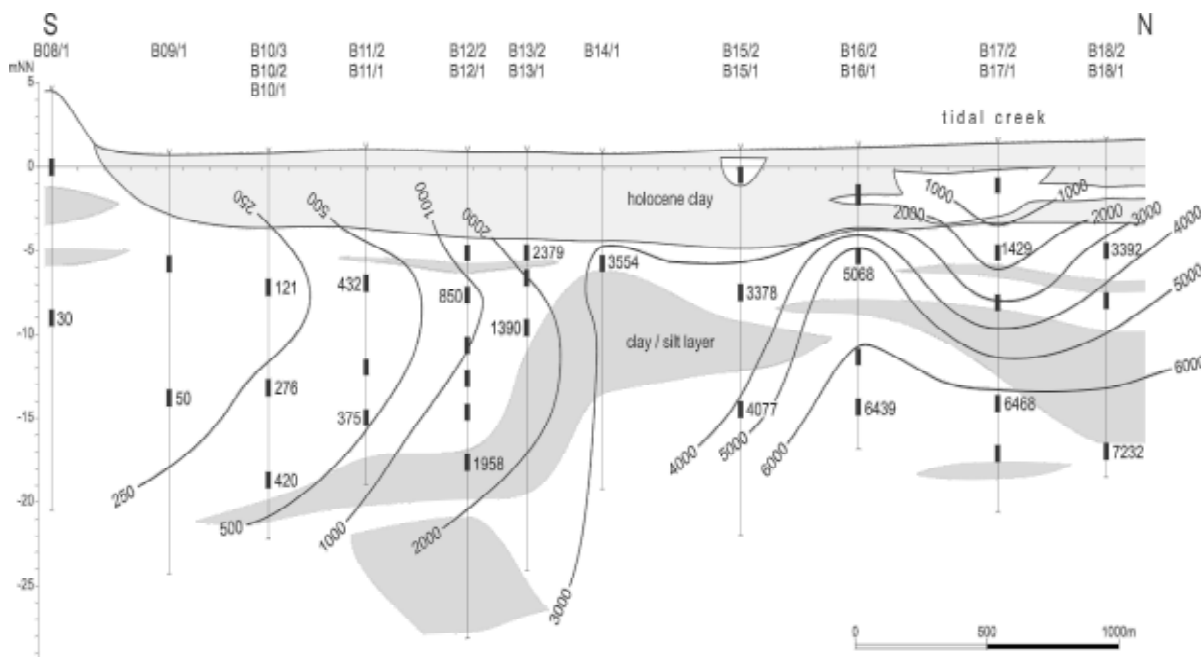


Figure 4. cross section 2 showing the interpolated distribution of Chloride (mg/l) in the marsh, section 2 (loc. 8 – 18)

CONCLUSIONS

In addition to previous surveys a combination of drillings, direct push measurements and ground water sampling has proven as a cost-efficient method to gather additional data in the marsh and on the tidal flats where still a lack of information exists. The outcome of the investigations has shown that the prediction of future climate change and sea level rise impacts on the island of Föhr will first of all be dependent on reliable data of the geohydraulic and geochemical situation especially in the marsh area.

REFERENCES

- Burschil, T., Scheer, W., Kirsch, R., Wiederhold, H. 2012, Compiling geophysical and geological information into a 3-D model of the glacially-affected island of Föhr. *Hydrol. Earth Syst. Sci.*, 16, 3485 – 3498.
- Jørgensen, F., Scheer, W., Thomsen, S., Sonnenborg, T.O., Hinsby, K., Wiederhold, H., Schamper, C., Burschil, T., Roth, B., Kirsch, R., Auken, E. 2012. Transboundary geophysical mapping of geological elements and salinity distribution critical for the assessment of future sea water intrusion in response to sea level rise. *Hydrol. Earth Syst. Sci.*, 16, 1845 – 1862.
- LLUR CLIWAT working group 2012. *Der Untergrund von Föhr: Geologie, Grundwasser und Erdwärme.* – Schriftenreihe LLUR – Geologie und Boden 18, Flintbek
- CLIWAT project group 2011. *Groundwater in a future climate.* – Central Denmark Region, Horsens

Contact Information: Wolfgang Scheer, Agency for Agriculture, Environment and rural Areas Schleswig-Holstein, Geological Survey, Hamburger Chaussee 25, D-24220 Flintbek, GE, Phone: 0049-4347-704-525, Fax: 0049-4347-704-502, Email: wolfgang.scheer@llur.landsh.de

Density-driven flow modelling using d³f

A. Schneider¹, L. Stoeckl^{2,3}, J. Wolf¹, M. Howahr⁴, L. Brand¹

¹ Gesellschaft für Anlagen- und Reaktorsicherheit mbH (GRS)

² Federal Institute for Geosciences and Natural Resources Germany (BGR)

³ Institute of Fluid Mechanics in Civil Engineering, Leibniz University Hannover

⁴ Oldenburgisch-Ostfriesischer Wasserverband (OOWV)

ABSTRACT

The finite volume code d³f (distributed density driven flow) has been developed with a view to modelling large, complex, density-influenced aquifer systems. The use of cutting-edge numerical methods and their parallelisation enables simulations over long time periods with feasible computational effort. Developed for long-term safety analyses for nuclear waste repositories, d³f is applied here to a series of laboratory experiments regarding fresh water lenses of islands, as well as to a coastal aquifer near the German North Sea (work in progress.)

INTRODUCTION

The code d³f (distributed density driven flow) has been developed to meet the needs of far field modelling as a part of long-term safety analyses for nuclear waste repositories in rock salt. It is able to model density-driven flow in the overburden of salt domes, i.e. in areas up to 10 000 km² with complex hydrogeological situations over time periods of some ten thousands of years. The development began in 1995 as a joint project of GRS together with five university institutes, funded by BMWi, and is still ongoing. The result is a powerful tool that is able to handle salt and heat transport in porous as well as fractured media, salt concentrations up to saturation and complex hydrogeological structures with high permeability contrasts. Besides safety analyses, d³f has been applied to other fields, too, such as laboratory and field experiments or coastal aquifers.

THE MODEL

The finite volume code d³f is based on the UG toolbox, uses fast numerical solvers such as multigrid methods and is completely parallelized (Fein 1999). Currently, d³f solves the following equation system describing thermo-haline flow:

$$\partial_t(\phi\rho) + \nabla \cdot (\rho\mathbf{q}) = 0 \quad (1)$$

$$\partial_t(\phi\omega\rho) + \nabla \cdot (\rho\omega\mathbf{q} + \mathbf{J}_\omega) = 0 \quad (2)$$

$$\mathbf{J}_\omega = -\rho\mathbf{D}\nabla\omega, \quad \mathbf{D} = D_m\boldsymbol{\tau} + \mathbf{D}_a \quad (3)$$

$$\partial_t[(\phi\rho C_f + (1-\phi)\rho_s C_s)\Gamma] + \nabla \cdot (\rho C_f T\mathbf{q} + \mathbf{J}_T) = 0 \quad (4)$$

$$\mathbf{J}_T = -\Lambda\nabla T \quad (5)$$

$$\mathbf{q} = -\frac{k}{\mu}(\nabla p - \rho\mathbf{g}) \quad (6)$$

where (1) describes the mass conservation of the fluid, (2) the mass conservation of the brine, (3) diffusive/dispersive flow, (4) energy conservation, (5) heat flow and (6) Darcy's law. Hereby, ϕ is the porosity [-], ω the solute mass fraction [-], $\rho(\omega)$ the fluid density [kg m^{-3}], t the time [s], \mathbf{q} the Darcy velocity [m s^{-1}], k the permeability [m^2], $\mu(\omega)$ the dynamic viscosity [Pa s], p the pressure [N m^{-2}] and \mathbf{g} the gravitation vector [m s^{-2}]. D_m represents the molecular diffusion constant, $\boldsymbol{\tau}$ the tortuosity tensor, and \mathbf{D}_d the dispersion tensor [$\text{m}^2 \text{s}^{-1}$] according to Scheidegger's law (Bear 1972). C_f is the specific heat capacity of the fluid [$\text{J kg}^{-1} \text{K}^{-1}$], C_s the specific heat capacity of the solid (rock) [$\text{J kg}^{-1} \text{K}^{-1}$], ρ_s the rock density [kg m^{-3}], T the temperature [K] and $\boldsymbol{\Lambda}$ the hydrodynamic thermal dispersion tensor [$\text{m}^2 \text{s}^{-1}$]. The fluid density ρ and the dynamic viscosity μ are depending on salt mass fraction and temperature. It should be mentioned that the complete equations for flow and salt transport are solved without simplifications such as the Boussinesq approximation. The application of d^3f is restricted to saturated conditions. A free groundwater surface is represented by means of a level set method. For detailed description see Fein (1999), Schneider (2012).

RESULTS

Reported here is the modelling of a couple of quasi-2d laboratory experiments performed by BGR to investigate the dynamics of freshwater lenses. Hereby, an acrylic sand box with a size of 2 m x 0.3 m x 0.05 m was used to simulate formation and degradation of freshwater lenses. Based on the experimental results a benchmark was defined, consisting of the lens formation by applying, and lens degradation after stopping recharge. For a description of the experiments and parameters in detail see Stoeckl (2012) and (2014). The benchmark was simulated numerically by five computer codes. Thereby, all codes had to use the same computational grid as well as the same numerical parameters. In the first step, a very coarse grid was used, consisting of 7380 nodes. Regarding concentration, d^3f results fitted very well with FEFLOW results, see figure 1. Remarkable was the very thin transition zone between fresh- and saltwater that was calculated by d^3f in spite of the prescribed coarse discretization.

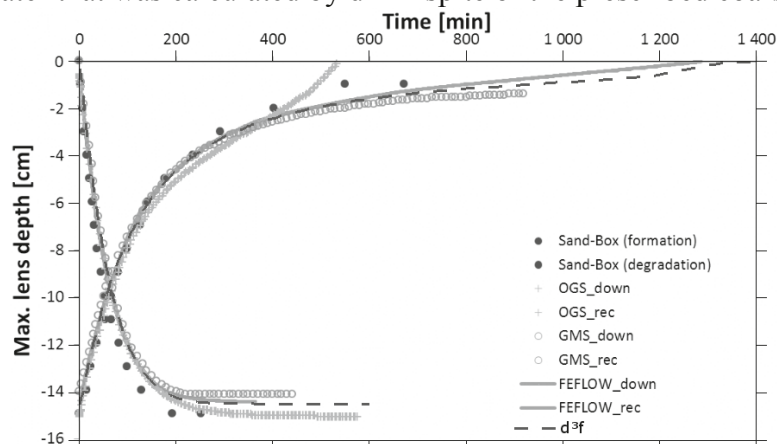


Figure 1: Depth of the saltwater-freshwater interface over time (deepest point) – comparison of the results of OpenGeosys, Seawat (GMS), FEFLOW and d^3f with the measurements (source: preliminary results after L. Stoeckl, modified)

In a second step the simulations were repeated on a finer grid consisting of 121 362 nodes (results see Stoeckl 2014). Because d^3f numerics are based on multigrid methods, we performed additional simulations on a multigrid from 1 617 to 394 497 nodes. Furthermore, the sensitivity to various factors was investigated, such as solving the full equation system in comparison to using the Boussinesq approximation, the influence of different variations of boundary conditions and the level of grid refinement.

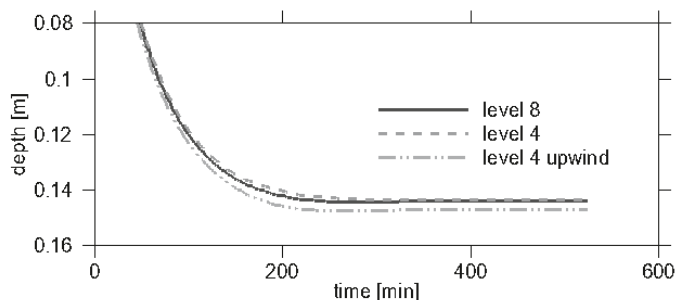


Figure 2: Depth of the saltwater-freshwater interface over time
 results on 394 497 (level 8) and 1 617 nodes (level 4) as well as using upwind methods

The results on the 121 362 nodes grid and on multigrid level 8, 7 and 6 almost completely coincide. Using Boussinesq approximation had also no observable influence. Figure 2 shows the relatively low influence of the grid refinement on the depth of the lens, whereas using upwind methods on relatively coarse grids may distort the result significantly. In figure 3 is illustrated, that the transition zone and especially the width of the outflow zone may easily be overestimated without an appropriate grid refinement or using upwind methods.

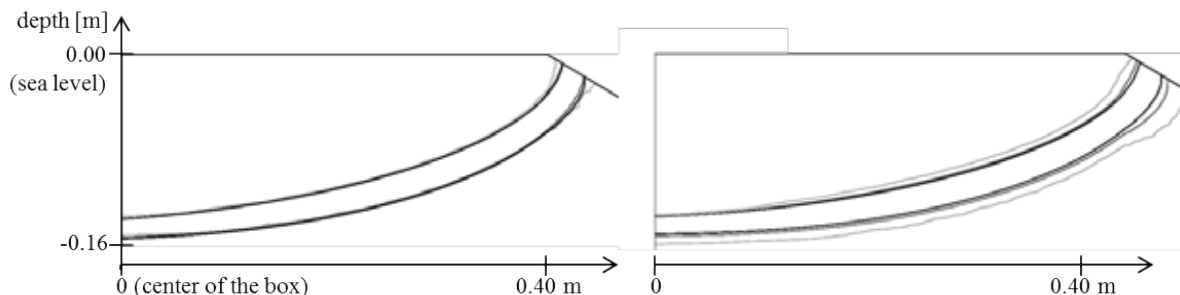


Figure 3: Thickness of the saltwater-freshwater transition zone
 isolines of 10 % (upper lines) and 90 % concentration, results on grid level 8 (black line), 6 (grey line) and 4 (light grey line); left: without upwind, right: with upwind method

Additionally, some variations of the experiment were simulated as well, such as changes in recharge and the introduction of less permeable zones in horizontal as well as in vertical direction (Dose et al. 2013.) Here, only one example is shown, where the left part of the sand box was filled with a more than 10 times lower permeable material ($k = 2.15 \cdot 10^{-10} \text{ m}^2$) than the right ($k = 2.35 \cdot 10^{-9} \text{ m}^2$). This inhomogeneity strongly influences the shape of the freshwater lens and the situation of the watershed. After reaching steady-state the lens is much deeper in the left hand part, and a change in its slope at the boundary between the two permeability sectors is clearly visible in the results (see Figure 4). The results of d³f and FEFLOW are almost identical. The experimental results could also be reproduced satisfactorily, except for the fact that both numerical codes overestimated the extension of the outflow zone on the higher permeable side.

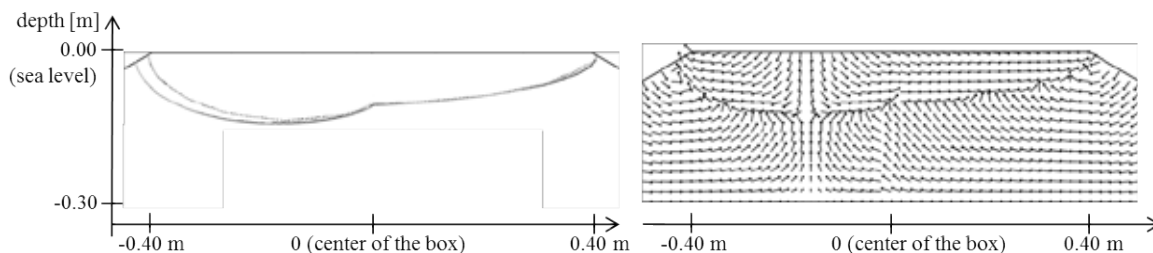


Figure 4: Left: Depth of the freshwater lens (50 % seawater concentration)
 grey line: d³f, black line: FEFLOW, dotted line: measurements; Right: velocity vectors (d³f)

In an ongoing project, d³f is applied to coastal aquifers near the German North Sea. The aim of this work is forecasting the impact of different climatic and demographic scenarios on the freshwater supply (see also Eley et al 2014). A regional 3d density-driven flow model will be set up, including pumping wells of three waterworks. Scenarios to be simulated are sea-level elevation as a consequence of climate change, shifts of the seasonal distribution of precipitation and changes in the fresh water demand caused by demographic and economic factors.

For now, a 2d vertical cross-section is extracted and adapted for d³f. Simulations are started with the objective of getting acquainted with the hydraulic processes in the model domain as well as testing the interaction of the various features and instruments. First results will be presented here.

CONCLUSIONS

It is shown that the density-driven flow code d³f is applicable to saltwater intrusion problems in laboratory and field scale.

For this type of problem solving the complete set of equations has no advantage over using the Boussinesq approximation because only low salt concentrations are involved. However one has to be very careful in using numerical parameters as grid refinement and upwind methods.

REFERENCES

Fein, E., Schneider, A. (eds.): d³f—Ein Programmpaket zur Modellierung von Dichteströmungen. FKZ-02 C 0465 379, final report. Gesellschaft für Anlagen- und Reaktorsicherheit (GRS) mbH, GRS-139, Braunschweig 1999.

Dose, E. J., Leonard Stoeckl, Houben, G. J., Vacher, H. L., Vassolo, S., Dietrich, J., Himmelsbach, T.: Experiments and modeling of freshwater lenses in layered aquifers: Steady state interface geometry. *Journal of Hydrology* 509 2013, (621-630).

Eley, M., Howahr, M., Schneider, A., Schöniger, M., Ullmann, A., Wolf, J.: Potential Consequences of Saltwater Intrusion at the German North Sea Coast for the water supply (same issue) 2014.

Schneider, A. (ed.): Enhancement of d³f und r³t (E-DuR). FKZ 02 E 10336 (BMW), final report, Gesellschaft für Anlagen- und Reaktorsicherheit (GRS) mbH, GRS-292, Braunschweig 2012.

Stoeckl, L., Houben, G.: Flow dynamics and age stratification of freshwater lenses: experiments and modeling. *Journal of Hydrology* 21 2012, (458-459), pp. 9-15.

Stoeckl, L., Walther, M., Schneider, A., Yang, J. and Graf, T. Comparison of numerical models using a two-dimensional benchmark of density-driven flow (same issue) 2014.

Contact Information: Anke Schneider, GRS mbH, Department Safety Assessment, Theodor-Heuss-Str., 38122 Braunschweig, Germany, Phone: +49-531-8012-248, Fax: +49-531-8012-248, Email: anke.schneider@grs.de

SUBMARINE GROUNDWATER DISCHARGE IN THE SOUTHWESTERN BALTIC SEA

Jan Scholten¹, M. Kreuzburg¹, K. Knoeller², J. Rapaglia³, M. Schlüter⁴, M. Schubert²

¹Institute for Geosciences, University Kiel, Germany

²Helmholtz Centre for Environmental Research, Leipzig, Germany

³Department of Biology, Sacred Heart University, US;

⁴Alfred-Wegener Institute, Bremerhaven, Germany

ABSTRACT

The protection of the coastal environment in the Baltic Sea relies on the correct identification of the sources and fluxes of pollutants. Although the main transport routes of pollutants (atmosphere, rivers) are well monitored, several studies indicate that a considerable part of unmonitored waters flow to the Baltic Sea. One of these, to date, unmonitored water flows to the sea is submarine groundwater discharge (SGD). SGD is defined here as the flow of meteoric water from the seabed to the coastal ocean and is a ubiquitous phenomenon at ocean margins. SGD occurs whenever the hydraulic gradient on land is above mean sea-level and permeable paths connect continental aquifers to the seafloor. So far very few SGD locations have been described in the Baltic Sea. Here we report from a systematic survey for SGD in the Southwestern Baltic Sea (Mecklenburg Bay, Lübeck Bay, Kiel Bay, Eckernförde Bay). Based on geochemical tracer measurements (radon, radium isotopes, salinity) in seawater, and measurements of pore water salinity in marine surface sediments, we could identify SGD locations related to coastal aquifers discharging directly at the beachfront. More frequently, diffuse discharge from near shore sediments was observed. Such SGD was characterized by significantly lower pore water salinities compared to ambient sea water. Pore water salinity was monitored using an in situ CTD. Interstitial water salinity was marked by strong variation, with generally lower values during periods of low sea level. This relationship indicates that diffusive SGD is largely controlled by the sea level, which, in turn, controls the hydraulic gradient between land and sea. In the Southwestern Baltic Sea the sea level is mainly determined by the wind regime. Within this study, several locations were identified in which SGD is associated with high nitrate concentrations indicating the importance of SGD for the nutrient balance of the Southwestern Baltic Sea.

Seawater intrusion in fractured coastal aquifers: preliminary investigation using a discretely fractured Henry problem

Megan L. Sebben^{1,2}, Adrian D. Werner^{1,2} and Thomas Graf³

¹National Centre for Groundwater Research and Training, Flinders University, Adelaide, SA, Australia

²School of the Environment, Flinders University, Adelaide, SA, Australia

³Institute of Fluid Mechanics and Environmental Physics in Civil Engineering, Leibniz Universität, Hannover, Germany

ABSTRACT

Coastal aquifers globally are under threat from seawater intrusion (SWI) (Chang and Yeh 2010). The extent of saltwater and of SWI in heterogeneous (e.g. fractured) aquifers is not well-understood relative to homogeneous (unfractured) aquifers (Allen et al. 2002). SWI in fractured coastal aquifers has been observed at several field sites (e.g. Caswell 1979; Barcelona et al. 2006), where fractures provide preferential flow paths that either facilitate or inhibit the inland migration of seawater. Despite this, numerical investigations that explore SWI processes and the persistence of seawater in fractured versus unfractured aquifers, are rare. Groundwater flow in fractured systems can be approximated using an equivalent porous media (EPM) model if the representative elementary volume is large enough (Pankow et al. 1986; Scanlon et al. 2003). However, accurate simulation of transport processes remains problematic due to difficulties with establishing the geologic controls on these systems (e.g. fracture spacing and fracture aperture) (Krásný and Sharp 2007). For this reason, discrete fracture network (DFN) models are useful tools for investigating groundwater flow and solute transport in fractured aquifers because they allow the validity (or otherwise) of EPM approximations to be tested (e.g. Vujević et al. submitted).

The purpose of this study is to determine how the structural properties of fracture networks influence both groundwater flow and solute transport processes (i.e. SWI) in fractured coastal aquifers. We examine the role of fracture location, orientation and density in SWI by applying DFNs to modified forms of the Henry (1964) seawater intrusion benchmark problem. Groundwater flow and solute transport are simulated for aquifers containing either a single fracture (anisotropic problem) or a network of regularly spaced, continuous, orthogonal fractures (isotropic problem) embedded within a permeable matrix. Simulations are carried out using HydroGeoSphere (Therrien et al. 2009), which solves 3D variable-density flow and solute transport in discretely fractured porous media. We compare metrics of SWI (e.g. the saltwater wedge toe location and width of the mixing zone) in the fractured cases with an EPM model, for steady-state groundwater flow conditions.

Our results show that the EPM model can predict reasonably well the inland extent of seawater (i.e. the saltwater wedge toe location) in the anisotropic, fractured Henry problem if the aquifer contains a single horizontal, centrally located fracture. The toe location in the fractured Henry problem is either under or overestimated (5-60%) by the EPM model if the horizontal fracture is positioned in the top or bottom halves of the aquifer, respectively. Horizontal fractures in the upper half of the aquifer facilitate the landward intrusion of seawater beneath the fracture. Conversely, horizontal fractures positioned in the lower half of the aquifer inhibit seawater intrusion and increase the width of the seawater-freshwater mixing zone.

We further demonstrate that predictions using the EPM model overestimate (4-10%) the toe location and underestimate the width of the seawater-freshwater mixing zone in aquifers containing a single, continuous vertical fracture. Vertical fractures in the saltwater wedge enhance transverse dispersion, increasing the width of the mixing zone. The EPM model predictions fail to capture the enhanced vertical mixing of incoming seawater and outgoing freshwater.

EPM model predictions do not represent adequately the extent of SWI in the isotropic, fractured Henry problem (containing networks of continuous, orthogonal fractures). Our simulations show that the steady-state seawater distribution is influenced strongly by the fracture density, i.e. the saltwater wedge typically retreats seawards and the width of the mixing zone increases as the fracture density increases. Predictions from the EPM model overestimate the position of the saltwater wedge toe by 10-20%.

Our results provide insight into how SWI is influenced by the structural properties of fracture networks. Further, we demonstrate that knowledge of the fracture network geometry is required to predict adequately the extent of saltwater contamination in fractured coastal aquifers.

REFERENCES

- Allen, D.M., D.G. Abbey, D.C. Mackie, R.D. Luzitano and M. Cleary. 2002. Investigation of Potential Saltwater Intrusion Pathways in a Fractured Aquifer using an Integrated Geophysical, Geological and Geochemical Approach. *Journal of Environmental and Engineering Geophysics* 7, no. 1: 19-36.
- Barcelona, M.J., M. Kim, C. Masciopinto and R. La Mantia. 2006. A Gypsum-Barrier Design to Stop Seawater Intrusion in a Fractured Aquifer at Salento (Southern Italy). In *Proceedings of SWIM-SWICA '06 Conference at the Hotel Le Meridien Chia Laguna, Cagliari, Italy*. v. 1: 263-272.
- Caswell, W.B. 1979. Maine's Groundwater Situation. *Ground Water* 17, no. 3: 235-243.
- Chang, C-M and H-D. Yeh 2010. Spectral approach to seawater intrusion in heterogeneous coastal aquifers. *Hydrology and Earth System Sciences* 14: 717-727.
- Henry, H.R. 1964. Effects of dispersion on salt encroachment in coastal aquifers. US Geological Survey Water Supply Paper 1613-C, 70-84.
- Krásný, J. and J.M. Sharp, Jr. 2007. Hydrogeology of fractured rocks from particular fractures to regional approaches: State-of-the-art and future challenges. In *Groundwater in Fractured Rocks – IAH Selected Papers*, eds J. Krásný and J.M. Sharp, Jr., 1-30. London, UK: Taylor and Francis Group.
- Pankow, J.F., R.L. Johnson, J.P. Hewetson and J.A. Cherry. 1986. An evaluation of contaminant migration patterns at two waste disposal sites on fractured porous media in terms of the equivalent porous medium (EPM) model. *Journal of Contaminant Hydrology* 1, no. 1-2: 65-76.

Scanlon, B.R., R.E. Mace, M.E. Barrett and B. Smith. 2003. Can we simulate regional groundwater flow in a karst system using equivalent porous media models? Case study, Barton Springs Edwards aquifer, USA. *Journal of Hydrology* 276, no. 1-4: 137-158.

Therrien, R., R.G. McLaren, E.A. Sudicky and S.M Panday. 2009. HGS - A three-dimensional numerical model describing fully-integrated subsurface and surface flow and solute transport. Groundwater Simulations Group.

Vujević, K., T. Graf, C.T. Simmons and A.D. Werner. Impact of fracture network geometry on free convective flow patterns (submitted).

Contact Information: Megan L. Sebben, Flinders University/National Centre for Groundwater Research and Training, Sturt Road, Bedford Park, SA 5042 Australia, Phone: +61-08-82012064, Email: Megan.Sebben@flinders.edu.au.

Submarine groundwater discharge at the Dead Sea

Christian Siebert¹, U. Mallast¹, T. Rödiger¹, M. Strey², D. Ionescu³, S. Häusler³, B. Noriega³, T. Pohl², B. Merkel²

¹Dept. Catchment Hydrology, Helmholtz Centre for Environmental Research – UFZ, Halle, Germany

²Dept. of Geology, TU Bergakademie Freiberg, Freiberg, Germany

³Microsensor Group, Max-Planck-Institute for Marine Microbiology, Bremen, Germany

ABSTRACT

Recent studies focused on the occurrence and mechanisms of submarine groundwater discharge along the Dead Sea. These springs are fed by groundwater from the Judean Mountains, which pass the unconsolidated sequence of clay minerals and evaporates (e.g. aragonite, gypsum, halite) forming the lakeshore and are able to pass the flat dipping Ghyben-Herzberg interface (Yechieli et al. 2006). Diving campaigns in Kane/Samar region revealed strong submarine springs emerging along distinct lines, of which orientation resembles those of onshore lineaments, while seeping springs mostly occur randomly.

To disclose pathways and transport mechanisms from the feeding mountain aquifers to the springs, hydrochemical and microbial investigations were carried out both, onshore and submarine and were combined with 2D hydraulic modelling. Microbial studies in these submarine springs revealed strong microbial reduction of dissolved sulphate and previously 'karstification' of the carbonatic minerals of the Dead Sea Sediment by sulphuric acid. The waters have their origin in a variety of hard rock aquifers of Cretaceous age. After draining into the Dead Sea sediments, groundwater (i) carry the easily soluble components (gypsum, halite) and the abundant organic matter, (ii) erodes and transports the hardly soluble minerals (clay and aragonite) and (iii) admix with briny pore water and ascending brines.

Finally, the individual processes and the directly influenced groundwater flow within the quaternary sediment of the Dead Sea (DS) were intended to be evaluated by applying a 2D numerical flow simulation. We introduced a statistical hydraulic 2D-flownet of primary and secondary flow paths (chaotic flow network). Assumptions include unidirectional flow, constant water inflow or constant concentration input. The mixing processes of fresh and salt water belong to the core interest of the density model. The investigation also focuses on the kind and the intensity of processes that are responsible for large differences in the output mass concentration to the DS. The study outlines the quantitative and qualitative share between terrestrial and submarine discharge to the Dead Sea and its responsible transport mechanisms.

INTRODUCTION

The lake level of the endoreic Dead Sea, situated within the Syrian-East-African Rift System, is dropping since decades. As a result, average groundwater levels in the aquifers of the surrounding mountain ranges follow that trend, due to their hydraulic connection to the lake level. The successively dry fallen lakebed exposes nowadays clayey and salty sediments, saturated with brines of comparable composition as the Dead Sea (TDS: 343 g/l; $\rho = 1,24 \text{ g/cm}^3$). Away from wadi fans, clay minerals dominate the sedimentary body, forming an aquiclude in general which blocks free groundwater discharge from the mountain aquifers in its back. Though, neotectonic disruptions (Mallast et al. 2011) and sulfuric acid and salt karst (Ionescu et al. 2012) lead to open fractures and pipes, which act as preferential flow paths. Consequently, springs are observable along the shoreline both, on- and offshore. Mostly, such springs occur concentrated in well-known areas, i.e. Feshkha, Kane/Samar or Ein Gedi. The

clustering of the observable lakeshore springs may be the higher abundance of groundwater upstream, which in turn is the result of higher fracture network that channels groundwater flow in the hardrock aquifers (Mallast et al., 2011). However, neither the hydraulic conditions that lead to these springs nor their discharge are analysed yet. This is the reason why it is one of the most doubtful variables in existing balances of the lake's water budget and strongly requires improvement.

The groundwater flow in the hard rocks of the Judea Group Aquifers (JGA) of the western DS drainage basin was at least partly numerically simulated (Laronne Ben-Itzhak and Gvirtzman 2005; Gräbe et al. 2013). The sensitivity analysis of the respective models showed that the hydrological system is mainly controlled by the distribution of hydraulic conductivities in the Upper and Lower JGA, respectively and important, by the Quaternary Dead Sea Group (DSG) sediments along the lakeshore. Gräbe et al. (2013) demonstrated that the DSG sediments control the release of groundwater from the JGA to the lake.

METHODS AND RESULTS

In general, the bulk composition of DSG sediment consists of highly heterogeneous deposited fine-grained clastic and evaporitic minerals. Where wadis release their surface runoff into the lake, the DSG-sediments are intercalated with coarser clastics. However, during low-stands of the former lakes, coarse sediments were also deposited in broader areas. The groundwaters, recharged in the JGA and in deeper geological strata (Ionescu et al., 2012) migrate through the DSG-sediment, where hydraulic features may allow their passage (e.g. Ein Feshkha, Kane/Samar, Ein Gedi) (Figure 1). In the framework of the multilateral SUMAR project (funded by the German Ministry of Education and Research BMBF, support code: 02WM0848) investigations revealed, the quantity of submarine discharge is comparable to that of onshore springs. Additionally, extensive hydrochemical and isotopic investigations (major elements; rare earths; stable and radiogenic isotopes of water, sulfur, carbon, strontium and chlorine) illustrate, submarine spring waters are not a simple mixture of freshwater and DS water.

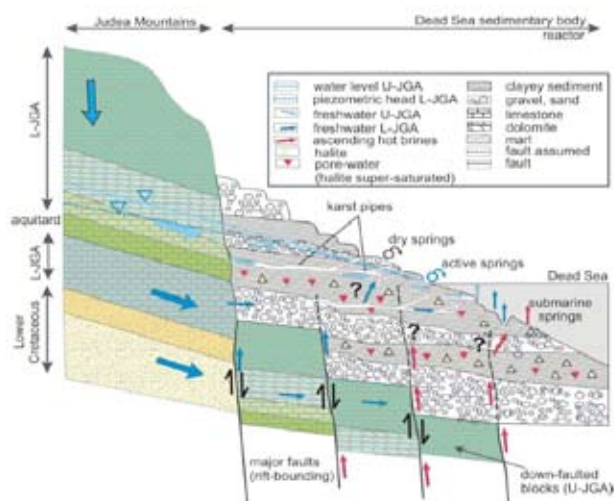


Figure 1. Conceptual cross-section through the hard-rock graben flank and the Dead Sea Group sediments with indicated preferential water pathways in the DSG sediment with resulting onshore and offshore discharges.

The analyses show that the mixing of water is mainly controlled by chemical solution processes of evaporites (e.g. anhydrite, halite) and carbonatic minerals (e.g. aragonite, strontianite) in the DSG sediment, and admixture of residual brines in the pore space. The mineralisation of the passing groundwaters increase with (a) residence time, which is mainly

controlled by the opening of conduits and (b) the ratio between discharge and aperture of the conduits. As a consequence of the solution process and the consistent groundwater discharge of the JGA, it is still unclear, whether the conduit network follows chaotic solution patterns or regulated pathways inside the DSG sediments.

Hence, the claim was to model the groundwater flow and transport in the sediments of the DS as a statistical hydraulic 2D-flownet of primary and secondary flow paths (chaotic flow network) by *FEFLOW 6.1*. Therefore, the cross-section was placed cutting the DSG sediments north of the impressive Wadi Darga fan (Figure 2). Assumptions include unidirectional flow, constant water inflow or constant concentration input. The mixing processes of fresh and salt water belong to the core interest of the density model. The investigation also focuses on the kind and the intensity of processes that are responsible for large differences in the output mass concentration to the DS. The study outlines the quantitative and qualitative share between terrestrial and submarine discharge to the DS and its responsible transport mechanisms.

Model setup

Dependent on available underground information of the sediment of the DS (drilling records of Mineral-2 (after Stein et al. 2010), Mineral-4 (after Yechieli 2005), Dragot-4 (after Yechieli 2005), M1 (after Torfstein et al. 2008 and Torfstein et al. 2013) and PZ-2 (after Waldmann et al. 2007 and Haliva-Cohen et al. 2012) the location of the cross-section was decided to be north of the outlet of Wadi Darga (Figure 2).

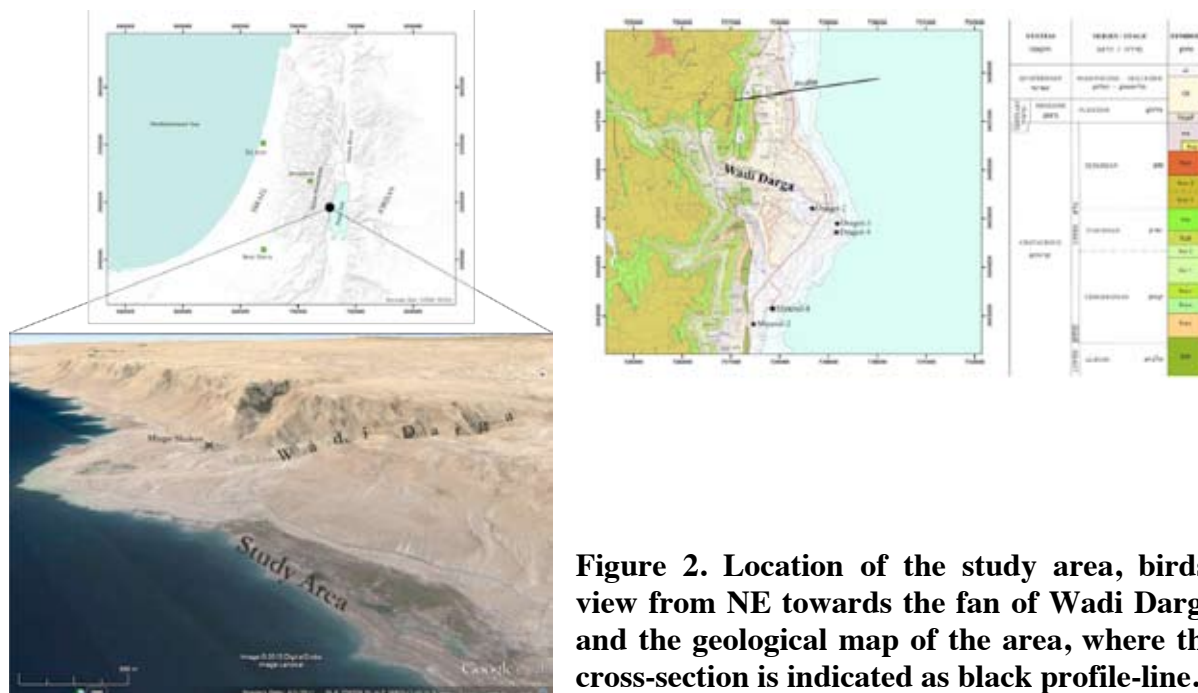


Figure 2. Location of the study area, bird's-eye view from NE towards the fan of Wadi Darga and the geological map of the area, where the cross-section is indicated as black profile-line.

The first concept of the numerical model setup and the corresponding parameterization of the hydrological settings were assumed from literature values and the general understanding of the area (Figure 3). The solution network features inside the sediments of the DS were realized by discrete elements (DE). During the calibration and finally in the simulation process the main task was to correctly parameterize the dimensions of the discrete elements.

Model results

The sensitivity analysis of the solution network revealed that small DE cross-section areas and low values of hydraulic aperture facilitate the supply of freshwater to the DS. Comparable to an aquitard, a considerable amount of freshwater flow from the JGA to the DS can only occur if the nearly impermeable sediment of the DS minimizes saltwater intrusion. Consequently,

large conduits in the lower part of the DSG sediment will favour salinity intrusion (pull mechanism) due to the low opposing pressure on the freshwater supply side and cause high saline pore waters in the DSG sediment. A depth of -528 m msl is the deepest point for a subsurface spring (revealed by the used DE frequency). Below, the dominance of seawater intrusion exacerbates freshwater outlets. The larger freshwater springs have been observed on the shoreline only a few meters below the DS surface till -433 m msl. Larger tubes, either in hydraulic aperture or cross-section area, govern these outlets. However, they can only occur in shallow areas where saltwater pressure does not prevail over the inflowing freshwater pressure (push mechanism). Consequently, the discharge system is particularly susceptible if conduits are permanently developing in the upper part of the DSG sediment. There, dissolution processes may result in small increases of cross-section areas or breakthrough of strongly tortuous pathways and effectively change the amount and frequency of springs on the shoreline of the DS to higher values. Especially, cross section areas and hydraulic apertures in the range of 5 mm to 5 cm result in surface and subsurface springs. Opposite, precipitation may effectively decrease the discharge to the DS. To summarize, the variability of discharge to the DS is larger in the upper DSG sediment. Figure 4 reflects the main model results.

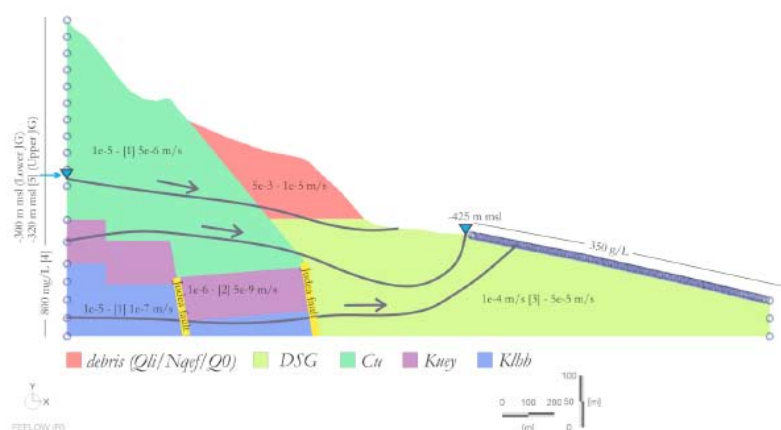


Figure 3. Shows the concept of hydrogeological properties (hydraulic conductivities and mass concentrations are based on literature values). Flow potentials and expected flow lines are denoted.

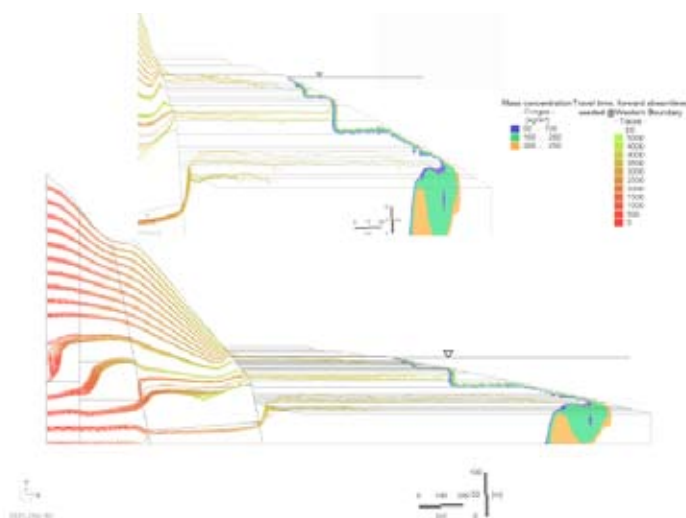


Figure 4. Simulated streamlines and mass concentration pattern inside the Cretaceous and Quaternary sediments of the Dead Sea area.

REFERENCES

- Gräbe, A., T. Rödiger, K. Rink, T. Fischer, F. Sun, W. Wang, C. Siebert and O. Kolditz 2013. Numerical analysis of the groundwater regime in the western Dead Sea escarpment, Israel + West Bank, *Env. Earth Sci*, no. 69 (2): 571-585.
- Haliva-Cohen, A., Stein, M., Goldstein, S.L., Sandler, A. and Starinsky, A. 2012. Sources and transport routes of fine detritus material to the Late Quaternary Dead Sea basin. *Quat Sci Rev*, no. 50: 55–70.
- Ionescu, D., Siebert, C., Polerecky, L., Munwes, Y.Y., Lott, C., et al. 2012. Microbial and Chemical Characterization of Underwater Fresh Water Springs in the Dead Sea. *PLoS ONE* 7(6): e38319. doi:10.1371/journal.pone.0038319
- Laronne Ben-Itzhak L. and H. Gvirtzman 2005. Groundwater flow along and across structural folding: an example from the Judean Desert, Israel. *J Hydrol*, no. 312: 51–69
- Mallast, U., Gloaguen, R., Geyer S., Rödiger T. and Siebert C. 2011. Derivation of groundwater flow-paths based on semi-automatic extraction of lineaments from remote sensing data. *HESS*, no. 15: 2665-2678.
- Stein, M., Torfstein, A., Gavrieli, I. and Yechieli, Y. 2010. Abrupt aridities and salt deposition in the post-glacial Dead Sea and their North Atlantic connection. *Quat Sci Rev*, no. 29 (3-4): 567–575.
- Strey, M. 2014. 2-D numerical flow and density modeling in Dead Sea Group sediments (Darga, Israel). Master thesis TU Bergakademie Freiberg, 134 pages (unpublished).
- Torfstein, A. Gavrieli, I., Katz, A., Kolodny, Y. and Stein, M. 2008. Gypsum as a monitor of the paleo-limnological–hydrological conditions in Lake Lisan and the Dead Sea. *GCA*, no. 72 (10): 2491–2509.
- Torfstein, A., Goldstein, S.L., Kagan, E.J. and Stein, M. 2013. Integrated multi-site U–Th chronology of the last glacial Lake Lisan. *GCA*, no. 104: 210–231.
- Waldmann, N., Starinsky, A. and Stein, M., 2007. Primary carbonates and Ca-chloride brines as monitors of a paleo-hydrological regime in the Dead Sea basin. *Quat Sci Rev*, no. 26 (17–18): 2219–2228.
- Wollman, S. et al. 2003. Summary of results for the test pumping in Nahal Arugot, Dead Sea sinkholes project: Stage B. Geological Survey of Israel Report GSI/42/2003.
- Yechieli, Y. 2005. Geological and hydrological findings from wells near the Dead Sea. Sinkhole Project -Phase Two. Geological Survey of Israel Report TR-GSI/06/2005.
- Yechieli, Y., Abelson, M., Bein, A., Crouvi, O. & Shtivelman, V. 2006. Sinkhole ‘swarms’ along the Dead Sea coast: Reflection of disturbance of lake and adjacent groundwater systems. *Geological Society of America Bulletin*, no. 118:1075–1087.

Airborne clay mapping at the East Frisian coast

Bernhard Siemon¹, Wolfgang Voß¹, Jörg Elbracht², Nico Deus² and Helga Wiederhold³

¹Federal Institute for Geosciences and Natural Resources (BGR), Hannover, Germany

²State Authority for Mining, Energy and Geology (LBEG), Hannover, Germany

³Leibniz Institute for Applied Geophysics (LIAG), Hannover, Germany

ABSTRACT

Airborne geophysical methods enable economic and ecological mapping of subsurface natural resources. Besides groundwater and mineral exploration, the investigation of non-mineral resources is an important task. Electromagnetic methods are able to map lithological units if these are correlated with electrical conductivity. Particularly resistive sands and gravels can be distinguished from conductive clayey materials. Currently most of our recent airborne surveys were flown in the coastal areas of Northern Germany, where saltwater intrusion and clay mapping are the principal topics. The helicopter-borne system operated by BGR was used to survey several areas in Eastern Friesland together with LIAG. The spatial conductivity distribution, which was derived from six-frequency helicopter-borne electromagnetic (HEM) data, provides information on both lithology and water salinity. Onshore, the HEM results clearly outline a rather complex pattern of higher conductivity which coincides with many boreholes provided by LBEG, in which clayey material was found particularly down to about 20 m depth. This pattern continues offshore and thus obviously outlines areas where fresh groundwater flows into the Wadden Sea. On the islands, the HEM results show some indications for thin clay layers within the freshwater lenses.

INTRODUCTION

The knowledge on saltwater intrusion and distribution of clayey sediments is important for understanding the current status of the dynamic setting in coastal areas, where large storms, rising sea level, and human activity may affect the hydrogeological conditions, and the impact of climate change effects is of particular interest (Hinsby et al. 2011).

Geophysical methods such as electromagnetics (EM) are able to map hydrogeological units if these are correlated with the electrical conductivity (or its inverse, the resistivity). Particularly conductive saltwater can be distinguished from resistive freshwater as well as conductive clayey materials from resistive sands and gravels (Kirsch 2006). Helicopter-borne geophysical methods enable economic and ecological mapping of near-surface natural resources and environmental settings (Siemon et al. 2009). One of the first successful airborne groundwater investigation surveys was conducted on the island of Spiekeroog, Germany, in 1978 (Sengpiel and Meiser 1981) using an early frequency-domain helicopter-borne electromagnetic (HEM) system (DIGHEM II) operated by BGR. Since then, many airborne surveys have demonstrated the applicability of airborne EM in coastal areas, e.g. for mapping of saltwater intrusions, freshwater outlets, or freshwater lenses on islands (e.g. Fitterman and Deszcz-Pan 1998; Siemon and Steuer 2011; Siemon et al. 2014).

Two surveys flown in Northern Germany in 2008-2009 cover an area of 20 km by 31 km including the island of Langeoog, the western half of the island of Spiekeroog, the Wadden Sea, and the onshore area to the north of Aurich. The aim of these surveys was the investigation of saltwater intrusion and the distribution of clayey sediments, and on the islands, the freshwater lenses and the lithological structure were studied.

METHODS

The BGR airborne geophysical system enables simultaneous measurements of three geophysical methods: electromagnetics, magnetics, and gamma-ray spectrometry. The electromagnetic sensors are housed in a 10 m long tube, which is towed by a Sikorsky S-76B helicopter on parallel flight lines about 30–40 m above ground level. The processed HEM data are converted to half-space parameters, which are used to define individual multi-layer starting models at each data point for an iterative Marquardt-Levenberg inversion process (Siemon et al. 2009; Steuer et al. 2014). As man-made effects caused by power lines, railway tracks, highways, wind parks or urban areas are able to distort nearby HEM measurements, these data have to be corrected (Siemon et al. 2011).

RESULTS

Assuming that clay/silt is represented by a resistivity ranging from 12 to 35 Ωm , the thicknesses of model layers fulfilling this condition were summed up and displayed on a map (Figure 1). In order to reduce misinterpretation caused by saltwater, only the upper four of six model layers were taken into account as they represent shallow clay/silt layers sufficiently well and the coastal saltwater intrusion mainly affects the lower two model layers. The thicknesses of clayey or silty layers at shallow depths (around 10 m bsl) obtained from the boreholes as well as the location of boreholes without clay and silt layers (LBEG 2014) are also shown on this map. It is obvious that the clay/silt thicknesses estimated from the HEM results are sufficiently correlated with clay/silt thicknesses of most of the boreholes. Some discrepancies occur, for example, at the location boreholes A, B, or C, which are often caused by man-made effects or insufficient borehole descriptions. This finding encourages the use of the airborne results for mapping of shallow clay occurrences.

The freshwater-saltwater interface in this survey is located rather close to the coastline, particularly at shallow depths (Steuer et al. 2014). At greater depth, a straggly distribution of resistive and conductive features crossing the coastline appears (Figure 2). On both sides of the sea dyke, finger-shaped conductivity features appear, which seem to be a continuation of the shallow clay/silt deposits onshore. Therefore, it is likely that the saltwater is linked to clayey sediments and that the fresh groundwater flows out to the Wadden Sea area. This detailed information is necessary for correctly setting-up geological and hydrogeological models (Deus and Elbracht 2014).

On the islands, the HEM results reveal the freshwater lenses (white colours on Figure 2) and show some indications for thin clay layers, which are investigated in detail by ground geophysical methods (Costabel et al. 2014).

DISCUSSION AND CONCLUSIONS

The application of helicopter-borne EM in coastal areas helps to map saltwater intrusion, offshore freshwater outlets and/or clayey sediments. The spatially acquired airborne data are able to close gaps resulting from sparse borehole density and enables improved geological and/or hydrogeological modelling. In this survey area, the knowledge about the distribution of medium to low resistivities was mandatory to successfully map clay/silt occurrences and freshwater-saltwater interfaces as these rather complex patterns were not sufficiently imaged by borehole interpretation alone.

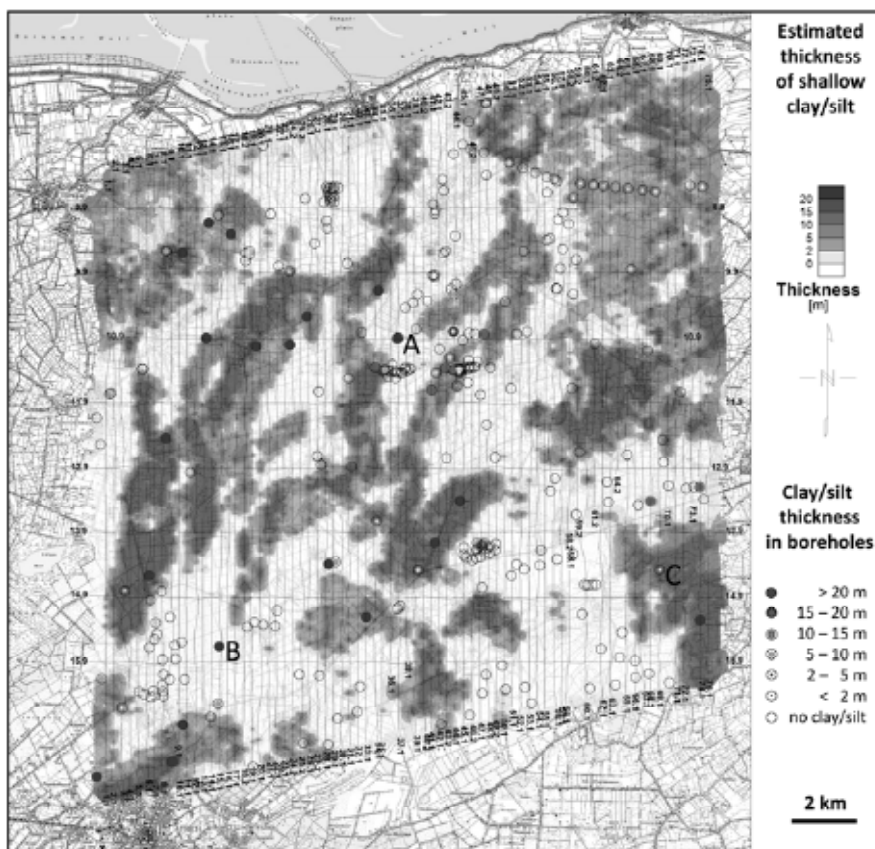


Figure 1. Comparison of clay thicknesses derived from HEM data and found in boreholes at shallow depth plotted on a topographic map (BKG 2008).

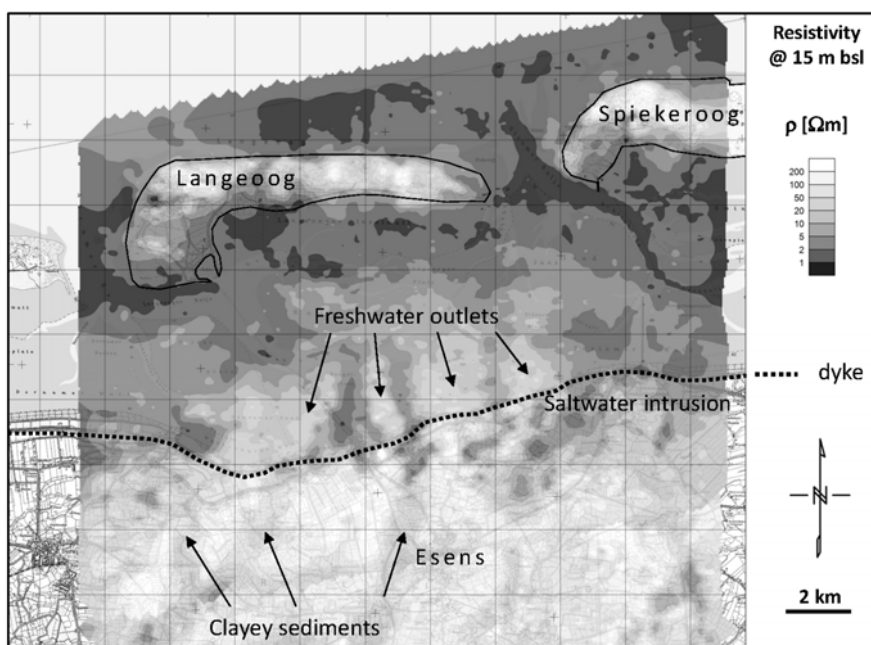


Figure 2. Resistivity at 15 m bsl revealing complex freshwater-saltwater interfaces at the North German coast and on the islands plotted on a topographic map (BKG 2008).

REFERENCES

- BKG. 2008. Digitale Topographische Karte 1:50 000 (DTK50-V): Geobasisdaten © BKG 2008, <http://www.bkg.bund.de/>.
- Costabel, S., U. Noell, T. Günther, G. Houben, W. Voß, and B. Siemon. 2014. Geophysical investigation of a managed freshwater lens on the North Sea island of Langeoog. In Proceedings of the 23rd Salt Water Intrusion Meeting, Husum, Germany.
- Deus, N., and J. Elbracht. 2014. 3D-Modelling of the salt-/fresh water interface in coastal aquifers of Lower Saxony (Germany) based on airborne electromagnetic measurements (HEM). In Proceedings of the 23rd Salt Water Intrusion Meeting, Husum, Germany.
- Fitterman, D.V., and M. Deszcz-Pan. 1998. Helicopter EM mapping of saltwater intrusion in Everglades National Park, Florida. *Exploration Geophysics* 29: 240–243.
- Hinsby, K., E. Auken, G.H.P. Oude Essink, P. de Louw, F. Jørgensen, B. Siemon, T.O. Sonnenborg, A. Vandenbohede, H. Wiederhold, A. Guadagnini, and J. Carrera. 2011. Assessing the impact of climate change for adaptive water management in coastal regions. Special Issue of Hydrology and Earth System Sciences, http://www.hydrol-earth-syst-sci-discuss.net/special_issue69.html.
- Kirsch, R. 2006. Hydrogeophysical properties of permeable and low permeable rocks. In *Groundwater Geophysics – A Tool for Hydrogeology*, ed R. Kirsch, 1-22. Springer.
- LBEG. 2014. Borehole database of Lower Saxony (BDN). Data set accessed 11 February 2014 at <http://nibis.lbeg.de/cardomap3/>.
- Sengpiel, K.-P., and P. Meiser. 1981. Locating the freshwater/salt water interface on the island of Spiekeroog by airborne EM resistivity/depth mapping. *Geologisches Jahrbuch C* 29, 255-271.
- Siemon, B., A.V. Christiansen, and E. Auken. 2009. A review of helicopter-borne electromagnetic methods for groundwater exploration. *Near Surface Geophysics* 7: 629-646.
- Siemon, B., and A. Steuer. 2011. Airborne geophysical investigation of groundwater resources in northern Sumatra after the tsunami of 2004. In *The tsunami threat – research and technology*, ed N.-A. Mörner, 575-594. InTech, Rijeka, ISBN 978-953-307-552-5.
- Siemon, B., A. Steuer, A. Ullmann, M. Vasterling, and W. Voß. 2011. Application of frequency-domain helicopter-borne electromagnetics for groundwater exploration in urban areas. *Journal of Physics and Chemistry of the Earth* 36: 1373-1385.
- Siemon, B., H. Wiederhold, A. Steuer, M.P. Miensopust, W. Voß, M. Ibs-von Seht, and U. Meyer. 2014. Helicopter-borne electromagnetic surveys in Northern Germany. In Proceedings of the 23rd Salt Water Intrusion Meeting, Husum, Germany.
- Steuer, A., B. Siemon, U. Meyer, and H. Wiederhold. 2014. Helicopter-borne electromagnetics: A powerful tool for the mapping of coastal aquifers. In Proceedings of the 23rd Salt Water Intrusion Meeting, Husum, Germany.

Contact Information: Bernhard Siemon, Federal Institute for Geosciences and Natural Resources, Department Groundwater and Soil Science, Stilleweg 2, 30655 Hannover, Germany, Phone: +49-511-6433488, Fax: +49-511-6433662, Email: bernhard.siemon@bgr.de

Helicopter-borne electromagnetic surveys in Northern Germany

Bernhard Siemon¹, Helga Wiederhold², Annika Steuer¹, Marion P. Miensopust¹, Wolfgang Voß¹, Malte Ibs-von Seht¹ and Uwe Meyer¹

¹Federal Institute for Geosciences and Natural Resources (BGR), Hannover, Germany

²Leibniz Institute for Applied Geophysics (LIAG), Hannover, Germany

ABSTRACT

For more than three decades BGR has conducted helicopter-borne geophysical surveys worldwide. Currently most of these surveys were flown in Northern Germany, where saltwater intrusion and clay mapping are the principal topics. Particularly airborne electromagnetics (AEM) is suitable for these mappings. Two helicopter-borne systems were used, a frequency-domain system (HEM) operated by BGR and a time-domain system (SkyTEM) developed at the university of Aarhus. The spatial conductivity distribution, which was derived from AEM data provides information on both lithology and water salinity.

INTRODUCTION

The airborne geophysical system operated by BGR for more than three decades enables simultaneous frequency-domain electromagnetic (HEM), magnetic and radiometric data acquisition. The project D-AERO, which is conducted by BGR in collaboration with State Geological Surveys of Germany and research institutes, merges existing airborne survey areas and appends new areas with respect to focusing on scientific and/or regional aspects. Several airborne geophysical surveys have been carried out by BGR in Northern Germany within the last two decades (Figure 1). In 2008-2009, LIAG supported these surveys by co-financing a number of BGR surveys and commissioning time-domain helicopter-borne electromagnetic surveys using the Danish SkyTEM system (Sørensen and Auken 2004). These systems were used to investigate the coastal areas of the North and Baltic Sea and some of the Frisian Islands (Wiederhold et al. 2010).

LIAG and BGR are building up a geophysics database (www.geophysics-database.de) which contains all airborne geophysical data sets. However, the more significant effort is to create a reference data set as basis for monitoring climate or man-made induced changes of the saltwater/freshwater interface at the German North Sea coast. The significance of problems for groundwater extraction and treatment caused by groundwater salinization is increasing and particularly coastal areas are affected by a latent risk for the sustainable usage of aquifers.

METHODS

The electromagnetic systems (DIGHEM, RESOLVE) operated by BGR are towed by a helicopter on parallel flight lines about 30–40 m above ground level. The processed HEM data are converted to half-space parameters, which are used to define individual multi-layer starting models at each data point for an iterative Marquardt-Levenberg inversion procedure (Steuer et al. 2014). The HEM inversion results are displayed as (apparent) resistivity maps and vertical resistivity sections (VRS) showing the 1D resistivity models along a survey profile with respect to the topographic relief (in m above mean sea level). As man-made effects caused by power lines, railway tracks, highways or urban areas are able to distort

nearby HEM measurements, these data have to be corrected (Siemon et al. 2011). Similarly, the processed time-domain data are converted to resistivity models (Viezzoli et al. 2008). Both systems as well as processing and interpretation schemes are described in detail by Siemon et al. (2009) and Steuer et al. (2009).

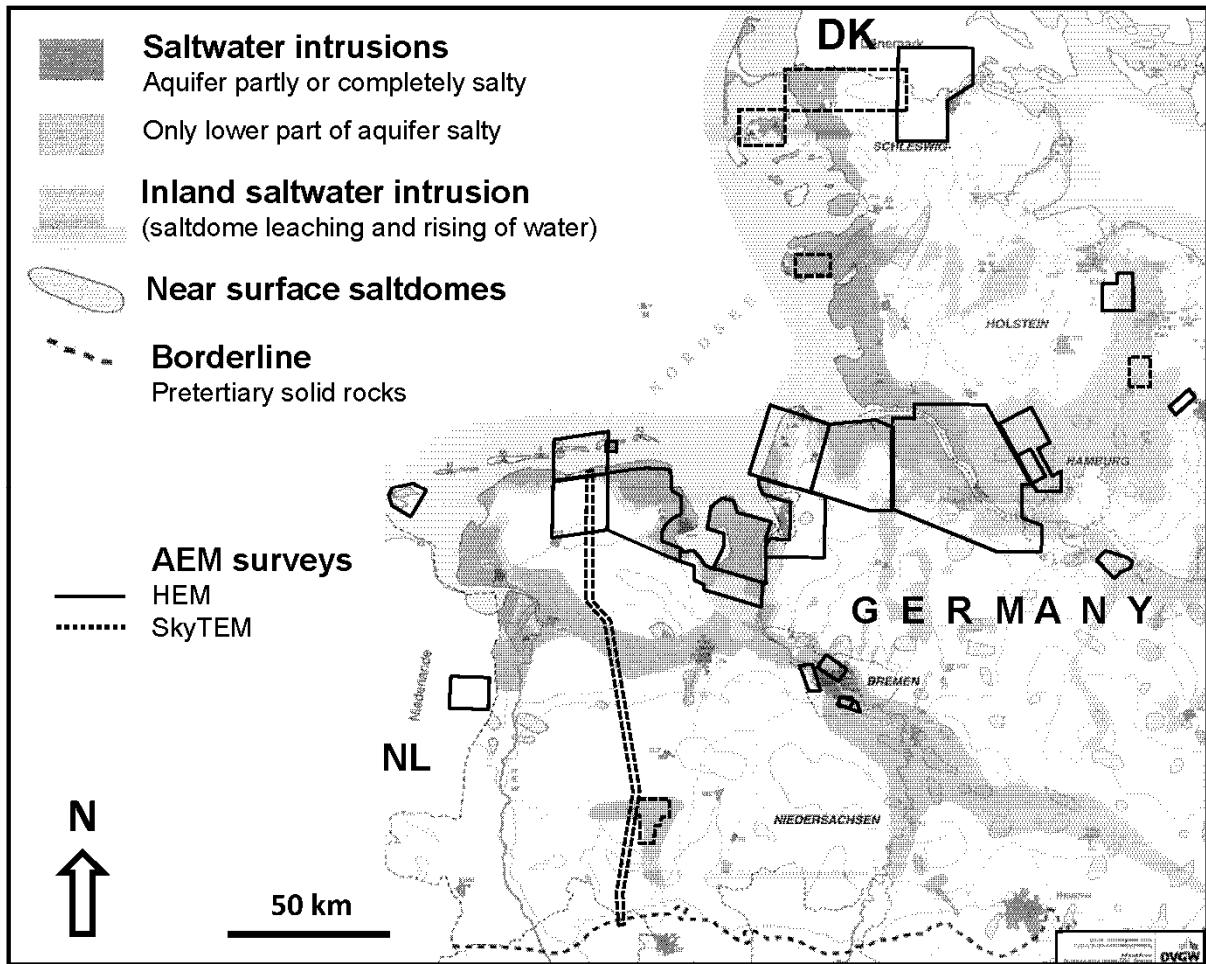


Figure 1. HEM surveys in Northern Germany. Background map: Groundwater salinization (modified after Grube et al., 2000).

RESULTS

Resistivities at a depth of 15 m bsl (below sea level) derived from 1D inversion are displayed on the map of Figure 2. Low resistivities ($\rho < 0.5 \Omega\text{m}$ or $\rho < 3 \Omega\text{m}$) clearly outline areas of saltwater or saltwater intrusion, respectively. High resistivities $\rho > 50 \Omega\text{m}$ indicate freshwater saturated sandy sediments. The resistivities in-between are typical for clayey sediments. Due to the sensitivity to the lithology and water salinity, rather low resistivities ($\rho = 3\text{-}10 \Omega\text{m}$) could also represent sandy sediments saturated with brackish water.

Comparison with Figure 1 demonstrates that the low resistivities derived from AEM data are suitable for mapping areas of the saltwater intrusion in great detail along the coast (Siemon et al. 2014) and inland (Klimke et al. 2013). Furthermore, AEM enables spatial mapping of freshwater lenses on islands (Burschil et al. 2012; Sulzbacher et al. 2012) and shallow submarine freshwater outlets (Rodemann et al. 2005). As AEM is also suitable for clay vs.

sand mapping (Siemon et al. 2014), buried tunnel valley can be outlined if the channel fill, e.g. clay, differs from the host material, e.g. sand (Eberle and Siemon 2006).

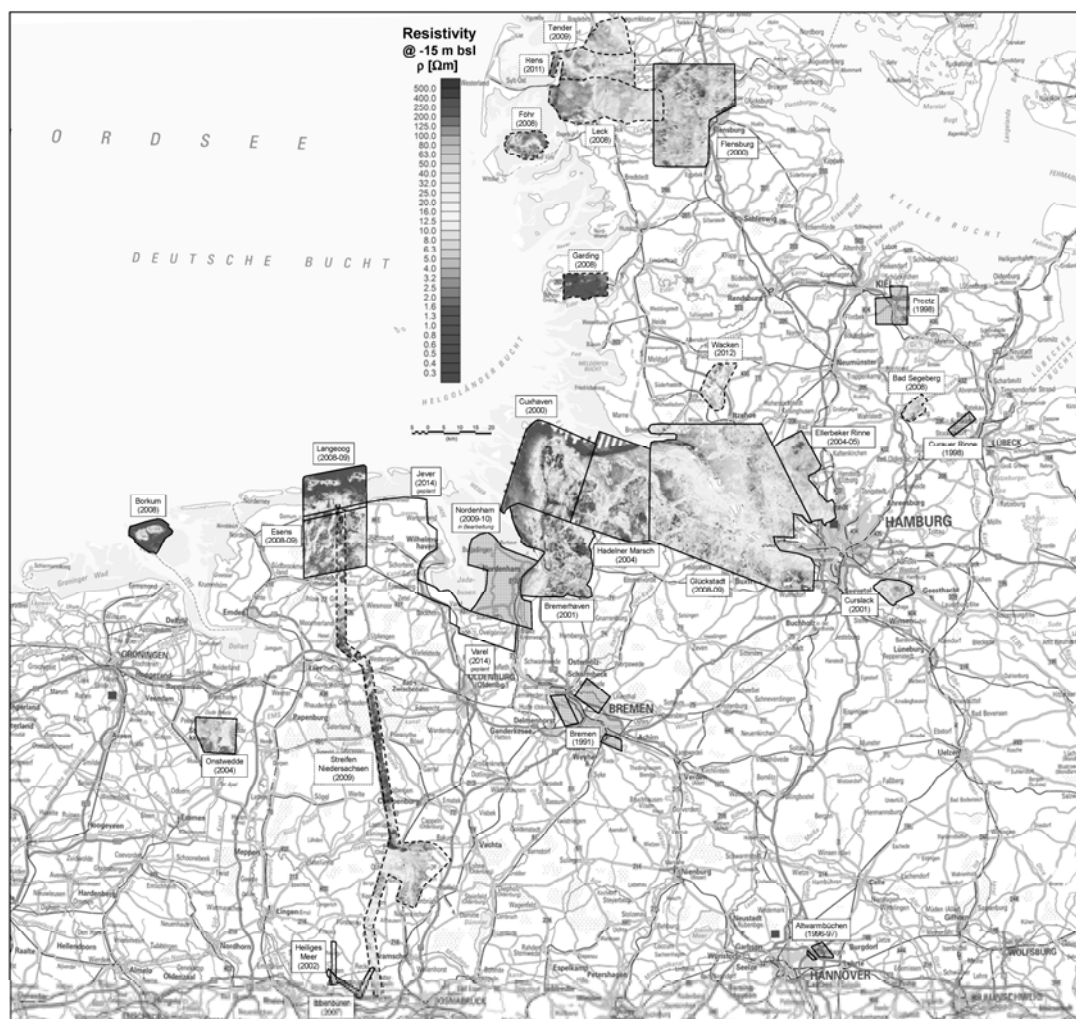


Figure 2. Resistivities at 15 m bsl derived from HEM (solid frames) and SkyTEM (dashed frames) data are plotted on a topographic map (BKG 2014).

DISCUSSION AND CONCLUSIONS

Airborne geophysical methods enable economic and ecological mapping of subsurface natural resources. Besides groundwater and mineral exploration the investigation of non-mineral resources is an important task. Electromagnetic methods are able to map lithological units if these are correlated with electrical conductivity. Particularly resistive sands and gravels can be distinguished from conductive clayey materials as well as freshwater from saltwater.

REFERENCES

BKG. 2014. Digitale Topographische Karte 1:1 000 000 (DTK1000): Geobasisdaten © BKG 2014. Map accessed at 20 February 2014 at <http://www.bkg.bund.de/>.

Burschil, T., W. Scheer, R. Kirsch, and H. Wiederhold. 2012. Hydrogeological characterisation of a glacially affected barrier island – the North Frisian Island of Föhr. *Hydrology and Earth System Sciences* 16: 3485-3498.

Eberle, D.G., and B. Siemon. 2006. Identification of buried valley using the BGR helicopter-borne geophysical system. *Near Surface Geophysics* 4, no. 2: 125-133.

Grube, A., K. Wichmann, L. Hahn, and K. H. Nachtigall. 2000. Geogene Grundwasserversalzung in den Poren-Grundwasserleitern Norddeutschlands und ihre Bedeutung für die Wasserwirtschaft: TZW (Technologiezentrum Wasser) Schriftenreihe 9.

Klimke, J., H. Wiederhold, J. Winsemann, G. Ertl, and J. Elbracht. 2013. Three-dimensional mapping of Quaternary sediments improved by airborne electromagnetics in the case of the Quakenbrück Basin, Northern Germany. *Zeitschrift der Deutschen Gesellschaft für Geowissenschaften* 164: 369-384.

Rodemann, H., E. Brost, J. Schünemann, U. Noell, B. Siemon, and F. Binot. 2005. Gleichstromgeoelektrische Untersuchungen eines mit aéroelektromagnetischen Messungen kartierten Süßwasservorkommens im Sahlenburger Watt unter Berücksichtigung von Äquivalenzfällen und 2D/3D-Modellrechnungen. *Zeitschrift für angewandte Geologie* 1/2005: 43-51.

Siemon, B., A.V. Christiansen, and E. Auken. 2009. A review of helicopter-borne electromagnetic methods for groundwater exploration. *Near Surface Geophysics* 7: 629-646.

Siemon, B., A. Steuer, A. Ullmann, M. Vasterling, and W. Voß. 2011. Application of frequency-domain helicopter-borne electromagnetics for groundwater exploration in urban areas. *Journal of Physics and Chemistry of the Earth* 36: 1373-1385.

Sørensen, K.I., and E. Auken. 2004. SkyTEM - a new high-resolution helicopter transient electromagnetic system: *Exploration Geophysics* 35: 191-199.

Steuer, A., B. Siemon, and E. Auken. 2009. A comparison of helicopter-borne electromagnetics in frequency and time-domain at the Cuxhaven valley in Northern Germany. *Journal of Applied Geophysics* 67: 194-205.

Siemon, B., W. Voß, J. Elbracht, N. Deus, and H. Wiederhold. 2014. Airborne clay mapping at the East Frisian coast. In *Proceedings of the 23rd Salt Water Intrusion Meeting, Husum, Germany*.

Steuer, A., B. Siemon, U. Meyer, and H. Wiederhold. 2014. Helicopter-borne electromagnetics: A powerful tool for the mapping of coastal aquifers. In *Proceedings of the 23rd Salt Water Intrusion Meeting, Husum, Germany*.

Sulzbacher, H., H. Wiederhold, B. Siemon, M. Grinat, J. Igel, T. Burschil, T. Günther, and K. Hinsby. 2012. Numerical modelling of climate change impacts on freshwater lenses on the North Sea Island of Borkum using hydrological and geophysical methods. *Hydrology and Earth System Sciences* 16: 3621-3663.

Viezzoli, A., A.V. Christiansen, E. Auken, and K.I. Sørensen. 2008. Quasi-3D-modeling of airborne TEM data by Spatially Constrained Inversion: *Geophysics* 73: F105-F113.

Wiederhold, H., B. Siemon, A. Steuer, G. Schaumann, U. Meyer, F. Binot, and K. Kühne. 2010. Coastal aquifers and saltwater intrusions in focus of airborne electromagnetic surveys in Northern Germany. In *Proceedings of the 21th Salt Water Intrusion Meeting, S. Miguel, Azores, Portugal*.

Contact Information: Bernhard Siemon, Federal Institute for Geosciences and Natural Resources, Department Groundwater and Soil Science, Stilleweg 2, 30655 Hannover, Germany, Phone: +49-511-6433488, Fax: +49-511-6433662, Email: bernhard.siemon@bgr.de

Geochemical and isotopic evidence of the aquifer-lagoon interaction during Holocene (Almería, SE Spain)

Fernando Sola¹, Ángela Vallejos¹, Linda Daniele^{2,3} & Antonio Pulido-Bosch¹

¹Water Resources and Environmental Geology – University of Almería, Spain

²Department of Geology – FCFM – University of Chile, Chile

³Andean Geothermal Center of Excellence (CEGA), Fondap-Conicyt, Chile

ABSTRACT

Variations in sea level along the Quaternary have affected both the piezometric level and the position of the mixing zone in coastal aquifers throughout the world. At the end of the Last Glacial, these salts have been washed, although in confined or low-permeability coastal aquifers part of the saline water can be retained. The study area corresponds to the small coastal aquifer of Cabo de Gata, which has surface area of only 16 km², located in south-eastern Spain. It is a multi-layer aquifer, formed by Plio-quaternary sands and conglomerates, which means that the unconfined aquifer becomes semi-confined towards its base, comprises Pliocene silts lying at 80 m depth. The hydrogeochemical characteristics of this aquifer were studied in an attempt to explain the anomalous salinity of its groundwater; in some cases the salinity exceeds that of seawater. Two groups of water have been identified. Group 1 is represented in the upper part of the aquifer (samples taken in the top 30 m of the aquifer), where the proportion of seawater, calculated with its ¹⁸O concentration, varies between 10-60%, while waters identified as Group 2, taken from the lower part of the aquifer, contain 60-70% seawater. In addition, hydrogeochemical modelling was applied, which reveals that the waters have been subject to evaporation between 25-35%. There was good agreement between the modelled results and the observed water chemistry. For SO₄, the results of the modelling were not optimal. The aquifer has suffered antropogenic pollution from the intense agricultural activity in the area, which contributes an additional source of SO₄.

The rates of evaporation modelled would imply that the water corresponding to Group G2 was, at some point in the past, surface water. This evaporation would have occurred during the Holocene, in a coastal lagoon environment. Sediments characteristic of this type of environment have been identified in this location; this lagoon would have been active between 8 and 3 kyr BP. The hydrogeochemical and isotopic results have allowed to identify this lagoon and reconstruct its interaction with the aquifer.

Contact Information: Fernando Sola, Water Resources and Environmental Geology. University of Almería. 04120 Almería, SPAIN, Phone: 34-950-015-874, Email: fesola@ual.es

Evidence of Pleistocene submarine discharges in the Aguadulce cliffs (Almería, SE Spain)

Fernando Sola¹, Ángela Vallejos¹, Jorge Currás², Linda Daniele^{3,4} & Antonio Pulido-Bosch¹

¹Water Resources and Environmental Geology – University of Almería, Spain

²IES Albaida – Almería, Spain

³Department of Geology – FCFM – University of Chile, Chile

⁴Andean Geothermal Center of Excellence (CEGA), Fondap-Conicyt, Chile

ABSTRACT

Submarine Groundwater Discharge (SGD) can be defined as the flow of water through continental margins from the seabed into the ocean. In the discharge area, the mixture of continental freshwater and marine saltwater, with very different properties, favours that a wide variety of physical and chemical processes occurs. Although the studies examining these processes in current mixing zones are common, there are few studies investigating the influence of these processes in the fossil record. The proposed criteria for recognizing these mixing zones in the sedimentary record are (Baceta et al., 2001): (1) the existence of evidences that materials have been under the phreatic surface, (2) development of porosity by dissolution, (3) formation of sulfides or oxides precipitates as indicators of different redox conditions, and (4) evidence of an alternation between dissolution and precipitation of carbonates. The town of Aguadulce (Almería, SE Spain), is named Aguadulce - freshwater in Spanish – due to the historical submarine groundwater discharges in this area, which disappeared due to overexploitation of the aquifer from the 60s. In this work, a cliff located just above those ancient springs is studied. The observations have been made in a band at the height of 30 - 40 m above sea level, in which a strong rock dissolution that can overcome 60 % is observed. Dissolution surfaces are impregnated by manganese oxides, on which grow precipitates of calcite, dolomite and finally, aragonite crystals, indicators of changes in the redox conditions and the saturation index of carbonates over time. All this karst development is beneath a Pleistocene marine terrace located 40 m a.s.l., and it is interpreted as dissolution reactions and mineral precipitation occurred in a zone of freshwater-seawater mixing during the Pleistocene.

Contact Information: Fernando Sola, Water Resources and Environmental Geology. University of Almería. 04120 Almería, SPAIN, Phone: 34-950-015-874, Email: fesola@ual.es

Coupled hydrogeophysical inversion on synthetic example of seawater intrusion

Eldad Haber^{1,2}, Klara Steklova¹

¹ Earth and Ocean Sciences, The University of British Columbia, Vancouver, BC, Canada

² Mathematics, The University of British Columbia, Vancouver, BC, Canada.

ABSTRACT

Seawater intrusion (SWI) is a complex process, where 3D modeling is often necessary in order to monitor and manage the effected aquifers. Unfortunately obtaining good quality groundwater data to support these models is difficult. Geophysics has become a common tool in the last two decades to supplement the lack of groundwater (GW) data. Geophysical methods are nonintrusive and less costly compared to standard drilling and offer an attractive alternative. Combining these two different sources of data, however, is still subject of ongoing investigation. One of the caveats is the different scales of geophysical and groundwater models, as well as the empirical petrophysical relationships that relate geophysical and groundwater states. Solving the parameter estimation problem in this field adds even more complexity, and careful analysis of the potential and the limitations of such an inverse problem should therefore precede the collection of field data.

We used Matlab to develop a 3D groundwater model for variable density flow, which is based on discretized flow and solute mass balance equations. In conjunction with the GW model, a geophysical model was developed for 3D electromagnetic (EM) modeling and inversion in the time domain. Having both models in the same environment gives space to implementing different coupling concepts.

Depending on the tightness of coupling between the two models in the inversion framework the approaches go from fully coupled framework to uncoupled approach, where the latter one was a focus of this work. With our models we can evaluate both sources of data at the same time, as well as within the inversion algorithms. In order to test the different coupling concepts for estimating the seawater intrusion process we started with a numerical test on a synthetic example. Seawater intrusion was simulated with our groundwater model code, for the geophysical application we use a time domain EM system with a loop source and receivers on surface. In our coupled framework the estimates of initial solute distribution served as a reference model for EM inversion and vice versa.

INTRODUCTION

The terminology differs among authors, usually as uncoupled inversion is meant inversion where geophysics and hydrogeology stay independent. Geophysical data are inverted to estimate the spatial distribution of some property, the outcomes are then converted with some petrophysical relationship, and then used as input data for the groundwater models. This is sometimes referred to as a sequential hydrogeophysical inversion. The big plus of this approach is that hydrogeological and geophysical models run independently, the disadvantage is that the geophysical inverse problem needs a regularization term, and therefore *a priori* information has to be entered in a form of smoother or a reference model.

By coupled approach we consider the framework where the geophysical and groundwater models are linked together during the inversion. For example, the GW model is often used as a form of regularization, providing realistic models for geophysical inversion. An example of field study with this approach is in Bauer-Gottwein (2009). In Herckenrath (2013) they further distinguish joint hydrogeophysical inversion when groundwater and geophysical model are simultaneously inverted.

In the following synthetic experiment we create a seawater intrusion scenario, with some propagation of saltwater front between time t_0 and t_1 . In the inverse problem we then want to estimate previous solute fraction (at time t_0) using coupled framework with both sources of data, GW well data and time t_1 , and EM data from t_0 .

METHODS

Numerical models

A 3D groundwater model developed in Matlab is based on discretized flow and solute mass balance equations. Finite difference scheme was used for the pressure equation and Semi-Lagrangian method for solute transport equation. This enables us to choose an arbitrarily large time step without losing stability (up to some accuracy requirement) due to the coupled character of governing equations. We assumed steady state for groundwater flow; however the GW flow equation still has to be resolved throughout the computation to update the pressure and velocity field as a result of solute content dynamic. For the state equations the density dependency is considered in a linear form, and the viscosity is kept constant, not dependent on solute fraction or temperature. Both governing partial differential equations were discretized on a 3D staggered grid.

We derive analytical sensitivities of actual solute mass with respect to initial solute fraction and permeability based on the discretized governing equations. Analytically derived sensitivities not only reduce the computations cost of an inverse problem, but also give insight for maximizing information in collected data.

The geophysical model is based on the Maxwell's equations in the time domain; the quasi-static approximation can be used due to shutting of the source initially, and assuming low permittivity and small changes for electric field. The change of magnetic field was measured at given time steps for all receivers, which provides the geophysical data. The geophysical model is also discretized on a staggered grid, but has to be solved on a larger padded grid compared to groundwater model due to no flow boundaries of the EM model.

Archie's law was used for converting the solute fraction values to conductivity, assuming the knowledge of its parameters and that the bulk conductivity is affected only by electrolytic conductivity of water in the porous matrix and the surface conductivity of porous material is negligible. This or any other empirically based connection can be used for this inner coupling between the two models and enables anytime switch between the solute fraction and soil bulk conductivity in the idealized case. Generally the Archie's law parameters are unknown but we can afford this luxury due to synthetic example setup.

Inversion

Both inverse EM and GW model were solved with a Gauss - Newton method. Since both inverse problems are ill-posed regularization has to be added. The objective function is:

$$\phi(m) = \phi_d + \beta\phi_m = \frac{1}{2} \|Q(d(m) - d_{obs})\|^2 + \frac{1}{2}\tau \|m - m_{ref}\|^2 + \frac{1}{2}\beta \sum_i \|G_{x_i}(m - m_{ref})\|^2$$

The m in EM model is soil bulk conductivity, in GW model is the solute fraction (saltwater content). The regularization parameters β and τ differs in each model as well as the data projection matrix Q . The weights of gradients (G_{x_i}) in the regularization term are favoring the expected direction of groundwater flow in both models.

RESULTS

To set up the seawater intrusion synthetic experiment, we chose GW boundary conditions corresponding to simple Henry problem setup with heterogeneous permeability field and a pumping well. We run the model with a different parameter setup up to time t_0 , which became an initial “unknown” solute content ω_0 . The groundwater model then goes from time t_0 to a final state at time t_1 , giving the “true” solute content ω_0 and ω_1 . Two transects of few wells is placed along the flow direction in the east and west part of the domain and solute fractions are “measured” in some depth intervals at time t_1 (43 observation points). Next to that EM imaging was done at time t_1 with a large loop source in the center and receivers placed uniformly and densely on the surface over the area of interest (33 x 33 receivers).

Coupled inversion starts with EM inversion, the estimate of bulk conductivity at t_1 is transferred via Archie’s law into ω_1 , and serve as additional data for GW inversion with smaller weight and only in some data points across the area.

GW inversion then runs with this extra data and final estimate is again transformed into soil bulk conductivity via Archie’s law to serve as a reference model for the next EM inversion. The result of the EM inversion is then again an entry model for the GW inversion. This loop cycle can keep going as long as the estimate of initial/final solute fraction changes. In Fig.1 you can see the scheme. At the end we have an estimate of solute fraction ω_1 and bulk conductivity σ_1 at time t_1 as well as groundwater estimate of ω_0 at time t_0 . Since this is a synthetic experiment we can also record the actual errors and not only the data misfit.

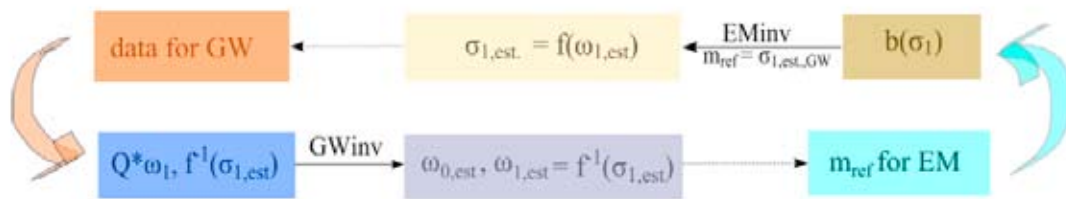


Figure 1. The coupled scheme used for inversion

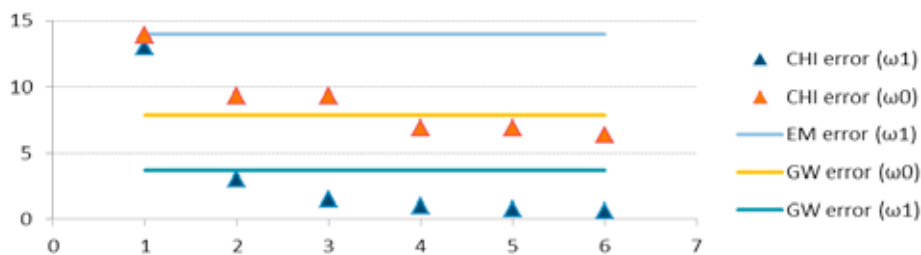


Figure 2. The actual error and data misfit decrease

After 3 runs of both GW and EM inversion we obtained estimate of the saltwater distribution at time t_1 as it can be seen in Fig.3 (also the uncoupled GW inversion result). Fig.2 shows the decrease of the actual error in the estimate of ω_0 and ω_1 as well as the error of $\omega_{0/1}$ when only uncoupled inversion is applied.

CONCLUSIONS

The coupled inversion gave visually the best estimate of saltwater front shape and also produced the best actual error compared to poorly constrained EM or GW inversions. Adding more GW data makes the difference in the initial estimates smaller, in these cases we could say we have enough information in the GW model and the geophysical model can therefore just confirm its validity. We can expect similar results once the joint inversion is implemented, where weighting between the two data sets will probably have a strong effect on the final result.

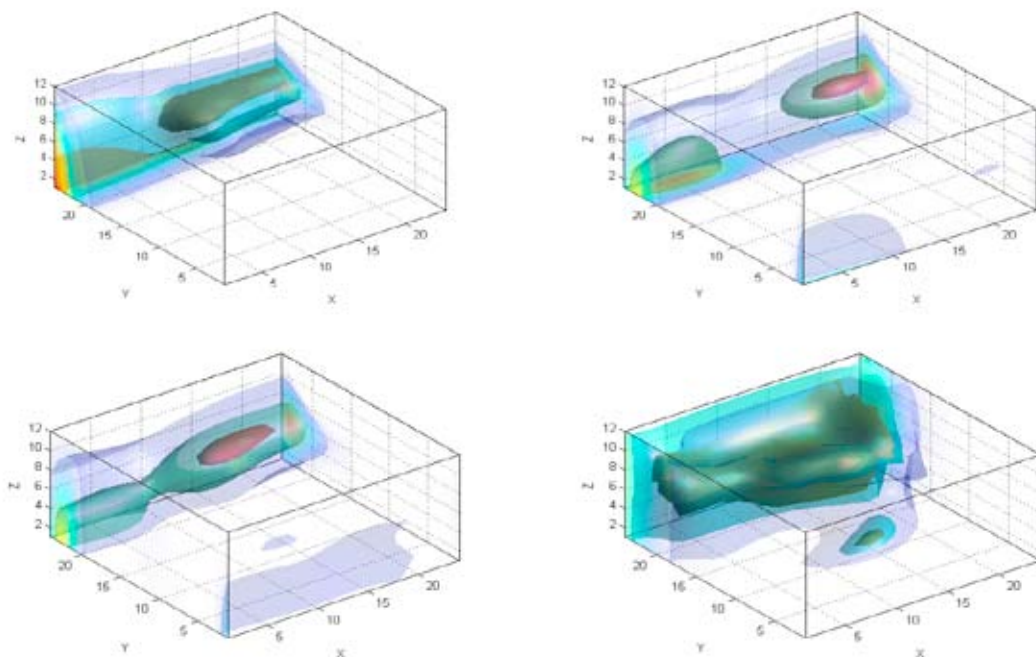


Figure 3. Upper left: the true initial seawater front shape ω_0 ; upper right: the estimate of ω_0 based solely on GW model; left bottom: the result of hydrogeophysical inversion for ω_0 ; right bottom: EM inversion only for ω_1 . The level sets of solute fraction: $\omega = 0.1, 0.4$ and 0.7 are displayed (red - 0.7 down to light blue - 0.1).

REFERENCES

- D. Herckenrath, G. Fiandaca, E. Auken, P. Bauer-Gottwein 2013. Sequential and joint hydrogeophysical inversion using a field-scale groundwater model with ERT and TDEM data. Hydrology and Earth System Sciences, Discussions
- P. Bauer-Gottwein, B. N. Gondwe, L. Christiansena, D. Herckenrath, L. Kgotlhangb, S. Zimmermann 2009. Hydrogeophysical exploration of three-dimensional salinity anomalies with the time-domain electromagnetic method (TDEM). Journal of Hydrology, Volume 380, Issue 3 – 4

Contact Information: Klara Steklova, Earth and Ocean Sciences, The University of British Columbia, Vancouver, BC, Canada, Phone: 778-829-5527, Email: ksteklova@ubc.eos.ca

Helicopter-borne electromagnetics: A powerful tool for the mapping of coastal aquifers

Annika Steuer¹, Bernhard Siemon¹, Uwe Meyer¹ and Helga Wiederhold²

¹Federal Institute for Geosciences and Natural Resources (BGR), Hannover, Germany

²Leibniz Institute for Applied Geophysics (LIAG), Hannover, Germany

ABSTRACT

In recent years airborne geophysical methods have turned out to have great potential in delineating subsurface information down to some hundred metres depth. This information is essential for planning purposes for manifold geoscientific, economic or environmental questions, like, e.g., utilization and protection of freshwater resources, land utilization or industrial planning. These data integrated into a three-dimensional geographic information system provide a perfect tool for spatial planning. Beside the geologic or geophysical basic information also changes of surface and subsurface data in time and space may be documented by repeated surveys. Here, a methodical introduction to helicopter-borne electromagnetics (HEM) is given and the advance of HEM in mapping of coastal aquifers is shown. Emphasis is placed on the mapping of freshwater-saltwater interfaces, saltwater intrusions, submarine freshwater outlets as well as on the mapping of clay occurrences.

INTRODUCTION

The problem of groundwater salinization is becoming more important within the context of groundwater extraction and treatment, and is a latent risk for the sustainable use of aquifers. The intrusion of seawater is a natural source of coastal groundwater salinization. Onshore salinization is attributable to the leaching of salt domes close to the earth's surface and the upwelling of deep saline water. These natural sources of salinization are exacerbated by man-made hydraulic activities such as groundwater extraction and drainage systems. Further risks are the long-term rise in sea level, storm floods, and – in some areas – flooding caused by tsunamis. These events will also have an impact on the distribution of saltwater in the subsurface and can also jeopardise aquifers used to produce potable water.

Airborne geophysical surveys enable huge areas to be surveyed almost completely in a relatively short time at economic cost. The results can generally be used for geological and hydrogeological mapping. Particular the data collected by airborne electromagnetic surveys is very important for hydrogeological interpretation as the derived electrical conductivities respond to both lithological and water-chemistry variations down to depths of the upper hundred metres (Siemon et al. 2009; Steuer et al. 2009).

METHODS

The helicopter-borne electromagnetic system

The electromagnetic system operated at BGR is a RESOLVE system consisting of six transmitter-receiver coil pairs. The electromagnetic sensors are installed in a 10 m long tube, which is towed by a Sikorsky S-76B helicopter on parallel flight lines at about 30–40 m above ground level (Figure 1).

The transmitter signals, the primary magnetic fields, induce eddy currents into the subsurface which depend on the electrical conductivity distribution. The relative secondary magnetic

fields from these induced currents are measured at the receiver coils in parts per million (ppm) as they are related to the primary fields. The use of different frequencies ranging from 387 Hz to 133 kHz enables investigation of different depths: High frequencies resolve the shallower parts of the subsurface and lower frequencies the deeper parts. The depth of investigation also depends on the subsurface conductivity distribution: The higher the conductivity the lower the penetration of the electromagnetic fields into the subsurface. Typical maximum investigation depths of the RESOLVE system range from about 30 m (saltwater saturated sediments) to about 150 m (freshwater saturated sandy sediments or hard rock).

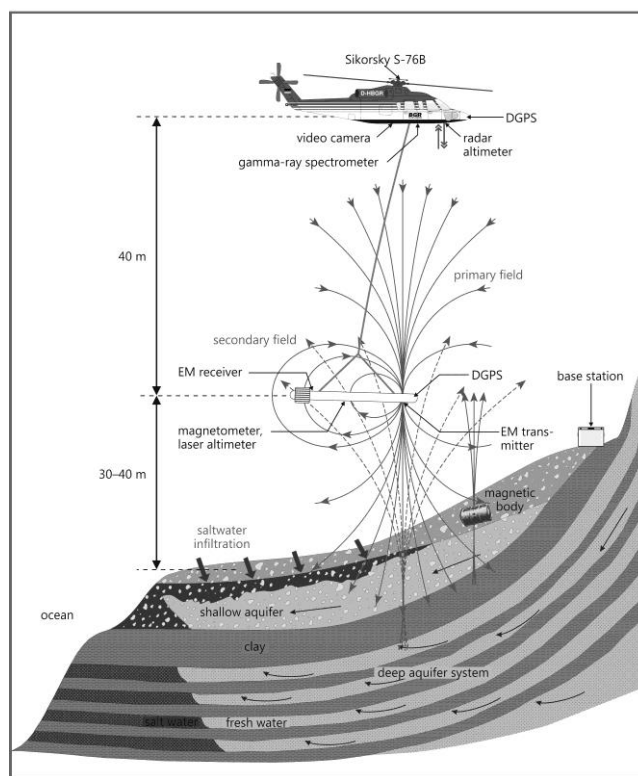


Figure 1. BGR helicopter-borne geophysical system and typical hydrogeological situation at a coast.

Modelling of the electromagnetic data

In the standard analysis, the in-phase (I) and quadrature (Q) components of the measured secondary magnetic fields are converted into resistivities (inverse of electrical conductivity) based on half-space models. Apparent resistivity ρ_a [Ωm] and centroid depth z^* [m] of a homogeneous half-space (Figure 2, Model 1) are derived from the data of each single frequency (f). The resulting sounding curves, $\rho_a(z^*)$, provide the initial approximation of the vertical resistivity distribution. They are used to derive appropriate starting models for the one-dimensional (1D) inversion. A Marquardt–Levenberg inversion procedure iteratively calculates the model parameters, resistivity ρ and thickness d of the model layers (Figure 2, Model 2), from the data of all frequencies available. The inversion procedure stops when a given threshold (e.g. 10%) is reached, which is defined as the differential fit of modelled and measured HEM data. Another approach is to use many layers with fixed thicknesses as starting model for a smooth inversion what results in more continuous intersections between geological units.

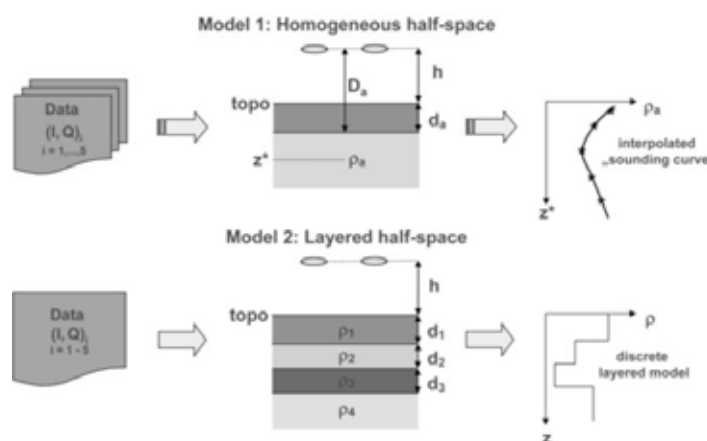


Figure 2. HEM inversion scheme based on the model of a homogeneous half-space and of a layered half-space model (Siemon and Steuer 2011).

Advanced analysis is optional and includes a priori information, e.g. borehole data, conductivities of water samples or results of other geophysical measurements, and/or constrained inversion (Gunnink et al. 2012). A further step is the integration of resistivity models into a geological or hydrogeological model and vice versa. The results of the 1D inversion are generally presented as vertical resistivity sections (VRS), resistivity and thickness/depth maps.

MAPPING OF COASTAL AQUIFERS

BGR initiated an airborne geophysical mapping project (D-AERO) in 2007, supported by LIAG for two years, in order to investigate coastal aquifers in Northern Germany (Siemon et al. 2014a). Exemplarily, Figure 3 shows some HEM applications.

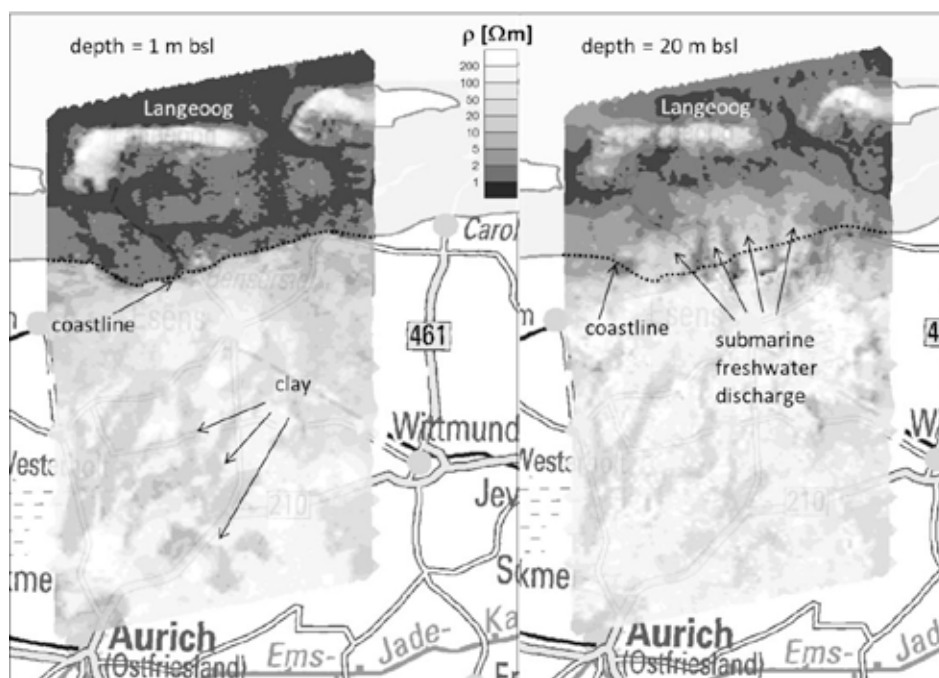


Figure 3. HEM resistivity maps at 1 and 20 m bsl plotted on a topographic map (BKG 2014). Dark colours indicate conductive areas, like saltwater. White colours indicate more resistive areas, like freshwater saturated sandy sediments.

The resistivity map at 1 m depth below sea level (bsl) clearly shows the freshwater-saltwater interface at the North Sea island of Langeoog and along the coastline. The clay distributions mapped onshore are discussed in more detail by Siemon et al. (2014b). At 20 m bsl, however, the freshwater-saltwater interface at the coast appears rather inhomogeneous. The finger-shaped interface indicates submarine freshwater discharge to the North Sea. The freshwater lens of the island of Langeoog is still present, but less extended.

DISCUSSION AND CONCLUSIONS

Mapping of coastal aquifers using HEM comprises mapping of freshwater-saltwater interfaces to outline saltwater intrusions and submarine freshwater occurrences, as well as mapping of clay distributions to estimate the vulnerability of the groundwater to pollution and to outline potential flow paths. HEM resistivity models are often used as base for further geophysical investigation (e.g. Costabel et al. 2014) or for hydrogeological modelling (e.g. Deus and Elbracht 2014). Therefore, HEM results are imported into a geographical information system (www.geophysics-database.de) which provides the data and the models.

REFERENCES

- BKG. 2014. Digitale Topographische Karte 1:1 000 000 (DTK1000): Geobasisdaten © BKG 2014. Map accessed at 20 February 2014 at <http://www.bkg.bund.de/>.
- Costabel, S., U. Noell, T. Günther, G. Houben, W. Voß, and B. Siemon. 2014. Geophysical investigation of a managed freshwater lens on the North Sea island of Langeoog. In Proceedings of the 23rd Salt Water Intrusion Meeting, Husum, Germany.
- Deus, N. and J. Elbracht. 2014. 3D-Modelling of the salt-/fresh water interface in coastal aquifers of Lower Saxony (Germany) based on airborne electromagnetic measurements (HEM). In Proceedings of the 23rd Salt Water Intrusion Meeting, Husum, Germany.
- Gunnink, J., J.H.A. Bosch, B. Siemon, B. Roth, and E. Auken. 2012. Combining ground-based and airborne EM through Artificial Neural Networks for modelling glacial till under saline groundwater conditions. *Hydrology and Earth System Sciences* 16: 3061-3074.
- Siemon, B., A.V. Christiansen, and E. Auken. 2009. A review of helicopter-borne electromagnetic methods for groundwater exploration. *Near Surface Geophysics*, 7: 563-580.
- Siemon, B., and A. Steuer. 2011. Airborne geophysical investigation of groundwater resources in northern Sumatra after the tsunami of 2004. In *The tsunami threat – research and technology*, ed N.-A. Mörner, 575-594. InTech, Rijeka, ISBN 978-953-307-552-5.
- Siemon, B., H. Wiederhold, A. Steuer, M. P. Miensopust, W. Voß, M. Ibs-von Seht, and U. Meyer. 2014a. Helicopter-borne electromagnetic surveys in Northern Germany. In Proceedings of the 23rd Salt Water Intrusion Meeting, Husum, Germany.
- Siemon, B., W. Voß, J. Elbracht, N. Deus, and H. Wiederhold. 2014b. Airborne clay mapping at the East Frisian coast. In Proceedings of the 23rd Salt Water Intrusion Meeting, Husum, Germany.
- Steuer, A., B. Siemon, and E. Auken. 2009. A comparison of helicopter-borne electromagnetics in frequency and time-domain at the Cuxhaven valley in Northern Germany. *Journal of Applied Geophysics* 67: 194-205.

Contact Information: Annika Steuer, Federal Institute for Geosciences and Natural Resources, Department Groundwater and Soil Science, Stilleweg 2, 30655 Hannover, Germany, Phone +49-511-6432148, Fax: +49-511-6433662, Email: annika.steuer@bgr.de

Comparison of numerical models using a two-dimensional benchmark of density-driven flow

Stoeckl, L.^{1,2}, Walther, M.³, Schneider, A.⁴, Yang, J.² and Graf, T.²

¹ Federal Institute for Geosciences and Natural Resources Germany (BGR)

² Institute of Fluid Mechanics in Civil Engineering, Leibniz University Hannover

³ Helmholtz Centre for Environmental Research (UFZ)

⁴ Gesellschaft für Anlagen- und Reaktorsicherheit mbH (GRS)

Keywords: freshwater lens, numerical modeling, benchmark, physical experiment

ABSTRACT

We compare five numerical models to a physical benchmark of density-driven flow of a freshwater lens. Freshwater flow paths, velocity and salinity distributions as well as the propagation of the saltwater-freshwater interface were observed and analyzed in detail. Steady-state as well as transient results reveal certain differences of the numerical models, even though the model settings and boundary conditions are kept as identical as possible.

INTRODUCTION

Today, a great variety of groundwater modeling software is available. Due to differences in structure, solver types and features implemented in the models, it is assumed that differences in modeling results should occur. We therefore investigate five numerical models capable of solving the partial differential equations of density-driven coupled flow and transport and compare them to a physical benchmark experiment. Describing the capabilities and revealing differences and limitations, as well as advantages of the different models, is the aim of this study.

METHODS

The test case used to compare the different codes is an artificially generated two-dimensional freshwater lens in a homogeneous sandy aquifer with horizontal and vertical extensions of approximately 80 cm and 30 cm, respectively. The benchmark is described in more detail in Stoeckl and Houben (2012), who used an acrylic glass box to simulate such a cross section of an infinite strip island. Salt water with a density of 1021 kg m^{-3} was injected, saturating the sand from bottom to top. Saltwater was continuously displaced by infiltrating freshwater at the top, developing a lens until equilibrium was reached. To visualize the flow pattern of the fresh water with a density of 997 kg m^{-3} , different fluorescent tracer dyes were added.

The models used for comparison are: *d3f* (Fein and Schneider 1999), *Feflow* (Diersch 2005), *HydroGeoSphere* (Therrien et al. 2007), *OpenGeoSys* (Kolditz et al. 20012), and *Spring* (König et al. 2012). To ensure the highest level of comparability for the numerical groundwater flow models, the setup is defined as similar as possible for all models, with identical temporal and spatial resolution (triangular grid with 241,400 elements and a constant time step size of 8.64 s). Additionally, the same boundary conditions and

parameters are used (Fig. 1). The output of each model is then converted into the same format and post-processed using the open-source program ParaView.

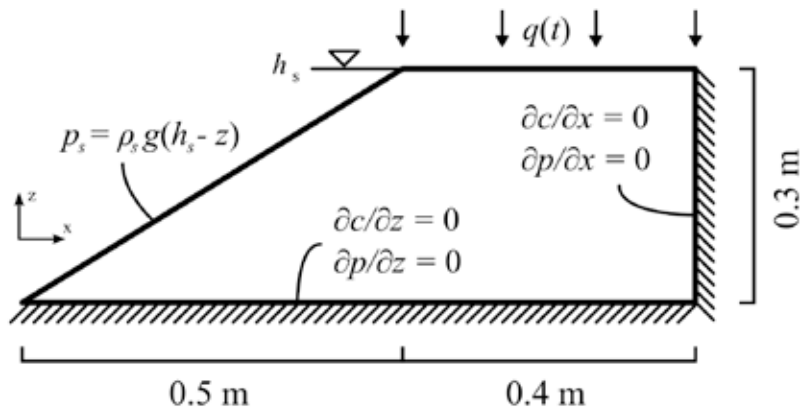


Figure 1: Sketch of model domain and boundary conditions used for the five different numerical models (Walther submitted, after Stoeckl and Houben 2012).

Table 1: Model geometry and parameters (based on Stoeckl and Houben 2012)

	acronym	value	unit
Model geometry			
Half width of island (top)	L	0.4	m
Bottom half width	B	0.9	m
Height of island	H	0.3	m
Number of elements (triangular)	-	241,400	-
Number of nodes	-	121,362	-
Measured parameters			
Hydraulic conductivity	K	$4.5 \cdot 10^{-3}$	$\text{m} \cdot \text{s}^{-1}$
Intrinsic permeability = $(K_f \cdot \mu) / (g \cdot \rho_f)$	k	$4.6 \cdot 10^{-10}$	m^2
Effective porosity	n_e	0.39	-
Density saltwater	ρ_s	1021	$\text{kg} \cdot \text{m}^{-3}$
Density freshwater	ρ_f	997	$\text{kg} \cdot \text{m}^{-3}$
Saltwater-freshwater ratio	a	0.02407	-
Salt concentration	c	1	-
Recharge rate	R	1.152	$\text{m} \cdot \text{d}^{-1}$
Estimated parameters			
Longitudinal dispersivity	α_L	$5 \cdot 10^{-3}$	m
Transversal dispersivity	α_T	$5 \cdot 10^{-4}$	m
Molecular diffusion	d	10^{-9}	$\text{m}^2 \cdot \text{s}^{-1}$
Specific storage (compressibility)	S_s	$1 \cdot 10^{-4}$	m^{-1}
Viscosity	μ	$1 \cdot 10^{-3}$	$\text{Pa} \cdot \text{s}$

RESULTS

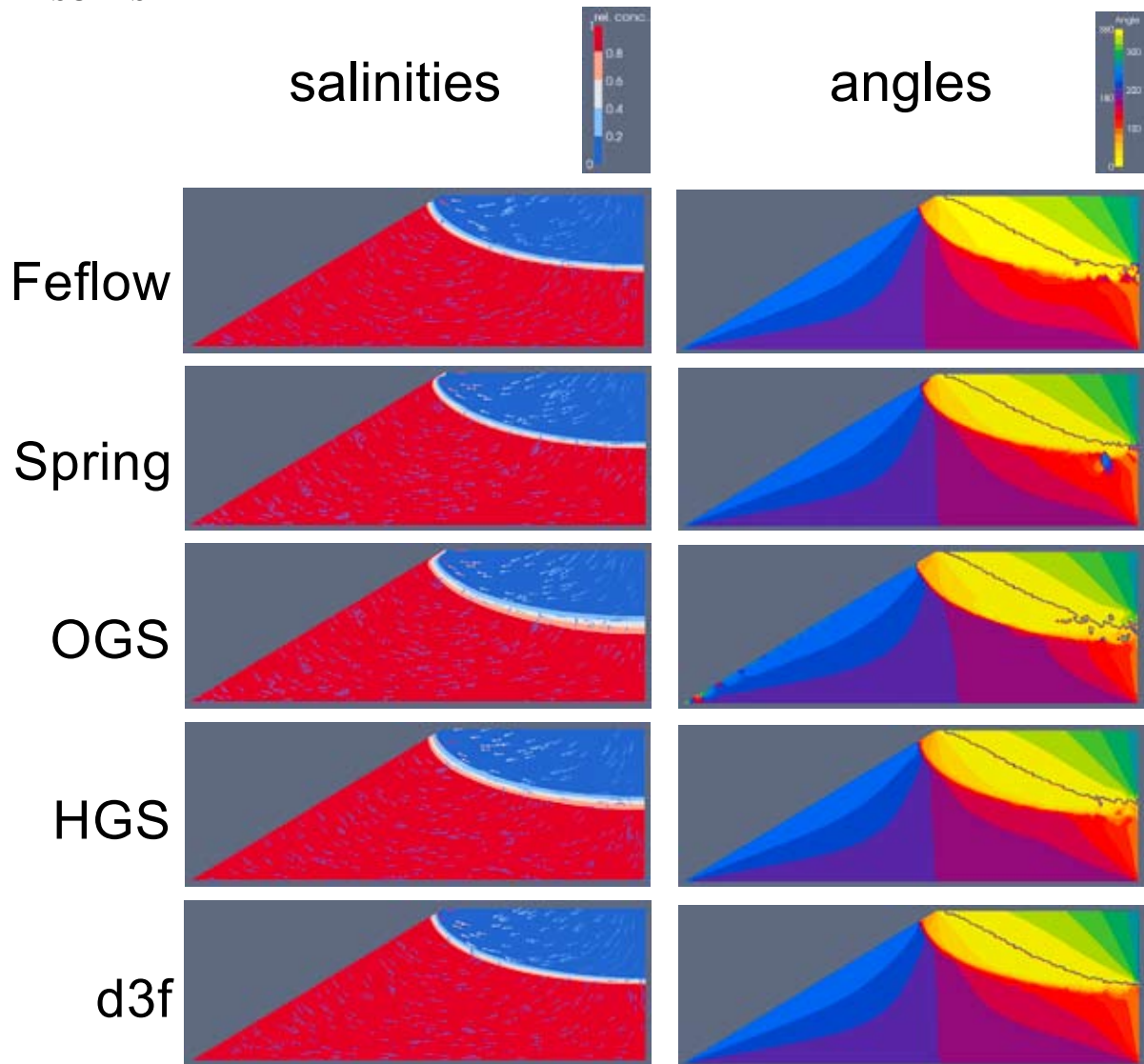


Figure 2: Steady-state simulation results for the five different models showing (left) salinity concentrations normalized to 1 (= seawater) and (right) angles of velocity vectors, clockwise from 0° (horizontal) to 360°.

Figure 2 demonstrates that the thickness of the saltwater-freshwater transition zone shows differences with thinner interfaces for Feflow, Spring and d3f. Spring and OpenGeoSys show an interface bended upwards at the outflow zone where the mass boundary condition at the slope cannot be disabled when water leaves the model domain. This is, however, a graphical artifact, as water is still exiting through this zone. The distribution of the angles of the velocity vectors shows a similar picture for all models (Fig. 2, right side). In Feflow and Spring slight deviations at the right boundary close to the interface are visible (darker spots) indicating a local disturbance. Results obtained for OpenGeoSys show local circulations at the slope.

Transient model results show small differences in the position of the saltwater-freshwater interface over time. Final interface depth positions at steady-state are also very similar at 14.5 cm b.s.w.l. with a deviation of ± 0.1 cm.

DISCUSSION AND CONCLUSIONS

Steady-state flow fields and concentration distributions, as well as the transient propagation of the interface at the centre of the island, are compared for five models. All models are capable of representing the benchmark of a developing freshwater lens reasonably well.

As expected, smaller deviations in the results exist as shown for e.g. the thickness of the transition zone or the alignment of the velocity vectors. Reasons for this behavior might be on the one hand program-specific techniques of solving the partial differential equations. On the other hand, the basic conditions are kept as similar as possible but not completely identical due to technical reasons (e.g. the implementation of a constraint turning off the mass-boundary condition).

REFERENCES

Diersch, H.-J.G., 2005. FEFLOW: Finite Element Subsurface Flow and Transport Simulation System WASY GmbH Institute for Water Resources Planning and Systems Research, Berlin, 292p.

Fein, E., Schneider, A. (eds.), 1999: d³f—Ein Programmpaket zur Modellierung von Dichteströmungen. FKZ-02 C 0465 379, final report. Gesellschaft für Anlagen- und Reaktorsicherheit (GRS) mbH, GRS-139, Braunschweig 1999.

König, C., Becker, M., Diehl, A., Rosen, B., Rüber, O., Seidel, T., Werth, B., Zimmermann, C., 2012. SPRING Benutzerhandbuch, Ausgabe 4.1, ISBN 978-3-00-040369-9; delta h Ingenieurgesellschaft mbH; Witten, Germany.

Kolditz, O., Bauer, S., Bilke, L., Böttcher, N., Delfs, J.O., Fischer, T., Görke, U.J., Kalbacher, T., Kosakowski, G., McDermott, C.I., Park, C.H., Radu, F., Rink, K., Shao, H., Shao, H.B., Sun, F., Sun, Y.Y., Singh, A.K., Taron, J., Walther, M., Wang, W., Watanabe, N., Wu, Y., Xie, M., Xu, W., Zehner, B. (2012): OpenGeoSys: an open-source initiative for numerical simulation of thermo-hydro-mechanical/chemical (THM/C) processes in porous media. *Environmental Earth Sciences*, 67(2), pp 589-599.

Stoeckl, L., Houben, G. 2012. Flow dynamics and age stratification of freshwater lenses: experiments and modeling. *Journal of Hydrology* 21 (458-459), pp 9-15.

Therrien, R., McLaren, R.G. and Sudicky, E.A. (2007): HydroGeoSphere - a three-dimensional numerical model describing fully integrated subsurface and surface flow and solute transport (Draft ed.). Groundwater Simulations Group, University of Waterloo. <http://www.science.uwaterloo.ca/~mclaren/public/hydrosphere.pdf>.

Walther, M. submitted. Variable-Density Flow Processes on Small, Medium and Regional Scales. Technical University Dresden. Dissertation.

Contact Information: Leonard Stoeckl, Federal Institute for Geosciences and Natural Resources, Stilleweg 2, 30165 Hanover, Germany, Phone: +49(0)511-643-3375, Email: leonard.stoeckl@bgr.de

Influence of geological heterogeneity on the saltwater freshwater interface position in coastal aquifers – physical experiments and numerical modeling

Anis S. Chowdhury¹, L. Stoeckl^{1,2} and G. Houben²

¹Institute of water resources and environmental management, Leibniz University, Hannover.

²Bundesanstalt für Geowissenschaften und Rohstoffe, Hannover.

ABSTRACT

Three realizations of a heterogeneous coastal aquifer were simulated by sand tank experiments, using three types of sands with different hydraulic properties. For each of the three experiments, the horizontal dimension (length) of the sand compartments was varied (9 cm, 18 cm, and 27 cm). It was observed that an increase in the lateral dimension of the sand compartments caused the salt water wedge to intrude further inland. For each set-up, five sea level heights were applied and the resulting wedge geometry monitored until steady-state was reached. As expected, an increase of the sea level led to a farther inland saltwater propagation. The results obtained from the physical model were successfully compared to numerical simulations. The numerical results for a homogeneous case with averaged hydraulic properties show an overall farther saltwater intrusion than for the heterogeneous cases.

INTRODUCTION

The influence of different length scales in geological heterogeneity on the salt- and freshwater interface (SFI) position was studied. Regarding the interface and the wedge toe position, as a measure of the saltwater intrusion length, aquifers with larger hydraulic conductivities are clearly more prone to saltwater intrusion than aquifers with lower conductivity. Considering geological heterogeneities of an aquifer, the research question we address here is how the lateral extent of sedimentary compartments with different hydraulic conductivities affects the intrusion of saltwater. This is especially interesting for deltaic coastal zones, e.g. the Ganges Delta, Bangladesh, with its strongly heterogeneous sedimentation patterns.

METHODS

The experimental set-up was based on Stoeckl and Houben (2012). An acrylic tank with a width of 5 cm was filled with three types of sand of different hydraulic conductivity, which were determined by granulometric analysis in the lab: fine sand ($K = 165 \text{ m}\cdot\text{d}^{-1}$), medium sand ($K = 355 \text{ m}\cdot\text{d}^{-1}$), and coarse sand ($K = 1229 \text{ m}\cdot\text{d}^{-1}$). The sands were separately backfilled into the tank, forming a trapezoidal shaped aquifer with a top-length of 1.18 m, a bottom-length of 0.62 and a height of 0.35 m. An angle of 32° was measured for the sloping beach face at the left side of the aquifer, where the ocean was simulated by colored (red) saltwater with a density of $1025 \text{ kg}\cdot\text{m}^{-3}$. Freshwater recharge (yellow, blue) with a density of $1000 \text{ kg}\cdot\text{m}^{-3}$ was applied to the top of the aquifer, using a peristaltic pump (Ismatec BVP, Germany). A constant pumping rate of 1.8 liter/hour was used. Four different saltwater-levels were applied in each experiment (0.210 m, 0.245 m and 0.280 m and 0.315 m above model bottom).

Three different experiments were conducted, varying the horizontal length of the rectangular sand compartments of the aquifer. Keeping the height of 3.5 cm constant for all compartments, a length of 9 cm, 18 cm and 27 cm was chosen for the first, second and third experiment, respectively. This, in turn, increased the anisotropy of the system. Care was taken, that compartments of the same type of sand did not overlay each other.

A numerical model was set up in FEFLOW 6.1 (Diersch, 2005). The finite element mesh with 10,000 elements was generated using the triangular grid builder. The initial time step length was 1 s and the maximum time step length was 3 s. A constant fluid flux boundary condition was assigned to the top of the trapezoidal polygon. The recharge rate was assigned to -1.73 m d^{-1} . The saltwater heads assigned to the left boundary were 0.210 m, 0.245 m, 0.280 m and 0.315 m. For modeling flow in the unsaturated zone, van Genuchten parameters of $\alpha = 20, 25$ and 30 and $n = 2, 2.5$ and 3 were assigned for the fine, medium and coarse sand, respectively (van Genuchten, 1980). Coordinates of the SFI geometry were read off manually.

RESULTS

Figure 1 shows a relationship between the length of the sand compartments and the extent of saltwater intrusion: Increasing the compartment length resulted in a movement of the interface (and the wedge toe position) farther into the aquifer, reducing the volume of freshwater.

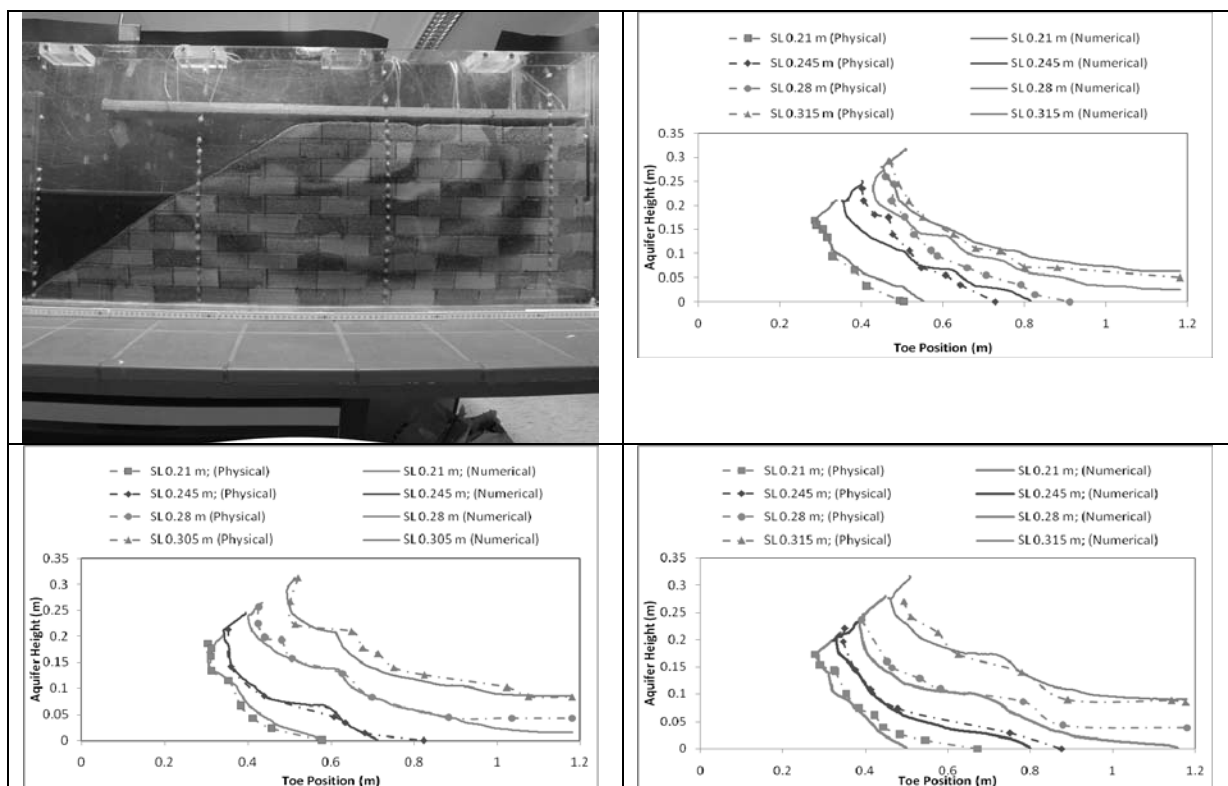


Figure 1: SFI geometry as a function of compartment length and for different sea levels in a) physical model with a compartment length of 9 cm (Experiment 1); results: b) Experiment 1 (compartment length 9 cm); c) Experiment 2 (18 cm); d) Experiment 3 (27 cm).

Further, it was found that by increasing the saltwater-level the interface became less steep, finally leading to its detachment from the impermeable bottom. The interface also became smoother indicating the influence of the length scale of the anisotropy (longer compartments, less bending of the SFI).

Figure 2 shows the SFI for experiments 1, 2 and 3, separated by the applied sea levels (a to d). In addition, the SFI geometry derived from a numerical model of a homogeneous aquifer, having an average hydraulic conductivity of the fine, medium and coarse sand is shown (Fig. 2). The results show, that a) with increasing sea level, the differences between the simulated homogeneous and observed heterogeneous intrusion length were reduced. Interestingly the interface position of the homogeneous aquifer always showed farther saltwater intrusion than for the heterogeneous cases.

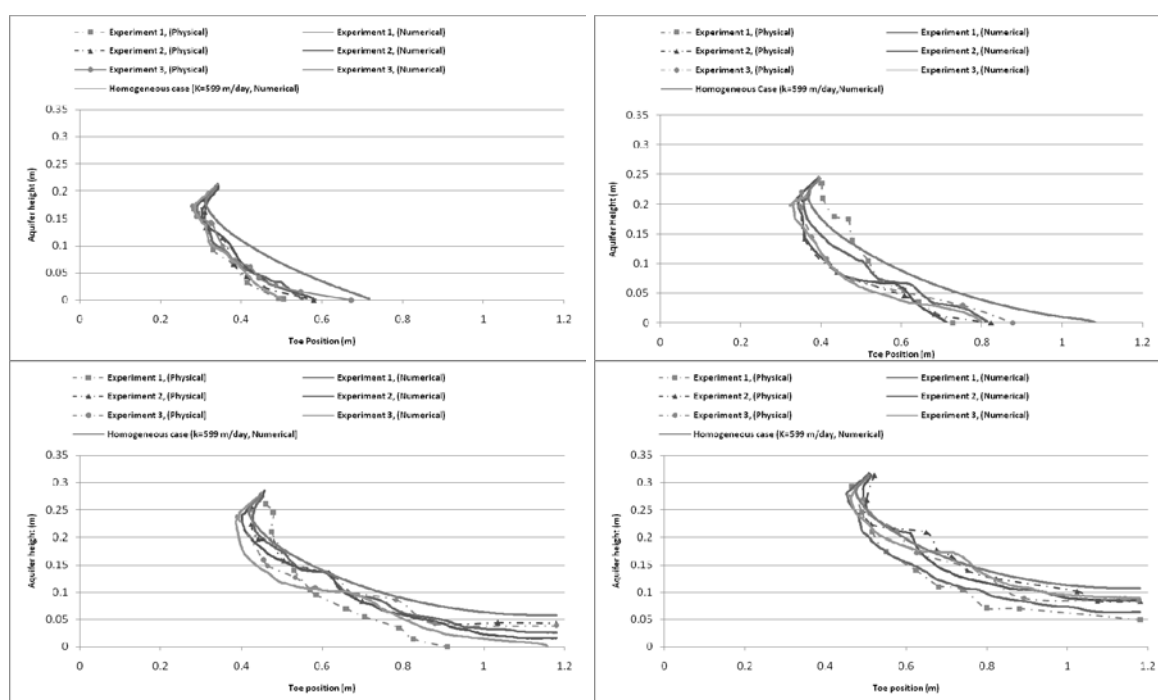


Figure 2: SFI positions in physical and numerical models as a function of sea level a) sea level 0.210 m, b) 0.245 m, c) 0.280 m, and d) 0.315 m with a constant recharge of 1.73 m/day (a simulated interface geometry of a homogeneous case is also included, orange curve)

DISCUSSION AND CONCLUSIONS

Results of sea level rise scenarios showed that with a higher sea level, the saltwater intrusion reached further inland. A good agreement between the physical and numerical model results was observed.

Results for the three different experiments with different compartment lengths (9 cm, 18 cm and 27 cm) showed that the saltwater intrusion reached further inland with longer compartment sizes. This on the other hand means that aquifers with smaller heterogeneities (short horizontal compartment length) are less vulnerable to saltwater intrusion.

The numerical model results, however, revealed that for a homogeneous aquifer with average aquifer properties, sea water intrusion reached even farther than for all

heterogeneous cases. This lead to the assumption that a “tipping point” separating homogeneous and heterogeneous aquifers should exist: when compartments fall below a certain length scale and the representative elementary volume is small enough, the system becomes a “homogeneous” aquifer. Therefore it is assumed that the wedge toe length increases again when compartment sizes are further shortened. This, however, could not be resolved with our limited set of experiments.

REFERENCES

van Genuchten, M. T. V. and Nielsen, D. R., 1985, On describing and predicting the hydraulic properties of unsaturated soils *Annales Geophysicae*, 615-628.

Diersch, H.J.G. 2005. FEFLOW: Finite Element Subsurface Flow and Transport Simulation System. WASY GmbH Institute for Water Resources Planning and Systems Research, Berlin. pp.292.

Stoeckl, L., Houben, G., 2012. Flow dynamics and age stratification of freshwater lenses: Experiments and modeling, *Journal of Hydrology*, 2012, pp 458-459.

Problems and solutions when storing fresh water in brackish aquifers for later use

Pieter J. Stuyfzand^{1,2}, Koen G. Zuurbier^{1,2} and Andreas Antoniou^{1,2}

¹KWR Watercycle Research Institute, Nieuwegein, Netherlands

²Faculty of Earth and Life Sciences, VU University, Amsterdam, Netherlands

ABSTRACT

Typical problems during storage and recovery of fresh water in a brackish or saline aquifer consist of (i) upward bubble drift by density driven flow, (ii) lateral bubble drift, and (iii) undesired water quality changes due to mobilization of Fe, Mn and As by redox reactions and of Na by cation exchange.

In unique field pilots, the effectiveness was tested of 2 smart well systems which are expected to mitigate the effects of bubble drift: a MUltiple Partially Penetrating ASR well (MUPPA) and a HOrizontal Salinization Protected ASR well (HOSPA; also called 'Freshmaker').

The prevention of undesired redox reactions was tested via PHREEQC-2 simulations of adding O₂ and Na₂CO₃ to the infiltration water, and via a unique ASR-simulating column study, in which KMnO₄ was added to the infiltration water. The results obtained show that the problems can be satisfactorily mitigated, which amplifies ASR applicability to brackish and saline aquifers.

INTRODUCTION

Aquifer Storage and Recovery (ASR) of fresh (often surface or rain) water is a well-known method to overcome seasonal or periodical water scarcity problems in areas with periodical water excess in contra-phase with peak demands. When the only suitable target aquifer is brackish or saline, ASR becomes more difficult to apply due to (i) upward bubble drift by density driven flow, (ii) earlier negative effects of lateral bubble migration (less mixing allowed for Cl than for constituents that sorb), and (iii) potentially more severe water quality problems by water-aquifer interactions, due to clay mobilization, enhanced cation and anion exchange, and enhanced redox and dissolution reactions. As a result, the recovery efficiency (RE) of the ASR system can become insufficient.

Storage in brackish or saline aquifers is however very attractive, because of several advantages: availability of huge, additional subterranean storage volumes, less interference with other aquifer users, lower pollution levels of admixed ambient groundwater (salt excluded), and direct reversal of salt water intrusion.

In this contribution, we present methods tested in pilots, to solve or mitigate the above mentioned problems, so as to amplify ASR applicability in a salinizing world.

METHODS

Upward bubble drift was studied and mitigated in 2 ASR pilots, each with a different approach. The first consisted of a Multiple Partially Penetrating ASR well (MUPPA) in a semi-confined, brackish (TDS 3,300, Cl 1,000 mg/L) sandy aquifer near Nootdorp (W-Netherlands). This MUPPA enabled injection at the base of the aquifer and recovery at the top (Fig.1), thus buffering the buoyancy effects. The well was fed with rainwater (TDS 60, Cl 5 mg/L) from the roof of a large greenhouse, after pretreatment by subsequently storage in a tank, rapid and slow sand filtration. Infiltration occurred whenever rainfall was sufficient to surpass a specific level in the storage tank. Infiltrated fresh water was recovered in dry periods, whenever available and needed for irrigation of crops in the greenhouse.

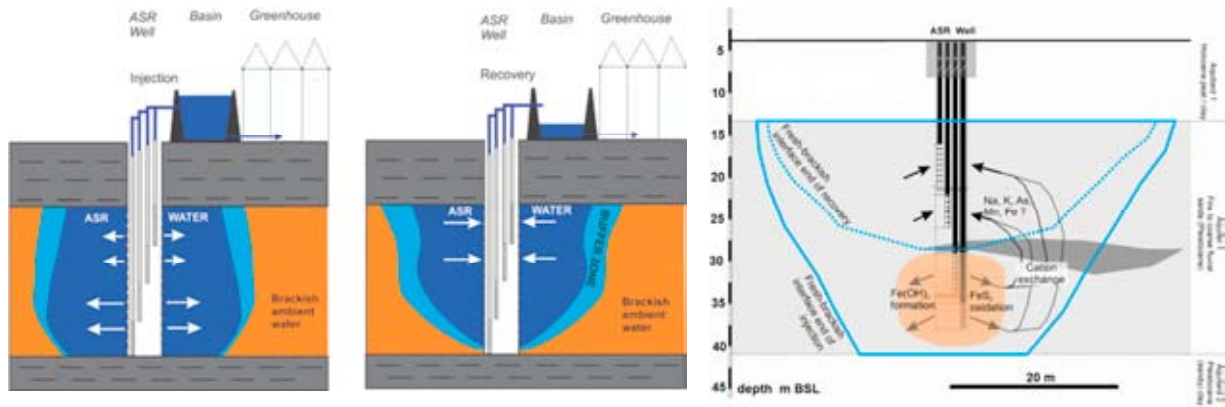


FIG. 1. Left and middle: Use of multiple partially penetrating ASR well for significant improvement of freshwater recovery from a confined brackish aquifer in coastal Netherlands. Right: Shift in position of the fresh water bubble after injection and after recovery, with important hydrogeochemical processes and zones.

The Maximum Permissible Concentration (MPC) for crops ($\text{Na} < 11 \text{ mg/L}$, monitored as $\text{EC} < 25 \text{ mS/m}$) determined when to stop recovery. The pilot was intensively monitored in 2012 (Zuurbier et al. 2014a).

The second pilot (Fig.2) is running since 2013, in an elongated, narrow creek ridge aquifer near Ovezande (SW-Netherlands), using a HORIZONTAL Salinization Protected ASR well (HOSPA; also called ‘Freshmaker’). It consists of 2 parallel, superimposed Horizontal Directional Drilled Wells (HDDWs) 70 m long, the upper one (at 7 m BSL) being the ASR well and the lower one (at 14.5 m BSL) being the interception well of underlying saltwater. Surface water is taken in from a local water course (fresh when significant rainfall), and is pretreated by sedimentation in a small basin. The saline groundwater (TDS 39,000, Cl 16,800 mg/L) is pumped out continuously ($40 \text{ m}^3/\text{d}$), and discharged downstream of the water course which discharges to the Scheldt estuary. The fresh water recovered is used for irrigation in an apple orchard. The MPC was set at 250 mg Cl/L, monitored as $\text{EC} < 150 \text{ mS/m}$. The pilot is being intensively monitored (Zuurbier et al. 2014b).

Results of the fresh/salt interface monitoring were simulated with SEAWAT, and used to extrapolate recovery efficiencies (REs) of future ASR scenario’s, and to demonstrate that REs would have been 50% lower with normal ASR wells.

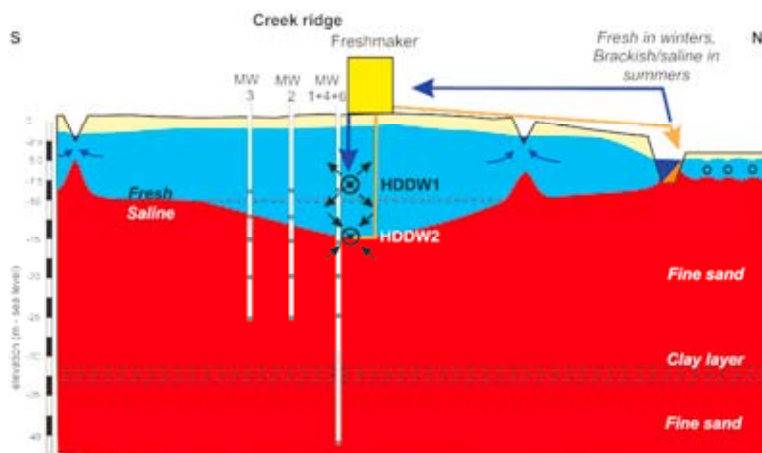


FIG. 2. Cross section over the creek ridge near Ovezande where a HOSPA is enlarging the fresh water reserve while saline groundwater is pumped out continuously. HDDW1 = horizontal ASR well; HDDW2 = horizontal interception well. MW = vertical Monitor Well.

A unique ASR column setup was developed to simulate oxic tap water injection and recovery from originally deeply anoxic sand saturated with brackish groundwater (Fig.3; Table 1). Undisturbed cores from the brackish aquifer at the Nootdorp pilot were thus tested via 2 series of 4 conventional ASR cycles, in which tap water was injected (Antoniou et al. submitted). The tests revealed a persisting Mn(II), Fe(II) and As mobilization due to pyrite oxidation and manganous siderite dissolution, as happened in field pilot Nootdorp (Fig.1) and in field pilot Herten (see Antoniou et al. 2013). This mobilization is feared because the recovered water needs to be distributed without post-treatment. In order to temper the mobilization, the cores were flushed during the second ASR cycle (of the second series) with a dilute 0.02 M KMnO_4 solution (Table 1), and after its recovery the column was flushed with tap water again. In addition, the effects of adding extra O_2 and Na_2CO_3 to oxic tap water were modeled using a calibrated flow-tube PHREEQC-2 model.

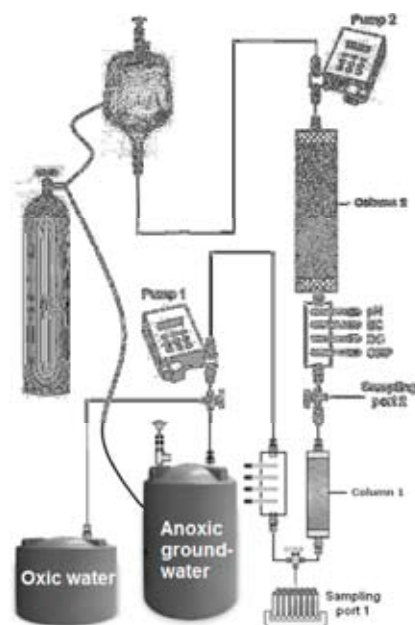


FIG. 3. A unique ASR column setup, showing reservoirs of oxic tap water and (deeply) anoxic groundwater, column 1 simulating the ASR proximal aquifer zone, and column 2 simulating the remote buffer zone.

RESULTS AND DISCUSSION

The MUPPA and HOSPA (Freshmaker) pilots showed that a sufficiently high RE (>50% and 100% respectively) could be realized, while the SEAWAT modeling indicated a far lower RE (<20% and <50% respectively) for both, if a normal ASR well (without buoyancy buffering and without salt water interception, respectively) had been used.

The realized RE's are excellent, considering the very stringent MPC for Na (11 mg/L) on the Nootdorp pilot, and MPC for Cl (250 mg/L) on the Ovezande pilot. These values correspond with an allowed admixing of only 3% brackish and 0.9% saline groundwater, respectively.

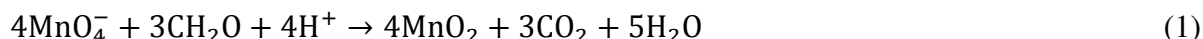
The MUPPA's RE could be further improved by a steady, slow abstraction of brackish groundwater (which could be used after desalination via RO), and by periodically also using the upper ASR well screen for infiltration. The latter helps to build up more ferrihydrite coatings which sorb the Fe, Mn and As mobilized in the deeper parts of the aquifer (Fig.1).

TABLE 1. Overview of water quality parameters for the brackish groundwater in the sand cores from Nootdorp (native groundwater), tap water (normal source water), and the diluted KMnO_4 solution.

	pH	EC	Alkalinity	NH ₄	Cl	SO ₄	Na	K	Ca	Mg	Fe	Mn	As
		μS/cm					mg/L						μg/L
Native water	6.8	3540	1102	12.3	1120.5	0.7	618.0	25.9	267.0	66.7	15.2	1.4	1.0
Normal source water	8.0	392	235	0.0	8.8	0.1	13.2	1.1	69.9	5.4	0.0	0.0	0.0
KMnO_4 source solution 0.02M	8.4	2400	56	-	-	0.1	1.6	782.0	1.6	0.0	0.0	1098.8	2.2

The horizontal wells in the HOSPA could also form a solution in case of lateral bubble drift, if aligned in the direction of regional groundwater flow. In that case the wells should be equipped with valves that can be closed so as to infiltrate via the upgradient section and recover in the downgradient parts.

The KMnO₄ treatment helped to increase RE from 15 to 84 % during the next conventional ASR cycle using tap water. This beneficial result is due to the combination of (i) the very strong oxidizing activity of KMnO₄, (ii) the increase of sorption capacity through the generation of Mn-oxide precipitates, (iii) the coating (inactivation) of reactive pyrite, and (iv) the resulting pH increase, which helps to immobilize Fe and Mn. The reactions with pyrite (FeS₂) and organic matter (CH₂O) are schematized as follows:



Although the use of KMnO₄ in water treatment is well established, in ASR some further research is required to solve questions regarding the dose, treatment frequency and costs.

Addition of only O₂ provoked an undesired pH decline, which stimulated Mn mobilization. When combined with a pH raising solute like Na₂CO₃ much better results in immobilizing Fe and Mn were obtained (Antoniou et al. 2013).

CONCLUSIONS

Even brackish and saline aquifers can be used to store fresh water for later use, if ASR wells are properly designed to reduce or buffer bubble drift, and if adverse water quality changes in an anoxic aquifer are mitigated by an oxidizing and pH increasing treatment.

REFERENCES

Antoniou, E.A., P.J. Stuyfzand & B.M. van Breukelen 2013. Reactive transport modeling of an aquifer storage & recovery (ASR) pilot in an anoxic sandy aquifer. *Applied Geochemistry* 35 (2013) 173–186.

Antoniou, E.A., N. Hartog, B.M. van Breukelen & P.J. Stuyfzand 2014. Aquifer pre-oxidation using permanganate to mitigate water quality deterioration during aquifer storage and recovery. Submitted to *Applied Geochemistry*.

Stuyfzand, P.J., P. Nienhuis, A. Anthoniou & K. Zuurbier 2012. Feasibility of subsurface storage through A(S/T)R in Dutch coastal dunes. Report KWR 2012.082, 107p (in Dutch).

Zuurbier, K.G., W.J. Zaadnoordijk, P.J. Stuyfzand 2014a. How multiple partially penetrating wells improve the freshwater recovery of coastal aquifer storage and recovery (ASR) systems: A field and modeling study. *Journal of Hydrology* 509 (2014) 430–441.

Zuurbier K.G., Kooiman J.W., Maas B., Groen M.M.A., Stuyfzand P.J., 2014b. Enabling successful aquifer storage and recovery using horizontal directional drilled wells (HDDWs) in coastal aquifers. Accepted *Journal of Hydrologic Engineering*.

Contact Information: Pieter J. Stuyfzand, KWR Watercycle Research Institute, Water Systems Department, P.O. Box 1072, 3430 BB Nieuwegein, Netherlands, Phone: 0031-6-10945021, Fax: 0031-30-6061-165, Email: Pieter.stuyfzand @kwrwater.nl

Predicting the effects of sea spray deposition and evapoconcentration on shallow coastal groundwater salinity under various vegetation types

Pieter J. Stuyfzand^{1,2}

¹Faculty of Earth and Life Sciences, VU University, Amsterdam, Netherlands

²KWR Watercycle Research Institute, Nieuwegein, Netherlands

ABSTRACT

Shallow groundwater in coastal areas can be brackish purely due to sea spray deposition followed by evapoconcentration, thus without any sea water intrusion. But when and where? A simple analytical model is presented, capable of predicting the mean chlorinity of shallow groundwater under various vegetation types in a sandy recharge area.

INTRODUCTION

Groundwater recharged by precipitation in temperate climates can become brackish when sea spray deposition and evapoconcentration (concentration rise by evapotranspiration losses) are high. For instance, the upper groundwater under pine forests close to the sea shore with frequent storms blowing inland may show Cl concentrations in the Netherlands as high as 1,100 mg/L (Stuyfzand 1993, Stuyfzand & Rambags 2011).

It is important to be able to predict the Cl concentration of rain fed groundwater for 4 reasons: (i) chloride, which is mainly (>95%) linked to sea spray inputs, determines also a very significant part of the concentrations in groundwater of Na, K, Mg, SO₄, Br, B, I, Li, Mo and Rb (Stuyfzand, 1993); (ii) climate change, sea level rise, coastal erosion or progradation (by e.g. beach nourishment) affect the quantity of sea spray deposition and vegetation composition, and thereby groundwater quality; (iii) Cl peaks in vertical logs of rain fed, coastal groundwater can be used to date shallow groundwater and to derive actual evapotranspiration rates via the chloride mass balance (Stuyfzand 1993 and 2014); and (iv) the observation of brackish groundwater in wells does not necessarily indicate salt water intrusion, so that an atmospheric origin needs to be excluded before panic is justified.

METHOD

The annual mean Cl concentration of rain-fed groundwater (Cl_G) in natural recharge areas is predicted by the following set of semi-empirical equations that were tested on a huge population of data (Stuyfzand 2010 and 2014):

$$Cl_G = f_E^{1.5} Cl_P \quad (1)$$

$$\begin{aligned} \text{if } E/P < 0.95 & \quad f_E = P / (P - E) \\ \text{if } 0.95 \leq E/P < 1 & \quad f_E = 20 E / P \\ \text{if } E/P \geq 1.00 & \quad f_E = 20 \end{aligned} \quad (2)$$

$$Cl_P = (Cl_M / 16,800) f_W \Sigma (v_W^{3.4} 550 [X_{WIND}]^{-0.45}) / 365.25 + 0.1 \quad (3)$$

where:

P = annual total of gross precipitation [mm/y]; E = annual total of evapotranspiration [mm/y]; Cl_P, Cl_M = chloride in bulk precipitation, coastal sea water [mg/L]; f_E =

evapoconcentration factor according to Eq.2; Σ = summation of daily values during calendar year under consideration; v_w = daily mean wind velocity measured at 10 m altitude [m/s]; X_{WIND} = daily mean distance of the Cl monitoring site to the beach high water line (HWL) as measured along each day's mean wind direction [m]; f_w = empirical correction factor to obtain the best overlap of the calculated or reconstructed Cl_P signal (based on wind data) with the measured Cl_P time series on site.

The above given approach requires the daily measurement of X_{WIND} , which can be automatized by using GIS or as follows, in case of a straight coastline (Fig.1):

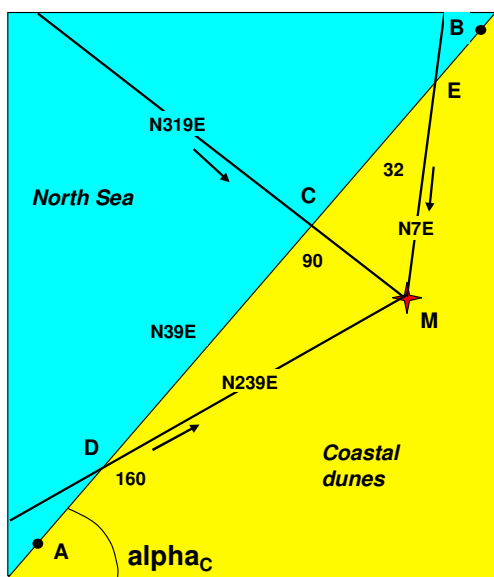
In case of offshore wind, thus if $(90 - \arctan(a_C)) < W_D < (180 + \arctan(a_C))$:

$$X_{WIND} = 200,000 \text{ [m]} \tag{4}$$

In case of onshore wind:

$$X_{WIND} = \text{sqrt} [\{a_C (b_C - b_M)/(a_M - a_C) + b_C - Y_M\}^2 + \{(b_C - b_M)/(a_M - a_C) - X_M\}^2] \tag{5}$$

Where: W_D = wind direction [e.g. west = 270]; $a_M = 90 - \tan(W_D)$; $b_M = Y_M - a_M X_M$; $a_C = \tan(\alpha_C)$ = slope of straight line between A and B in Fig.1 [-].



Annual mean values for frequently occurring vegetation types are listed in Table 1. The factor f_w is 0.0015 for KNMI's meteorological station De Kooy (North Holland). This value yields the best fit of calculated with measured Cl data at De Kooy in the period 1978-1987 (both annual and monthly data).

FIG. 1. Spatial relations between the location of monitoring site M, a straight coastline (between A and B) and 3 wind directions with fetch over land from the HWL up to monitor point M, being EM (N7°E), CM (N319°E) and DM (N239°E) respectively. From Stuyfzand (2010).

The power factor 3.4 corresponds with observations by Monahan & O'Muircheartaigh (1980). The theory behind Eqs.1-5 is that wind velocity determines the amount of sea spray in the atmosphere (Monahan & O'Muircheartaigh, 1980), and the wind direction determines the amount of sea spray in the atmosphere that disappears by sedimentation, impaction etc., in between the HWL and monitoring point M (X_M, Y_M).

As we know from literature (Leeflang 1938; Stuyfzand 1993), a decreasing distance to the coastline leads to an exponential increase of sea spray deposition. That distance is shortest when the wind is blowing perpendicularly to the coastline, and increases when the wind angle deviates from that (Fig.1).

TABLE 1. Relations between gross precipitation (P), evapotranspiration (E), groundwater recharge (R) and evapoconcentration factor (f_E), as function of 10 characteristic (dune) vegetation types. The values shown for E/P and f_E hold for $P = 0.845$ m/y.

VEGETATION		EVAP			Conc.
Type	Code	$R = (p \ln(P)-c)/1000$			factor Evap
Prec (P) m/y =	0.845	p	c	E/P	$f_E = P/R$
Bare	1	750.0	4330	0.143	0.725
Bare + some mosses/grasses	2	741.6	4338	0.219	0.660
Mosses	3	730.0	4360	0.338	0.560
Poor dry dune veg, mix of mosses+grasses+bare	4	720.0	4370	0.429	0.482
Dry shrubs (open), <50% mosses/grasses	5	710.0	4383	0.524	0.402
Rich dry dune veg, Heather, Dry deciduous	6	702.4	4398	0.603	0.335
Dense shrubs, Wet tall grasses, Oaks	7	641.6	3977	0.590	0.347
Wet dune slack, Deciduous forest (wet)	8	600.0	3750	0.653	0.294
Pines, dense dry	9	550.0	3500	0.755	0.207
Pines	9.5	504.3	3251	0.825	0.148
Pines, wet and dense	10	475.0	3100	0.880	0.101

Effects of evapoconcentration and interception deposition (= additional atmospheric, mainly dry deposition by vegetation compared to a bulk precipitation collector) are combined in the term $f_E^{1.5}$ of Eq.1.

Alternatives to using Eqs.3-5 are: (i) measuring the annual inland Cl gradient in bulk precipitation, or (ii) using the following approximation:

$$Cl_P = (Cl_M / 16,800) A [f_A X_{HWL}]^{-B} + 0.1 \quad (6)$$

Where: X_{HWL} = shortest distance to the High Water Line of the sea [m]; f_A = correction factor for a longer distance to HWL when measured along the azimuth of the predominant wind direction, along which on average during a year the strongest winds blow (with velocity >5 Beaufort) and with which the highest amount of sea spray is deposited; A, B = constants depending on storm frequency and intensity during calendar year.

In the Western Netherlands near Haarlem for instance, the following values hold: $f_A = 1.20$ (with azimuth = N260E); $A = 550$, $B = 0.45$ during windy years like 1981, and $A = 101.89$, $B = 0.3437$ during calm years like 1938-1939 and 2010-2011 (Stuyfzand 2014). The strength of Eq.6 is, that in principle only one coastal rain monitoring station may suffice to establish the annual windiness.

RESULTS AND DISCUSSION

The model shows an excellent fit with annual mean data from 28 monitoring plots collected in the early 1980s in the Western Netherlands, with vegetation types ranging from very scanty (nearly bare) to full-grown pine stands, and with distances to the HWL of 0.2 – 100 km (Fig.2).

The advantage of using wind data is, that (i) they have been measured much more frequently and for a longer time than Cl measurements in bulk or wet-only precipitation, and (ii) climate models do generate information on changes in wind climate, but not on sea spray deposition. Sometimes a correction factor (f_{LOC}) for location specific deviations from the normal inland Cl deposition gradient is needed, for instance due to an extremely high exposition to seawinds along the windward border of a forest ($f_{LOC} > 1$), or due to shielding from salty winds in the interior parts of a forest ($f_{LOC} < 1$).

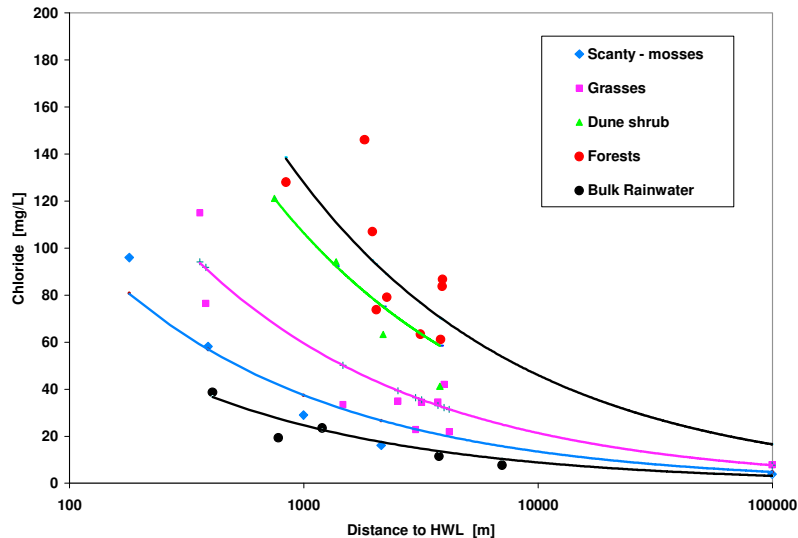


FIG. 2. Measured and with Eqs.1-5 calculated mean Cl concentrations of bulk precipitation and shallow dune groundwater under 4 vegetation types, as function of the distance of the monitoring plots to the North Sea high water line (HWL). Data points = measured in the early 1980s in coastal dunes of the Western Netherlands and National Park Veluwe (~100 km inland); Curves = calculated relations.

CONCLUSION

The validated analytical model can be used to predict the effects of for instance coastal erosion by sea level rise, coastal extension by sand nourishment, climate change or vegetation changes. And also, they can strengthen the chloride mass balance approach in estimating evaporation losses.

REFERENCES

- Leefflang, K.W.H. 1938. The chemical composition of precipitation in the Netherlands. Chem. Weekblad 35, 658-664 (in Dutch).
- Monahan, E.C. & I. O'Muircheartaigh 1980. Optimal power-law description of oceanic whitecap coverage dependence on wind speed. J. Phys. Oceanography 10, 2094-2099.
- Stuyfzand, P.J. 1993. Hydrochemistry and hydrology of the coastal dune area of the Western Netherlands. Ph.D Thesis Vrije Univ. Amsterdam, published by KIWA, ISBN 90-74741-01-0, <http://dare.uvu.vu.nl/handle/1871/12716>, 366 p.
- Stuyfzand, P.J. 2014. Effects of climate and environmental change on shallow groundwater quality and quantity in Dutch coastal dunes. KWR report BTO.2014.0?? (s) in prep.
- Stuyfzand, P.J. & F. Rambags 2011. Hydrology and hydrochemistry of the 4 lysimeters near Castricum; overview of results and feasibility of reanimation of the lysimeter station. KWR Rapport BTO 2011.020 (s), 111p (in Dutch).

Contact Information: Pieter J. Stuyfzand, KWR Watercycle Research Institute, Water Systems Department, P.O. Box 1072, 3430 BB Nieuwegein, Netherlands, Phone: 0031-6-10945021, Fax: 0031-30-6061-165, Email: Pieter.stuyfzand@kwrwater.nl

Effect of Dispersivity on Saltwater Intrusion and Removal Processes

Masahiro Takahashi¹ and Kazuro Momii²

¹Research and Development Center, Nippon Koei Co., Ltd., Tsukuba, JAPAN

²Department of Environmental Sciences and Technology, Kagoshima University, Kagoshima, JAPAN

ABSTRACT

This study focuses on the behavior of residual saltwater trapped in the storage area upon installation of the cut-off wall based on the laboratory experiments and numerical simulation. The longitudinal and transverse dispersivities, α_L and α_T , respectively, are estimated using image analysis of pulse and continuous injection experiments with tracers, and numerical analyses. The saltwater intrusion and removal experiments are numerically reproduced by the SEAWAT numerical model with the estimated α_L and α_T . Sensitivity analyses carried out by varying the α_L and α_T values prove the effect on removal time of the residual saltwater. The transverse dispersivity, consequently, plays an important role in the dilution and removal of residual saltwater due to the groundwater flow along the mixing zone between the freshwater and saltwater.

INTRODUCTION

The report of the fifth IPCC predicts a rise in sea level by global warming by up to 82 cm in 2100, and, as a result, it is expected that the progress of the seawater intrusion is accelerated in the coastal areas. A deterioration of water quality by the saltwater intrusion and a decrease in pump discharge have a potential for the large impact on people's life and their productive activities because there are in general a lot of groundwater exploitations in the coastal areas. Therefore, that is the significant issue to overcome. Seven subsurface dams, which have a storage function for securing water resource and also suppressing the saltwater intrusion, have already been constructed in the Southwest Islands in Japan. In many of the traditional research on subsurface dam, the freshwater storage has been discussed, and the saltwater behavior at storage area enclosed by the cut-off wall has been hardly discussed (Luyun et al. 2009). It is considered that the quantitative evaluation of residual saltwater removal is extremely important for the saltwater management with the cut-off wall. In this study, the behavior of saltwater remained at storage area after installation of the cut-off wall is quantitatively investigated by laboratory experiments and numerical analyses for unconfined groundwater.

METHOD

Laboratory experiment and image analysis

Acrylic laboratory equipment is the size 100 cm×40 cm×1.5 cm. It has storage tanks where water is supplied in both ends of the device, and 1.2 mm diameter glass beads were filled in the device. A tracer colored with food dye or fluorescent dye was poured from injection hole and others of the equipment, and its dynamic state was taken images with a fixed digital camera in a darkroom. An imaging time interval was 0.5 to 30 minutes. Further details of the experimental setup can be found in Luyun et al. (2009).

First, after filling the device with pure water, provided a difference in water-level, generating a flow field of freshwater. After the flow became a steady state, the tracer was injected in pulsed or continuously from 6 mm diameter injection hole. Second, a flow of pure water was generated and stabilized after the experimental device was filled with pure water, and started the saltwater intrusion. After the saltwater intrusion had reached an equilibrium state, the cut-off wall of 28 cm height was inserted between the left saltwater tank and a permeability layer, and the saline water was excluded. The dynamic state of the saltwater at this time was saved in images. Two EC sensors were installed in the saltwater intrusion area, and EC changes at the time of invasion and exclusion were measured.

Images of each experiment were split into RGB values using the software of IMAGEJ (NIH). The concentration was determined using G value for fluorescent dye, and R/B value for food dye. In addition, a relationship between individual concentration and G, R/B values was determined by calibration test.

Numerical analysis

From the image of the results of the first experiment, positions of center nodes and spreads of longitudinal and transverse directions of the tracer were read with time. Their values were assigned to an estimation equation and an analytical solution, and the α_L and α_T values was calculated. To verify the experimental outcomes, the numerical analysis by MT3D was performed. Furthermore, a reproduction of the experiments were made by inputting the α_L and α_T values to SEAWAT.

RESULTS

Pulse and continuous injection experiments

The α_L and α_T were presumed using the estimation equation from the experimental outcomes of the pulse injection. As a result, the α_L values were within a range of 0.19 to 0.22 cm, and the α_T values a range of 0.011 to 0.007 cm. In the continuous injection test (Figure 1), the α_T value was estimated to be 0.007 cm, and became almost equivalent to the result of the pulse injection test. The ratio of α_L/α_T obtained by the pulse injection test was 20 to 27. The experimental results were verified by inputting the estimated α_L and α_T values to MT3D, and an image of the experiment was approximately reproduced.

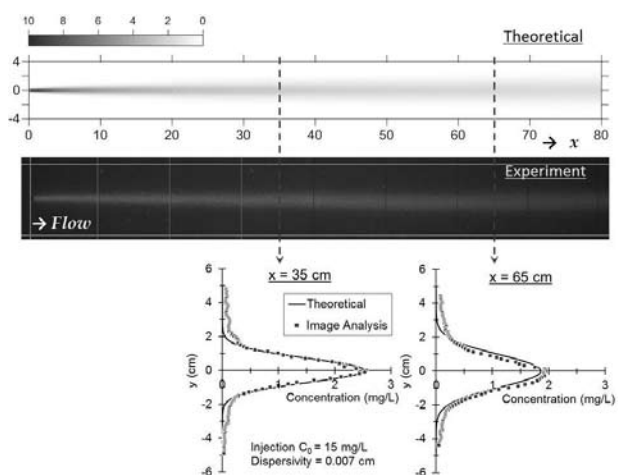


Figure 1. Result of continuous injection test.

Results of saltwater intrusion and removal experiments

Figure 2 shows the changes in the salt concentrations measured by two electrical conductivity probes EC1 and EC2 and the image analysis for the laboratory experiments of the saltwater intrusion and removal processes. Concentration estimated from EC1 reached

the saltwater concentration in a minute or two, and in case of EC2, concentration increased from six minutes and arrived at the max salt concentration in about 12 minutes. As with the EC probes, the concentrations of EC1 obtained by the image analysis reached the saltwater concentration in approximately one minute, at EC2, rose from five minutes to slightly faster than the measured values, leading to the salt concentration in about 15 minutes.

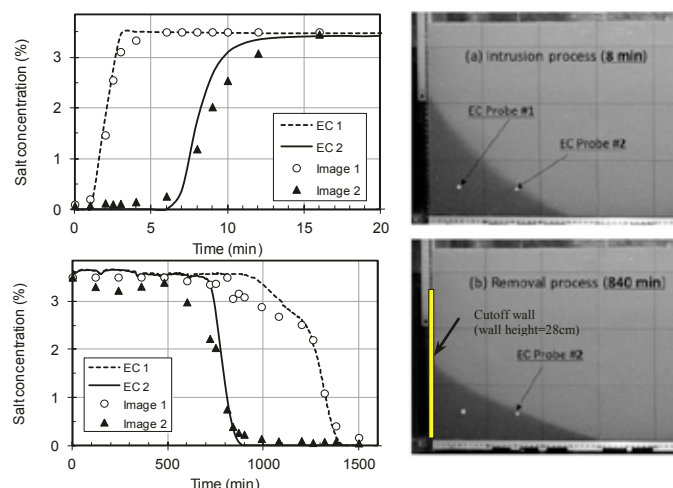


Figure 2. Changes in salt concentration by experiments.

In the removal process, the concentration began to change from approximately 700 minutes at EC2 after inserting the cut-off wall, and it altered to freshwater substantially in 900 minutes. On the other hand, the concentration began to decrease from 900 minutes and it became freshwater in 1400 minutes at EC1. The concentration change at EC1 with time has two gradients. The first gradient is smaller than the second one, and the similar trend was also observed in the image analysis.

Numerical analysis

As a result of conducting a reproduction analysis of the saltwater intrusion and the removal experiments by SEAWAT, the experimental outcome has been almost reproduced (Figure 3). Taking a more detailed look at it, the time-dependent change of the concentrations at EC1 and EC2 indicated the approximately the same tendency as that of EC sensor also in the analysis result. However, the concentration gradient in the invasion process was slightly looser than the EC measurements, and resulted in similar to the image analysis. In the removal process, the concentration change has two gradients at EC1 was reproduced, except that the gradient was also gradual than the EC measurements.

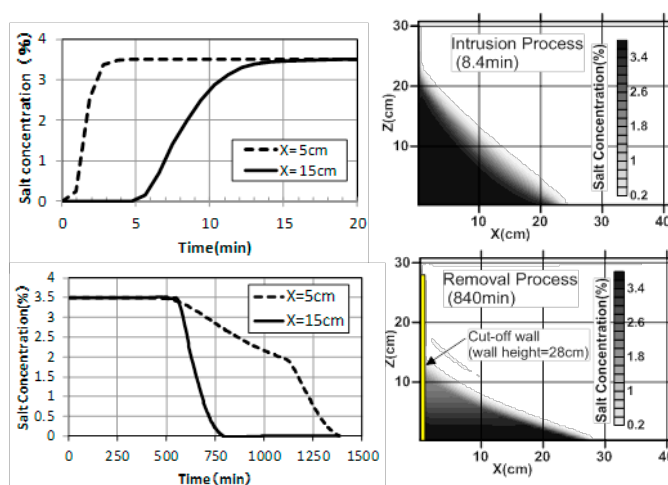


Figure 3. Changes in salt concentration with time by numerical simulation.

In the analysis of the exclusion experiment, in order to make a smooth insertion of the cut-off wall and to reinforce intensity, the porous acrylic board about 3 mm in thick was inserted between the cut-off wall and the glass beads. Since this must be considered to reproduce the measured values in the analysis, the reproduction analysis was performed by applying a high permeability to the left mesh corresponding to the porous acrylic plate. Then, the α_L/α_T was varied to 10, 27 and 100, and the change of the salt concentration was predicted (Figure 4). The high permeability of the left-end mesh is not taken into account in the predictive

analysis. Figure 4 shows that no significant differences are found in the concentration change from saltwater to freshwater at the location of EC2 in the invasion process even if the α_T is changed. On the other hand, the difference of removal time was as large as about 1000 minutes in the removal process. It was recognized that the width of mixing zone became thick as the α_T increased and concentrations was diluted on the whole.

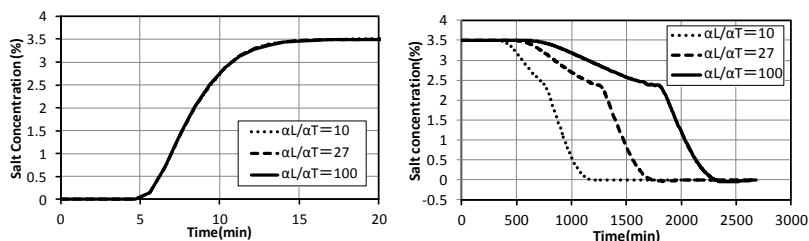


Figure 4. Changes in concentration with time for the ratio of $\alpha_L/\alpha_T=10, 27, \text{ and } 100$.

DISCUSSION AND CONCLUSIONS

Although the difference in the α_T value does not affect the invasion time in the saltwater intrusion process, the removal time becomes short as the α_T value increases in the removal process. In the removal process, saltwater is excluded along the groundwater flowing through the mixing zone between the freshwater and saltwater, and the concentration changes in an orthogonal direction to the groundwater flow along the mixing zone. The spread range of concentration change is evaluated in the α_T . Thus, the transverse dispersivity has a profound effect on the concentration change in the exclusion process.

When the ratio of α_L/α_T was altered, the simulated intrusion and removal processes indicated that the ratio of α_L/α_T contributes significantly to the retreating process because it took about 1.3 times removal time in case of $\alpha_L/\alpha_T = 27$ compared with $\alpha_L/\alpha_T = 10$. In the removal process, steep and gentle gradients can be seen in the concentration curves. Not all the saltwater flowing along the mixing zone moves upward and is removed, but a part of it moves downward and forms a circulating flow (Figure 5). This causes that the concentration in the upper part of the wedge is reduced gradually. It is considered that this generates the gentle slope in the concentration curve with respect to time shown in the experiment (Figure 3) and the analysis (Figure 4). The subsequent steep slope is interpreted as the exclusion by the flow along the mixing zone.

The numerical and image analyses of the experiments are effective to evaluate the ratio of α_L/α_T . The experimental results show that the evaluated ratio of α_L/α_T was larger than the general ratio of 10, indicating 20 or more. As a result, analysis of the saltwater removal process using the general ratio is found to predict a result that the complete removal will finish in a shorter time than reality. Therefore, it is considered that a comprehension of the α_L/α_T is required to develop more precise predictions.

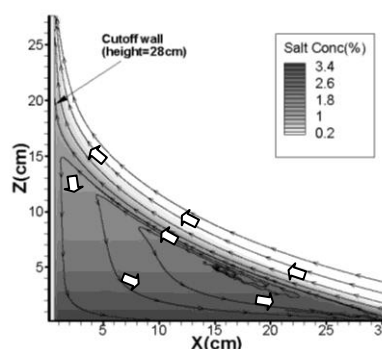


Figure 5. Streamlines and concentration distribution in removal process.

REFERENCE

Luyun Jr. R., K. Momii, and K. Nakagawa. 2009. Laboratory-scale saltwater behavior due to cutoff wall. *Journal of Hydrology* 377: 227-236.

Estimation of preferential recharge and saltwater intrusion to a coastal groundwater system in the North Central Coast of Vietnam by means of 3D hydrostratigraphical modeling

Vu Thanh Tam¹, Okke Batelaan², Tran Thanh Le¹ and Pham Quy Nhan¹

¹ Center for Water Resources Planning & Investigation of Vietnam (CWRPI)

²School of the Environment, Flinders University, Australia

ABSTRACT

Saltwater intrusion is worldwide regarded as a major threat to groundwater resources. Mostly, saltwater intrusion problems are related to sea water level rise or induced intrusion due to excessive groundwater extraction in coastal aquifers. However, the hydrogeological heterogeneity of the subsurface might play an important role in (non-)intrusion as well. This study focuses on local (hydro)geological conditions for preferential recharge as well as saltwater intrusion to a coastal groundwater system in Vietnam where geological formations exhibit highly heterogeneous lithologies. For that purpose, a 3D hydrostratigraphical solid model of the study area is constructed by a recursive and cluster analysis – based process combined with a chronographic marker. The cluster analysis is carried out on lithological composition, distribution depth and thickness of each lithological distinctive drilling interval of 47 boreholes to distinguish and map well-log intervals of similar lithological properties in different geological formations. A 3D hydrostratigraphical fence diagram is then generated from the constructed solid model and is used as a tool to estimate preferential recharge paths and saltwater intrusion to the groundwater system under study. Available data on groundwater level, water sample chemical analysis, and geophysical DC resistivity measurements are also used to support the estimation. Result of this research work contributes to the interpretation of why the aquifer system of the study area is almost uninfluenced by saltwater intrusion which is relatively common in coastal aquifers of Vietnam.

Keywords: stratigraphic modeling, coastal aquifer, cluster analysis, Vietnam.

Contact Information: Vu Thanh Tam, Center for Water Resources Planning & Investigation of Vietnam (CWRPI). Email: vttam@monre.gov.vn

Okke Batelaan, Strategic Professor Hydro(geo)logy, School of the Environment, Flinders University. Email: okke.batelaan@flinders.edu.au

Optimization of Subsurface Fresh Water Storage in New Land Developments

Marianne L. Tijs^{1,2}, Marloes van Ginkel^{1,2} and Theo N. Olsthoorn^{1,3}

¹Civil engineering, Delft University of Technology, Delft, The Netherlands

²Rivers, Deltas and Coasts, Royal HaskoningDHV, Rotterdam, The Netherlands

³Waternet, Amsterdam, The Netherlands

ABSTRACT

Coastal cities worldwide are dealing with the effects of rapid urbanization and climate change, yet most cities infrastructure and resources are barely able to cope. In many cases, further expansion of a city into the mainland is no longer possible for geographical and financial reasons, so developers turn to the sea. Land reclamation projects are currently underway in several cities such as Jakarta in Indonesia, Singapore and Lagos in Nigeria. While these new land developments may face the same resource problems as on the mainland, they also present new possibilities.

The case study area for this research is one of a number of new islands, which are planned in the Jakarta Bay as part of the Jakarta Coastal Development Strategy. The island is named Pluit 1 and is designated for residential and commercial use. Like on the mainland, providing fresh water for the island will not be easy or straightforward but this research may provide developers with an innovative water management strategy that will help solve that problem.

The storage of fresh water in the subsurface for later recovery (aquifer storage and recovery) provides a storage method which makes use of the purification properties of the subsurface, the geological characteristics of the aquifer and the density difference between fresh and saline water. We propose a further optimization of ASR systems by applying the possibilities presented by new land developments, allowing us to include dredging materials and techniques in the optimization of fresh water infiltration, storage and extraction.

A conceptual hydrological model is used to simulate infiltration and groundwater recharge in the island's urban environment. Then, using the calculated recharge as an input, several theories on how to best store fresh water in and extract it from the subsurface are tested using the groundwater modelling environment mFLab. Modelled scenarios include the simulation of sustainable urban drainage systems (SUDS) to increase infiltration rates, the use of different hydraulic fill materials to optimize the subsurface storage capacity and the implementation of impermeable barriers along the island borders to minimize losses.

The scenarios are tested and described, using the new island development in the bay of Jakarta, Indonesia as a case study but the ultimate goal is to develop a set of design criteria for subsurface fresh water storage in land developments worldwide.

Seawater intrusion characterization in the coastal section of Sfax superficial aquifer (Tunisia)

R. Trabelsi⁽¹⁾ and M. Zairi⁽¹⁾

⁽¹⁾Laboratoire Eau, Energie et Environnement, Ecole Nationale d'Ingénieurs de Sfax, Sfax University, Sfax, Tunisia.

ABSTRACT

In southern Tunisia, groundwater constitutes the main water resource for agriculture development, industry and drinking water. Consequently, the high demand induces the increase of groundwater quality degradation risk. The salinization and contamination are the main sources of pollution, especially in coastal area, where the potential risk of sea water intrusion, due to over-exploitation, is highly present.

The knowledge of the historical and present rate of movement of the seawater and the determination of the present location of the interface between freshwater and seawater are needed to provide the information required by the authorities to make decisions on changes of management operations.

The shallow aquifer system of the Sfax region, Tunisia is located in the Mio-Pliocene layers formed by sand and clay and with several permeable zones separated by less-permeable beds. During the last 30 years, the intensive pumping combined to the absence of integrated water resources management plan, resulted in the permanent decline of the piezometric head and the degradation of the groundwater quality. The decrease of the well-level appears mainly in the coastal region parallel with the increase of groundwater salinity. We performed a regional hydro chemical study on a total of 1400 shallow groundwater samples within 180 km length and till 10 Km far from the coastline.

The total dissolved solids content of groundwater is highly variable (750–21000 mg/l).

Hydrochemical diagrams and ion balance demonstrated that the salinization is controlled by several intermixed processes such as seawater mixing, anthropogenic contamination, and water–rock interaction. To evaluate the relative degree of seawater mixing, we used the 'Seawater Mixing Index' (SMI) based on the concentration of Na, Mg, Cl, and SO₄ and geophysical logs.

Keywords: Coastal aquifer; Salinization; Seawater Mixing Index; vertical sampling, Tunisia.

INTRODUCTION

In such arid and semi-arid environments, groundwater is a significant part of the total water resource, and plays an important role as a water supply both for drinking and irrigation. Aquifers in the coast are generally fragile and in most of the regions the shallow aquifers are easily depleted due to over exploitation of groundwater.

The present study concerns the coastal area of the Sfax region, Tunisia that is a typical Mediterranean coastal aquifer system. The shallow aquifer system is located in the Mio-Pliocene layer formed by sand and clay and it consists of several permeable zones separated by discontinuous aquitards.

Because of rapid economic growth and lack of precipitation, the use of groundwater resources has increase dramatically. In some region, substantial over-exploitation of groundwater create serious problems, for example, intense mineralization of groundwater, land desertification and salinization, degeneracy of vegetation, lowering of the regional

water table and modification of the natural flow system that induces lateral flow from seawater to the continent. If such situation continues, further deterioration of the environment and ecosystem of the vast area is unavoidable. Some safeguarding measures for groundwater resource protection must be undertaken.

The knowledge of the historical and present rate of the seawater intrusion and the determination of the present location of the interface between freshwater and seawater are needed to provide the information required by the authorities to make decisions of management operations.

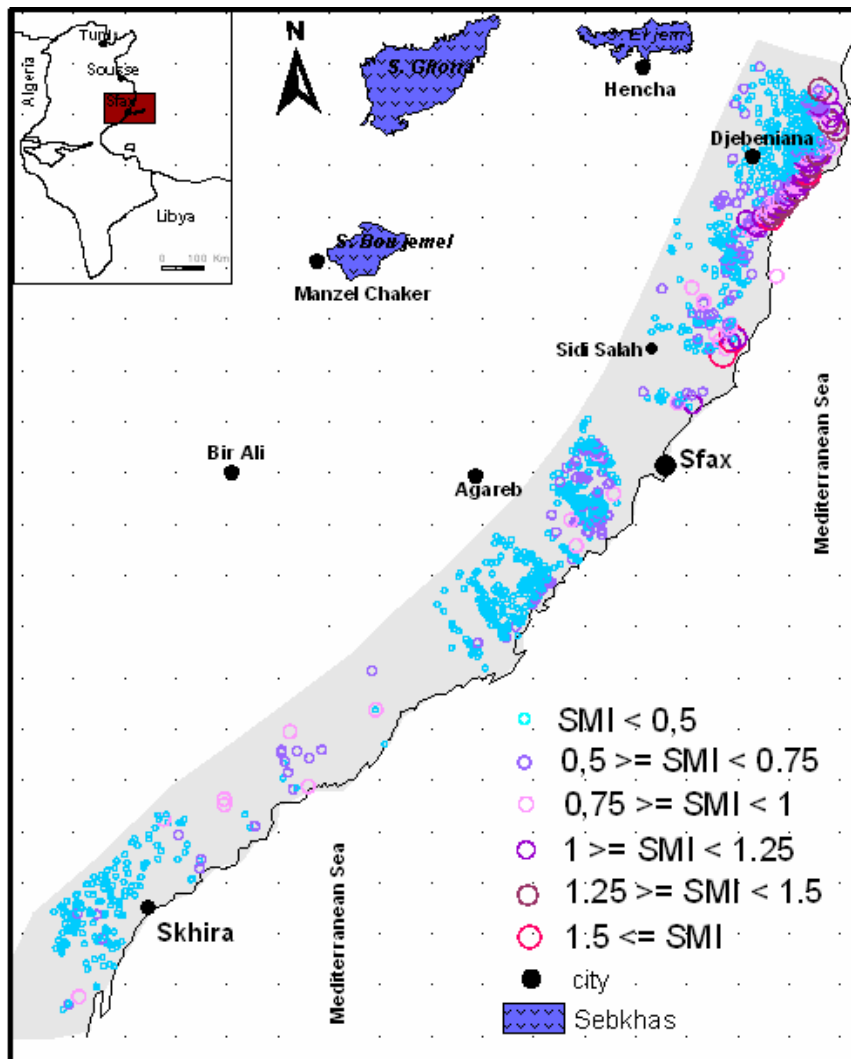


Figure1. Location of study area and spatial distribution of the SMI index.

METHODS

To check the conditions and provide a reasonable assessment of changes and variations in the quantity and quality of groundwater, the historical study presents an important and necessary step. To attempt this aim, we use monitoring data collected by the general direction of water resources (DGRE) during 35 years. More than 180 wells and 50 piezometers are selected to assess the piezometric level and 30 wells to control salinity parameter [CRDA 1970, 1979, 1990, 2001, 2005].

For evaluating the relative degree of seawater mixing, we propose the utilisation of 'Seawater Mixing Index' (SMI) [Park et al. 2005]. This parameter is based on the concentrations of four major ionic constituents in seawater (Na, Cl, Mg, and SO₄) as follow.

$$SMI = a \times \frac{C_{Na}}{T_{Na}} + b \times \frac{C_{Mg}}{T_{Mg}} + c \times \frac{C_{Cl}}{T_{Cl}} + d \times \frac{C_{SO_4}}{T_{SO_4}}$$

Where the constants a, b, c, and d denote the relative concentration proportion of Na, Mg, Cl, and SO₄ in seawater; C is the measured concentration in mg/l; and T represents the regional threshold values of the considered ions, which can be estimated from the interpretation of cumulative probability curves. If the calculated SMI value is greater than 1, the water may be considered to obviously record the effect of seawater mixing.

To apply this methods, we performed a regional hydrochemical study (DGRE, 2003) on a total of 1400 shallow groundwater sampled in coastal band within 180 km length and 10 Km distance from the coastline.

RESULT AND DICUSSION

During the last 30 years, the intensive pumping together with the absence of any integrated water resources management plan, resulted in the permanent decline of the piezometric head and the degradation of the groundwater quality. The decrease of the well-level appears mainly in the coastal region and essentially in coastal zones of Djebeniana, Sidi Abid - El Hajeb (Sfax), Gargour, Sidi Mhadheb, Chaffar and Skhira. The total dissolved solid contents of groundwater are highly variable (750–21000 mg/l). The lowering of the level goes in parallel with the increase of salinity (lower piezometric head in the order of 0.3 m/year and the salinity in the order of 0.15 g/l).

Generally, we note that the intensive exploitation and its effects are very local, they manifest especially in the coastal regions where access is easy to the groundwater. This state is in relation with the important thickness of the aquifer (greater than 75m) and the hydrodynamic characteristics that play in favor of the exploitation.

The effect of the seawater intrusion is visible with a progression of SMI values in direction of the sea, values pass to 0.75 to higher 1.5. The samples from coastal band are affected by the mixture and the phenomenon has a direct impact in the quality of the groundwater and presents the more critical state generally along the entire coastline.

The values of SMI greater than 0.75 are recorded in the areas of Skhira, El Hajeb, the east of the regions of Sidi Salah and Djebeniana region. This observation indicates a sensitivity of these areas to the effect of the seawater intrusion but the more important mixture (SMI>1) is manifested in the northern zone (east of Djebeniana city).

The continuing decline of the piezometric level in the eastern part of Djebeniana city (12 m/ 30 years) and the individualisation of a permanent regional cone of depression confirm the results obtained by the SMI.

In the second step, to examine the lateral and vertical distribution of the SMI in term of distance in relation to the coastline and the depth of each well the charts presentations of figures (2 and 3) are achieved.

On the figure 2, we note that the samples with a SMI greater than 1 have a tendency of preferential localisation at a distance less than 8 km from the coast line. Also, the correlation between SMI and the depths of the wells shows that the influence of seawater intrusion (SMI>1) is virtually absent to a depth greater than 40 m (figure 3).

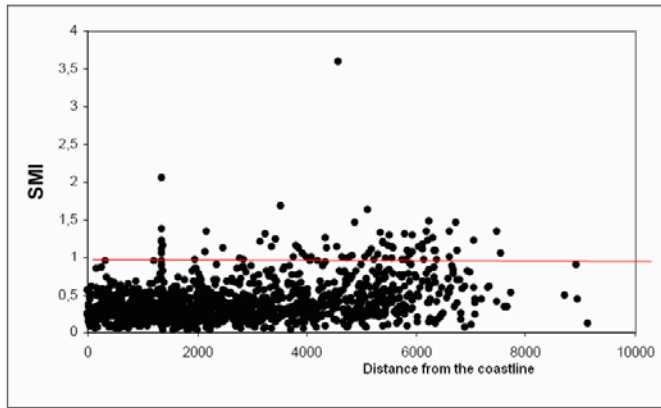


Figure 2. Lateral distribution of SMI index.

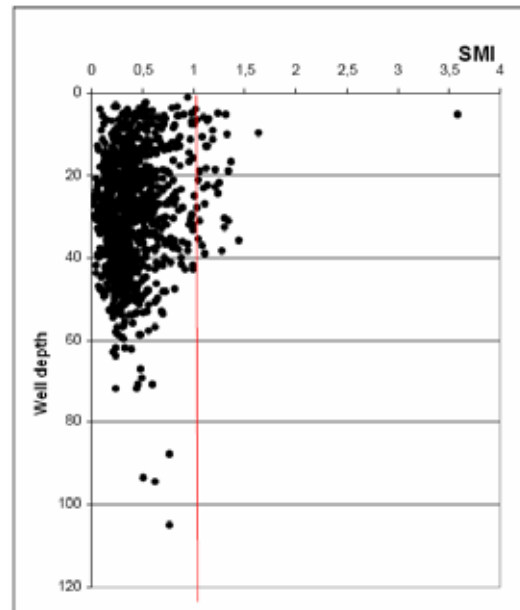


Figure 3. Vertical distribution of SMI index.

CONCLUSION

The interval of current influence of sea water along the groundwater system of the Sahel of Sfax does not exceed the 8 km laterally and 40 m vertically.

The geophysical and hydrochemical logs confirm that seawater intrusion processes and its importance in coastal aquifers is not linked only to the state of the exploitation but it is heavily influenced by the geological complexity of the site (technical, lithology ...) and topographical features, idea confirmed in the work of Pulido-Leboeuf et al (2003) and Barlow (2003).

REFERENCES

Commissariat régional au développement agricole de Sfax. Rapport annuel 1979, 1990, 2001, 2005. *Notes C.R.D.A Sfax*, Tunisie.

Direction générale des ressources en eaux (DGRE). 2005. Etude des nappes aquifères de Sfax : Thème des nappes phréatiques. *Rapport de la société SGF-INC filiale de la Tunisie*, Tunisie, pp 460.

Seh-Ch. Parka., S-T. Yuna., G-T. Chaea., I-S. Yooa., K-S. Shina., Ch-H. Heoa., S-K. Lee. 2005. Regional hydrochemical study on salinization of coastal aquifers, western coastal area of South Korea. *Journal of Hydrology* 313 (2005) 182–194

A.Pulido Bosch., P. Leboeuf., J. Gisbert., F. Sánchez Martos. and A. Vallejos. 2003. Forages littoraux et usines de dessalement. *Coastal aquifers intrusion technology : Mediterranean countries, TIAC03, Espagne*.

P.M. Barlow. 2003. Ground Water in Freshwater-Saltwater Environments of the Atlantic Coast. *U.S. Department of the Interior, U.S. Geological Survey, Circular 1262*, pp 113.

Contact Information: Trabelsi R, University of Sfax, Département sciences de la terre, Route de Soukra km 3.5 - B.P. n° 1171 – 3000, Sfax, Tunisie. Phone: (+216) 74 27 64 00 - 74 27 67 63, Fax: (+216) 74 27 44 37, Email:trabrouaida@yahoo.fr

Evidence and causes of groundwater level fluctuations in a semiconfined mediterranean coastal aquifer. The ocean tide effect

Angela Vallejos¹, Fernando Sola¹ and Antonio Pulido-Bosch¹

¹Water Resources and Environmental Geology, University of Almería, Spain

ABSTRACT

Coastal aquifers are complex because of the combined influences of marine oscillations and landward groundwater forces. The piezometric level is affected by these natural processes, each of which has its own cyclicity and range, resulting in a complex sequence of water level. This paper reports a field study that was conducted from May 2012 to July 2013, monitoring salinity using electrical conductivity (EC) measurements and groundwater levels in a coastal detrital aquifer in Almería (SE Spain). The monitoring wells used were installed near the top of the tidal zone on the beach front. Data on tidal level and the significant wave height were collected by the National Oceanographic Administration. The major objective of this study is to analyse the groundwater level fluctuations affected by rainfall, tides and waves, and to determine their implications on seawater intrusion dynamics.

Infiltration of precipitation is the most common and immediate cause of groundwater level rise. The study period was particularly dry and during this period the rise in groundwater level was approximately 25-30 cm, not identifying a seasonal cyclicity. Sea level fluctuations due to tidal action have had a clear influence on groundwater level. The maximum amplitude of sea level variations due to tides was 40 cm, causing groundwater level variations up to 15 cm. Tide-induced groundwater fluctuations were modeled using the analytical solution for unconfined coastal aquifers proposed by Li et al. (2000). To establish the degree of confinement in the studied aquifer the analytical solution proposed by Jiao and Tang (1999) has also been used. Respect to the influence of waves, there is a clear correlation between maximum wave height and the peaks corresponding to water table elevation. The main conclusion arrived at in this work is the greatest effect of precipitation on piezometric level, followed by the wave action, while tidal cycles caused variations of smaller amplitude in the piezometric logs. All these oscillations affect the position of the fresh water-seawater interface. The attenuation of tidal amplitude at the monitoring wells compared to the simulations calculated reveals certain differences, and this is due to the semiconfined nature of the aquifer. Groundwater conductivity and temperature are also seen to change with respect to the phase of the tides, with a symmetrical lag similar to that of water level in the well.

Contact Information: Angela Vallejos, Water Resources and Environmental Geology. University of Almería. 04120 Almería, SPAIN, Phone: 34-950-015-874, Email: avallejo@ual.es

Lessons learned from a regional variable density groundwater flow model and implemented climate change scenarios: a Dutch case

E.S. van Baaren¹, G.H.P. Oude Essink¹, G.M.C.M. Janssen¹, P.G.B. de Louw¹ and J. Verkaik¹

¹Subsurface and Groundwater Systems, Deltares, Utrecht, The Netherlands

ABSTRACT

The fresh groundwater resources of the Province of Zeeland, The Netherlands, are jeopardized by various causes. Floods, droughts and salinisation of the ground and surface waters are some pressing topics. Sea level rise and climate change threaten the fresh groundwater resources even more. For Zeeland, a 3D-model for density-dependent groundwater flow and coupled solute transport was developed to assess the impact of sea level rise and changing precipitation and evapotranspiration patterns on the freshening and salinisation processes of shallow groundwater systems. SWIM21, the building of the 3D numerical model was presented with the focus on the determination of the complex initial chloride distribution, using different types of (geophysical) techniques (Van Baaren et al). SWIM22, the use of the model as an interpolator to improve the 3D fresh-brackish-saline distribution was presented (Oude Essink et al). For SWIM23, the focus will be on the steps we have taken to improve the quality of this regional model (15 million model cells), and subsequently, on the results of the climate change scenario's. The first problem we had to tackle was the model size. We used a 64-bits computer, converted the MOCDENS3D software to 64-bits, and made sub-models to speed up the simulation time. The next step would be to use the beta version of a parallel computing version of SEAWAT. On top of these ICT-technological changes, we had a close hydrogeological look at the top of the groundwater system in order to decrease the largest fluxes which –through stability criteria– largely determine the length of the transport time steps. In order to improve the accuracy of the modelling results to monitoring values, we did tests with the number of particles and transient versus steady state groundwater flow. By building this model, we think we found a balance between simulation time and accuracy for regional variable-density groundwater flow models that use the particle tracking method for advective transport (like SEAWAT). At the end of this learning process, we implemented climate scenarios in order to predict the effects on the groundwater system. With this model we can offer two results for other low-lying saline deltaic areas: 1. the lessons learned and research questions for the balance between calculation time and accuracy for regional variable-density groundwater flow models and 2. the effects of climate change on the groundwater system.

Contact Information: Esther (E.S.) van Baaren, Deltares, unit Subsurface and Groundwater systems, Princetonaan 6-8, 3584 CB Utrecht, Postbus 85467, 3508 AL Utrecht, the Netherlands, Phone: +31(0)615609982, Email: Esther.vanBaaren@Deltares.nl

Sharing precious water volumes in The Water Farm: from concept towards practice

E.S. van Baaren¹, B.T. Ottow², G.H.P. Oude Essink¹ and P. Pauw^{1,3}

¹Subsurface and Groundwater Systems, Deltares, Utrecht, The Netherlands

²Scenarios and Policy Analysis, Deltares, Utrecht, The Netherlands

³Wageningen University, Wageningen, The Netherlands

ABSTRACT

On the Walcheren peninsula in the Netherlands, the majority of the groundwater and surface water is saline. As a consequence, the area suffers from drought and salt damage to agricultural crops. Farmers are used to accept these damages because no solution seemed available. In addition, climate change scenarios predict decrease of the available fresh water. Though investments for climate change are not common business for farmers, solutions need to be invented today for a climate robust fresh water supply. To explore potential solutions, the concept of the Water Farm was founded in 2007. The Water Farm is a cooperation of farmers, landowners, water board, etc. to manage (e.g., receive, store, use, process, deliver) fresh water in the region in such a way that no water from elsewhere needs to be invoked. It has been applied in practice in 2010, in a 3 km² area on Walcheren. Applied research is combined with the practical knowledge of farmers and the policies and regulations of the government. We introduced a framework of interaction between (geo)hydrological knowledge and process for participation. The technological input was the start of the process. Researchers presented their knowledge of the watersystem and possible measures to improve the fresh water supply. By participation of the farmers in the technological input (measurements, input numerical models by local knowledge), the technological insights increased and farmers found out that acceptance of salt and drought damage is not necessary. Tools in this framework are participative monitoring of (ground)water, workshops with maps, field excursions and participative decision making. We used various groundwater monitoring techniques and variable density groundwater models to design measures and to explain and understand the system. So far, the following improvements in the water system have been achieved: 1) isolation of saline seepage by simple dams, 2) storage of groundwater in the subsoil by controlled drainage, 3) installation and testing of an innovative artificial recharge system to increase a fresh water lens, 4) change in the water management (store instead of flush away fresh water) and 5) 'green deal' with the national government and consideration of change of regulations for managed aquifer recharge and recovery. We believe that the concept of the Water Farm could be used in all kinds of water problems worldwide and will help to bring (applied) scientific results into practice.

Contact Information: Esther (E.S.) van Baaren, Deltares, unit Subsurface and Groundwater systems, Princetonlaan 6-8, 3584 CB Utrecht, Postbus 85467, 3508 AL Utrecht, the Netherlands, Phone: +31(0)615609982, Email: Esther.vanBaaren@Deltares.nl

Cone Penetration Tests with electrical conductivity for fresh-salt water investigations

Kees-Jan van der Made¹, Michel Groen² and Frans Schaars³

¹ Wiertsema & Partners, Tolbert, the Netherlands

² Vrije Universiteit, Amsterdam, the Netherlands

³ Artesia BV, Schoonhoven, Netherlands

ABSTRACT

For fresh – salt water investigations in river deltas and other coastal areas, geophysical methods, based on contrasts in the electric conductivity of salt - and fresh water are commonly used. Ground truth is often derived from borehole logs and chemical analysis of groundwater samples obtained from monitoring wells. Cone Penetration Tests with simultaneous measurement of the soils electrical conductivity offer a cost effective alternative for investigations in areas with a soil profile consisting of unconsolidated sediments, providing an almost continuous profile with a resolution that does not diminish with depth. The technique has recently been applied in several projects ranging from groundwater exploration studies, ASR projects for storage of fresh water in salt water aquifers to environmental impact studies related to large scale coastal protection projects. In these case studies the CPT data have been compared to data from different geophysical techniques obtained from measurements carried out at the surface, airborne measurements, lithological and geophysical borehole logs and chemical analysis from monitoring wells, proving the accuracy of the in situ CPT measurements and added value for the interpretation of the data obtained by other geophysical techniques.



Figure 1. CPT investigation on the beach at the Dutch coast.

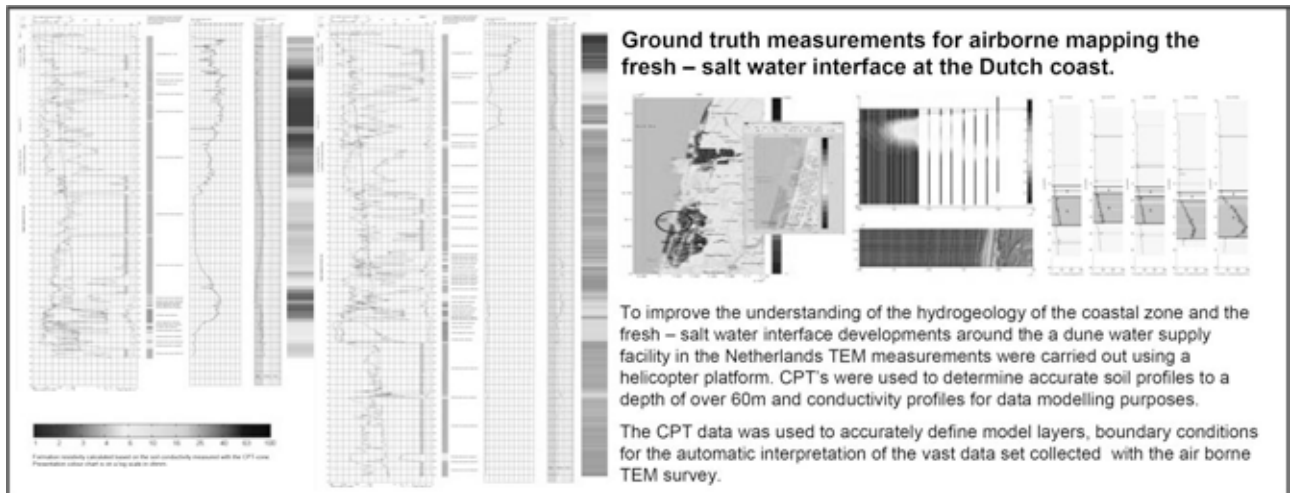


Figure 2. CPT results including soil conductivity to 60m depth with a resolution of 2cm.

Contact Information: Kees-Jan van der Made, Wiertsema & Partners, Feithspark 6
9356 BZ Tolbert, the Netherlands, Email: c.made@wiertsema.nl

Guiding Principles for Fresh Water Lens Development, Exploitation and Maintenance in Artificial Islands

Marloes van Ginkel^{1,2}, Th.N. Olsthoorn^{1,3}, M.L. Tijs^{1,2}

¹ Water Resources Department, Delft University of Technology, Delft, the Netherlands

² Rivers Deltas Coasts, Royal HaskoningDHV, Rotterdam, the Netherlands

³ Hydrology, Waternet, Amsterdam, the Netherlands

ABSTRACT

A fresh water lens may develop under newly constructed artificial islands in the ocean. The thus developed fresh water lens can be incorporated in the water supply system of the envisaged development on the island. The conditions for fresh water lens development can be optimized in artificial islands, since these islands are designed from scratch and the technical possibilities of dredging material and dredging equipment are large.

However, there is currently little guidance on methods for optimizing artificial islands for fresh water lens development. We address this gap looking at the factors affecting 1) the development, 2) the exploitation and 3) the maintenance of fresh water lenses. Based on numerical analysis of fresh water lens development in three land reclamation projects, we present design principles regarding the shape and characteristics of artificial islands and the capacity and continuity of recharge.

We conclude that optimization of artificial islands for fresh water lens development, exploitation and maintenance is technically feasible.

INTRODUCTION

An artificial island, also called land reclamation, is a newly constructed island in the ocean; the most well-known are the World Islands in Dubai with a mainly touristic purpose. The port of Rotterdam in the Netherlands has a history of land reclamations for port development; the latest is Maasvlakte II which was officially opened in May 2013. The port of Rotterdam is not unique for its reclamation sites since all over the world artificial islands are constructed for port and industrial development.

In recent years, we see a trend of land reclamations for urban expansion in densely populated delta cities. Population growth, urbanization and economic development result in an increasing pressure on available space. Land reclamations are used to meet this growing need. An example is Pluit City in Jakarta.

Water demand on the newly constructed islands includes water for domestic purposes, drinking water, irrigation and industrial purposes like firefighting and dust prevention. Safeguarding the fresh water supply is one of the major challenges. Since the island is constructed in the ocean, there is no fresh water available to meet the water demand of the future land use. Fresh water is usually supplied by pipeline from the main land, or by

desalination of seawater, and some small-scale rainwater harvesting and reuse. It is interesting to have seasonal or emergency storage of fresh water on the island to decrease the dependency on supply from the mainland and/or to decrease the costs related to desalination.

A fresh water lens may develop under newly constructed artificial islands in the ocean. The thus developed fresh water lens can be incorporated in the water supply system of the envisaged development on the island. The conditions for fresh water lens development can be optimized in artificial islands, since these islands are designed from scratch and the technical possibilities of dredging material and dredging equipment are large. However, there is currently little guidance on methods for optimizing artificial islands for fresh water lens development. We address this gap looking at the factors affecting the development, the exploitation and the maintenance of fresh water lenses.

METHODS

Generally loose, medium grained quartz sand is considered to be most suitable for the construction of artificial islands if it is available within an acceptable haulage distance from the project location. The properties of the sand change during the dredging process. The choices for dredging equipment are dependent on water depth, soil type, volume and required accuracy. Depending on site-specific conditions mechanical or hydraulic suction dredging is applied. The sand is transported through a pipeline or by ship from the borrow site to the project site. Ground improvement techniques are often applied to improve the geotechnical properties of the island.

There are no general geotechnical design guidelines. The required geotechnical properties of the island follow from the performance requirements of the future land use and are therefore site-specific. These properties include the strength (bearing capacity), stiffness (settlement), density (resistance against liquefaction), permeability (drainage capacity) and elevation (safety against flooding).

In this research the geotechnical properties and hydrological characteristics of three land reclamation projects are used to study the potential fresh water lens development in land reclamations. The SEAWAT computer code (Langevin et al. 2008) in the mLab environment (Olsthoorn 2013) was applied for numerical simulations. The three land reclamations are The World in Dubai, Maasvlakte II in the Netherlands and Pluit City in Jakarta.

RESULTS

Island G19 in Dubai is part of the World archipelago. It is a circular island of 3 ha which was constructed in the period 2003-2008. It is composed of sand dredged from the shallow coastal waters. Dubai has a tropical desert climate; hot, humid and extremely dry with five days rainfall per year on average. On the island are an estate and a palm plantation which is irrigated with desalinated water.

Maasvlakte II in the Netherlands was constructed in the period 2008-2013. It is an island of 2000 ha composed of sand from a borrow pit 11 km off the Dutch coast. Canals of 20 m depth for sea-going vessels are dredged and therefore Maasvlakte II may be considered as

strip islands with typical widths of 1000 m. The Netherlands have a moderate climate with a relatively equal precipitation distribution throughout the year. At the moment three container terminals are constructed on Maasvlakte II. Water for industrial purposes is supplied by pipeline.

Several islands will be constructed in Jakarta Bay as part of the Jakarta Coastal Development Strategy. Pluit City is designed for commercial and residential purposes; it is envisaged to inhabit 200.000 inhabitants. Jakarta has a tropical monsoon climate with distinct wet and dry seasons. Water for the future city will be supplied by pipeline or desalination.

The specific characteristics of the islands and the results of the numerical simulations of lens development will be presented at the Salt Water Intrusion Meeting for the three reclamation projects including measures for optimization. One of the optimizations is the application of subsurface cut-off walls (Des Tombe et al. 2012). Based on the numerical analysis, we will present general design principles regarding the shape and characteristics of artificial islands and the capacity and continuity of recharge. The best solution for a specific case is dependent on site-specific circumstances.

An especially interesting aspect is how the fresh water lens can be exploited and maintained. The modeling results show that the fresh water lens in the three land reclamations is thin and fresh water recovery will soon result in salt water upconing. From literature we know that horizontal wells (for example Stoeckl and Houben 2012), shallow skimming wells (see for example Sufi et al. 1998 and Zuurbier et al. 2014) can be applied to diminish the effect of salt water upconing. This effect can also be reduced by horizontal layering with layers of higher and lower conductivity, which can be constructed during the reclamation works. Simulation results will be presented at the Salt Water Intrusion Meeting.

It is worthwhile to have a permanent measurement system to operate and maintain the fresh water lens as optimally as possible. Options for a permanent measurement system with electromagnetic cables constructed in the subsurface of the island will be presented.

DISCUSSION AND CONCLUSIONS

In this research the geotechnical properties and hydrological characteristics of three land reclamation projects were used to study the potential fresh water lens development in land reclamations. We conclude that optimization of artificial islands for fresh water lens development, exploitation and maintenance is technically feasible. The best solution for a specific case is dependent on site-specific circumstances. It is worthwhile to link the civil engineering design and water management for future functions in an early design phase. The business case determines whether the optimizations for fresh water lens development, exploitation and maintenance will actually be applied in specific cases.

REFERENCES

Des Tombe, B., M. van Ginkel, Th.N. Olsthoorn, 2012. Aquifer Storage Recovery, the Storage Tank Method. In Proceedings of Salt Water Intrusion Meeting 22, October 2012, Buzios Brazil.

Langevin, C.D., D.T. Thorne, Jr., A.M. Dausman, M.C. Sukop, and W. Guo. 2008. SEAWAT Version 4: A Computer Program for Simulation of Multi-Species Solute and Heat Transport: U.S. Geological Survey techniques and Methods Book 6, Chapter A22, 39.

Olsthoorn, T.N. 2013. <http://code.google.com/p/mflab>

Stoeckl, L. and Houben, G. 2012. Flow dynamics and age stratification of fresh water lenses: experiments and modeling. *Journal of Hydrology*, 458-459: 9-15.

Sufi, A.B., M. Latif and G.V. Skogerboe. 1998. Simulating skimming well techniques for sustainable exploitation of groundwater. *Irrigation and Drainage Systems* 12: 203-226.

Zuurbier, K.G., W.J. Zaadnoordijk, P.J. Stuyfzand. 2014. How multiple partially penetrating wells improve the fresh water recovery of coastal aquifer storage and recovery (ASR) systems: A field and modeling study. *Journal of Hydrology* 509: 430-441.

Contact Information: Marloes van Ginkel, Delft University of Technology, Water Resources Department & Royal HaskoningDHV, Rivers Deltas Coasts. Email: Marloes.vanginkel@gmail.com

eMOD : a MATLAB application for MODFLOW-based groundwater flow and solute transport models

Alexander Vandenbohede

Department Geology and Soil Science, Ghent University, Gent, Belgium

ABSTRACT

eMOD, or elementary MODFLOW, is a freeware software package to prepare input files and handle output for the groundwater flow model MODFLOW2005, the density dependent multi-species solute transport model SEAWAT and the reactive transport model PHT3D.

INTRODUCTION

eMOD (Vandenbohede, 2013) provides a no-nonsense approach to simulations. ‘Elementary’ means that the interface to work with MODFLOW based simulations is simple and easy to use and learn. It also means that input not essential to the simulation is kept to a minimum. The user works directly with the different packages which implies that there is no handling of data which is not controlled by the user. Therefore models can be made in a flexible way and can be easily modified to experiment with different conceptual models or parameter combination. The aim of eMOD is to apply simulations straightforward to gain insight in a groundwater system, without losing oneself unnecessary in a complex user interface.

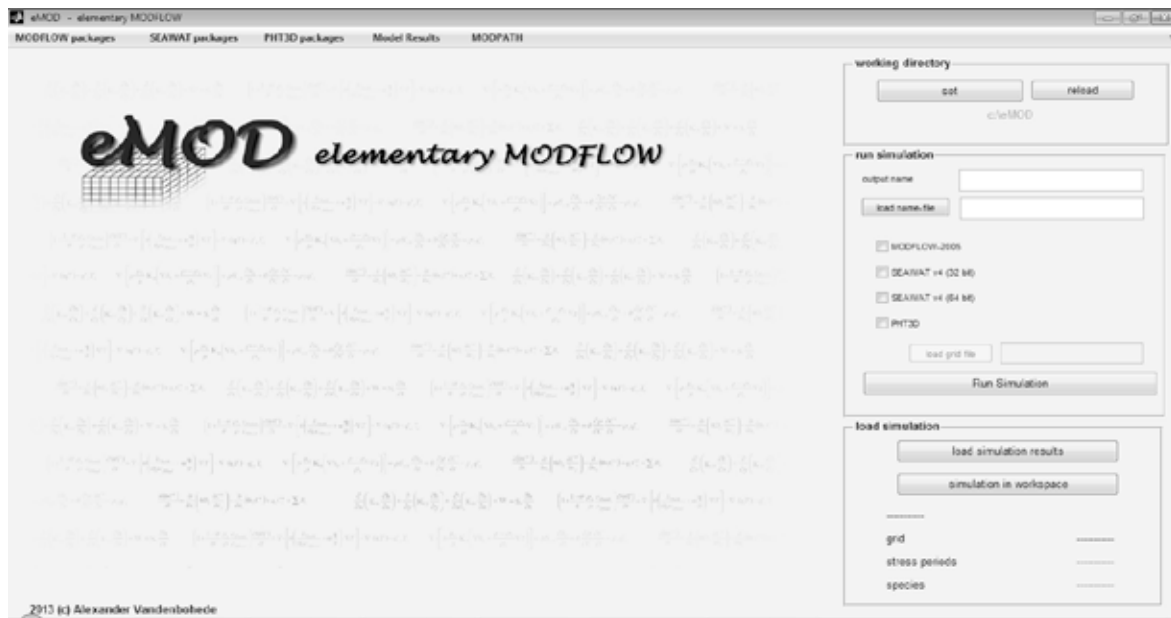


Figure 1. Main window of eMOD.

Possible disadvantage of this approach is that no GIS system is provided to define simulation input or to visualize output. However, model output can be easily exported in a format which can be loaded in GIS software. Also, the input can be made with the assistance of GIS software using xls(x)-files as a link between GIS and eMOD.

INPUT AND OUTPUT

The current eMOD version supports following MODFLOW2005 (Harbaugh, 2005) packages: discretization (dis), basic (bas), block centered flow (bcf), layer property flow (lpf), horizontal barrier flow (hfb), constant head boundary (chd), recharge (rch), well (wel), evapotranspiration (evt), multi-node well (mnw1 and mnw2), river (riv), drainage (drn), lake (lak), streamflow-routing (sfr), unsaturated-zone flow (ufz), general head boundary (ghb), strongly implicit procedure (sip), preconditioned conjugate-gradient (pcg) and, direct solver (de4) package. It supports following MT3D-MS packages: basic transport (btn), advection (adv), dispersion (dsp), sink-source mixing (ssm) and, generalized conjugate-gradient (gcg) package. It supports following SEAWAT (Langevin et al., 2007) packages: variable-density flow (vdf) and viscosity (vsc) package. It supports following PHT3D (Prommer and Post, 2010) packages: interface package and database file.

Input to prepare these packages is via interactive GUIs (figure 2a) combined with excel spread sheets (xls(x)-files). Hereby, for instance, MATLAB, PYTHON or a GIS program can be used to make the spread sheets in a flexible way in case the input becomes large or complicated. A special package is included to prepare input for radial flow cases (i.e. aquifer tests, upconing, aquifer storage and recovery) which automatically recalculates relevant parameters from a radial geometry to the Cartesian geometry used by MODFLOW (Langevin, 2008; Louwyck et al., 2012; Vandenbohede et al., 2014; Wallis et al., 2013).



Figure 2. Example of an input GUI, here for the btn package (a) and an example of a GUI to plot simulation output, here to plot horizontal cross-sections (b).

Output can be visualized with cross-sections (Figure 2b), movies and graphs showing aquifer heads, concentrations and/or flow vectors. Pathlines and capture zones can be calculated using MODPATH and be visualized in a number of ways.

AVAILABILITY

eMOD is programmed as a MATLAB tool but can also be used as a stand-alone application. The advantage of using eMOD as a MATLAB application is that full use of the functionalities of MATLAB can be made. The advantage of using eMOD as a stand-alone application is, of course, that MATLAB is not needed.

eMOD is freeware and is available for download at the repository on <https://github.com/eMOD/> where you find a folder containing a manual and the software.

REFERENCES

Harbaugh, A.W. 2005. MODFLOW-2005, the U.S. Geological Survey modular ground-water model - the Ground-Water Flow Process, U.S. Geological Survey Techniques and Methods 6-A16.

Langevin, C.D. 2008. Modeling axisymmetric flow and transport. *Ground Water* 46(4):579-590.

Langevin, C.D., D.T. Thorne, A.M. Dausman, M.C. Sukop, W. Gu., 2007. SEAWAT Version 4: a computer program for simulation of multi-species solute and heat transport. US Geol. Surv. Tech. Methods, Book 6, chap. A22, US Geological Survey Reston, VA.

Louwyck, A., A. Vandenbohede, M. Bakker, L. Lebbe. 2012. Simulation of axi-symmetric flow towards wells: a finite-difference approach. *Computers & Geosciences* 44:136-145.

Prommer, H., V. Post. 2010. PHT3D, a reactive multicomponent transport model for saturated porous media. User's Manual v2.10, <http://www.pht3d.org>.

Vandenbohede, A. 2013. eMOD - elementary MODFLOW: a MATLAB Application for MODFLOW-based Groundwater Flow and Solute Transport Models. Department Geology and Soil Science, Ghent University.

Vandenbohede, A., A. Louwyck, N. Vlamynck. 2014. SEAWAT-based simulation of axisymmetric heat transport. *Groundwater*:doi: 10.1111/gwat.12137.

Wallis, I., H. Prommer, V. Post, A. Vandenbohede, C.T. Simmons. 2013. Simulating MODFLOW-based reactive transport under radially symmetric flow conditions. *Ground Water* 51(3):398-413.

Contact Information: Alexander Vandenbohede, Ghent University, Department Geology and Soil Sciences, Krijgslaan 281 (S8), Gent, Belgium, Phone: 32-9-2644652, Fax: 32-9-2644653, Email: avdenboh@yahoo.co.uk

Seawater intrusion in the southern Po Plain, Italy: managing a geologic and historical heritage

Alexander Vandenbohede¹, Pauline N. Mollema², Nicolas Greggio², and Marco Antonellini²

¹ Department Geology and Soil Science, Ghent University, Gent, Belgium

² Integrated Geoscience Research Group, University of Bologna, Ravenna, Italy.

ABSTRACT

Irrigation in low-lying coastal plains may enhance the formation of fresh groundwater lenses and counteract salinization of groundwater and soil. This is discussed for the unconfined aquifer in the coastal plain near Ravenna, Italy. In this study area for example, a freshwater lens originates from an infiltration ditch used as a water reservoir for spray irrigation. Such incidental aquifer recharge practice from irrigation currently provides the only active freshening of an overall saline to brackish aquifer. The extend of the freshwater lens is controlled by the presence of drainage ditches, water level in ditches and rate of sea level rise. An integrated planning of irrigation within the water management of the coastal zone is necessary to have maximum benefits for freshening of the aquifer and making optimal use of the existing water and irrigation infrastructure.

INTRODUCTION

In low-lying coastal areas, groundwater is saline because of many interacting natural and human causes. The result is a complex distribution of freshwater and saltwater whereby the freshwater resources are often limited or under threat. This is not different for the coastal aquifer of the southern Po plain, Italy (Antonellini, 2008; Mollema et al., 2012). The study area (figure 1a) is located along the Adriatic coastline, south of Ravenna. From Roman times onward, human activity altered the layout of the Po plain and the coastline is currently characterized by river and canal mouths, wetlands, lagoons, developed areas with industrial facilities and reclaimed agricultural land.

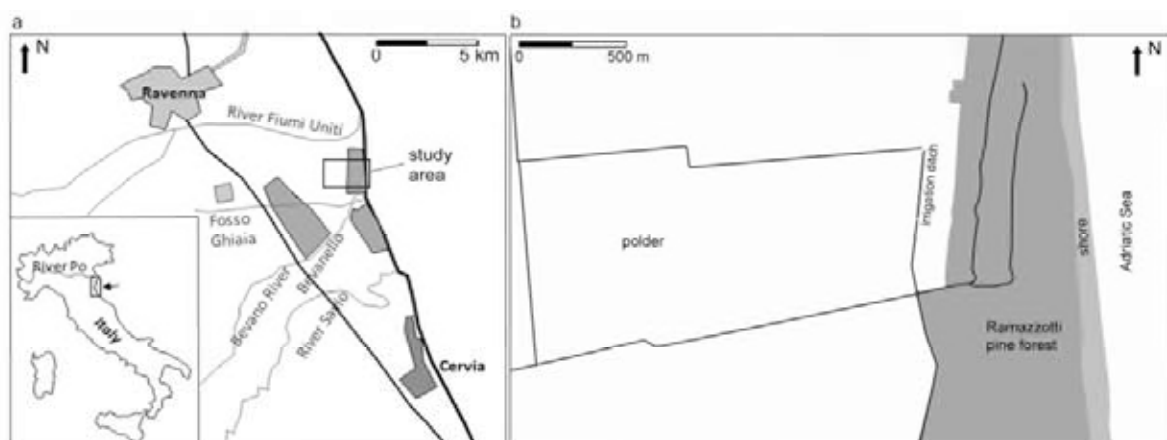


Figure 1. Location of the study area in the Po river plain (a) and detailed map of the field site (b) with indication of the major ditches (black lines).

FRESHWATER LENSES FROM IRRIGATION

Irrigation results in the formation of freshwater lenses via infiltration from irrigation water storage reservoirs into the aquifer. This, nowadays, is the only active freshening process of the aquifer (Greggio et al., 2012). A field example illustrates that a relatively large volume of freshwater can accumulate in the subsurface (Vandenbohede et al., 2014). The system is located in the polder bordering a coastal pine forest. It consists of a ditch used as a water reservoir (figure 1b). The water is used to irrigate the adjacent farmland with a sprinkler installation. Besides the ditch used for irrigation, a number of other ditches are used for drainage. Two such examples are present in the pine forest. A freshwater body accumulates in the aquifer between the irrigation ditch and the drainage ditches (figure 2). The freshwater body exhibits a clear seasonality. The level in the irrigation ditch is raised during the irrigation season (April to August) and water can freely infiltrate the aquifer. This results in an increase of the freshwater volume below the ditch up to a low permeable layer located at -8 m asl (above sea level). In between irrigation seasons, there is a flow reversal whereby there is an upward flow towards the ditch. Consequently, there is an up-coning of the fresh-saltwater interface towards the ditch and the amount of fresh water in the aquifer decreases. In terms of budget, however, there is an overall surplus of freshwater infiltration, which creates a permanent freshwater lens. Field observations (infiltration estimates, geophysical survey, water balance calculations) and numerical modelling, show that this freshwater lens is solely due to infiltration from the irrigation ditch whereby the contribution of the water sprinkled on the farmland is negligible.

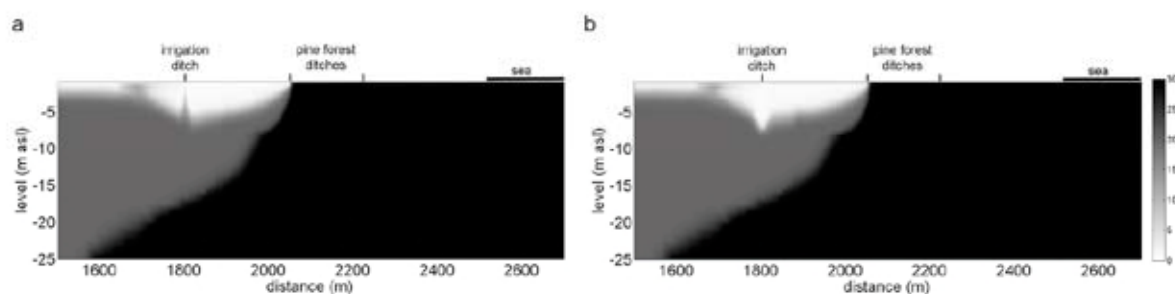


Figure 2. Simulated salinity (g/L) at the end of March (a) and at the end of August (b). The irrigated farmland is located between the irrigation ditch and the pine forest.

SCENARIO MODELING

A number of alternative scenarios were simulated. First, the water level in the irrigation ditch is kept high and freshwater can infiltrate into the aquifer during a whole year period (figure 3a). Evidently, the amount of freshwater increases with respect to the reference case of figure 2. After 30 years, there is twice more freshwater in the aquifer than by applying only a seasonal increase of the water level in the drainage ditch. The seaward extension of the freshwater lens remains defined by the pine forest drainage ditch. The aquifer between the drainage ditch in the pine forest and the irrigation ditch is now completely fresh down to the low permeable layer.

Case 2 differs from the baseline situation by a 30 cm lower level in the irrigation ditch during the irrigation season. The result is a similar seasonal change in freshwater volume but with the difference that the lens is smaller (figure 3b), because of the lower infiltration rate. Freshwater under the ditch nearly extends to the low permeable layer by the end of August

and freshwater between the irrigation and drainage ditches is only present in the shallow part of the aquifer.

Case 3 aims to investigate the impact of multiple ditches where freshwater can infiltrate. The intention, here, is to increase the lateral extension of the freshwater lens by increasing also the water level in the landward ditch within the pine forest. In this case, the pine forest ditch works as an irrigation ditch during the irrigation season and as a drainage ditch otherwise (figure 3c). The seaward ditch in the pine forest remains a drain throughout the year. This results in a freshwater lens that extends seaward under the pine forest towards the seaward drainage ditch. Freshwater, in this simulation, is present between the two ditches in the pine forest. Aquifer recharge from the ditches, however, is limited and the freshwater lens develops in the shallow part of the aquifer and its lateral extension west of the irrigation ditch is small.

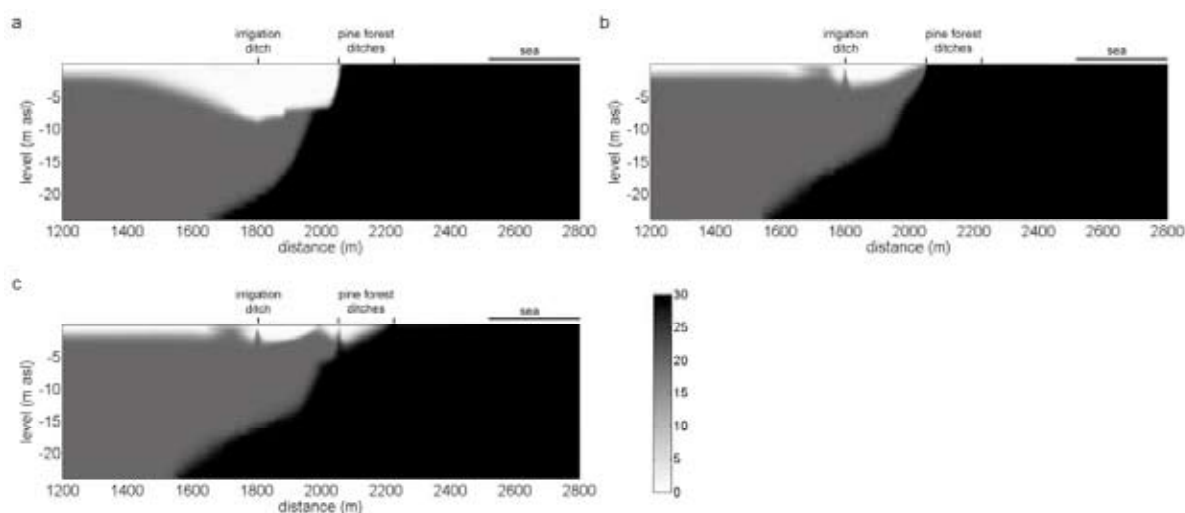


Figure 3. Salinity (g/L) after 30 years for case 1 (a), case 2 (b) and case 3(c) using alternative irrigation scenarios and water level management in the ditches.

In general, sea level rise decreases the volume of freshwater in coastal areas and this is not different here. The influence of a sea level rise of 60 cm and of 100 cm per century was simulated. Initially, the extension of the freshwater lens increases, because the lens is not yet in equilibrium. The volume decreases, however, after 20 and 50 years of sea level rise, respectively for a rate of 60 and 100 cm per century. Sea level rise causes a larger inland-directed hydraulic gradient compared to the current situation. Consequently, there is an increase in the landward groundwater flux and an increased saline seepage to the artificially drained agricultural fields.

DISCUSSION AND CONCLUSIONS

Irrigation could have important implications in terms of mitigation of the saline seepage to shallow groundwater and surface water as well as to soil quality preservation of low-lying coastal zones with a (semi)-arid or subhumid climate. The monitoring and modeling results from the Ravenna field site illustrate that a relatively large volume of freshwater can be accumulated provided that this type of irrigation with recharge from a storage pond is maintained over several years. By making use of the existing hydraulic infrastructure of irrigation and drainage ditches, the freshwater lenses can be maintained and even forced to increase. Different engineering measures (e.g. managed aquifer recharge using injection wells or infiltration ponds, deep drainage instead of surficial drainage) are applied to

enhance freshwater recharge but these are often costly options. Freshening of the aquifer as side-effect from irrigation could be a low-cost alternative to these other techniques.

Careful planning and managing of the water levels is necessary as is shown by the simulation of the different scenarios. Such managed irrigation and aquifer recharge practices should be included in long-term coastal zone development integrating groundwater extraction, drainage, irrigation, geomorphologic changes (e.g. to the coastline), and relevant socio-economic and environmental factors. The management of these irrigation water lenses should be considered within the principles of integrated water resources management aimed to address typical water quality and quantity concerns by optimizing water management and sustainability under the provisions of the Water Framework Directive implementation.

In the specific case of the Ravenna coastal plain, this means, for instance, taking into account the relative sea level rise. The necessary low water levels in the agricultural fields form a pre-conditioned constrained situation that will cause further stresses from saltwater seepage due to a rising sea level and a subsiding land surface over the next decades. This means that the currently present freshwater lenses will become smaller. A good planning, taking into account sea level rise, is necessary if surplus irrigation water is used for freshening the aquifer at new locations.

REFERENCES

Antonellini, M., P. Mollema, B. Giambastiani, K. Bishop, L. Caruso, A. Minchio, L. Pellegrini, M. Sabia, E. Ulazzi, and G. Gabbianelli. 2008. Salt water intrusion in the coastal aquifer of the southern Po Plain, Italy. *Hydrogeology Journal* 16:1541-1556.

Greggio, N., P. Mollema, M. Antonellini, G. Gabbianelli. 2012. Irrigation management in coastal zones to prevent soil and groundwater salinization. In: Abrol V, Peeyush S (edt.) *Resource management for sustainable agriculture*, Intech.

Mollema, P., M. Antonellini, G. Gabbianelli, M. Laghi, V. Marconi, and A. Minchio A. 2012. Climate and water budget change of a Mediterranean coastal watershed, Ravenna, Italy. *Environmental Earth Sciences* 65, 1:257-276.

Vandenbohede, A., P. Mollema, N. Greggio, M. Antonellini. 2014. Seasonal dynamic of a shallow freshwater lens due to irrigation in the coastal plain of Ravenna, Italy. *Hydrogeology Journal*, doi: 10.1007/s10040-014-1099-z.

Contact Information: Alexander Vandenbohede, Ghent University, Department Geology and Soil Sciences, Krijgslaan 281 (S8), Gent, Belgium, Phone: 32-9-2644652, Fax: 32-9-2644653, Email: avdenboh@yahoo.co.uk

Military inundations at the Yser front: the groundwater perspective

Alexander Vandenbohede

Department Geology and Soil Science, Ghent University, Gent, Belgium

ABSTRACT

The last week of October 1914 was a decisive period during the Great War. The German advance through Belgium could only be stopped by a military inundation of the polders near the river Yser. A number of hydro(geo)logical questions about this famous inundation are discussed. It is shown how water management of the polder area, composition of the subsurface and a chance factor, i.e. the weather, all contributed to the efficient realization of the inundation and the successful maintenance of it until 1918.

INTRODUCTION

On 9 October 1914, after two months of constant retreat for the Belgian and Entente armies, the Belgian king elected to make a stand at the river Yser to defend the last part of Belgian soil (figure 1). However, the situation was desperate: the worn-out Belgian army faced a far better equipped German IVth army. Therefore a plan to inundate part of the polders was implemented.

The coastal town of Nieuwpoort was of crucial importance since it is the location of a lock complex (Ganzeput, translated as ‘goose foot’) where six waterways come together (figure 1a): three canals used for shipping and three canals used to discharge drainage water from the polders. Consequently, the Ganzeput provided the key to inundate the polder. This was put into effect when on the night of 21 to 22 October the polder of Nieuwendamme was flooded by opening a spring sluice of the Ganzeput during high tide. The objective was to protect the left flank of the Belgian army from German attacks. But the main action to stop the German advance was to inundate the polder between the Yser and the Nieuwpoort to Diksmuide railway. The inundation combined with the topographical height of the railway embankment would form a strong defensive position. After less successful attempts starting on 26 October, an effective inundation started on the early morning of 30 October. Seawater was able to enter the area during a number of consecutive nights during high tide. This was right on time to initiate a retreat of the German army to the right bank of the Yser. An initial period of open warfare evolved into a dead-end positional warfare whereby the inundation was maintained until 1918. Although the military history and operation of the lock system during these dramatic days is known (Van Pul, 2006), a number of hydro(geo)logical questions remain.

CURRENT DAY GROUNDWATER QUALITY

The water quality distribution was mapped by De Breuck et al. (1974) 50 years after the conflict using a geophysical survey. It shows a fresh-saltwater distribution which is typical for the coastal plain (figure 1b): saline water is close to the surface in topographical low areas and freshwater lenses occur under the higher areas. This is a result of the displacement

of old saline water by freshwater due to the impoldering which occurred during the Middle Ages. The topographical lower areas contain a dense drainage system which means that almost no recharge takes place to flush the saltwater. The topographical low areas have also less permeable sediments (peat, mud and clay) in the subsurface than the higher grounds (loam and sand). A top clay layer is in general thicker in the topographical low areas. Interestingly, the observed distribution does not provide evidence of (relatively) recent recharge by saltwater.

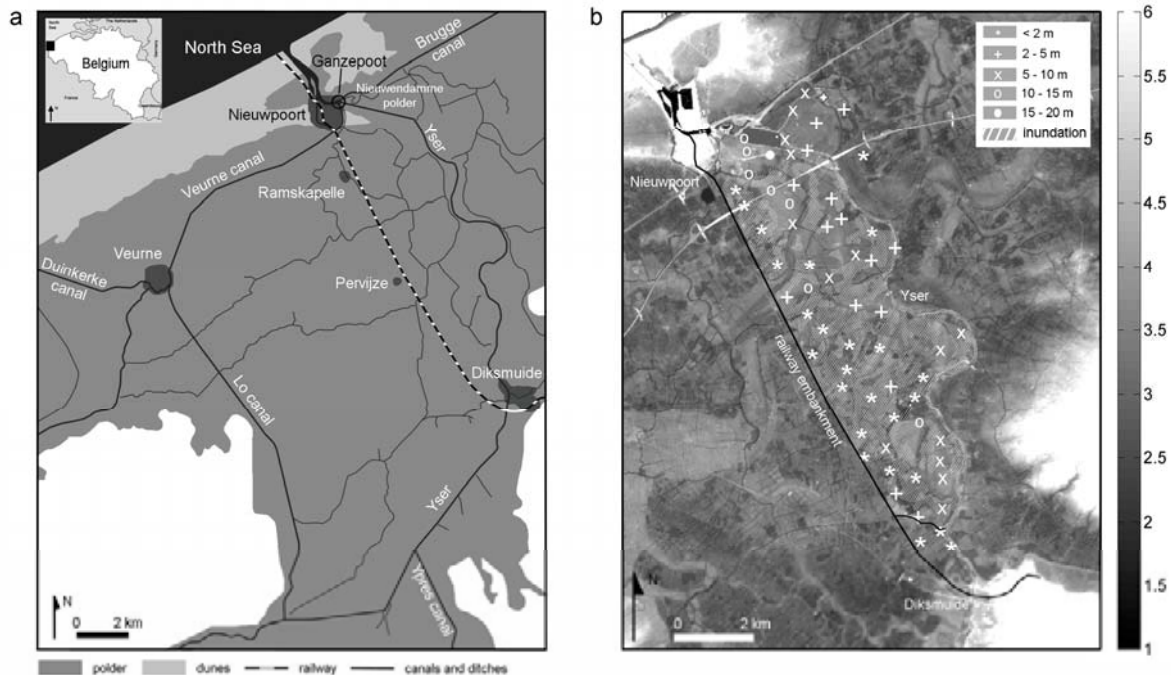


Figure 1. General map of the study area (a) and topographic map (m TAW, whereby 0 mTAW corresponds with low sea water level) of the inundated area with indication of the depth of the 1.5 g/L interface (symbols) (b).

Also, a more detailed look at water samples does not show recent salinization due to the inundation or freshening due to the restored freshwater recharge after the war. Water chemistry, and base exchange index is in line with what is found in the remainder of the coastal plain typified by the freshening due to the impoldering. Moreover, the brackish and saline samples indicate a lagoonal type, characterized by high alkalinity combined with extremes in sulphate reduction. This is in line with the mud-flat landscape present before the impoldering.

A 2D conceptual groundwater flow model (using SEAWAT) was made to better understand the lack of remnants of the inundation in the current water quality. It represents an east-west cross-section through the inundated area at a location where the current topography is considered more or less equal to the 1914 levels. In a first step, the formation of freshwater lenses due to the Medieval impoldering is simulated using the data of De Breuck et al. (1974) as an indication of the interface location. Interestingly, the top clay layer must be assigned a very low permeability to obtain the observed thicknesses for the freshwater lenses. Otherwise, almost the complete aquifer becomes fresh to brackish. Consequently, almost no saltwater recharges the aquifer when the effects of the inundation are simulated. It is therefore not surprising that no remnants of the inundation become obvious in the current-day salinity distribution.

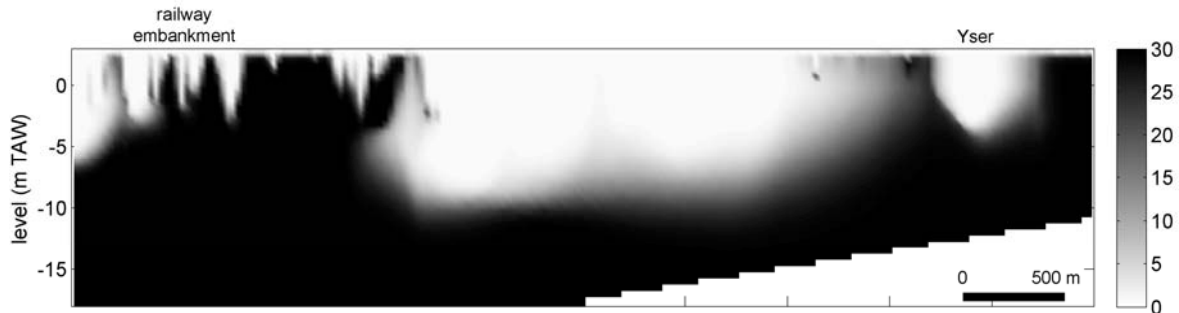


Figure 2. Simulated salinity distribution (g/L) before the inundation.

EFFICIENCY OF THE INITIAL INUNDATION

In the night of 29 to 30 October, a gate at the Ganzepoot was opened for the first time. Surprisingly, German soldiers near Ramskapelle already stood ankle-deep in mud and water during the morning hours of 30 October. The next day, only the higher grounds protruded above the water almost up to Diksmuide. The speed and the effect of the inundation is intriguing.

A number of factors contributed here. Although October 1914 was not exceptionally wet (42 mm at Ukkel), a number of days with heavy rain occurred: 13, 19, 25, 26 and 28 October. The low permeability of the top clay layer hampered infiltration of this rainwater and the soil was thus saturated. Rainwater must normally be collected by the different ditches and be discharged at low-tide through the Ganzepoot system. However, the lock staff left the construction on 18 or 19 October because it became too dangerous to stay. This meant that the polder between the Yser and the railway embankment was not drained for more than a week at the time of the inundation. Letters from German soldiers describe indeed the difficulty caused by the waterlogged fields during this period. So, the combination of a number of factors resulted in an already water saturated polder when the seawater was allowed to enter, explaining the efficiency of the inundation. It should be noted that the sea level was not especially high. Moreover, the inundation was realized during a period of neap tide. The minor importance of the sea level can be explained by the fact that the amount of water discharged into the polder was mainly determined by the dimensions of the gate.

PRESERVING THE INUNDATION

The inundation was preserved until the final offensive in 1918 and the crucial Ganzepoot was only destroyed by artillery fire in October 1918. The maintenance of the different hydraulic constructions is well-known (Thys, 1922). However, details of how the inundation was maintained are lacking. A key question is for instance how rainwater contributed relative to sea water.

The fact that the hydrography of the area is completely artificial already provide an answer. Without drainage and discharge of surplus water to the sea, the polder is flooded. This suggests that addition with rainwater was sufficient to maintain water levels during winter. During summer, due to the higher evaporation, water levels lowered, urging the need to bring additional seawater in the area. The low permeability of the subsurface is also an important factor since it prevents the infiltration (and loss) of large amounts of water. It also prevents important seepage of water in the adjacent fields, for instance west of the railway

where the Belgian positions were. Descriptions of when extra seawater was allowed to enter the inundated area are scant. However, in the winter of 1914-15, water had to be evacuated from the inundated area because stability of the railway embankment was at risk, endangering Belgian positions. During summer 1915, it is known that sea water had to be routed to another inundation southwest of Diksmuide. It would be surprising if this was different for the inundation between Nieuwpoort and Diksmuide. Finally, Massart (1920) identified gradients of fauna and flora in the area. He argued that the area north of Pervijze was dominated by saltwater. An in time variable water quality, i.e. because of rainwater, was present between Pervijze en Diksmuide.



Figure 3. View on the inundated land near Ramskapelle (Thys, 1922).

DISCUSSION AND CONCLUSIONS

The subsurface and the water management system made the polder at the Yser an ideal environment for an inundation. Low permeability of the soil, rainy weather, inactivity at the Ganzepoot to discharge drainage water during the preceding week and the audacity of a few men to operate the gate in full view of an enemy all contributed to the efficient inundation realized at the end of October 1914. The with rainwater waterlogged fields, provided a welcome chance factor to obtain a rapid inundation. The same factors made that the inundation could be sustained until 1918. Careful water management, i.e. managing the surplus rainwater in winter and adding seawater during summer but meanwhile maintaining the drainage of unoccupied polder land, was thereby the key issue.

REFERENCES

- De Breuck, W.,G. De Moor, and R. Tavernier. 1974. Depth of the fresh-salt water interface in the unconfined aquifer of the Belgian coastal area (1963-1973). Proc. 4th Salt Water Intrusion Meeting, Gent, annex-map, scale 1/100000.
- Massart, J. 1920. La biologie des inondations de l'Yser et la flore des ruines de Nieuport. Extrait du Bulletin de l'Institut de botanique Leo Errera: 11-429.
- Thys, R. 1922. Nieuport 1914-918. Les inondations de l'Yser et la Compagnie des Sapeurs-Pontoniers du Génie Belge.
- Vandenbohede, A., and L. Lebbe. 2012. Groundwater chemistry patterns in the phreatic aquifer of the central Belgian coastal plain. Applied Geochemistry 27:22-36.
- Van Pul,P.. 2006. In Flanders flooded fields. Before Ypres there was Yser. Barnsley, South Yorkshire: Pen & Swords Military.

Contact Information: Alexander Vandenbohede, Ghent University, Department Geology and Soil Sciences, Krijgslaan 281 (S8), Gent, Belgium, Phone: 32-9-2644652, Fax: 32-9-2644653, Email: avdenboh@yahoo.co.uk

Actualization of a 40 year old salinization map of the eastern Belgian coast using airborne time-domain electromagnetic survey (SkyTEM)

Dieter Vandeveld¹, Frans Schaars², Andrea Viezzoli³ and Per Gisseloe⁴

¹Flemish Environment Agency (VMM), Brussels, Belgium

²Artesia BV, Schoonhoven, the Netherlands

³Aarhus Geophysics ApS, Aarhus C, Denmark

⁴SkyTEM Surveys ApS, Aarhus N, Denmark (pgg@skytem.com)

ABSTRACT

The Belgian eastern coastal plain, bounded by the Dutch border in the east and the Boudewijn-channel in the west, is a region with diverse economic and social activities including seaports, agriculture, tourism, recreation, housing and nature. The groundwater is partly intruded with salt water, resulting in the occurrence of fresh, salt and brackish groundwater. This fresh- salt water distribution was mapped in the 60s - 70s, and published as the so-called salinity map. It has been used for many studies relating to groundwater. Half a century later, there is a need for a new map. The area has undergone many developments where the freshwater saltwater distribution was affected (especially the expansion of the port and the urban area). In addition to that there are large-scale projects planned in which the fresh-salt water distribution is an important aspect. The present freshwater lenses are also used for drinking water. The new map will contribute to the knowledge of the size of these freshwater lenses and provide a reference situation for short -and long- term projects. The comparison with the old map will also give insight into the autonomous development of the freshwater - saltwater distribution in relation to sea level rise and climate change.

The new map is made based on airborne geophysics, using the SkyTEM system attached to a helicopter. We will show how we incorporated prior information (such as borehole logs and sample analysis) to produce the final map. In addition to that we will analyze the difference with the 40 year old map, taking into account the difference between the methods used then, and the advanced possibilities we have now.

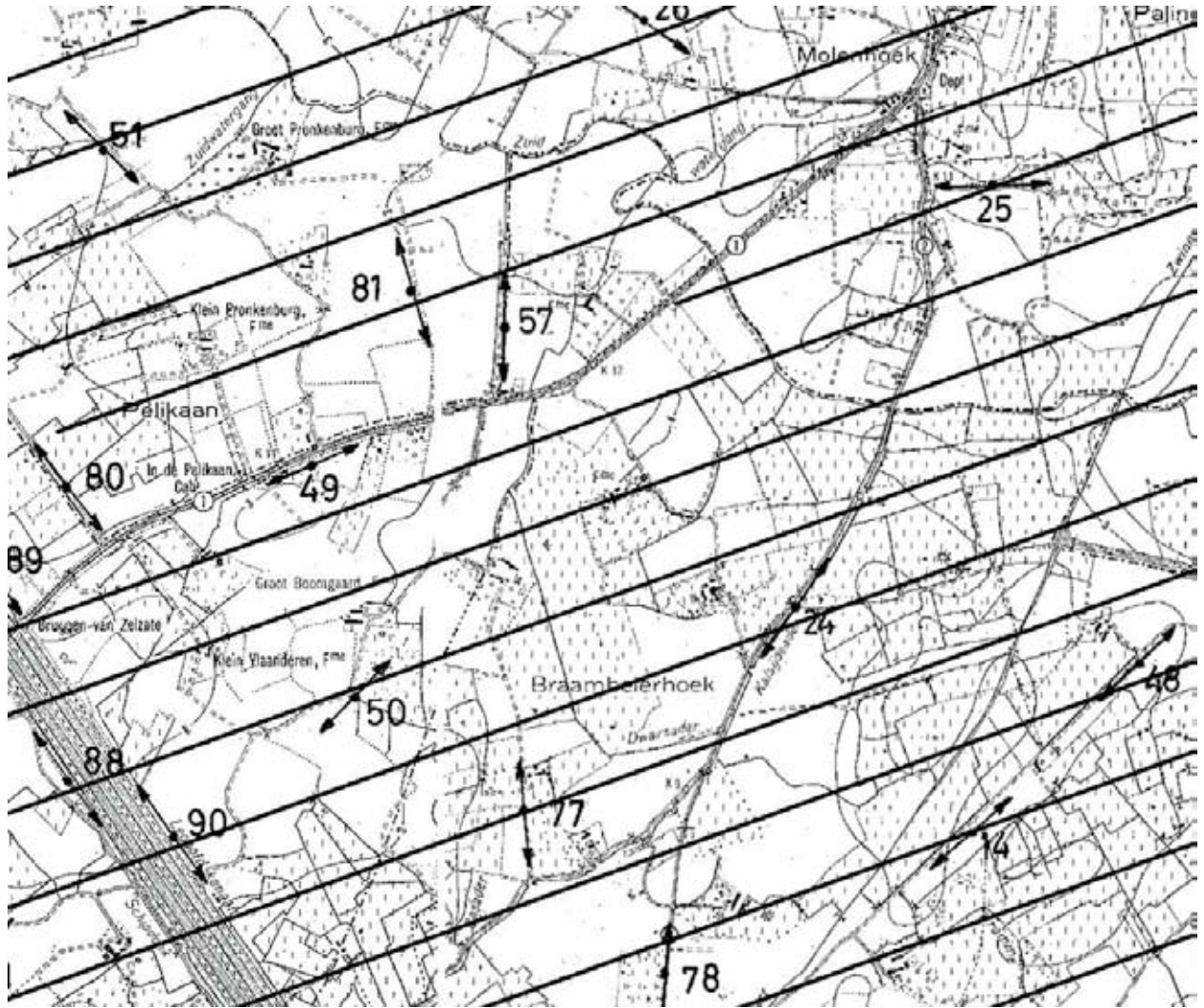


Figure 1. Flight lines of the SkyTEM survey (black lines, distance 250 m) projected on the old map with numbered VES locations.

Contact Information: Dieter Vandevelde, Flemish Environment Agency (VMM), Brussels, Belgium, Email: di.vandevelde@vmm.be

iMOD: A high performance open source framework for SEAWAT

Verkaik, J., Vermeulen, P., van Baaren, E., Janssen, G., de Louw, P., Faneca Sanchez, M., Oude Essink, G.
Deltares, Unit of Subsurface and Groundwater Systems, Utrecht, The Netherlands

ABSTRACT

At Deltares, a high performance open source framework for groundwater modeling is being developed, called iMOD. iMOD has originally been developed for high resolution groundwater modeling with MODFLOW, focusing on performance and user-friendliness. Since last year, SEAWAT has been successfully modified for iMOD. This means that the SEAWAT in- and output routines have been modified to incorporate fast binary read, where the code internally clips and scales (up- or down) the input data to the resolution and extent of the computational domain (subdomain). In that way the user can work from one expandable data set covering all possible future areas of interest, and easily generate consistent subdomain models. The iMOD graphical user interface is used to visualize and edit all the large datasets in a fast way. It incorporates a wide range of easy-to-use tools for visualization (e.g. 2D cross sections, 3D, time series) and model building (e.g. a 3D subsurface tool). For running SEAWAT, the code has been modified to read a driver input file. This file is key-word driven and enables the user to set up a model in a flexible and user friendly way. The iMOD version of SEAWAT is currently being used in projects in The Netherlands, Singapore and Bangladesh.

Saltwater contamination in the lowlying coastland of the Venice Lagoon, Italy

Rita Deiana¹, Francesco Morari², Pietro Teatini³, Luigi Tosi⁴ and **Andrea Viezzoli**⁵

¹Department of Cultural Heritage, University of Padova, Padova, Italy

²Department of Agronomy, Food, Natural resources, Animals, and Environment, University of Padova, Legnaro (PD), Italy

³Department of Civil, Environmental, and Architectural Engineering, University of Padova, Padova, Italy

⁴Institute of Marine Sciences, National Research Council, Venezia, Italy

⁵Aarhus Geophysics APS, Aarhus, Denmark

ABSTRACT

The southern portion of the Venice coastland includes a very precarious environment. Due to an elevation down to 4 m below msl, the Venice Lagoon and Adriatic Sea proximity, and the encroachment of seawater from the mouth of the river network up to 20 km inland, salt contamination of land and groundwater is a severe problem that is seriously affecting the farmland productivity. An interdisciplinary multi-scale research is ongoing with the aim of understanding the contamination process, quantifying the effect of the saltwater intrusion of the crop production, and proposing possible mitigation strategies. A 21-ha representative basin has been selected and deeply monitored from the hydrogeological and agricultural points of view. It has been clearly outlined that in the upper 5 to 10 m mainly the low-permeable soils are contaminated by salt. Conversely, fresh to brackish waters are located in the sandy elongated paleo-channels. This is likely due to the origin of the area which was a salty marshland since one century ago. The freshwater supplied for almost 100 years by the rainfall and leakage from the river and channel beds has been able to reduce the salt concentration only in the highly permeable deposits.

INTRODUCTION

Understanding the hydrogeological processes is critical for a sound management of groundwater resources in coastal areas. Here lie majority of human settlements, industrial production, and fish farming. Human pressure on the coastland environment is constantly increasing, and many studies predict a rising of seawater level in the next 50 years ranging from few cm up to several tens of cm, with expected threatening consequences (e.g., Carbognin et al., 2009). If these are common characteristics of most coastal areas, wetlands, lagoons and estuaries also have often unique flora and fauna depending on the groundwater-surface water processes.

The hydrologic setting of the transitional environments is complicated by their Late Quaternary subsoil architecture. The deposits represents the transition through the fluvial in tide-dominated depositional systems triggered by the sea level changes. In particular, in the Venice area numerous geomorphological features representing i.e. fluvial paleoriver beds, ancient tidal channels, and paleobeach ridges occur (Tosi et al., 2009). These features are generally filled by sandy deposits and can be considered preferential path for the groundwater flow, both in the horizontal and vertical directions.

The area under investigation is part of the coastal plain between the lower stretches of the Brenta and Adige rivers, south of the Venice Lagoon (Figure 1). The coastal plain lies almost completely below the mean sea level. The main hydrogeological problems of this part of the Venice area are the advancing of saltwater contamination into the phreatic aquifer yielding a reduction of the soil productivity (Braga et al., 2012). Geological and geomorphological features can favor or mitigate these processes.

METHODS

The study site (Figure 1) is a ca. 21 ha field located at Chioggia, Venice, Italy (45°10'57"N; 12°13'55"E) along the southern margin of the Venice Lagoon. With an elevation ranging between 1 and 3.3 m below asl, the soil is mainly silt-clay with the presence of peat and sandy drifts (i.e. paleochannels). In particular, two well preserved-paleochannels (i.e. western and eastern), generally characterized by coarse texture, cross the study site in a SW-NE direction (Rizzetto et al., 2003). A pumping station and a dense network of ditches control the depth to the water table (Manoli et al., 2013), which is generally maintained at ~0.6 m during the summer season in order to promote subirrigation.

Both undisturbed and disturbed soil samples were collected in May 2010 at 41 points selected according to an apparent electrical conductivity (ECa)-directed sampling scheme based on simulated spatial annealing. Disturbed samples were taken at 4 depth increments: 0–0.15, 0.15–0.45, 0.45–0.8, and 0.8–1.2 m. Undisturbed cores were extracted with a hydraulic sampler from the upper 1-m profile and then analyzed at 0–0.15, 0.15–0.45, 0.45–0.8, and 0.8–1.00 m for bulk density (Scudiero et al., 2011; 2013).

ECa at three different investigation depths (from 0 to 0.75 m; from 0 to 1.50 m; from 0 to 6.00 m) was measured from April 2010 to September 2012 by a ground-based electromagnetic conductivity meter (GEM). We applied an airborne electromagnetic technique (AEM) equipped by a dual moment bandwidths that allow to investigate the soil response from shallow to intermediate depths particularly suitable for our target (Teatini et al., 2011). EM data are then inverted using the Spatially Constrained Inversion (SCI) technique (Viezzoli et al., 2008). The traces of the surveys are provided in Figure 1. Water level and conductivity (ECw) have been systematically measured in a number of boreholes and in the watercourses crossing and bounding the farmland. In addition, five continuous cores have been taken down to 20-m depth for a detail hydrostratigraphic characterization. Finally, a few electrical resistivity tomographies and seismic sections have been acquired crossing the paleo-channels to delineate the geomorphological architecture and the related groundwater salinity.

RESULTS

Geophysical and hydrogeological investigations allowed improving the conceptual model of the processes responsible for the saltwater intrusion. It has been clearly outlined that in the upper 5 to 10 m mainly the low-permeable soils are contaminated by salt. Conversely, fresh to brackish waters are located in the sandy elongated paleo-channels. This is likely due to the origin of the area which was a salty marshland since one century ago. The freshwater supplied for almost 100 years by the rainfall and leakage from the river and channel beds has been able to reduce the salt concentration only in the highly permeable deposits. Below this upper layer, salt concentration is generally very high (ECw ranges between 10'000 and 45'000 mS/cm) in the whole area. Saltwater intrudes from the lagoon bottom, which is 2 to 3 m above the farmland, passes underneath the rivers and canals, and extends landward.

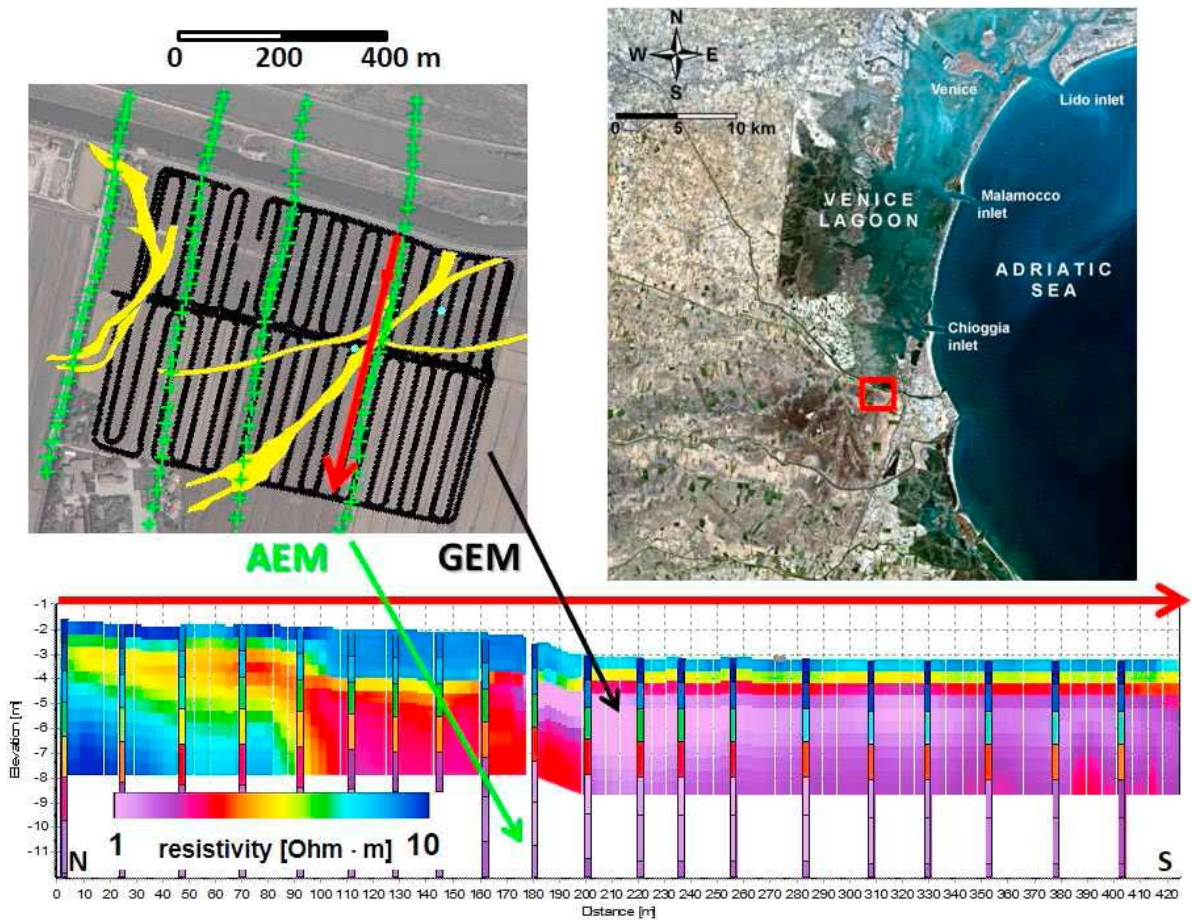


Figure 1. (top right) Location of the study area at the southern margin of the Venice Lagoon. (top left) Study area with the trace of the airborne EM (green) and ground EM (black) surveys together with the trace of the main paleorivers (in yellow). (bottom) North-south resistivity section obtained by AEM and GEM along the red alignment shown above.

DISCUSSION AND CONCLUSIONS

The study shows the importance of a 3D large-scale view of subsurface water and soil characteristics for the hydrogeological characterization of large fresh-salt transitional environments such as wetlands, lagoons, deltas. Considering the complex physiographic, morphologic and hydraulic setting, this is achieved by an integrated approach combining various methods, i.e. airborne and ground-based electromagnetic acquisitions, electrical resistivity tomographies, seismic surveys, lithological analyses on shallow cores and deep boreholes, piezometric and water conductivity measurements, and lab physical-chemical tests on water and soil samples.

From a general perspective, the integrated approach has a strong hydrogeological relevance both to define conceptual hydrogeological models (e.g. characteristic geometries, boundary conditions, major natural and anthropogenic forcing factors) and to provide the input for the simulation of the groundwater flow/transport by numerical models.

ACKNOWLEDGMENTS

The work has been developed within the Research Programme "GEO-RISKS: Geological, morphological and hydrological processes: monitoring, modelling and impact in the north-eastern Italy", WP4, funded by the University of Padova, Italy. A particular thanks to the Adige-Euganeo Water Reclamation Authority for the substantial help to develop the in-situ activities.

REFERENCES

- Braga, F., F. Morari, F. Rizzetto, E. Scudiero, P. Teatini, L. Tosi and Q. Xing. 2012. Characterizing the saltwater effect on soil productivity by WorldView-2 images. The southern margin of the Venice Lagoon, Italy. In: 7th EUREGEO, European Congress on Regional Geoscientific Cartography and Information Systems, ed S. Scappini and S. Zapparoli, Vol. I, 361-362. Centro Stampa Regione Emilia-Romagna Publ.
- Carbognin, L., P. Teatini, A. Tomasin and L. Tosi. 2010. Global change and relative sea level rise at Venice: what impact in term of flooding. *Climate Dynamics* 35:1039-1047.
- Manoli, G., S. Bonetti, E. Scudiero, P. Teatini, P. J. Binning, F. Morari, M. Putti, and M. Marani. 2013. Monitoring and modeling farmland productivity along the Venice coastland, Italy. *Procedia Environmental Sciences* 19: 361-368.
- Rizzetto, F., L. Tosi, L. Carbognin, M. Bonardi and P. Teatini. 2003. Geomorphological setting and related hydrogeological implications of the coastal plain south of the Venice Lagoon (Italy). In: *Hydrology of the Mediterranean and Semiarid Regions*, ed E. Servat et al., 463-470, IAHS Publ. n.278.
- Scudiero, E., Deiana, R., Teatini, P., Cassiani, G., Morari, F., 2011. Constrained optimization of spatial sampling in salt contaminated coastal farmland using EMI and continuous simulated annealing. *Procedia Environmental Sciences* 7: 234-239.
- Scudiero, E., P. Teatini, D. L. Corwin, A. Berti, and F. Morari. 2013. Delineation of site-specific management units in a saline region at the Venice Lagoon margin, Italy, using soil reflectance and apparent electrical conductivity. *Computers and Electronics in Agriculture* 99: 54-64.
- Teatini, P., L. Tosi, A. Viezzoli, L. Baradello, M. Zecchin, and S. Silvestri. 2011. Understanding the hydrogeology of the Venice Lagoon subsurface with airborne electromagnetics. *Journal of Hydrology* 411: 342-354.
- Tosi, L., P. Teatini, L. Carbognin, and G. Brancolini. 2009. Using high resolution data to reveal depth-dependent mechanisms that drive land subsidence: The Venice coast, Italy. *Tectonophysics* 474: 271-284.
- Viezzoli, A., A. V. Christiansen, E. Auken, and K. Sørensen. 2008. Quasi-3D modeling of airborne TEM data by spatially constrained inversion. *Geophysics* 73: F105-F113.
- Contact Information:** Andrea Viezzoli, Aarhus Geophysics APS, Hoegh-Guldbergs Gade 2, Aarhus DK-8000, Denmark, Email: andrea.viezzoli@aarhusgeo.com

Science, policy decision making and public participation – the challenge of climate change at the coast

Hans von Storch and Norddeutsches Klimabüro of HZG.
Institute for Coastal Research, Helmholtz Zentrum Geesthacht (HZG), Germany

ABSTRACT

Climate is changing, and we can only understand the causes of a minor part of the change, if we do not use the emission of radiatively active substances into the atmosphere as a key driver. Climate - that is the statistics of the “weather” in the atmosphere, in the groundwater, in the sea etc. Change means that these statistics are changing. It means we have less often cold winters, but not that we have no cold winters, for instance.

Even if significant changes cannot be comprehended without the action of greenhouse gases, it is not so that all changes have, or may have a causal link to the emission of greenhouse gases. Some are within the normal variations of climate; others, such the heavily increased storm surge heights in Hamburg, have their dominant origin in modifications of the estuary. In short: climate change is a serious issue, but not the only one.

In the presentation, the general situation of climate change - which variables, how strong, which changes are inconsistent with natural variability and need “external” explanation, and what are such possible external drivers – are discussed. First for the present situation, then for the expectation we have for the future. Among the presently changing variables, which need a reference to greenhouse gases, are all temperature-related variables. For storms we have no such signal; for heavy rainfall events, the situation is still under examination, and if the present rise in sea level is really beyond what has previously been recorded, is also still under debate. For the future, we expect a clear greenhouse-gas related increase in temperature and related variables, in sea level, and in heavy rainfall events, but not necessarily in storminess.

The discussion and the policy decision process is about the question of what to do about the present changes and the expected future changes. We name the situation “post-normal”, because the issue is serious, needs urgent decisions, which would involve many resources, and is embedded in ethical world views. In this situation, science can only to a limited extent help in the decision process, namely by analyzing what is going on, and by describing which consequences which policy decision would go along with. The decision itself is a political matter of balancing societal values, perceptions of risk and preferences of outcomes.

This is a challenging situation for scientists, who find themselves often enough in a position that they should provide truth from which the decisions would result – as some head of governments like to say “there is no alternative”. We have set up our “Norddeutsches Klimabüro” of the Helmholtz Institut für Küstenforschung in Geesthacht. This Klimabüro is a “farmshop” for our regional clients, many of them in coastal defense but also off-shore activities. It supports social actors (authorities, civil society, public at large, media, and economic actors) in better understanding perspectives and options. The Klimabüro is also feedback means to find out if our insights and products have any bearing for practical issues.

In the presentation, a number of products of the Norddeutsches KLimabüro will be presented, namely the IPCC-like “Hamburger Klimabericht” (which covers also the Schleswig Holstein. Westküste), and the internet-tools “Norddeutscher Klimaatlas“, the “Norddeutscher Klimamonitor” and “Küstenschutzbedarf”.

Contact Information: Hans von Storch, Institute for Coastal Research, Helmholtz Zentrum Geesthacht, Germany. Email: hvonstorch@web.de, <http://www.hvonstorch.de/klima>

Saltwater intrusion in fractured rock – a study of the proposed high-level nuclear waste repository at Forsmark, Sweden

Clifford I. Voss¹, Georg A. Lindgren² and Joel Geier³

¹ US Geological Survey, Menlo Park, CA, USA

² Swedish Radiation Safety Authority, Solna, Sweden

³ Clearwater Hardrock Consulting, Corvallis, OR, USA

ABSTRACT

Intrusion of highly saline formation brines through fractures may adversely impact the isolation ability of Sweden's high-level nuclear waste repository. The repository should isolate copper-steel canisters containing used nuclear fuel rods from groundwater flow and should prevent any leakage of radioactive nuclear waste from reaching the human ecosystem. Canisters will be placed in cylindrical deposition holes on the bottom of tunnels excavated at about 500 m depth in the fractured granitic bedrock. Each canister should be wrapped in a 'buffer' of relatively-impermeable bentonite clay, completely filling the deposition hole. Upon completing emplacement of all canisters, the tunnels will be backfilled and closed with a bentonite-rock mixture. Initially, bentonite is placed in deposition holes in dry form and it does not fill the entire hole volume around the canister. After repository closure, the bentonite will absorb groundwater that naturally leaks into deposition holes and must swell until it completely fills each deposition hole, providing the intended waste isolation. However, bentonite swelling requires absorption of relatively fresh groundwater but the repository is underlain by highly saline groundwater (brine). Should saline groundwater enter the repository during swelling, it would reduce swelling, possibly leaving gaps around canisters through which groundwater can reach the canister and through which groundwater can transport any leaking radionuclides out of the repository, reducing its isolation ability.

Numerical simulation analysis of variable-density groundwater flow through fracture zones that intersect repository tunnels at the proposed repository site at Forsmark, Sweden, is carried out. Results reveal the main controls on brine intrusion (upconing) to the repository and on brine flushing ('downconing'), and provide a range of time delays before brine reaches the open repository and an understanding of how long brine may remain in the repository rock surrounding the canisters. Simulations indicate that upconing is driven primarily by the pressure gradient created by open tunnels at 500 m depth, but downconing is driven exclusively by fluid density differences. This is similar to the behavior of seawater intrusion in coastal water-supply wells. Upconing is strongly affected by the ratio of permeability to porosity in each fracture zone, quantities that are not well known in fractured rock. Within the full range of parameter values that may describe the Forsmark site, simulations yield either no significant upconing at all during the canister emplacement period or rapid intrusion of brines within a few decades. After initial intrusion, brine remains in the repository while the pressure is low (until it resaturates with groundwater, perhaps 1000's of years after closure). This is a case in which saltwater intrusion may adversely affect the performance of a nuclear waste repository.

Complete reference:

Lindgren GA, Voss CI, Geier J (2013) Brine intrusion by upconing for a high-level nuclear waste repository at Forsmark, Sweden: Scoping calculations. Swedish Radiation Safety Authority (SSM) Report 2013:28, ISSN: 2000-0456, 47p (available at www.stralsakerhetsmyndigheten.se)

Contact Information: Clifford I. Voss, U.S. Geological Survey, 345 Middlefield Rd, Menlo Park, CA 94025 USA, Phone: 650-329-5885

Email: cvoss@usgs.gov

Hydrogeological and Hydrogeochemical Investigation of the Coastal Area of Jifarah Plain, NW Libya

Nawal Al Farrah^{1,2} and Kristine Walraevens¹

¹ Ghent University, Department of Geology and Soil Science, Laboratory for Applied Geology and Hydrogeology, Krijgslaan 281-S8, 9000 Gent, Belgium

² Az Zawia University, Geology Department, Az Zawia, Libya

INTRODUCTION

Nowadays, groundwater reserves are exposed to intensive exploitation, which may create serious problems in coastal areas where some hydraulic connection exists between the water reservoirs and seawater (Van Dam, 1996). The main objective of this research was to characterize and assess the geology, hydrogeology, hydrodynamics and water quality of the Upper Miocene-Pliocene-Quaternary aquifer in Jifarah Plain in order to identify the sources of groundwater salinization. An additional objective was to construct, calibrate and develop a groundwater flow model that could be used in future assessment and development processes (Al Farrah, 2011).

The study area covers the coastal part of the Jifarah Plain in NW of Libya (Fig. 1). The Jifarah Plain is a flat area of triangle shape of about 20,000 km². It is bordered by the Mediterranean Sea in the north, the Tunisian border in the west and Jebal Naffusah border in the south and east. The studied coastal area is a coastal strip of around 105 km length and 18 km wide in the north of central Jifarah comprising Tripoli city, where more than 50% of the country's population are concentrated.

The principle aquifer used by the population in the plain is the Upper Miocene-Pliocene-Quaternary aquifer, which is called the upper aquifer. Groundwater in the upper aquifer is mostly discharged through pumping wells and to some extent, loss from sebkhas, in addition to leakage to the lower aquifer. In the Jifarah, there are more than 30,000 abstraction wells. Hundreds of wells are being drilled every year to meet the growing demand. The wells are spread over the central and northern parts of the upper aquifer, where agricultural activities are more intensive. The available recharge in the plain was calculated at $633.55 \cdot 10^6$ m³/year. The discharge of $1433.33 \cdot 10^6$ m³/year is more than two times higher than the recharge. This clearly show an unbalanced situation which leads to important water level decline and water quality deterioration.

METHODOLOGY

Sampling and analytical methods

This study assesses the quality of groundwater from 134 different borehole locations in the coastal area of the plain. The methods employed for this study are field measurements, sampling and laboratory analysis. In the coastal area, a total of 134 shallow and deep wells (mostly 30-180 m deep), located at different distances from the Mediterranean Sea, were selected for groundwater sampling and water level measurement across the major cities. Chemical parameters analyzed are Na⁺, K⁺, Ca²⁺, Mg²⁺, Fe²⁺, Mn²⁺, Cl⁻, NO₃⁻, SO₄²⁻, HCO₃⁻, CO₃²⁻ and PO₄³⁻. Water level was measured from the ground surface using water level meter, and pH was analyzed using a pH meter and glass electrode.

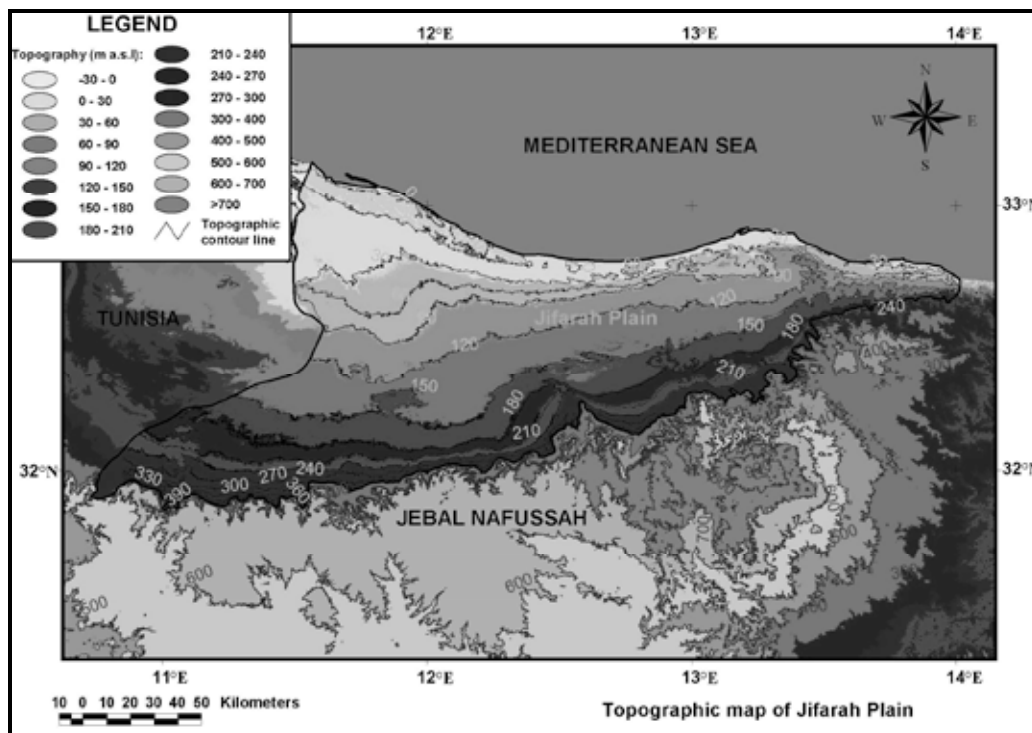


Figure 1: Location map of the Jifarah Plain.

Hydrochemical evaluation methods

The interpretation process is mainly based on ion deviation Δm_i from a conservative seawater-freshwater mixture, saturation indices calculation, graphical illustration methods including Piper diagram, classification of water according to Stuyfzand (1986), calculation of ionic ratios, and elaboration of maps and cross-sections showing the spatial and vertical distribution of water quality parameters in the study area.

The PHREEQC 2.16 program for Windows was used to calculate saturation indices for calcite, dolomite, halite and gypsum based on the chemical analytical results and measured field temperatures for all samples.

Construction of groundwater flow model

The natural groundwater system in Jifarah Plain was investigated in three dimensions using Visual MODFLOW model code to certify the hydraulic parameters by minimizing the difference between the observed and calculated values and to determine the adverse effect of overextraction. The steady state model and transient flow model in 50 stress periods (1957-2007) were successfully run for the unconfined Upper Miocene-Pliocene-Quaternary aquifer system of Jifarah Plain.

RESULTS AND DISCUSSION

Major hydrochemical parameters

The results show that: temperature ranges between 18 - 26 °C, pH range is 6.71 - 9.94, electrical conductivity between 510 -15,650 $\mu\text{S}/\text{cm}$ (25 °C), TDS range is 360 - 11,141 mg/l and chloride concentration ranges from 2 - 5285 mg/l. This high Cl⁻ concentration is probably due to mixing with seawater. High concentrations of chloride occur in all wells at a few kilometres from the coast and the concentration of Cl⁻ decreases gradually towards the south. However, in many farther inland wells, it is

still the dominant anion. TDS is high (>1500 mg/l) for most samples, where high Cl^- , SO_4^{2-} , Mg^{2+} and Na^+ contents are mainly due to mixing with seawater and/or upconing of deep saline water. This occurs as a result of overexploitation of the upper aquifer and scarcity of rainfall. Increase in SO_4^{2-} can also arise from the dissolution of sebkha sediments and gypsum. In addition, high application of fertilizers causes NO_3^- pollution in some areas.

Hydrochemical processes

The major hydrogeochemical processes occurring in the upper aquifer are: cation exchange during salinization due to mixing with the seawater end member, dissolution of gypsum and sebkha sediments. The salinization phenomenon occurs stronger in the coastal zone than in the upstream zone. In the downstream zone, next to mixing with salt water, cation exchange reaction is the most important process that modifies the concentration of ions in the groundwater. A large number of sampling points belong to the brackish and brackish-saline major type ($\text{Cl}^- > 300$ mg/l), and are very hard to extremely hard due to strong seawater admixture (with cation exchange code “-“ or “0”). A lower number of samples are fresh to fresh-brackish and moderately hard to hard (cation exchange code “+”).

The saturation index shows mostly a tendency to precipitation for calcite and dolomite. Gypsum and anhydrite are undersaturated, but with higher SI values in the area south of Sabratah, where the dissolution of gypsum has increased the concentrations of SO_4^{2-} and Ca^{2+} .

Stuyfzand (1986) classification and Piper (1944) plot (Fig. 2) show that NaCl and CaCl types are the main hydrochemical facies for the groundwaters, while CaHCO_3 and MgHCO_3 water types are found only for several wells mostly towards the recharge area in the south or in the north nearby a local high topographic area.

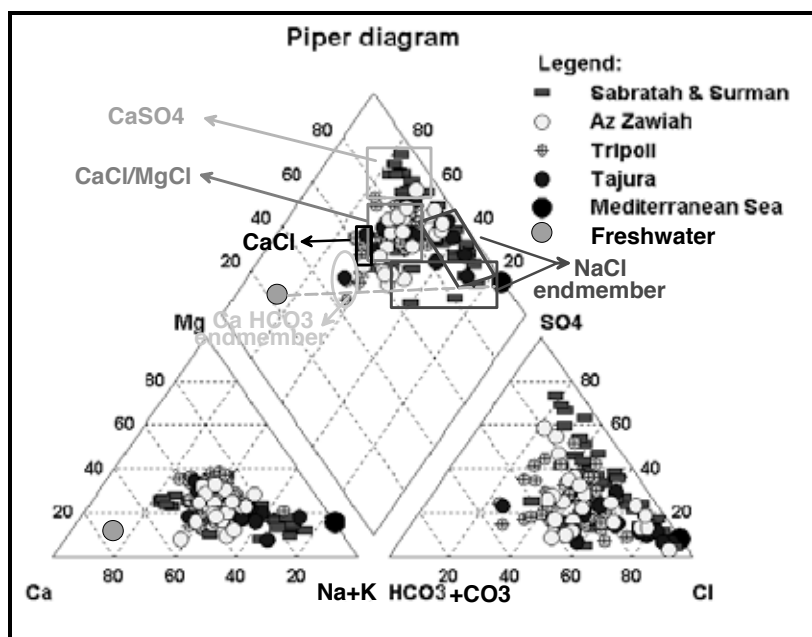


Figure 2: Water types according to Piper diagram.

Groundwater flow model

The steady state simulation has indicated that groundwater flow direction is from higher topography in the south to the north, towards the Mediterranean Sea in the north and sebkha drains in the north west of the plain.

The non-steady state simulation has indicated that groundwater levels in the upper aquifer are most sensitive to discharge from wells. The general direction of groundwater flow in 1957 is to the north to the Mediterranean Sea and sebkha drains. This pattern has changed gradually with time, forced by high pumping rate in the region, where the interaction between groundwater and seawater has increased gradually for every time step, due to high exploitation of the aquifer in the coastal plain. Figure 3 shows a calculated piezometric map for 2007.

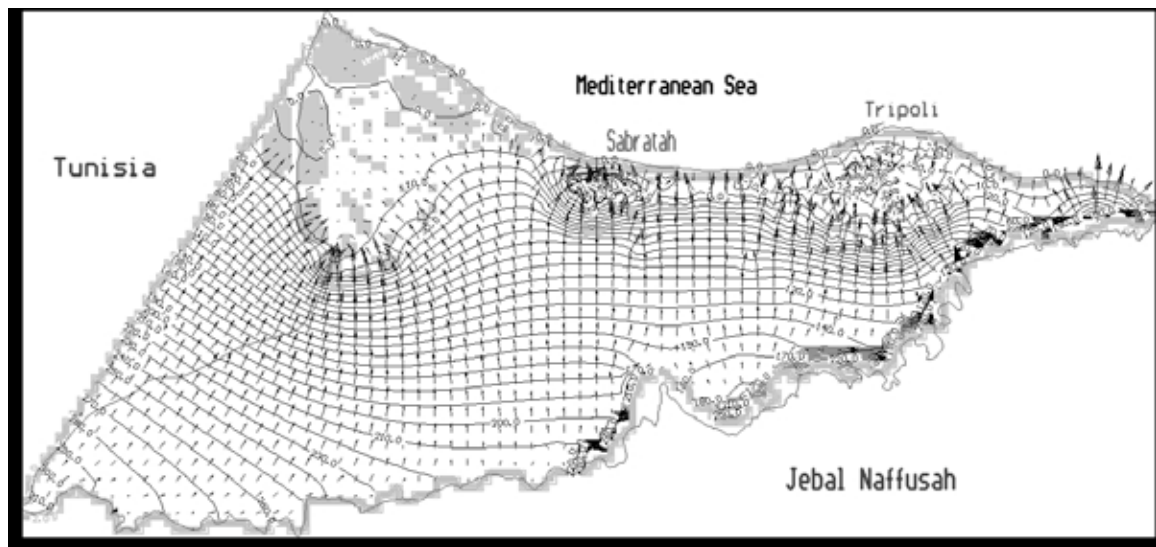


Figure 3: Transient state calculated piezometric map with flow vectors for 2007 (equidistance 10m).

CONCLUSION

The overpumping for groundwater has contributed to the deterioration of the water quality by marine intrusion and exposing the deep saline water. A majority of the groundwaters (80%) shows a composition that is indicative of seawater intrusion according to the Stuyfzand classification. Types of water that are indicative for saltwater intrusion are NaCl, MgCl and CaCl. CaCl is the typical water type appearing during the salinization processes, due to cation exchange.

REFERENCES

- AL FARRAH, N., 2011. Hydrogeological and hydrogeochemical investigation of the coastal area of Jifarah Plain, NW Libya. PhD thesis, Laboratory of Applied Geology and Hydrogeology, Ghent University, Belgium.
- STUYFZAND, P.J., 1986. A new hydrogeochemical classification of water types: principles and application to the coastal dunes aquifer system of the Netherlands. Proceedings 9th SWIM, Delft (The Netherlands), pp. 641-656.
- PIPER, A.M., 1944. A graphic procedure in the geochemical interpretation of water analyses. Transactions of the American Geophysical Union, 25: 914-928 Press, Boca Raton.
- VAN DAM, J. C., 1996. The shape and position of the salt water wedge in coastal aquifers. In: Proc. Hamburg Symposium of Relation of Groundwater Quantity and quality. IAHS, pp. 146.

Evaluating Remediation Potential of a Salinized Heterogeneous Aquifer System Using Three-Dimensional, Density-Dependent Groundwater Modeling

Walther, M.¹, Bilke, L.¹, Delfs, J.-O.², Graf, T.³, Grundmann, J.⁴, Liedl, R.⁵, Kolditz, O.^{1,6}

¹ Helmholtz-Centre for Environmental Research, Department Environmental Informatics, Leipzig, Germany

² Christian-Albrechts-Universität zu Kiel, Institute of Geosciences, Kiel, Germany

³ Leibniz Universität Hannover, Institute of Fluid Mechanics and Environmental Physics in Civil Engineering, Hannover, Germany

⁴ Technische Universität Dresden, Institute of Hydrology and Meteorology, Dresden, Germany

⁵ Technische Universität Dresden, Institute for Groundwater Management, Dresden, Germany

⁶ Technische Universität Dresden, Applied Environmental Systems Analysis, Dresden, Germany

ABSTRACT

This extended abstract shortly describes numerical modeling activities for a density-dependent groundwater model in a coastal arid region. The numerical modeling tool is benchmarked and used to calibrate the regional domain setup with its heterogeneous hydrogeology. Afterwards, the model is used to assess remediation potential of the local aquifer system. Results show that remediation actions will require a long-term strategy to retrieve the already salinized regions of the aquifer.

INTRODUCTION

This extended abstract presents a groundwater case study in the Al-Batinah, the northern coastal region of Oman. As in other arid regions, groundwater is the most reliable source for freshwater within the two catchments chosen for studying (wadis Ma'awil and Bani Kharus). Within this agriculturally used coastal region, where water consumption nowadays exceeds annual recharge, water table drawdown and subsequent saline intrusion are problems that need to be addressed in order to ensure sustainable water availability in terms of quality and quantity.

The work at hand shortly portrays modeling activities with respect to variable density flow in coastal areas and summarizes results of the case study. Relevant publications with more detailed information can be found for the development and application of the hydrogeological model (Walther et al 2012a), the regional groundwater model setup and steady state calibration (Walther et al 2012b), as well as for the transient calibration, water budgets and scenario simulation (Walther et al 2014, in review).

METHODS

Modeling Tools

To simulate groundwater flow and mass transport, the numerical modelling tool OpenGeoSys was utilized (OGS, Kolditz et al 2012; www.opengeosys.org). The numerical model is based on the Galerkin-FEM method. OGS was used before for several density-driven flow applications (Kalbacher et al 2011; Park and Aral 2008). Governing equations follow common standards for groundwater flow and mass transport in porous media and are given in Walther et al (2012b). Equation of state for density is a linear relationship which is reported to be sufficient for marine water density (Park 2004).

Benchmarking

To verify modeling capabilities of OGS for saltwater intrusion, the Goswami-Clement problem was used (Goswami and Clement 2007). The problem features a horizontally intruding and withdrawing saltwater front in an initially present freshwater environment. The conceptual model is depicted in Figure 1. For comparability reasons, the model setup and parameterization was followed as described by Goswami and Clement (2007). Exemplarily, Figure 2 compares results for the intruding case between experimental data and SEAWAT simulation output (by Goswami and Clement), and our own OGS simulations. All numerical results are in good accordance with experimental data.

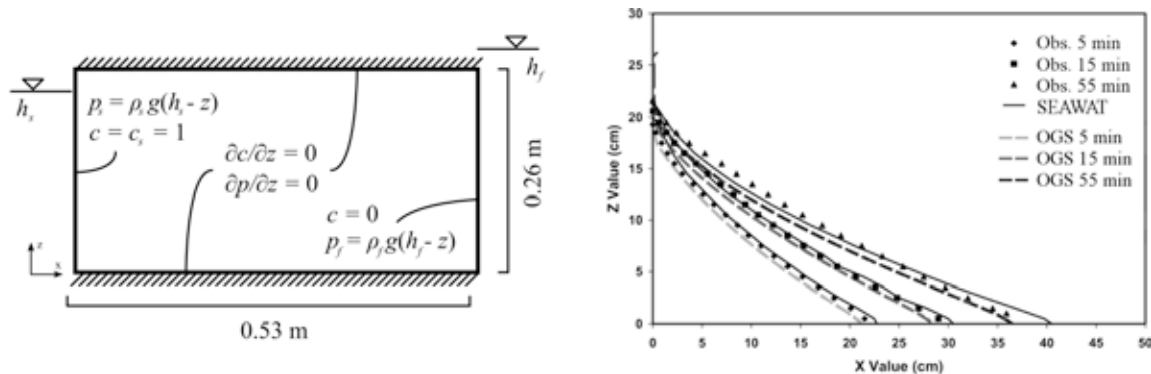


Figure 1 – Conceptual model of benchmark, from Walther et al (2014, in review), not to scale.

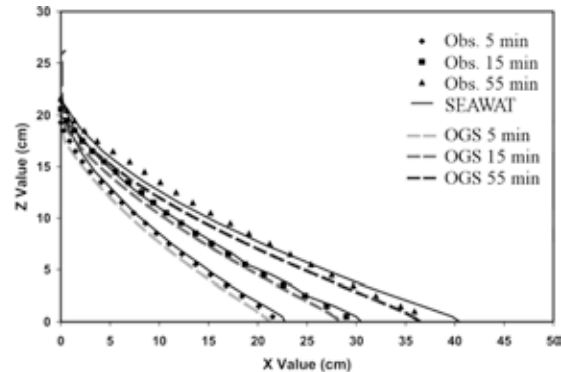


Figure 2 – Results for intruding state, from Walther et al (2014, in review).

Furthermore, Stoeckl et al (2014) compare results of several numerical models, among these OGS, to experimental data of development and degradation of a fresh water lens (see also Stoeckl and Houben 2012). Preliminary results show no significant deviations for either of the used models from the experimental data.

Regional Model Setup

The near coastal groundwater study area consists of a three-dimensional, heterogeneous aquifer with an extent of ca. 20·30 km² and a maximum depth of 450 m in the center of the domain (“Ma’awil trough”). The hydro-geological model mainly consists of twelve distinct material groups of different material properties (from gravel to clay). Above a less permeable secondary aquifer, a thin and highly permeable primary aquifer is present at the coast, increasing in depth to the south until the Ma’awil trough. The hydro-geological model is visualized in <http://youtu.be/jx0wt6Q1Ow>.

Boundary conditions of the numerical model are upstream subsurface inflow from mountainous recharge regions, spatially distributed pumping abstraction near the coast, and given sea water level and salinity. More details on the characteristics of the study area and the setup of the hydro-geological and numerical model are described in Walther et al (2012b) figures 4, 6, 7 and table 3.

RESULTS

Pre-development and Active Pumping State

Before the 1970s, groundwater abstraction was primarily achieved through hand-dug wells, and the aquifer system was supposed to be in a steady state. Simulations for this pre-development state could be calibrated with high correlation (correlation coefficient $R^2 = 0.83$). When cultural changes and industrialization made modern pumping wells available to

local farmers, water abstraction increased dramatically. Within this transient calibration time, i.e. 1974-2005, the correlation coefficient of groundwater levels reduced to $R^2 = 0.61$ until the year 2005. Deviations may result from several reasons, including low input data quality, or wide ranges of unknowns for calibration.

Simulation results for saline intrusion are similar to published measurement data concerning temporal development and spatial variability along the coast (Walther et al 2014, in review). A video (<http://youtu.be/-xBQJ9WWPJY>) shows the salinity distribution and flow paths through stream tracers originating in the southern and near coastal model domain exemplary for 1985. The effect of the heterogeneous permeability distribution can be recognized through the interlaced flow paths of the stream tracers that eventually merge into convection cells at the salt-freshwater interface.

Future Projection

In order to assess the remediation potential of the aquifer, a “best-case” scenario simulation was carried out with the assumption, that all pumping activity was ceased after year 2005. Additionally, we assume that the withdrawal of the saltwater will not involve any retention processes (e.g. reversible adsorption, double porosity continuum). The scenario simulation time was 500 years. We define the remediation potential Φ as

$$\Phi = 1 - c_{rel} \frac{\lambda}{\lambda_{max}} \quad (1)$$

with c_{rel} is relative concentration of salinity 10 m below groundwater level in 2005, λ is half-life of c_{rel} , and λ_{max} is maximum of λ . Comparable to the well-known half-life of a decaying element, the salinity half-life λ describes the time until the concentration of a mesh node reaches half of its value in the year 2005.

Figure 3 shows heterogeneous patterns of Φ . Some areas show a high remediation potential, while others do not reach half of the concentration value from 2005 after 500 years (striped areas). Differences between the eastern and western parts of the model domain are most likely due to a combination of spatially variable aquifer properties (e.g. permeability, yield) and corresponding preferred area of high abstraction activity. Although a “pump stop” might not be a practicable action, the best-case scenario simulation reveals a temporal dimension for remediation and overall salinization risk in the study area.

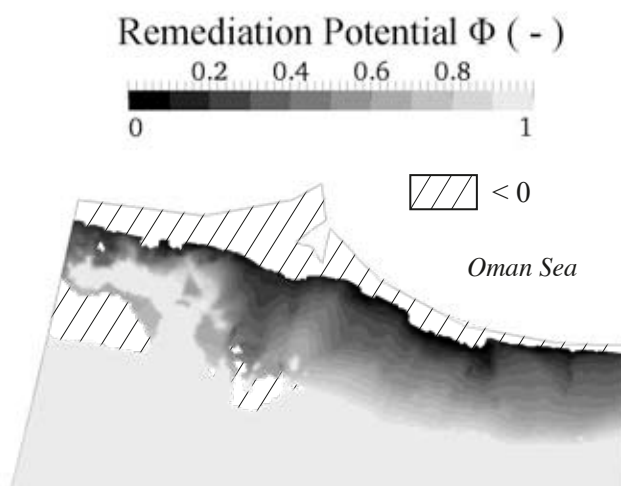


Figure 3 – Map of remediation potential in coastal area; from Walther et al (2014, in review).

CONCLUSIONS AND OUTLOOK

Although the data base was relatively weak compared to the typical requirements for this type of modeling including hydro-geological heterogeneities, the numerical model proved to be a useful tool. Calibrations show similar values as measurements and scenario results stress the vulnerability of the local aquifer system with its sensitive balance of the fresh-saltwater interface. In particular, the outcome underlines the necessity of an immediate action plan to prevent further saline intrusion or even total loss of the usability of the aquifer's groundwater resources.

ACKNOWLEDGEMENTS

The authors acknowledge the funding by the German Federal Ministry of Education and Research (BMBF Number: FKZ 02WM1166, IWAS), and by the Ministry of Science, Research and Arts of Baden-Württemberg (AZ Zu 33-721.3-2). The authors are grateful for the sincere cooperation of the Omani colleagues from the Ministry of Regional Municipalities and Water Resources, Muscat.

REFERENCES

- Goswami, R.R., Clement, T.P., 2007. Laboratory-scale investigation of saltwater intrusion dynamics. *Water Resour. Res.* 43, 1–11.
- Kalbacher, T., Delfs, J.O., Shao, H., Wang, W., Walther, M., Samaniego, L., Schneider, C., Musolff, A., Centler, F., Sun, F., Hildebrandt, A., Liedl, R., Borchardt, D., Krebs, P., Kolditz, O., 2011. The IWAS-ToolBox: Software Coupling for an Integrated Water Resources Management. *Environ. Earth Sci.*, doi:10.1007/s12665-011-1270-y.
- Kolditz, O., Bauer, S., Bilke, L., Böttcher, N., Delfs, J.O., Fischer, T., Görke, U.J., Kalbacher, T., Kosakowski, G., McDermott, C.I., Park, C.H., Radu, F., Rink, K., Shao, H.B., Sun, F., Sun, Y.Y., Singh, a. K., Taron, J., Walther, M., Wang, W., Watanabe, N., Wu, Y., Xie, M., Xu, W., Zehner, B., 2012. OpenGeoSys: an open-source initiative for numerical simulation of thermo-hydro-mechanical/chemical (THM/C) processes in porous media. *Environ. Earth Sci.* 67, 589–599.
- Park, C.-H., 2004. SALTWATER INTRUSION IN COASTAL AQUIFERS. Georgia, USA.
- Park, C.-H., Aral, M.M., 2008. Saltwater intrusion hydrodynamics in a tidal aquifer. *J. Hydrol. Eng.* 13, 863.
- Stoeckl, L., Houben, G., 2012. Flow dynamics and age stratification of freshwater lenses: Experiments and modeling. *J. Hydrol.* 458-459, 9–15.
- Stoeckl, L., Walther, M., Schneider, A., Yang, J. and Graf, T. Comparison of numerical models using a two-dimensional benchmark of density-driven flow (same issue) 2014.
- Walther, M., Böttcher, N., Liedl, R., 2012a. A 3D interpolation algorithm for layered tilted geological formations using an adapted inverse distance weighting approach, in: *ModelCare2011, Models - Repositories of Knowledge*. IAHS Publ. 355 (2012) ISBN 978-1-907161-34-6, 374, Leipzig, pp. 119–126.
- Walther, M., Delfs, J.-O., Grundmann, J., Kolditz, O., Liedl, R., 2012b. Saltwater intrusion modeling: Verification and application to an agricultural coastal arid region in Oman. *J. Comput. Appl. Math.* 236, 4798–4809.
- Walther, M., Bilke, L., Delfs, J.-O., Graf, T., Grundmann, J., Kolditz, O., Rudolf, L., 2014. Assessing the Saltwater Remediation Potential of a Three-Dimensional, Heterogeneous, Coastal Aquifer System: Model Verification, Application and Visualization for Transient Density-Driven Seawater Intrusion. *Env. Earth Sci.* In review.

Contact Information: Marc Walther, Helmholtz-Centre for Environmental Research, Department Environmental Informatics, Permoserstraße 15, 04318 Leipzig, Germany, mail: marc.walther@ufz.de

Saltwater intrusion in porous aquifers in Northern Germany

Helga Wiederhold¹, Reinhard Kirsch², Bernhard Siemon³

¹Leibniz Institute for Applied Geophysics (LIAG), Hannover, Germany

²Agency for Agriculture, Environment and Rural Areas Schleswig-Holstein (LLUR), Flintbek, Germany

³Federal Institute for Geosciences and Natural Resources (BGR), Hannover, Germany

BACKGROUND

In Northern Germany the primary source for drinking water supply is groundwater from porous Quaternary and Tertiary aquifers. After Grube (2000) around 25% of North German aquifers show inland salinization (upconing deeper saltwaters and salt diapir dilution) and about 5% seawater intrusion. The latter is expected to become more important in future due to climatic and demographic change. About 500 km coastal region (roughly measured) at the North Sea are concerned plus several barrier islands but also the metropolitan area of Hamburg.

INTRODUCTION

Availability of freshwater (in coastal areas) has been a challenge for long time. In the beginning of the settlement of the German coast water was collected in cisterns. Since the beginning of tourism and increasing of bather in the seaside resorts a more sustainable water supply has been necessary. That was the time when Herzberg made his studies on freshwater lenses on top of saltwater saturated sediments on the island of Norderney (Herzberg 1901). International discussion on groundwater salinization resulted in the first Salt Water Intrusion Meeting SWIM in Hannover (1968). Efforts were made to develop and apply geophysical methods to identify salinization. At the 6th SWIM first results of locating the freshwater/saltwater interface on the German North Sea island of Spiekeroog by airborne electromagnetic resistivity mapping were presented by Sengpiel and Meiser (1981). Since 2000 these airborne techniques have been applied to larger coastal regions also having in mind to create a reference data set as basis for monitoring climate or anthropogenic induced changes of the freshwater/saltwater interface at the German North Sea coast (Siemon et al. 2014a). Recently, several projects were dealing with saltwater intrusion and groundwater modelling, e.g., CLIWAT, KLIMZUG-NORD, KLIFF, NAWAK.

The objective of this paper is to summarize recent research activities on seawater intrusion in Northern Germany.

GEOLOGY

The hydrogeological situation of the upper 300 meter in northwestern Germany that is part of the North German Basin is dominated by Tertiary and Quaternary coarse grained, sandy sediments (aquifer) and fine grained, clayey strata (confining layer). Due to salt tectonics as well as glacial erosion and glacial tectonics the geological situation is very complex. In the coastal areas and where salt domes are close to the surface aquifer salinization is an issue.

The southern North Sea coast developed after the last glaciations in the Holocene. Today the German North Sea coastal area is dominated by low-lying marshland and higher elevated Geest ridges, estuaries of the rivers Ems, Weser, Elbe and Eider, the East Frisian barrier

islands and the North Frisian Geest core islands. Beside natural processes dike construction, land reclamation and water catchment affect the freshwater/saltwater environment.

GEOPHYSICAL METHODS

For geophysical methods to recognize salt water intrusion see Kirsch and Wiederhold (2014).

RESULTS / PROJECTS

Since 2000 the research borehole Cuxhaven Lüdningworth is focal point of coastal research and the basis of a “coastal aquifer test field” established by Leibniz Institute for Applied Geophysics (e.g., Wiederhold et al. 2005; Noell and Panteleit 2004). An airborne geophysical survey enabled a unique and large-area view to coastal seawater intrusions and freshwater aquifers as well as offshore freshwater springs (Siemon et al. 2004). Recognition of buried glacial valleys in these data provides the basis for the EU-project BurVal, where methods for mapping structures under the aspect of groundwater supply are developed and applied in pilot areas (BURVAL Working Group 2006). Building on these results and knowledge a general airborne survey of the German North Sea coastal area has been projected and started in 2008. Emphasis is placed on the mapping of freshwater/saltwater interfaces, saltwater intrusions and the evaluation of the coastal aquifers as well as on the mapping of submarine freshwater discharges (Siemon et al. 2014a). An example is given in Figure 1. With the mapping also a basis for monitoring should be set up. Interpretation strategies for airborne electromagnetic data are given, e.g., by Klimke et al. (2013), Siemon et al. (2014b).

With the EU-project CLIWAT groundwater dynamics came into focus as well as the effects of climate change on coastal groundwater systems and through this on surface water and water supply. Corresponding pilot areas for numerical groundwater modelling were the German North Sea islands Borkum (Sulzbacher et al. 2012) and Föhr (Scheer et al. 2014; Wiederhold et al. 2012). Also, to investigate the dynamics of the freshwater/saltwater transition zone at the North Sea island Borkum two vertical electrode systems of about 20 m length were installed in two water catchment areas in depths between 44 m and 65 m, i.e. in the freshwater/saltwater transition zone below the pumps. Data are transferred to LIAG in 5-hour rhythm (Grinat et al. 2014).

Similar groundwater modelling studies were performed for the Elbe estuary in the BMBF (Federal Ministry of Education and Research)-project KLIMZUG-NORD (www.klimzug-nord.de) or for the Weser estuary in the MWK-Niedersachsen (Ministry of Economy and Culture of the State of Lower Saxony)-project KLIFF (www.kliff-niedersachsen.de). For further studies on barrier islands see the BGR-project FLIN (e.g., Houben et al. 2014; Costabel et al. 2014).

Currently, the State Authority for Mining, Energy and Geology (LBEG) plans to generate a statewide “salt water map” for Lower Saxony (Deus et al. 2014). For actual maps see NIBIS® MAPSERVER.

A planning tool for coastal aquifers at the German North Sea Coast is under development in the project NAWAK. This tool takes into account the hydrodynamic and hydrochemical evolution of the aquifer as well as groundwater recharge and hydrological impacts of open drainages. Also specified targets and options of the regional water suppliers and other stakeholders are included (Eley et al. 2014).

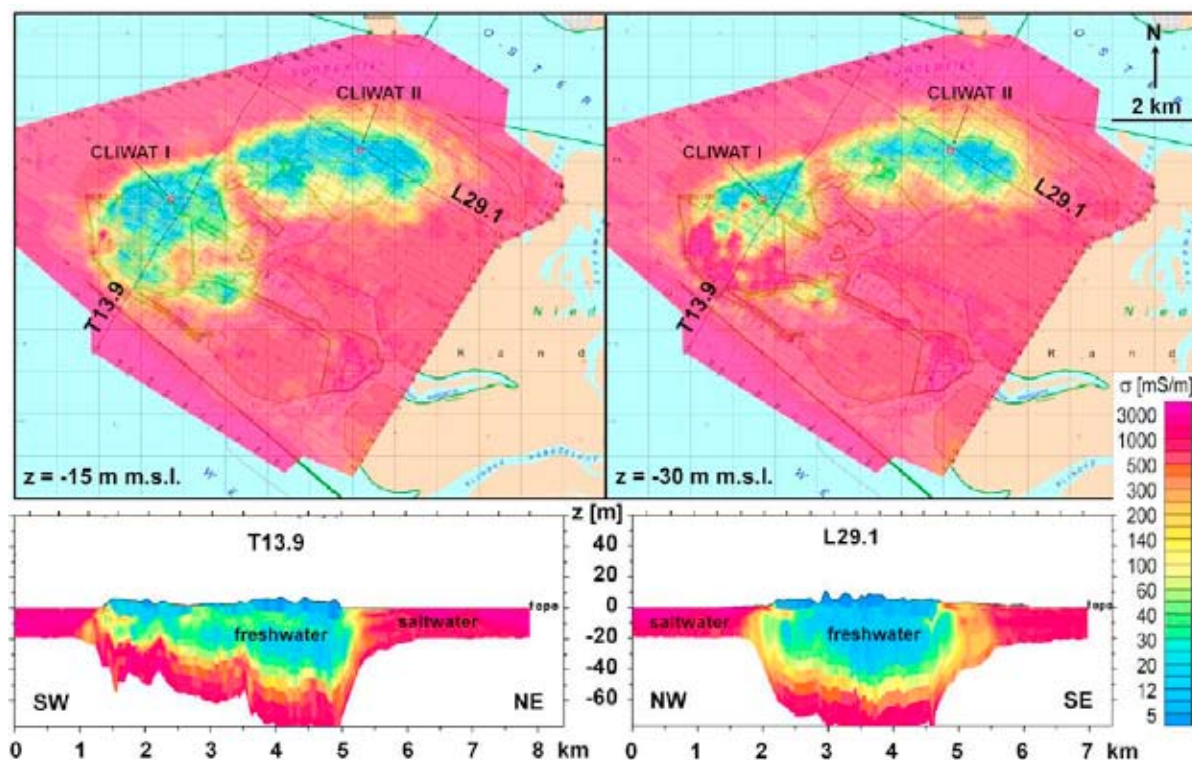


Figure 1. Top panel: Electrical conductivity (σ) maps for the North Sea island Borkum at different depths derived from helicopter-borne electromagnetic survey (saltwater saturated = high conductivity, freshwater saturated = low conductivity), bottom panel: cross sectional view along transects T13.9 and L29.1 (from Sulzbacher et al. 2012).

REFERENCES

- BURVAL Working Group. 2006. Groundwater Resources in Buried Valleys - A Challenge for Geosciences. Leibniz Institute for Applied Geophysics, 314 pp., 190 figs, Hannover:LIAG.
- Costabel, S., U. Noell, T. Günther, G. Houben, and W. Voß. 2014. Geophysical investigation of a managed freshwater lens on the North Sea island of Langeoog. In Proceedings of the 23rd Salt Water Intrusion Meeting, Husum, Germany.
- Deus, N. and J. Elbracht. 2014. 3D-Modelling of the salt-/fresh water interface in coastal aquifers of Lower Saxony (Germany) based on airborne electromagnetic measurements (HEM). In Proceedings of the 23rd Salt Water Intrusion Meeting, Husum, Germany.
- Eley, M., M. Howahr, A. Schneider, H.M. Schöniger, A. Ullmann, J. Wolf, and G. Meon. 2014. Potential Consequences of Saltwater Intrusion at the German North Sea Coast for the water supply. In Proceedings of the 23rd Salt Water Intrusion Meeting, Husum, Germany.
- Grinat, M., W. Südekum, D. Epping, and R. Meyer. 2014. Measurements with an automated electrical resistivity tomography system in a freshwater/saltwater transition zone. In Proceedings of the 23rd Salt Water Intrusion Meeting, Husum, Germany.
- Grube, A. 2010. Widespread geogenic salt water occurrence in North Germany - demonstrated on the basis of a generalized map. In Proceedings of the 16th Salt Water Intrusion Meeting, Wolin Island, Poland.

Herzberg, B. 1901. Die Wasserversorgung einiger Nordseebäder. *J. Gasbel. Wasservers.*, 44: 815–819.

Houben, G., P. Koeniger, and J. Sültenfuß. 2014. Freshwater lenses as archives for climate history and hydrochemical evolution - insights from depth-specific age dating and stable water isotope analysis, Langeoog Island, Germany. In *Proceedings of the 23rd Salt Water Intrusion Meeting*, Husum, Germany.

Kirsch, R. and H. Wiederhold. 2014. Saltwater intrusions - a challenge for geophysics. In *Proceedings of the 23rd Salt Water Intrusion Meeting*, Husum, Germany.

Klimke, J., H. Wiederhold, J. Winsemann, G. Ertl, and J. Elbracht. 2013. Three-dimensional mapping of Quaternary sediments improved by airborne electromagnetics. *Z. dt. Ges. Geowiss.*, 164: 369-384.

NIBIS® MAPSERVER (<http://nibis.lbeg.de/cardomap3>)

Noell, U. and B. Panteleit. 2004. Geophysical detection and hydrochemical analysis of an isolated shallow salt water body near Cuxhaven, Lower Saxony, Germany. In *Proceedings of the 18th Salt Water Intrusion Meeting*, Cartagena, Spain.

Scheer, W., B. Nommensen, and B. König. 2014. The fresh-saltwater distribution of the Island of Föhr - assembling of a data base for the assessment of climate change impact. In *Proceedings of the 23rd Salt Water Intrusion Meeting*, Husum, Germany.

Sengpiel, K.-P. and P. Meiser. 1981. Locating the freshwater/saltwater interface on the Island of Spiekeroog by airborne EM resistivity/depth mapping. *Geologisches Jahrbuch C29*: 255-271. Hannover: BGR.

Siemon, B., D.G. Eberle, and F. Binot. 2004. Helicopter-borne electromagnetic investigation of coastal aquifers in North-West Germany. *Z. geol. Wissen* 32: 385-395.

Siemon, B., H. Wiederhold, A. Steuer, M.P. Miensopust, W. Voß, M. Ibs-von Seht, and U. Meyer. 2014a. Helicopter-borne electromagnetic surveys in Northern Germany. In *Proceedings of the 23rd Salt Water Intrusion Meeting*, Husum, Germany.

Siemon, B., W. Voß, J. Elbracht, N. Deus and H. Wiederhold. 2014b. Airborne clay mapping at the East Frisian coast. In *Proceedings of the 23rd Salt Water Intrusion Meeting*, Husum, Germany.

Sulzbacher, H., H. Wiederhold, B. Siemon, M. Grinat, J. Igel, T. Burschil, T. Günther, and K. Hinsby. 2012. Numerical modelling of climate change impacts on freshwater lenses on the North Sea Island of Borkum using hydrological and geophysical methods. *Hydrology and Earth System Sciences* 16: 3621-3663.

Wiederhold, H., F. Binot, and W. Kessels. 2005. The Cuxhaven research borehole and the “Coastal Aquifer Test Field (CAT-Field)” – a test field for applied geoscientific research. *Zeitschrift für Angewandte Geologie* 51(1): 3-6.

Wiederhold, H., W. Scheer, R. Kirsch, T. Burschil, and M. Lilienfein. 2012. Effects of climate change to the groundwater body of the German North Sea Island of Föhr. In *Proceedings of the 22nd Salt Water Intrusion Meeting*, Armacao dos Buzios, Brazil.

Contact Information: Helga Wiederhold, Leibniz Institute for Applied Geophysics, Stilleweg 2, 30655 Hannover, Germany, Email: helga.wiederhold@liag-hannover.de

Modelling the Climate Change Impact on Seawater Intrusion in the Coastal Aquifer of Bremerhaven, North Germany

J. Yang¹, T. Graf¹ and T. Ptak²

¹Institute of Fluid Mechanics and Environmental Physics in Civil Engineering, Leibniz Universität Hannover, Germany

²Applied Geology, Geosciences Center, Georg-August-Universität Göttingen, Germany

ABSTRACT

Climate change is expected to induce sea level rise in the German Bight, which is part of the North Sea, Germany. Climate change may also modify river discharge of the river Weser flowing into the German Bight, which will alter both pressure and salinity distributions in the German Bight. To study the long-term interaction between sea level rise, discharge variations, and coastal aquifer flow dynamics, a three-dimensional saltwater intrusion model was designed using the fully coupled surface-subsurface numerical model HydroGeoSphere. The model simulates the coastal aquifer as an integral system considering complexities such as: (i) hydrodynamic factors (e.g. tidal fluctuations, variable-density flow, irregular land surface, boundary conditions), and (ii) anthropogenic factors (e.g. dyke, drainage canals, gates). The model simulates a real case of tidal activity for the period from April-08 to April-22 2009. In addition, three climate change scenarios are simulated until the year 2100 where the seaside boundary condition is obtained from an external hydrodynamic model: (i) mean sea level rise (MSLR) of 1 m, (ii) decrease of river Weser discharge (yearly average) from $326 \text{ m}^3 \text{ s}^{-1}$ to $200 \text{ m}^3 \text{ s}^{-1}$, and (iii) increase of river Weser discharge from $326 \text{ m}^3 \text{ s}^{-1}$ to $2000 \text{ m}^3 \text{ s}^{-1}$. Results demonstrate that the position of the seawater-freshwater interface as well as drainage discharge will be affected by climate change. The obtained results are useful for coastal engineering practices and drinking water resource management.

Keywords: seawater intrusion, climate change, coupled approach

INTRODUCTION

The German Bight, as part of the North Sea, has shown a MSLR of about 20 cm during the last 100 years. The river Weser discharges into the German Bight. That river Weser estuary is heavily influenced by the tides. Altered tidal dynamics is also expected due to the MSLR (Pickering et al., 2012). Climate change also leads to the change of river discharge from hinterland (Huang et al., 2013) and therefore the salinity of the estuary. Those processes change the sea level or salinity of the estuary, and consequently influence the seawater intrusion to the coastal aquifer belonging to the estuary. Yang et al. (2013) numerically simulated two-dimensional coastal flow dynamics, assuming a fully coupled surface-subsurface approach of the coastal aquifer Unterweser, accounting for all processes relevant to coastal flow dynamics. Zorndt and Zhang (2013) investigated the impact of climate change and tidal activity on hydrodynamics and salinities in the river Weser and its estuary using SELFE, which is a semi-implicit Eulerian-Lagrangian finite-element model for hydrodynamic cross-scale ocean circulation (Zhang and Baptista, 2008).

The aquifer under investigation has an area of around 108 km^2 . The west boundary contacts to the river Weser estuary. Flow and transport boundary conditions are obtained from results

provided by Zorndt and Zhang (2013). The inland is protected by a dyke along the shoreline. Drainage canals drain inland water via two outlet gates through the dyke to the estuary. The operation of the gates is tide-dependent and one-way, which means that seaward water flow is allowed during low-tide, but during high-tide, landward flow is inhibited and the gates are closed.

Using the fully coupled surface-subsurface approach of the numerical model HydroGeoSphere (Therrien et al. 2010), objectives of this study are: (i) to apply the coupled surface-subsurface HydroGeoSphere model to the 3D coastal aquifer considering hydrodynamic factors (e.g. tides) and anthropogenic factors (e.g. dyke, drainage canals), and (ii) to use the 3D model to predict and evaluate seawater intrusion effects on groundwater resources under climate change. The results of this study are potentially important for coastal engineering, protection practice of coastal infrastructure, and coastal aquifer water management.

MATHEMATICAL MODEL

HydroGeoSphere is a 3D numerical model describing fully-integrated variably-saturated subsurface and surface flow and variable-density solute transport. HydroGeoSphere uses the diffusive-wave approximation of the St. Venant equation for surface water flow. In order to represent the drainage canals, HydroGeoSphere is adapted to include a 1D canal domain, which is composed by 1D segments. Flow and transport in the canal domain share the same equations with the 2D surface domain, which are the diffusive-wave approximation of the St. Venant equation for flow and the advective-dispersive-diffusive transport equation. The one-way canal water flow through the gates is achieved by monitoring the hydraulic gradients at the gates.

SIMULATION AND RESULTS

In this study, the subsurface domain is discretized by vertically oriented 3D prisms, the surface domain is discretized by 2D triangular faces, and the canal domain is discretized by 1D segments. Parameter values are chosen from previous work for the investigated site (Yang et al., 2013). Time-variable heads and salinity during tidal activity are prescribed to the sea side boundary. Recharge is prescribed to the land surface. The model firstly ran for the year 2009 to reach a steady state for flow and transport, using the average sea levels and salinity of the year 2009. The steady state results of the year 2009 were calibrated using 111 groundwater level measurements. The modelling shows good fit between observed and simulated groundwater levels after calibration with PEST. The calibrated results were used as initial conditions for the following three climate change scenarios: (i) MSLR of 1 m, (ii) decrease of river Weser discharge (yearly average) from $326 \text{ m}^3 \text{ s}^{-1}$ to $200 \text{ m}^3 \text{ s}^{-1}$, and (iii) increase of river Weser discharge from $326 \text{ m}^3 \text{ s}^{-1}$ to $2000 \text{ m}^3 \text{ s}^{-1}$.

Result 1. Change of groundwater table

The simulated results show that 1 m of MSLR causes a groundwater table rise of 50 cm for most of the aquifer. Decrease of the river Weser discharge to $200 \text{ m}^3 \text{ s}^{-1}$ has relative little to no effect on the groundwater table, while increasing the river Weser discharge to $2000 \text{ m}^3 \text{ s}^{-1}$ causes 10 cm decrease of groundwater table for most of the land area because larger discharge of freshwater into the Weser estuary leads to a decrease of water pressure in the estuary. As a consequence of dropping pressure, subsurficial flow rates into the estuary increase and, hence, the groundwater table drops.

Result 2. Change of salinity

The simulated results (Figure 1) show that 1 m of MSLR results in about 200 m advance of the contaminated area in the deeper aquifer. Decrease of the river Weser discharge to $200 \text{ m}^3 \text{ s}^{-1}$ has no significant effect on the contaminated aquifer area, while, increasing the river Weser discharge to $2000 \text{ m}^3 \text{ s}^{-1}$ causes about 1400 m retreat of contaminated area in deeper aquifer.

Result 3. Change of discharge rates at gates

Simulated results (Figure 2) indicate that about 150% increase of discharge rate will result from 1 m of MSLR, and 60% of decrease of discharge rate will result from the increase of the river Weser discharge to $2000 \text{ m}^3 \text{ s}^{-1}$. Decreasing the river Weser discharge to $200 \text{ m}^3 \text{ s}^{-1}$ has not significant effect on changing the discharge rate.

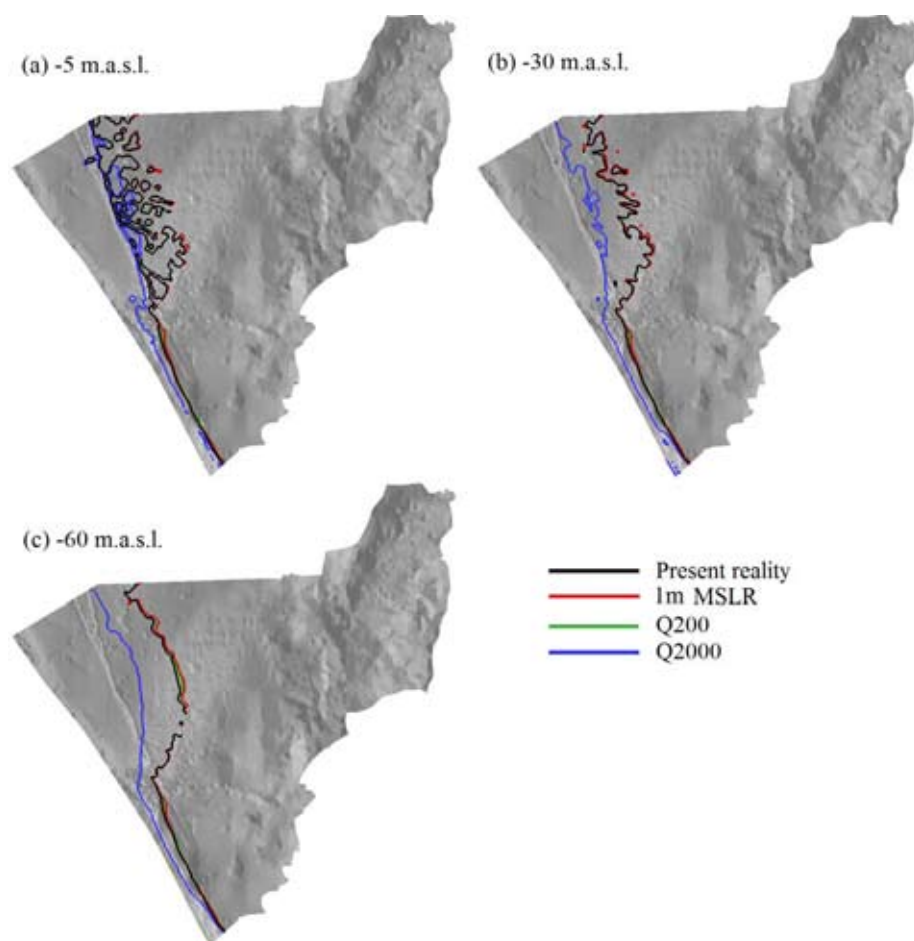


Figure 1. The iso-salinity lines of salinity = 0.671 PUS (drinking water standard) for each climate change scenario at different aquifer depths. For a colored figure please refer to an electronic version.

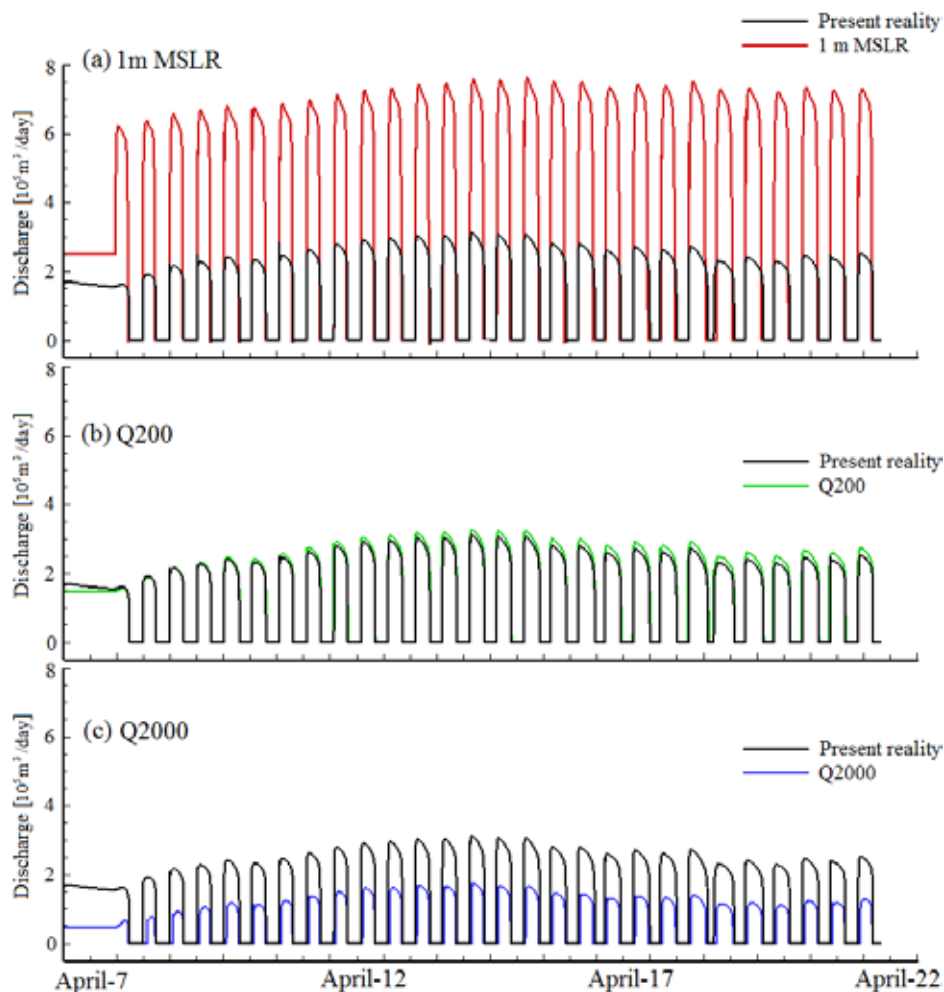


Figure 2. Comparison of the discharge rate at the south gate between “present reality” and each climate change scenario. For a colored figure please refer to an electronic version.

REFERENCES

- Huang S, Hattermann FF, Krysanova V, Bronstert A, 2013. Projections of climate change impact on river flood conditions in Germany by combining three different RCMs with a regional eco-hydrological model. *Climate Change*. 116, 631-663.
- Pickering M, Wells N, Horsburgh K, Green J, 2012. The impact of future sea-level rise on the European Shelf tides. *Continental Shelf Research*. 35, 1-15.
- Therrien R, McLaren R, Sudicky E, Panday S, 2010. *HydroGeoSphere - A three-dimensional numerical model describing fully-integrated subsurface and surface flow and solute transport*. University of Waterloo and Université Laval, Canada.
- Yang J, Graf T, Herold M, Ptak T, 2013. Modelling the effects of tides and storm surges on coastal aquifers using a coupled surface-subsurface approach. *Journal of Contaminant Hydrology*. 149, 61-75.
- Zhang YL, Baptista AM, 2008. SELFE: A semi-implicit Eulerian-Lagrangian finite-element model for cross-scale ocean circulation. *Ocean Modelling* 21 (3-4): 71-96.
- Zorndt AC, Zhang YJ, 2013. Modelling salt intrusion into the Weser Estuary with semi-implicit Eulerian-Lagrangian finite-element approach. *Ocean Dynamics*.

Dating of saline groundwater from several Israeli aquifers, indication for paleo seawater intrusion and comparison with results of numerical simulations

Yecheili Y.^{1,2}, Zilberbrand M.³, Burg A.¹, Weinstein Y.⁴, Wollman S.¹, Sivan O.²

¹Geological Survey of Israel

²Ben Gurion University

³Israeli Water Authority, Hydrological Service

⁴Bar Ilan University

ABSTRACT

This study deals with dating of saline groundwater, with salinity closed to that of seawater (mostly >75% seawater). Such dating was seldom conducted before since, in most cases, even the most saline water samples have a significant component of fresh water. Moreover, since the carbon concentration in the fresh groundwater is usually significantly larger than that of seawater, dating of the saline component with the radiocarbon method is difficult even in cases where the fresh component is 25% of the mixture.

We attempt to date saline groundwater in two of the main aquifers in Israel (the Coastal Aquifer and the Mountain Aquifer), using the most saline samples that could be obtained (some are >90% seawater) and correcting with the NetPath geochemical code, in order to estimate the time of seawater intrusion into these aquifers.

In the Coastal Aquifer, most of the saline water was found to be young (>50 years, tritium containing, ~60 PMC) indicating recent seawater intrusion. However, in some of the deeper sub-aquifers older saline water was found (5-10 PMC, i.e. older than ~10000 years), implying penetration of seawater at older time. Complementary age determinations were conducted on the fresh groundwater, some of which were found to be very old.

In the Mountain Aquifer, old saline water bodies were found in several locations. Estimation of the age of the different end members (fresh and saline) showed that the seawater component is older than 30000 year, probably beyond radiocarbon dating. The isotopic values of this old seawater component is similar to that of the present seawater (e.g. $\delta^{18}\text{O}$ of ~1.5‰ and 1.8‰ in old and recent seawater) which implies that the intrusion took place in similar sea conditions to that of the present ones. An attempt to determine the age of this old seawater will be done with noble gases.

Numerical simulations were conducted with FEFLOW in order to examine the flow regime in the different parts of the coastal aquifer. At this stage, only some preliminary steady state simulations were conducted and were found to fit quite well with ages of saline groundwater. Transient simulations are planned to be conducted in the next stage in order to simulate the effect of sea level changes (e.g. the rise of 120 meters at the end of the glacial period) on the rate of seawater intrusion into the coastal aquifers. These preliminary data show that dating of seawater component can be conducted provided high salinity groundwater is found.

Fresh keeper without reverse osmosis: can we prevent upconing by pumping brackish water to a deeper aquifer?

Willem J. Zaadnoordijk¹, Ate Oosterhof², Mark Houweling³, and Klaasjan Raat¹

¹KWR Watercycle Research Institute, Nieuwegein, the Netherlands

²Vitens, Zwolle, the Netherlands

³BAM de Ruiter, Hoofddorp, the Netherlands

ABSTRACT

At the former well field of Noardburgum in the Northern part of the Netherlands, a new pilot is started with a Fresh keeper well. Three well screens are placed in a single borehole: a fresh water extraction, a brackish water extraction, and injection of the brackish water. The fresh extraction will be pumping at a constant rate, while the combined brackish extraction and injection will adjusted to keep the fresh/brackish interface stable in between the two extraction well screens.

INTRODUCTION

Noardburgum is a village in the Northern Part of the Netherlands (see Figure 1). The well field of Noardburgum had been abandoned in 1993 due to salinization by upconing of deep brackish paleo groundwater. The water supply company Vitens wants to re-open the well field using Fresh keeper wells to obtain a stable extraction of fresh water.

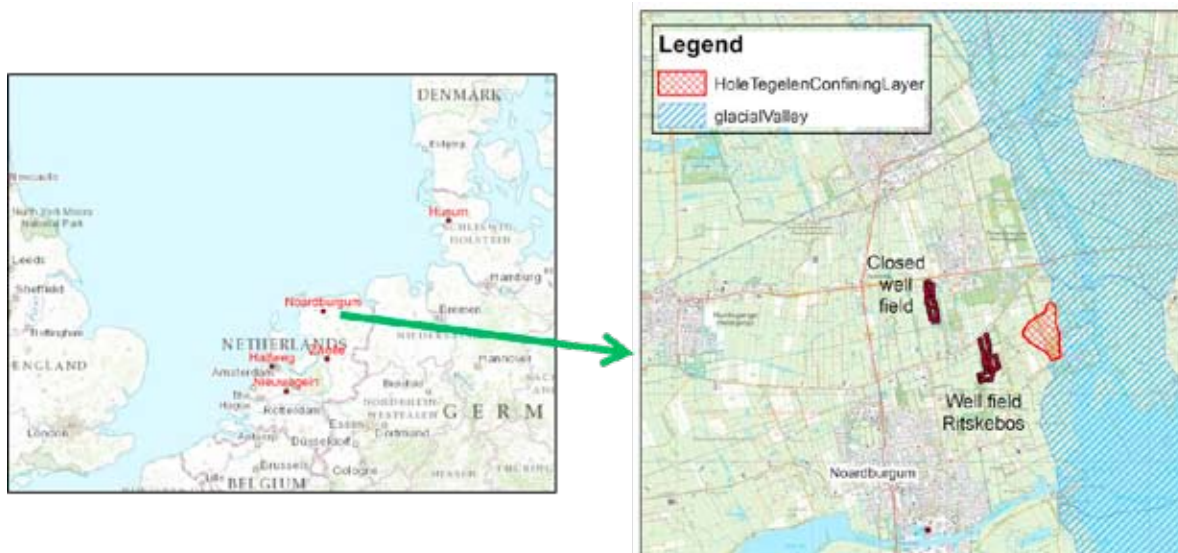


Figure 1. Location of Noardburgum and important geological features.

The philosophy of Fresh keeper wells is to prevent salinization of extraction wells by pumping also in the saline water. This reduces the head in saline water and prevents it from flowing toward the fresh extraction. A question to answer is what to do with the extracted saline water. Usually, discharge into surface water is not feasible. An option is to use reverse osmosis and use part of the water, but then the question becomes what to do with the

concentrate. In several pilots this has been injected deeper into the subsurface (Raat & Kooiman, 2012).

A first pilot with a Fresh keeper well has been operated at the former Noardburgum well field between 2009 and 2011 (Oosterhof & Raat, 2010, Raat et al., 2012, Oosterhof et al., 2013). The water from the saline extraction was treated with reverse osmosis (BWRO – Brackish Water Reverse Osmosis) so that part could be used as drinking water and the concentrate was injected below a regional aquitard. For full scale operation, reverse osmosis would require a large investment in the installation and relatively high energy costs for operation. Therefore, Vitens has started a new pilot in which all abstracted saline water is injected in a deeper aquifer to investigate whether this would be a better option for revitalizing the well field. Moreover, several aspects of the technical implementation of monitoring and operation of the Fresh keeper are developed and tested.

HYDROGEOLOGICAL SITUATION AND WELL SETUP

Noardburgum is located in an area with a lot of controlled surface water (see figure 1). The surface waters are separated from the aquifer system by a Holocene confining layer. To the East, a deep glacial valley is present in the subsurface, which is filled with tight clays. The aquifer system at Noardburgum consists of two main aquifers separated by a clay layer belonging to the Tegelen Formation (see Figure 2). The upper aquifer consists of two parts (1A and 1B) which are not separated by a resistance layer like the two parts of the lower aquifer (2). The properties of this resistance layer are not well known because only a few bore holes have been drilled to this depth. The inversions in the Chloride concentration indicate that this layer has a significant resistance and presence. The regional presence of the Tegelen clay is better documented, including a hole near the glacial valley (see Figure 1).

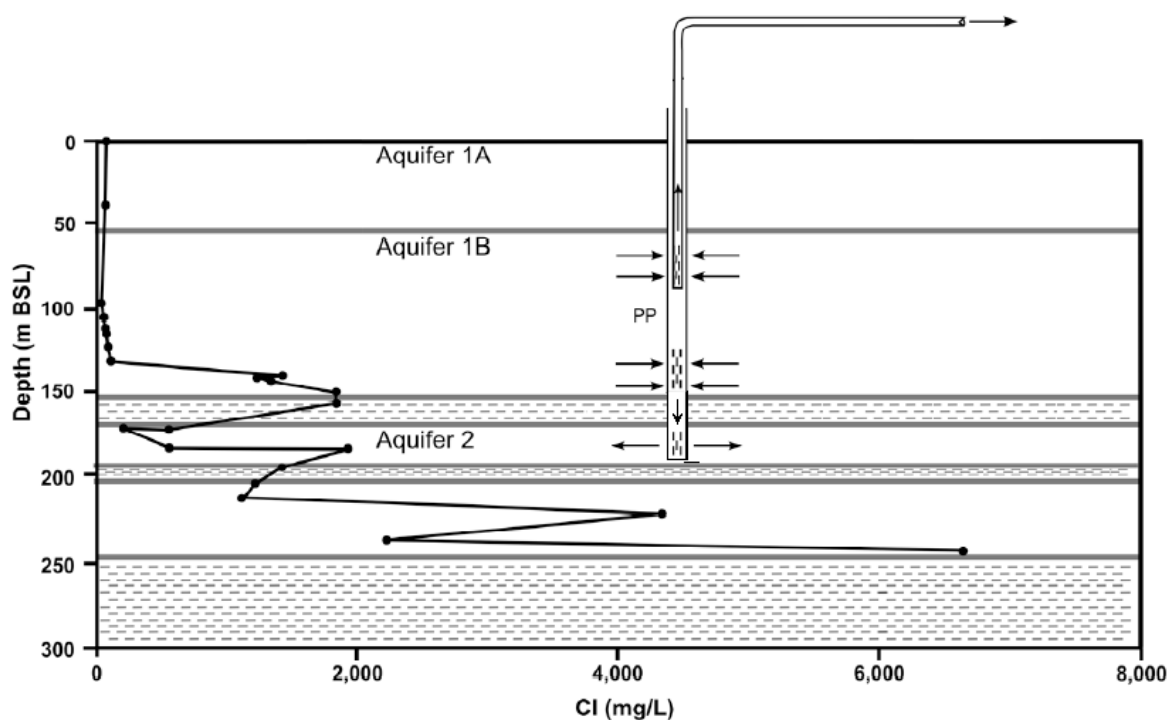


Figure 2. Hydrogeology at Noardburgum.

The fresh keeper well has three well screens in a single borehole (see Figure 2). Moreover, several monitoring wells will be installed of which one is wide enough for an EM-39 probe. The upper well screen is located above the fresh-brackish interface. The middle well screen is located near the base of Aquifer 1B below this interface. All water abstracted from the middle well screen will be injected into aquifer 2 through the lower well screen underneath the Tegelen confining layer.

MODELLING

An existing groundwater flow and transport model (Royal Haskoning, 2007) has been updated and refined to determine the effects of the new Freshkeeper at Noardburgum. The model can also be used to interpret the monitoring results. The upward flow through the hole in the Tegelen confining layer is the most sensitive aspect toward the existing well field of Ritskebos (see Figure 3).

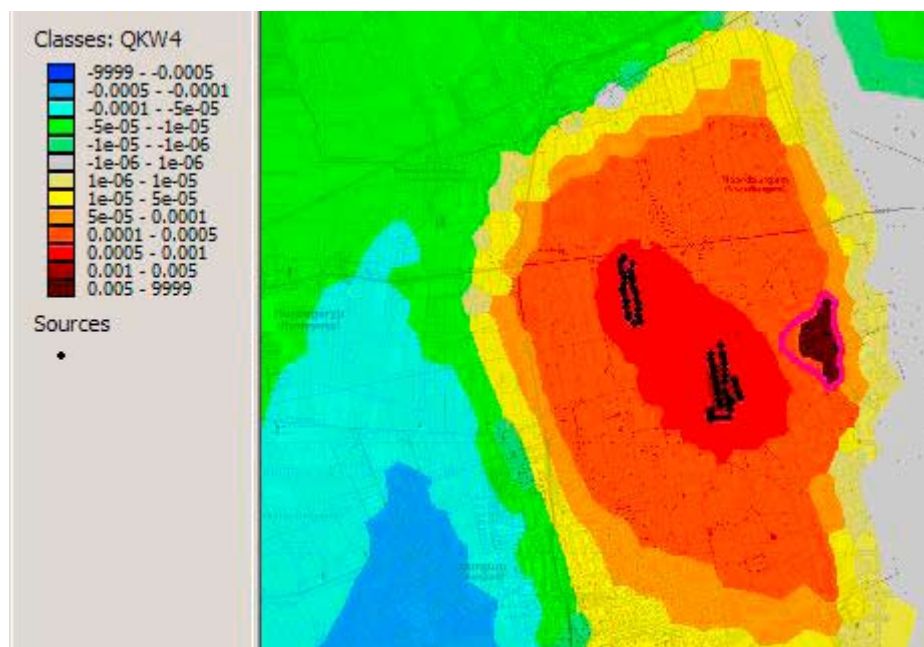


Figure 3. Flux from injection aquifer (2) to pumped (1B) through Tegelen clay.

DISCUSSION

The fresh abstraction will have a constant rate for the production of drinking water. The brackish abstraction will vary. The aim is to pumped at the minimum rate required to prevent upconing of brackish water toward the upper well screen. The brackish discharge will be adjusted automatically based on the signal from an electric conductivity sensor. The sensor will be placed in a monitoring well outside the well screen near its top. The brackish pumping rate will be decreased, when the electric conductivity (Ec) declines and increased when the Ec goes up. The control values will be established based on the values encountered during the installation of the well and will be adjusted when necessary based on the monitoring information.

CONCLUDING REMARKS

The new aspects of the Freshkeeper well to test in this pilot at Noardburgum are 1) three well screens with separate standpipes in a single borehole 2) monitoring the fresh/brackish interface between two extraction well screens 3) automatic control of the brackish extraction/injection to stabilize the interface, and 4) injection of the full amount of the brackish extraction instead of reducing its volume (and increasing the concentrations) by applying reverse osmosis.

REFERENCES

- Stuyfzand, P.J. & Raat, K.J. 2010 Benefits and hurdles of using brackish groundwater as a drinking water source in the Netherlands. *Hydrogeology Journal*, 18, 117-130. DOI 10.1007/s10040-009-0527-y.
- Grakist G., Maas, C., Rosbergen, W. & Kappelhof, J. 2002 Keeping our wells fresh. *Proceedings 17th Salt Water Intrusion Meeting*, 6–10 May 2002, Delft. pp. 337-340.
- Oosterhof, A.T. & Raat, K.J. 2010 Keep it Fresh! Field test results of the fresh keeper concept. *Proceedings ISMAR-7*, 9-13 October 2010, Abu Dhabi.
- Oosterhof, A.T., Raat, K.J. and Wolthek, N.B.A. (2013). Reuse of salinized well fields for the production of drinking water by interception and desalination of brackish groundwater. *IWA International Conference on Water Reuse*, October 27-31, 2013, Windhoek, Namibia.
- Raat, K.J., Stuyfzand, P.J. Boukes, H. & Oosterhof, A.T. 2011 Water quality changes following deep well injection of BWRO concentrate. Results from the BWRO pilots Noardburgum and Zevenbergen. Report number BTO 2011.105(s). KWR Watercycle Research Institute, Nieuwegein, the Netherlands.
- Raat, Klaasjan J., and Jan Willem Kooiman. 2012. Brackish groundwater: not avoid, but use! Final report pilots Noardburgum (Vitens) and Zevenbergen (Brabant Water) (in Dutch: Brak groundwater: niet mijden, maar gebruiken! Eindrapport BTO onderzoek pilots Noardburgum (Vitens) en Zevenbergen (Brabant Water)), Report 2011.48, KWR Watercycle Research Institute, Nieuwegein, the Netherlands.

Contact Information: Willem J. Zaadnoordijk, KWR Watercycle Research Institute, Geohydrology team, Groningenhaven 7, P.O. Box 1072, 3430 BB Nieuwegein, the Netherlands, Phone: +31 (30) 6069 597,
Fax: +31 (30) 6061165, Email: willemjan.zaadnoordijk@KWRwater.nl

Overview: management of groundwater at salinisation risk

Polemio M., Zuffianò L.E.

Istituto di Ricerca per la Protezione Idrogeologica – CNR, Bari, Italy,

ABSTRACT

Natural waters contain dissolved minerals from interactions with atmospheric and soil gases, mixing with other solutions, and/or interactions with the biosphere and lithosphere. In many cases, these processes result in natural waters containing solute or salinity above concentrations recommended for a specified use, which creates significant social and economic problems.

Groundwater salinization can be caused by natural phenomena and anthropogenic activities. For the first case, we can distinguish terrestrial and marine phenomena. Approximately 16% of the total area of continental earth is potentially involved in groundwater salinization. Seawater intrusion can be considered to be the primary phenomenon for study in terms of groundwater salinization.

The primary marine phenomena are (a) seawater intrusion and (b) downward intrusion.

Major underground sources of salt water of terrestrial origin can be distinguished as (c) connate groundwater, (d) juvenile groundwater, (e) the dissolution of soluble minerals of natural soils and rocks, (f) evapotranspiration effects in shallow groundwater, and (g) saline fluids from anthropogenic activities.

There are different measures, actions and practices for managing groundwater when the natural resource is exposed to salinization. Some of these measures have a mitigation objective. Other measures have a more adaptive approach and accept the high groundwater salinity but adjusting the groundwater use so that it is not harmful.

The complexity of these approaches generally increases due to difficulties caused by groundwater quality and quantity degradation and increased demand for quality water. Moving from the lowest to the highest complexity, these approaches are the engineering approach, the discharge management approach, and the water and land management approach.

The engineering approach is realized on the local scale with the purpose of controlling the salinization, optimizing the well discharge with specific technical solutions and/or completing works to improve the quality and/or quantity of the discharged fresh groundwater.

The discharge management approach includes a coastal aquifer and defines rules concerning groundwater utilization and well discharge.

The water and land management approach should be applied on the regional scale. This approach becomes necessary when one or more need creates an overall framework of high-quality water scarcity. These conditions, sometimes combined with an awareness of negative environmental effects, force people to accept new water saving practices and land use modifications. As the natural effects of salinization can be enhanced by a multiplicity of human actions, the discharge management approach and the water and land management approach should generally be applied by water authorities or institutional and governmental organizations that are responsible for groundwater quality and availability.

This research classifies the sources of groundwater salinization and defines in detail different management approaches to protecting the groundwater through salinization mitigation and/or groundwater salinity improvements. By focusing the attention on the effect of seawater intrusion, practical solutions are proposed.

Bold numbers indicate presenting authors

Abou Najem, M.	311	Daniele, L.	379, 380
Ahmed, A.	323, 327	Danskin, W.	71
Al Bitar, A.	204	De Giglio, M.	75
Al Farrah, N.	445	de Haas, S.	79
al Hagrey, S.	20	de la Torre, B.	343
Al-Raei, A.	42	de Louw, P.	83, 87 , 91, 199, 281, 416, 417, 437
Alam, N.	24 , 269	De Rosa, R.	297
Alameddine, I.	311	Deiana, R.	438
Allen, D.	25 , 168	Delfs, J.	449
Alves, M.	67	Dellwig, O.	46
Antonellini, A.	25	Delsman, J.	91
Antonellini, M.	125, 248, 427	Denchik, N.	288
Antoniou, A.	397	Deus, N.	95 , 371
Apollaro, C.	297	Devriese, G.	99 , 221
aus der Beek, M.	31	Dlugosch, R.	150
Bakker, M.	32 , 256, 350	Dragone, V.	235
Banda, K.	33	Duque, C.	339, 343
Banton, O.	62, 261	Eeman, S.	87
Baque, L.	288	El Fadel, M.	311
Barbarella, M.	75	Elbracht, J.	95, 371
Barrocu, G.	34	Eley, M.	103
Basso, A.	235	Elnaiem, A.	107
Batelaan, O.	409	Epping, D.	134
Bauer-Gottwein, P.	33	Ergul, S.	344
Beekman, W.	54	Erkul, E.	108
Bellot, J.	288	Escher, P.	42
Bierkens, M.	91, 189	Faneca Sanchez, M.	275, 417, 437, 109
Bilke, L.	449	Ferranti, F.	344
Boehme, J.	154	Fidelibus, M.	113, 117
Boluda-Botella, N.	38	Gavrieli, I.	279
Böning, P.	42	Geeraert, M.	288
Böttcher, E.	46	Geier, J.	444
Böttcher, M.	42, 46	Ghabayen, S.	121
Böttcher, T.	46	Giambastiani, B.	125
Bourhane, A.	50	Gingerich, S.	129
Brand, L.	358	Gisseloe, P.	435
Burg, A.	461	Glaeser, C.	154
Butler, A.	239	Goldau, N.	144, 148
Caljé, R.	54	Gómez Fontalva, J.	343
Calvache, M.	339, 343	Gouze, P.	288
Campana, C.	113	Gräber, M.	108
Capo, D.	25	Graf, T.	144, 148, 363, 449, 457
Casarano, D.	235	Greggio, N.	25, 75, 125, 427
Cassidy, R.	62	Greskowiak, J.	132
Chalikakis, K.	261	Grinat, M.	134
Chan, C.	243	Groen, J.	285
Chowdhury, A.	393	Groen, M.	138 , 285, 310, 418
Chripim, Z.	67	Grossmann, J.	140
Cianflone, G.	297	Grundmann, J.	449
Claus, J.	58 , 99, 221	Guevara, C.	144, 148
Comte, J.	50, 62	Günther, T.	63, 150, 195, 331, 335
Condesso de Melo, M.	67, 310	Gvirtzman, H.	225, 279
Costabel, S.	63 , 150	Haber, E.	381
Coviello, M.	344	Hamill, G.	323, 327
Craig, S.	309	Hanh, H.	154
Cremer, C.	144, 148	Häusler, S.	366
Crespo, K.	243	Heiss, J.	158
Curras, J.	380	Henneberg, M.	108
da Silva Jr., G.	67 , 164	Henry, G.	288
Daniel, M.	261	Herckenrath, D.	162, 163 , 215

Herut, B.....	121	Liu, H.....	164
Hinsby, K.....	164 , 319	Lods, G.....	288
Hoang, H.....	220	Lofi, J.....	288
Holding, S.....	168	López Chicano, M.....	339, 343
Houben, G.....	63, 172 , 176 , 180 , 393	Ma, Z.....	164
Houweling, M.....	462	MacAllister, D.....	239
Howahr, M.....	103, 358	Makokha, M.....	62
Hu-a-ng, K.....	91	Mallast, U.....	366
Hughes, J.....	184	Mara, T.....	50
Hugman, R.....	185	Marçais, J.....	310
Huizer, S.....	189	Mariner, K.....	176
Hussain, M.....	191	Marobhe, I.....	62
Hutson, J.....	246	Massmann, G.....	132
Ibrahim, K.....	62	Mayer, A.....	261
Ibs-von Seht, M.....	375	Melchioly, S.....	62
Igel, J.....	195	Meon, G.....	103
Iodice, A.....	125	Merkel, B.....	366
Ionescu, D.....	366	Meyer, R.....	134
Jackson, M.....	239	Meyer, U.....	375, 385
Jacobsen, C.....	164	Michael, H.....	158, 243
Jakobsen, R.....	33	Michaelsen, J.....	315
Jakovovic, D.....	199	Miensopust, M.....	375
Janssen, G.....	58, 109, 437	Miraldo Ordens, C.....	246
Javadi, A.....	191	Mjemah, I.....	62
Jazar, M.....	204	Mohamed, I.....	62
Johnsen, A.....	164	Molinari, P.....	297
Join, J.....	50, 62	Mollema, P.....	25, 248 , 427
Kaczor-Kurzawa, D.....	200	Momii, K.....	405
Kaland, L.....	58	Monteiro, J.....	185
Kalaoun, O.....	204	Montenegro, S.....	164
Kamps, P.....	265	Moore, W.....	252
Kathmann, S.....	315	Morari, F.....	438
Kim, G.....	208	Morgan, L.....	162, 255 , 256
Kim, Y.....	208	Müller-Petke, M.....	150
Kirby, J.....	243	Mushtaha, A.....	121, 257
Kirsch, R.....	211, 453	Mwega, B.....	62
Knoeller, K.....	362	Nakayama, K.....	262
Knowling, M.....	162, 215 , 246	Neyens, D.....	288
Koeniger, P.....	172	Nguyen, B.....	261
Köhn, D.....	20	Nguyen, H.....	262
Kolditz, O.....	449	Ni, C.....	229
König, B.....	354	Nienhuis, P.....	265
Krause, F.....	31, 218	Noell, U.....	63
Kreuzburg, M.....	362	Nommensen, B.....	354
Kroeger, K.....	243	Nyambe, I.....	33
Kuntzer, M.....	195	Obando, J.....	62
Langevin, C.....	184, 219	Ogroske, A.....	218
Larsen, F.....	33, 220	Olsthoorn, T.....	24, 265, 269 , 410, 420
Lazareva, O.....	243	Oosterhof, A.....	462
Lebbe, L.....	58, 99, 221	Oppermann, F.....	335
Levannier, A.....	288	Ottow, B.....	417
Levanon, E.....	225	Oude Essink, G... 58, 87, 91, 109, 189, 275 , 281, 416, 417, 437	
Li, W.....	229	Oz, I.....	279
Liebezeit, G.....	42	Pacella, K.....	125
Liedl, R.....	449	Palladino, G.....	301
Limoni, P.....	235	Panciroli, L.....	75
Limoni, P.....	301	Pauw, P.....	281 , 285 , 416, 417
Lindgren, G.....	444	Perroud, H.....	288
Liotta, D.....	301	Pezard, P.....	288
Lipka, M.....	46	Pham, N.....	220

Phuc, H.	154, 292	Stuyfzand, P.	91, 248, 397, 401
Pohl, T.	366	Südekum, W.	134
Polemio, M.	235, 297, 301, 305, 466	Sültenfuß, J.	172
Pool, M.	309	Sulzbacher, H.	195
Popp, M.	218	Takahashi, M.	405
Post, V.	87, 199, 246, 285, 310	Teatini, P.	438
Postma, D.	164	Thanh Le, T.	409
Ptak, T.	457	Thanh Tam, V.	409
Pulido-Bosch, A.	379, 380, 415	Thomas, G.	389
Quy Nhan, P.	409	Thullner, M.	176
Raat, K.	462	Tijs, M.	410, 420
Rabbel, W.	20, 108	Tosi, L.	438
Rachid, G.	311	Trabelsi, R.	411
Radmann, K.	315	Tran, L.	220
Rapaglia, J.	362	Tulipano, L.	117
Rasmussen, P.	319	Ullmann, A.	103
Rizzo, E.	301	Vallejos, A.	379, 380, 415
Robins, N.	62	van Baaren, E.	281, 416, 417, 437
Robinson, G.	323, 327	van der Made, K.	285, 418
Rödiger, T.	366	van Ginkel, M.	410, 420
Rolf, H.	79	Vandenbohede, A.	424, 427, 431
Romanazzi, A.	297, 305	Vandevelde, A.	58
Ronczka, M.	331, 335	Vandevelde, D.	435
Röper, T.	132	Verkaik, J.	416, 437
Russoniello, C.	243	Vermeu, E.	87
Sánchez Úbeda, J.	339, 343	Vermeulen, P.	437
Santaloia, F.	235, 301	Vespasiano, G.	297
Sappa, G.	344	Viezzoli, A.	435, 438
Sawyer, A.	243	Vincent, P.	309
Schaars, F.	54, 79, 350, 418, 435	Vinogradov, J.	239
Schäfer, D.	20	Visser, M.	281, 417
Schäfer, S.	31, 218	Vogels, M.	109
Scheer, W.	354	von Storch, H.	442
Schlegel, C.	315	Vos, P.	91
Schlüter, M.	362	Voss, C.	129, 444
Schmidt, T.	31	Voß, W.	63, 371, 375
Schmiedinger, I.	46	Walraevens, K.	121, 257, 445
Schneider, A.	103, 358, 389	Walther, M.	389, 449
Schneider, B.	42	Waterloo, M.	310
Scholten, J.	362	Watson, T.	162
Schöniger, H.	103	Weinstein, Y.	121, 461
Schubert, M.	362	Werner, A.	162, 199, 215, 246, 255, 256, 363
Sebben, M.	363	White, J.	184
Shalev, E.	225	Wiederhold, H.	195, 211, 371, 375, 385, 453
Shalev, E.	279	Wieggers, C.	20
Shauri, H.	62	Wilken, D.	108
Shi, F.	243	Winde, V.	42, 46
Siebert, C.	366	Wolf, J.	103, 358
Siemon, B.	63, 371, 375, 385, 453	Wollman, S.	461
Sivan, O.	461	Wu, J.	164
Skowronek, F.	140	Yang, J.	389, 457
Sola, F.	379, 380, 415	Yaqubi, A.	121
Sonnenborg, T.	319	Yechieli, Y.	121, 225, 279, 461
Sørensen, S.	164	Yoon, H.	208
Soule, H.	62	Zaadnoordijk, W.	462
Steklova, K.	381	Zairi, M.	411
Steuer, A.	375, 385	Zamrsky, D.	275
Stieglitz, T.	243	Zilberbrand, M.	461
Stigter, T.	185	Zuffianò, L.	235, 301, 466
Stoekli, L.	176, 331, 358, 389, 393	Zurbier, K.	397

